

Copyright

by

Lindsay Ann Szramek

2010

The Dissertation Committee for Lindsay Ann Szramek certifies that this is the approved version of the following dissertation:

BASALTIC VOLCANISM:  
DEEP MANTLE RECYCLING, PLINIAN ERUPTIONS, AND COOLING-INDUCED  
CRYSTALLIZATION

Committee:

---

James Gardner, Supervisor

---

John Lassiter, Co-Supervisor

---

William Carlson

---

Bruce Houghton

---

Michael Rowe

**Basaltic Volcanism:**  
**Deep Mantle Recycling, Plinian Eruptions, and Cooling-Induced Crystallization**

by

**Lindsay Ann Szramek, B.A.; M.S.**

**Dissertation**

Presented to the Faculty of the Graduate School of

The University of Texas at Austin

In Partial Fulfillment

of the Requirements

for the Degree of

**Doctor of Philosophy**

The University of Texas at Austin

August 2010

This dissertation is dedicated to:

Jake Szramek

Natalie Szramek

&

Kati Szramek



## **Acknowledgements**

This dissertation has been made possible by many people and funding sources. I have received funding from NSF grants and the Jackson School of Geosciences to do the work contained in this volume. I have been employed on NSF grants as an RA and as a TA for the Jackson school. My summers have been funded so that I could make it out, 6 years after starting.

The first group of people that I would like to thank are my committee members. Jim Gardner, my advisor who I first started working with back in 2002 in Fairbanks, AK. I followed him to Texas where I learned more about experiments than I thought I would ever know. John Lassiter, my co-advisor who taught me to look beyond the surface and into the mantle. Bill Carlson, while a metamorphic petrologist has the best zoned labradorite in his kitchen island I have ever seen. Bruce Houghton, one of the nicest volcanologists I have ever met and someone who is going to help the community figure out these pesky mafic eruptions! Mike Rowe, who went from the post-doc who knew everything about melt inclusions to my committee member who still knows everything about melt inclusions. Mike stepped in at the last minute as a replacement committee member and I was worried having a friend as a member would be a problem, but it all went smoothly and I can't fathom not having him on my committee. The last member, who is no longer with us, Todd Housh, was a great man who knew how to balance science with an outside life. I learned a lot from him in the few short years I knew him

and will always wonder what more I would have learned had he lived. I will always miss him, but I am glad I was able to know him.

Next, I would like to thank the faculty and staff of the Jackson School that were there for me. First of all Sharon Mosher, without her I am sure I would have quit before I finished. She helped me deal with the realities that are geology graduate school. Chris Bell, whom I also considered a graduate advisor during my time. Marc Cloos, whose enthusiasm about geology was catching. Dennis Trombatore the most awesome librarian in the entire world. All the office staff-Kathy, Nicole, Lou, and any others I have forgotten, for taking care of me.

Philip gets his own paragraph. He knows everything about UT Austin. He has an adorable dog. He is a great softball pitcher. He gets things done. Did I mention he knows everything. Oh yes and he is just awesome. The department without Philip would fall apart in about 24 hours, if that long.

Now on to the friends that have helped me stay a bit sane while in the heat of Texas. Of course there are the other volcanologists-Giovanni, Abby, Nicole, Francine, and Kathy. I will never go to Mexico without Giovanni and will miss getting to see Mayra and the kids when they come to see him at school. I have become a FOP-friend of paleo and Kerin and Jen have taught me things about fossils and dead things I never thought I would know. My fellow hard-rockers-Miss Jamie and Miriam-the upstairs office Stephanie, Emily, Eric, and Jad. Of course I have forgotten many people in this list, but I thank them also.

I have saved my greatest thanks for last, my family. Mom, Dad, and Kati. Mom and Dad have been there for support and bought plane tickets home when I needed a break. They have been there when I needed to talk or complain and supported me in any decision I made. Kati who went through it all right before I did understood things that parents were not able to. Now there are two Dr. Szramek's...and I am ok with being number two as long as Kati is number one.

## **Basaltic Volcanism:**

### **Deep Mantle Recycling, Plinian Eruptions, and Cooling-Induced Crystallization**

Lindsay Ann Szramek, Ph.D

The University of Texas at Austin, 2010

Supervisors: James E Gardner and John C. Lassiter

Mafic magma is the most common magma erupted at the surface of the earth. It is generated from partial melting of the mantle, which has been subdivided into end-members based on unique geochemical signatures. One reason these end members, or heterogeneities, exist is subduction of lithospheric plates back into the mantle. The amount of elements, such as Cl and K, removed during subduction and recycled into the deep mantle, is poorly constrained. Additionally, the amount of volatiles, such as Cl, that are recycled into the deep mantle will strongly affect the behavior of the system. I have looked at Cl and K in HIMU source melts to see how it varies. Cl/Nb and K/Nb suggest that elevated Cl/K ratios are the result of depletion of K rather than increased Cl recycled into the deep mantle.

After the mantle has partially melted and mafic melt has migrated to the surface, it usually erupts effusively or with low explosivity because of its low viscosity, but it is possible for larger eruptions to occur. These larger, Plinian eruptions, are not well understood in mafic systems. It is generally thought that basalt has a viscosity that is too

low to allow for such an eruption to occur. Plinian eruptions require fragmentation to occur, which means the melt must undergo brittle failure. This may occur if the melt ascends rapidly enough to allow pressure to build in bubbles without the bubbles expanding. To test this, I have done decompression experiments to try to bracket the ascent rate for two Plinian eruptions. One eruption has a fast ascent, faster than those seen in more silicic melts, whereas the other eruption is unable to be reproduced in the lab, however it began with a increased viscosity in the partly crystallized magma.

After fragmentation and eruption, it is generally thought that tephra do not continue to crystallize. We have found that crystallinity increases from rim to core in two basaltic pumice. Textural data along with a cooling model has allowed us to estimate growth rates in a natural system, which are similar to experimental data.

## Table of Contents

List of Figures.....	xiii
List of Tables.....	xv
Chapter 1: Introduction to Dissertation.....	1
Introduction.....	2
Chapter 2: Deep Mantle Recycling of Cl and K: Insights from	
HIMU melt inclusions from Raivavae Island.....	6
Abstract.....	7
Introduction.....	8
Background .....	12
Previous Studies on Cl.....	12
Recycled Oceanic Crust and HIMU.....	14
Austral.....	15
Melt-Inclusions.....	16
Methods.....	18
Sample Preparation.....	18
Electron Microprobe analysis of major elements and Cl.....	19
SIMS.....	23
Results.....	28
Major-Elements.....	28
Trace-Elements.....	28

Discussion.....	30
Elemental Trends.....	30
HIMU Source.....	31
Recycling Efficiency.....	33
Chapter 3: Mafic Plinian Eruptions: Is Fast Ascent Required? .....	97
Abstract.....	98
Introduction.....	99
Geologic Background.....	102
Basaltic Andesite-Fontana Lapilli, Masaya Volcano.....	102
Hawaiite-122 BC Mt Etna.....	103
Methods.....	105
Starting Material.....	105
Decompressions.....	107
Textural Analysis.....	108
Results.....	110
Natural Groundmasses.....	110
Experimental Textures.....	111
Discussion.....	113
Experimental Results.....	113
Magma Ascent During the Fontana Plinian Eruption.....	114
Magma ascent During the Etna Plinian Eruption.....	116
Fragmentation During Mafic Plinian Eruptions.....	119

Chapter 4: Cooling Induced Crystallization of Microlite Crystals	
in two Basaltic Pumice.....	136
Abstract.....	137
Introduction.....	138
Methods.....	140
Results.....	143
Phenocryst Assemblage and Glass Compositions.....	143
Groundmass Textures.....	144
Discussion.....	147
Implications.....	150
Chapter 5: Conclusion to Dissertation.....	161
Conclusion.....	162
Appendix 1.....	164
Appendix 2.....	227
Appendix 3.....	264
Bibliography.....	304
Vita.....	314



## List of Figures

<i>Figure</i>	<i>Page</i>
Figure 2.1.....	36
Figure 2.2.....	37
Figure 2.3.....	38
Figure 2.4.....	39
Figure 2.5.....	40
Figure 2.6.....	41
Figure 2.7.....	42
Figure 2.8.....	43
Figure 2.9.....	44
Figure 2.10.....	45
Figure 2.11.....	46
Figure 2.12.....	47
Figure 2.13.....	48
Figure 2.14.....	49
Figure 2.15.....	50
Figure 2.16.....	51
Figure 2.17.....	52
Figure 2.18.....	53
Figure 3.1.....	121
Figure 3.2.....	122

Figure 3.3.....	123
Figure 3.4.....	124
Figure 3.5.....	125
Figure 3.6.....	126
Figure 3.7.....	127
Figure 3.8.....	128
Figure 3.9.....	129
Figure 3.10.....	130
Figure 4.1.....	152
Figure 4.2.....	153
Figure 4.3.....	154
Figure 4.4.....	155
Figure 4.5.....	156
Figure 4.6.....	157
Figure 4.7.....	158
Figure 4.8.....	159

## List of Tables

<i>Tables</i>	<i>Page</i>
Table 2.1.....	54
Table 2.2.....	59
Table 2.3.....	62
Table 2.4.....	63
Table 2.5.....	65
Table 2.6.....	68
Table 2.7A.....	69
Table 2.7B.....	77
Table 2.7C.....	85
Table 2.8A.....	91
Table 2.8B.....	94
Table 3.1.....	131
Table 3.2.....	132
Table 3.3.....	133
Table 3.4.....	134
Table 3.5.....	135
Table 4.1.....	160

# **Chapter 1**

## **Introduction to Dissertation**

## Introduction

Mafic magma is the most common magma erupted at the surface of the earth and typically occurs as effusive eruptions, although more explosive Plinian and sub-Plinian eruptions are known to occur (Williams, 1983; Coltelli et al., 1995; Gurenko et al., 2005; Walker et al., 1984; Sable et al., 2006). Volatiles play a large role in the behavior of the eruptions and therefore are important to understand, from concentration in mantle heterogeneities to magma ascent, degassing, and fragmentation. To understand how volcanic processes are modulated by the role of volatiles, we must also understand the volcanic products that we have available to examine. The next three chapters will be an exploration of (1) how volatiles and other elements, Cl and K in particular, are recycled through the subduction process; (2) if rapid ascent can account for brittle failure and fragmentation in low viscosity melts; and (3) post-eruptive alteration of groundmass in a mafic sub-Plinian deposit.

Project one focuses on basaltic magma, which is generated from partial melting of the mantle. The mantle has been subdivided into end-members based on unique isotopic and geochemical signatures (Zindler and Hart, 1986). One reason these end members, or heterogeneities, exist is subduction of plates into the mantle. The concentration of elements, such as Cl and K, removed during subduction and recycled into the deep mantle, is poorly constrained. To understand recycling into the deep mantle better, I have looked at the elements Cl and K in HIMU (high  $\mu$ ;  $\mu = {}^{238}\text{U}/{}^{204}\text{Pb}$ ) mantle. Characteristics of HIMU mantle include a high  ${}^{238}\text{U}/{}^{208}\text{Pb}$  ratio, radiogenic Os and Pb isotopes, unradiogenic Sr isotopes, and depletions in fluid-mobile elements such as K. It is

modeled as containing ancient subducted, dehydrated oceanic crust and therefore its trace-element abundances provide information on chemical cycling at subduction zones and recycling into the deep mantle. Melt inclusions trapped at depth can provide information on the abundance of volatiles such as Cl not available from surface samples that have experienced subaerial degassing. I have examined melt inclusions from 12 samples from the Austral Islands whose isotopic compositions span a wide range, from HIMU compositions to EM-like values. I have determined that that elevated Cl/K ratios are the result of a decrease of K, rather than increased Cl.

Project two investigates how a low viscosity mafic magma can erupt in Plinian style. The viscosity of basalt is generally considered to be too low to allow for Plinian eruptions. For an eruption to be Plinian, fragmentation, where brittle failure breaks the magma into pieces (Papale, 1999; Wright and Weinberg, 2009; Zhang, 1999; Alidibirov and Dingwell, 2000), must occur. It has been hypothesized that for a Plinian eruption of mafic magma to occur, brittle failure will only happen if the ascent of the magma is fast enough to trap pressure in the vesicles without allowing them to expand. To determine how fast basaltic Plinian magmas need to travel from the chamber to the level of fragmentation, I carried out a number of decompression experiments on hydrous mafic magmas and compared the results to two well-documented basaltic Plinian eruptions: the basaltic andesite of Fontana eruption of Masaya (Nicaragua) and the hawaiite of 122 BC eruption of Etna (Italy). Comparing experimental textures to natural textures, I have been able to bracket decompression of the basaltic andesite between  $0.2 \text{ MPa s}^{-1}$  and  $0.1 \text{ MPa s}^{-1}$ . This bracketed decompression rate is faster than those experimentally determined for

more siliceous melts. In the case of the hawaiiite, I was unable to experimentally reproduce the textures seen in the natural sample, however I have determined that the viscosity of this magma was 1-2 orders of magnitude higher than the pure melt because of microlite growth prior to eruption. It appears that fast ascent is not required for mafic Plinian eruptions.

In the third and final project I look at how textures vary across two basaltic pumice. One assumption made about pumice deposits of Plinian eruptions is that the groundmass stops crystallizing after fragmentation. If this is the case, then I would expect to see no variation across a pumice with relation to distance from the rim. In my two samples, I see that textures do vary from the rim to the core of each pumice. Pairing this variation with a cooling model that is dependant on pumice size, I have been able to determine growth rates for natural plagioclase. I find that our rates are similar to those determined via experiments for similar cooling rates.

While each project is distinct and looks at a portion of the eruptive process, together they all are trying to understand what happens in mafic volcanism. The amount of volatiles present in a source will have a large effect on melting and style of eruption. The behavior of volatiles within that magma during ascent will either produce an effusive or explosive eruption, yet we do not understand how mafic magmas can produce a Plinian style eruption. Mafic Plinian eruptions are rare and therefore we must study the deposits left behind by the eruptions. To study these deposits, we can either look at there physical aspects or we can look on a smaller scale at there petrology. To study the minerals within the pumice, we must know how and where the minerals formed.

Knowing if the minerals grew during ascent or during cooling allows us to understand the deposits better.



## **Chapter 2**

**Deep Mantle Recycling of Cl and K:**

**Insights from HIMU melt inclusions from Raivavae Island**

## Abstract

The amount of chlorine and potassium that is recycled into the deep mantle through subduction processes is poorly constrained. Estimates of the chlorine content in recycled, dehydrated oceanic crust range from <50 ppm (Lassiter et al., 2002) up to ~200 ppm (Philippot et al., 1998; Stroncik and Haase, 2004). The amount of potassium that is recycled into the deep mantle varies from 5% (Becker et al., 2000) to 71% (Eiler et al., 2000).

In order to better constrain the Cl and K content in subducted crust, we have examined Cl concentrations as well as Cl/K<sub>2</sub>O, Cl/Nb and K/Nb ratios in olivine-hosted and plagioclase-hosted melt inclusions in HIMU lavas from the island of Raivavae, Austral Islands. Raivavae lavas span a wide range of lead isotopic values, with <sup>206</sup>Pb/<sup>204</sup>Pb ranging from ~19.3 to 21.3. Previous isotopic and trace element studies suggest that Raivavae lavas derive from a mantle source containing ancient dehydrated oceanic crust.

Melt-inclusions from 12 samples from the Austral Islands have been examined, whose isotopic compositions span a wide range, from HIMU compositions to EM-like values. Chlorine and K<sub>2</sub>O concentrations range from 40-1070 ppm and 0.22-3.5 wt.% respectively. The majority of Cl/K<sub>2</sub>O ratios range from 0.01-0.12, Cl/Nb ratios range from 5-25, and K/Nb ratios range from 50-300. Cl/Nb has no correlation with Nb/Zr (a source signature) whereas K/Nb has a general negative correlation. This suggests the elevated Cl/K<sub>2</sub>O ratios seen in HIMU basalts are caused by a depletion of K because Cl/Nb ratios do not appear to vary between mantle sources.

## Introduction

Although it has been recognized since the early 1980's that subduction plays a major role in the generation of mantle heterogeneities (e.g. White and Hofmann 1982; Cohen and O'Nions 1982; Morris and Hart, 1983), there is still little consensus on how subduction affects the composition of subducted materials (e.g. Willbold and Stracke, 2006; Rapp et al., 2008; Dasgupta et al., 2004; Philippot et al., 1998; Ludden, 2009; Kent et al., 2002; Saal et al., 2005). Subduction of plates can introduce sediments, continental crust, and oceanic crust into the mantle (Ludden, 2009; Willbold and Stracke, 2006), creating heterogeneities within the mantle (Rapp et al., 2008; Willbold and Stracke, 2006; Roux et al., 2006). Volatiles (e.g., H<sub>2</sub>O, CO<sub>2</sub>) introduced into the mantle during subduction of crustal materials may have a number of effects including changing the rheology and lowering the melting temperature of the mantle (Portnyagin et al., 2007; Behrens and Gaillard, 2006). However, the extent to which processes such as dehydration or partial melting that may occur in association with plate subduction modify the compositions of subducted materials returned to the deep mantle is poorly constrained. In particular, the degree to which volatile species such as water, Cl, CO<sub>2</sub>, or S are retained in recycled components during subduction is poorly understood. Because these species play an important role in controlling rheology and melting processes, further constraining the geochemical cycling of these species in the Solid Earth is an important goal.

The removal of volatiles during subduction and dehydration can be seen in enrichments present in arc lavas (Wallace, 2005; Benjamin et al., 2007; Münker et al.,

2004; Vigouroux et al., 2008). For example, melt-inclusions in high-Mg andesite arc lavas in northern California have water contents up to 8-10 wt. % H<sub>2</sub>O (Grove et al., 2002, Wallace, 2005). Additionally, melt inclusions from arc lavas show enrichments over MORB lavas in CO<sub>2</sub>, Cl, and S (Wallace, 2005). However, whether water and other volatile species are quantitatively removed from subducted slabs during processing in the “subduction factory”, or whether a portion of these species is returned to the deep mantle, remains a matter of debate. For example, although arc lavas typically have elevated water contents, Ito et al. (1983) pointed out that arc lavas do not account for all of the volatiles that are contained in the sub-arc wedge or the subducted crust and sediment. This raises the possibility that a portion of the volatile budget contained in recycled components may be returned to the deep mantle, and that variations in the concentration of species such as water or Cl may therefore be useful for tracking the presence and quantity of recycled material in different mantle reservoirs.

Chlorine and K are potentially useful species for evaluating the chemical processes that affect recycled components during subduction. Recycled components such as sediments and hydrothermally altered oceanic crust are enriched in Cl and K (Michael and Schilling, 1989; Plank and Langmuir, 1998; Rapp et al., 2008). In addition, both of these species are likely to strongly partition into aqueous phases produced during dehydration reactions that occur as crustal material is subducted and heated in the mantle (Pearce and Peate, 1995; Sun et al., 2007). Previous studies have shown that lavas derived from arc and back-arc environments often have elevated Cl and K concentrations relative to MORB, as seen in high Cl/Nb and K/Nb ratios (c.f., Kent et al., 2002, Sun et

al., 2007), reflecting transfer of these elements to the sub-arc mantle wedge during slab melting or dehydration (eg., Kent et al., 2002; Sun et al., 2007; Bouvier et al., 2008). More recently, Rowe & Lassiter (2009) reported elevated Cl/Nb ratios in lavas derived from subduction-modified continental lithosphere beneath the Colorado Plateau and Rio Grande Rift. Thus, preferential transfer of these species from subducted slabs into the sub-arc mantle wedge is well established. However, the amount of Cl or K that remain in slab restite after subduction is more contentious, and different studies have provided greatly varying estimates of the recycling efficiency of Cl (c.f., Stroncik and Haase, 2004; Philippot et al., 1998; Lassiter et al., 2002) and K (Becker et al., 2000; Eiler et al., 2000). The extent to which concentrations of Cl or K vary in different mantle reservoirs, and whether these variations track the type and amount of recycled material present, is therefore unclear.

To investigate the issue of Cl and K recycling to the deep mantle, melt-inclusions from lavas found on Raivavae Island, Austral Islands have been examined. This location has lavas with isotopic values that reflect mixture of HIMU (high  $\mu$ ;  $\mu = {}^{238}\text{U}/{}^{204}\text{Pb}$ ) and DMM (depleted mantle) reservoirs (Lassiter et al., 2003), which allows us to investigate how Cl and K vary with source composition. Because HIMU mantle is thought to contain ancient, recycled oceanic crust that has been dehydrated during subduction (Hauri and Hart, 1993), estimating the concentrations of Cl and K in HIMU mantle will allow greater constraint on the concentrations of these species in recycled crust *after* subduction and dehydration, and thus the overall recycling efficiency of these species to the deep

mantle. 12 samples spanning a range in isotopic compositions have been analyzed, with major-elements on 235 inclusions and trace-elements on a subset.

## **Background**

### *Previous Studies on Cl*

Many previous studies have focused on the enrichment of Cl seen in lavas that result from subduction (Rowe et al., 2009; Wallace, 2005; Kent et al., 2002). Wallace (2005), looking at lavas worldwide, found that Cl is present in high concentrations in arc and back-arc lavas. Kent et al. (2002) reported a decrease in Cl/H<sub>2</sub>O and Cl/K<sub>2</sub>O ratios with increasing distance from the arc front in lavas from the Lau Basin. More recently, Rowe and Lassiter (2009) reported elevated Cl/Nb ratios in melt inclusions from lavas from the Rio Grande Rift, and argued that the elevated Cl content in these lavas reflected melt generation from subduction-modified continental lithosphere, possibly in response to shallow subduction of the Farallon slab. However, none of these studies directly constrain how large a fraction of Cl or K are removed from recycled crust during subduction. To do this, it is necessary to examine the composition of recycled materials *after* they have passed through the subduction factory.

Several studies have attempted to constrain the efficiency of Cl recycling to the deep mantle (e.g., Philippot et al., 1998; Stronck and Haase, 2004; Lassiter et al., 2002). Philippot et al. (1998) examined eclogites that experienced little or no interaction with external fluid sources. Analysis of the fluid inclusions and oxygen isotopes in a number of eclogites and comparison to unmetamorphoized protoliths suggests that the variability of the original rock is preserved. Extrapolating the eclogite data to subducted oceanic crust suggests that 100-200 ppm of Cl are recycled into the mantle during subduction.

Lassiter et al. (2002) and Stronck and Hasse (2004) examined Cl concentrations

in melt inclusions and submarine glasses from several plume-related settings to constrain the role of recycling in generating Cl concentration variations in the mantle. Stroncik and Haase (2004) examined basaltic glasses with isotopic compositions ranging from EM- to HIMU-like compositions. They found that Cl/K ratios in submarine glasses correlated with isotopic composition, with HIMU samples possessing higher Cl/K ratios than samples with either EM or DMM compositions, and estimated that 11-160 ppm of Cl is contained in recycled oceanic crust (assumed to be a major component in the HIMU source). The large uncertainty reflected uncertainty in the proportion of K in the subducted slab that is returned to the deep mantle, where estimates range from 5% (Becker et al., 2000) to 71% (Eiler et al., 2000). In contrast, Lassiter et al. (2002) found only a small range of Cl/K ratios in a global comparison of oceanic basalts, with little difference between basalts from MORB and OIB settings. In particular, Lassiter et al. (2002) found low Cl/K ratios in a small suite of HIMU lavas from Raivavae, Austral Islands, and estimate only ~50 ppm Cl in the HIMU source. A significant difference between these two studies is that Lassiter et al. (2002) assumed a lower K content for the HIMU source, based on low observed K/U ratios in HIMU lavas relative to MORB. The chlorine recycling estimates of both the Stroncik & Haase (2004) and Lassiter et al. (2002) studies are dependant on the inferred efficiency of K recycling in the mantle during subduction, which is problematic because the amount of K that recycled in the deep mantle is itself poorly constrained, with estimates ranging between 5% (Becker et al., 2000) to 71% (Eiler et al., 2000). Furthermore, Sun et al. (2007) recently suggested that Cl is more incompatible than K during mantle melting, with a bulk distribution



coefficient similar to Nb (Sun et al., 2007). As a result, variations in degree of partial melting will result in variations in Cl/K, but not Cl/Nb. Therefore, in order to better constrain the behavior of both Cl and K during slab subduction and dehydration, we examine the variation of Cl/Nb and K/Nb ratios in suites of inclusions from the island of Raivavae for host lavas spanning a wide range in isotopic compositions.

#### *Recycled Oceanic Crust and HIMU*

HIMU basalts are characterized by a distinctive isotopic and trace-element signature. HIMU basalts have very radiogenic Pb-isotopes ( $^{206}\text{Pb}/^{204}\text{Pb} > 20$ ), reflecting long-term enrichment in the HIMU source in U and Th with respect to Pb. The  $^{187}\text{Os}/^{188}\text{Os}$  ratio of HIMU basalts is also much higher than found in other mantle end-members (Hauri and Hart, 1993), with  $^{187}\text{Os}/^{188}\text{Os}$  ratios of  $\sim 0.150$ . This radiogenic signature indicates that the HIMU source has evolved with a high Re/Os ratio. However, HIMU basalts typically have relatively unradiogenic Sr-isotopes ( $^{87}\text{Sr}/^{86}\text{Sr}$  ratio of  $\sim 0.7029$ ; Zindler and Hart, 1986), reflecting a low source Rb/Sr ratio. HIMU basalts are also depleted in K, Rb, and Ba, reflected for example in low K/U and K/Nb ratios. The trace-element mantle-normalized pattern mirrors that for MORB with a steady decrease from niobium (Nb) to cesium (Cs) (Sun and McDonough, 1989), although HIMU basalts have much higher trace element abundances than MORB and are LREE-enriched rather than depleted.

Several studies have proposed ancient recycled oceanic crust as the source of HIMU basalts (e.g., Zindler and Hart, 1986; Woodhead, 1996; Hauri and Hart, 1993, Lassiter et al., 2003). The specific evidence that suggests recycled crust as the source of

HIMU is as follows. HIMU has radiogenic Os-isotopes, which indicate a high time-integrated source Re/Os ratio. During partial melting, Os is compatible whereas Re is incompatible during partial melting (Dale et al., 2007). Therefore, mafic lithologies (e.g., recycled basalt) should have much higher Re/Os than mantle peridotite. Additionally, element ratios such as low Rb/Sr, K/U, and Pb/U (high U/Pb) all suggest depletion of fluid-soluble elements relative to insoluble elements. This depletion can be explained by removal of these elements during dehydration reactions accompanying subduction.

Ancient subducted oceanic crust is not the only model that has been proposed for HIMU. Other models, including mantle metasomatism by low-degree partial melts have been suggested (Hart, 1988). However, mantle metasomatism cannot account for the observed fractionation of soluble from insoluble elements (e.g., low K/U). Although there is still debate on the origin of HIMU, the recycled crust model is best able to account for the observed characteristics and this model has therefore been used as a basis for the subsequent analysis.

### *Australis*

HIMU lavas occur as end-member compositions, rather than within a mixture, in only a few localities, including St. Helena (Chaffey et al., 1989) and the Austral Islands (Woodhead, 1996). The Austral Islands make an excellent location to study the effect of oceanic crust recycling on Cl and K concentration variations in the mantle because lavas from the Austral Islands span a wide range in isotopic composition (Lassiter et al, 2003). In particular, lavas from the island of Raivavae span a wide range in composition reflecting mixing of HIMU and depleted mantle components (e.g.,  $^{206}\text{Pb}/^{204}\text{Pb}$  ratios

range from ~19-21.5; Fig 2.1). This range makes Raivavae an excellent location to study the efficiency of recycling of Cl and K during subduction through characterization of melt-inclusions hosted in olivine or plagioclase, because variations in the relative abundance of Cl or K can be correlated with isotopic variations in the host lavas.

### *Melt-Inclusions*

Volatile concentrations in subaerially-erupted lavas are affected by low-pressure magma degassing processes, and therefore do not directly provide information about source volatile content. However, Cl degassing at pressures greater than ~4 MPa is minor (Unni and Schilling, 1978). Therefore, melt-inclusions trapped at greater pressures can be used to examine the concentration of Cl in magmas prior to shallow degassing. Melt-inclusions can provide a sample of melt that has been ‘closed’, not allowed to degas, from the time it was entirely trapped within a crystal. A simple definition of a melt-inclusion is: a bleb of silicate melt trapped inside an incompressible phenocryst host that acts as a pressure vessel (Lowenstern, 2003). If no cracks are present in the incompressible phenocryst host, the trapped melt records the composition of the magma at the time of entrapment including any volatile species present. An analysis of this quenched melt provides insight into the magma composition at depth.

Although melt-inclusions are a direct record of pre-eruptive volatile content and magma composition, a number of issues exist in measuring and interpreting the data. One of the major issues is the size of the inclusions, ranging from 100’s of microns in diameter to less than a micron. Small inclusions are often not analyzed because of machine limitations. If the inclusion is not quenched rapidly enough to produce only

glass, crystals may be present. The amount of crystals can range from only a few to completely crystalline. Also, vapor bubbles or fluids may be present in the inclusion (Lowenstern, 2003). In these cases, melt inclusions are typically rehomogenized to produce a glass prior to analysis. However, this process must be done in a matter of minutes, as hydrogen has been shown to diffuse out of inclusions at elevated temperature, altering the water composition (Hauri, 2002). Furthermore, over or underheating of the inclusion during rehomogenization may result either in melting and assimilation of the host phenocryst, or incomplete melting of daughter crystals, respectively. Volatiles may also escape the inclusion during rehomogenization if the inclusion is breached. This can usually be detected optically by the presence of cracks or fractures intersecting the target melt inclusion, or analytically by measurement of anomalously low Cl or S abundances in the homogenized melt. If no S or Cl is present, it is assumed that the inclusion was breached and is not a good study candidate. Finally, diffusion of Fe from the trapped melt into host olivines during slow magma cooling has also been shown to affect the major element compositions of olivine-hosted melt inclusions, requiring correction for melt/host interaction (Danyushevsky et al., 2000).

## Methods

### *Sample Preparation*

Rock samples were lightly crushed in a steel mortar and pestle and groundmass was magnetically separated. The resulting crystal concentrates were examined under a binocular microscope and all olivine  $\pm$  plagioclase crystals were separated. Melt inclusions were then rehomogenized in a gas-mixing Deltech vertical tube furnace at temperatures ranging from 1050-1250°C, selected to match the 1-atm liquidus temperature of the bulk rock composition for each sample as determined via MELTS (Asimow and Ghiorso, 1998; Ghiorso and Sack, 1995). Because most of the whole-rock samples selected for study contained cumulous olivine, this resulted in an overheating of most inclusions and some melting of the host phenocryst during melt inclusion homogenization (see below). The sample apparatus, consisting of oxygen probe, thermocouple, and sample, was placed in the gas-mixing furnace, with the sample raised near the water-cooled region until the gases had reached an oxygen fugacity of QFM. The fugacity was monitored from the voltage output of the oxygen probe. After the  $fO_2$  and temperature had stabilized, the sample was lowered into the hot zone of the furnace for 17 minutes, 5 minutes to warm up and 12 minutes to rehomogenize. The sample was then quenched rapidly in water.

Individual inclusions were exposed and prepared for analysis using a procedure similar to that described in Hauri (2002). Individual inclusion-bearing crystals were first attached with crystalbond to the stubs of a 4-post sample holder. Grains were rough polished with silica carbide grit paper (80-600 grit) to expose inclusions, which were

identified using a binocular microscope and a reflected light monocular petrographic microscope. Once an inclusion was intersected, the stub that contained the crystal+inclusion was removed and a new post was inserted. Crystals with intersected inclusions were removed from the stubs by soaking in acetone and then cleaned in methanol. Multiple crystals were then re-mounted in epoxy, inclusion side down, in ¼" Aluminum tubing. The mounts were then polished with 3 µm and 1 µm diamond paste and finally cleaned in water and methanol. Each sample was then imaged in reflected light at low magnification to identify and map exposed inclusions for subsequent analysis.

#### *Electron Microprobe analysis of major elements and Cl*

Mineral and glass electron microprobe analyses were done at Oregon State University on a Cameca SX-100 and at The University of Texas at Austin on a JEOL 8200 Superprobe. Glass analysis conditions were 15 kV, 30 nA current, and a defocused beam that ranged from 5 to 10 microns in diameter. Most major elements were analyzed for 20 seconds on peak and 10 seconds off-peak. Cl was analyzed for 100 seconds on peak and 50 seconds off-peak. To maximize spectrometer usage, some elements were occasionally counted for longer than 20 seconds on peak and 10 seconds off peak. Backgrounds were measured above and below the peak and a line was fit for background subtraction. VG-2G basalt glass was used as a secondary standard for sulfur and chlorine and BHVO-2G basalt glass as a secondary standard for the major-elements. Secondary standards were run every 15-20 analyses to check for instrument drift. Because of beam size and interactions, only inclusions larger than ~10 microns in diameter were analyzed.

Sodium loss was monitored and corrected for following the methods of Nielsen and Sigurdsson (1981). Major element compositions of minerals hosting non-degassed inclusions (inclusions containing measurable S and Cl) were analyzed using separate routines for olivine and plagioclase. Operating conditions consisted of 15 kV, 50 nA current, and a focused beam. Major elements were analyzed for 20 seconds on peak and 10 seconds off-peak. To maximize spectrometer usage, some elements were occasionally counted for longer than 20 seconds on peak and 10 seconds off peak. Measurements were taken no further than 100 microns from the melt inclusions. As with the glass routine, secondary standards, San Carlos and Springwater (USNM 2566) for olivine and An50 (University of Texas at Austin) for plagioclase, were run every 15-30 analyses.

The accuracy and precision of the microprobe data were evaluated from repeat analyses of secondary standards (Tables 2.1, 2.2, and 2.3) during each run as well as duplicate measurements of unknowns (Table 2.4). The relative standard deviations (RSD) for duplicate analyses average less than 7 % for elements present at > 0.1 wt. % whereas elements present at <0.1 wt. % have average RSDs in the 20-30 % range (Fig. 2.2). To obtain better data on Cl, more counts were obtained. Data precision was evaluated by comparison of average standard analyses with accepted values. For glass analyses (VG-2G and BHVO-2G), SiO<sub>2</sub>, Al<sub>2</sub>O<sub>3</sub>, S, K<sub>2</sub>O, MnO, CaO, FeO, Na<sub>2</sub>O, MgO and TiO<sub>2</sub> had average measured values within 10% of the canonical values, whereas P<sub>2</sub>O<sub>5</sub> showed greater departure from canonical values, up to 12% (Table 2.1). Cr<sub>2</sub>O<sub>3</sub> and NiO both had large deviations from accepted values, and these data for the melt inclusions are not considered further in the subsequent discussion. In plagioclase, average measured values

for  $\text{SiO}_2$ ,  $\text{Al}_2\text{O}_3$ ,  $\text{CaO}$ , and  $\text{Na}_2\text{O}$  in the AN50 standard were all within 3 % of the canonical values (Table 2.3). Measured values for  $\text{SiO}_2$ ,  $\text{FeO}$ , and  $\text{MgO}$  in olivine are similar to canonical values for the San Carlos and Springwater olivine standards whereas  $\text{MnO}$ ,  $\text{CaO}$ , and  $\text{Cr}_2\text{O}_3$  are more variable, possibly as a result of their low abundances (Table 2.2). Repeat analyses of melt inclusions have average RSD's < 5% for all but elements except Cl and  $\text{MnO}$ , which have average RSD's of 6-7 % , and  $\text{Cr}_2\text{O}_3$  and  $\text{NiO}$ , which have average RSD's of 23-25 % (Table 2.4).

Major-element compositions in each melt-inclusion could be affected by a number of factors and therefore need to be corrected. Olivine-hosted melt inclusions were first corrected for iron loss (Rowe et al., 2006; Danyushevsky et al., 2000). The average iron concentration present in the whole-rock; ~12 wt. %  $\text{FeO}$  (Lassiter et al., 2003), is assumed to be the amount that would be in the inclusion if no iron loss had occurred. To correct the iron composition of each inclusion to 12 wt. %  $\text{FeO}$ , a number of steps were taken. First, the microprobe data was converted to moles and then mole fractions. Next, total  $\text{FeO}$  was converted to ferrous iron by assuming that 85% of the iron reported was ferrous based on typical ratios found in basalts. At this point, ferrous iron was added and magnesium was subtracted on a 1:1 molar basis until the final wt. %  $\text{FeO}$ =12 wt. %. The next major correction was addition or subtraction of the olivine host until equilibrium was reached. Equilibrium was defined when the Mg # of the melt and the Fo content of the host olivine fell on a curve that defined a  $K_d$  of 0.3 (Ford et al., 1983). If olivine needed to be removed from the melt composition, an olivine host composition was used, if olivine needed to be added to the melt composition, a



stoichiometric olivine composition, in equilibrium with the melt, was added. Steps used in the corrections processes added or subtracted 0.1 wt. % olivine. Each step, regardless of addition or subtraction of olivine was preformed as follows:

$$C_{i_{new}^{melt}} = \frac{C_{i_{melt}} X_m + C_{i_{ol}} X_{ol}}{X_m + X_{ol}}$$

When olivine was added, the host olivine for each individual inclusion was used. When olivine was subtracted, a stoichiometric olivine was used and the composition was varied to maintain equilibrium with the latest melt composition. Adding or subtracting host olivine to the melt composition would change the iron concentration in the melt inclusion. Therefore, the proceeding process, including iron correction and host addition/subtraction, was preformed in iterative steps, until the final iron concentration was ~12 wt. %.

Plagioclase-hosted melt-inclusions, in samples RVV312, RVV343, and RVV362, do not experience iron loss and therefore the FeO wt. % was not altered. However, the host mineral can still have crystallized or melted into the melt-inclusion, changing the composition. Typically, adding or subtracting the host plagioclase composition will bring the melt and the host plagioclase into equilibrium. Equilibrium in the plagioclase/melt system can be simply defined from a plagioclase/melt binary diagram, where the plagioclase has a higher An content than the melt it is in equilibrium with. The An composition from plagioclase-hosted melt-inclusions in RVV312, RVV343, and RVV362 is similar to the An composition of the plagioclase that the inclusions are hosted in. Therefore, adding or subtracting the plagioclase host composition does not bring the

melt and host into equilibrium. Additionally, the An content of the whole-rock is similar to the An content of plagioclase and melt composition. Therefore, it is reasonable to not correct the plagioclase-hosted melt-inclusions. This will affect the absolute concentrations, but will not affect the ratios.

Altering the composition of each melt-inclusion to account for iron loss and addition/subtraction of host mineral adds another layer of error to the microprobe data. For the majority of the data, the composition of the melt-inclusion was changed  $\pm 10\%$ , however in some instances the change was larger, up to 30%. This change was determined by the number of steps (1 step=0.1 %) required to reach equilibrium between host and melt. If the required change to bring the melt-inclusion and host into equilibrium was too great ( $>30\%$ ), then that data point was discarded as it was determined to be unreliable.

### *SIMS*

Trace-element analysis was performed at Arizona State University on a Cameca 6F

Secondary Ion Mass Spectrometer (SIMS) over three sessions. Two different operating conditions were used. For the first and third operating sessions, a 12.5 KeV beam of mass filtered  $^{16}\text{O}^-$  at 1-5 nA (focused to  $\sim 25$  microns) and secondary ions accelerated to  $\sim 10\text{KeV}$  was used. For some analyses with melt inclusions smaller than 30 by 30 microns, a field aperture, with variable size, was also used in order to reduce the beam size. The second session used a beam of mass filtered  $\text{Cs}^+$  focused to  $\sim 30$  microns in an attempt to collect hydrogen. All sessions employed conventional energy filtering, where

ions with  $75 \pm 20$  eV excess kinetic energy were allowed into the mass spectrometer (Shimizu, 1978). During each session, BHVO-2G and BCR-2G were analyzed as secondary standard and standard, respectively. To monitor for changes between sample mounts, standards were analyzed at the start, middle, and end of each set of analyses on a sample when more than 10 inclusions were present. If fewer inclusions were present, standards were only analyzed at the start and end of each sample sequence. Each analysis lasted between 30 and 45 minutes, depending on the instrument setup. Measurements were done in ratio mode, with all masses ratioed to  $^{30}\text{Si}$ . Masses analyzed are as follows:  $^{47}\text{Ti}$ ,  $^{88}\text{Sr}$ ,  $^{89}\text{Y}$ ,  $^{90}\text{Zr}$ ,  $^{93}\text{Nb}$ ,  $^{138}\text{Ba}$ ,  $^{139}\text{La}$ ,  $^{140}\text{Ce}$ ,  $^{144}\text{Nd}$ ,  $^{147}\text{Sm}$ ,  $^{151}\text{Eu}$ ,  $^{158}\text{Gd}$ ,  $^{162}\text{Dy}$ ,  $^{166}\text{Er}$ ,  $^{174}\text{Yb}$ , and  $^{180}\text{Hf}$ .

To evaluate the accuracy and precision of the SIMS data, secondary standards were analyzed (Table 2.5). In addition, measurements of inclusions analyzed during this study are compared with measurements made on the same inclusion suite (Table 2.6) reported previously by Lassiter et al. (2002). Because of variations in machine setup during different analytical sessions, standard data for each session are reported separately. The RSD for standard measurements made during run one averaged  $\sim 10\%$  except for Rb, which had a high value of 82%. Because of the poor reproducibility of the standard Rb data, Rb data are not reported for inclusions analyzed during this session. Average standard measured values are within 10 % of reported standard values for all elements except Nb, which is accurate to within 14 %. For the second analytical session average standard measured values are within 10 % of reported standard values for all elements except Li, Y, Eu, Yb, and Hf, which are accurate to within 20 %. RSD values

for replicate standard measurements were again ~10%. For the third analytical session average standard measured values are within 6 % of reported standard values for all elements except Ca, Gd, Dy, Er, Yb, and Hf, which are accurate to within 32 %. Session three had a slightly better average RSD, at ~9%, but more variation in accepted/measured especially for Ca. To compare the suite of data collected by Lassiter (2002) for sample RVV 310 to the three points collected in this study a spider diagram was used (Fig. 2.3). From the spider diagram, it appears that the data collected overlaps well with the data previously collected. Two of the samples overlay the high range of the data, whereas one sample is in the middle of the data, with the elements from Hf-Yb showing more variation.

Data reduction was performed in a number of steps. To correct for interferences in the initially measured ratios that arose from complexes that formed during the analysis, the methods described by Shimizu and Hart (1982) were used. This method is done by using measurements collected on the SIMS on elements that are known to form complexes and contribute to the counts on the desired element. By using the counts on the elements that form the complexes with the known ratio at which they occur, the contribution can be subtracted. Next, olivine-hosted inclusions were corrected for any analysis that overlapped both host olivine and inclusion. This correction was done by a comparison of Ca microprobe data to the Ca value as determined by SIMS. For inclusions where the Ca microprobe ( $Ca_{probe}$ ) data gave a higher concentration than seen in the Ca SIMS ( $Ca_{sims}$ ) data, it was assumed that this was a result of ion beam overlap with inclusion host during analysis. If the Ca SIMS ( $Ca_{sims}$ ) data gave a higher

concentration than seen in the Ca microprobe ( $Ca_{probe}$ ) data, an overlap of 0 was assumed because it was assumed that overlap with the olivine would dilute, not increase, the  $Ca_{SIMS}$  measurement. The overlap was calculated by  $Ca_{SIMS} = Ca_{olivine}X_{olivine} + Ca_{Melt\ from\ probe}(1-X_{olivine})$ , with  $X_{olivine}$  equal to the overlap. With the calculated overlap,  $Si_{SIMS}$  was recalculated by  $Si_{SIMS} = Si_{melt}X_{melt} + Si_{olivine}X_{olivine}$ . Using the new value of  $Si_{SIMS}$  in equation 1 below,  $Ca_{SIMS}$  was recalculated.

$$X_{Unknown\ ppm} = \left( \frac{X}{Si} \right)_{measured} (SiO_2)_{sims} * \left( \frac{X_{std\ ppm}}{\left( \frac{X}{Si} \right)_{std} * SiO_{2std}} \right)$$

Equation 1

where  $(X/Si)_{measured}$  is the corrected ratio as measured,  $(SiO_2)_{sims}$  is the wt.%  $SiO_2$  corrected for beam overlap,  $X_{std\ ppm}$  is standard concentration of the element,  $(X/Si)_{std}$  is the average measured ratio of the std, and  $SiO_{2std}$  is the wt.% of the standard.

This process was repeated until  $X_{olivine}$  and  $X_{melt}$  converged to a stable value. Once the extent of overlap was determined, the trace element abundances were corrected for overlap using the following equation:

$$C_{melt} = \frac{C_{SIMS} - C_{ol}(X_{ol})}{1 - X_{ol}}$$

Plagioclase-hosted inclusions were corrected in a similar manner, except the Ca in the host was incorporated into the calculation of the overlap value. Also, because of

uncertainties with Sr in plagioclase-hosted inclusions, that data will not be used. After correcting for overlap with the host mineral, the melt inclusions then had to be corrected for the dilution that produced. This was done by  $[\text{conc. element X in melt}] = [\text{conc. calculated for SIMS analysis}]/(X_{\text{melt}})$ . Values of  $X_{\text{melt}}$  less than 0.5 were considered too dilute to use and are not reported. Plagioclase-hosted melt inclusions also were corrected for trace-elements that were contributed from host overlap. This was done using a trace-element analysis from a representative plagioclase host mineral (Table 2.8).

The final trace-element correction was for the dilution/enrichment produced from host addition or subtraction. The dilution/enrichment values were determined as percentages, therefore, the corrections were also done as percentages. If melt inclusion had addition of X% host mineral, that would dilute the trace element values by X%, so the final trace-element concentrations would be increased. Because only olivine-hosted melt inclusions were corrected for addition or subtraction, only olivine-hosted melt inclusions had this final correction.

## Results

### *Major-Elements*

Corrected melt inclusion major element variations are presented in Table 2.7 and selected element pairs vs. whole rock data are illustrated in figure 2.4 (Fig. 2.4, Table 2.7).  $\text{Al}_2\text{O}_3$  vs.  $\text{CaO}$  shows a general negative correlation in the melt inclusion data. Likewise, whole rock data shows a similar negative trend that overlaps with the melt inclusion data (Fig. 2.4).  $\text{Al}_2\text{O}_3$  vs.  $\text{Na}_2\text{O}$  shows a general positive trend in both the melt inclusion and whole rock data. A similar positive trend is observed in  $\text{Na}_2\text{O}$  vs.  $\text{TiO}_2$  for both the melt inclusion and whole rock data (Fig. 2.4). Overall whole rock compositions are shifted to lower concentrations of Ca, Al, Na, and Ti, which may reflect variable addition of cumulus olivine to many whole rock samples.

### *Trace-Elements*

Trace-elements measured in the inclusion suite correlate well with whole-rock trace-elements for a majority of our samples (Fig. 2.8, Table 2.8). Overall, both the whole-rock samples and individual inclusions are light rare earth element (LREE) enriched. The majority of the inclusions have higher concentrations of incompatible trace elements than in the host whole-rock, most likely reflecting the presence of cumulate olivine and clinopyroxene in the whole rocks. However, two samples, RVV312 and RVV344, contain inclusions with lower trace element concentrations than found in the host whole-rock (Fig. 2.8). The plagioclase-hosted inclusion population contains more outliers than for the olivine-hosted inclusions.

### *Source Signatures*

A general positive correlation between whole-rock  $^{206}\text{Pb}/^{204}\text{Pb}$  and average inclusion Cl/K, with high Cl/K ratios correlating with high  $^{206}\text{Pb}/^{204}\text{Pb}$  values, is observed (Fig. 2.9), consistent with the correlation reported by Stroncik and Haase (2004). However, different inclusions from the same sample often show a very wide range in Cl/K, suggesting that erupted lavas reflect mixture of different melts with varying chemical and possibly isotopic composition. Because whole-rock  $^{206}\text{Pb}/^{204}\text{Pb}$  and whole-rock Nb/Zr are positively correlated, correlations of Nb/Zr with Cl/K and Cl/Nb in the inclusions were examined. When average inclusion suite Nb/Zr is plotted against whole-rock  $^{206}\text{Pb}/^{204}\text{Pb}$ , the correlation observed in whole-rock data is maintained, but there is more spread in the data (Fig. 2.11).

No trend is observed between Nb/Zr and Cl/Nb, with or without outliers removed (Fig. 2.12). For K/Nb versus Nb/Zr, a general negative trend emerges when outliers are removed from the dataset, with high Nb/Zr ratios corresponding to low K/Nb ratios (Fig. 2.12). Cl/K<sub>2</sub>O vs. Nb/Zr shows a general positive correlation (Fig. 2.12).

Within the melt-inclusion and whole-rock datasets, a positive trend is observed between La/Sm and Nb/Zr (Fig. 2.13). In the melt-inclusions, La/Sm vs. Cl/Nb shows no correlation, with or without outliers (Fig. 2.14). La/Sm vs. K/Nb shows a broad negative correlation, with outliers removed (Fig. 2.14). CaO/Al<sub>2</sub>O<sub>3</sub> vs. Nb/Zr in the melt-inclusion data lacks any trends whereas the whole-rock data has a positive correlation (Fig. 2.15). SiO<sub>2</sub> vs. Nb/Zr, in both melt-inclusion and whole-rock data has a general negative correlation (Fig. 2.16).



## Discussion

### *Elemental Trends*

The variation seen in the Harker diagrams for  $\text{Na}_2\text{O}$ ,  $\text{TiO}_2$ , and  $\text{P}_2\text{O}_5$  is also seen in some of the individual inclusion suites (Fig. 2.4, 2.5, 2.6, and 2.7). Compared to the trends in whole-rock dataset, some of the sample suites mimic the whole-rock data. The correlation suggests that several of the individual sample suites are composed of a mix of different end member melts similar to those seen in the whole-rock data set.

Trace-element data for melt-inclusions are similar to trace-element data from whole-rock samples (Fig. 2.3). As expected, the trace-elements in the melt-inclusions have higher trace-element concentrations than the whole-rock (Fig. 2.3), which would be diluted by minerals within the lava.

Lead isotopes are a defining characteristic of HIMU-sourced lava (Zindler and Hart, 1986); therefore plots that incorporate  $^{206}\text{Pb}/^{204}\text{Pb}$  can show source signatures. One of the issues with this is that  $^{206}\text{Pb}/^{204}\text{Pb}$  is known only for the whole-rock data set; therefore to use Pb isotopes it must be assumed that the isotopic value characterizes the entire sample. As major-element trend suggest that some samples may be a mixture of different end members, this is not a valid way to interpret the data. Therefore, the positive correlation seen in the whole-rock data between  $^{206}\text{Pb}/^{204}\text{Pb}$  vs. Nb/Zr has been used as a proxy for source, suggesting that an elevated Nb/Zr ratio is indicative of a HIMU-source. Examining the whole-rock  $^{206}\text{Pb}/^{204}\text{Pb}$  vs. inclusion Nb/Zr, a trend is observed. However, there is much spread in the data suggesting that  $^{206}\text{Pb}/^{204}\text{Pb}$  values from the whole-rock for a suite of inclusions may not be an ideal ratio to use when

comparing whole-rock and individual inclusion data.

Using the Nb/Zr ratio for individual inclusions, how Cl/Nb and K/Nb vary with involvement of the HIMU source can be examined. From Figure 2.12 it is apparent that Cl/Nb has no variation with Nb/Zr whereas K/Nb does appear to have an overall negative correlation. This negative correlation seen in Figure 2.12 may just be the result of Nb being on each axis. As previously determined, Nb/Zr varies with the source, therefore that ratio has been used for comparison purposes. It is observed that La/Sm vs. Nb/Zr, in both the whole-rock and melt-inclusion data shows a positive correlation (Fig. 2.13). Using this relationship, La/Sm ratios can also be used as an indicator of source. La/Sm vs. Cl/Nb show no relationship whereas La/Sm vs. K/Nb shows a negative correlation (Fig. 2.14). This suggests that the depletion in K is real and not an artifact of Nb on both axes of the plot. If major-elements are looked at, CaO/Al<sub>2</sub>O<sub>3</sub> vs. Nb/Zr has a positive correlation in the whole-rock data but lacks any trend in the melt-inclusion data (Fig. 2.15). Also SiO<sub>2</sub> vs. Nb/Zr, in both melt-inclusion and whole-rock data has a general negative correlation (Fig. 2.16). These last two observations suggest that SiO<sub>2</sub>, in these lavas can be used as a proxy for HIMU-source region.

#### *HIMU Source*

The Austral Islands are one of only a few localities where HIMU basalt occurs (Chaffey et al., 1989; Woodhead, 1996). Additionally, Raivavae spans a wide range of lead isotopic values (Fig. 2.1) and shows a decrease in K/U ratios with increasing <sup>206</sup>Pb/<sup>204</sup>Pb and an increase with increasing <sup>143</sup>Nd/<sup>144</sup>Nd (Fig. 2.17). These factors, along with the geochemical signature of HIMU basalts present at Raivavae, suggest that the

basalts are sourced from ancient recycled oceanic crust. Therefore, the basalts that have the HIMU signature of  $^{206}\text{Pb}/^{204}\text{Pb}$  can be assumed to be a proxy for recycled oceanic crust whereas the other basalts present can be thought of as originating from a different mechanism or mixing of different sources. By examination of the trends that exist in the geochemistry of Raivavae lavas, or rather melt-inclusions, inferences of the geochemical characterization of the HIMU source can be made.

If the assumption that Nb/Zr is a good proxy for source region is valid, then different element ratios can be examined. In figure 2.12, Cl/Nb vs. Nb/Zr plots as a cloud of data, without any correlation. This data suggests that the HIMU source has a similar Cl/Nb ratio compared to other basalt sources at Raivavae Island. The data cloud varies from a high Cl/Nb ratio of 15 to a low of 5, with an average of  $\sim 10$ . In Figure 2.12, K/Nb vs. Nb/Zr, also plots as a cloud of data, however there is a general negative correlation. If the outliers at Nb/Zr > 0.5 are ignored, a general negative correlation with a high K/Nb ratio correlating to a low Nb/Zr ratio is observed. This results in an estimate that HIMU has a K/Nb ratio of  $\sim 75$  based on figure 2.12.

Using the estimates of Cl/Nb and K/Nb in HIMU it is possible to convert those values into concentrations of Cl and K in the HIMU source using the following equations:

$$(\text{Cl/Nb})_{\text{HIMU}} * [\text{Nb}]_{\text{oc}} \approx [\text{Cl}]_{\text{RC}} \quad \text{Equation 2}$$

$$(\text{K/Nb})_{\text{HIMU}} * [\text{Nb}]_{\text{oc}} \approx [\text{K}]_{\text{RC}} \quad \text{Equation 3}$$

The values for  $(\text{Cl/Nb})_{\text{HIMU}}$  and  $(\text{K/Nb})_{\text{HIMU}}$  correspond to the average value of each from figure 2.12, and are respectively  $\sim 10$  and  $\sim 75$ , with 5.6 ppm Nb in oceanic crust (Hoffman, 1988). Using these values, estimates of  $\sim 56$  ppm Cl and  $\sim 420$  ppm K in the recycled crust or HIMU source are obtained.

Estimations of Cl in the HIMU source have previously been made (Philippot et al., 1998; Stroncik and Haase, 2004; Lassiter et al., 2002), however they relied on the concentration of K. Our estimate, which relies on Nb, is able to provide a different method for Cl concentration as well as provide an estimate for K. This work has found that Cl/Nb ratios not vary between mantle end members and variations reported for Cl/K previously (Philippot et al., 1998; Stroncik and Haase, 2004) are likely caused by depletion of K rather than increased Cl. Lassiter et al. (2002) found similar results using Cl/K. The other two previous studies estimated that Cl was elevated in the HIMU source, with concentrations up to  $\sim 160$  ppm (Philippot et al., 1998; Stroncik and Haase, 2004).

### *Recycling Efficiency*

With estimates of Cl and K in the HIMU source, the efficiency of deep mantle recycling through the process of subduction can be addressed. The subducting plate is oceanic crust and it will have been altered by seawater, thus changing its composition from its initial creation. Therefore the concentrations of Cl and K in altered oceanic crust have been used as initial starting values for both Cl and K. In altered oceanic crust, Cl concentration is estimated at 157-322 ppm (Philippot et al., 1998). With the estimate of 56 ppm Cl in the HIMU source and the estimate of Cl in altered oceanic crust an estimate

of 64-83% removal of Cl during subduction is calculated. A similar estimate can be made for K, which has ~4650 ppm in altered oceanic crust (Staudigel et al., 1995). Using the estimate of 420 ppm K present in the HIMU source and the amount in altered oceanic crust an estimate of 91% removal of K during subduction is calculated.

The values of removal obtained are consistent with high Cl and K values that are observed in Arc lavas (Wallace, 2005, Benjamin et al., 2007; Münker et al., 2004; Vigouroux et al., 2008). Additionally, the data suggests very efficient removal of K during recycling, which means that very little is recycled into the deep mantle during subduction. Previous estimates range from 5% (Becker et al., 2000) to 71% (Eiler et al., 2000) making it past subduction and into the mantle. This study supports the lower value of Becker et al. (2000), with only 9% recycled.

The net influx of Cl and K into the mantle can also be addressed by comparing how the HIMU source varies from MORB or fresh oceanic crust. MORB contains 20-50 ppm Cl (Oppenheimer, 2004) and ~880 ppm K (Hofman, 1988) whereas this study estimates ~56 ppm Cl and ~420 ppm K in the HIMU source. Using the above values for Cl concentration, it appears that there may be a net influx of Cl or steady state to the mantle through subduction over geologic time. K concentrations, on the other hand, show that there may be a net decrease into the mantle over time through subduction.

If Cl is in a steady state with the mantle over geologic time, then other mantle reservoirs should have similar Cl/Nb ratios. To investigate if this is valid or not, data from depleted mantle (DMM), Primitive Mantle (PM), Mid Ocean Ridge Basalt (MORB), Hawaii, and the Canary Islands have been compared to data on HIMU from

this study (Fig. 2.18). Because it is not common to have studies that gather both Cl and trace-element data, average data for each reservoir was used (GERM). While Cl/Nb for DMM and MORB is on average lower than that found in HIMU, it does overlap with the lower values observed in HIMU (Fig. 2.18). This suggests that Cl is not being added to the mantle in an appreciable amount. Rather, during subduction, Cl appears to be effectively removed from the down-going slab as suggested by the previous data comparisons. Primitive mantle, on the other hand, has double the ratio seen in HIMU, suggesting that initially the mantle contained more Cl. This implies that the observations of Stroncik and Haase (2004), who saw a range of Cl/K ratios in HIMU sourced lavas and inferred that the HIMU source has a elevated Cl/K ratio because of increased Cl is incorrect. Cl does not vary from source to source, implying that variation in Cl/K ratios must be caused by variation in K rather than variation in Cl.

When average K/Nb ratios for DMM, MORB, and PM are compared to HIMU, HIMU has a much lower K/Nb ratio (Fig. 2.18). This suggests that HIMU does have a lower concentration of K, which would lead to high Cl/K ratios observed by previous workers (Phillippot et al., 1998; Stroncik and Haase, 2004). It also implies that if HIMU is mixed back into the mantle, the overall concentration of K should decrease with geologic time. The higher the percent of the mantle that is involved in subduction, the greater the effect will be.

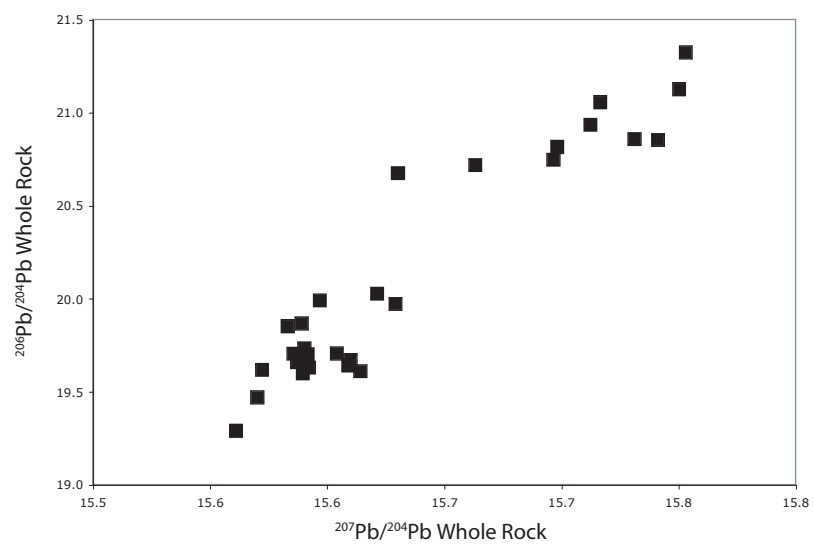


Figure 2.1. Lead isotopic range from whole-rock data at Raivavea Island.

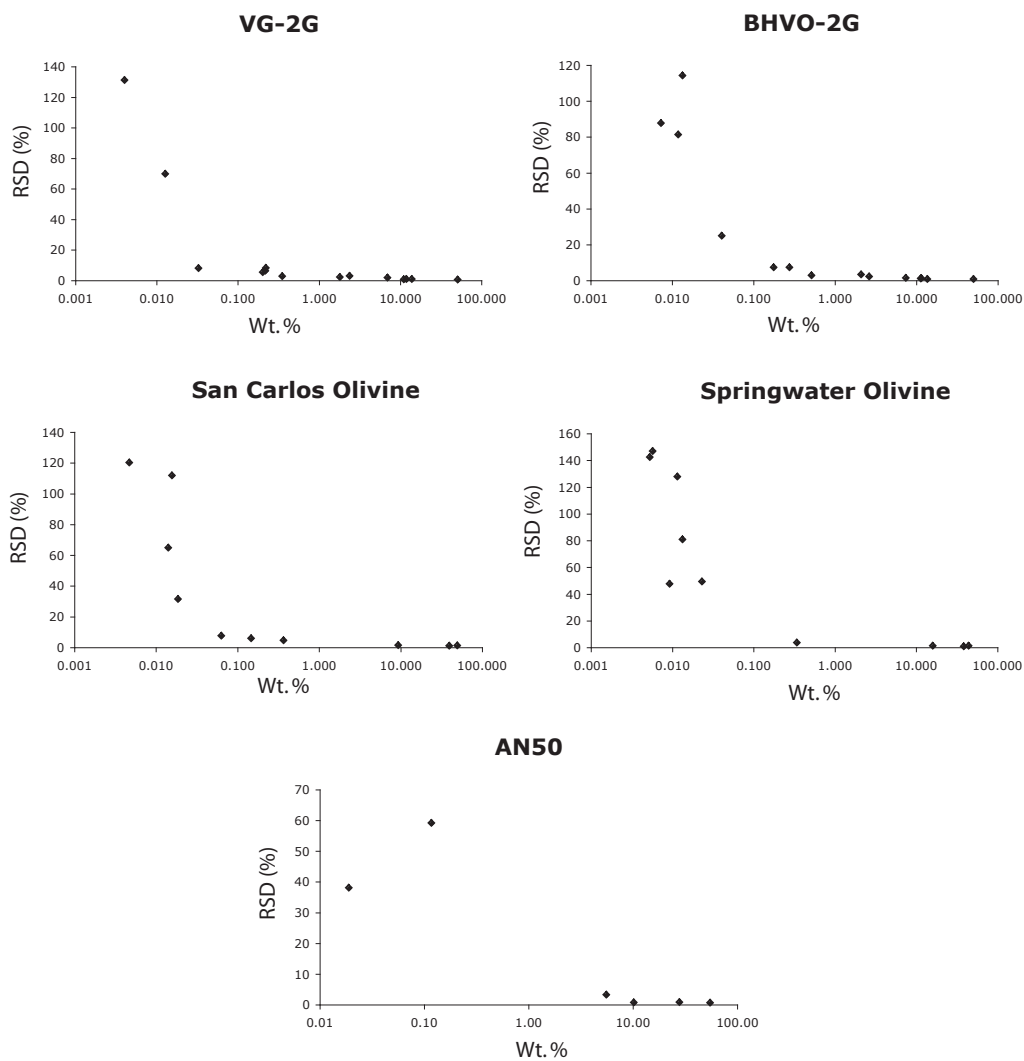


Figure 2.2. RSD's vs wt. % for Glass, Olivine, and Plagioclase Secondary Standards.



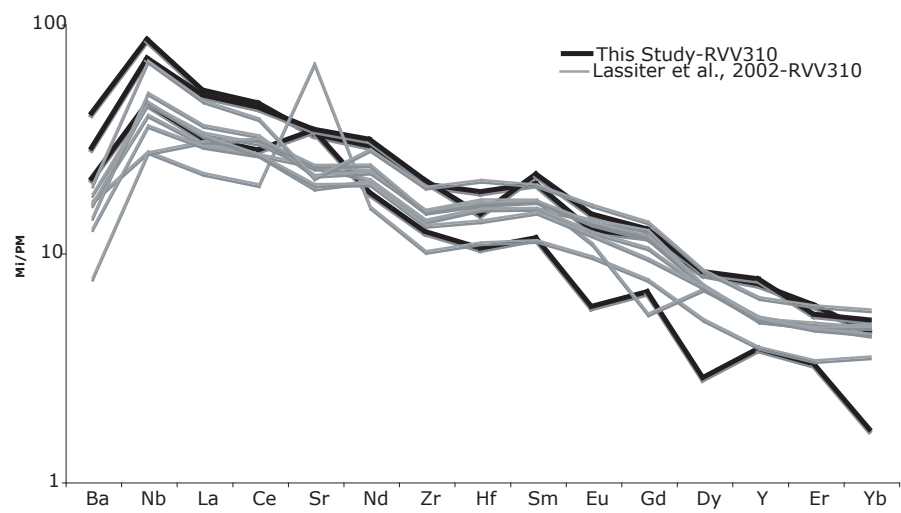


Figure 2.3. Spider Diagram of RVV310 with samples collected this study and by Lassiter et al., 2002.

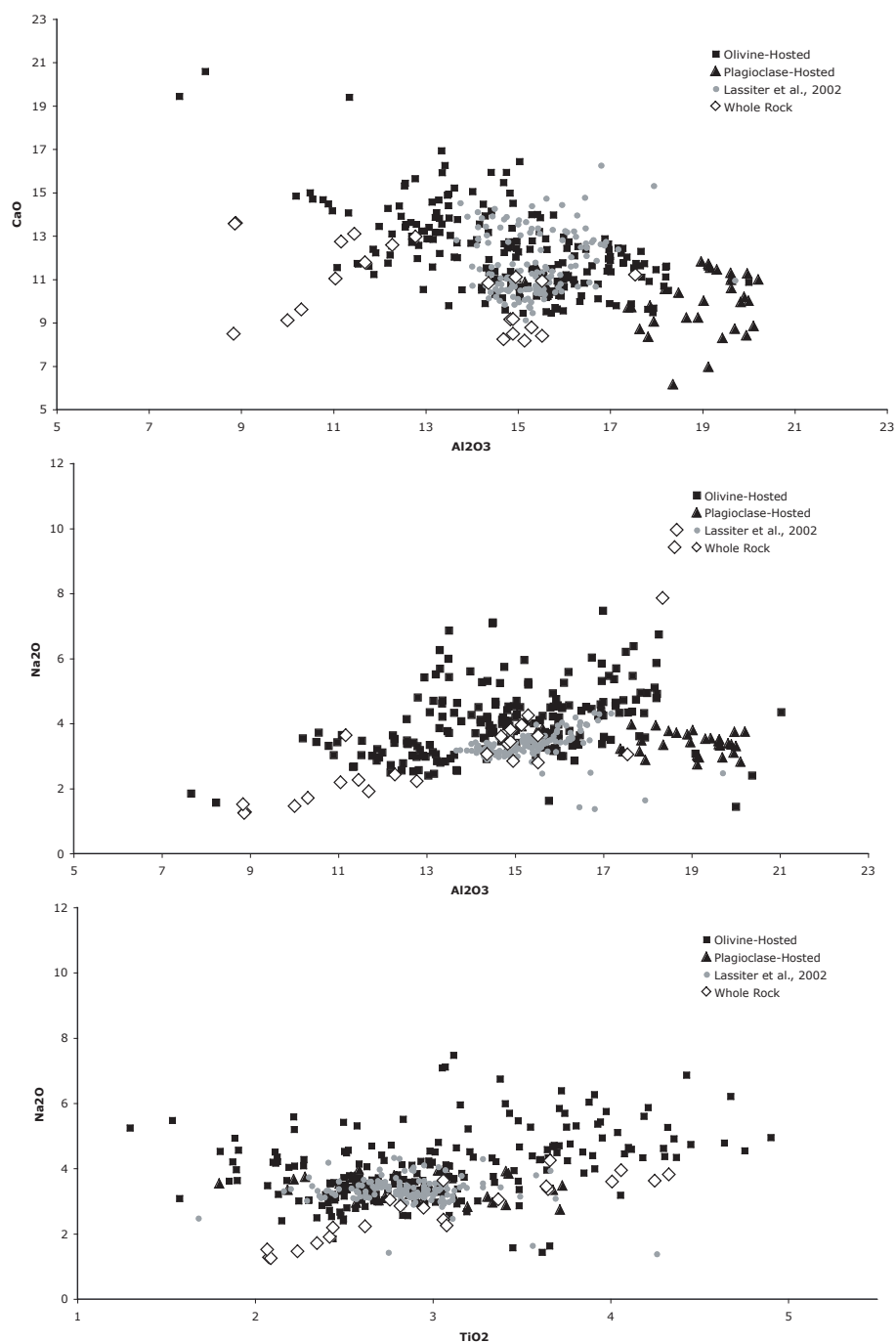


Figure 2.4. Element Pairs for the Major-elements.

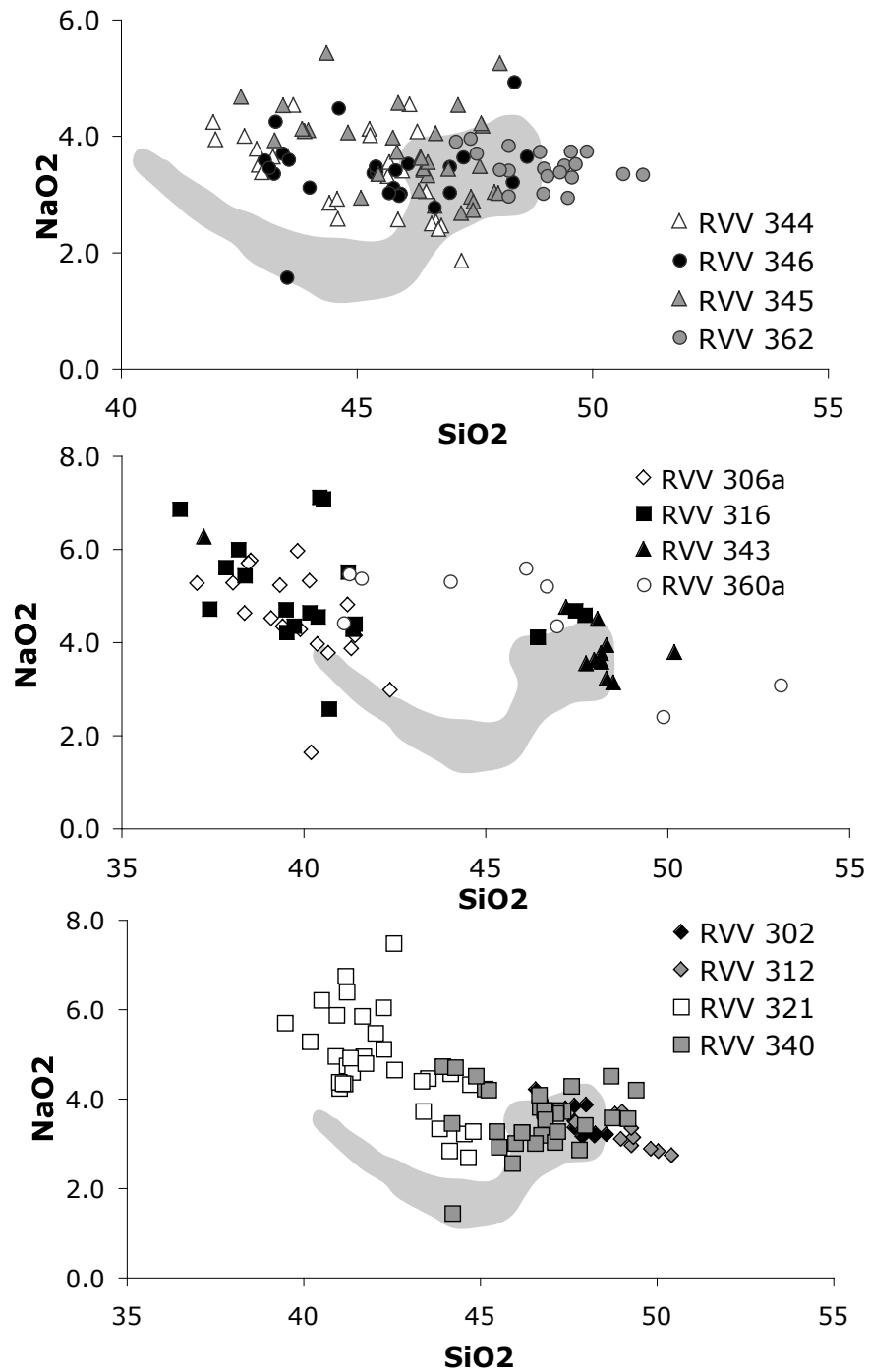


Figure 2.5. Individual Inclusion suites NaO2 vs. SiO2 as well as whole-rock data

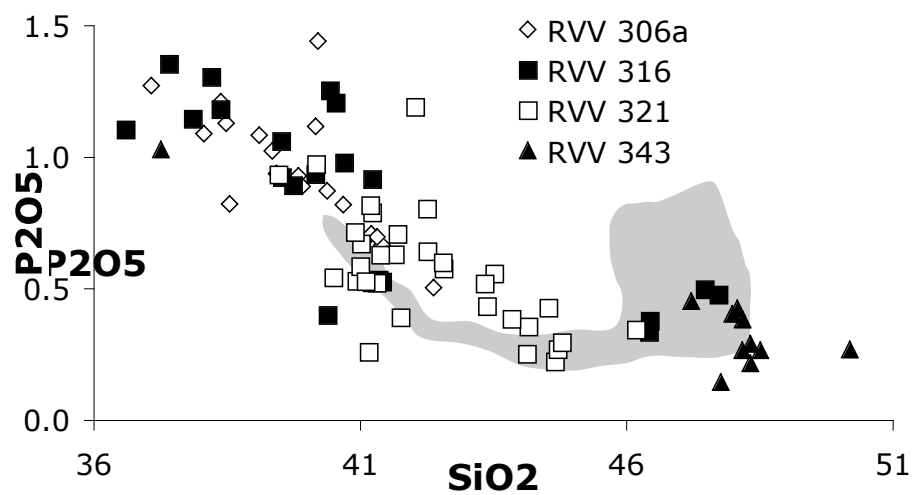
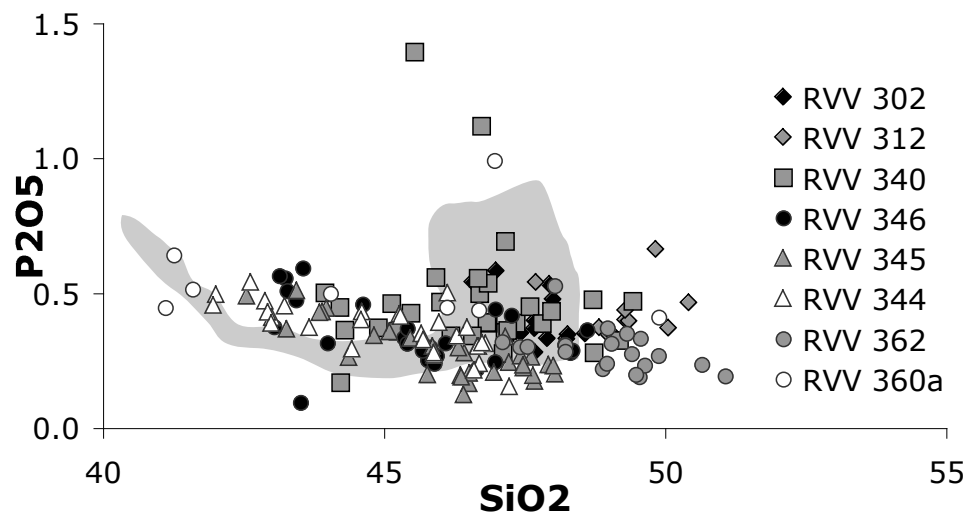


Figure 2.6. Individual Inclusion suites P2O5 vs. SiO2 as well as whole-rock data

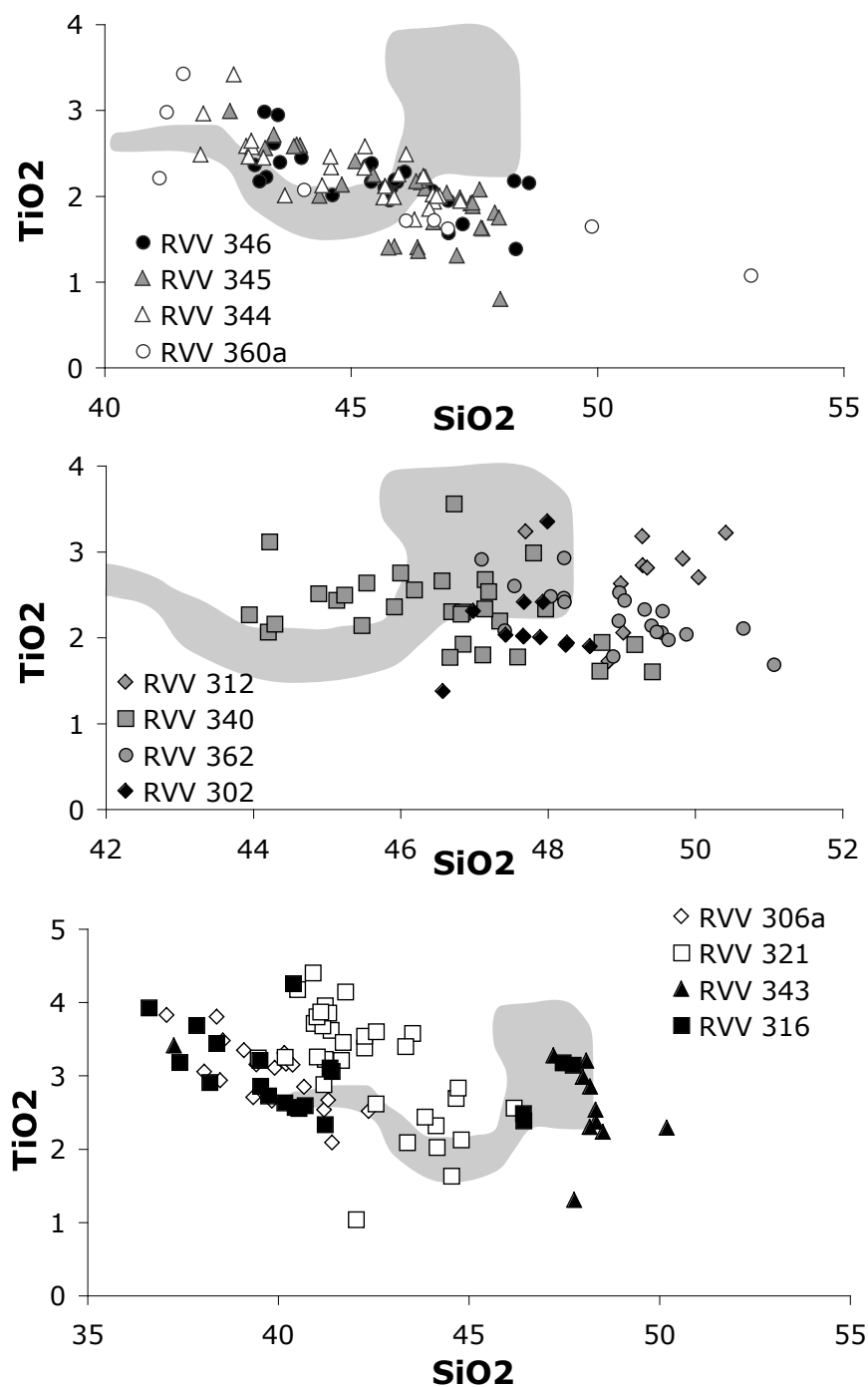


Figure 2.7. Individual Inclusion suites  $\text{TiO}_2$  vs.  $\text{SiO}_2$  as well as whole-rock data

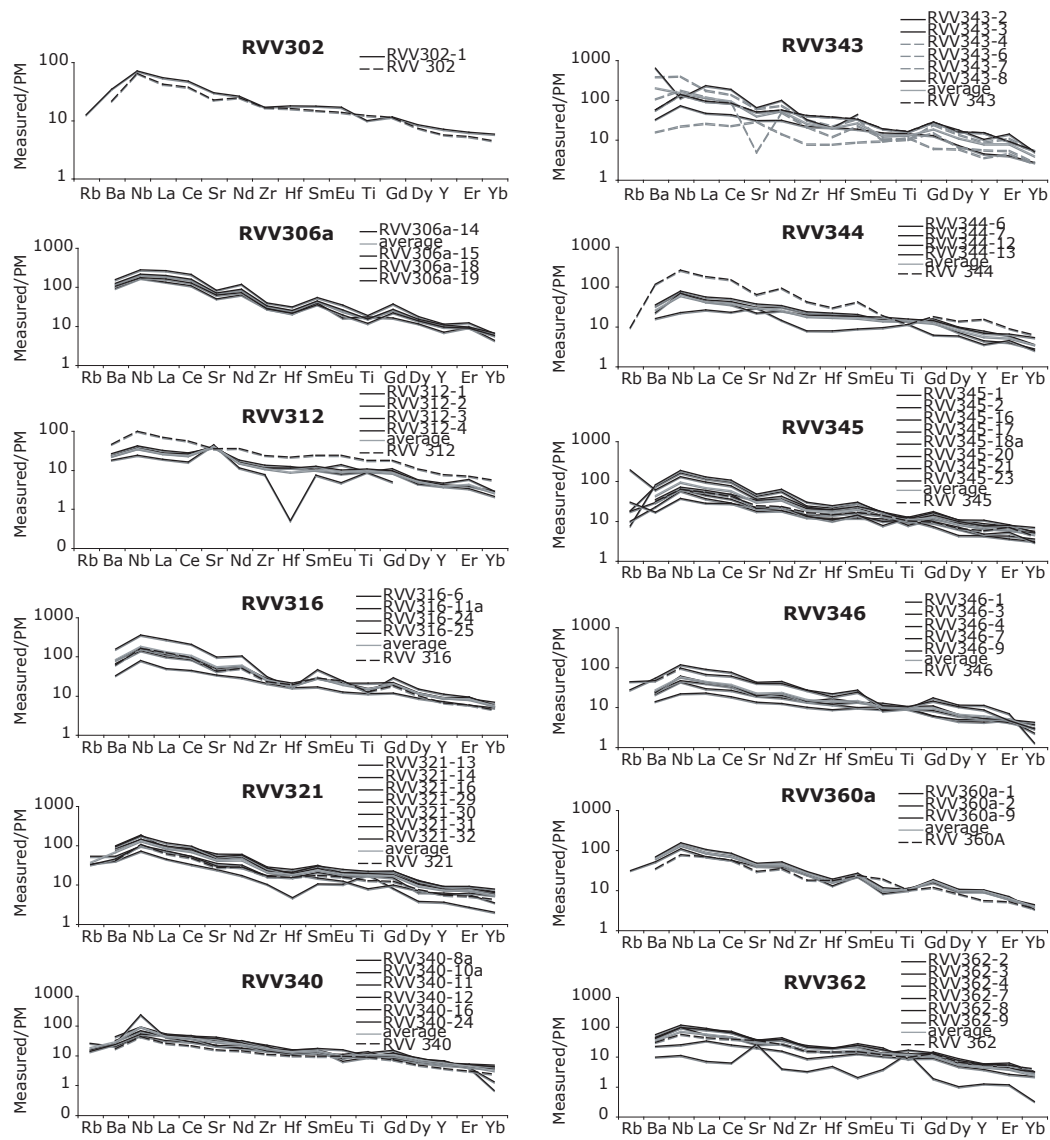


Figure 2.8. Individual Inclusion suites Spider Diagrams. Black Lines are samples, gray line is the average of the samples, and black dashed line is the whole-rock data.

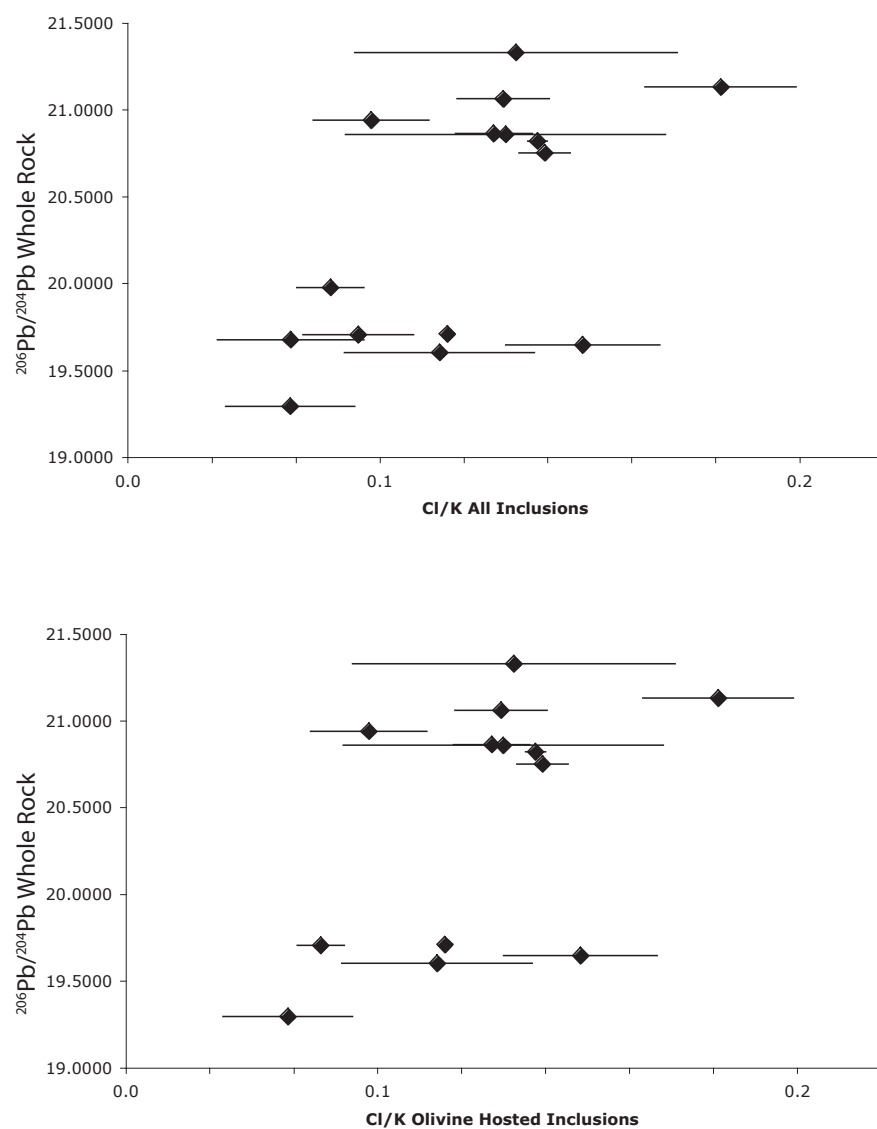


Figure 2.9. Average inclusion Cl/K ratios vs whole-rock  $^{206}\text{Pb}/^{204}\text{Pb}$ .

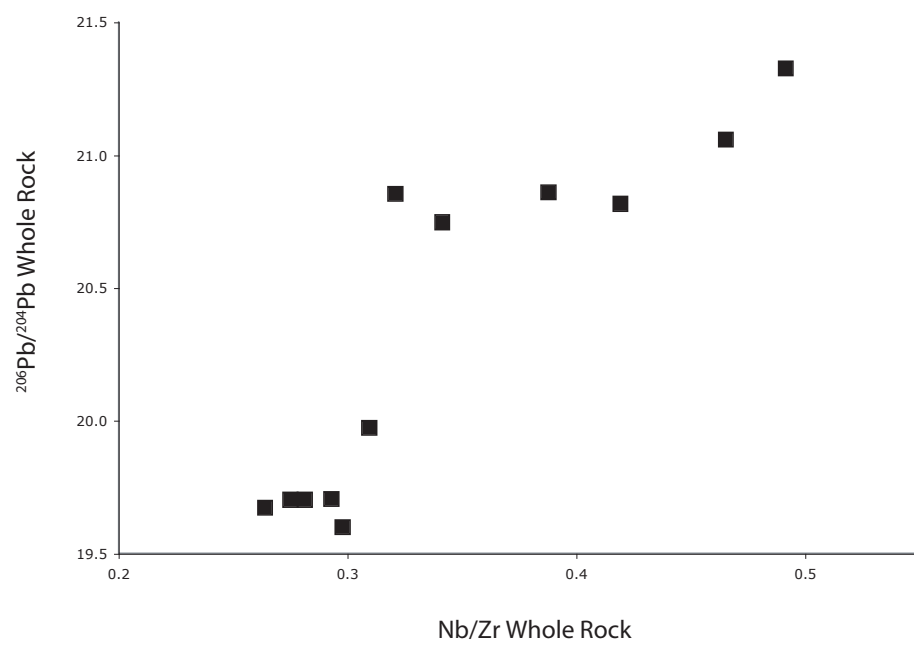


Figure 2.10. Whole-rock  $^{206}\text{Pb}/^{204}\text{Pb}$  vs. whole-rock Nb/Zr.



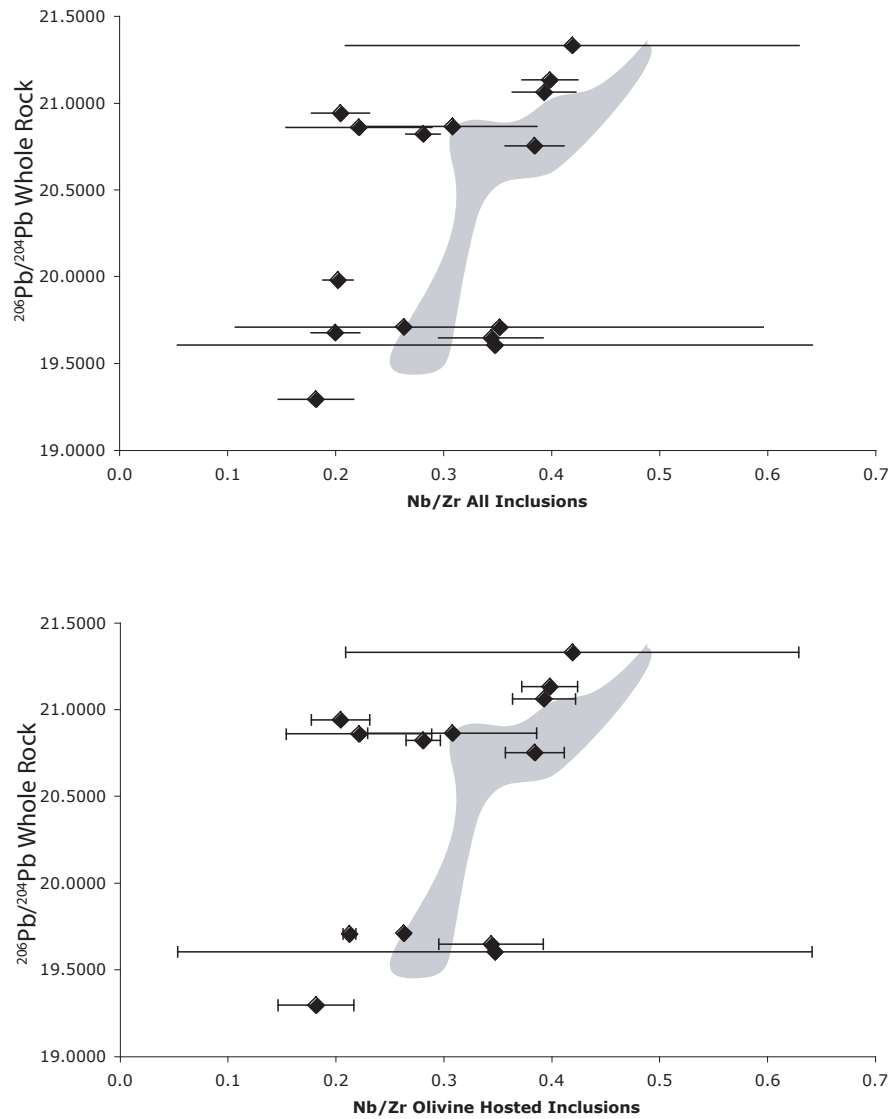


Figure 2.11. Whole-rock  $^{206}\text{Pb}/^{204}\text{Pb}$  vs. average inclusion Nb/Zr, both with and without plagioclase data. Shaded area is whole-rock data.

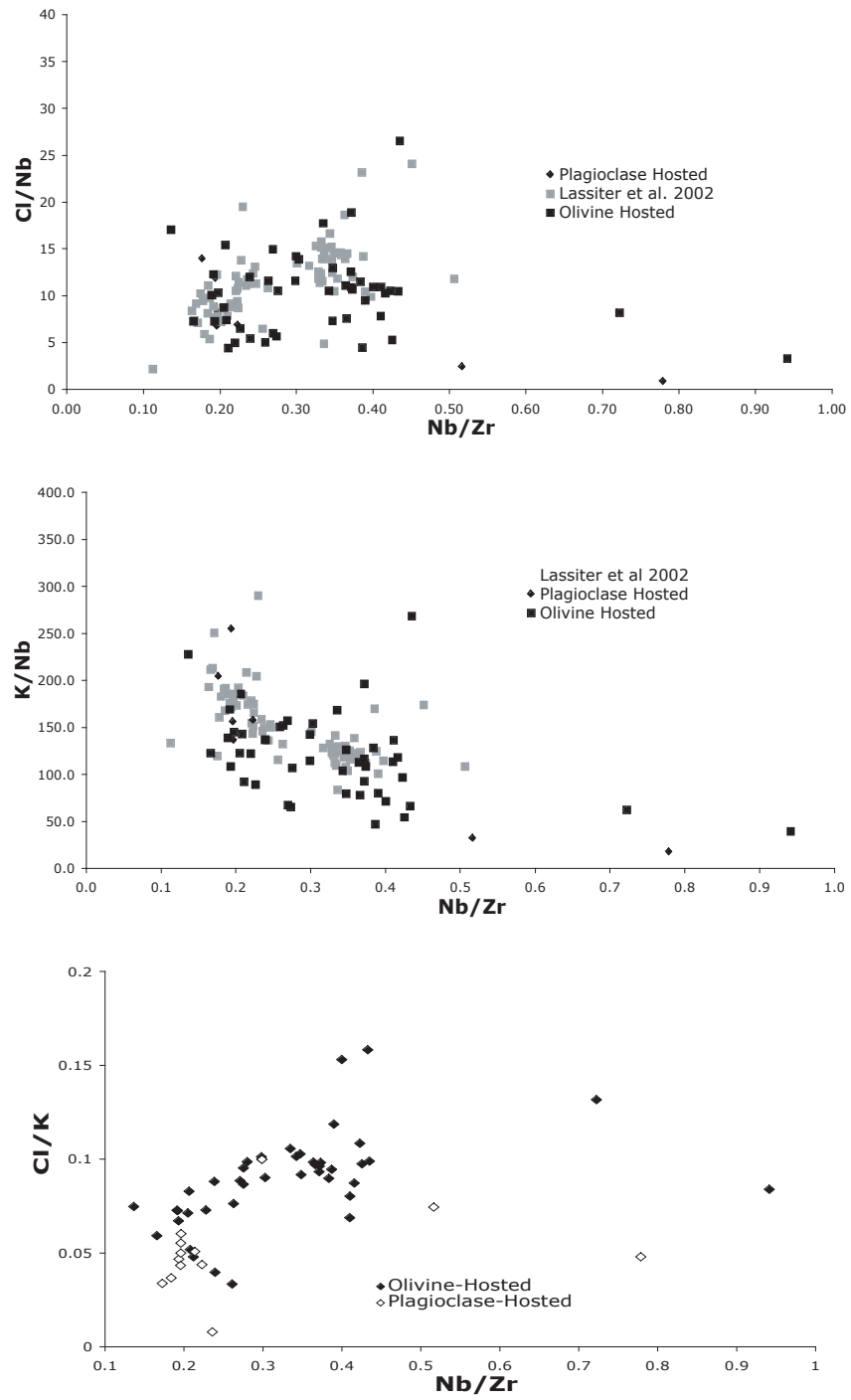


Figure 2.12. Individual melt-inclusion Nb/Zr vs Cl/Nb and K/Nb.

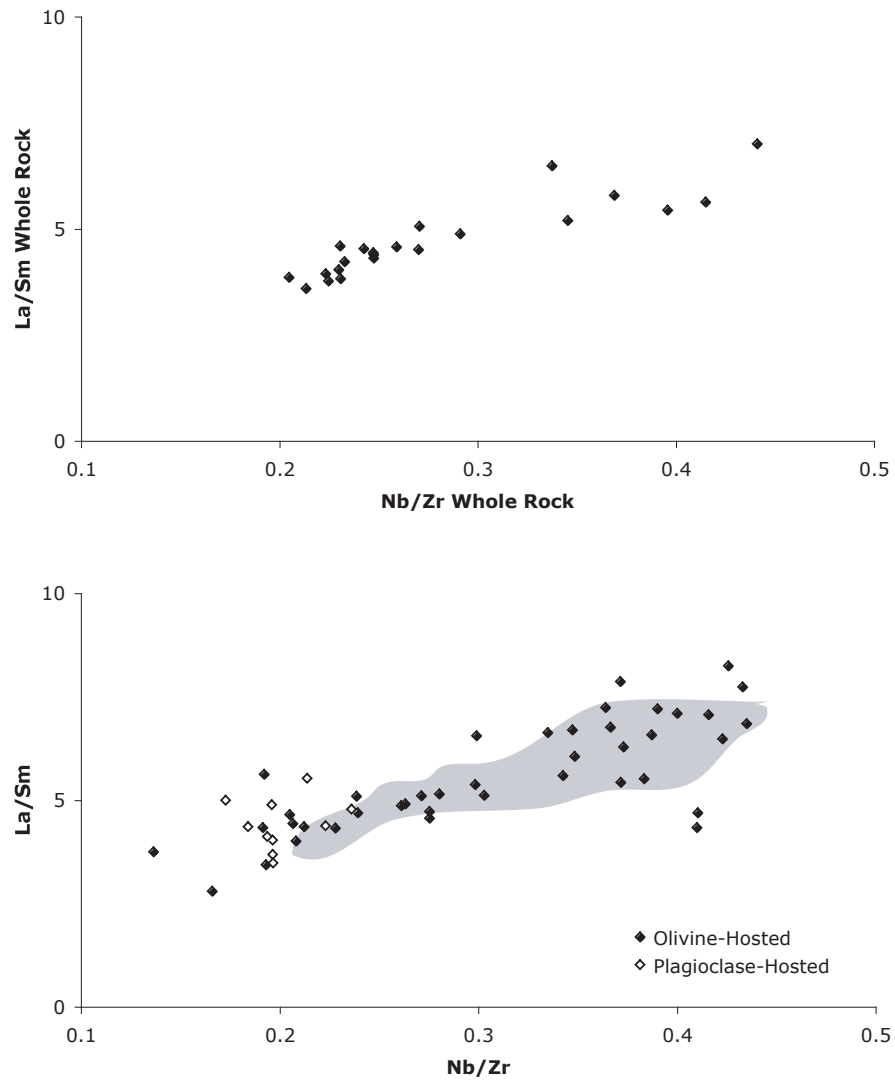


Figure 2.13. La/Sm vs. Nb/Zr in whole-rock data and inclusion data. Gray field is whole-rock data.

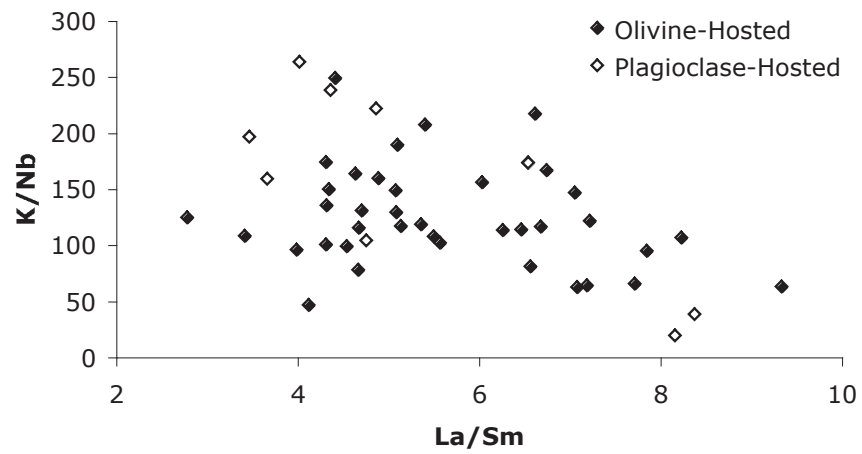
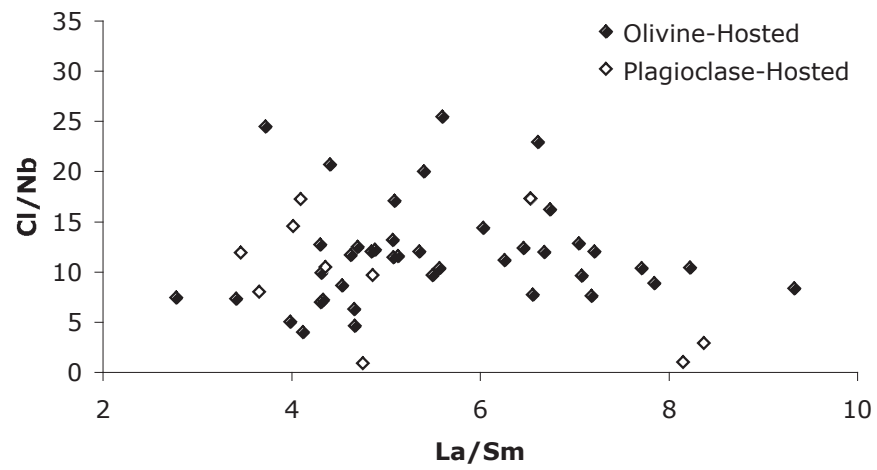


Figure 2.14. La/Sm vs Cl/Nb and K/Nb in inclusion data

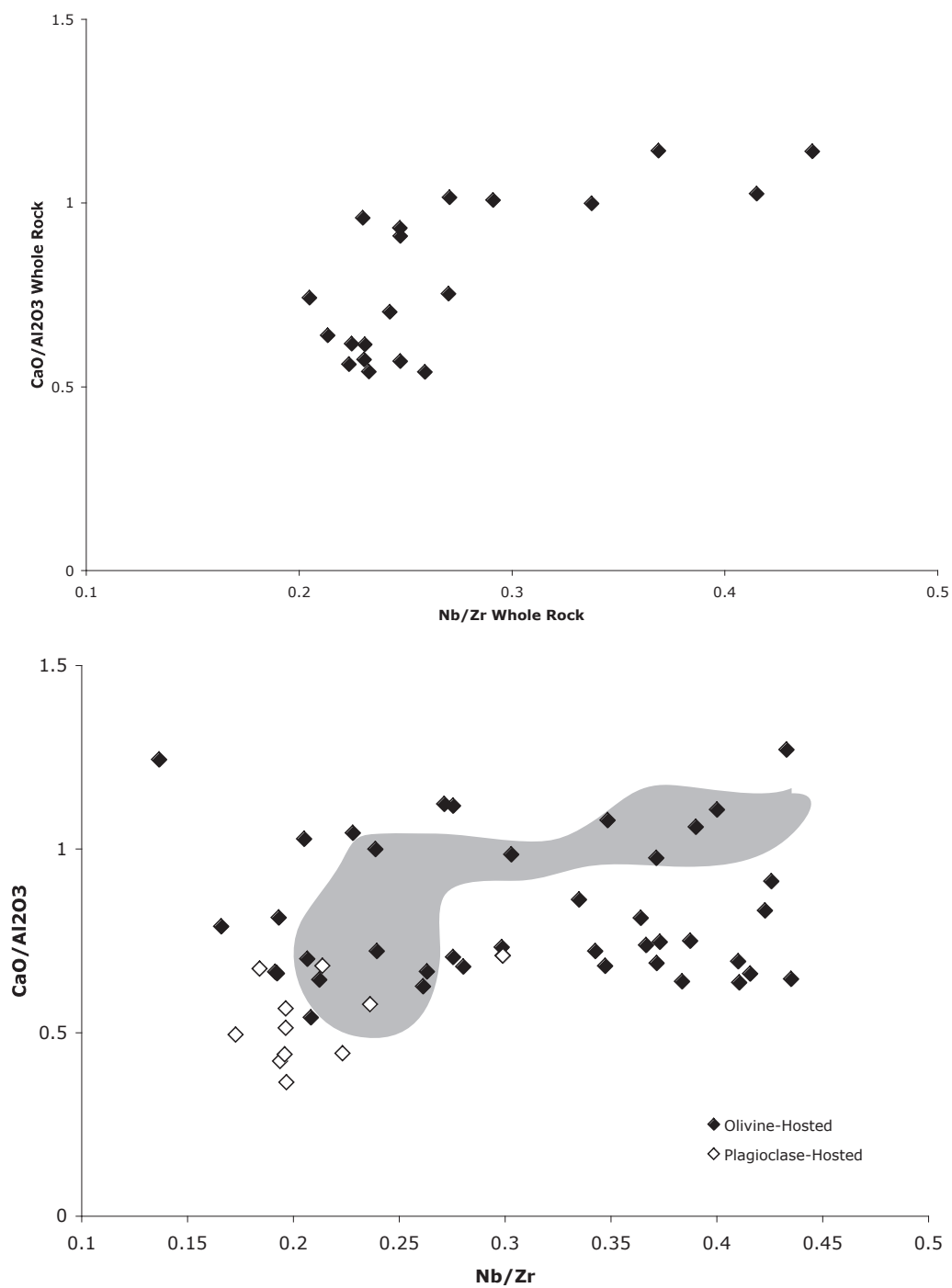


Figure 2.15.  $\text{CaO}/\text{Al}_2\text{O}_3$  vs.  $\text{Nb}/\text{Zr}$  in whole-rock and inclusion data. Gray field is whole-rock data

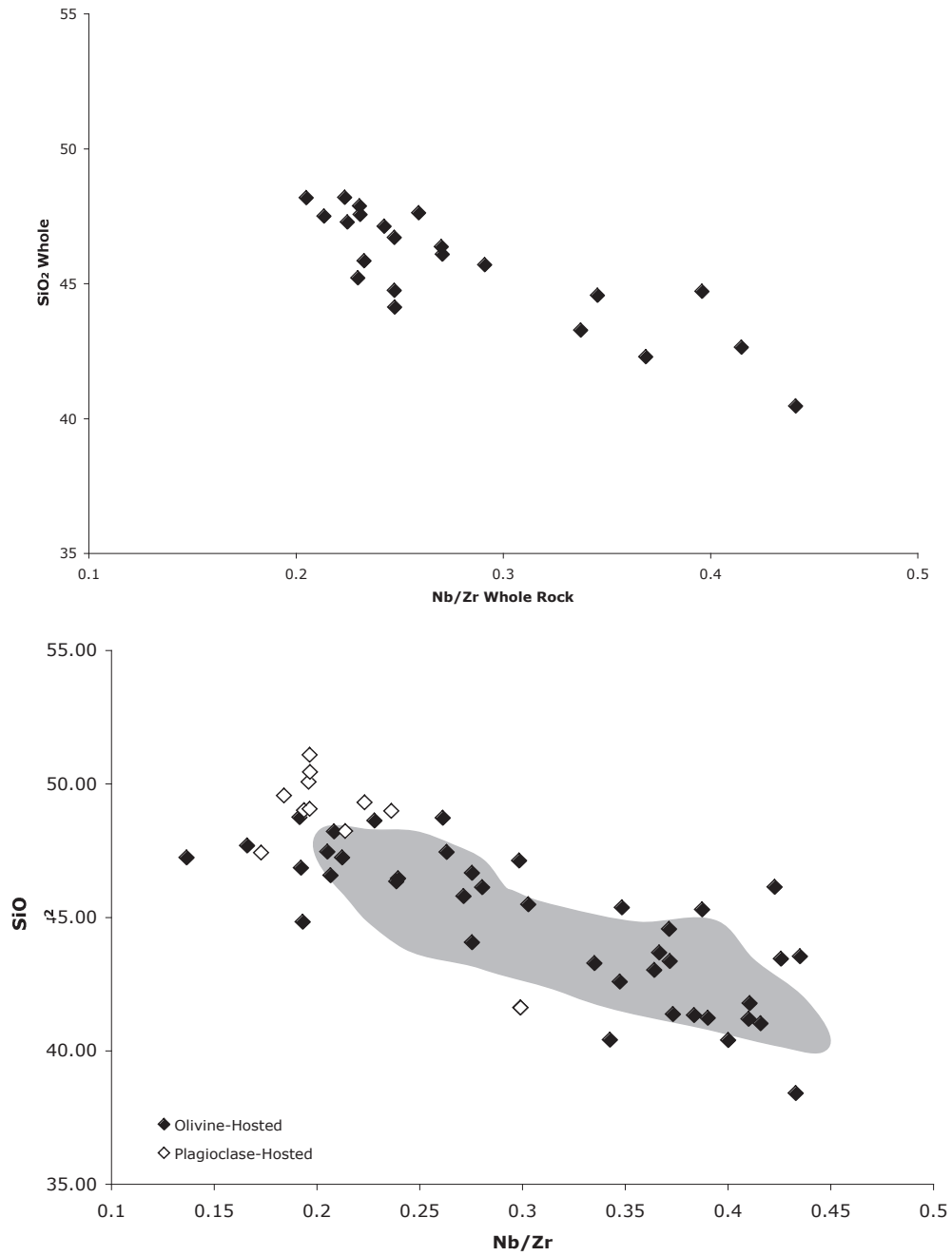


Figure 2.16.  $\text{SiO}_2$  vs.  $\text{Nb/Zr}$  in whole-rock and inclusion data. Gray field is whole-rock data

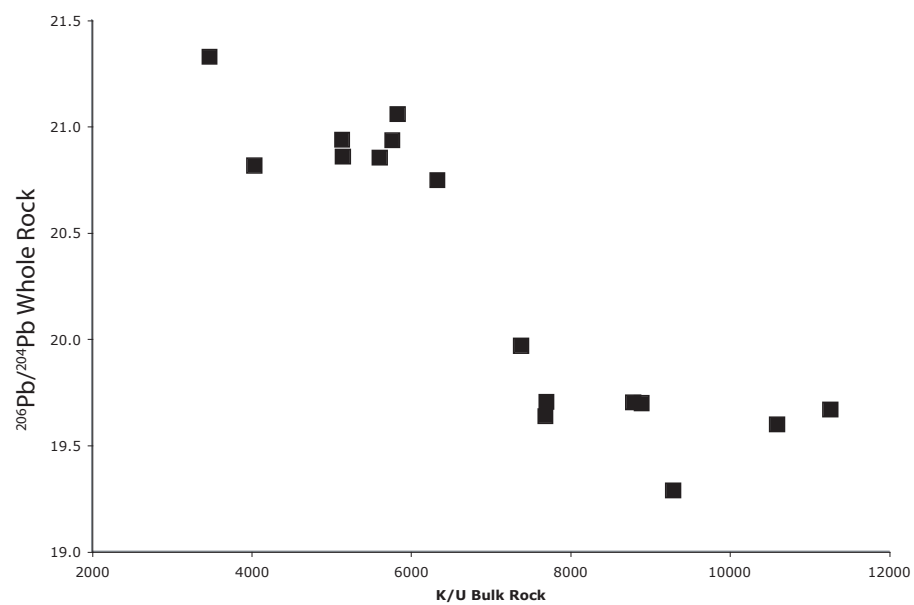


Figure 2.17. Whole-rock  $^{206}\text{Pb}/^{204}\text{Pb}$  vs. whole-rock K/U.

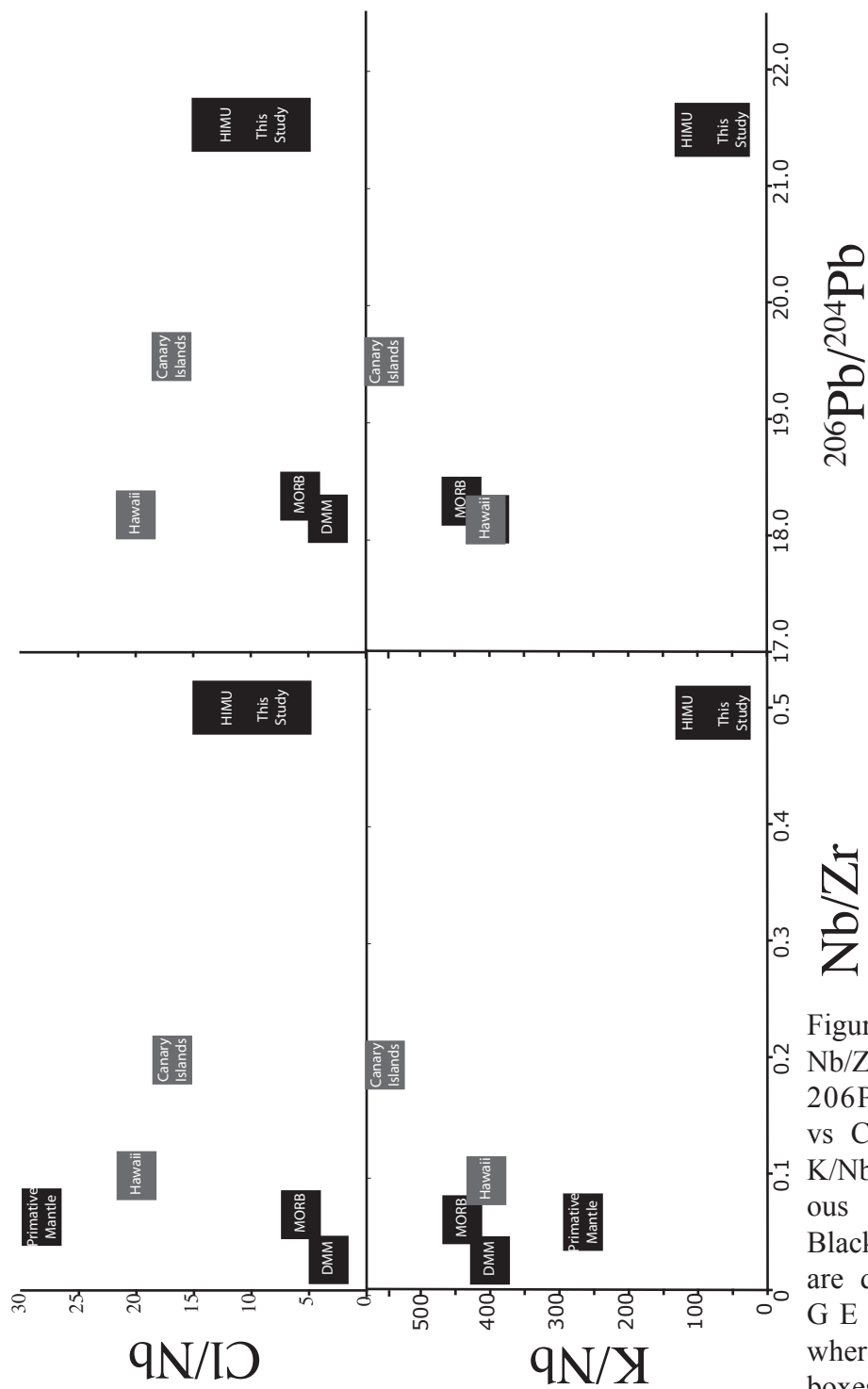


Figure 2.18. Nb/Zr and  $^{206}\text{Pb}/^{204}\text{Pb}$  vs Cl/Nb and K/Nb for various locations. Black boxes are data from GERO whereas grey boxes are from GERM



Table 2.1: Glass Standard Measurements  
VG-2G

Run	SiO <sub>2</sub>	Al <sub>2</sub> O <sub>3</sub>	P <sub>2</sub> O <sub>5</sub>	SO <sub>3</sub>	Cl	K <sub>2</sub> O	CaO	MnO	Cr <sub>2</sub> O <sub>3</sub>	FeO*	NiO	Na <sub>2</sub> O	MgO	TiO <sub>2</sub>	Total
1	51.10	14.09	0.25	0.35	0.03	0.18	11.18	0.24	0.02	12.07	0.00	2.37	6.98	1.80	100.65
1	51.21	14.15	0.24	0.34	0.03	0.19	11.26	0.21	0.01	12.13	0.00	2.41	6.96	1.83	100.97
1	51.08	14.10	0.22	0.36	0.03	0.19	11.26	0.23	0.02	12.05	0.01	2.32	7.07	1.82	100.76
1	50.94	13.93	0.23	0.34	0.03	0.20	11.28	0.20	0.03	11.99	0.00	2.46	6.71	1.81	100.13
1	51.13	14.03	0.24	0.37	0.03	0.20	11.17	0.22	0.02	11.98	0.01	2.39	6.98	1.83	100.58
1	51.10	13.91	0.20	0.34	0.04	0.20	11.15	0.19	0.00	12.00	0.01	2.37	7.07	1.85	100.40
1	51.15	14.04	0.19	0.37	0.03	0.20	11.14	0.22	0.00	11.99	0.00	2.43	7.03	1.82	100.61
1	51.10	14.01	0.23	0.36	0.04	0.20	11.09	0.20	0.02	12.02	0.01	2.48	7.09	1.81	100.62
1	51.16	14.04	0.24	0.37	0.03	0.20	11.08	0.23	0.01	12.00	0.00	2.38	6.97	1.82	100.54
1	51.08	14.07	0.21	0.34	0.03	0.20	11.22	0.23	0.01	11.98	0.00	2.39	7.17	1.82	100.75
1	51.17	14.16	0.23	0.37	0.03	0.20	11.18	0.22	0.00	12.11	0.01	2.27	7.11	1.80	100.84
1	51.14	14.05	0.24	0.34	0.03	0.21	11.14	0.19	0.02	11.97	0.00	2.38	7.09	1.82	100.61
1	51.11	14.00	0.20	0.35	0.04	0.21	11.16	0.22	0.03	12.00	0.01	2.38	7.15	1.81	100.64
1	50.87	13.98	0.22	0.35	0.03	0.21	11.17	0.22	0.03	11.93	0.02	2.37	6.96	1.80	100.15
1	51.26	14.11	0.24	0.35	0.04	0.21	11.19	0.22	0.00	12.02	0.00	2.22	6.92	1.84	100.59
1	50.97	14.01	0.20	0.36	0.04	0.21	11.25	0.23	0.01	11.90	0.01	2.42	6.71	1.84	100.13
1	51.02	14.04	0.19	0.36	0.04	0.21	11.20	0.22	0.01	12.05	0.00	2.37	7.17	1.84	100.70
1	51.05	14.02	0.20	0.35	0.03	0.22	11.24	0.21	0.00	12.00	0.01	2.47	7.00	1.83	100.61
1	50.88	13.95	0.20	0.36	0.03	0.22	11.15	0.23	0.02	12.02	0.00	2.37	7.00	1.84	100.26
1	51.09	14.02	0.25	0.35	0.03	0.22	11.17	0.22	0.01	11.87	0.01	2.45	6.98	1.85	100.50
1	51.14	14.00	0.22	0.38	0.03	0.22	11.25	0.23	0.02	12.02	0.00	2.41	6.84	1.83	100.56
1	51.20	13.92	0.20	0.36	0.03	0.22	11.13	0.22	0.02	12.19	0.00	2.21	6.95	1.82	100.46
1	50.81	14.03	0.22	0.35	0.04	0.23	11.20	0.23	0.01	11.91	0.00	2.40	6.75	1.87	100.05
2	51.40	13.82	0.23	0.36	0.03	0.19	11.15	0.23	0.00	11.93	0.01	2.37	7.14	1.70	100.52
2	51.28	13.87	0.22	0.36	0.03	0.19	11.09	0.23	0.02	11.79	0.01	2.38	7.15	1.84	100.46
2	51.40	13.80	0.21	0.35	0.04	0.20	11.15	0.20	0.01	11.90	0.00	2.40	7.02	1.75	100.41
2	51.32	13.86	0.26	0.36	0.03	0.20	11.15	0.23	0.02	12.00	0.01	2.49	6.89	1.79	100.60
2	51.20	13.95	0.23	0.36	0.03	0.20	11.08	0.19	0.01	11.91	0.00	2.44	7.06	1.88	100.53
2	51.24	13.76	0.22	0.37	0.03	0.20	11.08	0.24	0.00	11.80	0.00	2.40	7.12	1.74	100.19
2	51.26	13.81	0.21	0.35	0.03	0.20	11.04	0.23	0.02	11.78	0.00	2.43	7.15	1.74	100.25

2	51.60	13.91	0.23	0.36	0.03	0.21	11.16	0.22	0.02	12.02	0.00	2.26	7.00	1.88	100.88
2	51.07	13.81	0.24	0.34	0.03	0.21	11.13	0.21	0.02	11.81	0.00	2.50	7.10	1.82	100.27
2	51.30	13.94	0.22	0.35	0.03	0.21	11.14	0.23	0.02	11.93	0.01	2.41	6.87	1.84	100.49
2	51.45	13.85	0.25	0.36	0.03	0.21	11.14	0.21	0.02	11.95	0.00	2.42	7.04	1.84	100.76
2	51.41	13.78	0.23	0.37	0.03	0.21	11.08	0.22	0.00	11.96	0.00	2.42	7.01	1.78	100.49
Average	51.16	13.97	0.22	0.36	0.03	0.20	11.16	0.22	0.01	11.97	0.00	2.39	7.01	1.82	100.51
stdev	0.17	0.11	0.02	0.01	0.00	0.01	0.06	0.01	0.01	0.09	0.01	0.07	0.12	0.04	0.22
RSD	0.33	0.77	8.12	2.70	7.87	5.19	0.54	6.15	69.67	0.77	130.96	2.79	1.75	2.15	0.22
Standard															
Value	50.51	14.06	0.20	0.33		0.19	11.12	0.22		11.84		2.62	6.61	1.82	
Std/Avg	0.99	1.01	0.90	0.92		0.93	1.00	1.01		0.99		1.10	0.94	1.00	

#### BHVO-2G

Run	SiO2	Al2O3	P2O5	SO3	Cl	K2O	CaO	MnO	Cr2O3	FeO*	NiO	Na2O	MgO	TiO2	Total
1	50.85	13.90	0.34	0.01	0.01	0.49	11.48	0.19	0.04	11.44	0.01	2.09	7.61	2.71	101.16
1	50.70	13.85	0.29	0.00	0.01	0.50	11.48	0.16	0.06	11.34	0.02	2.12	7.56	2.72	100.81
1	50.79	13.81	0.29	0.01	0.01	0.50	11.56	0.19	0.05	11.33	0.01	2.02	7.46	2.68	100.69
1	50.66	13.84	0.28	0.01	0.01	0.50	11.46	0.19	0.04	11.30	0.03	2.05	7.34	2.67	100.38
1	50.74	13.83	0.27	0.00	0.01	0.50	11.61	0.19	0.04	11.28	0.01	2.10	7.42	2.67	100.66
1	50.81	13.86	0.31	0.00	0.01	0.50	11.51	0.18	0.04	11.32	0.01	2.07	7.59	2.67	100.86
1	50.43	13.77	0.28	0.02	0.01	0.50	11.42	0.17	0.02	11.35	0.02	2.09	7.55	2.71	100.32
1	50.60	13.74	0.24	0.01	0.05	0.50	11.54	0.18	0.05	11.25	0.01	2.12	7.29	2.63	100.18
1	50.70	13.81	0.28	0.01	0.01	0.50	11.42	0.18	0.04	11.36	0.00	2.08	7.55	2.68	100.65
1	50.87	13.78	0.27	0.00	0.01	0.50	11.49	0.19	0.03	11.30	0.02	2.11	7.37	2.70	100.63
1	50.78	13.87	0.28	0.01	0.01	0.50	11.54	0.19	0.04	11.26	0.02	2.06	7.51	2.67	100.74
1	50.74	13.78	0.28	0.00	0.01	0.51	11.56	0.19	0.03	11.33	0.00	2.09	7.24	2.70	100.44
1	50.74	13.83	0.29	0.00	0.01	0.51	11.49	0.18	0.05	11.32	0.02	2.13	7.35	2.67	100.60
1	50.70	13.83	0.29	0.03	0.01	0.51	11.43	0.17	0.04	11.29	0.02	2.14	7.44	2.67	100.57
1	50.63	13.79	0.29	0.01	0.01	0.51	11.45	0.18	0.04	11.34	0.03	2.07	7.42	2.64	100.38
1	50.81	13.80	0.29	0.02	0.01	0.51	11.51	0.19	0.04	11.38	0.01	2.05	7.54	2.68	100.84
1	50.81	13.81	0.33	0.01	0.01	0.51	11.61	0.18	0.06	11.39	0.01	2.06	7.47	2.67	100.91
1	50.65	13.79	0.28	0.02	0.01	0.51	11.38	0.18	0.04	11.37	0.01	2.12	7.43	2.68	100.49

1	50.66	13.82	0.24	0.01	0.01	0.51	11.51	0.18	0.05	11.34	0.02	2.11	7.41	2.66	100.52
1	50.73	13.79	0.28	0.00	0.01	0.51	11.55	0.17	0.03	11.22	0.00	2.04	7.37	2.67	100.36
1	50.77	13.85	0.29	0.00	0.01	0.52	11.54	0.18	0.05	11.37	0.03	2.09	7.56	2.69	100.94
1	50.66	13.76	0.26	0.00	0.01	0.52	11.48	0.20	0.04	11.33	0.02	2.13	7.41	2.68	100.48
1	50.34	13.74	0.28	0.00	0.01	0.52	11.45	0.16	0.03	11.26	0.01	2.08	7.53	2.68	100.10
1	50.85	13.88	0.27	0.00	0.01	0.52	11.54	0.18	0.05	11.35	0.02	2.06	7.57	2.68	100.95
1	50.68	13.80	0.28	0.02	0.01	0.52	11.51	0.20	0.06	11.32	0.00	2.14	7.40	2.67	100.58
1	50.68	13.81	0.28	0.00	0.01	0.52	11.49	0.18	0.04	11.27	0.02	2.05	7.50	2.65	100.48
1	50.74	13.76	0.25	0.01	0.01	0.52	11.56	0.17	0.06	11.33	0.02	2.17	7.38	2.67	100.64
1	50.66	13.74	0.29	0.00	0.01	0.52	11.39	0.19	0.05	11.36	0.03	2.11	7.40	2.72	100.46
1	50.73	13.86	0.26	0.01	0.01	0.52	11.46	0.19	0.03	11.33	0.01	2.09	7.44	2.69	100.63
1	50.70	13.83	0.26	0.00	0.01	0.52	11.52	0.17	0.04	11.33	0.02	2.09	7.30	2.70	100.49
1	50.87	13.83	0.25	0.02	0.01	0.52	11.46	0.18	0.04	11.39	0.01	2.04	7.49	2.68	100.79
1	50.85	13.88	0.28	0.00	0.01	0.53	11.48	0.15	0.03	11.30	0.02	2.08	7.48	2.67	100.74
1	50.77	13.79	0.30	0.01	0.01	0.53	11.45	0.18	0.05	11.26	0.01	2.00	7.50	2.66	100.50
1	50.63	13.80	0.29	0.02	0.08	0.53	11.59	0.18	0.03	11.20	0.03	2.12	7.40	2.71	100.58
1	50.80	13.79	0.29	0.01	0.01	0.53	11.52	0.18	0.03	11.37	0.00	2.05	7.44	2.67	100.68
1	50.82	13.91	0.28	0.01	0.01	0.53	11.45	0.16	0.04	11.42	0.00	2.11	7.54	2.69	100.97
1	50.81	13.87	0.31	0.00	0.01	0.53	11.58	0.18	0.04	11.35	0.00	2.05	7.55	2.67	100.93
1	50.91	13.89	0.31	0.01	0.01	0.53	11.68	0.19	0.06	11.43	0.03	2.00	7.52	2.70	101.26
1	50.76	13.83	0.29	0.01	0.01	0.53	11.43	0.18	0.04	11.27	0.00	2.09	7.54	2.72	100.67
1	50.74	13.81	0.25	0.01	0.01	0.53	11.58	0.16	0.02	11.23	0.00	2.04	7.37	2.68	100.43
1	50.71	13.90	0.29	0.00	0.01	0.54	11.37	0.20	0.04	11.41	0.02	2.13	7.55	2.71	100.86
1	50.61	13.84	0.30	0.01	0.01	0.54	11.42	0.16	0.03	11.36	0.01	2.18	7.37	2.67	100.51
2	50.77	13.66	0.31	0.01	0.01	0.49	11.58	0.19	0.02	11.34	0.00	2.18	7.50	2.74	100.80
2	50.69	13.68	0.28	0.02	0.01	0.49	11.78	0.18	0.06	11.44	0.02	2.12	7.27	2.64	100.68
2	51.10	13.65	0.28	0.00	0.01	0.50	11.72	0.18	0.04	11.52	0.00	2.06	7.51	2.54	101.10
2	50.47	13.71	0.25	0.01	0.01	0.50	11.75	0.17	0.05	11.48	0.01	2.08	7.59	2.55	100.63
2	50.16	13.54	0.28	0.02	0.01	0.50	11.56	0.19	0.05	11.36	0.00	2.17	7.47	2.55	99.85
2	50.61	13.88	0.27	0.00	0.01	0.50	11.68	0.17	0.04	11.47	0.01	2.19	7.54	2.54	100.90
2	51.24	13.82	0.27	0.01	0.01	0.50	11.72	0.18	0.05	11.44	0.01	2.16	7.47	2.57	101.46
2	51.63	13.97	0.29	0.01	0.01	0.51	11.77	0.18	0.05	11.51	0.02	1.68	7.66	2.66	101.94
2	50.75	13.68	0.27	0.01	0.01	0.51	11.62	0.18	0.06	11.43	0.01	2.14	7.39	2.60	100.65

2	50.66	13.64	0.25	0.01	0.01	0.51	11.64	0.21	0.05	11.36	0.00	2.14	7.39	2.59	100.44
2	51.12	13.68	0.28	0.01	0.01	0.51	11.66	0.20	0.04	11.40	0.00	2.06	7.58	2.57	101.10
2	51.27	13.71	0.28	0.00	0.01	0.51	11.65	0.17	0.04	11.51	0.01	2.07	7.61	2.59	101.41
2	50.97	13.66	0.29	0.01	0.02	0.51	11.77	0.19	0.04	11.49	0.02	2.10	7.29	2.65	100.98
2	50.78	13.74	0.27	0.01	0.01	0.51	11.65	0.16	0.04	11.50	0.01	2.08	7.33	2.65	100.73
2	50.29	13.84	0.27	0.01	0.01	0.51	11.67	0.17	0.05	11.45	0.00	2.12	7.48	2.61	100.47
2	51.32	13.77	0.27	0.00	0.01	0.51	11.54	0.18	0.03	11.48	0.01	2.13	7.57	2.60	101.41
2	50.70	13.69	0.28	0.00	0.02	0.51	11.61	0.18	0.02	11.37	0.01	2.08	7.37	2.60	100.43
2	50.32	13.68	0.27	0.01	0.02	0.51	11.60	0.17	0.04	11.43	0.03	2.03	7.41	2.62	100.13
2	50.27	13.73	0.28	0.00	0.01	0.51	11.69	0.19	0.04	11.46	0.02	2.12	7.45	2.66	100.40
2	51.26	13.77	0.30	0.00	0.01	0.51	11.80	0.19	0.04	11.59	0.00	2.10	7.55	2.57	101.68
2	51.42	13.81	0.29	0.01	0.01	0.51	11.72	0.18	0.05	11.38	0.00	2.10	7.55	2.56	101.59
2	51.26	13.74	0.26	0.01	0.01	0.51	11.68	0.17	0.05	11.43	0.01	2.10	7.57	2.59	101.37
2	50.22	13.86	0.28	0.01	0.01	0.51	11.73	0.17	0.03	11.41	0.00	2.09	7.39	2.58	100.28
2	51.07	13.60	0.29	0.01	0.01	0.52	11.70	0.19	0.04	11.49	0.01	2.07	7.48	2.60	101.06
2	50.28	13.75	0.26	0.02	0.01	0.52	11.74	0.19	0.05	11.45	0.01	2.08	7.54	2.58	100.48
2	50.22	13.80	0.25	0.01	0.02	0.52	11.65	0.21	0.06	11.41	0.03	2.17	7.67	2.53	100.52
2	51.06	13.72	0.28	0.00	0.02	0.52	11.63	0.18	0.03	11.44	0.01	2.08	7.39	2.58	100.91
2	51.10	13.70	0.31	0.00	0.01	0.52	11.64	0.17	0.05	11.35	0.00	2.08	7.45	2.61	100.98
2	51.08	13.82	0.28	0.01	0.01	0.52	11.79	0.18	0.04	11.47	0.02	2.06	7.45	2.59	101.31
2	50.83	13.68	0.28	0.01	0.01	0.52	11.79	0.17	0.06	11.42	0.00	2.14	7.47	2.60	100.98
2	50.38	13.83	0.25	0.01	0.01	0.52	11.66	0.16	0.04	11.46	0.00	2.17	7.53	2.59	100.61
2	50.88	13.77	0.24	0.01	0.01	0.52	11.56	0.20	0.02	11.42	0.02	2.22	7.50	2.69	101.06
2	50.31	13.76	0.30	0.00	0.10	0.52	11.60	0.20	0.04	11.28	0.02	2.17	7.54	2.61	100.42
2	51.15	13.77	0.28	0.01	0.01	0.52	11.71	0.18	0.05	11.55	0.01	2.18	7.43	2.69	101.53
2	51.21	13.83	0.31	0.00	0.01	0.52	11.69	0.18	0.04	11.35	0.00	2.14	7.46	2.61	101.36
2	50.87	13.70	0.27	0.01	0.01	0.52	11.59	0.18	0.06	11.49	0.00	2.18	7.44	2.71	101.02
2	50.78	13.76	0.25	0.01	0.01	0.52	11.66	0.19	0.03	11.40	0.01	2.11	7.36	2.60	100.69
2	51.23	13.75	0.26	0.02	0.01	0.52	11.62	0.17	0.04	11.46	0.00	2.18	7.43	2.63	101.32
2	51.11	13.67	0.30	0.00	0.01	0.52	11.70	0.16	0.04	11.41	0.00	2.17	7.45	2.56	101.10
2	50.70	13.69	0.27	0.00	0.02	0.52	11.77	0.17	0.05	11.43	0.01	2.17	7.52	2.57	100.87
2	50.13	13.78	0.27	0.01	0.01	0.52	11.65	0.18	0.03	11.37	0.02	2.11	7.48	2.53	100.07
2	51.17	13.81	0.30	0.01	0.01	0.53	11.63	0.20	0.03	11.47	0.02	2.18	7.52	2.60	101.44

2	50.90	13.77	0.26	0.00	0.01	0.53	11.66	0.19	0.06	11.47	0.03	2.15	7.43	2.63	101.08	
2	51.01	13.78	0.33	0.01	0.00	0.53	11.64	0.17	0.06	11.51	0.02	2.06	7.47	2.59	101.18	
2	50.85	13.69	0.29	0.00	0.03	0.53	11.75	0.18	0.05	11.45	0.00	2.14	7.30	2.63	100.86	
2	50.47	13.92	0.30	0.00	0.01	0.53	11.62	0.20	0.05	11.48	0.01	2.14	7.60	2.59	100.91	
2	50.85	13.82	0.26	0.00	0.01	0.53	11.73	0.17	0.02	11.45	0.02	2.12	7.37	2.62	100.97	
2	50.19	13.77	0.27	0.00	0.01	0.53	11.70	0.17	0.04	11.40	0.01	2.13	7.57	2.58	100.36	
2	50.25	13.75	0.28	0.02	0.01	0.53	11.58	0.18	0.05	11.36	0.03	2.07	7.39	2.61	100.09	
2	50.39	13.84	0.26	0.01	0.01	0.53	11.62	0.17	0.05	11.39	0.02	2.05	7.56	2.56	100.44	
2	50.26	13.66	0.25	0.02	0.06	0.54	11.61	0.18	0.04	11.23	0.01	2.19	7.39	2.56	99.97	
2	51.09	13.68	0.27	0.01	0.02	0.54	11.66	0.18	0.03	11.35	0.03	2.12	7.39	2.57	100.92	
2	50.83	13.63	0.25	0.02	0.02	0.54	11.65	0.17	0.04	11.45	0.01	2.05	7.34	2.64	100.61	
2	50.28	13.82	0.28	0.00	0.01	0.54	11.59	0.17	0.03	11.48	0.02	2.12	7.51	2.61	100.46	
2	50.67	13.72	0.26	0.01	0.03	0.55	11.60	0.17	0.05	11.48	0.01	2.24	7.57	2.62	100.96	
2	50.85	13.78	0.23	0.01	0.01	0.55	11.80	0.17	0.05	11.33	0.01	1.89	7.34	2.66	100.67	
2	50.37	13.60	0.31	0.02	0.09	0.56	11.50	0.18	0.05	11.18	0.01	2.18	7.54	2.58	100.15	
3	49.89	13.78	0.25	0.00	0.01	0.48	11.28	0.15	0.02	10.93	0.05	2.13	7.52	2.75	99.25	
3	49.91	13.76	0.29	0.00	0.01	0.51	11.25	0.15	0.04	11.04	0.00	2.13	7.51	2.74	99.33	
3	49.70	13.77	0.27	0.00	0.01	0.52	11.29	0.18	0.04	11.04	0.01	2.13	7.54	2.76	99.26	
3	49.89	13.74	0.29	0.00	0.01	0.47	11.33	0.13	0.05	10.95	0.00	2.18	7.54	2.78	99.36	
<hr/>																
Average		50.72	13.77	0.28	0.01	0.01	0.52	11.58	0.18	0.04	11.37	0.01	2.10	7.47	2.64	100.70
Stddev		0.34	0.08	0.02	0.01	0.02	0.01	0.12	0.01	0.01	0.11	0.01	0.07	0.09	0.06	0.48
RSD		0.68	0.56	7.23	87.53	114.08	2.79	1.06	7.22	24.75	0.98	81.19	3.20	1.21	2.15	0.48
Standard																
Value		49.90	13.50	0.27		0.52	11.40		0.03	11.10	0.03	2.22	7.23	2.73		
Std/Avg		0.98	0.98	0.97		1.01	0.98		0.73	0.98	2.52	1.06	0.97	1.03		
*FeO reported as total Fe																

\*FeO reported as total Fe

Table 2.2: Olivine Standard Measurements  
San Carlos Olivine

Run	SiO2	Al2O3	MnO	FeO*	NiO	Na2O	MgO	CaO	TiO2	Cr2O3	Total
1	39.84	0.03	0.14	9.46	0.38	0.01	50.13	0.06	0.00	0.03	100.08
1	39.82	0.02	0.14	9.25	0.35	0.00	49.60	0.07	0.05	0.02	99.30
1	39.55	0.02	0.15	9.34	0.41	0.02	49.24	0.06	0.02	0.01	98.81
1	39.94	0.01	0.13	9.28	0.36	0.00	50.09	0.06	0.00	0.01	99.88
1	39.71	0.02	0.14	9.33	0.37	0.02	50.57	0.06	0.04	0.02	100.29
1	39.76	0.01	0.14	9.28	0.35	0.00	50.35	0.06	0.00	0.03	99.99
1	39.06	0.01	0.14	9.23	0.36	0.00	50.71	0.06	0.04	0.01	99.62
1	39.08	0.01	0.16	9.08	0.33	0.00	50.92	0.07	0.01	0.02	99.68
1	39.06	0.02	0.14	9.16	0.36	0.01	51.30	0.06	0.00	0.00	100.10
2	40.09	0.03	0.16	9.44	0.37	0.00	49.34	0.06	0.02	0.02	99.52
2	40.17	0.02	0.14	9.34	0.37	0.00	49.02	0.07	0.00	0.01	99.15
2	39.98	0.02	0.16	9.48	0.37	0.02	49.47	0.06	0.00	0.01	99.56
2	40.12	0.02	0.14	9.48	0.36	0.00	49.21	0.07	0.00	0.02	99.43
2	40.22	0.02	0.14	9.49	0.39	0.00	49.36	0.06	0.00	0.01	99.67
2	40.20	0.01	0.15	9.44	0.34	0.00	49.63	0.06	0.03	0.02	99.88
2	39.58	0.01	0.15	9.43	0.37	0.00	49.09	0.07	0.00	0.00	98.70
2	39.78	0.03	0.16	9.62	0.37	0.01	49.68	0.06	0.04	0.01	99.76
2	39.78	0.02	0.15	9.49	0.37	0.01	49.33	0.07	0.01	0.00	99.22
2	39.62	0.02	0.15	9.43	0.36	0.01	49.21	0.06	0.04	0.03	98.91
2	39.67	0.02	0.16	9.56	0.37	0.00	49.40	0.07	0.03	0.01	99.28
2	39.67	0.02	0.14	9.47	0.38	0.00	49.50	0.06	0.03	0.02	99.29
2	39.98	0.02	0.16	9.57	0.37	0.01	49.41	0.06	0.00	0.01	99.58
2	39.86	0.01	0.14	9.52	0.37	0.01	49.51	0.08	0.00	0.03	99.52
2	39.22	0.03	0.15	9.38	0.37	0.00	49.30	0.07	0.05	0.02	98.57
2	39.42	0.02	0.15	9.46	0.38	0.02	49.30	0.07	0.00	0.01	98.83
2	39.27	0.02	0.15	9.46	0.40	0.00	49.00	0.07	0.00	0.02	98.37
2	39.37	0.03	0.15	9.59	0.37	0.01	49.52	0.06	0.03	0.01	99.14
2	39.46	0.03	0.15	9.43	0.36	0.01	49.24	0.06	0.02	0.00	98.76
2	39.40	0.02	0.15	9.51	0.39	0.00	49.54	0.06	0.00	0.00	99.07
Average	39.68	0.02	0.15	9.41	0.37	0.00	49.65	0.06	0.02	0.01	99.38
Stdev	0.35	0.01	0.01	0.13	0.02	0.01	0.59	0.00	0.02	0.01	0.49
RSD	0.87	31.30	5.85	1.36	4.50	120.13	1.19	7.39	111.73	64.76	0.50
Standard Value	40.81		0.14	9.55			49.42	0.05			
Std/Avg	1.03		0.95	1.01			1.00	0.79			

Springwater Olivine

Run	SiO2	Al2O3	MnO	FeO*	NiO	Na2O	MgO	CaO	TiO2	Cr2O3	Total
1	38.86	0.00	0.34	16.17	0.04	0.00	44.54	0.01	0.04	0.02	100.03
1	39.02	0.00	0.35	16.01	0.01	0.00	45.05	0.01	0.00	0.03	100.48
1	39.06	0.00	0.34	15.95	0.02	0.01	45.68	0.01	0.00	0.06	101.13
1	38.63	0.01	0.35	16.21	0.00	0.00	44.08	0.01	0.01	0.01	99.30
1	38.83	0.01	0.35	16.03	0.02	0.00	44.00	0.01	0.00	0.02	99.27
1	38.52	0.01	0.35	16.00	0.02	0.00	44.59	0.01	0.01	0.02	99.52

1	39.02	0.00	0.33	16.12	0.00	0.02	44.85	0.01	0.01	0.01	100.37
1	38.97	0.01	0.33	16.24	0.00	0.00	44.78	0.01	0.00	0.01	100.35
1	38.87	0.02	0.35	16.15	0.02	0.01	44.36	0.00	0.00	0.02	99.78
1	38.90	0.02	0.34	16.40	0.00	0.00	43.95	0.02	0.01	0.01	99.65
1	38.72	0.01	0.33	16.21	0.02	0.03	43.72	0.01	0.00	0.01	99.08
1	39.14	0.02	0.35	16.36	0.00	0.01	44.71	0.01	0.00	0.04	100.63
1	38.97	0.00	0.34	16.06	0.00	0.00	44.38	0.00	0.02	0.03	99.80
1	38.78	0.01	0.31	16.35	0.01	0.01	44.42	0.02	0.01	0.02	99.92
1	38.67	0.03	0.36	15.98	0.00	0.00	43.83	0.02	0.01	0.03	98.93
1	38.66	0.02	0.34	16.11	0.00	0.00	43.93	0.01	0.02	0.03	99.12
1	38.73	0.01	0.33	15.86	0.00	0.00	43.48	0.01	0.01	0.01	98.45
1	38.91	0.01	0.33	16.17	0.01	0.00	43.78	0.01	0.00	0.00	99.22
1	39.17	0.01	0.34	16.12	0.01	0.00	44.66	0.01	0.03	0.02	100.36
1	38.69	0.02	0.34	16.54	0.01	0.01	44.33	0.01	0.00	0.03	99.99
1	38.82	0.02	0.33	16.05	0.01	0.01	44.10	0.00	0.01	0.02	99.38
1	39.02	0.01	0.35	16.08	0.01	0.00	43.80	0.01	0.00	0.02	99.30
1	38.38	0.01	0.35	15.94	0.00	0.00	43.19	0.02	0.01	0.02	97.93
1	38.54	0.02	0.34	16.24	0.00	0.00	43.76	0.01	0.01	0.03	98.94
1	38.54	0.00	0.36	15.85	0.00	0.00	44.31	0.01	0.00	0.03	99.09
1	38.98	0.01	0.34	16.02	0.00	0.02	44.71	0.00	0.00	0.03	100.12
1	39.08	0.02	0.35	15.94	0.00	0.00	44.84	0.01	0.00	0.04	100.27
1	39.13	0.00	0.34	15.81	0.00	0.00	44.65	0.01	0.00	0.02	99.96
1	38.64	0.00	0.34	16.11	0.00	0.00	43.95	0.01	0.00	0.03	99.09
1	38.86	0.00	0.35	16.02	0.01	0.01	43.90	0.01	0.03	0.04	99.23
1	38.77	0.00	0.34	16.05	0.01	0.00	44.41	0.01	0.00	0.04	99.63
1	39.16	0.01	0.35	16.25	0.00	0.00	45.16	0.01	0.00	0.01	100.95
1	39.03	0.01	0.34	15.95	0.00	0.00	44.76	0.01	0.00	0.03	100.14
1	38.72	0.01	0.34	16.02	0.02	0.01	44.47	0.01	0.00	0.02	99.61
1	38.98	0.00	0.35	16.23	0.00	0.01	44.28	0.01	0.00	0.01	99.86
1	38.49	0.01	0.34	16.04	0.00	0.00	43.82	0.02	0.00	0.00	98.72
1	38.91	0.00	0.34	15.95	0.03	0.00	44.60	0.01	0.01	0.01	99.85
1	38.76	0.01	0.34	16.04	0.00	0.01	44.37	0.01	0.00	0.05	99.59
1	38.89	0.01	0.34	15.88	0.00	0.00	44.79	0.01	0.01	0.03	99.96
1	38.66	0.00	0.31	16.25	0.00	0.03	44.43	0.02	0.03	0.03	99.75
1	39.04	0.01	0.33	16.08	0.01	0.01	44.55	0.00	0.02	0.01	100.07
1	38.68	0.00	0.35	16.23	0.00	0.01	44.26	0.01	0.05	0.02	99.61
1	39.13	0.01	0.34	16.16	0.01	0.02	44.44	0.00	0.01	0.00	100.11
1	38.80	0.02	0.33	16.32	0.00	0.00	44.49	0.01	0.00	0.04	100.00
1	38.98	0.02	0.34	16.06	0.00	0.00	44.97	0.01	0.03	0.01	100.43
1	38.45	0.03	0.33	15.92	0.03	0.01	43.82	0.02	0.00	0.04	98.63
1	38.80	0.01	0.33	16.05	0.01	0.00	44.01	0.01	0.00	0.02	99.25
1	39.29	0.02	0.35	16.32	0.00	0.00	44.52	0.01	0.03	0.02	100.55
1	38.81	0.02	0.34	15.95	0.00	0.02	43.64	0.01	0.00	0.03	98.83
1	38.38	0.06	0.36	15.90	0.00	0.00	43.51	0.01	0.01	0.03	98.25
1	38.40	0.00	0.34	16.19	0.00	0.01	44.06	0.01	0.01	0.04	99.05
1	38.38	0.05	0.32	16.20	0.01	0.00	43.85	0.01	0.00	0.02	98.84
1	38.91	0.00	0.34	16.11	0.00	0.00	44.23	0.01	0.01	0.03	99.65

1	38.32	0.02	0.34	16.07	0.00	0.01	43.37	0.01	0.03	0.03	98.18
1	38.58	0.00	0.35	16.28	0.00	0.00	43.48	0.00	0.03	0.04	98.76
1	38.78	0.00	0.35	16.24	0.00	0.01	43.64	0.01	0.00	0.02	99.06
1	38.93	0.02	0.33	16.03	0.01	0.00	44.35	0.00	0.03	0.01	99.71
1	38.85	0.03	0.34	16.04	0.00	0.00	44.23	0.02	0.04	0.02	99.56
1	38.85	0.01	0.34	16.15	0.00	0.01	44.30	0.00	0.03	0.01	99.69
1	39.18	0.02	0.34	16.15	0.00	0.00	44.74	0.01	0.00	0.03	100.47
1	38.71	0.04	0.32	15.92	0.01	0.04	43.37	0.01	0.03	0.03	98.45
1	38.76	0.01	0.35	15.73	0.00	0.00	43.77	0.01	0.00	0.01	98.63
1	38.98	0.01	0.34	16.23	0.01	0.00	44.42	0.01	0.00	0.02	100.02
2	38.93	0.02	0.34	16.30	0.00	0.00	44.28	0.01	0.03	0.01	99.92
2	38.80	0.02	0.37	16.53	0.01	0.02	44.03	0.01	0.01	0.03	99.83
2	39.00	0.01	0.36	16.31	0.00	0.00	44.42	0.01	0.03	0.03	100.17
2	38.74	0.02	0.36	16.23	0.00	0.01	44.08	0.01	0.05	0.02	99.50
2	38.78	0.01	0.35	16.21	0.01	0.01	44.33	0.01	0.00	0.01	99.72
2	38.81	0.01	0.37	16.41	0.00	0.00	44.49	0.00	0.00	0.03	100.13
2	38.66	0.01	0.35	16.29	0.02	0.01	44.28	0.01	0.04	0.02	99.68
2	38.79	0.02	0.36	16.04	0.03	0.01	44.23	0.01	0.04	0.03	99.57
2	38.64	0.02	0.38	16.35	0.00	0.01	43.93	0.00	0.00	0.03	99.35
2	38.61	0.02	0.35	16.30	0.00	0.00	44.30	0.01	0.01	0.02	99.61
2	38.59	0.01	0.36	16.37	0.00	0.00	44.13	0.01	0.00	0.04	99.52
2	38.94	0.01	0.36	16.46	0.00	0.01	44.47	0.01	0.03	0.04	100.32
2	38.33	0.02	0.35	16.27	0.00	0.00	43.68	0.01	0.00	0.02	98.66
2	38.55	0.01	0.35	16.40	0.00	0.01	44.25	0.00	0.00	0.04	99.61
2	38.46	0.02	0.35	16.40	0.00	0.01	44.30	0.02	0.00	0.02	99.57
2	38.53	0.04	0.36	16.19	0.00	0.00	44.10	0.02	0.00	0.02	99.24
2	38.43	0.04	0.37	16.36	0.01	0.00	43.97	0.01	0.04	0.01	99.24
2	38.71	0.02	0.35	16.43	0.02	0.00	44.27	0.01	0.00	0.02	99.83
2	38.59	0.00	0.37	16.36	0.01	0.00	44.22	0.01	0.00	0.04	99.60
2	39.11	0.02	0.36	16.26	0.00	0.01	44.83	0.01	0.04	0.01	100.64
Average	38.79	0.01	0.34	16.15	0.01	0.01	44.24	0.01	0.01	0.02	99.59
Stdev	0.23	0.01	0.01	0.17	0.01	0.01	0.44	0.00	0.01	0.01	0.64
RSD	0.58	80.63	3.44	1.08	146.70	142.27	1.00	47.44	127.52	49.16	0.64
Standard Value	38.95		0.30	16.62			43.58			0.02	
Std/Avg	1.00		0.87	1.03			0.99			0.86	

\*FeO reported as total Fe



Table 2.3: Plagioclase Standard Measurements  
An50

	SiO2	Al2O3	K2O	FeO*	Na2O	CaO	Total
	55.36	27.87	0.02	0.09	5.57	10.24	99.15
	55.25	27.64	0.02	0.10	5.07	10.19	98.25
	55.09	27.98	0.02	0.16	5.60	10.17	99.03
	55.31	27.84	0.01	0.06	5.35	10.18	98.74
	54.94	27.88	0.01	0.02	5.56	10.30	98.70
	55.48	28.16	0.03	0.07	5.55	10.24	99.53
	55.30	27.70	0.03	0.09	5.47	10.27	98.86
	55.37	27.76	0.02	0.00	5.45	10.24	98.84
	55.43	28.09	0.02	0.14	5.70	10.11	99.49
	54.90	28.12	0.02	0.23	5.73	10.22	99.23
	54.30	28.14	0.02	0.05	5.65	10.20	98.37
	54.69	27.99	0.02	0.18	5.70	10.29	98.87
	54.83	28.14	0.01	0.12	5.75	10.38	99.22
	55.02	27.90	0.01	0.15	5.72	10.38	99.19
	54.57	27.98	0.03	0.16	5.50	10.27	98.51
	54.84	28.51	0.02	0.15	5.68	10.28	99.48
	55.12	28.21	0.02	0.26	5.77	10.24	99.60
Average	55.05	28.00	0.02	0.12	5.58	10.25	99.00
Stdev	0.33	0.21	0.01	0.07	0.18	0.07	0.41
RSD	0.60	0.76	37.99	59.12	3.18	0.69	0.41
Standard							
Value	55.59	28.29			5.74	10.38	
Std/Avg	1.01	1.01			1.03	1.01	

\*FeO reported as total Fe

Table 2.4: Uncorrected Repeated Melt Inclusions Major Element Compositions

Sample	SiO <sub>2</sub>	Al <sub>2</sub> O <sub>3</sub>	P <sub>2</sub> O <sub>5</sub>	S	Cl	K <sub>2</sub> O	CaO	MnO	Cr <sub>2</sub> O <sub>3</sub>	FeO*	NiO	Na <sub>2</sub> O	MgO	TiO <sub>2</sub>	Total
RVV316-11	41.70	15.24	1.32	0.11	0.20	1.78	11.95	0.12	0.02	7.33	0.07	7.48	11.16	2.70	101.27
RVV316-11a	41.53	15.13	1.26	0.11	0.20	1.79	11.87	0.11	0.02	7.29	0.07	7.40	11.07	2.67	100.61
average	41.61	15.18	1.29	0.11	0.20	1.78	11.91	0.11	0.02	7.31	0.07	7.44	11.11	2.68	
stdev	0.12	0.07	0.04	0.00	0.00	0.00	0.05	0.00	0.01	0.03	0.00	0.06	0.06	0.02	
RSD	0.28	0.49	3.19	0.52	1.44	0.12	0.46	4.32	28.28	0.41	1.08	0.79	0.57	0.92	
RVV340-8	44.36	10.46	0.33	0.05	0.02	0.64	6.97	0.25	0.02	17.92	0.03	2.98	15.15	1.14	100.40
RVV340-8a	44.54	11.25	0.35	0.06	0.02	0.72	7.13	0.25	0.01	17.32	0.04	3.35	13.50	1.20	99.82
average	44.45	10.86	0.34	0.05	0.02	0.68	7.05	0.25	0.01	17.62	0.04	3.17	14.33	1.17	
stdev	0.13	0.56	0.01	0.00	0.00	0.06	0.11	0.00	0.00	0.42	0.01	0.26	1.17	0.04	
RSD	0.28	5.12	4.32	4.66	15.71	8.28	1.53	0.29	34.14	2.40	18.61	8.35	8.17	3.75	
RVV340-10	44.40	11.43	0.26	0.12	0.03	0.45	7.56	0.20	0.02	15.41	0.07	2.68	16.36	1.71	100.84
RVV340-10a	44.23	11.51	0.28	0.12	0.03	0.45	7.69	0.19	0.00	15.42	0.06	2.70	16.44	1.68	100.97
RVV340-10b	44.02	11.43	0.29	0.12	0.02	0.44	7.72	0.20	0.02	15.56	0.07	2.72	16.18	1.67	100.61
average	44.21	11.45	0.28	0.12	0.03	0.45	7.66	0.19	0.01	15.46	0.06	2.70	16.32	1.69	
stdev	0.19	0.05	0.02	0.00	0.00	0.00	0.08	0.00	0.01	0.08	0.00	0.02	0.13	0.02	
RSD	0.43	0.41	5.44	2.29	6.03	1.02	1.11	1.57	64.33	0.55	4.56	0.78	0.81	1.43	
RVV343-3	47.61	17.36	0.37	0.11	0.03	0.76	9.41	0.14	0.01	10.83	0.02	3.46	7.31	2.76	100.16
RVV343-3a	47.75	17.43	0.39	0.11	0.03	0.81	9.46	0.15	0.02	10.85	0.03	3.54	7.15	2.92	100.65
average	47.68	17.39	0.38	0.11	0.03	0.78	9.43	0.14	0.02	10.84	0.02	3.50	7.23	2.84	
stdev	0.11	0.05	0.02	0.00	0.00	0.04	0.04	0.01	0.01	0.02	0.00	0.06	0.11	0.11	
RSD	0.22	0.31	4.89	0.84	4.86	4.61	0.39	6.45	34.35	0.18	6.19	1.58	1.59	4.05	
RVV345-2	48.74	14.85	0.18	0.08	0.02	0.37	11.70	0.15	0.04	9.40	0.00	4.31	9.72	1.67	101.33
RVV345-2a	48.69	14.85	0.20	0.08	0.02	0.36	11.71	0.15	0.03	9.35	0.01	4.36	9.67	1.68	101.25
average	48.71	14.85	0.19	0.08	0.02	0.36	11.70	0.15	0.04	9.37	0.00	4.33	9.70	1.67	
stdev	0.03	0.00	0.02	0.00	0.00	0.00	0.01	0.01	0.00	0.04	0.00	0.03	0.03	0.01	
RSD	0.07	0.00	8.19	2.15	12.86	0.97	0.05	3.80	13.94	0.38	106.07	0.75	0.34	0.46	
RVV345-15	44.83	15.60	0.47	0.10	0.09	1.08	13.15	0.10	0.06	7.64	0.02	4.32	9.77	2.73	100.09
RVV345-15a	44.87	15.73	0.46	0.11	0.09	1.05	13.27	0.12	0.06	7.53	0.02	4.33	9.76	2.75	100.28
RVV345-15b	44.90	15.63	0.46	0.11	0.09	1.06	13.44	0.12	0.05	7.59	0.02	4.38	9.79	2.74	100.50

average	44.86	15.65	0.46	0.10	0.09	1.06	13.29	0.11	0.06	7.59	0.02	4.34	9.77	2.74
stdev	0.03	0.07	0.01	0.01	0.00	0.01	0.15	0.01	0.01	0.06	0.00	0.03	0.02	0.01
RSD	0.07	0.44	1.60	5.59	1.10	1.26	1.11	8.04	14.26	0.73	18.62	0.66	0.17	0.41
RVV345-16	46.62	14.30	0.36	0.15	0.06	0.85	14.08	0.11	0.06	8.02	0.06	3.65	9.51	2.46
RVV345-16a	45.82	14.54	0.38	0.15	0.07	0.84	14.00	0.12	0.04	7.88	0.05	3.15	9.86	2.58
average	46.22	14.42	0.37	0.15	0.07	0.84	14.04	0.11	0.05	7.95	0.06	3.40	9.69	2.52
stdev	0.56	0.17	0.01	0.00	0.00	0.01	0.05	0.00	0.02	0.10	0.01	0.36	0.24	0.09
RSD	1.22	1.19	3.57	3.01	5.02	1.33	0.36	3.57	28.50	1.25	11.40	10.49	2.51	3.42
RVV345-18	47.42	17.76	0.22	0.02	0.48	3.13	10.64	0.08	0.03	6.96	0.04	4.41	8.04	1.55
RVV345-18a	47.28	17.19	0.22	0.02	0.49	3.21	10.49	0.11	0.04	7.05	0.04	4.00	7.49	1.54
RVV345-18b	47.39	17.37	0.21	0.02	0.50	3.22	10.46	0.09	0.05	7.06	0.05	3.99	7.43	1.50
average	47.36	17.44	0.21	0.02	0.49	3.19	10.53	0.09	0.04	7.02	0.04	4.13	7.65	1.53
stdev	0.07	0.29	0.01	0.00	0.01	0.05	0.10	0.01	0.01	0.06	0.01	0.24	0.34	0.03
RSD	0.15	1.68	2.77	9.06	2.22	1.63	0.90	13.20	24.13	0.79	17.32	5.77	4.43	1.90
RVV345-25	50.38	13.84	0.27	0.13	0.03	0.52	13.67	0.09	0.11	6.38	0.05	3.55	9.37	2.05
RVV345-25a	49.45	14.06	0.27	0.12	0.04	0.52	13.58	0.12	0.12	6.46	0.07	3.14	9.93	2.21
average	49.91	13.95	0.27	0.13	0.03	0.52	13.62	0.11	0.11	6.42	0.06	3.34	9.65	2.13
stdev	0.66	0.15	0.00	0.00	0.00	0.00	0.07	0.02	0.00	0.06	0.01	0.29	0.39	0.11
RSD	1.32	1.07	0.66	3.64	13.49	0.95	0.50	23.13	4.34	0.88	19.41	8.58	4.05	5.27
RVV346-11	47.17	14.14	0.30	0.09	0.05	0.75	14.50	0.10	0.09	7.03	0.03	3.30	9.98	2.38
RVV346-11a	47.24	14.25	0.27	0.09	0.05	0.76	14.54	0.09	0.09	6.98	0.04	3.28	10.01	2.41
average	47.21	14.20	0.28	0.09	0.05	0.75	14.52	0.10	0.09	7.00	0.03	3.29	9.99	2.39
stdev	0.05	0.07	0.02	0.00	0.00	0.01	0.03	0.00	0.00	0.04	0.01	0.02	0.02	0.03
RSD	0.11	0.53	7.58	1.23	0.00	0.94	0.22	2.95	3.11	0.60	30.94	0.49	0.21	1.06

\*FeO reported as total Fe

Table 2.5: Repeat measurements on SIMS secondary standard

Run	Standard	Ca	Ti	Rb	Li	B	Sr	Y	Zr	Nb	Ba	La	Ce	Nd	Sm	Eu	Gd	Dy	Er	Yb	Hf
1	BHVO-2G	129797.9		14.1			396.4	28.0	174.8	15.8	130.8	16.4	38.7	23.5	6.5	2.0	6.7	5.7	3.5	2.2	4.8
1	BHVO-2G	122462.4		9.2			372.5	25.7	166.3	16.0	118.3	16.1	36.9	22.0	5.9	1.8	6.0	5.4	2.7	2.0	4.3
1	BHVO-2G	119732.6		7.6			365.1	24.5	160.9	16.4	119.6	16.3	34.7	20.8	4.7	2.1	6.7	5.1	2.8	1.7	3.6
1	BHVO-2G	119020.8		6.5			364.3	25.9	167.6	16.1	113.9	13.6	35.7	22.6	5.9	2.4	4.7	5.1	2.8	2.4	4.8
1	BHVO-2G	115478.5		7.2			353.6	24.4	161.1	16.8	122.3	14.7	32.2	19.2	5.7	1.8	5.2	5.3	1.9	1.9	3.3
1	BHVO-2G	112811.6		4.0			347.9	22.0	162.3	16.5	115.7	14.9	33.4	21.0	6.3	2.0	6.2	4.2	2.6	1.5	3.9
1	BHVO-2G	117777.9		14.0			364.7	25.3	167.2	17.4	114.9	15.8	37.3	21.8	6.5	1.7	4.6	4.4	2.5	2.2	4.2
1	BHVO-2G	125755.7		10.4			377.9	26.4	168.7	17.2	123.9	16.3	36.6	23.5	5.9	1.8	5.9	5.5	2.6	1.4	3.4
1	BHVO-2G	107579.4		1.0			329.1	22.2	147.4	14.7	106.8	13.6	28.8	16.3	4.8	1.3	4.5	3.6	1.9	1.2	3.5
1	BHVO-2G	122240.4		2.0			376.4	26.1	172.0	17.0	118.1	16.1	40.7	24.0	7.1	1.6	6.2	5.7	2.8	2.0	4.2
1	BHVO-2G	126196.7		8.2			385.6	27.1	173.4	16.3	119.5	17.0	39.5	24.5	7.2	2.4	6.2	5.9	3.1	1.8	4.7
1	BHVO-2G	124987.7		5.5			374.2	25.6	174.7	16.5	121.2	15.2	41.1	24.4	7.2	2.1	5.7	6.4	2.5	1.9	4.7
1	BHVO-2G	126907.6		2.8			389.7	26.8	179.3	16.7	124.4	16.6	43.9	25.3	6.1	2.4	6.2	5.0	2.5	2.3	3.7
1	BHVO-2G	124846.2		7.6			384.8	26.7	164.5	15.7	121.2	16.8	37.1	23.9	6.2	2.2	4.8	4.7	2.7	2.1	4.1
1	BHVO-2G	114473.8		7.5			351.2	23.5	158.4	16.4	110.2	15.0	35.0	19.9	4.8	1.6	4.3	4.4	2.4	1.9	2.9
1	BHVO-2G	121154.6		0.0			371.9	23.8	163.7	16.8	114.6	14.5	35.5	21.1	6.2	1.9	5.6	6.0	2.6	2.4	3.5
1	BHVO-2G	115957.7		-0.2			361.0	24.0	164.4	15.4	114.5	14.5	34.2	22.1	6.4	1.8	5.8	4.8	2.6	2.0	3.7
1	BHVO-2G	125329.7		6.4			390.0	27.1	178.5	16.9	123.7	16.6	42.0	24.2	6.7	1.9	5.4	6.1	3.1	2.5	4.3
1	BHVO-2G	130063.0		-3.9			407.0	28.9	183.0	16.9	123.0	19.0	40.9	25.3	6.8	2.4	5.7	6.4	2.9	2.2	4.3
1	BHVO-2G	128037.6		5.9			394.3	28.5	178.9	17.2	122.4	17.5	42.5	26.9	7.1	2.0	6.6	5.9	3.1	2.2	4.5
1	BHVO-2G	125052.4		0.6			388.8	28.0	174.5	16.2	124.2	17.0	39.9	24.7	6.6	1.7	5.0	5.5	2.9	2.1	5.1
1	BHVO-2G	124352.9		2.7			383.5	26.9	170.4	16.5	120.6	17.3	41.5	23.9	6.8	1.7	5.0	6.4	2.5	2.6	5.3
1	BHVO-2G	125396.1		6.3			389.3	27.8	180.6	16.6	125.3	17.3	42.5	25.0	6.9	2.3	6.2	5.5	2.9	2.2	5.0
1	BHVO-2G	120482.2		3.1			377.9	25.4	169.1	17.7	116.1	16.7	38.2	23.0	6.3	2.1	5.5	4.7	2.6	2.4	4.8
Average		121912.3		5.4			374.9	25.9	169.2	16.5	119.4	16.0	37.9	22.9	6.3	2.0	5.6	5.3	2.7	2.1	4.2
stdev		5655.3		4.4			17.9	1.9	8.3	0.7	5.4	1.3	3.8	2.3	0.7	0.3	0.7	0.7	0.4	0.3	0.6
RSD		4.6		81.7			4.8	7.3	4.9	4.1	4.5	8.1	9.9	10.2	11.5	14.8	12.8	14.0	13.1	16.3	15.1
Accepted		114000.0		9.8			389.0	26.0	172.0	19.2	129.0	15.3	37.9	24.4	6.0	2.0	6.2	5.3	2.5	2.0	4.1
Correction Factor		0.9		1.8			1.0	1.0	1.0	1.2	1.1	1.0	1.0	1.1	1.0	1.0	1.1	1.0	0.9	1.0	1.0
2	BHVO-2G	123283.7		4.1	2.2	442.7	33.0	182.9	20.6	135.7	19.1	45.7	29.9	6.3	1.9	6.7	6.6	2.6	2.5	4.6	

2	BHVO-2G	118100.1	4.0	2.6	424.6	28.5	173.7	18.8	135.9	15.7	40.8	26.2	7.3	1.7	5.9	5.9	2.1	2.6	4.2
2	BHVO-2G	115295.9	4.0	2.5	414.2	27.0	172.9	17.7	128.9	15.3	38.1	26.5	5.2	1.5	5.5	5.8	2.4	2.2	4.2
2	BHVO-2G	114263.2	3.9	3.6	403.1	26.8	176.0	19.3	124.3	15.3	37.0	25.2	5.6	1.6	6.4	4.9	2.4	1.8	4.5
2	BHVO-2G	106097.9	3.6	3.0	367.8	25.6	160.2	18.6	119.7	13.2	35.9	22.0	5.5	1.4	4.6	4.9	2.3	1.9	3.9
2	BHVO-2G	124746.4	3.9	2.2	448.0	34.6	187.3	20.5	138.8	18.9	48.1	31.1	7.2	1.8	6.9	6.7	2.5	2.5	5.5
2	BHVO-2G	109093.0	3.6	2.8	391.4	27.7	168.6	18.9	119.2	16.2	38.5	23.2	6.1	1.5	5.6	4.7	2.2	1.8	4.5
2	BHVO-2G	117394.1	3.6	2.3	408.1	30.9	176.2	19.7	130.0	17.6	41.5	28.9	6.1	1.7	6.0	5.0	2.9	2.3	4.8
Average			3.9	2.7	412.5	29.3	174.7	19.3	129.1	16.4	40.7	26.6	6.2	1.6	6.0	5.6	2.4	2.2	4.5
stdev			0.2	0.5	26.4	3.2	8.3	1.0	7.5	2.0	4.3	3.2	0.8	0.2	0.7	0.8	0.3	0.3	0.5
RSD			5.3	18.5	6.4	11.0	4.7	5.2	5.8	12.2	10.5	12.0	12.4	11.5	12.4	14.4	10.6	14.4	10.9
Accepted			4.4		389.0	26.0	172.0	19.2	129.0	15.3	37.9	24.4	6.0	2.0	6.2	5.3	2.5	2.0	4.1
Correction Factor			1.1		0.9	0.9	1.0	1.0	1.0	0.9	0.9	0.9	1.0	1.2	1.0	1.0	1.0	0.9	0.9

3	BHVO-2G	81669.5	16953.9	403.5	26.3	171.2	18.3	135.3	15.7	39.7	25.7	5.9	2.3	10.7	7.2	3.1	2.6	4.8
3	BHVO-2G	81669.5	16953.9	403.5	26.3	171.2	18.3	135.3	15.7	39.7	25.7	5.9	1.7	5.5	5.1	2.5	2.0	4.1
3	BHVO-2G	81916.0	17347.1	407.0	26.2	183.6	18.6	150.5	18.3	44.8	24.9	6.9	2.4	12.3	9.3	3.7	2.4	4.6
3	BHVO-2G	81916.0	17347.1	407.0	26.2	183.6	18.6	150.5	18.3	44.8	24.9	6.9	1.7	6.9	7.3	3.1	1.6	3.7
3	BHVO-2G	79784.8	17589.7	422.7	26.2	179.2	20.2	146.4	16.5	42.1	27.1	5.8	2.1	11.2	7.6	3.6	2.4	5.8
3	BHVO-2G	79784.8	17589.7	422.7	26.2	179.2	20.2	146.4	16.5	42.1	27.1	5.8	1.4	5.7	5.4	2.9	1.7	5.1
3	BHVO-2G	80168.3	16581.0	385.2	25.6	164.3	16.8	126.5	15.5	37.7	25.0	5.8	2.5	10.0	6.8	2.6	2.7	4.6
3	BHVO-2G	80168.3	16581.0	385.2	25.6	164.3	16.8	126.5	15.5	37.7	25.0	5.8	1.9	5.1	4.8	2.0	2.1	4.0
3	BHVO-2G	81221.6	16847.6	397.3	26.2	168.1	17.8	129.5	15.5	39.3	25.9	6.0	2.4	10.7	7.7	3.1	2.9	5.0
3	BHVO-2G	81221.6	16847.6	397.3	26.2	168.1	17.8	129.5	15.5	39.3	25.9	6.0	1.7	5.6	5.6	2.5	2.3	4.3
3	BHVO-2G	81322.7	17037.1	399.2	26.0	169.8	18.1	134.0	15.4	39.5	26.4	6.3	2.5	10.8	6.8	3.1	2.7	5.1
3	BHVO-2G	81322.7	17037.1	399.2	26.0	169.8	18.1	134.0	15.4	39.5	26.4	6.3	1.8	5.6	4.7	2.4	2.1	4.5
3	BHVO-2G	80928.4	16976.2	394.6	26.5	168.1	16.9	132.9	15.7	38.1	25.7	6.0	2.5	10.6	7.5	2.5	2.8	4.5
3	BHVO-2G	80928.4	16976.2	394.6	26.5	168.1	16.9	132.9	15.7	38.1	25.7	6.0	1.8	5.6	5.4	1.9	2.1	3.8
3	BHVO-2G	80692.8	16960.4	394.4	26.2	168.9	17.6	131.5	15.5	39.1	25.1	5.8	2.6	10.3	7.3	3.2	2.8	4.5
3	BHVO-2G	80692.8	16960.4	394.4	26.2	168.9	17.6	131.5	15.5	39.1	25.1	5.8	2.0	5.2	5.2	2.6	2.2	3.9
3	BHVO-2G	80228.5	16773.5	387.7	25.3	167.0	17.5	127.7	15.5	39.1	24.9	6.3	2.3	10.5	7.4	3.0	2.7	4.8
3	BHVO-2G	80228.5	16773.5	387.7	25.3	167.0	17.5	127.7	15.5	39.1	24.9	6.3	1.7	5.5	5.4	2.4	2.0	4.2
3	BHVO-2G	81136.4	17414.1	405.5	26.2	176.7	20.1	139.1	16.0	40.6	26.6	6.4	2.5	10.8	7.0	3.3	3.0	4.9
3	BHVO-2G	81136.4	17414.1	405.5	26.2	176.7	20.1	139.1	16.0	40.6	26.6	6.4	1.8	5.5	4.9	2.6	2.4	4.3

3	BHVO-2G	81105.3	17230.3	398.9	26.4	173.5	18.4	133.1	15.6	39.7	26.0	6.0	2.4	10.9	7.5	3.0	2.6	5.5
3	BHVO-2G	81105.3	17230.3	398.9	26.4	173.5	18.4	133.1	15.6	39.7	26.0	6.0	1.7	5.8	5.5	2.4	1.9	4.8
3	BHVO-2G	81323.0	16936.6	392.8	25.9	169.2	17.0	128.9	15.8	39.0	25.8	6.0	2.6	10.3	7.3	2.8	2.5	4.8
3	BHVO-2G	81323.0	16936.6	392.8	25.9	169.2	17.0	128.9	15.8	39.0	25.8	6.0	2.0	5.2	5.3	2.2	1.9	4.1
3	BHVO-2G	81137.3	17200.4	400.6	25.7	170.7	18.6	136.5	15.7	39.0	26.5	6.1	2.5	10.9	7.1	3.1	2.7	5.1
3	BHVO-2G	81137.3	17200.4	400.6	25.7	170.7	18.6	136.5	15.7	39.0	26.5	6.1	1.8	5.7	5.0	2.5	2.0	4.5
Average		80971.9	17065.2	399.2	26.0	171.6	18.2	134.8	15.9	39.8	25.8	6.1	2.1	8.2	6.4	2.8	2.3	4.6
stdev		596.4	273.8	9.3	0.3	5.3	1.1	7.0	0.8	1.8	0.7	0.3	0.4	2.7	1.2	0.5	0.4	0.5
RSD		0.7	1.6	2.3	1.3	3.1	5.9	5.2	4.8	4.5	2.7	4.9	17.1	32.7	19.1	16.4	16.5	11.1
Accepted		114000.0		389.0	26.0	172.0	19.2	129.0	15.3	37.9	24.4	6.0	2.0	6.2	5.3	2.5	2.0	4.1
Correction Factor		1.4		1.0	1.0	1.0	1.1	1.0	1.0	1.0	0.9	1.0	1.0	0.8	0.8	0.9	0.8	0.9

Table 2.6: Corrected Trace element compositions from this study and Lassiter et al., 2002 from RVV310

Sample	Study	Ba	Nb	La	Ce	Sr	Nd	Zr	Hf	Sm	Eu	Gd	Dy	Y	Er	Yb
RVV310-25	This Study	266	56	35	75	650	36	207	5	9	2	6	6	32	3	2
RVV310-37	This Study	138	29	22	47	677	23	128	3	5	1	4	2	17	2	1
RVV310-42	This Study	187	46	34	71	680	39	215	4	9	2	7	6	34	3	2
RVV310	Lassiter	111	18	15	33	1335	20	107	3	5	1	4	4	17	2	2
RVV310	Lassiter	109	26	21	45	478	26	146	4	7	2	7	5	23	2	2
RVV310	Lassiter	119	30	23	51	468	29	158	5	7	2	6	5	23	2	2
RVV310	Lassiter	95	33	25	54	434	28	162	5	7	2	3	5	24	2	2
RVV310	Lassiter	51	18	21	53	482	30	160	5	7	2	6	5	23	2	2
RVV310	Lassiter	84	24	20	45	382	26	145	4	7	2	6	5	23	2	2
RVV310	Lassiter	131	45	32	65	424	35	203	6	9	2	7	6	29	3	2
RVV310	Lassiter	107	30	23	45	397	25	139	4	7	2	5	5	23	2	2

Table 2.7A: Uncorrected Melt Inclusions Major Element Compositions

Sample	Host	SiO <sub>2</sub>	Al <sub>2</sub> O <sub>3</sub>	P <sub>2</sub> O <sub>5</sub>	S	Cl	K <sub>2</sub> O	CaO	MnO	Cr <sub>2</sub> O <sub>3</sub>	FeO*	NiO	Na <sub>2</sub> O	MgO	TiO <sub>2</sub>	Total
RVV302-1	Olivine	47.94	16.10	0.35	0.09	0.05	0.83	10.72	0.14	0.10	9.49	0.00	3.75	9.19	2.01	100.76
RVV302-2	Olivine	47.51	16.23	0.59	0.10	0.03	0.76	11.16	0.16	0.02	9.81	0.02	3.74	8.06	2.34	100.52
RVV302-3	Olivine	46.68	15.02	0.54	0.10	0.03	0.93	12.28	0.14	0.26	11.39	0.01	4.20	7.63	1.37	100.60
RVV302-4	Olivine	48.65	16.99	0.38	0.11	0.03	0.82	11.19	0.13	0.00	8.87	0.02	3.46	8.00	2.08	100.74
RVV302-5	Olivine	48.77	17.15	0.42	0.12	0.03	0.92	10.74	0.10	0.04	8.58	0.02	3.66	8.00	2.10	100.66
RVV302-6	Olivine	48.45	16.31	0.34	0.08	0.03	0.80	11.05	0.14	0.01	10.29	0.02	3.25	7.74	2.06	100.57
RVV302-7	Olivine	48.80	16.57	0.34	0.08	0.03	0.84	10.79	0.16	0.01	10.15	0.06	3.30	7.21	1.99	100.32
RVV302-8	Olivine	49.16	16.65	0.37	0.09	0.03	0.80	10.76	0.16	0.00	10.42	0.02	3.35	6.60	1.99	100.39
RVV302-9	Olivine	48.69	16.44	0.36	0.08	0.03	0.76	10.86	0.18	0.02	11.25	0.03	3.34	6.59	2.01	100.63
RVV302-10	Olivine	48.96	16.24	0.29	0.11	0.02	0.50	11.01	0.18	0.01	9.60	0.03	3.93	8.72	2.47	102.06
RVV302-11	Olivine	47.24	13.68	0.45	0.09	0.04	0.89	9.75	0.16	0.00	11.86	0.00	3.64	9.12	3.16	100.08
RVV302-12	Olivine	48.17	15.71	0.53	0.07	0.04	0.97	10.33	0.16	0.04	10.36	0.01	3.36	8.15	2.42	100.33
RVV302-13	Olivine	42.40	14.97	0.72	0.13	0.09	1.28	11.62	0.17	1.34	12.91	0.03	4.46	7.04	1.58	98.73
<i>RVV302 Average</i>		<i>47.80</i>	<i>16.00</i>	<i>0.44</i>	<i>0.10</i>	<i>0.04</i>	<i>0.85</i>	<i>10.94</i>	<i>0.15</i>	<i>0.14</i>	<i>10.38</i>	<i>0.02</i>	<i>3.65</i>	<i>7.85</i>	<i>2.12</i>	<i>100.49</i>
<i>RVV302 Stdev</i>		<i>1.78</i>	<i>0.96</i>	<i>0.12</i>	<i>0.02</i>	<i>0.02</i>	<i>0.17</i>	<i>0.60</i>	<i>0.02</i>	<i>0.37</i>	<i>1.21</i>	<i>0.02</i>	<i>0.37</i>	<i>0.85</i>	<i>0.43</i>	<i>0.71</i>
RVV306a-1	Olivine	37.09	12.90	0.72	0.21	0.15	1.13	13.97	0.19	0.02	16.70	0.05	5.02	8.23	3.04	99.69
RVV306a-2	Olivine	39.40	14.44	0.88	0.15	0.16	1.30	10.18	0.20	0.03	12.86	0.06	5.66	12.23	2.52	100.27
RVV306a-3	Olivine	38.03	14.02	1.19	0.17	0.17	1.39	13.88	0.10	0.04	10.17	0.07	6.00	10.63	3.09	99.14
RVV306a-4	Olivine	37.17	14.41	1.10	0.21	0.21	1.42	14.64	0.11	0.01	12.37	0.06	5.33	8.70	3.08	98.82
RVV306a-5	Olivine	39.45	16.89	1.13	0.15	0.09	1.51	14.11	0.10	0.03	10.78	0.03	5.76	7.66	2.98	100.67
RVV306a-6	Olivine	40.99	13.63	0.72	0.13	0.12	1.01	16.65	0.16	0.10	11.25	0.00	4.50	7.71	2.27	99.24
RVV306a-7	Olivine	39.63	14.74	0.93	0.16	0.14	1.03	15.85	0.11	0.08	10.65	0.04	4.49	8.30	3.26	99.44
RVV306a-8	Olivine	38.68	16.17	1.23	0.18	0.18	1.41	15.50	0.11	0.00	9.36	0.02	5.15	7.18	3.82	99.01
RVV306a-9	Olivine	39.51	14.84	1.02	0.08	0.11	1.08	16.59	0.09	0.09	11.06	0.04	4.72	8.02	3.43	100.68
RVV306a-10	Olivine	36.07	16.00	1.26	0.21	0.23	1.93	12.66	0.10	0.02	11.96	0.05	5.23	8.71	3.80	98.50
RVV306a-11	Olivine	39.64	14.90	1.36	0.16	0.06	0.54	13.22	0.15	0.00	11.15	0.05	1.54	13.19	2.99	99.14
RVV306a-12	Olivine	42.54	14.20	0.56	0.10	0.10	0.95	17.42	0.11	0.08	7.89	0.02	3.31	8.54	2.80	98.73
RVV306a-13	Olivine	39.76	15.59	1.21	0.16	0.23	1.88	12.95	0.09	0.01	10.39	0.04	5.77	7.44	3.59	99.28
RVV306a-14	Olivine	36.74	12.43	1.13	0.28	0.17	1.30	15.79	0.14	0.00	14.82	0.03	4.31	7.37	3.54	98.43
RVV306a-15	Olivine	32.24	22.30	0.63	0.16	0.12	1.06	11.99	0.13	0.32	15.07	0.13	3.77	9.67	3.18	100.99
RVV306a-16	Olivine	39.90	11.10	0.63	0.26	0.11	0.82	11.86	0.33	0.02	19.90	0.02	3.32	9.40	2.65	100.68
RVV306a-17	Olivine	39.69	10.73	0.58	0.26	0.11	0.79	11.21	0.34	0.02	21.55	0.00	3.33	9.18	2.67	100.84
RVV306a-18	Olivine	39.77	14.29	0.86	0.22	0.15	1.17	15.80	0.12	0.01	11.89	0.03	3.92	7.82	3.11	99.47
RVV306a-19	Olivine	41.02	14.29	0.79	0.19	0.12	1.25	15.14	0.12	0.01	10.50	0.04	5.36	7.78	2.83	99.70



RVV306a-20	Olivine	40.38	14.96	0.91	0.19	0.15	1.21	16.54	0.11	0.01	8.67	0.03	4.18	7.94	3.16	98.65
RVV306a-21	Olivine	41.33	14.87	0.78	0.16	0.13	1.18	16.43	0.13	0.03	8.55	0.02	4.32	8.02	2.98	99.14
<i>RVV306a Average</i>		39.00	14.65	0.93	0.18	0.14	1.21	14.40	0.14	0.04	12.26	0.04	4.52	8.75	3.08	99.55
<i>RVV306a Stdev</i>		2.23	2.31	0.25	0.05	0.04	0.33	2.03	0.07	0.07	3.56	0.03	1.08	1.57	0.40	0.82
RVV312-1	Plagioclase	47.83	19.12	0.39	0.14	0.03	0.73	8.46	0.16	0.01	10.82	0.00	2.86	3.76	2.75	97.04
RVV312-2	Plagioclase	48.63	19.81	0.34	0.13	0.03	0.68	8.34	0.14	0.01	11.25	0.00	3.07	4.21	2.60	99.26
RVV312-3	Plagioclase	48.95	19.67	0.36	0.13	0.03	0.71	8.64	0.16	0.00	10.18	0.01	2.76	3.56	2.64	97.80
RVV312-4	Plagioclase	49.67	18.85	0.46	0.14	0.03	0.54	6.85	0.18	0.00	11.89	0.01	2.69	4.04	3.17	98.52
RVV312-5	Plagioclase	48.38	17.47	0.39	0.14	0.04	1.05	8.18	0.20	0.00	11.70	0.00	3.07	4.46	2.75	98.03
RVV312-6	Plagioclase	47.36	17.74	0.54	0.16	0.05	0.87	9.70	0.22	0.00	11.53	0.00	3.45	4.21	3.21	99.28
RVV312-7	Plagioclase	49.20	18.33	0.44	0.14	0.02	0.56	6.14	0.18	0.02	12.40	0.01	3.33	5.68	3.17	99.82
RVV312-8	Plagioclase	48.56	18.80	0.37	0.12	0.03	0.82	9.17	0.19	0.02	11.67	0.00	3.64	4.17	1.71	99.45
RVV312-9	Plagioclase	49.14	18.70	0.36	0.12	0.03	0.85	9.24	0.22	0.00	11.61	0.00	3.71	4.02	2.06	100.24
RVV312-10	Plagioclase	49.78	17.93	0.66	0.17	0.05	1.07	9.03	0.21	0.00	11.70	0.00	2.87	3.27	2.91	99.89
<i>RVV312 Average</i>		48.75	18.64	0.43	0.14	0.03	0.79	8.38	0.19	0.01	11.47	0.00	3.15	4.14	2.70	98.93
<i>RVV312 Stdev</i>		0.76	0.78	0.10	0.02	0.01	0.18	1.11	0.03	0.01	0.61	0.01	0.37	0.65	0.49	1.04
RVV316-6	Olivine	47.75	16.61	0.40	0.09	0.03	0.91	11.97	0.09	0.03	6.76	0.00	4.39	8.55	2.55	100.25
RVV316-7	Olivine	47.67	16.55	0.36	0.09	0.03	0.91	11.88	0.11	0.04	6.80	0.01	4.37	8.59	2.64	100.18
RVV316-8	Olivine	47.91	14.35	0.47	0.12	0.03	0.95	10.87	0.15	0.03	9.38	0.00	4.52	8.22	3.10	100.26
RVV316-9	Olivine	48.12	14.45	0.49	0.12	0.04	0.97	10.94	0.14	0.02	9.33	0.01	4.64	8.57	3.16	101.16
RVV316-11	Olivine	41.70	15.24	1.32	0.11	0.20	1.78	11.95	0.12	0.02	7.33	0.07	7.48	11.16	2.70	101.27
RVV316-11a	Olivine	41.53	15.13	1.26	0.11	0.20	1.79	11.87	0.11	0.02	7.29	0.07	7.40	11.07	2.67	100.61
RVV316-12	Olivine	40.98	12.92	0.90	0.17	0.15	1.21	13.57	0.21	0.14	16.09	0.01	5.39	8.21	2.28	102.47
RVV316-13	Olivine	35.36	12.73	1.04	0.23	0.19	1.76	13.05	0.11	0.00	15.78	0.03	6.47	8.80	3.70	99.55
RVV316-14	Olivine	37.04	13.53	1.31	0.25	0.22	1.53	14.51	0.10	0.00	11.93	0.03	6.01	9.18	2.93	98.89
RVV316-15	Olivine	38.90	13.93	0.96	0.18	0.18	1.30	14.15	0.13	0.02	11.56	0.05	4.39	10.35	2.98	99.31
RVV316-16	Olivine	39.65	13.58	0.93	0.18	0.16	1.19	13.66	0.19	0.03	12.84	0.04	4.60	10.26	2.61	100.14
RVV316-17	Olivine	37.73	13.92	1.14	0.26	0.21	1.69	12.62	0.12	0.01	14.42	0.05	5.58	10.18	3.67	101.92
RVV316-18	Olivine	36.58	11.38	0.99	0.10	0.02	1.41	12.61	0.15	0.03	17.89	0.06	4.58	10.15	2.91	99.00
RVV316-19	Olivine	35.81	12.98	1.32	0.23	0.10	1.26	15.49	0.14	0.02	14.29	0.05	4.58	8.55	3.09	98.24
RVV316-20	Olivine	40.71	13.71	1.05	0.04	0.09	3.83	12.80	0.10	0.05	7.51	0.03	2.75	12.89	2.77	98.35
RVV316-21	Olivine	39.64	14.36	0.98	0.16	0.18	1.32	14.73	0.11	0.04	10.50	0.04	4.79	10.06	3.00	100.10
RVV316-22	Olivine	37.95	11.51	0.43	0.38	0.10	0.97	12.62	0.25	0.02	19.39	0.03	3.65	9.73	3.24	100.80
RVV316-23	Olivine	38.45	12.76	0.90	0.20	0.16	1.18	14.00	0.15	0.04	14.66	0.03	3.99	10.43	2.73	99.93
RVV316-24	Olivine	39.25	16.20	0.37	0.22	0.09	1.05	11.69	0.19	0.01	15.13	0.00	4.27	7.34	3.99	100.11
RVV316-25	Olivine	40.49	15.36	0.48	0.22	0.10	1.19	11.48	0.18	0.02	13.94	0.01	3.88	10.09	2.82	100.57

RVV316-26	Olivine	40.41	15.19	0.47	0.22	0.10	1.22	11.32	0.16	0.00	14.41	0.05	3.94	9.91	2.74	100.45
<i>RVV316 Average</i>		40.65	14.11	0.84	0.17	0.12	1.40	12.75	0.14	0.03	12.25	0.03	4.84	9.63	2.97	100.17
<i>RVV316 Stdev</i>		3.99	1.47	0.35	0.08	0.07	0.63	1.31	0.04	0.03	3.82	0.02	1.18	1.27	0.41	1.06
RVV321-1	Olivine	40.74	14.19	0.68	0.24	0.13	1.63	8.64	0.22	0.01	17.33	0.03	5.11	9.63	2.86	101.75
RVV321-2	Olivine	39.65	16.03	0.47	0.23	0.10	1.28	9.85	0.24	0.00	17.56	0.04	5.17	7.93	3.26	102.14
RVV321-3	Olivine	39.72	15.31	0.68	0.22	0.11	1.29	9.68	0.25	0.01	16.84	0.01	5.52	8.52	2.81	101.28
RVV321-4	Olivine	37.54	14.70	0.79	0.25	0.13	1.62	10.05	0.20	0.04	15.33	0.06	4.84	9.58	2.76	98.23
RVV321-5	Olivine	39.35	15.24	0.68	0.27	0.11	1.39	8.85	0.26	0.00	17.66	0.04	5.62	8.74	2.40	100.98
RVV321-6	Olivine	44.08	15.04	0.33	0.16	0.07	0.76	11.25	0.18	0.02	12.83	0.05	4.23	10.64	1.88	101.74
RVV321-7	Olivine	41.59	13.38	0.40	0.17	0.06	0.95	13.14	0.18	0.02	11.64	0.02	3.45	10.01	1.94	97.18
RVV321-8	Olivine	40.51	14.49	0.54	0.19	0.09	1.23	9.92	0.26	0.01	16.55	0.02	4.99	9.84	2.74	101.66
RVV321-9	Olivine	42.23	9.50	0.19	0.06	0.03	0.38	16.28	0.27	0.04	18.06	0.01	2.24	8.85	2.25	100.46
RVV321-10	Olivine	39.54	14.80	0.51	0.23	0.11	1.28	9.40	0.26	0.03	19.16	0.03	4.70	6.94	2.34	99.33
RVV321-11	Olivine	39.62	15.50	0.55	0.26	0.10	1.32	9.19	0.21	0.01	18.47	0.00	4.37	6.69	3.03	99.31
RVV321-12	Olivine	40.09	15.05	0.50	0.24	0.09	1.10	10.28	0.22	0.00	16.64	0.04	4.05	7.15	3.14	98.59
RVV321-13	Olivine	41.66	15.31	0.51	0.23	0.11	1.32	9.90	0.19	0.00	14.14	0.04	4.07	7.51	3.28	98.26
RVV321-14	Olivine	41.66	15.25	0.48	0.24	0.11	1.32	10.51	0.17	0.00	14.53	0.05	4.06	7.23	3.14	98.77
RVV321-15	Olivine	42.16	15.94	0.24	0.22	0.06	2.02	8.46	0.19	0.00	16.64	0.03	3.84	6.18	2.52	98.49
RVV321-16	Olivine	44.75	14.83	0.44	0.20	0.07	0.95	14.45	0.18	0.04	11.07	0.02	3.34	8.31	1.69	100.33
RVV321-17	Olivine	37.15	13.87	0.43	0.31	0.08	1.19	9.26	0.22	0.02	17.55	0.03	4.92	9.31	3.33	98.10
RVV321-18	Olivine	38.29	13.21	0.46	0.22	0.12	1.60	7.83	0.37	0.02	24.98	0.02	5.81	5.85	2.06	101.15
RVV321-19	Olivine	40.01	15.33	0.61	0.24	0.09	1.19	11.73	0.20	0.02	14.51	0.02	3.85	9.23	2.96	100.33
RVV321-20	Olivine	38.77	14.39	0.46	0.20	0.10	1.16	9.26	0.24	0.01	18.50	0.02	4.15	9.67	3.08	100.27
RVV321-21	Olivine	41.14	11.40	0.21	0.12	0.09	0.58	13.85	0.22	0.09	15.97	0.03	2.41	9.31	1.97	97.54
RVV321-22	Olivine	44.15	14.89	0.28	0.14	0.05	0.61	12.30	0.19	0.05	13.61	0.01	3.12	9.19	2.03	100.81
RVV321-23	Olivine	38.91	14.66	0.59	0.27	0.07	1.55	9.06	0.22	0.01	17.90	0.00	4.07	9.76	3.61	101.06
RVV321-24	Olivine	39.12	15.15	0.45	0.23	0.08	1.28	10.07	0.24	0.00	17.28	0.02	4.05	8.44	3.38	100.11
RVV321-25	Olivine	38.97	15.00	0.44	0.23	0.08	1.30	9.71	0.25	0.00	17.58	0.00	3.93	8.90	3.25	99.97
RVV321-26	Olivine	40.41	14.80	0.55	0.25	0.11	1.44	9.98	0.20	0.03	16.01	0.05	4.01	10.00	3.17	101.34
RVV321-27	Olivine	43.29	15.11	0.36	0.18	0.06	0.78	11.64	0.21	0.01	13.26	0.05	3.09	10.55	2.26	101.09
RVV321-28	Olivine	39.30	15.11	0.59	0.22	0.10	1.24	9.70	0.28	0.00	19.36	0.00	4.15	7.87	2.90	101.13
RVV321-29	Olivine	40.00	15.40	0.23	0.21	0.08	1.39	10.71	0.18	0.01	14.77	0.03	3.84	9.69	3.27	100.10
RVV321-30	Olivine	39.77	15.11	0.43	0.24	0.08	1.10	9.71	0.24	0.01	17.66	0.02	4.08	9.80	3.19	101.78
RVV321-31	Olivine	39.32	14.75	0.32	0.21	0.08	1.13	9.49	0.23	0.02	18.26	0.02	3.88	9.78	3.36	101.13
RVV321-32	Olivine	39.91	15.70	0.52	0.23	0.10	1.37	10.39	0.21	0.03	16.08	0.02	3.89	8.80	3.39	100.96
RVV321-33	Olivine	40.18	16.14	0.48	0.29	0.10	1.31	10.82	0.19	0.01	16.24	0.03	3.99	7.69	3.56	101.43

RVV321-34	Olivine	42.47	17.78	1.24	0.12	0.03	1.64	10.16	0.24	0.01	10.89	0.03	5.68	9.61	1.07	101.14
RVV321-35	Olivine	39.21	13.42	0.85	0.09	0.17	1.36	12.32	0.13	0.01	14.17	0.02	4.63	10.48	2.86	99.80
<i>RVV321 Average</i>		<i>40.44</i>	<i>14.74</i>	<i>0.50</i>	<i>0.21</i>	<i>0.09</i>	<i>1.23</i>	<i>10.51</i>	<i>0.22</i>	<i>0.02</i>	<i>16.26</i>	<i>0.03</i>	<i>4.20</i>	<i>8.79</i>	<i>2.76</i>	<i>100.22</i>
<i>RVV321 Stdev</i>		<i>1.81</i>	<i>1.38</i>	<i>0.20</i>	<i>0.05</i>	<i>0.03</i>	<i>0.33</i>	<i>1.79</i>	<i>0.04</i>	<i>0.02</i>	<i>2.71</i>	<i>0.01</i>	<i>0.84</i>	<i>1.26</i>	<i>0.61</i>	<i>1.34</i>
RVV340-1	Olivine	44.49	10.63	0.31	0.10	0.02	0.56	7.76	0.24	0.01	18.15	0.03	2.92	14.05	1.72	101.14
RVV340-2	Olivine	41.81	9.66	0.84	0.06	0.01	0.27	9.53	0.34	0.04	25.06	0.01	2.39	7.93	2.68	100.71
RVV340-3	Olivine	44.19	11.18	0.33	0.05	0.02	0.60	7.63	0.25	0.22	18.86	0.02	3.17	13.20	1.33	101.11
RVV340-4	Olivine	42.69	10.67	0.51	0.13	0.02	0.38	8.11	0.30	0.01	23.42	0.00	2.75	9.72	1.97	100.86
RVV340-5	Olivine	40.79	10.46	0.30	0.14	0.02	0.41	7.32	0.26	0.28	21.01	0.05	2.78	14.14	1.60	99.76
RVV340-6	Olivine	40.59	12.14	0.35	0.16	0.03	0.60	6.96	0.26	0.30	21.94	0.04	3.28	12.72	1.57	101.17
RVV340-7	Olivine	41.01	10.76	0.24	0.13	0.02	0.45	7.26	0.26	0.31	21.30	0.05	2.82	13.74	1.68	100.22
RVV340-8	Olivine	44.36	10.46	0.33	0.05	0.02	0.64	6.97	0.25	0.02	17.92	0.03	2.98	15.15	1.14	100.40
RVV340-8a	Olivine	44.54	11.25	0.35	0.06	0.02	0.72	7.13	0.25	0.01	17.32	0.04	3.35	13.50	1.20	99.82
RVV340-9	Olivine	43.40	11.00	0.37	0.21	0.03	0.70	7.89	0.22	0.22	17.29	0.07	2.79	14.64	1.69	100.80
RVV340-10	Olivine	44.40	11.43	0.26	0.12	0.03	0.45	7.56	0.20	0.02	15.41	0.07	2.68	16.36	1.71	100.84
RVV340-10a	Olivine	44.23	11.51	0.28	0.12	0.03	0.45	7.69	0.19	0.00	15.42	0.06	2.70	16.44	1.68	100.97
RVV340-10b	Olivine	44.02	11.43	0.29	0.12	0.02	0.44	7.72	0.20	0.02	15.56	0.07	2.72	16.18	1.67	100.61
RVV340-11	Olivine	45.98	14.74	0.32	0.12	0.04	0.59	10.35	0.14	0.02	11.65	0.03	2.76	11.24	2.45	100.41
RVV340-12	Olivine	46.85	14.33	0.59	0.11	0.05	0.73	12.57	0.13	0.17	9.02	0.01	2.67	11.00	2.47	100.70
RVV340-13	Olivine	46.25	14.67	0.35	0.14	0.02	0.61	9.01	0.16	0.01	12.48	0.01	2.57	10.45	2.68	99.40
RVV340-14	Olivine	45.81	16.25	0.47	0.10	0.04	0.70	11.29	0.16	0.03	12.38	0.00	3.04	7.23	2.78	100.29
RVV340-15	Olivine	45.16	14.23	0.49	0.16	0.04	0.86	10.45	0.12	0.27	13.35	0.03	3.20	8.88	1.74	98.99
RVV340-16	Olivine	48.42	15.06	0.27	0.11	0.04	0.66	10.01	0.18	0.02	12.02	0.02	3.49	8.20	1.90	100.40
RVV340-17	Olivine	40.29	10.66	0.25	0.12	0.03	0.43	7.47	0.28	0.20	22.78	0.05	2.99	12.86	1.69	100.29
RVV340-18	Olivine	45.25	13.92	1.30	0.14	0.07	0.78	11.24	0.17	0.10	11.74	0.01	2.72	10.89	2.45	100.99
RVV340-19	Olivine	41.92	13.52	0.39	0.13	0.05	0.71	11.58	0.16	0.18	13.98	0.04	3.02	10.28	1.80	97.95
RVV340-20	Olivine	44.54	13.86	0.40	0.21	0.04	0.65	11.90	0.18	0.09	14.70	0.03	3.05	9.28	2.00	101.26
RVV340-21	Olivine	44.25	12.76	0.48	0.11	0.05	1.09	9.83	0.22	0.10	16.35	0.03	3.51	9.74	1.52	100.20
RVV340-22	Olivine	47.93	14.41	0.42	0.14	0.04	0.83	9.96	0.15	0.00	12.39	0.04	3.27	9.79	2.24	101.82
RVV340-23	Olivine	43.07	16.89	0.14	0.09	0.00	0.28	9.24	0.30	0.01	16.69	0.04	1.22	11.45	2.63	102.17
RVV340-24	Olivine	47.53	15.34	0.28	0.10	0.05	0.60	11.23	0.14	0.08	10.08	0.03	3.00	10.63	1.79	101.02
RVV340-25	Olivine	45.91	15.02	0.32	0.13	0.05	0.78	10.33	0.18	0.10	11.93	0.03	3.07	10.79	2.42	101.25
RVV340-26	Olivine	44.39	12.99	0.36	0.17	0.09	1.19	11.45	0.17	0.11	13.82	0.03	4.64	9.91	2.13	102.29
RVV340-27	Olivine	49.67	13.94	0.32	0.12	0.17	0.81	9.68	0.19	0.00	11.26	0.02	3.48	10.62	1.87	102.34
RVV340-28	Olivine	47.39	15.18	0.35	0.12	0.04	0.87	9.86	0.15	0.02	11.17	0.01	3.18	10.63	2.46	101.61
<i>RVV340 Average</i>		<i>44.55</i>	<i>12.91</i>	<i>0.40</i>	<i>0.12</i>	<i>0.06</i>	<i>0.64</i>	<i>9.26</i>	<i>0.21</i>	<i>0.10</i>	<i>15.69</i>	<i>0.03</i>	<i>2.97</i>	<i>11.67</i>	<i>1.96</i>	<i>100.70</i>



RVV344-23	Olivine	48.50	15.05	0.34	0.06	0.03	0.60	13.81	0.10	0.12	5.79	0.04	3.16	10.12	2.28	100.09
RVV344-24	Olivine	47.63	14.75	0.36	0.07	0.03	0.54	14.59	0.08	0.12	5.57	0.02	2.71	9.03	2.26	97.83
RVV344-25	Olivine	45.84	15.45	0.49	0.08	0.08	0.90	14.35	0.13	0.09	6.96	0.02	2.90	9.93	2.63	99.96
RVV344-26	Olivine	47.87	14.86	0.41	0.07	0.06	0.85	13.14	0.11	0.12	6.74	0.03	3.32	10.04	2.43	100.13
RVV344-27	Olivine	45.68	15.44	0.43	0.09	0.08	0.90	14.17	0.12	0.12	7.12	0.04	3.13	10.07	2.64	100.14
<i>RVV344 Average</i>		<i>45.39</i>	<i>14.47</i>	<i>0.38</i>	<i>0.09</i>	<i>0.07</i>	<i>0.83</i>	<i>13.16</i>	<i>0.15</i>	<i>0.10</i>	<i>8.92</i>	<i>0.03</i>	<i>3.38</i>	<i>10.65</i>	<i>2.33</i>	<i>100.06</i>
<i>RVV344 Stdev</i>		<i>2.48</i>	<i>1.84</i>	<i>0.08</i>	<i>0.03</i>	<i>0.02</i>	<i>0.25</i>	<i>1.83</i>	<i>0.04</i>	<i>0.05</i>	<i>2.47</i>	<i>0.02</i>	<i>0.62</i>	<i>2.03</i>	<i>0.31</i>	<i>1.70</i>
RVV345-1	Olivine	44.80	15.52	0.35	0.12	0.03	0.54	12.60	0.16	0.01	10.34	0.01	4.13	8.81	2.17	99.75
RVV345-2	Olivine	48.74	14.85	0.18	0.08	0.02	0.37	11.70	0.15	0.04	9.40	0.00	4.31	9.72	1.67	101.33
RVV345-2a	Olivine	48.69	14.85	0.20	0.08	0.02	0.36	11.71	0.15	0.03	9.35	0.01	4.36	9.67	1.68	101.25
RVV345-3	Olivine	49.51	15.68	0.22	0.09	0.02	0.44	10.86	0.16	0.31	9.98	0.00	5.61	8.15	0.85	102.01
RVV345-4	Olivine	48.43	15.72	0.36	0.10	0.05	0.72	11.41	0.15	0.08	9.37	0.01	4.80	8.81	1.38	101.51
RVV345-5	Olivine	42.87	17.07	0.49	0.08	0.10	1.08	11.94	0.21	0.01	11.21	0.02	4.69	8.19	3.00	101.07
RVV345-6	Olivine	42.90	15.95	0.49	0.17	0.10	1.16	11.19	0.19	0.00	12.05	0.02	4.34	8.70	2.60	100.11
RVV345-7	Olivine	46.36	16.32	0.28	0.11	0.02	0.49	12.03	0.20	0.04	10.03	0.00	4.66	8.47	1.44	100.60
RVV345-8	Olivine	46.32	10.42	0.30	0.04	0.04	0.64	14.54	0.17	0.11	10.62	0.04	3.68	12.33	1.97	101.27
RVV345-9	Olivine	45.46	14.25	0.29	0.06	0.05	3.17	11.62	0.10	0.05	8.47	0.03	5.97	8.92	2.20	100.70
RVV345-10	Olivine	47.52	13.17	0.30	0.09	0.05	0.70	14.07	0.12	0.09	7.21	0.04	3.66	10.44	2.31	99.90
RVV345-11	Olivine	48.00	11.66	0.22	0.08	0.04	0.60	15.06	0.14	0.12	8.25	0.01	3.64	10.29	2.16	100.37
RVV345-12	Olivine	47.33	11.45	0.18	0.10	0.04	0.52	15.60	0.15	0.09	9.76	0.04	3.52	9.58	2.21	100.72
RVV345-13	Olivine	46.76	9.89	0.12	0.08	0.03	0.47	14.15	0.15	0.11	10.34	0.02	3.23	14.20	2.06	101.72
RVV345-14	Olivine	47.31	10.88	0.22	0.08	0.05	0.55	15.87	0.16	0.11	9.68	0.03	3.79	9.33	2.37	100.53
RVV345-15	Olivine	44.83	15.60	0.47	0.10	0.09	1.08	13.15	0.10	0.06	7.64	0.02	4.32	9.77	2.73	100.09
RVV345-15a	Olivine	44.87	15.73	0.46	0.11	0.09	1.05	13.27	0.12	0.06	7.53	0.02	4.33	9.76	2.75	100.28
RVV345-15b	Olivine	44.90	15.63	0.46	0.11	0.09	1.06	13.44	0.12	0.05	7.59	0.02	4.38	9.79	2.74	100.50
RVV345-16	Olivine	46.62	14.30	0.36	0.15	0.06	0.85	14.08	0.11	0.06	8.02	0.06	3.65	9.51	2.46	100.30
RVV345-16a	Olivine	45.82	14.54	0.38	0.15	0.07	0.84	14.00	0.12	0.04	7.88	0.05	3.15	9.86	2.58	99.48
RVV345-17	Olivine	44.07	15.93	0.40	0.15	0.09	1.01	13.72	0.11	0.05	9.14	0.04	4.22	8.97	2.75	100.63
RVV345-18	Olivine	47.42	17.76	0.22	0.02	0.48	3.13	10.64	0.08	0.03	6.96	0.04	4.41	8.04	1.55	100.77
RVV345-18a	Olivine	47.28	17.19	0.22	0.02	0.49	3.21	10.49	0.11	0.04	7.05	0.04	4.00	7.49	1.54	99.17
RVV345-18b	Olivine	47.39	17.37	0.21	0.02	0.50	3.22	10.46	0.09	0.05	7.06	0.05	3.99	7.43	1.50	99.33
RVV345-19	Olivine	47.48	14.99	0.32	0.03	0.27	2.68	11.09	0.12	0.05	8.84	0.01	4.26	8.23	1.78	100.15
RVV345-20	Olivine	47.74	14.62	0.33	0.12	0.06	0.76	14.61	0.11	0.06	6.64	0.05	3.38	9.01	2.40	99.89
RVV345-21	Olivine	48.90	12.48	0.27	0.09	0.03	0.43	15.51	0.14	0.10	7.67	0.03	2.94	10.05	2.18	100.82
RVV345-22	Olivine	48.96	12.99	0.30	0.11	0.04	0.69	13.20	0.10	0.21	7.23	0.06	3.92	9.26	2.33	99.39
RVV345-23	Olivine	49.32	13.65	0.31	0.13	0.03	0.58	14.02	0.11	0.10	6.69	0.07	3.38	9.55	2.19	100.13

RVV345-23a	Olivine	49.47	13.61	0.26	0.13	0.04	0.57	14.23	0.10	0.10	6.50	0.07	3.29	9.72	2.15	100.23
RVV345-24	Olivine	50.05	13.46	0.27	0.12	0.03	0.53	13.75	0.11	0.07	6.58	0.07	3.55	9.43	2.11	100.12
RVV345-25	Olivine	50.38	13.84	0.27	0.13	0.03	0.52	13.67	0.09	0.11	6.38	0.05	3.55	9.37	2.05	100.45
RVV345-25a	Olivine	49.45	14.06	0.27	0.12	0.04	0.52	13.58	0.12	0.12	6.46	0.07	3.14	9.93	2.21	100.08
<i>RVV345 Average</i>		<i>47.15</i>	<i>14.41</i>	<i>0.30</i>	<i>0.10</i>	<i>0.10</i>	<i>1.05</i>	<i>13.07</i>	<i>0.13</i>	<i>0.08</i>	<i>8.42</i>	<i>0.03</i>	<i>4.01</i>	<i>9.42</i>	<i>2.12</i>	<i>100.44</i>
<i>RVV345 Stdev</i>		<i>2.00</i>	<i>2.00</i>	<i>0.10</i>	<i>0.04</i>	<i>0.13</i>	<i>0.90</i>	<i>1.58</i>	<i>0.03</i>	<i>0.06</i>	<i>1.56</i>	<i>0.02</i>	<i>0.68</i>	<i>1.27</i>	<i>0.48</i>	<i>0.68</i>
RVV346-1	Olivine	47.14	13.40	0.28	0.08	0.05	0.70	15.04	0.12	0.10	7.55	0.04	3.48	10.06	2.18	100.32
RVV346-2	Olivine	44.96	14.29	0.34	0.07	0.08	0.96	15.85	0.13	0.09	8.61	0.03	3.40	9.09	2.66	100.64
RVV346-3	Olivine	44.36	15.24	0.51	0.10	0.11	1.40	13.88	0.10	0.07	8.36	0.03	4.00	9.51	2.83	100.62
RVV346-4	Olivine	50.22	12.14	0.40	0.07	0.05	0.75	12.66	0.12	0.12	7.68	0.02	4.00	9.87	2.36	100.56
RVV346-5	Olivine	46.78	13.77	0.33	0.06	0.05	0.80	13.80	0.11	0.40	8.25	0.02	3.70	9.66	2.28	100.08
RVV346-6	Olivine	43.20	14.82	0.37	0.08	0.10	1.11	14.44	0.15	0.10	10.19	0.03	3.57	9.62	2.35	100.24
RVV346-7	Olivine	48.11	13.40	0.24	0.11	0.04	0.60	14.96	0.11	0.09	7.18	0.05	2.99	10.47	2.22	100.72
RVV346-8	Olivine	44.50	6.01	0.20	0.06	0.03	0.41	6.15	0.15	0.10	10.37	0.17	1.78	31.80	0.84	102.64
RVV346-9	Olivine	46.73	13.54	0.36	0.10	0.07	0.91	14.59	0.10	0.07	7.91	0.03	3.63	10.34	2.55	101.05
RVV346-10	Olivine	46.78	13.55	0.40	0.10	0.07	0.87	14.49	0.13	0.09	7.93	0.02	3.66	10.22	2.57	101.03
RVV346-11	Olivine	47.17	14.14	0.30	0.09	0.05	0.75	14.50	0.10	0.09	7.03	0.03	3.30	9.98	2.38	100.02
RVV346-11a	Olivine	47.24	14.25	0.27	0.09	0.05	0.76	14.54	0.09	0.09	6.98	0.04	3.28	10.01	2.41	100.21
RVV346-12	Olivine	46.85	13.67	0.31	0.10	0.05	0.70	14.70	0.13	0.07	8.40	0.04	3.26	10.10	2.27	100.78
RVV346-13	Olivine	48.16	11.66	0.26	0.07	0.04	0.57	15.52	0.14	0.18	8.25	0.03	3.25	10.25	2.09	100.57
RVV346-14	Olivine	46.01	10.71	0.27	0.04	0.05	0.71	13.26	0.17	0.16	10.17	0.06	2.97	16.87	1.86	103.35
RVV346-15	Olivine	43.46	8.16	0.10	0.02	0.02	0.33	20.44	0.13	0.09	12.60	0.06	1.56	11.04	2.93	100.95
RVV346-16	Olivine	47.53	13.58	0.35	0.07	0.07	0.91	13.89	0.10	0.10	7.54	0.03	3.90	9.83	2.53	100.50
RVV346-17	Olivine	50.31	13.42	0.32	0.06	0.04	0.68	12.69	0.11	0.10	6.83	0.05	3.63	9.77	2.46	100.54
RVV346-18	Olivine	47.30	15.05	0.45	0.10	0.06	0.91	11.37	0.16	0.18	9.85	0.02	3.55	9.35	1.60	100.09
RVV346-19	Olivine	43.73	16.47	0.58	0.15	0.08	1.04	11.01	0.15	0.05	10.04	0.02	3.48	11.25	2.32	100.57
RVV346-20	Olivine	48.92	15.94	0.29	0.09	0.02	0.31	9.70	0.16	0.01	10.01	0.01	4.96	9.09	1.39	101.02
RVV346-21	Olivine	43.32	14.89	0.54	0.22	0.11	1.00	13.34	0.17	0.07	11.80	0.02	3.23	9.52	2.87	101.40
RVV346-22	Olivine	44.59	15.56	0.45	0.16	0.03	0.46	12.07	0.19	0.15	12.31	0.00	4.35	8.88	1.95	101.37
RVV346-23	Olivine	43.54	16.92	0.51	0.14	0.08	1.04	12.02	0.17	0.05	11.82	0.01	4.23	8.51	2.22	101.44
RVV346-24	Olivine	42.44	13.97	0.54	0.13	0.07	0.90	14.73	0.17	0.07	11.09	0.04	3.29	9.39	2.07	99.08
<i>RVV346 Average</i>		<i>46.13</i>	<i>13.54</i>	<i>0.36</i>	<i>0.09</i>	<i>0.06</i>	<i>0.78</i>	<i>13.58</i>	<i>0.13</i>	<i>0.11</i>	<i>9.15</i>	<i>0.04</i>	<i>3.46</i>	<i>10.98</i>	<i>2.25</i>	<i>100.79</i>
<i>RVV346 Stdev</i>		<i>2.22</i>	<i>2.41</i>	<i>0.12</i>	<i>0.04</i>	<i>0.02</i>	<i>0.25</i>	<i>2.55</i>	<i>0.03</i>	<i>0.07</i>	<i>1.79</i>	<i>0.03</i>	<i>0.70</i>	<i>4.60</i>	<i>0.46</i>	<i>0.84</i>
RVV360a-1	Olivine	43.65	16.68	0.49	0.12	0.07	0.92	11.76	0.14	0.07	10.51	0.05	5.22	7.46	2.04	99.20
RVV360a-2	Olivine	46.07	16.06	0.44	0.10	0.06	0.77	10.90	0.14	0.08	8.97	0.01	5.54	8.33	1.70	99.18
RVV360a-3	Olivine	46.66	15.08	0.43	0.13	0.08	0.92	11.35	0.14	0.12	9.61	0.01	5.13	8.26	1.70	99.62

RVV360a-4	Olivine	40.99	15.35	0.46	0.15	0.10	1.17	15.52	0.16	0.05	10.72	0.02	4.57	8.16	2.29	99.70
RVV360a-5	Olivine	41.32	17.62	0.64	0.18	0.12	1.41	12.28	0.10	0.00	10.98	0.02	5.45	7.23	2.97	100.34
RVV360a-6	Olivine	53.41	18.82	0.47	0.00	0.21	1.57	3.26	0.26	0.01	10.52	0.01	3.04	8.41	1.06	101.06
RVV360a-7	Olivine	48.21	22.04	1.04	0.04	0.13	4.19	3.01	0.18	0.00	8.95	-0.01	4.56	7.26	1.70	101.30
RVV360a-8	Olivine	49.35	19.40	0.39	0.06	0.10	1.90	4.72	0.31	0.03	12.61	-0.02	2.29	8.25	1.57	100.97
RVV360a-9	Olivine	41.43	16.78	0.50	0.15	0.10	1.21	11.88	0.15	0.03	10.47	0.03	5.22	8.30	3.33	99.57
<i>RVV360a Average</i>		<i>45.68</i>	<i>17.54</i>	<i>0.54</i>	<i>0.10</i>	<i>0.11</i>	<i>1.56</i>	<i>9.41</i>	<i>0.17</i>	<i>0.04</i>	<i>10.37</i>	<i>0.01</i>	<i>4.56</i>	<i>7.96</i>	<i>2.04</i>	<i>100.10</i>
<i>RVV360a Stdev</i>		<i>4.24</i>	<i>2.23</i>	<i>0.20</i>	<i>0.06</i>	<i>0.04</i>	<i>1.05</i>	<i>4.53</i>	<i>0.07</i>	<i>0.04</i>	<i>1.13</i>	<i>0.02</i>	<i>1.14</i>	<i>0.49</i>	<i>0.72</i>	<i>0.83</i>
RVV362-1	Plagioclase	48.55	15.49	0.31	0.12	0.01	0.34	11.68	0.15	0.04	11.27	0.04	3.43	6.78	2.48	100.69
RVV362-2	Plagioclase	49.58	15.51	0.19	0.10	0.01	0.39	10.43	0.15	0.03	11.22	0.03	3.74	6.64	2.06	100.08
RVV362-3	Plagioclase	47.89	15.52	0.31	0.14	0.03	0.63	10.57	0.10	0.02	11.90	0.02	3.81	5.49	2.91	99.33
RVV362-4	Plagioclase	47.61	17.72	0.30	0.11	0.02	0.62	8.73	0.18	0.01	12.61	0.01	3.98	6.44	2.09	100.44
RVV362-5	Plagioclase	46.58	14.99	0.32	0.22	0.03	0.54	10.73	0.19	0.01	12.47	0.02	3.87	6.06	2.88	98.90
RVV362-6	Plagioclase	47.21	15.44	0.30	0.12	0.03	0.48	10.64	0.17	0.00	12.00	0.00	3.68	6.64	2.59	99.29
RVV362-7	Plagioclase	49.69	19.91	0.38	0.14	0.00	0.47	11.45	0.14	0.01	9.24	0.00	3.50	3.78	2.56	101.48
RVV362-8	Plagioclase	51.81	20.19	0.20	0.10	0.02	0.51	10.32	0.13	0.02	8.26	0.00	3.39	4.63	1.71	101.45
RVV362-9	Plagioclase	49.14	19.68	0.32	0.13	0.02	0.53	11.10	0.13	0.00	9.66	0.00	3.33	3.53	2.44	100.20
RVV362-10	Plagioclase	49.72	20.07	0.33	0.16	0.02	0.58	10.03	0.12	0.00	9.91	0.00	3.31	3.51	2.32	100.33
RVV362-11	Plagioclase	49.71	19.76	0.28	0.11	0.02	0.47	10.65	0.10	0.02	9.16	0.00	3.52	4.51	2.15	100.63
RVV362-12	Plagioclase	50.52	20.47	0.27	0.12	0.02	0.47	11.12	0.11	0.00	8.24	0.01	3.79	3.91	2.07	101.28
RVV362-13	Plagioclase	50.37	19.60	0.24	0.11	0.02	0.39	11.61	0.12	0.01	8.64	0.01	3.57	4.62	2.01	101.48
RVV362-14	Plagioclase	48.53	18.81	0.20	0.09	0.01	0.47	11.30	0.12	0.00	9.35	0.01	2.89	4.15	2.03	98.09
RVV362-15	Plagioclase	49.46	19.90	0.35	0.16	0.03	0.57	9.97	0.12	0.01	10.07	0.01	3.39	3.68	2.34	100.31
RVV362-16	Plagioclase	49.46	20.21	0.22	0.12	0.02	0.57	11.39	0.12	0.01	9.48	0.00	3.78	3.80	1.80	101.18
RVV362-17	Plagioclase	48.27	19.07	0.53	0.14	0.02	0.42	11.87	0.13	0.00	9.79	0.00	3.44	4.10	2.50	100.49
RVV362-18	Plagioclase	49.39	19.30	0.24	0.15	0.02	0.46	11.81	0.13	0.02	9.49	0.00	3.04	4.41	2.22	100.89
RVV362-19	Plagioclase	50.96	19.74	0.24	0.16	0.02	0.48	11.04	0.10	0.00	8.47	0.00	3.38	3.67	2.12	100.62
RVV362-20	Plagioclase	48.55	19.28	0.29	0.16	0.02	0.52	11.71	0.14	0.00	10.23	0.00	2.99	4.13	2.43	100.68
<i>RVV362 Average</i>		<i>49.15</i>	<i>18.53</i>	<i>0.29</i>	<i>0.13</i>	<i>0.02</i>	<i>0.50</i>	<i>10.91</i>	<i>0.13</i>	<i>0.01</i>	<i>10.07</i>	<i>0.01</i>	<i>3.49</i>	<i>4.72</i>	<i>2.29</i>	<i>100.39</i>
<i>RVV362 Stdev</i>		<i>1.28</i>	<i>1.95</i>	<i>0.08</i>	<i>0.03</i>	<i>0.01</i>	<i>0.08</i>	<i>0.78</i>	<i>0.03</i>	<i>0.01</i>	<i>1.38</i>	<i>0.01</i>	<i>0.30</i>	<i>1.16</i>	<i>0.32</i>	<i>0.90</i>

Sample names ending in a or b are duplicate measurements

FeO\* is reported at total iron

Table 2.7B: Corrected Melt Inclusion Major Element Compositions

Sample	Host	Steps	SiO <sub>2</sub>	Al <sub>2</sub> O <sub>3</sub>	P <sub>2</sub> O <sub>5</sub>	S	Cl	K <sub>2</sub> O	CaO	MnO	Cr <sub>2</sub> O <sub>3</sub>	FeO*	NiO	Na <sub>2</sub> O	MgO	TiO <sub>2</sub>	Total
RVV302-1	Olivine	0.05	47.43	16.23	0.35	0.09	0.05	0.83	10.79	0.12	0.10	12.00	0.00	3.78	6.20	2.03	100.00
RVV302-2	Olivine	0.01	46.99	15.98	0.58	0.10	0.03	0.75	10.99	0.16	0.02	12.03	0.01	3.68	6.38	2.30	100.00
RVV302-3	Olivine	0.00	46.57	15.00	0.54	0.10	0.03	0.93	12.27	0.13	0.26	12.05	0.01	4.20	6.52	1.37	100.00
RVV302-4	Olivine	0.02	47.67	16.43	0.37	0.11	0.03	0.80	10.82	0.13	0.00	12.04	0.02	3.35	6.22	2.02	100.00
RVV302-5	Olivine	0.03	47.67	16.37	0.40	0.11	0.03	0.88	10.24	0.10	0.04	12.05	0.02	3.50	6.59	2.01	100.00
RVV302-6	Olivine	0.01	47.90	15.87	0.33	0.08	0.03	0.77	10.75	0.14	0.01	12.04	0.02	3.16	6.89	2.00	100.00
RVV302-7	Olivine	0.02	48.24	15.93	0.33	0.08	0.03	0.81	10.37	0.15	0.01	12.04	0.05	3.17	6.87	1.91	100.00
RVV302-8	Olivine	0.02	48.57	15.89	0.35	0.08	0.03	0.76	10.26	0.15	0.00	12.02	0.01	3.20	6.78	1.89	100.00
RVV302-9	Olivine	0.01	48.26	15.83	0.35	0.08	0.03	0.73	10.46	0.17	0.01	12.05	0.03	3.21	6.85	1.94	100.00
RVV302-10	Olivine	0.01	47.68	15.88	0.28	0.11	0.02	0.49	10.76	0.16	0.01	12.00	0.02	3.84	6.33	2.41	100.00
RVV302-11	Olivine	-0.02	48.00	14.50	0.48	0.10	0.04	0.95	10.30	0.15	0.00	12.00	0.00	3.86	6.29	3.35	100.00
RVV302-12	Olivine	0.01	47.94	15.67	0.53	0.07	0.04	0.96	10.30	0.15	0.04	12.02	0.01	3.35	6.49	2.41	100.00
<i>RVV302 Average</i>			47.74	15.80	0.41	0.09	0.03	0.81	10.69	0.14	0.04	12.03	0.02	3.53	6.53	2.14	100.00
<i>RVV302 Stdev</i>			0.56	0.55	0.10	0.01	0.01	0.13	0.56	0.02	0.08	0.02	0.01	0.34	0.26	0.47	0.00
RVV306a-1	Olivine	-0.07	38.56	14.75	0.82	0.24	0.17	1.30	15.94	0.17	0.02	12.00	0.03	5.75	6.79	3.48	100.00
RVV306a-2	Olivine	-0.01	39.85	15.21	0.93	0.16	0.16	1.37	10.71	0.20	0.03	12.01	0.05	5.96	10.71	2.65	100.00
RVV306a-3	Olivine	0.02	38.49	13.30	1.13	0.16	0.16	1.31	13.17	0.10	0.04	12.01	0.06	5.69	11.45	2.93	100.00
RVV306a-4	Olivine	0.00	38.07	14.25	1.09	0.21	0.21	1.40	14.48	0.11	0.01	12.01	0.06	5.27	9.79	3.05	100.00
RVV306a-5	Olivine	0.03	39.36	15.30	1.02	0.14	0.09	1.37	12.78	0.09	0.03	12.01	0.02	5.22	9.88	2.70	100.00
RVV306a-6	Olivine	0.02	41.42	12.54	0.66	0.12	0.11	0.93	15.32	0.14	0.09	12.01	-0.01	4.14	10.44	2.08	100.00
RVV306a-7	Olivine	0.02	39.92	14.01	0.89	0.15	0.13	0.98	15.06	0.10	0.08	12.02	0.04	4.27	9.26	3.10	100.00
RVV306a-8	Olivine	0.07	39.12	14.16	1.08	0.16	0.16	1.24	13.56	0.09	0.00	12.01	0.00	4.51	10.57	3.34	100.00
RVV306a-9	Olivine	0.02	39.44	13.62	0.94	0.07	0.10	0.99	15.22	0.07	0.08	12.01	0.03	4.33	9.94	3.15	100.00
RVV306a-10	Olivine	0.00	37.09	16.10	1.27	0.21	0.23	1.95	12.75	0.10	0.02	12.02	0.05	5.26	9.14	3.82	100.00
RVV306a-11	Olivine	0.00	40.22	15.77	1.44	0.17	0.06	0.57	13.97	0.14	0.00	12.01	0.04	1.63	10.84	3.16	100.00
RVV306a-12	Olivine	0.06	42.39	12.77	0.50	0.09	0.09	0.85	15.65	0.09	0.07	12.01	0.01	2.97	10.00	2.51	100.00
RVV306a-13	Olivine	0.04	40.18	14.37	1.12	0.15	0.21	1.73	11.93	0.07	0.01	12.02	0.02	5.31	9.57	3.31	100.00
RVV306a-14	Olivine	0.00	38.39	13.34	1.21	0.30	0.18	1.39	16.93	0.14	0.00	12.03	0.03	4.62	7.64	3.80	100.00
RVV306a-18	Olivine	-0.14	40.39	14.41	0.87	0.23	0.15	1.18	15.94	0.12	0.01	12.03	0.03	3.96	7.55	3.14	100.00
RVV306a-19	Olivine	-0.30	41.22	12.79	0.71	0.17	0.11	1.12	13.54	0.10	0.01	12.01	0.03	4.80	10.86	2.53	100.00
RVV306a-20	Olivine	-0.04	40.69	13.47	0.82	0.17	0.14	1.09	14.88	0.09	0.01	12.02	0.01	3.77	10.01	2.84	100.00
RVV306a-21	Olivine	-0.04	41.32	13.28	0.70	0.14	0.12	1.05	14.66	0.11	0.03	12.02	0.01	3.86	10.04	2.66	100.00
<i>RVV306a Average</i>			39.78	14.08	0.95	0.17	0.14	1.21	14.25	0.11	0.03	12.01	0.03	4.52	9.69	3.01	100.00
<i>RVV306a Stdev</i>			1.36	1.04	0.24	0.05	0.05	0.32	1.59	0.03	0.03	0.01	0.02	1.07	1.24	0.45	0.00



RVV312-1	Plagioclase	n/a	49.29	19.70	0.40	0.14	0.03	0.75	8.72	0.16	0.01	11.15	0.00	2.95	3.87	2.84	100.00
RVV312-2	Plagioclase	n/a	49.00	19.96	0.35	0.13	0.03	0.69	8.40	0.15	0.01	11.33	0.00	3.09	4.24	2.62	100.00
RVV312-3	Plagioclase	n/a	50.05	20.11	0.37	0.13	0.03	0.72	8.84	0.17	0.00	10.41	0.01	2.82	3.64	2.70	100.00
RVV312-4	Plagioclase	n/a	50.42	19.13	0.46	0.14	0.03	0.55	6.95	0.18	0.00	12.06	0.01	2.73	4.10	3.22	100.00
RVV312-5	Plagioclase	n/a	49.35	17.82	0.40	0.14	0.04	1.07	8.34	0.20	0.00	11.94	0.00	3.13	4.55	2.81	100.00
RVV312-6	Plagioclase	n/a	47.70	17.87	0.54	0.17	0.05	0.87	9.77	0.23	0.00	11.62	0.00	3.47	4.24	3.23	100.00
RVV312-7	Plagioclase	n/a	49.29	18.36	0.44	0.14	0.02	0.56	6.15	0.18	0.02	12.43	0.01	3.34	5.69	3.18	100.00
RVV312-8	Plagioclase	n/a	48.83	18.91	0.37	0.12	0.03	0.82	9.22	0.19	0.02	11.74	0.00	3.66	4.20	1.72	100.00
RVV312-9	Plagioclase	n/a	49.03	18.66	0.36	0.12	0.03	0.85	9.22	0.22	0.00	11.58	0.00	3.71	4.01	2.05	100.00
RVV312-10	Plagioclase	n/a	49.83	17.95	0.66	0.17	0.05	1.08	9.04	0.21	0.00	11.71	0.00	2.88	3.27	2.91	100.00
<i>RVV312 Average</i>			<i>49.28</i>	<i>18.85</i>	<i>0.43</i>	<i>0.14</i>	<i>0.03</i>	<i>0.80</i>	<i>8.47</i>	<i>0.19</i>	<i>0.01</i>	<i>11.60</i>	<i>0.00</i>	<i>3.18</i>	<i>4.18</i>	<i>2.73</i>	<i>100.00</i>
<i>RVV312 Stdev</i>			<i>0.75</i>	<i>0.86</i>	<i>0.10</i>	<i>0.02</i>	<i>0.01</i>	<i>0.18</i>	<i>1.11</i>	<i>0.03</i>	<i>0.01</i>	<i>0.55</i>	<i>0.01</i>	<i>0.35</i>	<i>0.64</i>	<i>0.50</i>	<i>0.00</i>
RVV316-6	Olivine	-0.20	46.44	15.55	0.38	0.08	0.03	0.86	11.20	0.08	0.03	12.05	0.00	4.11	6.84	2.38	100.00
RVV316-7	Olivine	0.05	46.43	15.56	0.33	0.08	0.03	0.85	11.16	0.10	0.04	12.02	0.01	4.11	6.79	2.48	100.00
RVV316-8	Olivine	0.00	47.74	14.55	0.48	0.12	0.03	0.96	11.01	0.13	0.03	11.97	-0.01	4.58	5.27	3.14	100.00
RVV316-9	Olivine	0.00	47.47	14.56	0.50	0.12	0.04	0.98	11.00	0.12	0.02	11.97	0.00	4.68	5.38	3.17	100.00
RVV316-11	Olivine	0.04	40.44	14.49	1.25	0.10	0.19	1.70	11.37	0.11	0.02	12.03	0.06	7.11	8.56	2.57	100.00
RVV316-11a	Olivine	0.02	40.55	14.49	1.20	0.10	0.19	1.71	11.37	0.11	0.02	12.02	0.06	7.08	8.55	2.55	100.00
RVV316-12	Olivine	-0.03	41.23	13.20	0.91	0.18	0.16	1.24	13.86	0.21	0.14	12.02	0.01	5.51	9.00	2.33	100.00
RVV316-13	Olivine	-0.04	36.61	13.50	1.10	0.24	0.20	1.87	13.84	0.11	0.00	12.01	0.02	6.86	9.69	3.93	100.00
RVV316-14	Olivine	-0.18	38.21	13.49	1.30	0.25	0.22	1.53	14.40	0.03	0.00	12.00	-0.02	5.99	9.70	2.91	100.00
RVV316-15	Olivine	0.01	39.54	13.35	0.92	0.17	0.17	1.25	13.56	0.13	0.02	12.00	0.04	4.21	11.78	2.85	100.00
RVV316-16	Olivine	-0.01	40.17	13.68	0.93	0.18	0.16	1.20	13.76	0.19	0.03	12.01	0.03	4.64	10.38	2.63	100.00
RVV316-17	Olivine	-0.02	37.86	13.98	1.14	0.26	0.21	1.70	12.68	0.11	0.01	12.01	0.05	5.61	10.69	3.69	100.00
RVV316-18	Olivine	-0.06	38.39	13.50	1.18	0.11	0.02	1.67	14.93	0.14	0.04	12.02	0.03	5.43	9.09	3.44	100.00
RVV316-19	Olivine	-0.02	37.42	13.35	1.35	0.24	0.11	1.29	15.93	0.14	0.02	12.01	0.05	4.71	10.19	3.18	100.00
RVV316-20	Olivine	0.04	40.71	12.82	0.98	0.03	0.09	3.58	11.97	0.10	0.05	12.00	0.03	2.57	12.49	2.59	100.00
RVV316-21	Olivine	0.02	39.75	13.07	0.89	0.15	0.16	1.20	13.40	0.10	0.04	12.00	0.04	4.35	12.13	2.73	100.00
RVV316-23	Olivine	-0.08	39.52	15.03	1.06	0.24	0.19	1.39	16.44	0.08	0.04	11.91	0.00	4.70	6.20	3.21	100.00
RVV316-24	Olivine	0.00	40.40	17.27	0.40	0.24	0.09	1.12	12.44	0.18	0.01	12.02	-0.01	4.55	7.03	4.26	100.00
RVV316-25	Olivine	0.07	41.35	16.96	0.53	0.24	0.11	1.32	12.64	0.16	0.02	12.00	-0.01	4.28	7.29	3.11	100.00
RVV316-26	Olivine	-0.05	41.42	16.95	0.52	0.25	0.11	1.37	12.60	0.14	0.00	12.00	0.03	4.39	7.17	3.06	100.00
<i>RVV316 Average</i>			<i>41.08</i>	<i>14.47</i>	<i>0.87</i>	<i>0.17</i>	<i>0.13</i>	<i>1.44</i>	<i>12.98</i>	<i>0.12</i>	<i>0.03</i>	<i>12.00</i>	<i>0.02</i>	<i>4.97</i>	<i>8.71</i>	<i>3.01</i>	<i>100.00</i>
<i>RVV316 Stdev</i>			<i>3.33</i>	<i>1.36</i>	<i>0.34</i>	<i>0.07</i>	<i>0.07</i>	<i>0.59</i>	<i>1.63</i>	<i>0.04</i>	<i>0.03</i>	<i>0.03</i>	<i>0.03</i>	<i>1.13</i>	<i>2.18</i>	<i>0.52</i>	<i>0.00</i>
RVV321-1	Olivine	-0.11	42.26	16.73	0.80	0.28	0.16	1.92	10.11	0.14	0.02	12.00	-0.01	6.04	6.17	3.38	100.00
RVV321-2	Olivine	-0.10	40.94	18.20	0.53	0.27	0.11	1.46	11.12	0.16	0.00	11.96	0.00	5.87	5.67	3.71	100.00

RVV321-3	Olivine	-0.10	41.23	17.68	0.79	0.26	0.12	1.49	11.10	0.16	0.02	11.93	-0.04	6.39	5.64	3.22	100.00
RVV321-4	Olivine	-0.06	39.48	17.29	0.93	0.29	0.15	1.91	11.78	0.18	0.05	12.00	0.03	5.70	6.99	3.24	100.00
RVV321-5	Olivine	-0.11	41.20	18.25	0.82	0.32	0.13	1.67	10.49	0.14	0.00	11.82	-0.02	6.75	5.56	2.88	100.00
RVV321-6	Olivine	-0.02	44.17	16.22	0.35	0.18	0.08	0.82	12.09	0.15	0.02	12.00	0.03	4.56	7.30	2.02	100.00
RVV321-7	Olivine	-0.01	43.39	14.42	0.43	0.18	0.07	1.02	14.15	0.17	0.02	12.02	0.01	3.72	8.30	2.09	100.00
RVV321-8	Olivine	-0.09	41.66	16.96	0.63	0.22	0.11	1.45	11.55	0.21	0.01	12.00	-0.02	5.85	6.17	3.21	100.00
RVV321-9	Olivine	-0.11	44.66	11.34	0.22	0.08	0.04	0.45	19.41	0.22	0.05	12.00	-0.04	2.68	6.19	2.69	100.00
RVV321-11	Olivine	-0.11	42.27	18.16	0.64	0.31	0.12	1.55	10.69	0.16	0.01	11.93	-0.04	5.11	5.55	3.54	100.00
RVV321-12	Olivine	-0.03	42.58	17.27	0.57	0.27	0.11	1.27	11.75	0.17	0.00	11.98	0.01	4.65	5.76	3.60	100.00
RVV321-13	Olivine	0.04	43.52	16.73	0.56	0.25	0.12	1.44	10.79	0.18	0.00	12.00	0.02	4.45	6.35	3.58	100.00
RVV321-14	Olivine	0.01	43.34	16.50	0.52	0.26	0.11	1.43	11.35	0.16	0.00	12.00	0.04	4.40	6.48	3.40	100.00
RVV321-15	Olivine	-0.07	44.72	17.92	0.27	0.25	0.06	2.28	9.48	0.17	0.00	11.94	0.01	4.32	5.75	2.83	100.00
RVV321-16	Olivine	-0.24	44.54	14.29	0.43	0.19	0.07	0.91	13.92	0.17	0.03	12.02	0.02	3.22	8.55	1.63	100.00
RVV321-17	Olivine	-0.13	40.51	17.51	0.54	0.39	0.10	1.50	11.54	0.04	0.03	11.77	-0.04	6.21	5.75	4.18	100.00
RVV321-18	Olivine	-0.18	42.56	16.99	0.60	0.29	0.15	2.06	9.89	0.20	0.03	11.59	-0.08	7.47	5.64	2.62	100.00
RVV321-19	Olivine	-0.04	41.02	16.88	0.67	0.26	0.10	1.31	12.89	0.19	0.02	12.00	0.00	4.24	7.15	3.26	100.00
RVV321-21	Olivine	-0.06	44.14	13.41	0.25	0.14	0.10	0.68	16.26	0.21	0.11	12.00	0.01	2.84	7.53	2.32	100.00
RVV321-22	Olivine	-0.02	44.80	15.60	0.29	0.15	0.05	0.63	12.87	0.18	0.05	12.02	0.01	3.27	7.95	2.12	100.00
RVV321-23	Olivine	-0.13	40.91	17.84	0.71	0.33	0.09	1.88	10.91	0.11	0.01	11.93	-0.05	4.95	5.97	4.40	100.00
RVV321-24	Olivine	-0.10	41.23	17.74	0.52	0.27	0.10	1.50	11.73	0.18	0.00	12.00	-0.01	4.74	6.05	3.95	100.00
RVV321-25	Olivine	-0.15	46.18	15.90	0.34	0.13	0.05	0.82	10.91	0.17	0.11	12.02	0.01	3.25	7.55	2.56	100.00
RVV321-26	Olivine	-0.06	41.39	16.93	0.63	0.28	0.12	1.65	11.38	0.18	0.03	12.00	0.02	4.59	7.18	3.62	100.00
RVV321-27	Olivine	-0.03	43.85	16.30	0.38	0.19	0.07	0.84	12.52	0.19	0.01	12.02	0.03	3.33	7.82	2.44	100.00
RVV321-28	Olivine	-0.13	41.71	17.99	0.71	0.26	0.12	1.48	11.45	0.18	0.00	11.85	-0.04	4.94	5.90	3.45	100.00
RVV321-29	Olivine	-0.09	41.17	17.36	0.26	0.24	0.09	1.56	12.03	0.16	0.01	12.00	0.01	4.33	7.11	3.68	100.00
RVV321-30	Olivine	-0.10	41.32	18.21	0.52	0.28	0.10	1.33	11.62	0.14	0.01	11.97	-0.03	4.92	5.75	3.86	100.00
RVV321-31	Olivine	-0.60	41.76	18.20	0.39	0.26	0.09	1.39	11.57	0.06	0.03	11.67	-0.05	4.79	5.70	4.14	100.00
RVV321-32	Olivine	0.23	41.01	17.65	0.58	0.26	0.11	1.54	11.63	0.19	0.04	12.00	0.00	4.37	6.81	3.80	100.00
RVV321-33	Olivine	-0.05	41.11	17.55	0.53	0.31	0.10	1.43	11.75	0.17	0.01	12.00	0.03	4.34	6.80	3.87	100.00
RVV321-34	Olivine	0.01	42.04	17.12	1.19	0.12	0.03	1.58	9.78	0.23	0.01	12.01	0.03	5.47	9.35	1.03	100.00
RVV321-35	Olivine	-0.05	40.18	15.30	0.97	0.10	0.19	1.55	13.99	0.10	0.01	12.00	0.00	5.28	7.09	3.25	100.00
<i>RVV321 Average</i>			42.33	16.74	0.56	0.24	0.10	1.39	11.95	0.16	0.02	11.95	0.00	4.76	6.65	3.14	100.00
<i>RVV321 Stdev</i>			1.61	1.54	0.22	0.07	0.04	0.42	1.92	0.04	0.03	0.10	0.03	1.14	0.99	0.79	0.00
RVV340-1	Olivine	-0.07	47.34	13.50	0.39	0.13	0.03	0.72	9.79	0.24	0.01	12.01	-0.03	3.72	9.95	2.19	100.00
RVV340-2	Olivine	-0.17	46.73	12.84	1.12	0.07	0.01	0.36	12.57	0.36	0.05	11.97	-0.05	3.18	7.22	3.56	100.00
RVV340-3	Olivine	-0.12	47.59	15.04	0.45	0.07	0.02	0.81	10.15	0.22	0.29	11.97	-0.07	4.28	7.40	1.77	100.00

RVV340-4	Olivine	-0.16	47.15	14.51	0.69	0.17	0.02	0.51	10.93	0.31	0.02	11.98	-0.10	3.74	7.39	2.68	100.00
RVV340-5	Olivine	-0.21	45.13	15.85	0.46	0.21	0.03	0.62	10.93	0.19	0.42	12.08	-0.09	4.22	7.51	2.43	100.00
RVV340-6	Olivine	-0.19	43.94	17.45	0.50	0.24	0.04	0.87	9.88	0.22	0.43	12.06	-0.06	4.72	7.45	2.27	100.00
RVV340-7	Olivine	-0.22	45.24	16.00	0.36	0.20	0.03	0.67	10.65	0.23	0.46	12.09	-0.06	4.20	7.46	2.50	100.00
RVV340-8	Olivine	-0.19	49.42	14.72	0.47	0.07	0.02	0.91	9.59	0.12	0.03	11.96	-0.14	4.20	7.02	1.60	100.00
RVV340-8a	Olivine	0.25	48.71	15.11	0.48	0.08	0.03	0.97	9.44	0.20	0.01	11.91	-0.05	4.51	6.99	1.61	100.00
RVV340-9	Olivine	-0.13	46.69	15.02	0.50	0.28	0.04	0.96	10.66	0.18	0.30	11.95	0.01	3.81	7.30	2.30	100.00
RVV340-10	Olivine	-0.10	47.14	15.64	0.36	0.16	0.03	0.62	10.23	0.14	0.02	11.98	-0.02	3.67	7.68	2.33	100.00
RVV340-10a	Olivine	0.29	46.84	15.76	0.39	0.16	0.04	0.62	10.41	0.14	0.00	11.98	-0.02	3.70	7.68	2.30	100.00
RVV340-10b	Olivine	-0.10	46.82	15.68	0.39	0.17	0.03	0.61	10.47	0.14	0.02	11.98	-0.02	3.74	7.68	2.27	100.00
RVV340-11	Olivine	0.14	46.56	16.04	0.34	0.13	0.04	0.65	11.22	0.13	0.02	12.00	0.00	3.01	7.20	2.66	100.00
RVV340-12	Olivine	-0.02	45.91	13.68	0.56	0.10	0.05	0.70	12.01	0.12	0.16	12.01	0.01	2.55	9.76	2.36	100.00
RVV340-13	Olivine	-0.04	47.81	16.34	0.39	0.15	0.02	0.68	9.99	0.14	0.01	11.99	-0.02	2.86	6.66	2.99	100.00
RVV340-14	Olivine	-0.01	46.00	16.09	0.47	0.10	0.04	0.69	11.17	0.16	0.03	12.04	0.00	3.01	7.45	2.75	100.00
RVV340-15	Olivine	-0.04	46.85	15.73	0.54	0.18	0.05	0.95	11.51	0.09	0.30	11.98	0.01	3.53	6.35	1.92	100.00
RVV340-16	Olivine	-0.23	48.73	15.40	0.28	0.11	0.04	0.67	10.23	0.17	0.02	12.02	0.02	3.57	6.79	1.94	100.00
RVV340-17	Olivine	-0.20	44.89	16.06	0.37	0.19	0.04	0.65	11.08	0.24	0.30	11.90	-0.08	4.51	7.35	2.51	100.00
RVV340-18	Olivine	-0.02	45.54	14.95	1.39	0.15	0.07	0.84	12.04	0.15	0.10	12.00	-0.01	2.92	7.22	2.64	100.00
RVV340-19	Olivine	-0.04	44.21	15.46	0.45	0.14	0.06	0.81	13.21	0.15	0.21	12.02	0.02	3.45	7.76	2.06	100.00
RVV340-20	Olivine	-0.04	45.47	14.84	0.43	0.22	0.05	0.69	12.73	0.17	0.10	12.02	0.01	3.27	7.86	2.14	100.00
RVV340-21	Olivine	-0.08	46.67	14.84	0.56	0.13	0.05	1.27	11.37	0.20	0.12	12.00	0.00	4.08	6.95	1.77	100.00
RVV340-22	Olivine	-0.02	47.97	15.03	0.43	0.15	0.04	0.86	10.36	0.14	0.00	12.02	0.03	3.41	7.22	2.33	100.00
RVV340-23	Olivine	-0.07	44.22	20.00	0.17	0.10	0.00	0.33	10.87	0.29	0.01	12.00	0.00	1.44	7.46	3.12	100.00
RVV340-24	Olivine	0.04	47.11	15.46	0.28	0.10	0.05	0.60	11.30	0.14	0.08	12.02	0.02	3.03	8.00	1.80	100.00
RVV340-25	Olivine	-0.02	46.18	15.90	0.34	0.13	0.05	0.82	10.91	0.17	0.11	12.02	0.01	3.25	7.55	2.56	100.00
RVV340-26	Olivine	-0.02	44.29	13.15	0.36	0.17	0.70	1.20	11.58	0.17	0.11	12.02	0.02	4.70	9.38	2.16	100.00
RVV340-27	Olivine	-0.01	49.18	14.29	0.33	0.13	0.17	0.83	9.89	0.17	0.00	12.02	0.00	3.56	7.51	1.92	100.00
RVV340-28	Olivine	-0.01	47.19	15.61	0.36	0.12	0.04	0.90	10.16	0.13	0.02	12.02	0.00	3.27	7.62	2.54	100.00
<i>RVV340 Average</i>			46.57	15.35	0.47	0.15	0.06	0.75	10.88	0.18	0.12	12.00	-0.02	3.58	7.57	2.32	100.00
<i>RVV340 Stdev</i>			1.46	1.30	0.23	0.05	0.12	0.20	0.93	0.06	0.14	0.04	0.04	0.69	0.79	0.44	0.00
RVV343-1	Olivine	-0.02	37.27	13.29	1.03	0.21	0.05	1.49	13.82	0.12	0.01	12.01	0.08	6.26	10.94	3.41	100.00
RVV343-2	Olivine	-0.19	47.22	15.93	0.45	0.12	0.04	0.97	10.24	0.09	0.00	11.96	0.02	4.75	4.93	3.27	100.00
RVV343-3	Olivine	-0.45	48.19	17.94	0.38	0.12	0.03	0.78	9.68	0.08	0.01	11.81	0.00	3.58	4.55	2.85	100.00
RVV343-3a	Olivine	-0.01	47.99	17.81	0.40	0.12	0.04	0.83	9.63	0.10	0.02	11.87	0.01	3.62	4.58	2.98	100.00
RVV343-4	Plagioclase	n/a	48.33	17.39	0.21	0.17	0.02	0.36	9.70	0.18	0.00	13.14	0.00	3.22	4.91	2.37	100.00
RVV343-5	Plagioclase	n/a	48.52	17.46	0.26	0.16	0.03	0.39	9.71	0.20	0.00	13.13	0.02	3.13	4.75	2.23	100.00

RVV343-6	Plagioclase	n/a	48.33	18.19	0.29	0.13	0.03	0.53	10.53	0.15	0.01	10.74	0.00	3.93	4.42	2.53	100.00
RVV343-7	Plagioclase	n/a	50.20	19.03	0.27	0.12	0.02	0.59	10.00	0.16	0.01	9.55	0.00	3.78	3.79	2.28	100.00
RVV343-8	Olivine	0.00	48.09	15.80	0.42	0.11	0.04	1.05	9.70	0.09	0.00	11.93	0.00	4.49	5.07	3.20	100.00
RVV343-9	Plagioclase	n/a	47.77	19.44	0.14	0.05	0.01	0.55	8.28	0.25	0.01	12.87	0.01	3.54	5.69	1.30	100.00
RVV343-10	Plagioclase	n/a	48.18	18.49	0.26	0.14	0.03	0.48	10.37	0.16	0.00	11.16	0.01	3.76	4.47	2.30	100.00
<i>RVV343 Average</i>			<i>47.28</i>	<i>17.34</i>	<i>0.38</i>	<i>0.13</i>	<i>0.03</i>	<i>0.73</i>	<i>10.15</i>	<i>0.14</i>	<i>0.01</i>	<i>11.83</i>	<i>0.01</i>	<i>4.01</i>	<i>5.28</i>	<i>2.61</i>	<i>100.00</i>
<i>RVV343 Stdev</i>			<i>3.40</i>	<i>1.75</i>	<i>0.24</i>	<i>0.04</i>	<i>0.01</i>	<i>0.34</i>	<i>1.35</i>	<i>0.05</i>	<i>0.01</i>	<i>1.07</i>	<i>0.02</i>	<i>0.89</i>	<i>1.94</i>	<i>0.61</i>	<i>0.00</i>
RVV344-1	Olivine	-0.03	42.01	14.87	0.50	0.16	0.10	1.06	13.36	0.21	0.08	12.02	0.00	3.94	8.74	2.96	100.00
RVV344-2	Olivine	-0.03	42.63	14.70	0.54	0.15	0.11	1.10	12.24	0.26	0.10	12.02	0.03	3.99	8.73	3.41	100.00
RVV344-3	Olivine	-0.02	47.23	7.66	0.15	0.06	0.03	0.27	19.44	0.23	0.26	12.02	0.02	1.85	8.85	1.94	100.00
RVV344-4	Olivine	0.02	41.96	15.62	0.46	0.11	0.08	1.08	12.39	0.11	0.02	12.02	0.04	4.24	9.40	2.48	100.00
RVV344-5	Olivine	0.02	44.42	13.23	0.29	0.09	0.05	0.62	14.08	0.15	0.06	12.01	0.06	2.85	9.96	2.12	100.00
RVV344-6	Olivine	0.09	43.66	15.87	0.37	0.12	0.09	1.09	11.69	0.16	0.05	12.02	0.04	4.53	8.29	2.00	100.00
RVV344-7	Olivine	-0.14	45.28	14.21	0.42	0.10	0.07	0.94	10.64	0.13	0.09	12.02	0.06	4.12	9.60	2.33	100.00
RVV344-8	Olivine	-0.03	45.29	15.42	0.41	0.12	0.07	0.88	13.99	0.02	0.09	11.81	0.02	4.01	5.29	2.57	100.00
RVV344-9	Olivine	0.02	45.67	12.78	0.35	0.07	0.04	0.56	12.79	0.12	0.16	12.01	0.08	3.30	10.07	1.98	100.00
RVV344-10	Olivine	-0.01	46.29	13.78	0.34	0.12	0.05	0.64	10.52	0.20	0.02	12.01	0.03	4.07	10.21	1.72	100.00
RVV344-11	Olivine	0.01	42.88	14.97	0.47	0.10	0.09	1.06	12.77	0.16	0.12	12.01	0.05	3.77	8.98	2.58	100.00
RVV344-12	Olivine	0.17	46.13	14.97	0.50	0.13	0.11	1.18	12.43	0.12	0.04	11.91	0.00	4.54	5.46	2.48	100.00
RVV344-13	Olivine	0.08	43.00	15.98	0.41	0.12	0.09	1.13	12.96	0.14	0.04	12.02	0.01	3.53	7.99	2.56	100.00
RVV344-14	Olivine	0.05	45.97	14.99	0.39	0.05	0.07	0.89	11.01	0.12	0.11	12.02	0.02	3.40	8.71	2.25	100.00
RVV344-15	Olivine	0.03	43.23	16.47	0.45	0.10	0.09	1.14	12.40	0.13	0.01	12.03	0.02	3.64	7.85	2.44	100.00
RVV344-16	Olivine	0.07	46.69	12.69	0.24	0.06	0.03	0.44	13.00	0.09	0.13	12.01	0.00	2.53	10.16	1.93	100.00
RVV344-17	Olivine	0.05	46.60	12.18	0.21	0.07	0.03	0.48	14.28	0.11	0.17	12.02	0.03	2.49	9.50	1.85	100.00
RVV344-18	Olivine	0.05	45.88	12.42	0.28	0.07	0.05	0.59	14.38	0.13	0.14	12.02	0.00	2.56	9.50	1.98	100.00
RVV344-19	Olivine	0.00	42.93	17.17	0.43	0.10	0.09	1.12	12.44	0.11	0.04	12.03	0.02	3.50	7.58	2.45	100.00
RVV344-20	Olivine	-0.02	42.99	16.97	0.39	0.08	0.10	1.04	12.38	0.14	0.08	12.00	-0.04	3.37	7.87	2.64	100.00
RVV344-21	Olivine	0.06	46.80	13.16	0.31	0.04	0.04	0.55	12.85	0.10	0.10	12.02	0.00	2.45	9.59	2.00	100.00
RVV344-22	Olivine	0.06	45.70	14.31	0.33	0.05	0.07	0.79	11.53	0.09	0.09	12.02	0.01	3.55	9.36	2.11	100.00
RVV344-23	Olivine	0.07	46.66	13.30	0.30	0.05	0.03	0.53	12.20	0.08	0.11	12.01	0.03	2.79	9.88	2.02	100.00
RVV344-24	Olivine	0.09	46.74	13.03	0.32	0.06	0.03	0.47	12.88	0.06	0.10	12.02	0.00	2.40	9.90	1.99	100.00
RVV344-25	Olivine	0.06	44.61	13.67	0.43	0.07	0.07	0.79	12.69	0.11	0.08	12.01	0.01	2.57	10.55	2.33	100.00
RVV344-26	Olivine	0.05	46.48	13.62	0.37	0.06	0.05	0.78	12.04	0.10	0.11	12.02	0.02	3.04	9.08	2.23	100.00
RVV344-27	Olivine	0.05	44.59	14.35	0.40	0.08	0.07	0.84	13.18	0.11	0.11	12.02	0.03	2.91	8.85	2.45	100.00
<i>RVV344 Average</i>			<i>44.90</i>	<i>14.16</i>	<i>0.37</i>	<i>0.09</i>	<i>0.07</i>	<i>0.82</i>	<i>12.84</i>	<i>0.13</i>	<i>0.09</i>	<i>12.01</i>	<i>0.02</i>	<i>3.33</i>	<i>8.89</i>	<i>2.29</i>	<i>100.00</i>
<i>RVV344 Stdev</i>			<i>1.68</i>	<i>1.89</i>	<i>0.09</i>	<i>0.03</i>	<i>0.03</i>	<i>0.27</i>	<i>1.64</i>	<i>0.05</i>	<i>0.05</i>	<i>0.04</i>	<i>0.02</i>	<i>0.73</i>	<i>1.28</i>	<i>0.37</i>	<i>0.00</i>

RVV345-1	Olivine	0.00	44.82	15.26	0.34	0.12	0.03	0.53	12.39	0.16	0.01	12.02	0.00	4.06	8.14	2.13	100.00
RVV345-2	Olivine	0.02	47.68	14.37	0.17	0.08	0.02	0.36	11.32	0.15	0.04	12.02	0.00	4.17	8.01	1.61	100.00
RVV345-2a	Olivine	0.02	47.65	14.37	0.19	0.08	0.01	0.35	11.33	0.14	0.03	12.02	0.01	4.21	7.99	1.62	100.00
RVV345-3	Olivine	0.02	48.04	14.66	0.20	0.09	0.02	0.41	10.15	0.15	0.29	12.03	0.00	5.24	7.92	0.80	100.00
RVV345-4	Olivine	0.03	47.16	14.85	0.34	0.09	0.05	0.68	10.78	0.14	0.07	12.02	0.01	4.53	7.98	1.30	100.00
RVV345-5	Olivine	0.00	42.55	16.99	0.49	0.08	0.10	1.08	11.88	0.20	0.01	12.03	0.02	4.67	6.91	2.99	100.00
RVV345-6	Olivine	-0.01	43.44	16.61	0.51	0.18	0.10	1.21	11.63	0.17	0.00	12.00	0.01	4.52	6.91	2.71	100.00
RVV345-7	Olivine	0.01	45.89	15.96	0.27	0.11	0.02	0.48	11.77	0.19	0.04	12.03	0.00	4.56	7.27	1.41	100.00
RVV345-8	Olivine	0.01	45.86	10.55	0.30	0.04	0.04	0.65	14.70	0.16	0.11	12.01	0.03	3.72	9.82	2.00	100.00
RVV345-9	Olivine	0.05	44.37	12.95	0.26	0.05	0.04	2.88	10.54	0.09	0.04	12.02	0.02	5.42	9.32	2.00	100.00
RVV345-10	Olivine	0.05	46.43	12.26	0.28	0.08	0.05	0.65	13.10	0.11	0.09	12.02	0.04	3.41	9.33	2.15	100.00
RVV345-11	Olivine	0.03	46.95	10.97	0.21	0.07	0.03	0.56	14.17	0.13	0.11	12.02	0.01	3.43	9.31	2.03	100.00
RVV345-12	Olivine	0.02	46.51	10.77	0.16	0.09	0.04	0.49	14.68	0.14	0.09	12.02	0.04	3.32	9.57	2.08	100.00
RVV345-13	Olivine	0.00	46.42	10.49	0.12	0.08	0.03	0.50	14.99	0.13	0.12	12.02	0.00	3.43	9.49	2.18	100.00
RVV345-14	Olivine	0.03	46.52	10.19	0.20	0.08	0.05	0.51	14.85	0.14	0.10	12.02	0.02	3.55	9.56	2.22	100.00
RVV345-15	Olivine	0.04	43.98	14.77	0.44	0.09	0.09	1.02	12.45	0.10	0.05	12.02	0.02	4.09	8.30	2.59	100.00
RVV345-15a	Olivine	0.04	43.90	14.81	0.43	0.10	0.08	0.99	12.49	0.11	0.06	12.03	0.01	4.08	8.30	2.59	100.00
RVV345-15b	Olivine	0.04	43.85	14.70	0.43	0.10	0.09	1.00	12.64	0.11	0.05	12.03	0.02	4.12	8.30	2.57	100.00
RVV345-16	Olivine	-0.05	45.46	13.07	0.33	0.14	0.06	0.78	12.86	0.10	0.06	12.02	0.05	3.34	9.49	2.25	100.00
RVV345-16a	Olivine	0.04	45.10	13.53	0.36	0.14	0.06	0.78	13.03	0.10	0.04	12.02	0.05	2.93	9.46	2.40	100.00
RVV345-17	Olivine	0.00	43.26	14.80	0.37	0.14	0.08	0.94	12.74	0.10	0.05	12.02	0.04	3.92	9.00	2.55	100.00
RVV345-18	Olivine	0.07	45.77	15.98	0.20	0.02	0.43	2.82	9.55	0.06	0.03	12.02	0.02	3.97	7.74	1.39	100.00
RVV345-18a	Olivine	0.07	46.36	15.61	0.20	0.02	0.45	2.92	9.51	0.08	0.03	12.03	0.02	3.63	7.74	1.40	100.00
RVV345-18b	Olivine	0.08	46.37	15.72	0.19	0.02	0.45	2.92	9.45	0.07	0.05	12.03	0.03	3.62	7.73	1.35	100.00
RVV345-19	Olivine	0.03	46.68	14.21	0.30	0.03	0.25	2.54	10.51	0.11	0.04	12.04	0.01	4.04	7.54	1.69	100.00
RVV345-20	Olivine	-0.06	46.33	13.20	0.30	0.11	0.05	0.69	13.18	0.09	0.06	12.03	0.04	3.05	8.72	2.17	100.00
RVV345-21	Olivine	-0.02	47.22	11.32	0.24	0.08	0.02	0.39	14.07	0.13	0.09	12.01	0.03	2.67	9.75	1.98	100.00
RVV345-22	Olivine	0.06	47.62	11.53	0.26	0.09	0.04	0.61	11.71	0.08	0.18	12.02	0.04	3.48	10.26	2.07	100.00
RVV345-23	Olivine	-0.07	47.43	11.91	0.27	0.11	0.03	0.50	12.23	0.09	0.09	12.01	0.05	2.95	10.41	1.91	100.00
RVV345-23a	Olivine	0.07	47.48	11.86	0.22	0.11	0.03	0.49	12.39	0.08	0.09	12.01	0.05	2.87	10.43	1.88	100.00
RVV345-24	Olivine	0.08	47.93	11.51	0.23	0.10	0.03	0.45	11.75	0.09	0.06	12.01	0.05	3.03	10.95	1.80	100.00
RVV345-25	Olivine	0.08	48.01	11.76	0.23	0.11	0.03	0.44	11.61	0.06	0.09	12.01	0.03	3.01	10.86	1.74	100.00
RVV345-25a	Olivine	0.07	47.48	12.18	0.23	0.11	0.03	0.45	11.76	0.10	0.10	12.01	0.05	2.72	10.87	1.92	100.00
RVV345-25a			46.08	13.45	0.28	0.09	0.09	0.97	12.19	0.12	0.07	12.02	0.02	3.75	8.89	1.98	100.00
RVV345 Average			1.54	1.98	0.10	0.04	0.12	0.82	1.53	0.04	0.05	0.01	0.02	0.69	1.17	0.47	0.00
RVV345 Stdev																	
RVV346-1	Olivine	-0.06	45.77	11.99	0.25	0.07	0.05	0.62	13.45	0.10	0.09	12.01	0.03	3.11	10.51	1.95	100.00

RVV346-2	Olivine	0.04	43.99	13.14	0.32	0.07	0.07	0.88	14.56	0.11	0.08	12.02	0.02	3.12	9.17	2.45	100.00
RVV346-3	Olivine	-0.03	43.43	14.10	0.48	0.09	0.10	1.29	12.84	0.09	0.06	12.02	0.03	3.70	9.16	2.62	100.00
RVV346-4	Olivine	-0.04	48.61	11.07	0.37	0.07	0.04	0.68	11.55	0.11	0.11	12.02	0.02	3.65	9.56	2.16	100.00
RVV346-5	Olivine	0.04	45.81	12.70	0.30	0.06	0.05	0.74	12.72	0.09	0.37	12.01	0.02	3.42	9.62	2.10	100.00
RVV346-6	Olivine	0.01	43.04	14.89	0.38	0.08	0.10	1.12	14.51	0.15	0.10	12.03	0.03	3.59	7.63	2.37	100.00
RVV346-7	Olivine	-0.32	46.64	12.46	0.22	0.11	0.04	0.56	13.91	0.10	0.08	12.02	0.04	2.78	8.98	2.06	100.00
RVV346-8	Olivine	-0.13	47.26	12.23	0.42	0.12	0.06	0.84	12.12	-0.06	0.20	12.00	0.05	3.64	9.44	1.68	100.00
RVV346-9	Olivine	0.04	45.35	12.57	0.34	0.09	0.06	0.84	13.54	0.10	0.06	12.02	0.03	3.37	9.27	2.36	100.00
RVV346-10	Olivine	0.04	45.41	12.55	0.37	0.09	0.07	0.81	13.41	0.12	0.09	12.02	0.02	3.39	9.27	2.38	100.00
RVV346-11	Olivine	0.05	45.93	12.91	0.27	0.08	0.05	0.68	13.23	0.08	0.08	12.02	0.02	3.01	9.46	2.17	100.00
RVV346-11a	Olivine	0.05	45.89	12.97	0.24	0.08	0.05	0.69	13.23	0.08	0.08	12.02	0.03	2.98	9.47	2.19	100.00
RVV346-12	Olivine	0.04	45.68	12.67	0.29	0.09	0.05	0.65	13.63	0.11	0.07	12.02	0.03	3.02	9.59	2.10	100.00
RVV346-13	Olivine	0.03	46.97	10.89	0.25	0.07	0.03	0.53	14.49	0.13	0.17	12.02	0.03	3.03	9.46	1.95	100.00
RVV346-14	Olivine	-0.04	45.40	12.55	0.31	0.05	0.06	0.83	15.45	0.08	0.19	12.00	-0.01	3.48	7.45	2.17	100.00
RVV346-15	Olivine	-0.01	43.51	8.22	0.10	0.02	0.02	0.33	20.59	0.13	0.09	12.01	0.05	1.57	10.41	2.95	100.00
RVV346-16	Olivine	0.05	46.09	12.27	0.32	0.06	0.06	0.82	12.54	0.09	0.09	12.01	0.02	3.53	9.82	2.28	100.00
RVV346-17	Olivine	0.06	48.31	11.88	0.28	0.05	0.04	0.60	11.23	0.09	0.09	12.01	0.04	3.21	10.00	2.18	100.00
RVV346-18	Olivine	0.01	46.97	14.73	0.44	0.09	0.06	0.89	11.12	0.16	0.18	12.03	0.02	3.48	8.26	1.57	100.00
RVV346-19	Olivine	0.00	43.55	17.01	0.59	0.16	0.08	1.07	11.35	0.14	0.05	12.02	0.01	3.60	7.97	2.40	100.00
RVV346-20	Olivine	0.01	48.34	15.85	0.29	0.09	0.02	0.30	9.64	0.15	0.01	12.03	0.00	4.93	6.96	1.39	100.00
RVV346-21	Olivine	-0.01	43.24	15.49	0.56	0.23	0.11	1.04	13.85	0.15	0.07	12.00	0.00	3.36	6.92	2.99	100.00
RVV346-22	Olivine	-0.02	44.62	16.06	0.46	0.16	0.03	0.48	12.43	0.17	0.16	12.02	-0.01	4.48	6.92	2.01	100.00
RVV346-23	Olivine	-0.01	43.27	17.00	0.51	0.14	0.08	1.05	12.06	0.16	0.05	12.02	0.00	4.25	7.18	2.23	100.00
RVV346-24	Olivine	-0.01	43.14	14.68	0.56	0.14	0.07	0.95	15.47	0.15	0.08	12.02	0.03	3.46	7.08	2.18	100.00
RVV346 Average			45.45	13.31	0.36	0.09	0.06	0.77	13.32	0.11	0.11	12.02	0.02	3.41	8.78	2.19	100.00
RVV346 Stdev			1.73	2.03	0.12	0.04	0.02	0.24	2.06	0.04	0.07	0.01	0.02	0.62	1.17	0.36	0.00
RVV360a-1	Olivine	0.03	44.04	16.96	0.50	0.13	0.07	0.93	11.95	0.13	0.07	12.00	0.05	5.31	5.78	2.07	100.00
RVV360a-2	Olivine	0.04	46.11	16.20	0.45	0.10	0.06	0.77	10.99	0.13	0.08	12.00	0.00	5.59	5.78	1.72	100.00
RVV360a-3	Olivine	0.01	46.68	15.29	0.44	0.13	0.08	0.93	11.49	0.13	0.13	12.00	0.00	5.20	5.77	1.72	100.00
RVV360a-4	Olivine	0.01	41.11	14.82	0.45	0.15	0.09	1.13	14.98	0.15	0.05	12.02	0.02	4.41	8.41	2.21	100.00
RVV360a-5	Olivine	0.00	41.26	17.67	0.64	0.18	0.12	1.41	12.30	0.10	0.00	12.00	0.02	5.46	5.86	2.98	100.00
RVV360a-6	Olivine	0.00	53.11	19.08	0.47	0.00	0.22	1.59	3.28	0.24	0.01	12.00	0.00	3.08	5.83	1.07	100.00
RVV360a-7	Olivine	0.03	46.96	21.03	0.99	0.04	0.12	4.00	2.87	0.16	0.00	12.04	-0.01	4.35	5.83	1.62	100.00
RVV360a-8	Olivine	-0.03	49.88	20.37	0.41	0.07	0.10	1.99	4.92	0.29	0.03	11.98	-0.04	2.40	5.94	1.65	100.00
RVV360a-9	Olivine	0.07	41.59	17.24	0.52	0.15	0.10	1.24	12.21	0.13	0.03	12.00	0.03	5.37	5.96	3.43	100.00
RVV360a Average			45.64	17.63	0.54	0.11	0.11	1.56	9.44	0.16	0.04	12.01	0.01	4.58	6.13	2.05	100.00



Table 2.7C: Uncorrected Host Mineral Major Element Compositions

Sample	SiO <sub>2</sub>	Al <sub>2</sub> O <sub>3</sub>	K <sub>2</sub> O	MnO	FeO*	NiO	Na <sub>2</sub> O	MgO	CaO	TiO <sub>2</sub>	Cr <sub>2</sub> O <sub>3</sub>	Total
RVV302-1	38.26	0.06	0.00	0.25	20.35	0.18	0.00	41.14	0.33	0.03	0.00	100.59
RVV302-2	38.17	0.04	0.00	0.26	19.86	0.15	0.00	41.35	0.34	0.01	0.00	100.18
RVV302-3	38.31	0.05	0.00	0.27	19.65	0.20	-0.01	41.59	0.33	0.03	0.00	100.43
RVV302-4	37.97	0.06	0.00	0.25	20.08	0.15	0.00	40.66	0.34	0.02	0.00	99.53
RVV302-5	38.39	0.05	0.00	0.24	19.35	0.19	0.00	41.44	0.33	0.01	0.00	100.02
RVV302-6	38.47	0.05	0.00	0.23	18.77	0.15	0.01	42.00	0.31	0.03	0.00	100.00
RVV302-7	38.50	0.06	0.00	0.29	18.79	0.22	0.01	42.06	0.30	0.01	0.00	100.24
RVV302-8	38.65	0.06	0.00	0.24	19.03	0.18	0.01	42.06	0.31	0.03	0.00	100.58
RVV302-9	38.60	0.04	0.00	0.26	18.84	0.24	0.00	42.06	0.30	0.01	0.00	100.37
RVV302-10	38.14	0.04	0.00	0.30	19.93	0.14	0.00	41.33	0.33	0.01	0.00	100.22
RVV302-11	37.47	0.03	0.00	0.20	20.21	0.14	0.01	41.19	0.34	0.05	0.00	99.64
RVV302-12	38.15	0.06	0.00	0.29	19.38	0.24	0.01	40.92	0.31	0.02	0.00	99.38
RVV302-13	38.53	0.06	0.00	0.25	19.59	0.20	0.01	41.10	0.31	0.03	0.00	100.06
<i>RVV302 Average</i>	<i>38.28</i>	<i>0.05</i>	<i>0.00</i>	<i>0.26</i>	<i>19.53</i>	<i>0.18</i>	<i>0.00</i>	<i>41.45</i>	<i>0.32</i>	<i>0.02</i>	<i>0.00</i>	<i>100.10</i>
<i>RVV302 Stdev</i>	<i>0.32</i>	<i>0.01</i>	<i>0.00</i>	<i>0.03</i>	<i>0.55</i>	<i>0.04</i>	<i>0.01</i>	<i>0.47</i>	<i>0.01</i>	<i>0.01</i>	<i>0.00</i>	<i>0.38</i>
RVV306a-1	37.66	0.07	0.00	0.29	18.80	0.16	0.02	41.47	0.35	0.03	0.02	98.87
RVV306a-2	39.27	0.05	0.00	0.21	13.24	0.25	0.02	46.35	0.22	0.02	0.01	99.64
RVV306a-3	39.77	0.06	0.00	0.19	12.79	0.31	0.02	47.81	0.21	0.04	0.04	101.25
RVV306a-4	39.03	0.05	0.00	0.17	14.14	0.31	0.03	45.11	0.29	0.02	0.00	99.14
RVV306a-5	39.64	0.04	0.00	0.21	14.15	0.31	0.01	45.70	0.24	0.00	0.00	100.30
RVV306a-6	38.93	0.05	0.01	0.17	13.51	0.25	0.00	46.09	0.34	0.01	0.00	99.37
RVV306a-7	39.05	0.05	0.00	0.19	14.78	0.27	0.00	44.67	0.39	0.01	0.00	99.40
RVV306a-8	39.46	0.04	0.01	0.15	13.22	0.25	0.01	45.71	0.34	0.02	0.00	99.22
RVV306a-9	39.53	0.05	0.01	0.20	14.21	0.28	0.01	46.10	0.36	0.02	0.00	100.77
RVV306a-10	39.24	0.04	0.00	0.23	15.14	0.17	0.02	45.20	0.25	0.02	0.00	100.30
RVV306a-11	39.80	0.03	0.00	0.21	13.35	0.23	0.02	47.29	0.20	0.05	0.03	101.22
RVV306a-12	39.30	0.04	0.00	0.22	14.11	0.24	0.02	46.17	0.36	0.02	0.03	100.52
RVV306a-13	39.13	0.03	0.00	0.19	14.58	0.23	0.00	45.61	0.18	0.00	0.03	99.96
RVV306a-14	38.78	0.04	0.00	0.27	17.68	0.19	0.00	43.94	0.36	0.01	0.03	101.28
RVV306a-15	38.72	0.04	0.00	0.27	16.98	0.16	0.00	43.18	0.39	0.03	0.00	99.77
RVV306a-16	36.92	0.03	0.00	0.48	25.57	0.09	0.01	35.67	0.27	0.03	0.01	99.08
RVV306a-17	37.21	0.03	0.00	0.46	24.69	0.05	0.04	36.84	0.27	0.03	0.00	99.61
RVV306a-18	38.52	0.03	0.00	0.24	17.60	0.15	0.02	43.40	0.28	0.04	0.00	100.28
RVV306a-19	39.67	0.05	0.00	0.18	13.33	0.28	0.00	47.27	0.24	0.02	0.04	101.08
RVV306a-20	39.04	0.03	0.00	0.24	14.19	0.25	0.00	46.33	0.27	0.03	0.02	100.40
RVV306a-21	39.04	0.03	0.00	0.24	14.19	0.25	0.00	46.33	0.27	0.03	0.02	100.40
<i>RVV306a Average</i>	<i>38.94</i>	<i>0.04</i>	<i>0.00</i>	<i>0.24</i>	<i>15.73</i>	<i>0.22</i>	<i>0.01</i>	<i>44.58</i>	<i>0.29</i>	<i>0.02</i>	<i>0.01</i>	<i>100.09</i>
<i>RVV306a Stdev</i>	<i>0.79</i>	<i>0.01</i>	<i>0.00</i>	<i>0.09</i>	<i>3.54</i>	<i>0.07</i>	<i>0.01</i>	<i>3.15</i>	<i>0.07</i>	<i>0.01</i>	<i>0.02</i>	<i>0.76</i>
RVV312-1	52.50	29.46	0.18	0.00	0.49	0.00	4.40	0.06	12.06	0.09	0.00	99.24
RVV312-2	52.53	29.58	0.21	0.00	0.53	0.00	4.31	0.06	12.06	0.10	0.00	99.38
RVV312-3	52.57	29.63	0.19	0.01	0.42	0.00	4.43	0.06	12.03	0.11	0.00	99.46
RVV312-4	52.16	29.22	0.21	0.01	0.44	0.00	4.31	0.06	12.10	0.09	0.00	98.61
RVV312-5	52.39	28.99	0.20	0.00	0.96	0.00	4.40	0.00	12.28	0.00	0.00	99.21
RVV312-6	51.34	28.10	0.19	0.00	0.85	0.00	4.31	0.00	12.40	0.00	0.00	97.19
RVV312-7	51.45	29.59	0.21	0.00	0.78	0.00	4.90	0.00	11.70	0.00	0.00	98.62
RVV312-8	52.70	29.46	0.20	0.00	0.87	0.00	4.59	0.00	12.11	0.00	0.00	99.93
RVV312-9	53.02	29.33	0.22	0.00	0.81	0.00	4.65	0.00	11.93	0.00	0.00	99.96
RVV312-10	52.57	29.29	0.24	0.00	1.03	0.00	4.70	0.00	12.02	0.00	0.00	99.84
<i>RVV312 Average</i>	<i>52.32</i>	<i>29.27</i>	<i>0.20</i>	<i>0.00</i>	<i>0.72</i>	<i>0.00</i>	<i>4.50</i>	<i>0.02</i>	<i>12.07</i>	<i>0.04</i>	<i>0.00</i>	<i>99.14</i>



<i>RVV312 Stdev</i>	<i>0.54</i>	<i>0.45</i>	<i>0.02</i>	<i>0.00</i>	<i>0.22</i>	<i>0.00</i>	<i>0.20</i>	<i>0.03</i>	<i>0.19</i>	<i>0.05</i>	<i>0.00</i>	<i>0.84</i>
RVV316-6	37.92	0.04	0.00	0.29	18.71	0.11	0.01	41.47	0.28	0.05	0.00	98.88
RVV316-7	37.94	0.05	0.00	0.30	18.70	0.14	0.00	41.41	0.28	0.04	0.00	98.85
RVV316-8	37.49	0.04	0.00	0.33	22.66	0.09	0.00	38.98	0.25	0.00	0.00	99.83
RVV316-9	37.82	0.04	0.00	0.32	22.07	0.12	0.00	38.80	0.25	0.06	0.01	99.51
RVV316-11	38.92	0.04	0.00	0.28	15.73	0.19	0.02	43.87	0.28	0.06	0.02	99.40
RVV316-11a	38.92	0.04	0.00	0.28	15.73	0.19	0.02	43.87	0.28	0.06	0.02	99.40
RVV316-12	39.77	0.08	0.00	0.25	15.10	0.20	0.01	44.30	0.28	0.03	0.03	100.05
RVV316-13	39.16	0.03	0.00	0.22	14.35	0.24	0.00	45.36	0.28	0.04	0.02	99.69
RVV316-14	39.16	0.03	0.00	0.22	14.35	0.24	0.00	45.36	0.28	0.04	0.02	99.69
RVV316-15	39.57	0.03	0.00	0.17	12.27	0.30	0.01	47.34	0.19	0.00	0.02	99.90
RVV316-16	39.16	0.01	0.00	0.20	13.60	0.24	0.01	46.16	0.21	0.02	0.03	99.64
RVV316-17	39.21	0.03	0.00	0.20	13.10	0.24	0.03	45.76	0.23	0.00	0.03	98.82
RVV316-18	39.36	0.03	0.00	0.23	15.08	0.29	0.02	44.79	0.21	0.05	0.05	100.10
RVV316-19	39.25	0.04	0.00	0.21	14.06	0.27	0.01	46.85	0.15	0.01	0.02	100.85
RVV316-20	40.01	0.03	0.00	0.18	11.88	0.33	0.02	48.48	0.20	0.00	0.02	101.15
RVV316-21	39.74	0.03	0.00	0.19	12.17	0.29	0.02	48.24	0.21	0.02	0.03	100.94
RVV316-22	38.30	0.02	0.00	0.41	22.16	0.08	0.01	40.56	0.36	0.02	0.01	101.92
RVV316-23	38.45	0.02	0.00	0.33	20.33	0.15	0.00	41.39	0.22	0.04	0.00	100.94
RVV316-24	38.83	0.05	0.00	0.29	19.29	0.15	0.01	44.20	0.24	0.04	0.01	103.09
RVV316-25	38.31	0.05	0.00	0.27	18.48	0.17	0.01	44.14	0.27	0.04	0.00	101.73
RVV316-26	38.20	0.04	0.00	0.27	18.40	0.17	0.02	43.08	0.26	0.03	0.00	100.46
<i>RVV316 Average</i>	<i>38.83</i>	<i>0.04</i>	<i>0.00</i>	<i>0.26</i>	<i>16.58</i>	<i>0.20</i>	<i>0.01</i>	<i>44.02</i>	<i>0.25</i>	<i>0.03</i>	<i>0.01</i>	<i>100.23</i>
<i>RVV316 Stdev</i>	<i>0.71</i>	<i>0.01</i>	<i>0.00</i>	<i>0.06</i>	<i>3.46</i>	<i>0.07</i>	<i>0.01</i>	<i>2.78</i>	<i>0.05</i>	<i>0.02</i>	<i>0.01</i>	<i>1.11</i>
RVV321-1	37.98	0.08	0.00	0.33	20.47	0.13	0.01	41.08	0.28	0.01	0.00	100.38
RVV321-2	37.10	0.09	0.00	0.37	21.57	0.12	0.03	39.97	0.28	0.00	0.02	99.56
RVV321-3	37.75	0.09	0.00	0.37	21.67	0.15	0.02	40.10	0.28	0.08	0.00	100.50
RVV321-4	37.82	0.08	0.00	0.26	18.56	0.22	0.00	42.17	0.24	0.04	0.02	99.39
RVV321-5	37.38	0.07	0.00	0.35	21.01	0.14	0.01	38.78	0.26	0.00	0.01	98.01
RVV321-6	39.64	0.06	0.00	0.33	17.84	0.18	0.02	42.71	0.38	0.00	0.01	101.17
RVV321-7	38.47	0.04	0.00	0.27	16.66	0.22	0.01	45.09	0.39	0.00	0.00	101.16
RVV321-8	38.40	0.08	0.00	0.32	20.35	0.14	0.01	40.93	0.26	0.00	0.01	100.50
RVV321-9	38.40	0.08	0.00	0.32	20.35	0.14	0.01	40.93	0.26	0.00	0.01	100.50
RVV321-10	37.95	0.05	0.01	0.35	22.89	0.18	0.00	39.08	0.26	0.02	0.00	100.80
RVV321-11	38.00	0.04	-0.01	0.30	21.97	0.15	0.02	39.93	0.26	0.03	0.00	100.70
RVV321-12	38.18	0.07	-0.01	0.36	21.59	0.17	0.01	40.66	0.27	0.02	0.00	101.33
RVV321-13	37.72	0.04	0.00	0.30	19.98	0.18	0.01	41.42	0.29	0.03	0.00	99.97
RVV321-14	38.24	0.05	0.00	0.30	19.91	0.17	0.00	42.15	0.27	0.03	0.00	101.12
RVV321-15	37.78	0.04	0.00	0.31	21.26	0.14	0.00	40.08	0.25	0.04	0.00	99.90
RVV321-16	39.00	0.04	0.00	0.25	15.83	0.17	0.01	44.15	0.41	0.01	0.00	99.87
RVV321-17	37.45	0.04	0.00	0.39	21.12	0.14	0.01	40.30	0.26	0.04	0.02	99.77
RVV321-18	37.45	0.04	0.00	0.39	21.12	0.14	0.01	40.30	0.26	0.04	0.02	99.77
RVV321-19	38.98	0.04	0.00	0.27	18.73	0.17	0.04	43.82	0.25	0.04	0.00	102.33
RVV321-20	37.95	0.05	0.00	0.33	22.05	0.10	0.01	40.39	0.25	0.04	0.01	101.17
RVV321-21	39.19	0.04	0.00	0.28	18.15	0.13	0.01	44.77	0.24	0.01	0.01	102.82
RVV321-22	39.17	0.04	0.00	0.28	17.52	0.15	0.01	45.37	0.31	0.01	0.00	102.85
RVV321-23	37.97	0.05	0.00	0.32	21.02	0.11	0.02	41.16	0.25	0.00	0.00	100.88
RVV321-24	38.12	0.05	0.00	0.32	21.32	0.10	0.00	41.91	0.25	0.04	0.00	102.10
RVV321-25	38.16	0.03	0.00	0.31	21.33	0.10	0.02	41.54	0.26	0.00	0.00	101.75
RVV321-26	39.10	0.06	0.00	0.26	18.43	0.18	0.02	43.24	0.26	0.06	0.02	101.60
RVV321-27	39.08	0.05	0.00	0.27	17.60	0.16	0.01	44.89	0.34	0.00	0.00	102.38

RVV321-28	38.25	0.04	0.00	0.35	21.94	0.10	0.01	41.14	0.26	0.01	0.01	102.10
RVV321-29	38.63	0.03	0.00	0.27	18.51	0.15	0.01	42.98	0.26	0.06	0.01	100.91
RVV321-30	38.65	0.05	0.00	0.33	21.25	0.11	0.02	41.32	0.24	0.00	0.00	101.97
RVV321-31	37.75	0.06	0.00	0.31	21.08	0.11	0.02	40.40	0.24	0.02	0.00	99.99
RVV321-32	38.48	0.04	0.00	0.30	19.19	0.13	0.00	42.44	0.27	0.02	0.00	100.87
RVV321-33	38.69	0.06	0.00	0.28	19.19	0.11	0.01	42.89	0.27	0.02	0.01	101.50
RVV321-34	39.37	0.04	0.00	0.25	15.05	0.23	0.02	45.99	0.29	0.04	0.02	101.30
RVV321-35	38.24	0.04	0.00	0.25	18.33	0.08	0.01	42.34	0.31	0.05	0.01	99.67
<i>RVV321 Average</i>	<i>38.30</i>	<i>0.05</i>	<i>0.00</i>	<i>0.31</i>	<i>19.85</i>	<i>0.14</i>	<i>0.01</i>	<i>41.90</i>	<i>0.28</i>	<i>0.02</i>	<i>0.01</i>	<i>100.87</i>
<i>RVV321 Stdev</i>	<i>0.62</i>	<i>0.02</i>	<i>0.00</i>	<i>0.04</i>	<i>1.92</i>	<i>0.04</i>	<i>0.01</i>	<i>1.86</i>	<i>0.04</i>	<i>0.02</i>	<i>0.01</i>	<i>1.07</i>
RVV340-1	38.63	0.07	0.00	0.22	13.96	0.25	0.00	45.33	0.31	0.00	0.05	98.81
RVV340-2	38.23	0.07	0.00	0.27	18.60	0.15	0.00	43.87	0.31	0.02	0.04	101.57
RVV340-3	38.58	0.10	0.00	0.26	17.58	0.20	0.01	42.54	0.30	0.04	0.03	99.64
RVV340-4	38.44	0.06	0.00	0.24	17.55	0.23	0.00	42.30	0.27	0.03	0.01	99.13
RVV340-5	38.63	0.07	0.00	0.26	17.42	0.22	0.01	42.43	0.26	0.00	0.03	99.34
RVV340-6	38.89	0.07	0.00	0.24	17.61	0.20	0.01	42.61	0.26	0.00	0.04	99.93
RVV340-7	38.74	0.08	0.00	0.23	17.67	0.19	0.02	42.73	0.26	0.02	0.03	99.96
RVV340-8	37.79	0.08	0.00	0.25	18.46	0.21	0.02	42.38	0.29	0.01	0.02	99.51
RVV340-9	38.72	0.10	0.00	0.23	18.16	0.16	0.01	43.33	0.28	0.02	0.02	101.01
RVV340-10	38.79	0.06	0.00	0.24	17.19	0.21	0.00	43.10	0.28	0.03	0.03	99.92
RVV340-11	38.70	0.05	0.00	0.22	18.08	0.17	0.02	42.72	0.29	0.03	0.00	100.28
RVV340-12	39.21	0.04	0.00	0.17	14.26	0.25	0.00	45.50	0.34	0.02	0.00	99.80
RVV340-13	37.42	0.03	0.00	0.23	19.06	0.23	0.01	41.51	0.29	0.03	0.00	98.81
RVV340-14	38.64	0.08	0.00	0.23	17.66	0.21	0.01	42.81	0.29	0.01	0.00	99.94
RVV340-15	37.83	0.04	0.01	0.29	19.45	0.16	0.01	40.34	0.32	0.02	0.00	98.47
RVV340-16	38.69	0.04	0.00	0.29	18.95	0.18	0.01	41.91	0.31	0.02	0.00	100.39
RVV340-17	38.43	0.05	0.00	0.26	17.77	0.21	0.02	42.94	0.28	0.06	0.03	100.05
RVV340-18	38.19	0.03	0.00	0.26	17.74	0.22	0.02	42.03	0.30	0.01	0.00	98.80
RVV340-19	38.00	0.06	0.00	0.25	17.18	0.20	0.02	43.51	0.28	0.00	0.02	99.52
RVV340-20	37.97	0.07	0.00	0.24	17.22	0.21	0.02	44.20	0.27	0.05	0.02	100.27
RVV340-21	37.98	0.04	0.00	0.28	19.12	0.20	0.01	43.36	0.29	0.00	0.00	101.27
RVV340-22	38.71	0.06	0.00	0.25	18.28	0.18	0.01	43.04	0.28	0.05	0.01	100.86
RVV340-23	38.93	0.04	0.00	0.25	17.77	0.18	0.02	43.21	0.28	0.00	0.02	100.69
RVV340-24	37.72	0.05	0.00	0.25	17.04	0.24	0.01	44.51	0.27	0.01	0.03	100.12
RVV340-25	38.11	0.04	0.00	0.26	18.03	0.20	0.03	44.42	0.28	0.01	0.02	101.41
RVV340-26	38.83	0.06	0.00	0.22	15.17	0.24	0.06	46.43	0.30	0.07	0.03	101.40
RVV340-27	37.95	0.03	0.00	0.26	17.97	0.20	0.05	44.04	0.30	0.00	0.01	100.82
RVV340-28	38.05	0.97	0.00	0.22	17.48	0.18	0.23	43.54	0.27	0.04	0.01	100.99
<i>RVV340 Average</i>	<i>38.39</i>	<i>0.09</i>	<i>0.00</i>	<i>0.25</i>	<i>17.59</i>	<i>0.20</i>	<i>0.02</i>	<i>43.24</i>	<i>0.29</i>	<i>0.02</i>	<i>0.02</i>	<i>100.10</i>
<i>RVV340 Stdev</i>	<i>0.44</i>	<i>0.17</i>	<i>0.00</i>	<i>0.02</i>	<i>1.28</i>	<i>0.03</i>	<i>0.04</i>	<i>1.27</i>	<i>0.02</i>	<i>0.02</i>	<i>0.01</i>	<i>0.87</i>
RVV343-1	39.06	0.03	0.00	0.21	13.00	0.30	0.02	46.40	0.18	0.04	0.02	99.26
RVV343-2	37.64	0.06	0.00	0.32	24.26	0.11	0.01	39.07	0.27	0.04	0.00	101.77
RVV343-3	36.88	0.04	0.01	0.37	24.89	0.14	0.01	37.52	0.28	0.02	0.00	100.17
RVV343-4	49.11	29.72	0.17	0.01	0.58	0.01	3.30	0.10	13.67	0.08	0.00	96.76
RVV343-5	50.37	29.85	0.16	0.00	0.55	0.02	3.60	0.11	13.42	0.07	0.00	98.17
RVV343-6	51.20	27.46	0.00	0.00	0.59	0.01	4.23	0.11	12.58	0.02	0.01	96.19
RVV343-7	51.20	27.46	0.00	0.00	0.59	0.01	4.23	0.11	12.58	0.02	0.01	96.19
RVV343-8	36.70	0.04	0.00	0.33	23.29	0.10	0.01	38.65	0.26	0.00	0.00	99.39
RVV343-9	48.15	29.60	0.00	0.00	0.61	0.00	2.81	0.09	14.96	0.11	0.02	96.34
RVV343-10	48.45	29.36	0.00	0.00	0.64	0.01	3.01	0.08	14.63	0.01	0.00	96.18
<i>RVV343 Average</i>	<i>44.88</i>	<i>17.36</i>	<i>0.03</i>	<i>0.12</i>	<i>8.90</i>	<i>0.07</i>	<i>2.12</i>	<i>16.22</i>	<i>8.28</i>	<i>0.04</i>	<i>0.01</i>	<i>98.04</i>

<i>RVV343 Stdev</i>	6.40	14.93	0.07	0.16	11.20	0.09	1.87	20.95	6.96	0.04	0.01	2.02
RVV344-1	39.49	0.09	0.00	0.28	15.50	0.18	0.01	44.26	0.39	0.00	0.01	100.20
RVV344-2	39.51	0.08	0.00	0.28	15.59	0.15	0.01	44.43	0.40	0.02	0.02	100.49
RVV344-3	39.43	0.10	0.00	0.28	15.26	0.21	0.04	44.13	0.41	0.04	0.02	99.91
RVV344-4	39.78	0.07	0.00	0.24	14.73	0.18	0.01	45.16	0.40	0.04	0.01	100.62
RVV344-5	40.32	0.06	0.00	0.24	14.32	0.21	0.02	46.66	0.38	0.06	0.04	102.30
RVV344-6	39.32	0.11	0.00	0.30	16.52	0.17	0.03	44.65	0.44	0.02	0.03	101.57
RVV344-7	39.24	0.06	0.00	0.23	14.35	0.23	0.01	44.94	0.31	0.04	0.04	99.45
RVV344-8	38.37	0.07	0.00	0.37	22.64	0.14	0.03	39.62	0.27	0.00	0.00	101.51
RVV344-9	39.81	0.07	0.00	0.22	14.04	0.28	0.02	46.18	0.39	0.03	0.03	101.08
RVV344-10	39.70	0.05	0.00	0.21	13.87	0.25	0.01	46.33	0.36	0.02	0.05	100.85
RVV344-11	39.22	0.07	0.00	0.24	15.28	0.18	0.00	44.87	0.42	0.00	0.03	100.31
RVV344-12	37.26	0.08	0.00	0.41	21.96	0.14	0.00	39.40	0.29	0.00	0.00	99.55
RVV344-13	39.60	0.08	0.00	0.30	17.14	0.18	0.01	44.71	0.40	0.02	0.02	102.46
RVV344-14	37.82	0.07	0.00	0.25	15.46	0.19	0.00	43.92	0.41	0.01	0.02	98.13
RVV344-15	37.70	0.07	0.00	0.31	16.99	0.18	0.01	43.39	0.40	0.02	0.00	99.07
RVV344-16	40.17	0.08	0.00	0.22	14.15	0.26	0.02	47.00	0.33	0.01	0.05	102.29
RVV344-17	39.56	0.06	0.00	0.25	14.83	0.22	0.02	45.99	0.35	0.00	0.03	101.29
RVV344-18	38.93	0.05	0.00	0.24	14.82	0.25	0.00	45.88	0.37	0.01	0.02	100.56
RVV344-19	38.63	0.09	0.00	0.30	17.52	0.16	0.00	43.22	0.41	0.00	0.02	100.34
RVV344-20	38.58	0.08	0.00	0.30	16.79	0.18	0.00	43.31	0.39	0.00	0.00	99.63
RVV344-21	38.67	0.10	0.00	0.23	14.42	0.25	0.01	45.06	0.36	0.03	0.05	99.17
RVV344-22	39.02	0.08	0.00	0.22	14.80	0.23	0.00	45.23	0.38	0.02	0.03	100.01
RVV344-23	39.02	0.08	0.00	0.21	14.09	0.24	0.02	45.42	0.33	0.00	0.04	99.44
RVV344-24	39.17	0.09	0.00	0.21	14.09	0.28	0.01	45.49	0.33	0.00	0.05	99.71
RVV344-25	39.08	0.10	0.00	0.22	13.39	0.32	0.02	46.10	0.34	0.01	0.03	99.60
RVV344-26	37.86	0.08	0.00	0.21	15.25	0.21	0.02	45.15	0.38	0.01	0.03	99.18
RVV344-27	38.08	0.10	0.00	0.25	15.43	0.22	0.01	44.54	0.41	0.10	0.03	99.19
<i>RVV344 Average</i>	39.01	0.08	0.00	0.26	15.68	0.21	0.01	44.63	0.37	0.02	0.03	100.29
<i>RVV344 Stdev</i>	0.77	0.02	0.00	0.05	2.19	0.05	0.01	1.77	0.04	0.02	0.02	1.10
RVV345-1	38.05	0.05	0.00	0.29	16.45	0.21	0.01	43.75	0.36	0.03	0.05	99.24
RVV345-2	37.55	0.05	0.00	0.29	16.50	0.19	0.02	43.08	0.33	0.02	0.04	98.08
RVV345-2a	37.55	0.05	0.00	0.29	16.50	0.19	0.02	43.08	0.33	0.02	0.04	98.08
RVV345-3	37.72	0.06	0.00	0.27	16.68	0.22	0.02	42.99	0.33	0.04	0.07	98.39
RVV345-4	38.05	0.06	0.00	0.30	16.48	0.20	0.03	42.88	0.33	0.00	0.02	98.34
RVV345-5	38.86	0.05	0.00	0.34	18.56	0.19	0.01	41.71	0.33	0.09	0.00	100.13
RVV345-6	37.06	0.06	0.00	0.33	18.38	0.17	0.01	41.66	0.34	0.04	0.01	98.06
RVV345-7	37.38	0.06	0.00	0.31	17.58	0.20	0.02	41.62	0.36	0.04	0.03	97.60
RVV345-8	38.90	0.09	0.00	0.24	14.08	0.24	0.02	45.19	0.36	0.00	0.02	99.14
RVV345-9	38.97	0.10	0.00	0.24	15.00	0.24	0.01	45.68	0.40	0.08	0.03	100.76
RVV345-10	38.75	0.21	0.00	0.24	14.82	0.24	0.00	45.19	0.43	0.04	0.06	99.97
RVV345-11	38.83	0.18	0.00	0.24	14.95	0.24	0.01	45.34	0.49	0.02	0.08	100.39
RVV345-12	38.78	0.18	0.00	0.22	14.43	0.23	0.01	45.03	0.60	0.01	0.14	99.63
RVV345-13	38.64	0.09	0.00	0.23	14.66	0.20	0.01	45.42	0.35	0.07	0.02	99.68
RVV345-14	38.78	0.18	0.00	0.22	14.43	0.23	0.01	45.03	0.60	0.01	0.14	99.63
RVV345-15	38.25	0.10	0.00	0.28	16.21	0.19	0.02	43.82	0.36	0.04	0.02	99.27
RVV345-15a	38.25	0.10	0.00	0.28	16.21	0.19	0.02	43.82	0.36	0.04	0.02	99.27
RVV345-16	39.01	0.05	0.01	0.20	14.54	0.26	0.01	44.97	0.33	0.01	0.00	99.38
RVV345-17	39.11	0.07	0.01	0.26	15.15	0.16	0.01	44.54	0.39	0.02	0.00	99.72
RVV345-18	38.10	0.08	0.00	0.29	16.99	0.18	0.00	42.87	0.36	0.01	0.00	98.86
RVV345-19	38.39	0.11	0.01	0.32	17.41	0.17	0.01	42.72	0.42	0.02	0.00	99.57

RVV345-20	38.70	0.08	0.00	0.22	15.54	0.25	0.00	44.16	0.30	0.02	0.00	99.29
RVV345-21	38.99	0.04	0.00	0.18	14.17	0.28	0.00	45.20	0.28	0.01	0.00	99.15
RVV345-22	39.59	0.07	0.00	0.22	13.74	0.31	0.00	45.95	0.28	0.01	0.00	100.16
RVV345-23	39.27	0.07	0.00	0.22	13.40	0.30	0.00	45.64	0.22	0.01	0.00	99.13
RVV345-23a	39.27	0.07	0.00	0.22	13.40	0.30	0.00	45.64	0.22	0.01	0.00	99.13
RVV345-24	38.96	0.09	0.00	0.11	12.84	0.32	0.01	45.93	0.30	0.01	0.00	98.58
RVV345-25	39.30	0.07	0.00	0.22	13.07	0.32	0.00	46.45	0.21	0.01	0.00	99.66
RVV345-25a	39.30	0.07	0.00	0.22	13.07	0.32	0.00	46.45	0.21	0.01	0.00	99.66
<i>RVV345 Average</i>	<i>38.56</i>	<i>0.09</i>	<i>0.00</i>	<i>0.25</i>	<i>15.35</i>	<i>0.23</i>	<i>0.01</i>	<i>44.34</i>	<i>0.35</i>	<i>0.03</i>	<i>0.03</i>	<i>99.24</i>
<i>RVV345 Stdev</i>	<i>0.65</i>	<i>0.04</i>	<i>0.00</i>	<i>0.05</i>	<i>1.62</i>	<i>0.05</i>	<i>0.01</i>	<i>1.46</i>	<i>0.09</i>	<i>0.02</i>	<i>0.04</i>	<i>0.75</i>
RVV346-1	39.44	0.10	0.00	0.21	13.45	0.24	0.00	46.17	0.30	0.01	0.02	99.94
RVV346-2	39.08	0.10	0.00	0.25	15.28	0.17	0.01	45.63	0.38	0.08	0.02	100.99
RVV346-3	39.08	0.10	0.00	0.25	15.28	0.17	0.01	45.63	0.38	0.08	0.02	100.99
RVV346-4	39.09	0.07	0.00	0.21	14.42	0.27	0.02	45.05	0.30	0.04	0.03	99.50
RVV346-5	39.25	0.07	0.00	0.23	14.37	0.23	0.01	45.08	0.31	0.00	0.01	99.56
RVV346-6	38.00	0.07	0.00	0.30	17.07	0.14	0.03	42.37	0.40	0.00	0.02	98.40
RVV346-7	38.69	0.11	0.00	0.24	15.18	0.21	0.02	44.46	0.33	0.00	0.02	99.26
RVV346-8	38.67	0.08	0.00	0.25	14.56	0.21	0.01	44.74	0.35	0.03	0.03	98.92
RVV346-9	38.70	0.08	0.00	0.25	14.82	0.25	0.01	44.82	0.36	0.02	0.03	99.34
RVV346-10	38.70	0.08	0.00	0.25	14.82	0.25	0.01	44.82	0.36	0.02	0.03	99.34
RVV346-11	38.33	0.07	0.00	0.25	14.61	0.22	0.02	45.10	0.29	0.06	0.04	98.99
RVV346-12	38.50	0.06	0.00	0.23	14.46	0.21	0.03	45.27	0.30	0.04	0.03	99.13
RVV346-13	38.53	0.07	0.00	0.25	14.58	0.21	0.02	44.93	0.33	0.03	0.06	99.00
RVV346-14	38.02	0.06	0.00	0.36	17.47	0.22	0.03	42.34	0.36	0.05	0.04	98.94
RVV346-15	38.41	0.05	0.00	0.21	13.30	0.34	0.03	45.27	0.26	0.01	0.04	97.92
RVV346-16	39.43	0.04	0.00	0.23	14.19	0.23	0.01	45.56	0.28	0.01	0.04	100.02
RVV346-17	39.02	0.14	0.00	0.24	13.90	0.34	0.02	45.46	0.32	0.00	0.08	99.50
RVV346-18	38.34	0.05	0.00	0.28	16.05	0.20	0.02	43.13	0.33	0.00	0.07	98.46
RVV346-19	38.34	0.06	0.00	0.28	16.56	0.20	0.02	43.14	0.33	0.00	0.02	98.96
RVV346-20	37.90	0.06	0.00	0.32	18.18	0.16	0.03	41.27	0.32	0.01	0.01	98.25
RVV346-21	37.26	0.04	0.00	0.33	17.99	0.16	0.02	40.75	0.35	0.02	0.00	96.90
RVV346-22	37.29	0.07	0.00	0.33	18.02	0.18	0.07	40.67	0.36	0.01	0.04	97.04
RVV346-23	37.74	0.07	0.00	0.31	17.76	0.21	0.02	41.63	0.36	0.04	0.00	98.14
RVV346-24	38.98	0.06	0.00	0.33	18.34	0.18	0.00	42.35	0.34	0.00	0.00	100.58
<i>RVV346 Average</i>	<i>38.53</i>	<i>0.07</i>	<i>0.00</i>	<i>0.27</i>	<i>15.61</i>	<i>0.22</i>	<i>0.02</i>	<i>43.98</i>	<i>0.33</i>	<i>0.02</i>	<i>0.03</i>	<i>99.09</i>
<i>RVV346 Stdev</i>	<i>0.61</i>	<i>0.02</i>	<i>0.00</i>	<i>0.04</i>	<i>1.63</i>	<i>0.05</i>	<i>0.01</i>	<i>1.73</i>	<i>0.03</i>	<i>0.02</i>	<i>0.02</i>	<i>1.03</i>
RVV360a-1	36.70	0.04	0.00	0.32	20.88	0.14	0.02	39.42	0.30	0.02	0.00	97.84
RVV360a-2	37.02	0.04	0.00	0.36	20.94	0.16	0.01	39.67	0.30	0.02	0.00	98.53
RVV360a-3	37.39	0.03	0.01	0.31	20.84	0.18	0.02	39.17	0.30	0.02	0.00	98.27
RVV360a-4	38.73	0.05	0.01	0.28	15.99	0.19	0.01	43.86	0.42	0.02	0.00	99.54
RVV360a-5	37.94	0.02	0.00	0.28	21.11	0.11	0.01	40.45	0.36	0.03	0.00	100.31
RVV360a-6	38.00	0.03	0.00	0.33	20.97	0.17	0.01	39.73	0.30	0.01	0.00	99.56
RVV360a-7	37.99	0.02	0.01	0.34	21.13	0.17	0.00	40.06	0.30	0.00	0.00	100.02
RVV360a-8	37.87	0.03	0.02	0.32	20.75	0.14	0.01	40.17	0.30	0.01	0.00	99.61
RVV360a-9	39.14	1.20	0.05	0.36	20.06	0.03	0.21	39.08	0.72	0.08	0.00	100.93
<i>RVV360a Average</i>	<i>37.87</i>	<i>0.16</i>	<i>0.01</i>	<i>0.32</i>	<i>20.30</i>	<i>0.15</i>	<i>0.03</i>	<i>40.18</i>	<i>0.37</i>	<i>0.02</i>	<i>0.00</i>	<i>99.40</i>
<i>RVV360a Stdev</i>	<i>0.77</i>	<i>0.39</i>	<i>0.02</i>	<i>0.03</i>	<i>1.65</i>	<i>0.05</i>	<i>0.07</i>	<i>1.45</i>	<i>0.14</i>	<i>0.02</i>	<i>0.00</i>	<i>1.01</i>
RVV362-1	49.03	31.61	0.16	0.00	0.61	0.00	2.88	0.07	14.82	0.05	0.00	99.22
RVV362-2	50.59	30.16	0.19	0.00	0.69	0.00	3.47	0.11	13.55	0.07	0.00	98.84
RVV362-3	48.00	30.28	0.15	0.00	0.63	0.00	3.19	0.10	14.12	0.07	0.00	96.54
RVV362-4	50.64	29.69	0.17	0.00	0.57	0.01	3.71	0.12	13.22	0.09	0.00	98.22

RVV362-5	48.18	31.10	0.11	0.06	0.61	0.00	2.97	0.09	14.76	0.07	0.00	97.94
RVV362-6	47.75	31.12	0.11	0.00	0.60	0.02	2.76	0.11	15.09	0.06	0.00	97.61
RVV362-7	52.79	29.35	0.17	0.00	1.10	0.00	3.94	0.00	12.68	0.00	0.00	100.02
RVV362-8	52.17	29.46	0.13	0.00	0.93	0.00	3.83	0.00	13.31	0.00	0.00	99.82
RVV362-9	51.67	29.97	0.14	0.00	1.16	0.00	3.57	0.00	13.47	0.00	0.00	99.98
RVV362-10	50.09	30.11	0.17	0.00	1.21	0.00	3.97	0.00	13.10	0.00	0.00	98.65
RVV362-11	51.74	29.98	0.15	0.00	1.00	0.00	3.80	0.00	13.33	0.00	0.00	100.00
RVV362-12	52.69	29.55	0.15	0.00	0.87	0.00	3.84	0.00	13.01	0.00	0.00	100.10
RVV362-13	51.61	30.76	0.12	0.00	1.20	0.00	3.53	0.00	13.75	0.00	0.00	100.96
RVV362-14	51.24	29.80	0.14	0.00	1.32	0.00	3.45	0.00	13.57	0.00	0.00	99.51
RVV362-15	50.07	31.01	0.15	0.00	1.13	0.00	3.91	0.00	13.57	0.00	0.00	99.83
RVV362-16	51.31	30.45	0.13	0.00	1.06	0.00	3.43	0.00	13.91	0.00	0.00	100.29
RVV362-17	51.78	29.90	0.14	0.00	1.05	0.00	3.78	0.00	13.40	0.00	0.00	100.05
RVV362-18	50.78	31.20	0.12	0.00	1.26	0.00	3.40	0.00	14.21	0.00	0.00	100.96
RVV362-19	51.71	29.69	0.15	0.00	1.08	0.00	3.92	0.00	13.04	0.00	0.00	99.59
RVV362-20	49.79	31.52	0.09	0.00	1.37	0.00	2.70	0.00	15.12	0.00	0.00	100.59
<i>RVV362 Average</i>	<i>50.68</i>	<i>30.33</i>	<i>0.14</i>	<i>0.00</i>	<i>0.97</i>	<i>0.00</i>	<i>3.50</i>	<i>0.03</i>	<i>13.75</i>	<i>0.02</i>	<i>0.00</i>	<i>99.43</i>
<i>RVV362 Stdev</i>	<i>1.50</i>	<i>0.71</i>	<i>0.02</i>	<i>0.01</i>	<i>0.27</i>	<i>0.01</i>	<i>0.41</i>	<i>0.05</i>	<i>0.72</i>	<i>0.03</i>	<i>0.00</i>	<i>1.15</i>

---

\*FeO reported as total iron

Table 2.8A: Uncorrected Melt Inclusions Trace Element Compositions-no host addition/subtraction

Sample	MELT	Ca	Li	B	Ti	Sr	Y	Zr	Nb	Ba	La	Ce	Nd	Sm	Eu	Gd	Dy	Er	Yb	Hf
RVV302-1	0.99	87284				589.6	30.7	174.3	45.9	223.6	37.1	77.5	31.9	7.6	2.5	6.1	6.0	2.9	2.5	4.9
<i>RVV302 Average</i>	<i>0.99</i>					<i>594.8</i>	<i>30.9</i>	<i>175.9</i>	<i>46.3</i>	<i>225.6</i>	<i>37.4</i>	<i>78.2</i>	<i>32.2</i>	<i>7.6</i>	<i>2.6</i>	<i>6.2</i>	<i>6.0</i>	<i>2.9</i>	<i>2.5</i>	<i>5.0</i>
<i>RVV302 Stdev</i>																				
RVV306a-14	0.72	148175			27010	1627.4	49.5	409.8	177.5	1006.1	178.3	344.6	144.8	23.1	5.3	19.8	12.4	5.7	2.8	8.7
RVV306a-15	0.62	101149			19962	986.2	30.8	291.0	108.1	606.7	91.7	178.2	77.9	17.1	2.4	8.7	8.2	4.3	1.9	5.8
RVV306a-18	0.86	155904			25147	1388.7	47.7	344.2	137.8	810.3	134.8	260.9	109.2	19.0	3.9	14.3	10.6	4.4	2.9	7.0
RVV306a-19	0.77	144015			21578	1215.0	41.4	287.6	112.3	682.0	109.6	209.1	88.5	15.2	2.9	11.8	9.6	4.2	2.5	6.0
<i>RVV306a Average</i>	<i>0.74</i>	<i>137311</i>			<i>23424</i>	<i>1304.3</i>	<i>42.3</i>	<i>333.1</i>	<i>133.9</i>	<i>776.3</i>	<i>128.6</i>	<i>248.2</i>	<i>105.1</i>	<i>18.6</i>	<i>3.6</i>	<i>13.6</i>	<i>10.2</i>	<i>4.7</i>	<i>2.5</i>	<i>6.9</i>
<i>RVV306a Stdev</i>	<i>0.10</i>	<i>24606</i>			<i>3226</i>	<i>271.2</i>	<i>8.5</i>	<i>57.3</i>	<i>31.9</i>	<i>174.8</i>	<i>37.6</i>	<i>72.8</i>	<i>29.5</i>	<i>3.4</i>	<i>1.2</i>	<i>4.7</i>	<i>1.8</i>	<i>0.7</i>	<i>0.4</i>	<i>1.3</i>
RVV312-1	0.78	65855				790.3	16.7	116.9	26.1	157.1	18.7	39.8	19.9	4.3	1.2	4.6	3.1	1.6	0.9	3.2
RVV312-2	0.79	66422				873.5	12.0	79.7	15.5	118.5	13.1	26.5	14.0	3.2	0.7	2.7	0.0	0.0	0.0	0.1
RVV312-3	0.72	57415				736.1	20.5	137.8	27.0	170.3	21.9	45.7	22.1	4.5	2.1	5.9	4.0	2.7	1.2	3.4
RVV312-4	0.73	53433				790.1	18.4	118.3	23.3	149.3	18.9	42.7	19.1	5.4	1.5	5.1	3.8	1.8	1.2	3.1
<i>RVV312 Average</i>	<i>0.76</i>	<i>60782</i>				<i>797.5</i>	<i>16.9</i>	<i>113.2</i>	<i>23.0</i>	<i>148.8</i>	<i>18.1</i>	<i>38.7</i>	<i>18.8</i>	<i>4.3</i>	<i>1.4</i>	<i>4.6</i>	<i>2.8</i>	<i>1.5</i>	<i>0.8</i>	<i>2.5</i>
<i>RVV312 Stdev</i>	<i>0.04</i>	<i>6400</i>				<i>56.7</i>	<i>3.6</i>	<i>24.3</i>	<i>5.3</i>	<i>22.0</i>	<i>3.7</i>	<i>8.5</i>	<i>3.4</i>	<i>0.9</i>	<i>0.6</i>	<i>1.4</i>	<i>1.9</i>	<i>1.1</i>	<i>0.6</i>	<i>1.6</i>
RVV316-6	0.67	105869			20238	665.3	31.3	214.0	51.3	214.5	33.9	73.3	35.3	7.2	1.9	6.3	6.1	2.7	2.2	4.5
RVV316-11a	0.80	113353			21414	1888.7	48.2	317.3	229.3	1001.7	184.8	338.6	127.8	19.8	3.7	15.4	10.7	4.4	2.3	4.6
RVV316-24	0.76	109997			30995	828.6	39.7	267.1	91.5	430.8	67.5	137.3	66.1	12.1	3.2	11.6	8.5	3.9	3.0	5.0
RVV316-25	0.83	110974			23067	948.8	38.2	278.6	104.0	531.6	77.0	154.1	70.6	12.3	3.2	10.6	8.4	4.3	2.5	5.9
<i>RVV316 Average</i>	<i>0.77</i>	<i>110048</i>			<i>23928</i>	<i>1082.8</i>	<i>39.3</i>	<i>269.2</i>	<i>119.0</i>	<i>544.7</i>	<i>90.8</i>	<i>175.8</i>	<i>74.9</i>	<i>12.9</i>	<i>3.0</i>	<i>11.0</i>	<i>8.4</i>	<i>3.8</i>	<i>2.5</i>	<i>5.0</i>
<i>RVV316 Stdev</i>	<i>0.07</i>	<i>3122</i>			<i>4852</i>	<i>549.6</i>	<i>6.9</i>	<i>42.6</i>	<i>76.9</i>	<i>332.2</i>	<i>65.3</i>	<i>114.0</i>	<i>38.5</i>	<i>5.2</i>	<i>0.8</i>	<i>3.7</i>	<i>1.8</i>	<i>0.8</i>	<i>0.3</i>	<i>0.6</i>
RVV321-12	1.00	92735				853.7	39.1	253.6	88.1	453.1	79.5	146.4	60.1	11.9	4.1	11.7	8.2	5.0	2.9	6.0
RVV321-13	0.51	37090				313.4	10.6	71.0	30.9	175.1	20.6	35.7	14.0	3.0	1.0	2.9	1.8	0.8	0.6	0.9
RVV321-14	0.93	69409				631.8	25.3	157.0	58.4	321.7	44.9	81.1	36.3	8.3	2.3	7.5	4.2	2.5	1.4	3.9
RVV321-16	1.00	116539				579.6	24.6	174.2	64.7	295.7	49.8	86.5	33.4	6.3	1.9	5.2	5.0	2.9	2.3	5.3
RVV321-29	0.84	104165			27310	1182.1	38.5	289.1	118.6	634.1	57.4	141.6	73.3	13.3	2.9	11.5	9.1	4.1	2.9	6.8
RVV321-30	0.88	93946			25313	863.4	38.8	244.1	93.7	496.5	66.2	134.1	61.1	12.0	3.0	11.1	7.5	3.8	2.8	5.7
RVV321-31	0.86	92034			27934	923.9	40.0	227.1	93.3	545.4	60.2	123.7	63.9	12.9	3.7	12.0	8.8	4.2	3.4	5.7
RVV321-32	0.62	87721			24303	1007.0	33.6	271.7	113.0	611.1	79.3	157.1	70.0	11.2	2.7	9.5	7.3	3.3	2.5	5.2
<i>RVV321 Average</i>	<i>0.83</i>	<i>86705</i>			<i>26215</i>	<i>794.3</i>	<i>31.3</i>	<i>211.0</i>	<i>82.6</i>	<i>441.6</i>	<i>57.2</i>	<i>113.3</i>	<i>51.5</i>	<i>9.9</i>	<i>2.7</i>	<i>8.9</i>	<i>6.5</i>	<i>3.3</i>	<i>2.3</i>	<i>4.9</i>
<i>RVV321 Stdev</i>	<i>0.18</i>	<i>24124</i>			<i>1695</i>	<i>273.7</i>	<i>10.4</i>	<i>72.6</i>	<i>29.5</i>	<i>163.2</i>	<i>19.4</i>	<i>41.6</i>	<i>21.1</i>	<i>3.7</i>	<i>1.0</i>	<i>3.4</i>	<i>2.6</i>	<i>1.3</i>	<i>0.9</i>	<i>1.8</i>
RVV340-8a	0.71	50992	5.6	3.5		402.7	14.8	114.6	30.0	140.5	18.5	37.1	18.9	3.8	0.8	3.7	3.0	1.3	0.5	2.5
RVV340-10a	0.68	52438	5.1	2.7		294.1	14.5	106.8	20.5	105.3	17.2	38.7	19.8	3.1	0.9	4.4	3.1	1.3	0.6	1.9
RVV340-11	0.81	68114				359.3	17.1	120.8	25.0	109.2	17.8	39.1	17.8	4.0	1.4	3.3	3.4	1.7	1.5	3.3

RVV340-12	0.79	78834	330.2	18.1	131.2	123.6	136.6	22.8	39.4	17.8	5.5	1.2	3.6	3.6	1.5	1.3	2.6
RVV340-16	1.00	88460	733.6	24.7	174.9	33.5	154.1	31.9	68.6	32.1	7.4	2.3	6.4	5.9	2.4	2.1	4.2
RVV340-24	0.66	98549	408.4	22.7	147.8	44.1	195.6	30.1	61.1	28.0	5.6	1.4	5.1	4.8	2.3	1.8	3.2
RVV340 Average	0.78	72898	421.4	18.7	132.7	46.1	140.2	23.0	47.3	22.4	4.9	1.3	4.4	3.9	1.7	1.3	3.0
RVV340 Stdev	0.12	19271	159.0	4.2	25.1	38.8	33.0	6.5	13.8	6.1	1.6	0.5	1.2	1.1	0.5	0.6	0.8
RVV343-2	0.70	71702	490.3	33.6	212.2	45.1	185.1	32.5	70.0	34.9	7.5	1.8	7.9	6.1	2.5	1.5	5.6
RVV343-3	0.67	83959	602.6	19.5	225.2	47.0	212.0	31.9	71.0	38.0	8.0	2.3	6.9	5.1	1.9	1.2	5.7
RVV343-4	0.80	78079	576.6	15.9	81.8	14.5	104.2	18.0	37.9	17.8	3.8	1.4	3.3	4.2	2.1	1.1	2.2
RVV343-6	0.48	4045	98.1	24.7	223.6	115.6	700.1	82.5	149.3	61.5	9.8	1.7	8.1	4.7	2.5	1.2	3.4
RVV343-7	1.00	115356	1198.3	39.2	334.1	260.3	2525.9	120.5	228.2	91.6	14.8	1.5	13.1	9.8	5.1	2.4	6.3
RVV343-8	0.97	95599	1273.0	45.0	332.6	73.1	4126.6	158.3	306.9	122.1	18.9	-0.1	14.7	12.7	6.5	2.2	5.6
RVV343 Average	0.77	74790	706.5	29.6	234.9	92.6	1309.0	74.0	143.9	61.0	10.5	1.4	9.0	7.1	3.4	1.6	4.8
RVV343 Stdev	0.20	37916	448.9	11.5	93.3	88.9	1655.8	56.5	105.6	39.4	5.5	0.8	4.2	3.4	1.9	0.5	1.6
RVV344-6	0.60	68314	485.3	25.0	162.8	59.7	253.6	42.6	84.9	37.2	6.3	1.4	5.0	3.8	2.4	1.2	4.3
RVV344-7	0.86	91897	621.4	34.2	218.8	84.8	377.0	61.8	124.1	57.3	9.4	1.8	5.2	5.3	2.5	1.8	4.5
RVV344-12	0.72	109564	820.3	37.6	247.4	104.7	485.4	78.0	157.8	67.5	12.0	2.5	9.3	7.5	3.5	2.2	5.9
RVV344-13	0.52	101256	696.8	32.4	230.8	84.1	394.0	65.6	125.9	51.3	9.1	2.0	6.7	6.3	3.2	2.4	5.2
RVV344 Average	0.68	92758	656.0	32.3	215.0	83.3	377.5	62.0	123.2	53.3	9.2	2.0	6.6	5.7	2.9	1.9	5.0
RVV344 Stdev	0.15	17822	140.2	5.3	36.7	18.4	95.3	14.7	29.9	12.7	2.3	0.5	2.0	1.6	0.5	0.5	0.7
RVV345-1	0.73	116890	656.1	33.4	211.6	40.9	192.5	34.3	76.7	43.9	10.0	2.6	7.6	6.9	3.7	3.0	5.4
RVV345-2	0.68	103903	435.3	28.8	145.5	24.2	109.9	19.3	45.5	27.3	6.9	2.1	6.0	6.2	2.8	2.2	4.0
RVV345-16	0.74	73671	323.1	15.0	108.0	32.7	149.9	24.3	46.4	18.0	4.8	1.2	3.1	2.5	1.3	1.1	2.2
RVV345-17	0.73	61759	322.9	16.3	107.1	35.9	177.3	32.0	60.9	22.2	4.8	0.9	4.1	3.9	1.9	1.0	2.4
RVV345-18a	1.00	78450	173.1	14.7	103.8	9.0	181.2	25.3	36.9	12.2	3.0	1.0	2.5	2.5	1.2	1.2	1.7
RVV345-20	0.88	105568	426.3	22.9	151.5	36.2	180.9	32.3	61.5	26.0	6.4	1.9	4.5	4.2	2.9	1.7	3.6
RVV345-21	0.57	70092	183.2	13.1	72.2	9.9	62.9	10.7	20.9	10.7	2.9	0.9	2.3	2.2	1.6	0.7	1.7
RVV345-23	0.93	104270	345.1	20.6	131.4	26.0	126.2	18.5	40.8	19.7	4.0	1.5	3.0	3.3	1.8	1.2	3.0
RVV345-25	0.82	88553	314.0	17.8	116.5	23.9	107.9	16.9	32.6	15.9	3.7	1.2	2.5	2.6	1.7	1.1	3.1
RVV345 Average	0.79	89240	353.2	20.3	127.5	26.5	143.2	23.7	46.9	21.8	5.2	1.5	4.0	3.8	2.1	1.4	3.0
RVV345 Stdev	0.13	19213	145.2	6.9	39.6	11.3	44.1	8.0	17.0	10.0	2.3	0.6	1.8	1.7	0.8	0.7	1.2
RVV346-1	0.67	94882	414.0	24.8	139.1	37.8	173.3	31.1	62.1	27.7	6.1	1.0	4.9	4.3	1.9	0.6	3.4
RVV346-3	0.67	92835	723.4	29.9	230.7	98.3	418.8	71.3	132.2	55.8	8.7	2.0	7.8	4.7	2.9	1.3	3.9
RVV346-4	0.57	72807	389.8	19.0	137.4	31.4	149.9	23.0	49.8	24.0	5.3	1.1	4.1	4.0	1.4	0.9	2.8
RVV346-7	0.71	102302	390.9	21.3	129.0	35.6	169.6	23.7	46.8	23.9	5.2	1.0	5.2	3.8	1.8	1.2	2.2
RVV346-9	0.54	78348	421.0	20.5	126.4	44.1	208.9	29.7	58.9	26.5	4.9	1.0	4.4	3.5	1.7	1.2	2.5
RVV346 Average	0.63	88235	467.8	23.1	152.5	49.4	224.1	35.8	70.0	31.6	6.0	1.2	5.3	4.1	1.9	1.1	3.0

<i>RVV346 Sdev</i>	<i>0.07</i>	<i>12237</i>	<i>1.4</i>	<i>1.2</i>	<i>143.6</i>	<i>4.3</i>	<i>44.0</i>	<i>27.7</i>	<i>110.9</i>	<i>20.2</i>	<i>35.4</i>	<i>13.7</i>	<i>1.5</i>	<i>0.4</i>	<i>1.5</i>	<i>0.5</i>	<i>0.6</i>	<i>0.3</i>	<i>0.7</i>
RVV360a-1	0.97	95778			704.4	25.5	221.2	61.0	281.7	56.3	118.9	53.8	11.9	3.0	7.7	6.0	2.9	1.4	5.4
RVV360a-2	1.00	96488			651.0	26.2	204.4	57.4	279.7	56.5	112.2	45.9	11.0	3.3	7.3	6.8	2.9	1.3	5.3
RVV360a-9	0.84	80195			641.9	21.3	213.6	63.9	314.0	53.2	92.5	38.0	8.1	1.7	6.3	3.4	1.7	1.1	4.9
<i>RVV360a Average</i>	<i>0.94</i>	<i>90820</i>			<i>665.7</i>	<i>24.3</i>	<i>213.1</i>	<i>60.7</i>	<i>291.8</i>	<i>55.3</i>	<i>107.9</i>	<i>45.9</i>	<i>10.4</i>	<i>2.7</i>	<i>7.1</i>	<i>5.4</i>	<i>2.5</i>	<i>1.3</i>	<i>5.2</i>
<i>RVV360a Sdev</i>	<i>0.08</i>	<i>9209</i>			<i>33.7</i>	<i>2.7</i>	<i>8.4</i>	<i>3.3</i>	<i>19.2</i>	<i>1.8</i>	<i>13.7</i>	<i>7.9</i>	<i>2.0</i>	<i>0.8</i>	<i>0.7</i>	<i>1.8</i>	<i>0.7</i>	<i>0.2</i>	<i>0.3</i>
RVV362-2	0.73	69266			396.8	16.3	88.4	16.3	148.2	23.4	41.1	19.2	5.4	1.5	4.8	3.3	1.2	1.0	2.9
RVV362-3	0.64	53335			517.3	5.5	33.0	7.1	64.0	4.8	10.2	4.8	0.9	0.6	1.0	0.7	0.5	0.1	1.3
RVV362-4	0.87	78980			522.8	18.3	98.8	17.1	116.9	20.3	38.6	18.3	4.1	1.3	3.0	3.1	1.3	1.2	2.5
RVV362-7	0.69	60522			685.8	23.6	155.3	36.7	200.6	29.8	64.5	32.0	6.3	1.8	6.7	4.7	2.4	1.7	4.0
RVV362-8	0.63	44824			388.3	19.9	133.1	26.2	118.4	19.5	43.6	23.4	5.3	1.4	4.5	3.9	2.0	1.6	3.4
RVV362-9	0.69	62153			672.5	12.0	84.1	16.5	93.5	12.4	27.2	14.5	3.1	1.0	2.9	2.3	1.1	0.8	2.4
<i>RVV362 Average</i>	<i>0.71</i>	<i>61513</i>			<i>530.6</i>	<i>15.9</i>	<i>98.8</i>	<i>20.0</i>	<i>123.6</i>	<i>18.4</i>	<i>37.5</i>	<i>18.7</i>	<i>4.2</i>	<i>1.3</i>	<i>3.8</i>	<i>3.0</i>	<i>1.4</i>	<i>1.1</i>	<i>2.7</i>
<i>RVV362 Sdev</i>	<i>0.09</i>	<i>11933</i>			<i>128.5</i>	<i>6.4</i>	<i>42.5</i>	<i>10.2</i>	<i>47.0</i>	<i>8.7</i>	<i>18.1</i>	<i>9.0</i>	<i>2.0</i>	<i>0.4</i>	<i>2.0</i>	<i>1.4</i>	<i>0.7</i>	<i>0.6</i>	<i>0.9</i>
Average																			
Plagiocase Host																			
					696.0	0.9	1.2	0.1	28.9	0.9	1.5	0.8	0.1	0.3	0.0	0.1	0.1	0.1	0.0



Table 2.8B: Corrected Melt Inclusions Trace Element Compositions

Sample	MELT	Ca	Li	B	Ti	Sr	Y	Zr	Nb	Ba	La	Ce	Nd	Sm	Eu	Gd	Dy	Er	Yb	Hf
RVV302-1	1.0	82632				558.2	29.0	165.0	43.5	211.7	35.1	73.4	30.2	7.2	2.4	5.8	5.7	2.7	2.4	4.7
RVV302 Average	1.0	88047				594.8	30.9	175.9	46.3	225.6	37.4	78.2	32.2	7.6	2.6	6.2	6.0	2.9	2.5	5.0
RVV302 Stdev																				
RVV306a-14	0.7	148087			26994	1626.5	49.4	409.5	177.4	1005.5	178.2	344.4	144.7	23.1	5.3	19.8	12.4	5.7	2.8	8.7
RVV306a-18	0.9	177799			28679	1583.8	54.4	392.5	157.2	924.1	153.8	297.5	124.6	21.7	4.5	16.3	12.1	5.0	3.3	8.0
RVV306a-19	0.8	187462			28088	1581.5	53.9	374.3	146.1	887.7	142.6	272.2	115.2	19.8	3.8	15.3	12.5	5.4	3.3	7.8
RVV306a Average	0.8	171116			27920	1597.2	52.6	392.1	160.2	939.1	158.2	304.7	128.2	21.5	4.5	17.1	12.4	5.4	3.1	8.2
RVV306a Stdev	0.1	20520			855	25.3	2.7	17.6	15.9	60.3	18.2	36.6	15.1	1.6	0.7	2.3	0.2	0.4	0.3	0.5
RVV312-1	0.8	65855				16.7	116.9	26.1	157.1	18.7	18.7	39.8	19.9	4.3	1.2	4.6	3.1	1.6	0.9	3.2
RVV312-2	0.8	66422				12.0	79.7	15.5	118.5	13.1	13.1	26.5	14.0	3.2	0.7	2.7	0.0	0.0	0.0	0.1
RVV312-3	0.7	57415				20.5	137.8	27.0	170.3	21.9	45.7	45.7	22.1	4.5	2.1	5.9	4.0	2.7	1.2	3.4
RVV312-4	0.7	53433				18.4	118.3	23.3	149.3	18.9	42.7	42.7	19.1	5.4	1.5	5.1	3.8	1.8	1.2	3.1
RVV312 Average	0.8	60782				16.9	113.2	23.0	148.8	18.1	38.7	18.8	4.3	1.4	4.6	2.8	1.5	0.8	2.5	
RVV312 Stdev	0.0	6400				3.6	24.3	5.3	22.0	3.7	8.5	3.4	0.9	0.6	1.4	1.9	1.1	0.6	1.6	
RVV316-6	0.7	127216			24319	799.4	37.6	257.1	61.6	257.7	40.8	88.1	42.4	8.7	2.3	7.6	7.4	3.2	2.6	5.4
RVV316-11a	0.8	111623			21087	1859.8	47.4	312.4	225.8	986.4	182.0	333.4	125.8	19.5	3.6	15.2	10.5	4.3	2.3	4.5
RVV316-24	0.8	109635			30893	825.9	39.5	266.2	91.2	429.4	67.2	136.9	65.9	12.1	3.2	11.6	8.5	3.9	3.0	5.0
RVV316-25	0.8	103190			21449	882.3	35.5	259.0	96.7	494.3	71.6	143.3	65.6	11.4	3.0	9.8	7.8	4.0	2.3	5.5
RVV316 Average	0.8	112916			24437	1091.8	40.0	273.7	118.9	542.0	90.4	175.4	74.9	12.9	3.0	11.0	8.5	3.9	2.5	5.1
RVV316 Stdev	0.1	10190			4540	513.2	5.2	26.1	73.0	312.7	62.5	108.2	35.6	4.6	0.6	3.2	1.4	0.4	0.3	0.4
RVV321-12	1.0	95705				881.0	40.3	261.8	91.0	467.6	82.1	151.1	62.0	12.3	4.2	12.1	8.5	5.2	3.0	6.2
RVV321-13	0.5	35495				299.9	10.1	67.9	29.6	167.6	19.7	34.2	13.4	2.9	1.0	2.8	1.7	0.8	0.6	0.8
RVV321-14	0.9	68388				622.5	24.9	154.7	57.5	317.0	44.2	79.9	35.8	8.2	2.2	7.4	4.1	2.4	1.4	3.9
RVV321-16	1.0	144390				718.1	30.5	215.8	80.2	366.4	61.7	107.2	41.3	7.9	2.3	6.5	6.2	3.6	2.8	6.6
RVV321-29	0.8	113944			29874	1293.1	42.1	316.3	129.8	693.6	62.7	154.8	80.2	14.5	3.2	12.6	9.9	4.5	3.1	7.4
RVV321-30	0.9	103293			27832	949.3	42.6	268.4	103.0	545.9	72.8	147.4	67.2	13.2	3.3	12.2	8.3	4.2	3.0	6.2
RVV321-31	0.9	147285			44704	1478.5	64.0	363.4	149.3	872.9	96.3	198.0	102.2	20.6	5.9	19.1	14.1	6.8	5.4	9.2
RVV321-32	0.6	67805			18785	778.3	26.0	210.0	87.4	472.3	61.3	121.4	54.1	8.7	2.1	7.3	5.6	2.6	1.9	4.1
RVV321 Average	0.8	97038			30299	877.6	35.1	232.3	91.0	487.9	62.6	124.2	57.0	11.0	3.0	10.0	7.3	3.7	2.7	5.5
RVV321 Stdev	0.2	38834			10745	372.8	16.0	92.8	37.9	220.7	23.3	50.7	27.6	5.4	1.5	5.0	3.8	1.8	1.4	2.6
RVV340-8a	0.7	38370	4.2	2.6		303.0	11.1	86.2	22.5	105.7	13.9	27.9	14.2	2.9	0.6	2.8	2.2	0.9	0.4	1.9
RVV340-10a	0.7	37285	3.6	1.9		209.1	10.3	75.9	14.6	74.9	12.2	27.5	14.1	2.2	0.7	3.1	2.2	0.9	0.4	1.3
RVV340-11	0.8	58862				310.5	14.8	104.4	21.6	94.4	15.3	33.8	15.4	3.5	1.2	2.9	3.0	1.5	1.3	2.9
RVV340-12	0.8	80257				336.2	18.5	133.6	125.8	139.0	23.3	40.1	18.1	5.6	1.2	3.7	3.6	1.6	1.3	2.6



<i>RVV360a Average</i>	0.9	87004	637.3	23.3	203.9	58.1	278.9	53.0	103.4	44.0	9.9	2.5	6.8	5.2	2.4	1.2	5.0
<i>RVV360a Stdev</i>	0.1	10517	44.7	3.0	10.3	2.5	12.6	2.8	15.3	8.5	2.1	0.8	0.8	1.8	0.7	0.2	0.4
RVV362-2	0.7	69266	16.3	88.4	16.3	148.2	23.4	41.1	19.2	5.4	1.5	4.8	3.3	1.2	1.0	2.9	
RVV362-3	0.6	53335	5.5	33.0	7.1	64.0	4.8	10.2	4.8	0.9	0.6	1.0	0.7	0.5	0.1	1.3	
RVV362-4	0.9	78980	18.3	98.8	17.1	116.9	20.3	38.6	18.3	4.1	1.3	3.0	3.1	1.3	1.2	2.5	
RVV362-7	0.7	60522	23.6	155.3	36.7	200.6	29.8	64.5	32.0	6.3	1.8	6.7	4.7	2.4	1.7	4.0	
RVV362-8	0.6	44824	19.9	133.1	26.2	118.4	19.5	43.6	23.4	5.3	1.4	4.5	3.9	2.0	1.6	3.4	
RVV362-9	0.7	62153	12.0	84.1	16.5	93.5	12.4	27.2	14.5	3.1	1.0	2.9	2.3	1.1	0.8	2.4	
<i>RVV362 Average</i>	0.7	61513	15.9	98.8	20.0	123.6	18.4	37.5	18.7	4.2	1.3	3.8	3.0	1.4	1.1	2.7	
<i>RVV362 Stdev</i>	0.1	11933	6.4	42.5	10.2	47.0	8.7	18.1	9.0	2.0	0.4	2.0	1.4	0.7	0.6	0.9	

## **Chapter 3**

**Mafic Plinian Eruptions:**

**Is Fast Ascent Required?**

## **Abstract**

It has been hypothesized that for a Plinian eruption of mafic magma to occur, that magma must rise rapidly from the chamber to cause it to fragment into a dusty jet. To determine how fast mafic Plinian magmas need to travel to the level of fragmentation, a number of decompression experiments were carried out on two hydrous mafic magmas, and the results are compared to the products of two well-documented mafic Plinian eruptions: the basaltic andesite Fontana eruption of Masaya (Nicaragua) and the hawaiiite 122 BC eruption of Etna (Italy). Comparison of natural and experimental textures show that the Fontana eruption can be replicated in the lab at decompression rates between  $0.2 \text{ MPa s}^{-1}$  and  $0.1 \text{ MPa s}^{-1}$ . This decompression rate is faster than any determined experimentally for more silicic eruptions. The hawaiiite was unable to be reproduced in the lab. The natural groundmass is highly crystalline, which would have raised the viscosity of the initial melt by 1-2 orders of magnitude, which may not be enough to cause fragmentation.

## Introduction

Fragmentation of magma, the dynamic change from a bubbly magma to a dusty gas, occurs in explosive eruptions, but not in effusive ones (Thomas et al., 1994; Papale, 1999; Houghton and Gonnermann, 2008). Acceleration of the dusty gas will, upon exiting the conduit, produce an eruption column. The interplay between high viscosity and volatile content is thought to control fragmentation (Houghton and Wilson, 1989; Roggensack et al., 1997; Papale, 1999).

Whereas there are various models for fragmentation, many models for silicic volcanic systems rely on some form of brittle failure criteria (Papale, 1999; Zhang, 1999; Alidibirov and Dingwell, 2000; Gaonac'h et al., 2003; Koyaguchi and Mitani, 2005; Wright and Weinberg, 2009). Brittle fragmentation is thought to occur when the structural relaxation of the melt is overcome by strain induced on the melt (Dingwell and Webb 1989; Sparks et al., 1994; Mader, 1998, Papale, 1999, Zhang, 1999). Within the general framework of brittle failure fragmentation, there are different explanations as to the processes leading to the failure. In the strain-induced fragmentation model, the magma undergoes strain, raising its viscosity until the glass transition is reached, and brittle fracture of the melt occurs (Papale, 1999). It is thought that melt viscosities of  $\sim 10^{6.5}$  Pa s or greater are needed for brittle fragmentation (Papale, 1999). The other explanation invokes overpressure in bubbles. In this model, the tensile strength of the bubble stresses the shell of melt surrounding the bubble until the melt breaks (Zhang, 1999). For bubbles to become overpressured, the viscosity of the melt must be high enough to inhibit the bubble from expanding at equilibrium rates (Thomas et al., 1994;

Proussevitch and Sahagian, 1996). A melt viscosity of  $10^6$  Pa s or greater is again required for fragmentation to occur (Namiki and Manga, 2008).

If viscosity needs to exceed  $10^6$  Pa s for fragmentation to occur, then Plinian, or highly explosive, eruptions of low-viscosity melts should not occur. There are, however, well-documented examples of nominally low-viscosity magma erupting in Plinian fashion (Williams, 1983; Coltelli et al., 1995; Gurenko et al., 2005; Walker et al., 1984; Sable et al., 2006). Those eruptions imply that either special conditions are required for such magmas to behave as if they were highly viscous, or there must be another mechanism that leads to their fragmentation. Most models based on brittle failure require relatively fast ascent, and so one possibility is that low viscosity magma ascends faster than their highly viscous counterparts, allowing such magmas to either be strained very quickly or to trap bubbles that are unable to expand in the melt and lead to large overpressures.

To examine ascent rates of low viscosity Plinian eruptions a series of decompression experiments on two separate mafic magmas were performed. One is a basaltic andesite erupted from Masaya, whereas the other is a hawaiite erupted from Etna, both of which erupted in sub-Plinian to Plinian style (Costantini et al., 2009; Wehrmann et al., 2006; Coltelli et al., 1995; Del Carlo, 2001). Using groundmass textures, comparison of experimental results to natural samples allows inferences to be made regarding the most likely decompression rates of those magmas. The microlites in the basaltic andesite can be reproduced experimentally, and bracket the decompression rate between  $0.2 \text{ MPa s}^{-1}$  and  $0.1 \text{ MPa s}^{-1}$ . That rate is faster than rates determined for more

silicic magmas erupted in Plinian fashion (e.g., Geschwind and Rutherford, 1995; Devine et al., 1997; Szramek et al., 2006; Castro and Gardner, 2008; Andrews and Gardner, in review). In contrast, microlites in the hawaiiite cannot be reproduced experimentally by a single decompression, possibly pointing to a more complicated ascent history.



## Geologic Background

### *Basaltic Andesite-Fontana Lapilli, Masaya Volcano*

One of our target samples is from the Fontana Lapilli, which erupted near Masaya volcano in the Late Pleistocene (60 ka) (Costantini et al., 2009). Wehrmann et al. (2006) divided the Fontana Lapilli into seven units, labeled A-G. Units A, B, and C, attributed to the opening stages of the eruption, are characterized by thin, moderately sorted, graded, and poorly sorted beds (Costantini et al., 2009). The main portion of the deposit consists of units D, E, F, and lower G, which are composed of many alternating beds of moderately sorted, massive-to-weakly stratified, and non-graded layers (Costantini et al., 2009). The upper portion of unit G represents the closing stage of the eruption, and is characterized by moderately stratified layers that alternate with fine and coarse layers (Costantini et al., 2009). The entire deposit is also characterized by thin layers of ash, which occur at regular intervals (Wehrmann et al., 2006). The eruption is interpreted to have begun with Hawaiian-type explosions (units A and B), followed by a pyroclastic surge (unit C), and then the main Plinian phase (units D-F). The eruption ended with short-lived eruption pulses (upper part of unit G) (Wehrmann et al., 2006). Although Wehrmann et al. (2006) suggested that meteoritic water played a minor role in a few stages of the eruption, later reinterpretation by Costantini et al. (2009) suggests that the eruption was purely magmatic. The Plinian eruption column that deposited layers D-lower G is estimated to have obtained a maximum height of 30-32 km, at a mass eruption rate of  $1.4 \times 10^8 \text{ kg s}^{-1}$  (Costantini et al., 2009). The total volume of tephra is estimated at 2.9-3.8 km<sup>3</sup> (Costantini et al., 2009).

The magma is basaltic andesite in composition and contains less than 1 vol. % phenocrysts. The pre-eruptive conditions of the basaltic andesite were determined via hydrothermal phase-equilibria experiments, glass-inclusion analyses, and mineral compositions (Goepfert and Gardner, 2010). Glass inclusions contain a wide range of water contents, but because that range does not correlate with glass composition, much of it is thought to have resulted from leaking from glass inclusions. Goepfert and Gardner (2010) suggest that pre-eruptive water content was ~2.8 wt. %. Based on that water content and results of phase-equilibria, the basaltic andesite is thought to have been stored prior to erupting at 1010-1030°C and 40-80 MPa (Fig. 3.1).

#### *Hawaiiite-122 BC Mt Etna*

Although the eruptive style of Mt Etna is typically effusive (Del Carlo and Pompillo, 2004), over two dozen sub-Plinian and one Plinian eruptions have occurred during the Holocene (Coltelli et al., 1995). The Plinian eruption occurred in 122 BC, and was recorded by the Romans, and ash fell on what was the town of Catania, causing fires and roofs to collapse (Coltelli et al., 1995; Del Carlo, 2001).

The deposit has been divided into seven units, A-G (Coltelli et al., 1998). Unit A is characterized by coarse ash fallout resulting from strombolian activity.

Phreatomagmatic and phreatic eruptions resulted in the massive to bedded tuffs of units B, D, F, and G. Plinian units C and E are characterized by well sorted, graded, and stratified bedding. Based on isopach and isopleth maps, Coltelli et al. (1998) place the vent for the eruption in the Cratere del Piana, a 2-km-wide caldera that they believe

formed during the 122 BC eruption. The total volume of the deposit is  $0.4 \text{ km}^3$  ( $0.095 \text{ km}^3 \text{ DRE}$ ), and the Plinian phase is inferred to have erupted at a rate of  $5\text{-}8.5 \times 10^7 \text{ kg s}^{-1}$ , resulting in a 24-26 km high column (Coltelli et al, 1998).

Juvenile pumice are relatively homogeneous and hawaiitic in composition (Del Carlo, 2001). Like the basaltic andesite, the pre-eruptive conditions for the hawaiite were determined via hydrothermal phase-equilibria experiments, glass-inclusion analysis, and mineral compositions (Goepfert and Gardner, 2010). Glass inclusions in the hawaiite contain a wide range of water contents, like that of the basaltic andesite, which is thought to have resulted from partial leaking. Goepfert and Gardner (2010) suggest that pre-eruptive water content was also  $\sim 2.8 \text{ wt. \%}$  for the hawaiite. Based on those water contents and results of phase equilibria, the hawaiite magma appears to have been stored prior to eruption at  $1000\text{-}1020^\circ\text{C}$  and  $60\text{-}75 \text{ MPa}$  (Fig. 3.1).

## **Methods**

### *Starting Material*

Hawaiite pumice from unit C (sample 128-07) of the 122 BC Mt Etna eruption were provided by Dr. Bruce Houghton. The basaltic andesite pumice from units E, F, and G of the Fontana Lapilli were provided by Dr. Heidi Wehrmann. Bulk and matrix glass compositions are reported in Table 3.1. For the hawaiite, the largest piece of pumice was chosen for experiments, whereas for the basaltic andesite a number of pumice fragments were used from units E, F, and, G. Each pumice used had an average vesicularity for its eruption phase. Thin sections were made for examination of textures from low, median, and high vesicularity pumice for each eruption (Goepfert and Gardner, 2010), resulting in 3 thin sections for the hawaiite and 9 (three for each unit) for the basaltic andesite. Pumice clasts were gently crushed in a steel mortar and pestle to a fine powder of no more than ~0.5 mm in diameter. The powder was examined under a binocular microscope to remove any flakes of steel from the mortar.

Platinum (Pt) tubing was used in all experiments. To minimize iron loss from the samples, all Pt tubes that were to be in contact with sample material were pre-saturated with that material. Pre-saturation was accomplished by welding each tube at one end, filling it with sample powder, and then lowering the tube into the hot zone of a furnace and holding it for 24+ hours at 1150°C. The tube was removed and quenched by placing it in a bucket of water. Glass was then removed by lightly tapping the tube with a hammer and shaking it out. Any remaining glass was removed by opening the tube and

scraping the sides clean. The cleaned and pre-saturated Pt tubing was then molded back into a tube shape for experimental use.

Starting materials for decompression experiments were prepared by adding sample powder into a pre-saturated Pt tube, which was crimped shut at both ends. A second Pt tube that contained nickel metal and nickel oxide powder (Ni+NiO) to buffer the experiments was made, with the ends crimped shut. Both the sample and buffer tubes were then placed inside a larger Pt-tube, which was welded at one end, to which 5 wt.% de-ionized water relative to sample powder was added, allowing for water saturation as well as water loss during welding. The large tube was then welded shut and checked for leaks by heating on a hot plate. Samples were run in externally heated Titanium-Zirconium-Molybdenum (TZM) pressure vessels for 24 hours with ~2 bars of methane added to the pressuring argon. Samples of basaltic andesite were run at 1030 °C and 70 MPa (Table 3.2). Samples of hawaiite were run at either 1035 °C or 1000 °C at 75 MPa. To minimize quench crystals, the pressure vessel was pulled out of the furnace and flipped, which caused the sample capsule to drop from the hot zone to the water-cooled end of the pressure vessel, quenching the sample rapidly (Mangan and Sisson, 2000). When successful, there is a small increase in pressure when the sample capsule falls to the water-cooled end of the pressure vessel. Additionally, the sample tube remains crushed, unlike if the sample remains in the hot portion of the bomb, where it expands as it cools. The samples that quenched rapidly were opened and the buffer tubing was checked to ensure that both Ni and NiO were present. The starting material was removed and examined petrographically before being used in decompression experiments.

### *Decompressions*

For each decompression, a split of starting material was added to a pre-saturated Pt-capsule, crimped at both ends, and placed within a larger Pt tube. Samples were run in externally heated TZM pressure vessels with ~2 bars of methane added to the pressuring argon. Each decompression experiment was held at the original starting conditions for ~1 hour before being decompressed. After one hour, pressure was released continuously to 10 MPa for the basaltic andesite and 12 MPa for the hawaiite. Those final pressures were chosen as approximate fragmentation pressures based on converting the water degassed from depth into vesicularity until it overlapped with the vesicularity of Etna (Houghton et al., 2004). Conversion of degassed water to vesicularity was done by converting H<sub>2</sub>O wt. % to H<sub>2</sub>O volume as pressure was decreased and determining the fraction of gas to melt, assuming no gas loss. The final pressure for Fontana was estimated as slightly higher as it has a lower vesicularity. We assumed that the natural vesicularities pressure was fragmentation pressure. The release of pressure took ~45 seconds, including fine-tuning to achieve the desired final pressure, as pressure increases up to 1 MPa after gas release is stopped, requiring additional pressure release. Experiments were held at final pressure for various times until a desired decompression rate was approximated, where the rate equals the total pressure drop divided by the time taken to release pressure plus the time held at final pressure (Table 3.2). Experiments were quenched by flipping the pressure vessel. A decompression experiment was determined a success if it remained crushed and fell into the water-cooled region of the pressure vessel during quenching. In addition,

one multi-step experiment was carried out using the basaltic andesite and two using the hawaiite. In those cases pressure was released in ten, roughly equal steps until final pressure was reached (Table 3.2). The sample was quenched as before, but immediately following the final step.

### *Textural Analysis*

Backscattered electron images (BSE Images) were collected of pumice from each eruption as well as each experiment. For analysis, the JEOL 8200 Superprobe at the University of Texas at Austin was used, at operating conditions of 15 keV and 10-20 nA with a focused beam. Conditions were optimized for analyzing groundmass crystallinity by varying magnification, brightness, and contrast. BSE images were also collected with a JEOL JSM -6490LV SEM at the University of Texas at Austin in high and low vacuum mode at operating conditions that optimized images.

To measure individual crystals, each microlite was first outlined digitally by hand and then its area was measured. An ellipse was fit to each crystal to calculate its short and long axis. Additionally, each microlite was assigned a morphology, based on the shapes described by Lofgren (1974, 1980). Tabular crystals are well-defined without embayments; hopper crystals resemble an empty box, filled with glass; skeletal crystals are poorly formed and can have one or more embayments; acicular crystals have high aspect ratios and resemble threads or needles; swallowtail crystals are tabular crystals that have growths off of their ends; dendritic crystals have multiple branches; and spherulies are clusters of crystals all radiating from a common point (Fig. 3.2).

Crystallinity ( $\phi_i$ ) was determined for each phase ( $i$ ) by summing the cumulative area of each phase and dividing by the total groundmass area (minus areas of vesicles and phenocrysts), then multiplying by 100. Area number density was also measured,  $N_A^i$  ( $\mu\text{m}^{-2}$ ), from which characteristic crystal size,  $S_n$ , was estimated, which equals  $\left[\left(\frac{\phi}{100}\right)(N_A)^{-1}\right]^{\frac{1}{2}}$ , and volumetric number density,  $N_V^i$ , which equals  $(N_A S_n^{-1})$ , following Hammer and Rutherford (2002).



## Results

### *Natural Groundmasses*

The basaltic andesite and hawaiite have the same groundmass mineral assemblage, but the phases occur in substantially different proportions and morphologies (Table 3.3). The basaltic andesite has a few, relatively large microlites, whereas the hawaiite is characterized by many small microlites. Additionally, plagioclase microlites in the basaltic andesite vary strongly in morphology, whereas those in the hawaiite are all tabular.

The basaltic andesite groundmass assemblage is dominated by glass and plagioclase, with trace amounts of pyroxene and Fe-Ti oxides. As pyroxene and Fe-Ti oxides occur in trace amounts only, and would not be statistically significant, we focus on plagioclase textures, such that plagioclase textures  $\approx$  total groundmass textures (Table 3.3). Overall, plagioclase crystallinity is found to be  $\sim 4$  vol. %, and occurs in an area number densities of  $8.4 \times 10^{-4} \mu\text{m}^2$  and volumetric number densities of  $1.3 \times 10^{-4} \mu\text{m}^3$  (Table 3.3). The characteristic crystal size is  $\sim 8 \mu\text{m}$ . The crystal size distributions of the major and minor axes of plagioclase are unimodal, ranging from 4-28  $\mu\text{m}$  and 4-16  $\mu\text{m}$ , respectively (Fig. 3.3). Plagioclase exhibits a wide range of textures, with dendritic, hopper, acicular, swallowtail, spherulitic, tabular, and skeletal shapes (Table 3.4). Although quantitative textural data on pyroxene and Fe-Ti oxides were not acquired, morphological data were gathered. Pyroxene morphologies include tabular, hopper, swallowtail, and dendritic, whereas the Fe-Ti oxides are either dendritic or tabular.

The hawaiiite groundmass assemblage consists of glass, plagioclase, pyroxene, and Fe-Ti oxides. The groundmass is highly crystallized, with crystals occurring in with an area number densities of  $1.4 \times 10^{-1} \mu\text{m}^2$  and volumetric number densities of  $8.3 \times 10^{-2} \mu\text{m}^3$  (Table 3.3). There is a relatively small characteristic crystal size overall, with plagioclase being the largest at  $\sim 3 \mu\text{m}$  (Table 3.3). Crystal size distributions of the major and minor axes of the plagioclase microlites are unimodal, ranging from 2-16  $\mu\text{m}$  and 2-6  $\mu\text{m}$ , respectively (Fig. 3.4). Plagioclase and pyroxene occur in similar crystallinities, whereas Fe-Ti oxides are  $\sim 6$ -7 times less abundant. Area number densities for all phases are similar, but their volumetric number densities differ because of their correspondingly smaller sizes. Plagioclase microlites are only tabular, whereas pyroxene microlites are hopper or tabular (Table 3.4). Fe-Ti oxides are too small to clearly distinguish morphology.

### *Experimental Textures*

The only microlite to nucleate and grow in the decompressed basaltic andesite is plagioclase (Table 3.5). The amount of plagioclase varies from 4 to 35 vol.%, with a general increase in crystallinity as decompression rate decreases (Fig. 3.5). Characteristic size varies from 7 to 260  $\mu\text{m}$ , and the crystal-size distributions are unimodal, but as the decompression rate decreases, the range in sizes generally increase, except in the longest experiment (Fig. 3.3).  $N_A^{\text{plag}}$  and  $N_V^{\text{plag}}$  both vary by 2 orders of magnitude, from  $10^{-2} - 10^{-4} \mu\text{m}^{-2}$  and  $10^{-4} - 10^{-6} \mu\text{m}^{-3}$ , respectively, but do not correlate with decompression rate (Fig. 3.6, 3.7). There is also a wide range of morphologies that broadly vary with

decompression rate. At the slowest decompression rate, only tabular plagioclase are present. As the decompression rate increases, acicular and skeletal crystals appear first, followed by hopper and spherulitic crystals.

In the hawaiiite, plagioclase is the only phase that grows, except for the two slowest decompressions, where pyroxene and then pyroxene plus Fe-Ti oxides occur. Overall, the amount of plagioclase crystallized varies from 3 to 44 vol. % and generally increases as decompression rate decreases (Fig. 3.5). Characteristic size ranges from 13 to 22  $\mu\text{m}$ . Crystal size distributions are unimodal and do not vary with decompression rate (Fig. 3.4). Area number densities are in the range of  $10^{-5} \mu\text{m}^{-2}$ , and volumetric number densities are in the range of  $10^{-6} \mu\text{m}^{-3}$ , with one outlier one order-of-magnitude less (Table 3.5). Neither characteristic crystal size nor number densities vary with decompression rate (Table 3.5, Fig. 3.6,3.7). Multistep decompression experiments overlap well with all microlite textures except for crystal content (vol. %) (Table 3.5). Regardless of decompression rate, all plagioclase are hopper, tabular, or skeletal in shape. When pyroxene and Fe-Ti oxides occur, they are tabular.

## Discussion

### *Experimental Results*

In general, the hawaiite has lower area number densities and smaller crystals than the basaltic andesite (Fig. 3.8). Plagioclase crystallinity in the two suites are equal at the same decompression rate (Fig. 3.5). At relatively slow decompression rates, both basaltic andesite and hawaiite have the highest plagioclase crystallinity. The  $N_A^{Plag}$  does not correlate with decompression rate for either the basaltic andesite or the hawaiite (Fig. 3.6). Total  $N_A$  does, however, increase in the hawaiite with decompression rate. The crystal size distributions for the basaltic andesite show that as the decompression rate slows, the minor axis length generally shrinks, whereas the major axis length becomes more variable (Fig. 3.3). In the hawaiite, the crystal size distributions, in contrast, show no correlation with decompression rate (Fig. 3.4). Differences in  $N_V$  are less between the melt compositions yet vary similarly to  $N_A$  (Fig. 3.7).

Only 5° C separate most of the decompression experiments, and the starting materials have similar water contents, suggesting that any differences result from either decompression rate or melt composition. To determine what causes the differences, we plotted both melt compositions vs. decompression rates. If data were offset by composition, then that was the cause of the difference. If data varied with decompression, then melt composition did not have a first-order effect on the property examined. Melt composition seems to be a second order effect in the control of crystal content (Fig. 3.5). The increase seen with decompression rate is likely caused by the increase of time allowed for growth of plagioclase microlites. The increase in  $N_A$  for

hawaiite likely results from crystallization of pyroxene and Fe-Ti oxides in the slower decompressions. The lack of correlation of  $N_A^{Plag}$  in the basaltic andesite cannot be explained by additional crystallization, as all experiments produced only plagioclase. The overall differences in  $N_A^{Plag}$  are likely related to differences in melt composition. The typically smaller crystals in the hawaiite and variations in the crystal size distributions are also likely caused by composition, whereas the variation in  $N_V$ , while in part a result of composition, is also caused by size differences.

According to over 30 years of observations and experiments, plagioclase morphology is linked to changes in cooling rate (e.g., Lofgren, 1974), which has been shown comparable to morphology changes from decompression rate (e.g., Hammer and Rutherford, 2002). Although similar results are found in basaltic andesite, the hawaiite always contains hopper, skeletal, and tabular morphologies, regardless of decompression rate. It does appear, however, that at the slowest decompression rate, the interiors of hopper plagioclase are beginning to fill with additional plagioclase growth. At decompression rates as high as  $0.6 \text{ MPa s}^{-1}$ , hopper plagioclase are found. That rate allowed for only  $\sim 105$  seconds of crystal nucleation and growth, suggesting that during decompression the morphologies are imprinted on the crystals. A similar phenomenon was observed by Szramek et al. (2010), who found that the ratio of hopper to tabular plagioclase did not vary in natural basaltic pumice, despite dramatic changes in cooling rate.

*Magma Ascent During the Fontana Plinian Eruption*

Comparing natural crystallinities with those in the decompression experiments (Fig. 3.5), it appears that the basaltic andesite decompressed rapidly, similar to the faster decompressed experiments. The only overlap in  $N_A^{Plag}$  between the experimental and natural samples of basaltic andesite occurs at the second fastest decompression rate (Fig. 3.6). Characteristic crystal sizes in the experiments are larger than those in the natural samples (Fig. 3.8). Crystal size distributions for the basaltic andesite match well for the minor axis at  $0.1 \text{ MPa s}^{-1}$  and  $0.2 \text{ MPa s}^{-1}$ , and match well for the major axis at  $0.1 \text{ MPa s}^{-1}$ .  $N_V^{Plag}$  for the natural samples overlap those of most decompression rates (Fig. 3.7).

The natural basaltic andesite has a wide range of morphologies present, including dendritic, hopper, swallowtail, skeletal, acicular, spherulitic, and tabular. The experimental samples show that as decompression rate increases, microlite morphology becomes more varied. At the fastest decompression rates, all microlite morphologies in the natural samples are present. Based on the above comparisons, it appears that the basaltic andesite decompressed faster than  $0.1 \text{ MPa s}^{-1}$ , but slower than  $0.2 \text{ MPa s}^{-1}$ .

Having bracketed a decompression rate for the basaltic andesite, comparison of that value to those determined experimentally for other eruptions of different compositions can be made (Fig. 3.9). Of the four Plinian eruptions that have experimental constraints on decompression rate, the determined rate for the basaltic andesite is faster than any previously reported. So what does this mean for the fragmentation of Fontana? The original hypothesis was that fragmentation is occurring in these low viscosity melts because they ascend faster allowing for brittle failure to occur

in the melt. The initial results suggest that this may be possible, but with only one data point it cannot be seen if this is a universal case.

### *Magma ascent During the Etna Plinian Eruption*

Comparing natural and experimental hawaiite data does not produce an overlap that allows for estimation a possible decompression rate. Comparing crystal contents (Fig. 3.5), it is apparent that the hawaiite could have decompressed over a large range of decompression rates, except for the slowest and fastest. For  $N_A^{Plag}$ , the hawaiite natural sample plots an order and a half higher than those of experiments (Fig. 3.6).

Characteristic crystal sizes are larger in the experiments than in the natural sample (Fig. 3.8), and none of the crystal size distributions from the experiments resemble the natural sample (Fig. 3.4).  $N_V^{Plag}$  in the hawaiite experiments are all lower than that of the natural sample (Fig. 3.7). Plagioclase morphologies in the natural hawaiite are only tabular, whereas the experiments contain hopper, skeletal, and tabular crystals, regardless of decompression rate. Natural and experimental hawaiite data do not overlap, except for total crystallinity, and therefore do not allow an inference to be made about decompression rate.

In the case of the hawaiite, we have no information on the probable decompression rate of the magma prior to the eruption, yet it did produce a Plinian eruption. One possibility that has been proposed to explain basaltic Plinian eruptions is that microlite crystallization prior to eruption raises the viscosity and allows for explosive eruptions (Houghton and Gonnermann, 2008). Such a model may explain the eruption of

122 BC Mt Etna with pumice that have extremely crystalline groundmasses, but it cannot explain all mafic Plinian eruptions, as Fontana pumice have an almost vitreous groundmass. If an increase in viscosity is the explanation for 122 BC Etna, a first-order approximation for the viscosity of the melt before eruption can be obtained to see if this explanation is plausible. The numerous small microlites suggest that they all nucleated and grew at a similar pressure and temperature, but those conditions are unknown. Using the estimated pre-eruptive temperature of 1010°C and varying pressure from 70-10 MPa, in increments of 10 MPa, an examination of microlite growth at different levels in the conduit has been made. For modeling purposes, it was assumed that all growth occurred at 20 MPa in the conduit. This assumption was made because the plagioclase microlites were relatively uniform in size, suggesting a similar time-scale for growth.

To examine how viscosity changes with the presence of microlites and pressure, a number of parameters have been used. The range of initial melt viscosities 200-1318 Pa s<sup>-1</sup> was determined from the model of Giordano et al. (2008), based on varying pressure and water content (Moore et al., 1998) as well as glass compositions and temperature (Goepfert and Gardner, 2010). Additionally, a phenocryst content of 1-10 vol. % (Sable et al., 2006) and a microlite content of 43 ± 12 vol. % was also used. Those crystallinities overlap potentially with where the presence of crystals becomes important in changing the viscosity, which is defined by Lejeune and Richet (1995) as ~ 40 vol. %. Up to a crystallinity of 40 vol. %, they claim it is valid to estimate magma viscosity ( $\eta$ ) using the Einstein-Roscoe equation (Roscoe, 1952). Such that:



$$\eta = \eta^o \left( 1 - \frac{f_c}{f_m} \right)^n$$

with  $\eta^o$ =viscosity of melt,  $f_c$ =fraction of crystals,  $f_m$ =0.6 or 0.7, and  $n=2.5$  (Lejeune and Richet, 1995). The value of  $f_m$  is based on maximum packing, where 0.6 applies when that the crystals are equant (Marsh, 1981) and 0.7 applies when the crystals are bimodal in size. For analysis purposes, both values of  $f_m$  are used as well as the maximum crystal content to determine the largest viscosity increase possible from microlite growth.

Figure 3.10 shows the results of the viscosity modeling as pressure, or conduit depth, is varied. As expected, when the microlites grow at lower pressure the increase of viscosity is larger, ranging from only one order of magnitude at maximum depth to over two orders of magnitude at the shallowest depth. Varying  $f_m$  results in about one order of magnitude increase in viscosity from, regardless of pressure. The reduction in pressure from 70 MPa to 30 MPa results in an order of magnitude increase in viscosity, which is twice that found for crystal-free melt. The reduction in pressure from 30 MPa to 10 MPa results in another order of magnitude increase in viscosity.

Brittle failure models suggest that a viscosity of  $10^6$  Pa s or more is needed for fragmentation (Papale, 1999; Namiki and Manga, 2008). A viscosity that high is only achieved when  $f_m=0.7$  at a pressure of 10 MPa. As pressure is decreased a two to three order of magnitude increase of viscosity is observed from the initial viscosity at depth. Is that increase enough to cause Plinian behavior? To answer that question, a better understanding of the viscosity at the time of fragmentation is required. Papale (1999) was able to model fragmentation of a crystal-rich basalt and additionally his model output

the vesicularity at time of fragmentation. He found that viscosity and gas volume fraction, vesicularity, are inversely correlated at the time of fragmentation. Thus at a lower viscosity, a higher vesicularity is expected. In the case of Etna, Houghton et al. (2004) found 64 % bulk vesicularity at maximum eruption intensity, which according to Papale (1999) would require a viscosity of  $\sim 10^8$  Pa s at the time of fragmentation.

By comparing the viscosity at fragmentation to the viscosity calculated from the vesicularity, we can ascertain if brittle failure was caused by viscosity alone. Using the microlite morphologies as an indicator of the storage level prior to eruption, it is likely that the magma was stored at a shallow pressure. If it is assumed that storage and then fragmentation occurred at  $\sim 20$  MPa, then the resulting viscosity is  $\sim 10^6$  Pa s. This viscosity is two orders of magnitude lower than the model of Papale (1999) predicts for brittle failure with the vesicularity seen in the tephra of the eruptive deposits.

Therefore, while the viscosity does increase from the growth of microlites, it is unlikely that that increase is enough to produce a Plinian eruption without additional complications. Both Plinian phases of the eruption were characterized by a transition in the eruptive style from phreatomagmatic activity to Plinian activity (Houghton et al., 2004). Therefore external water was involved in part of the eruption, although it is believed to have not been involved in the Plinian phases (Houghton et al., 2004).

#### *Fragmentation During Mafic Plinian Eruptions*

Although microlites in Etna suggest a complicated ascent history, those in Fontana suggest simple ascent and fragmentation resulting from decompression of 0.1 -

0.2 MPa s<sup>-1</sup>. Mafic Plinian eruptions have also occurred at Arenal and Shishaldin. At Arenal, relatively homogenous basaltic andesite has been erupting since 1968, but it started current its activity with a Plinian eruption. The erupted pumice contains ~40 vol. % microlites, but experiments were able to bracket the decompression rate between 0.0013 and 0.025 MPa s<sup>-1</sup> for that that eruption (Szramek et al., 2006). Shishaldin erupted in Plinian fashion in 1999 and tapped tholeiitic basalt, with a microlite content of 20 vol. % (Szramek et al., 2010). The plagioclase microlites present occur in a range of morphologies, similar to our experiments. Although experiments have not investigated, if we assume that crystal content gives a first-order approximation for decompression, it appears that the basalt decompressed  $0.5 \times 10^{-2} - 1 \times 10^{-1}$  MPa s<sup>-1</sup>. Shishaldin and Arenal appear to have decompressed at a range between 0.01 MPa s<sup>-1</sup> and 0.0013 MPa s<sup>-1</sup> (Fig. 3.9).

Low viscosity magmas appear to be able to fragment when they decompresses at rates of 0.0013 MPa s<sup>-1</sup> to 0.1 MPa s<sup>-1</sup> (Fig. 3.9). More silicic Plinian eruptions, such as those of Mount St. Helens and Ksudach, have decompression rates that range from 10<sup>-1</sup> MPa s<sup>-1</sup> to 10<sup>-2</sup> MPa s<sup>-1</sup>, with viscosities of 10<sup>5.1</sup> Pa s and 10<sup>3.8</sup> Pa s, respectively (Fig. 3.9). Those more silicic eruptions have decompression rates that overlap with the more mafic eruption, although they have higher viscosities. That suggests that fragmentation of low viscosity magma does not appear to require especially rapid decompression.

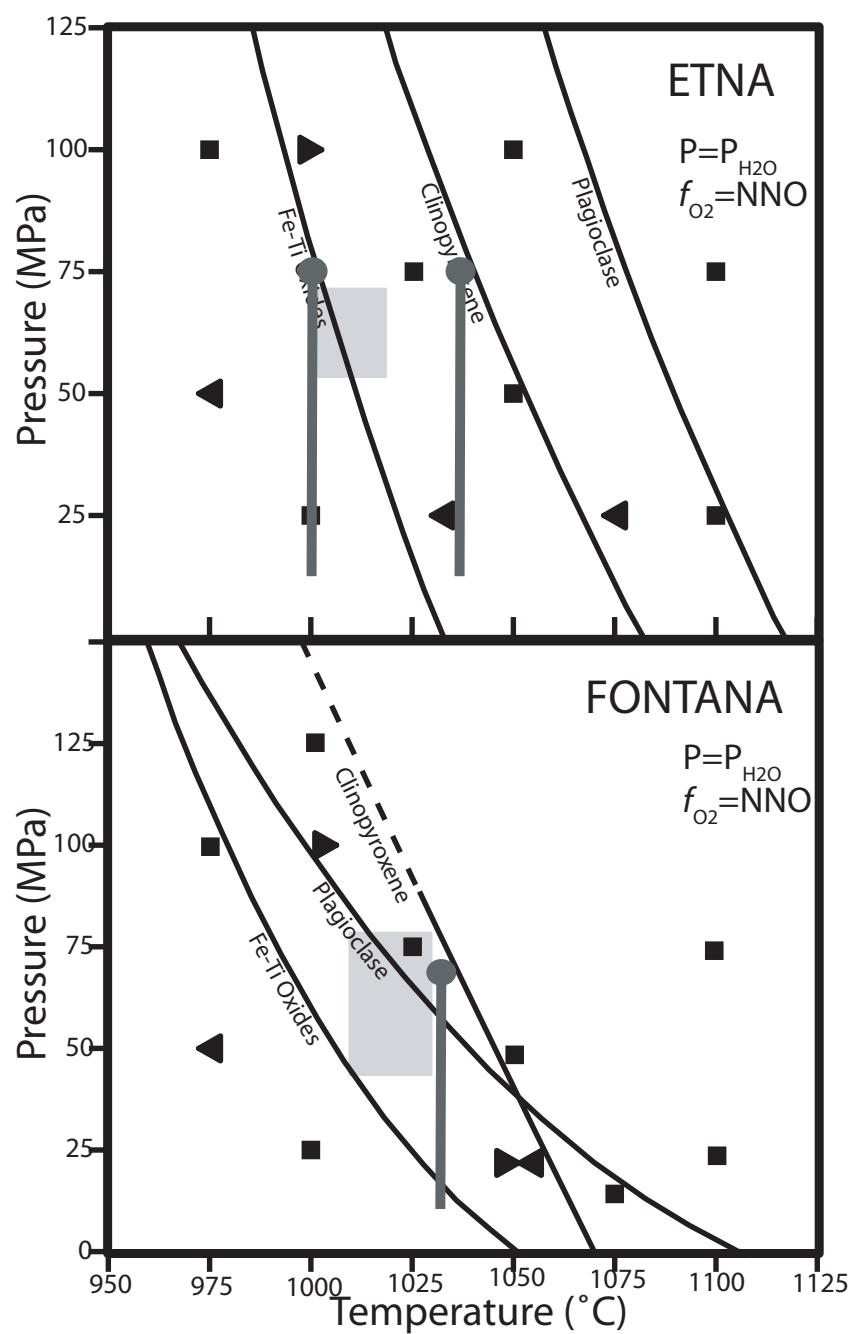


Figure 3.1. Phase diagrams modified from Goepfert and Gardner (2010). Gray boxes are starting conditions as determined from Goepfert and Gardner (2010). Dark gray vertical lines are decompression paths used in this study.

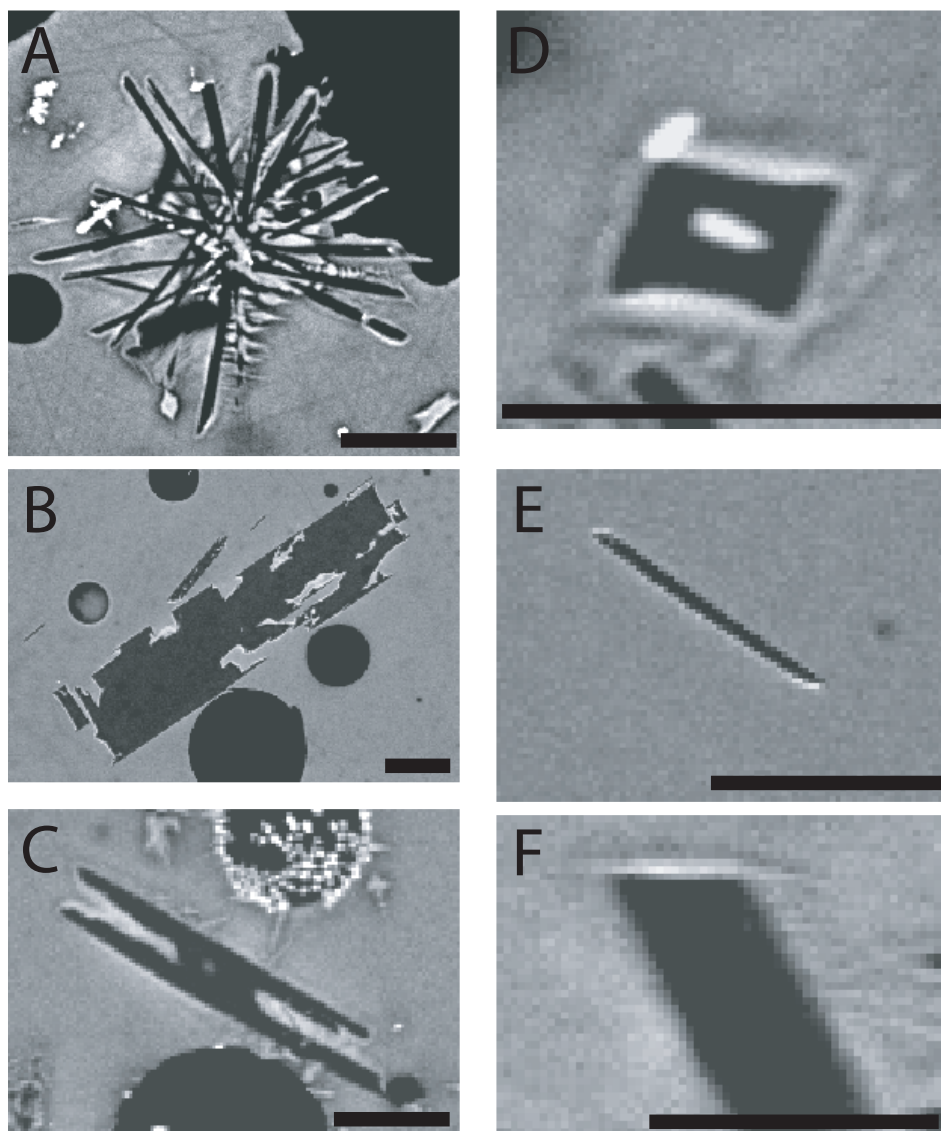


Figure 3.2. Plagioclase microlite morphologies as observed in BSE images, light gray color is glass and darker gray is plagioclase. (A) spherical, (B) skeletal, (C) swallowtail, (D) hopper, (E) acicular, and (F) tabular. Black scale bar is 10 microns in each image.

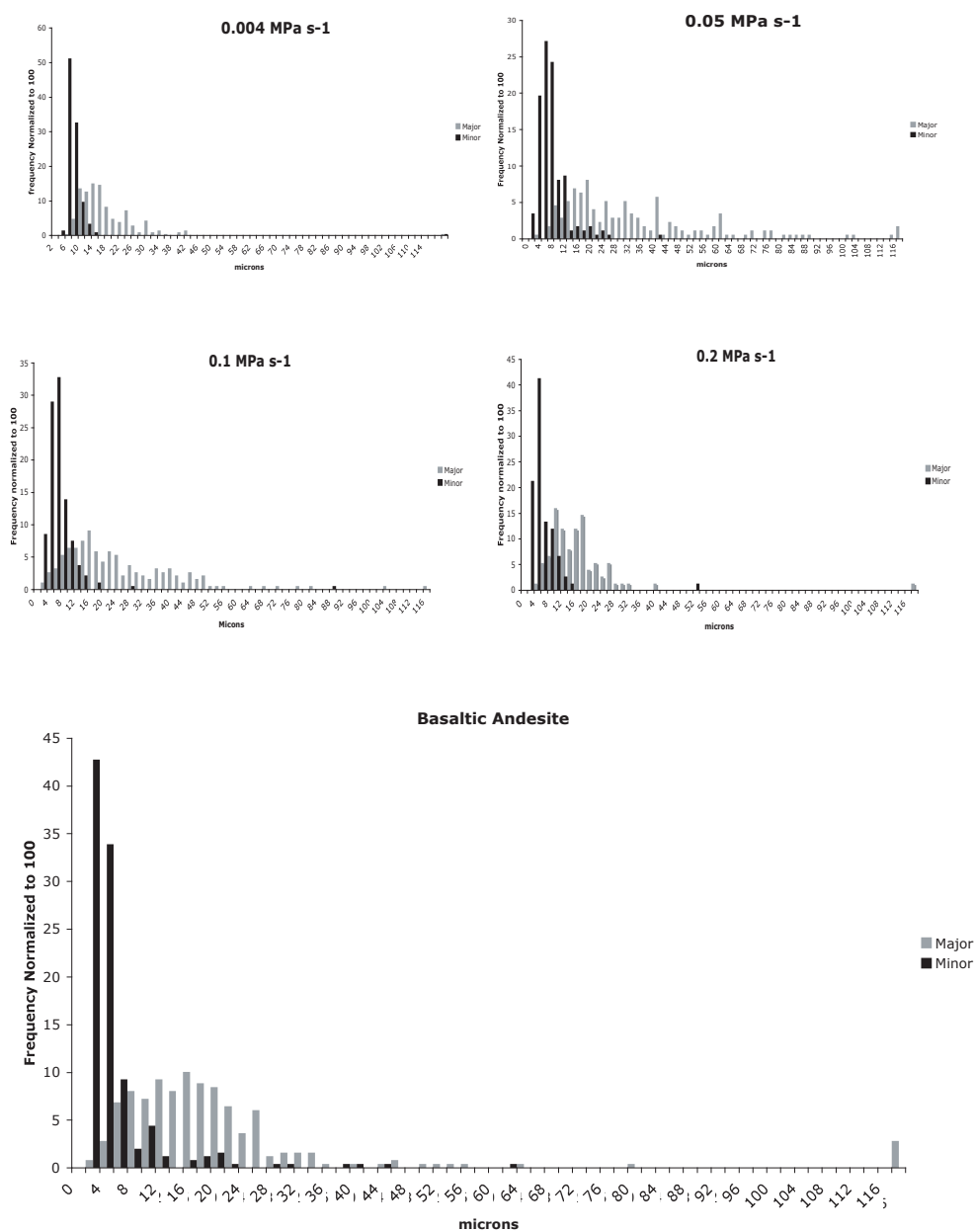


Figure 3.3. Normalized histograms of long and short crystal axes for selected experiments and basaltic andesite.

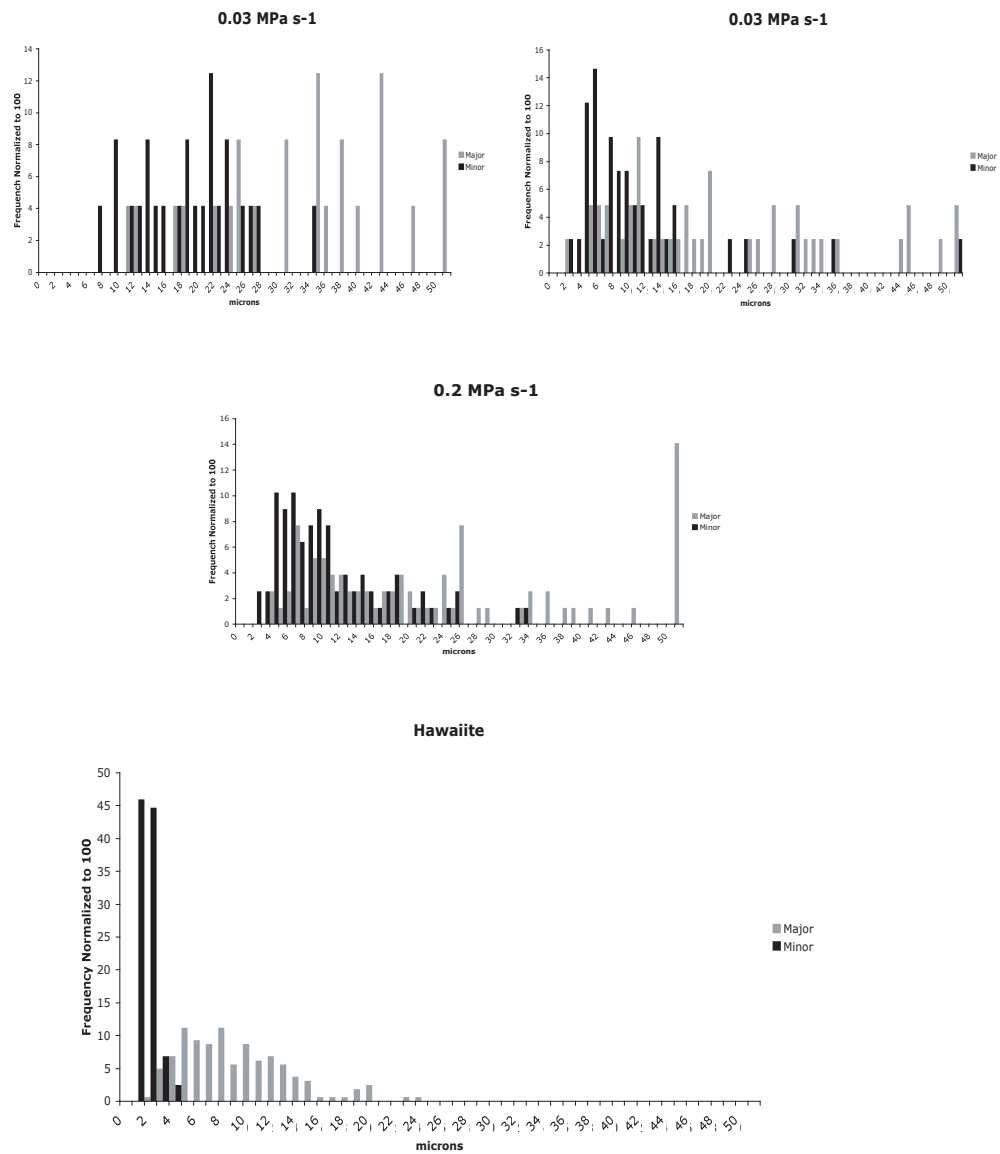


Figure 3.4. Normalized histograms of long and short crystal axes for selected experiments and Hawaiiite.

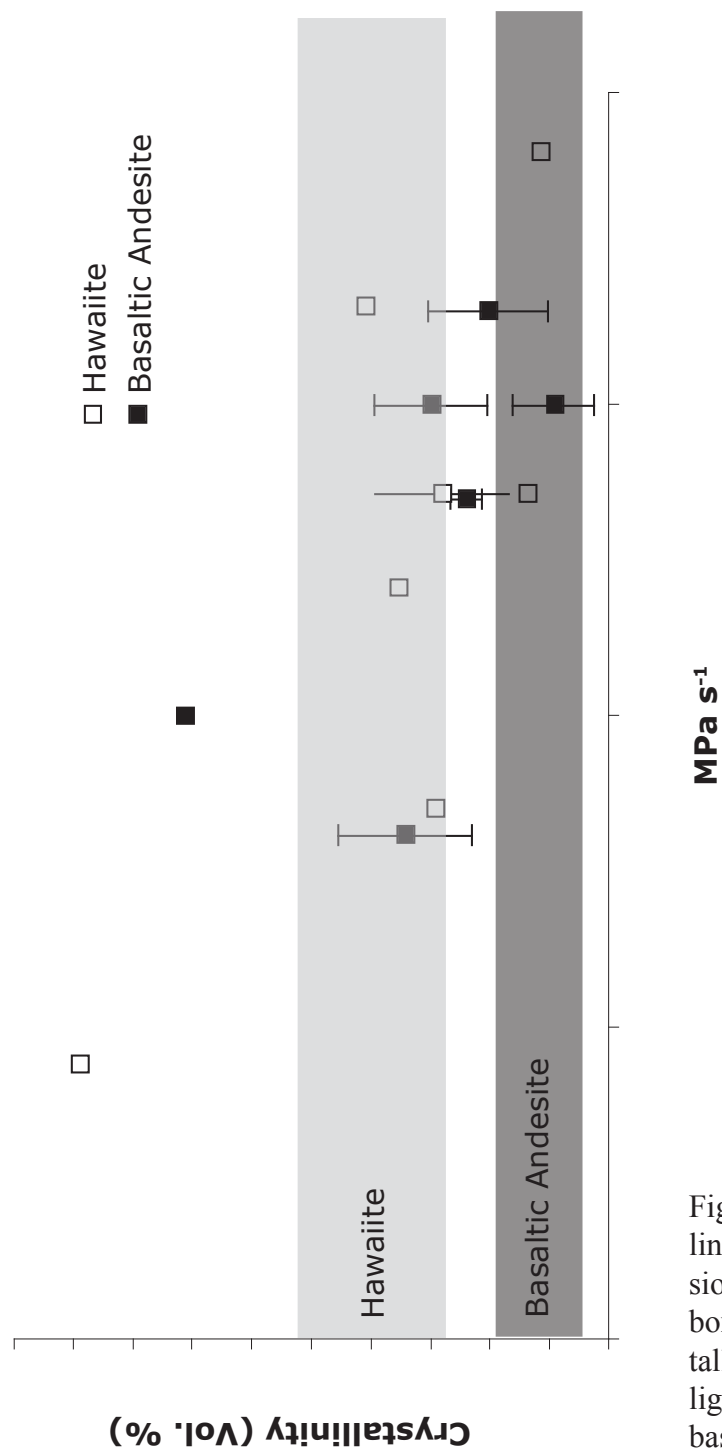


Figure 3.5. Crystallinity vs. decompression rate. Dark gray box is hawaiiite crystallinity range and light gray box is basaltic andesite crystallinity range.



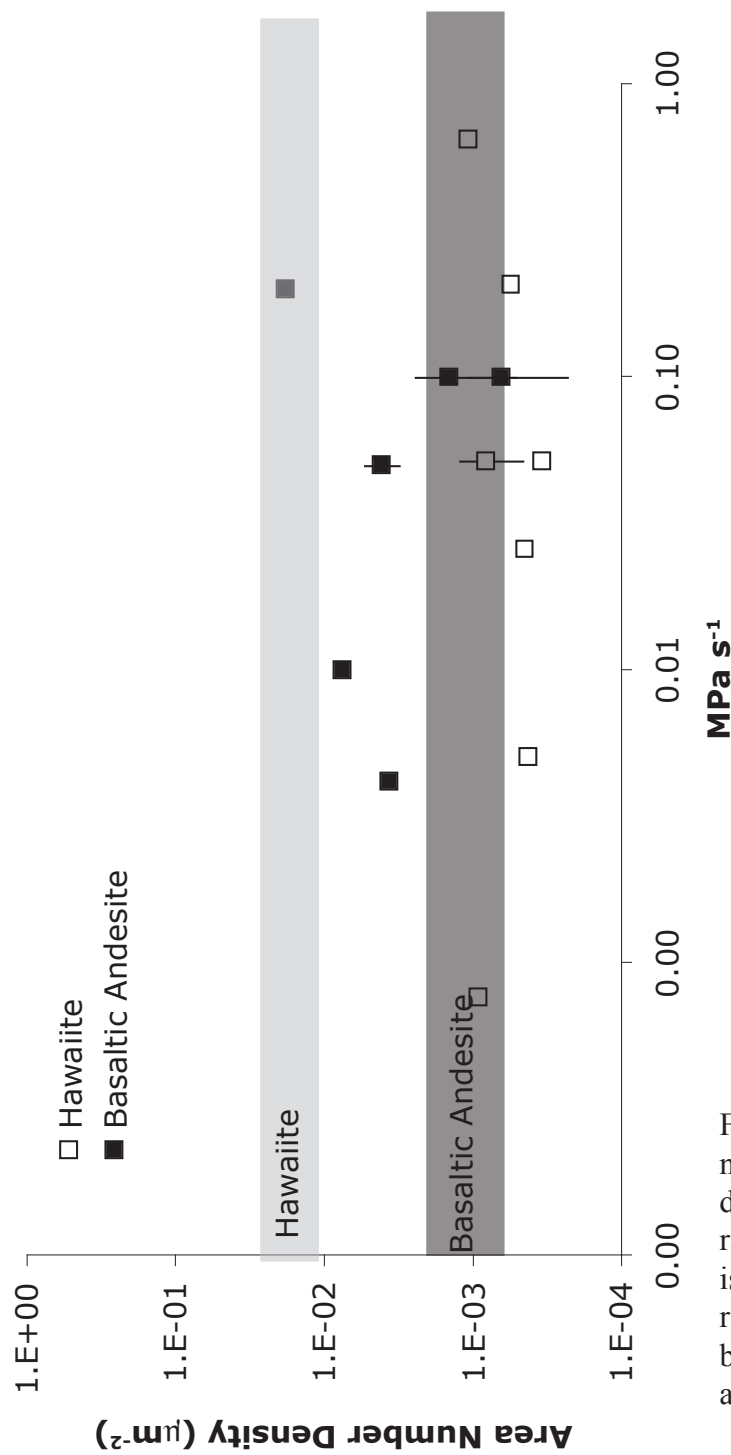


Figure 3.6. Area number density vs. decompression rate. Dark gray box is hawaiiite NA range and light gray box is basaltic andesite NA range.

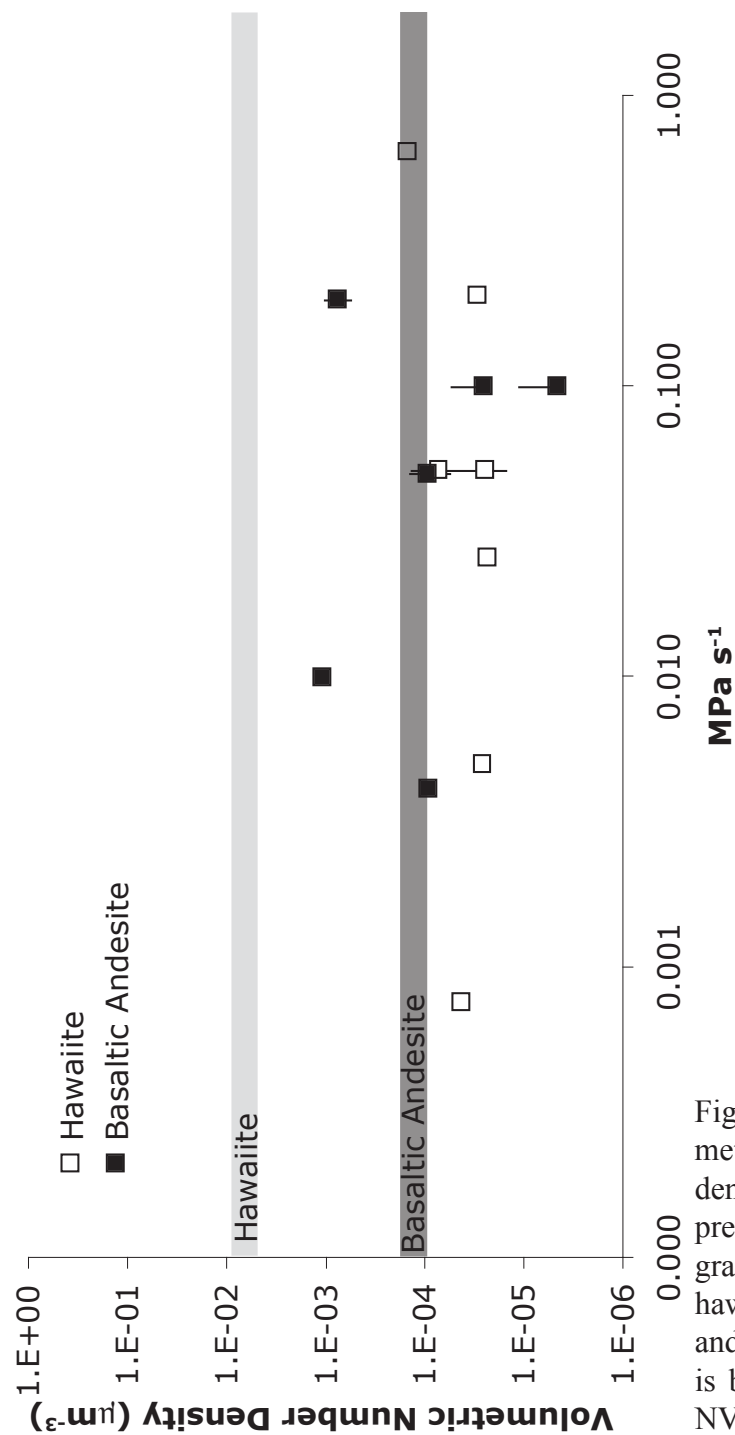


Figure 3.7. Volumetric number density vs. decompression rate. Dark gray box is hawaiiite NV range and light gray box is basaltic andesite NV range.

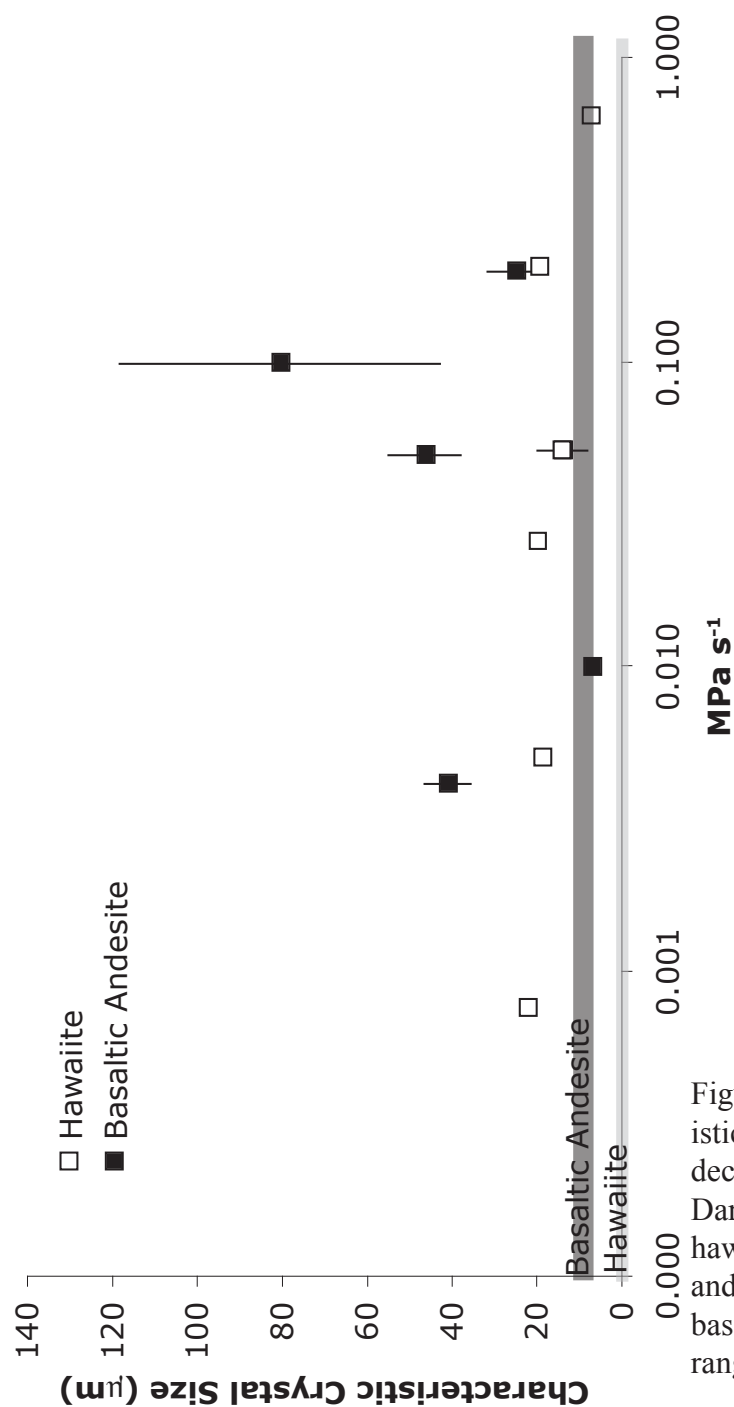


Figure 3.8. Characteristic crystal size vs. decompression rate. Dark gray box is hawaiite SN range and light gray box is basaltic andesite SN range.

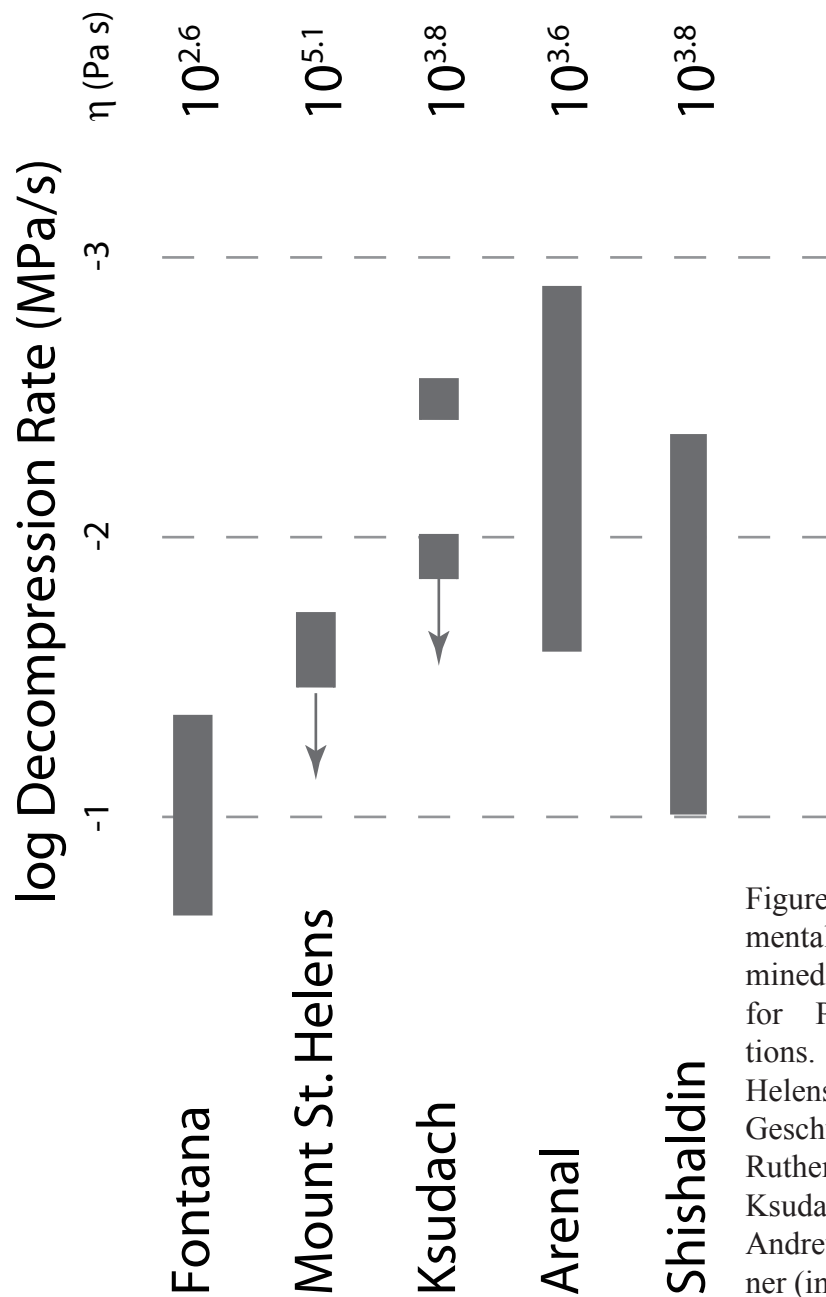


Figure 3.9. Experimentally determined ascent rates for Plinian eruptions. Mount St Helens data from Geschwind and Rutherford (1995), Ksudach data from Andrews and Gardner (in review), and Arenal data from Szramek et al. (2006).

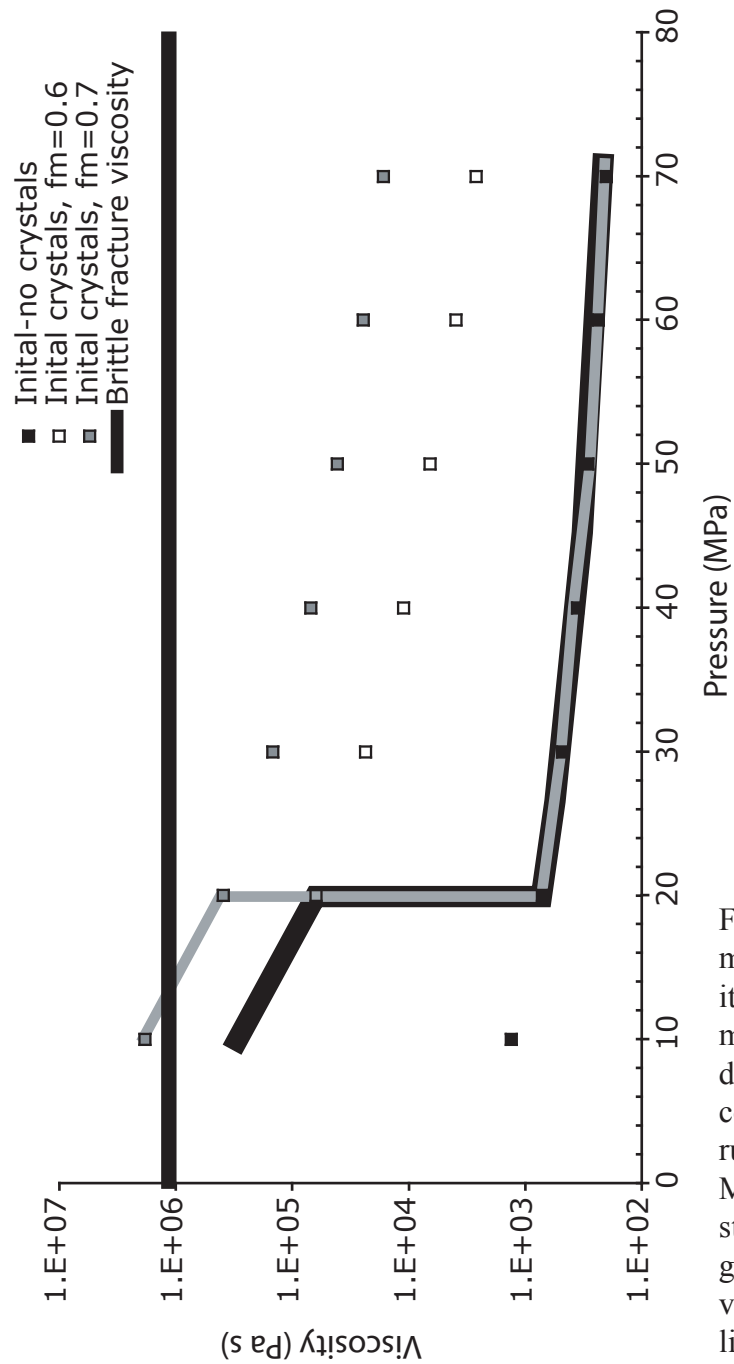


Figure 3.10. Etna modeling of viscosity changes when microlites grow at different levels in the conduit. Model was run at 70 MPa - 10 MPa in 10 MPa steps. Black and gray line follows viscosity for microlites growing at 20 MPa in the conduit. d (see Fig. 4.7).

Table 3.1: Bulk and matrix glass major element composition

	SiO <sub>2</sub>	TiO <sub>2</sub>	Al <sub>2</sub> O <sub>3</sub>	Fe <sub>2</sub> O <sub>3</sub>	FeO	MnO	MgO	CaO	Na <sub>2</sub> O	K <sub>2</sub> O	P <sub>2</sub> O <sub>5</sub>	H <sub>2</sub> O
Fontana Unit F*	52.74	1.24	15.53	13.41		0.23	3.96	8.40	2.80	1.49	0.32	
Fontana Matrix Glass"	53.56	1.34	15.01		13.54	0.28	3.58	7.93	2.06	1.71	0.35	
Etna 122b <sup>#</sup>	49.32	1.95	18.44	7.80	3.01	0.18	2.78	9.39	4.18	1.72	0.50	0.72
Etna Matrix Glass"	53.17	1.91	15.82		9.52	0.22	3.97	5.91	4.77	3.11	1.08	

\*Costantini et al., 2010

<sup>#</sup>Coltelli et al., 1998

"Goepfert, 2008

Table 3.2: Experimental Run Conditions

Run	Starting Material	Temperature(°C)	Starting Pressure (MPa)	Final Pressure (Mpa)	Experimental Duration (min)	Sample Weight (mg)	Water Weight (mg)	Decompression Rate (MPa/s)	Decompression Steps
F-S-1	Fontana pumice	1030	70	N/A	1440	108.9	7.6	N/A	N/A
F-1-D	F-S-1	1030	70	10	20	9.5	0.0	0.05	N/A
F-2-D	F-S-1	1030	70	10	40	7.0	0.0	0.03	N/A
F-3-D	F-S-1	1030	70	10	5	5.9	0.0	0.2	N/A
F-4-D	F-S-1	1030	70	10	240	7.6	0.0	0.004	N/A
F-6-D	F-S-1	1030	70	10	100	5.1	0.0	0.01	N/A
FSM	Fontana Pumice	1030	70	N/A	1440	46.5	8.0	N/A	N/A
F-8-D	FSM	1030	70	10	10	7.8	0.0	0.1	N/A
F-9-D	FSM	1030	70	10	10	6.6	0.0	0.1	10
ETNADST-2	ETNA Pumice	1035	75	N/A	1500	172.4	9.7	N/A	N/A
E-1	ETNADST-2	1035	75	13	20	13.5	2.5	0.05	N/A
E-2	ETNADST-2	1035	75	13	20	9.6	1.6	0.05	N/A
E-4	ETNADST-2	1035	75	13	5	14.2	1.2	0.2	N/A
E-5	ETNADST-2	1035	75	13	40	19.2	1.5	0.03	N/A
E-6	ETNADST-2	1035	75	13	204	14.3	1.3	0.01	N/A
E-7	ETNADST-2	1035	75	13	1.6	11.5	1.3	0.6	N/A
E-9	ETNADST-2	1035	75	13	1354	10.5	1.1	0.001	N/A
ETNADST-3	ETNA Pumice	1035	75	N/A	N/A	67.0	7.0	N/A	N/A
MSE-1	ETNADST-3	1035	75	13	41	7.1	0.8	0.03	10
MSE-2	ETNADST-3	1035	75	13	10.6	9.6	0.6	0.1	10
E-S-2	ETNA Pumice	1000	75	N/A	1560	98.8	10.1	N/A	N/A
E-2-1	E-S-2	1000	75	13	204	3.8	0.0	0.01	N/A
E-2-2	E-S-2	1000	75	13	20	6.1	0.0	0.05	N/A

Table 3.3: Natural Samples Textural Data									
122 Mt Etna									
Textural Data									
	$\Phi$ (vol. %)	Stdev	$N_A(\mu\text{m}^{-2})$	Stdev	$S_N(\mu\text{m})$	Stdev	$N_V(\mu\text{m}^{-3})$	Stdev	
Plagioclase	20	7	2.4E-02	1.0E-02	3.0	0.4	8.4E-03	3.9E-03	
Pyroxene	20	10	6.6E-02	1.2E-02	1.7	0.5	4.2E-02	1.9E-02	
Fe-Ti Oxides	3	1	5.0E-02	3.1E-02	0.9	0.3	6.5E-02	4.3E-02	
Total	43	12	1.4E-01	5.1E-02	1.8	0.4	8.3E-02	4.0E-02	
Fontana Lapilli									
Textural Data									
Total=Plagioclase	4	4	8.4E-04	1.0E-03	7.9	3.3	1.3E-04	1.7E-04	



Table 3.4. Groundmass Textures for Basaltic Andesite and Hawaiiite

	Basaltic Andesite Plagioclase vol. %	Hawaiiite Plagioclase vol. %	Hawaiiite Pyroxene vol. %
Dendritic			
Hopper	1		30
Acicular	3		
Swallowtail	11		
Spherulitic	16		
Tabular	33	100	70
Skeletal	36		

Table 3.5: Experimental Textures

Run	Decompression Rate (MPa/s)	Crystallinity (vol. %)	Stdev	Area		Stdev	Characteristic		Volumetric	
				Density (um- 2)	Number		Crystal Size (um)	Stdev	Number	Density (um <sup>-3</sup> )
F-1-D	0.05	12	1	4.1E-03	1	1.1E-03	46	8	9.4E-05	4.0E-05
F-3-D	0.2	10	5	1.8E-02	3.9E-04	3.9E-04	25	7	7.6E-04	2.2E-04
F-4-D	0.004	17	6	3.7E-03	2.5E-04	2.5E-04	41	5	9.1E-05	6.1E-06
F-6-D	0.01	35		7.5E-03			19		3.9E-04	
F-8-D	0.1	15	5	1.5E-03	9.5E-04	9.5E-04	80	38	2.5E-05	2.6E-05
F-9-D	0.1	5	3	6.4E-04	4.2E-04	4.2E-04	262	159	4.6E-06	6.0E-06
E-1	0.05	14	6	8.2E-04	3.7E-04	3.7E-04	14	6	7.2E-05	5.7E-05
E-2	0.05	7		3.4E-04			14		2.5E-05	
E-4	0.2	20		5.6E-04			19		2.9E-05	
E-5	0.03	18		4.5E-04			20		2.3E-05	
E-6-Pyroxene	0.01	5		1.4E-04			19		7.3E-06	
E-6-Plagioclase	0.01	15		4.3E-04			18		2.6E-05	
E-6-Total	0.01	19		5.6E-04			18		3.1E-05	
E-7	0.6	6		1.1E-03			7		1.5E-04	
E-9-Pyroxene	0.001	10		5.4E-04			13		4.1E-05	
E-9-Fe-Ti Oxides	0.001	1		2.0E-03			2		8.7E-04	
E-9-Plagioclase	0.001	44		9.3E-04			22		4.2E-05	
E-9-Total	0.001	55		3.5E-03			13		2.8E-04	
MSE-1	0.03	20	20	6.7E-05	7.5E-05	7.5E-05	43	32	1.3E-06	1.5E-06
MSE-2	0.1	3	8	6.7E-04	9.4E-05	9.4E-05	13	1	5.0E-05	3.2E-06

## **Chapter 4**

### **Cooling Induced Crystallization of Microlite Crystals in two Basaltic Pumice**

## Abstract

Microlites in pumice fragments can record the rate of magma decompression and ascent, but only if none grow while those fragments cool in the atmosphere. For highly viscous silicate melts such crystallization is unlikely, but more basic melts are known to crystallize rapidly, and thus could partially crystallize during cooling and overprint decompression textures. To examine whether post-fragmentation crystallization can occur, we examined two basaltic pumice from the sub-Plinian eruption of Shishaldin volcano, Alaska, in April, 1999. Radial sectioning shows that microlite content doubles from rim to core in both, mainly from growth of plagioclase. Dendrite magnetite also increases greatly in content, but only within the larger pumice. Such radial textures demonstrate that crystallization occurred after fragmentation and before deposition (no welding occurred). Using a conductive cooling model coupled with a model for temperature in the eruption column, we estimate that rims of the pumice cool to their glass-transition temperature in ~100-200 seconds, but their cores take ~500-2000 seconds to cool, which translate into cooling rates of ~0.2 to 2.5° C s<sup>-1</sup>. Using a conservative assumption that all plagioclase nucleated before cooling began, we estimate that both short and long axes grew at ~4.8(±2.7)×10<sup>-7</sup> cm s<sup>-1</sup>. Such rates match those determined experimentally for basaltic melts at similar cooling rates. Magnetite grew only at the slowest cooling rates, and the rate of bulk magnetite crystallization equals that of plagioclase. Our results demonstrate that groundmass crystallization can occur in basic melts on the time scale of explosive eruptions, and so pumice from such eruptions must be viewed with caution before being used to infer eruption dynamics.

## Introduction

The behavior of volcanic eruptions is controlled by how fast magma ascends towards the surface (Jaupart 2000). Ascent rates can only be inferred, however, because magma ascent cannot be witnessed. One potential record of how fast magma ascends are microlite crystals grown in the magma as it ascends, with more and larger ones linked to slower decompression rate, and hence ascent rates (e.g., Hammer and Rutherford 2002; Couch et al. 2003; Szramek et al. 2006). Indeed, changes in eruption dynamics in the 1968 eruption of Arenal volcano, Costa Rica, and the 1992 eruption of Mt. Spurr, USA, have been inferred from textural changes (Gardner et al. 1998; Szramek et al. 2006).

One assumption often used to interpret eruption dynamics from microlites is that all crystals nucleate and grow while the magma rises toward the surface and before it fragments, and none form while the magma cools in the atmosphere. Although that assumption may be valid for relatively silica-rich magma, in which nucleation and growth of crystals is slow, it may not be for more mafic melts, in which diffusion is rapid and viscosity is low. In fact, crystals can nucleate and grow in basaltic melts at cooling rates as fast as  $1000^{\circ}\text{C hr}^{-1}$  (Cashman 1993; Leshner et al. 1999). Interiors of relatively large pumice cool slower than that (Hort and Gardner 2000), and so their interior textures may be overprinted by cooling.

To investigate whether cooling can overprint pumice groundmass textures, we examine two large pumice from the 1999 eruption of Shishaldin, Alaska, which erupted tholeiitic basalt (Stelling et al. 2002). We show that significant crystallization occurred after fragmentation, imparting a radial pattern of crystal content inside the pumice. By

modeling the conductive cooling of pumice we use the sizes of microlites to estimate growth rates, and find that they are in line with experimental rates in basalt (Leshner et al. 1999). Our results suggest that caution must be used in inferring eruption dynamics from groundmass textures.

## Methods

Two pumice fragments were chosen from the ~20-cm-thick deposit on snow of the April 1999 activity at Shishaldin Volcano, Alaska. The larger one has dimensions of 10.8 x 8.9 x 7.6 cm, whereas the smaller one was 7.6 x 5.4 x 3.8 cm (Fig. 4.1). A series of polished thin sections were cut across each pumice, each orientated towards the center, and many included the exterior rim.

Petrographic microscope and Energy Dispersive X-Ray Spectroscopy (EDS) examination determined that the microlite assemblage consists of plagioclase and Fe-Ti oxides with trace amounts of olivine and pyroxene. Backscattered electron images (BSE Images) were collected at 5 positions from rim to core of each pumice, using the JEOL 8200 Superprobe at the University of Texas at Austin, at operating conditions of 15 keV and 10-20 nA with a focused beam (Fig. 4.2). Conditions were optimized for analyzing groundmass crystallinity by varying magnification, brightness, and contrast. The groundmass from a total of 39 BSE images was digitized and analyzed from the large pumice, and 30 from the small pumice (Table 1).

Crystallinity ( $\phi_i$ ) was determined for each phase ( $i$ ) by summing the total area of each phase and dividing by groundmass area (minus areas of vesicles and phenocrysts). We also measured an area number density,  $N_A$  (number  $\text{cm}^{-2}$ ), from which we estimated characteristic crystal size,  $S_n$ , which equals  $\left[\left(\frac{\phi}{100}\right)(N_A)^{-1}\right]^{\frac{1}{2}}$  and volumetric number density,  $N_V$ , which equals  $(N_A S_n^{-1})$ , following Hammer and Rutherford (2002). To measure individual sizes of plagioclase, each crystal was first outlined by hand, then its

area was measured. A best-fit ellipse was fit to each crystal to calculate its short and long axis. We report here sizes where more than 1000 crystals were measured (Table 1). In addition, plagioclase number density,  $N_P$  ( $\text{cm}^{-3}$ ), was calculated from our size measurements by dividing the plagioclase volume fraction by the sum of number of microlites of a certain size divided by total number of microlites multiplied by the volume of that size microlite, following the methods of Gardner et al. (1999). We estimated the volume of each plagioclase by assuming a tabular shape and that its intermediate axis equals the short axis, which probably slightly underestimates volume. On average, the error associated with  $N_P$  is  $\sim 20\%$ . Fe-Ti oxides, which are mainly dendritic and hence not conducive to individual crystal separation, were not measured separately.

Mineral and glass compositions were measured with the electron microprobe using operating conditions of 10 nA and 15 keV. Minerals were analyzed with a focused beam, whereas glasses were analyzed with a defocused beam ( $\sim 10 \mu\text{m}$ ). Most glass analyses were made near the rim because of increasing microlite occurrence towards the core. Sodium migration (Nielsen and Sigurdsson 1981) was monitored during every analysis, by measuring the count rate at the peak position, and then extrapolating to an initial count at time zero.

Dissolved water concentrations in glass inclusions hosted in plagioclase and pyroxene were determined via Fourier Transform Infrared Spectroscopy (FTIR) on doubly polished crystals. Crystals were separated by crushing several individual pumice, and hand picked using a binocular microscope with reflected light. Because of the dark color of adhering



basaltic glass, only crushed pieces of rock with visible crystal portions were chosen. Plagioclase and pyroxene were separated and each mineral was then mounted in epoxy, attached to a slide with crystal bond, and polished until a glass inclusion was intersected. The crystal was then removed by heating the crystal bond, flipped, and reattached to the slide, and the second side was polished until the same inclusion was intersected. The crystal was then separated from the slide with acetone and cleaned with ethanol.

FTIR analyses were made using a Nicolet Magna 750 FTIR spectrometer, using a KBr beam splitter, MCT-A detector, and a SpectraTech Analytical microscope, at the United States Geological Survey, Menlo Park, California. Seven spectra were collected in the mid-infrared region. Water concentration (in wt.%) was determined using a modified Beers-Lambert equation

$$c = \frac{18.02 A}{d \rho \epsilon} 100 \quad (1)$$

where  $A$  is absorbance,  $d$  is sample thickness (in cm),  $\rho$  is density (in g L<sup>-1</sup>), and  $\epsilon$  is molar absorptivity (in L mol<sup>-1</sup> cm<sup>-1</sup>), following Ihinger et al. (1994). We measured absorbance by total water at the 3550 cm<sup>-1</sup> band, assuming  $\epsilon = 63$  (Dixon et al. 1995) and  $\rho = 2800$  (Bouska 1993, p. 95). We did not iterate density for water content. A vertically mounted Mitutoyo micrometer was used to measure thickness, with an error of  $\pm 2\mu\text{m}$  as estimated by multiple measurements.

## Results

### *Phenocryst Assemblage and Glass Compositions*

The phenocryst assemblage consists of plagioclase, olivine, clinopyroxene, and Fe-Ti oxides. There is no change in either phenocryst content or composition from rim to core of either pumice. Plagioclase is complexly zoned, with a range of An<sub>50-90</sub>, but rim compositions (within 15  $\mu$ m) are relatively homogenous at An<sub>60.5</sub>. Clinopyroxene is Wo<sub>36.2</sub>Fs<sub>18.1</sub>En<sub>44.2</sub>, and olivine is Fo<sub>70.5</sub>. There are no observed compositional zonings in either olivine or clinopyroxene, but individual olivine phenocrysts differ in composition. Fe-Ti oxides were not analyzed in this study, but previous work found only magnetite (Stelling et al. 2002).

Regardless of position, glass is the dominant component of both pumice. Where crystallinity was low enough to allow microprobe analysis, usually less than ~30 vol.%, that glass is tholeiitic basalt, with ~50 wt.% SiO<sub>2</sub> and ~4.4 wt.% Na<sub>2</sub>O+K<sub>2</sub>O. Water contents in glass inclusions range from a low of 0.1 wt.% to a high of 1.4 wt.%, in agreement with estimates by Stelling et al. (2002). Given that no carbon was detected in the glass inclusions, minimum storage pressure would have been ~20 MPa, using the solubility model of Newman and Lowenstern (2002).

To estimate pre-eruptive temperature of the magma, we evaluated the bulk composition and phenocryst assemblage of the magma using the Melts model of Ghiorso and Sack (1995). Simulations were run at iterations in pressure and temperature, using a water content of 1.4 wt.% and an oxygen fugacity equal to the Ni-NiO buffer reaction. That fugacity is slightly lower than that estimated by Stelling et al. (2002) from a single

sulfur peak shift measurement, but should have no effect crystallization from cooling. When compared to the natural phase assemblage results from the Melts model indicate that the magma equilibrated at  $1060\pm 30^{\circ}\text{C}$  just before erupting.

#### *Groundmass Textures*

The outer 2-8 mm rind of the larger pumice is glassy with plagioclase and rare olivine and pyroxene (Fig. 4.2). Within that rind the abundance of plagioclase increases inward from ~20 to ~30 vol.% (Fig. 4.3), whereas there are no changes in the content of olivine or pyroxene. Further inwards to the core, plagioclase remains nearly constant in abundance. Magnetite first appears about 2 mm inside of the rim, and steadily increases in abundance to the core, reaching a maximum of 16 vol.%. Overall, crystallinity of the groundmass thus increases from 20 vol.% to 46 vol.% (Table 4.1). Throughout the pumice, ~96% of plagioclase are tabular, with the remaining ~4% hopper shaped (Fig. 4.2). Shallow-tailed plagioclase occur, but are extremely rare. Magnetite is always dendritic, but increases in size towards the core by having greater number of branches on each dendrite.

The outer ~5 mm rind of the small pumice appears very similar to that of the large pumice, with mainly plagioclase and rare olivine and pyroxene, except that the total amount of crystals is more variable (Fig. 4.3). Plagioclase abundance steadily increases to the core of the small pumice (Table 4.1). Plagioclase is dominantly tabular, with minor hopper plagioclase. In contrast to the large pumice, dendritic magnetite occurs only locally throughout the small one, never exceeding 1 vol.%.

Plagioclase size distributions appear similar at all positions within both pumice, being positively skewed with modal lengths of  $\sim 4\text{-}5\ \mu\text{m}$  and modal widths of  $\sim 0.5\ \mu\text{m}$  (Fig. 4.4). Plagioclase coarsens from rim to core in both pumice (Table 4.1), although differences in average sizes are slight, masked by the wide ranges in lengths and widths. In both pumice the characteristic size of plagioclase ( $S_n$ ) increases from the rim inwards, with most of the increase occurring between the rim and the mid-point (Table 4.1). In addition, we find that in both pumice the number of plagioclase shorter than  $8\ \mu\text{m}$  decrease from rim inward by  $\sim 8\text{-}16\%$ , whereas the number of those longer than  $10\ \mu\text{m}$  increase by  $\sim 33\text{-}50\%$ . In addition, the number of plagioclase narrower than  $5\ \mu\text{m}$  decrease slightly inward, especially in those narrower than  $2\ \mu\text{m}$ , whereas those wider than  $5\ \mu\text{m}$  increase by a factor of 2-4. The changes in sizes result in variations in plagioclase volumes with distance, with the number of plagioclase less voluminous than  $10\ \mu\text{m}^3$  decreasing by 15-20% in both pumice. Those 10 to  $100\ \mu\text{m}^3$  increase in number in both, by  $\sim 50\%$  in the small pumice but by only 7% in the large pumice. Plagioclase more voluminous than  $100\ \mu\text{m}^3$  also increase in number from the rim inward, by  $\sim 50\%$  in the small pumice and more than doubling in the large pumice. Importantly, much of the changes in length, width, and especially volume occur within the outer halves of both pumice (outer 9 mm in the small pumice; outer 18 mm in the large pumice).

There are no significant differences in either  $N_V$  or  $N_P$  for plagioclase in either pumice, with  $N_P$  averaging  $6.3(\pm 1.7) \times 10^9\ \text{cm}^{-3}$  (Table 1). We note that plagioclase in the outer part of the large pumice (0-8 mm) occur in numbers similar to the entire small

pumice, whereas they occur in slightly lower numbers in the inner part of the large pumice, although there is considerable overlap in number densities (Table 1).

The groundmass described above makes up more than 95% of all groundmass in both pumice. Both also contain minor pockets of four distinctly different groundmasses. Each variety comprises less than 1 vol.% of a pumice, and none vary systematically across either pumice. The first variety consists of relatively abundant pyroxene, olivine, and plagioclase with less than 5 vol.% glass, which is delimited from the surrounding groundmass by a thin line of magnetite. The glass in those pockets is basaltic andesite in composition, with ~54 wt.%  $\text{SiO}_2$  and ~5.1 wt.%  $\text{Na}_2\text{O}+\text{K}_2\text{O}$ . The second variety consists of dendritic magnetite that radiates outwards from vesicles, and overprints the nearby, otherwise normal groundmass. The third variety appears to be glass shards with sharp boundaries, and the fourth is holocrystalline aggregates. Those last two varieties are much rarer than the others.

## Discussion

Rims of both pumice are similar, containing ~13-20 vol.% of microlites (Fig. 4.3). Crystal content then increases from rim to core in both, and becomes less variable at a given general position (Table 4.1). In the small pumice, that increase results from coarsening plagioclase, whereas in the large pumice it results from both coarsening plagioclase and increasing amounts of magnetite. The appearance of magnetite in the large pumice is likely caused by slower cooling. Overall changes in groundmass crystallization are thus radial in both pumice.

For such radial variations to have formed in the flowing magma as it rises up the conduit, there would have to have been non-random nucleation and growth of crystals on the scale of centimeters or less. Although such small-scale fluctuations may occur, the radial distribution leads us to propose that instead they formed after the magma fragmented, and specifically while the pumice cooled in the atmosphere. Pumice cool from their exteriors inward, and so their interiors can potentially remain hot for significant amounts of time (Hort and Gardner 2000). If their interiors remain hot long enough, then they may crystallize, and so radial variations could be seen from rim to core. The main control on how long a pumice remains hot is its size, with larger ones able to remain hot longer. Such cooling has been invoked to explain radial variations in pumice color, magnetization, and vesicularity (Gardner et al. 1996; Tait et al. 1998).

Assuming that the observed textural variations resulted from radial cooling, we model the thermal history of the two pumice. To infer cooling rates at various locations within each, we utilize the model of Hort and Gardner (2000), which couples a cooling model

for pumice and ash with a steady-state eruption column model. The eruption column is modeled using the equations of Glaze and Baloga (1996) and Glaze et al. (1997), which balance mass, momentum, and energy. The model solves for both vertical mean velocity and mean temperature within the eruption column, and then estimates the position of a pumice with time by assuming that gas and particles move together. Using that position and its associated temperature, a conductive cooling model is then used to solve for the thermal profile in a spherical pumice.

We used the estimated column height, dense rock equivalent, and average mass flux for the sub-Plinian activity of April 1999 (Stelling et al. 2002) as input parameters in the model. The initial and final temperature for the pumice, however, had to be estimated. For the initial temperature we used the pre-eruptive temperature of 1060° C. As for the end of cooling, we assume as a first-order approximation that crystallization ceases when its glass transition temperature ( $T_g$ ) is reached. We use a value of 739(±1)° C (Giordano et al. 2005), which assumes that the groundmass glass degassed completely.

Having determined temperature bounds over which crystallization occurred, the amount of time that a portion of each pumice would remain above  $T_g$  can be estimated; we focus on the rim, middle, and core of each pumice (Fig. 4.5). Given those time scales for cooling, we use our textural data to estimate crystallization rates of plagioclase. We use the average of the 10 largest microlites (Table 1), following Leshner et al. (1999).

To estimate growth rates, we must assume that either all plagioclase formed during cooling or that some formed during ascent, before cooling began. If we assume all formed during cooling, then growth rates are simply size divided by the amount of time

above  $T_g$ . To instead allow for crystallization before the pumice erupted at the surface, we can assume that all microlites in the rim of each pumice formed during ascent. Crystallization rates for slower cooling interiors can then be estimated by first subtracting the sizes of microlites in the rim.

In the case where all crystallization is assumed to occur during cooling, we find that the groundmass crystallized at a rate of  $\sim 0.07 (\pm 0.05) \text{ vol.\% s}^{-1}$  (Fig. 4.6). Growth rates of long and short axes vary linearly with cooling rate (Fig. 4.7). Interestingly, the ratio of growth rates (long axis versus short axis) is relatively constant at  $3.3 \pm 0.5$ . If we instead assume that some crystallization occurred before the pumice began cooling, then the overall rate of crystallization is reduced to  $\sim 0.022 (\pm 0.019) \text{ vol.\% s}^{-1}$  (Fig. 4.6). At that rate the groundmass would completely crystallize in about 75 minutes. Growth rates are reduced by about an order of magnitude, with that for the long axis reduced more than for the short axis (Fig. 4.7). Interestingly, most of the modified growth rates fall within a narrow range and average  $4.8(\pm 2.7) \times 10^{-7} \text{ cm s}^{-1}$ , except for one anomalously slow rate.

Given that there is little variation in either  $N_V$  or  $N_P$  for plagioclase in either pumice, it seems more likely that at least some microlites nucleated before cooling. In addition, given the extreme cooling rates that we estimate for the pumice, more skeletal crystals would be expected (e.g., Lofgren 1980). Taking the extreme view that all crystals nucleated before cooling, we find that both long and short axes grew at rates of  $\sim 5 \times 10^{-7} \text{ cm s}^{-1}$  at cooling rates of  $0.2^\circ$  to  $3^\circ \text{ C s}^{-1}$ .

Experimental constraints on crystal growth at such fast cooling rates for terrestrial magmas are not common. Lesher et al. (1999) found that solitary plagioclase laths grew



in a basaltic melt at  $1.6 \times 10^{-7} \text{ cm s}^{-1}$  when cooled  $\sim 0.01^\circ \text{ C s}^{-1}$  and at  $\sim 2.2 \times 10^{-6} \text{ cm s}^{-1}$  when cooled  $\sim 0.3^\circ \text{ C s}^{-1}$  (Fig. 4.8). Conte et al. (2006) found similar rates, on order of  $10^{-6} \text{ cm s}^{-1}$  at  $\sim 0.25^\circ \text{ C s}^{-1}$ . Our growth rates compare favorably, although slower, with those experimental results, and thus appear reasonable. Our rates are slightly slower than those predicted by the empirical calibration of Cashman (1993), which may imply that our assumption that growth that occurred before cooling is recorded by all plagioclase found in the rims may be too conservative.

Although we did not quantify sizes of the magnetite dendrites, their radial change in abundance is consistent with cooling variations. Our model predicts that the interior of the large pumice cooled more slowly than the entire small pumice, and it is only in the interior of the large pumice that we find significant amounts of magnetite. At those cooling rates, magnetite grows at a rate similar rate as plagioclase (Fig. 4.6). The lack of significant crystallization of either olivine or clinopyroxene is probably related to the suppression of their crystallization at such high cooling rates (Leshner et al. 1999).

### *Implications*

We have shown that basaltic pumice can be affected by post-fragmentation cooling crystallization, which can potentially overprint crystallization during ascent. Inferring ascent histories for explosively erupted basic magmas can thus be difficult if such overprinting is significant. Indeed, a study that attempted to estimate ascent rates of basaltic andesite at Arenal volcano found that cooling overprinting made it impossible to constrain anything except that magma erupted in Plinian fashion ascended faster than that erupted in non-Plinian events (Szramek et al. 2006). Such overprinting is unlikely to

occur in more silicic melts, in which kinetics are slower and crystallization is unlikely to occur after fragmentation (Hammer and Rutherford 2002). Caution must, however, be taken when examining pumice from more basic magmas, such as basalt and basaltic andesite. For example, assuming that observed crystallinities found in the erupted products of basic magma could lead to erroneously high estimates for the rheology of such magma in conduit modeling. Finally, if groundmasses can crystallize on the timescale of pumice ejection in explosive eruptions, then bubble populations (i.e., vesicles) should even more easily adjust to post-fragmentation conditions (Gardner et al. 1996).

The radial variations in texture in the Shishaldin pumice suggest that rims of pumice are the best candidates for recording decompression histories. Even small lapilli, on order of a few centimeters, cool at rates similar to the rims of large pumice, which means that if crystallization can occur in the rims, it can occur in a wide range of pumice (Hort and Gardner 2000).

One interesting observation is that the ratio of tabular to hopper microlites remains unchanged between and across each pumice clast. This observation suggests that the morphology of the plagioclase was not determined via cooling-induced growth, as experimental and observational literature thus far has reported (Lofgren 1980). It is unclear why the ratio of tabular to hopper microlites does not change, although it may be related to the variation in cooling rate across each pumice clast. Although based only on two samples, the lack of a cooling overprint on crystal morphology may yet allow ascent rates to be inferred for basic magma.

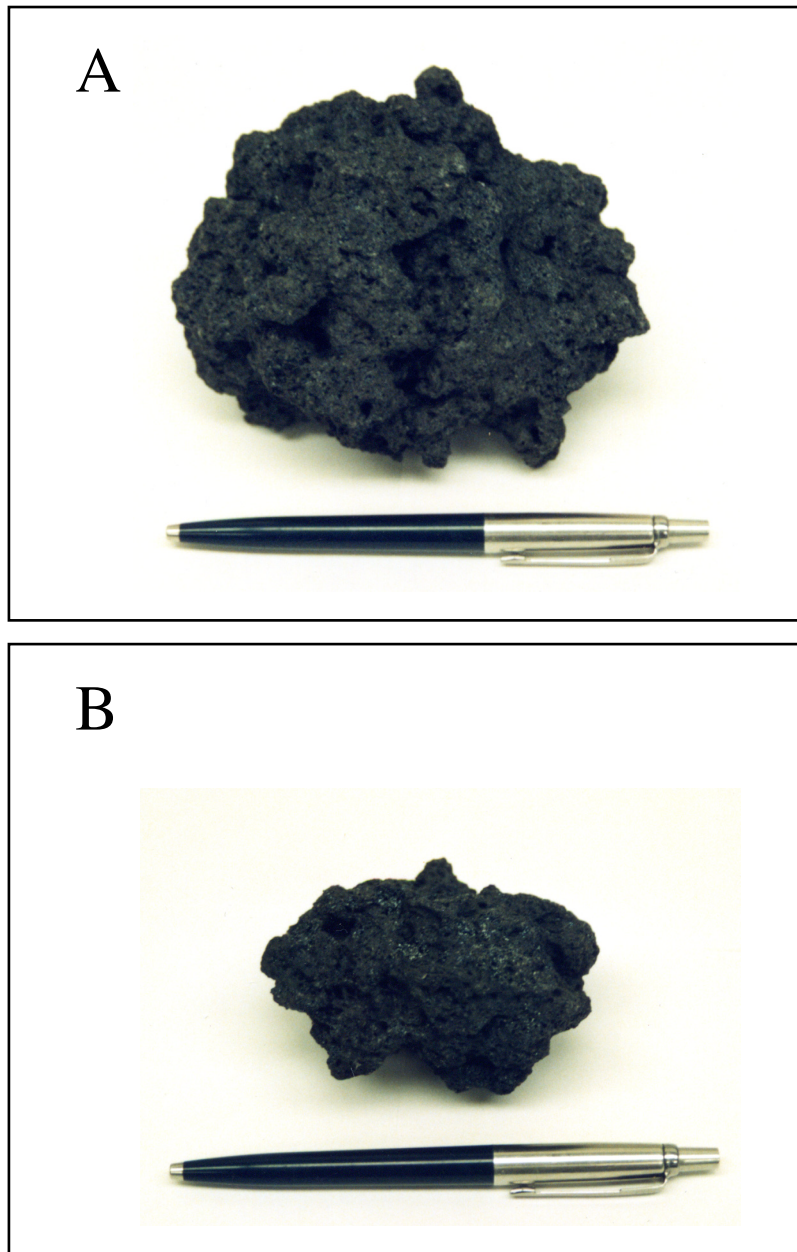


Figure 4.1. Photographs of (A) large and (B) small basaltic pumice from Shishaldin volcano, Alaska, used in this study. The pen in both pictures is approximately 14 cm long.

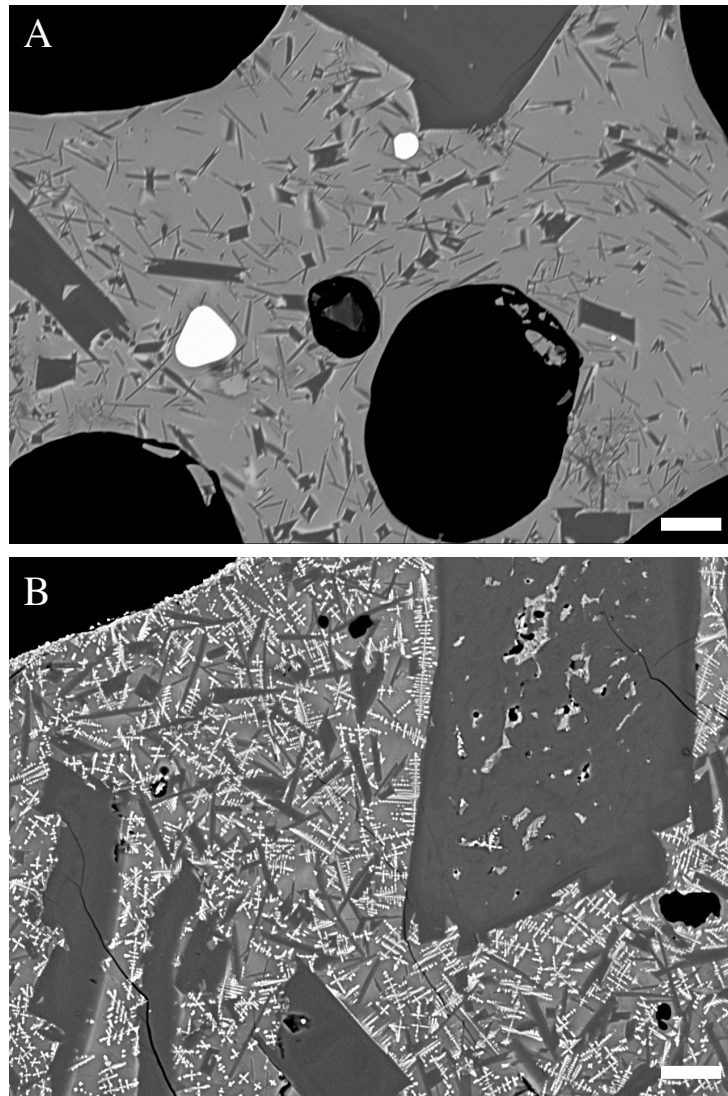


Figure 4.2. Representative backscattered electron images of (A) rim and (B) core of the large pumice. Plagioclase is in dark gray, magnetite is bright areas, glass is light gray, and vesicles are black. Note the dendritic shape of magnetite microlites. The scale bar in each image is 20  $\mu\text{m}$  long.

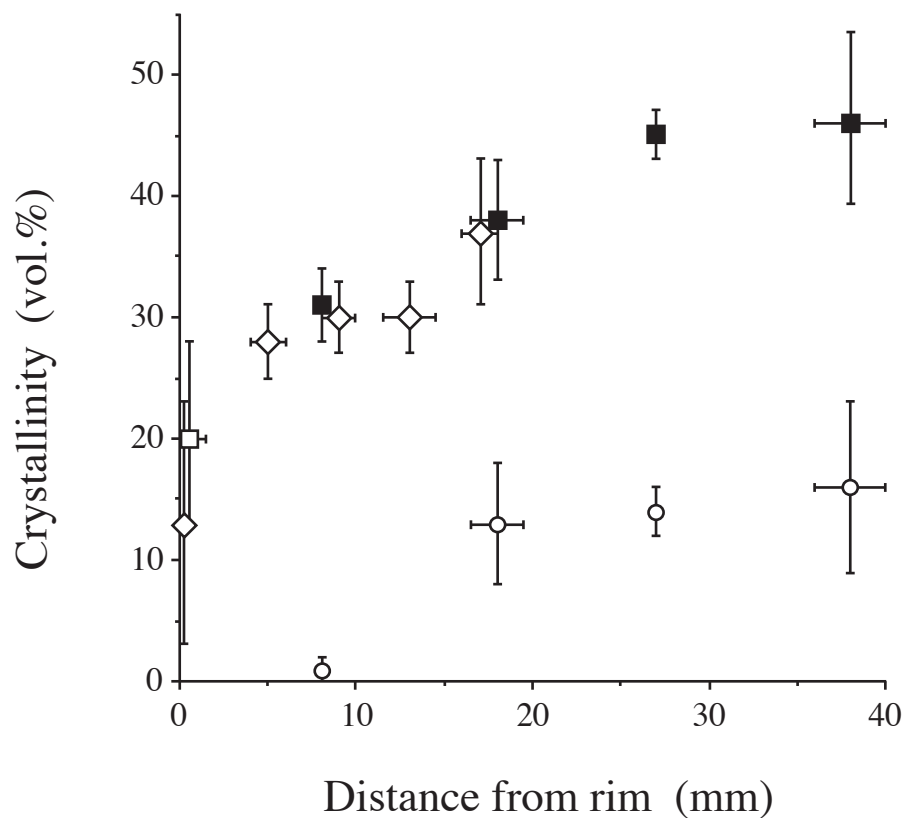


Figure 4.3. Groundmass crystallinity (in volume percent) as a function of position in either the large (squares) or small (diamonds) pumice. In the small pumice, crystal content is plagioclase only, but equals either plagioclase (open square) or plagioclase plus magnetite (filled squares) in the large pumice. Magnetite contents are shown as circles. Errors on content are from averaging multiple images at each position. The area covered by those images at each position is shown as horizontal error bars.

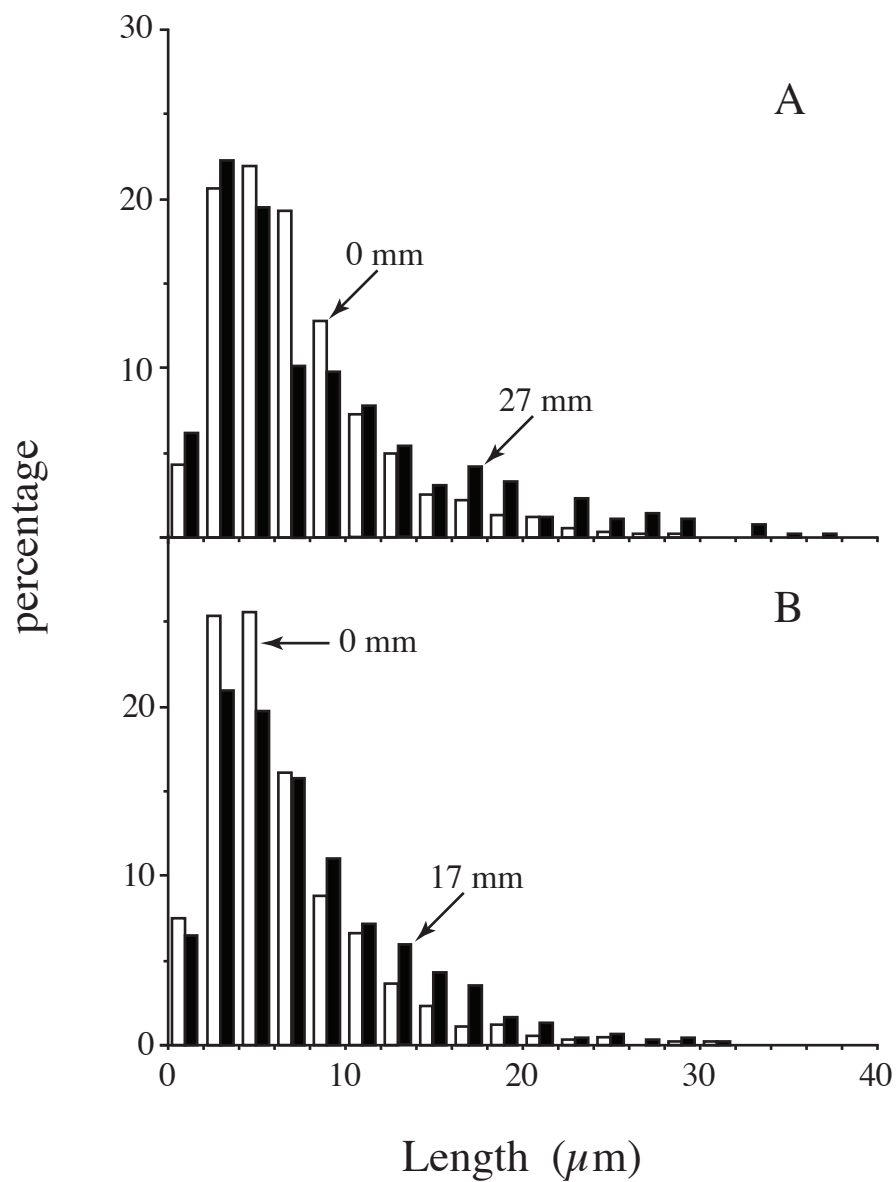


Figure 4.4. Representative size distributions of plagioclase microlites: (A) long axes (at 0 and 27 mm from the rim of the large pumice) and (B) short axes (at 0 and 17 mm from the rim of the small pumice).

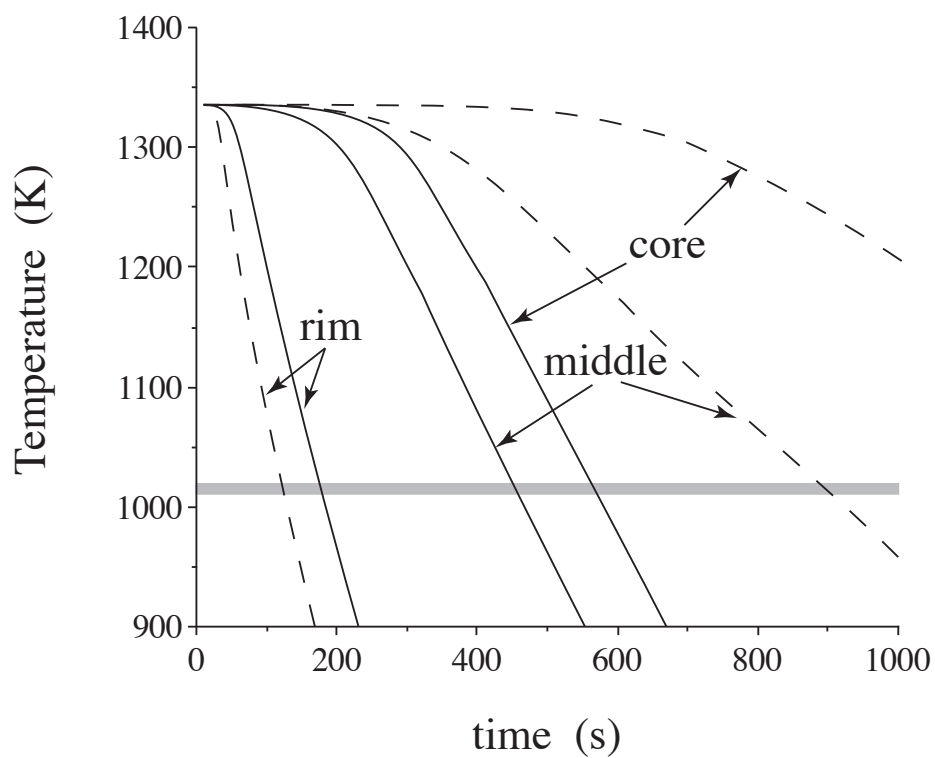


Figure 4.5. Modeled variations in temperature as a function of time at the rim, middle, and core of the small pumice (solid lines) and large pumice (dashed lines). The assumed final temperature for crystallization is shown by the horizontal gray bar.

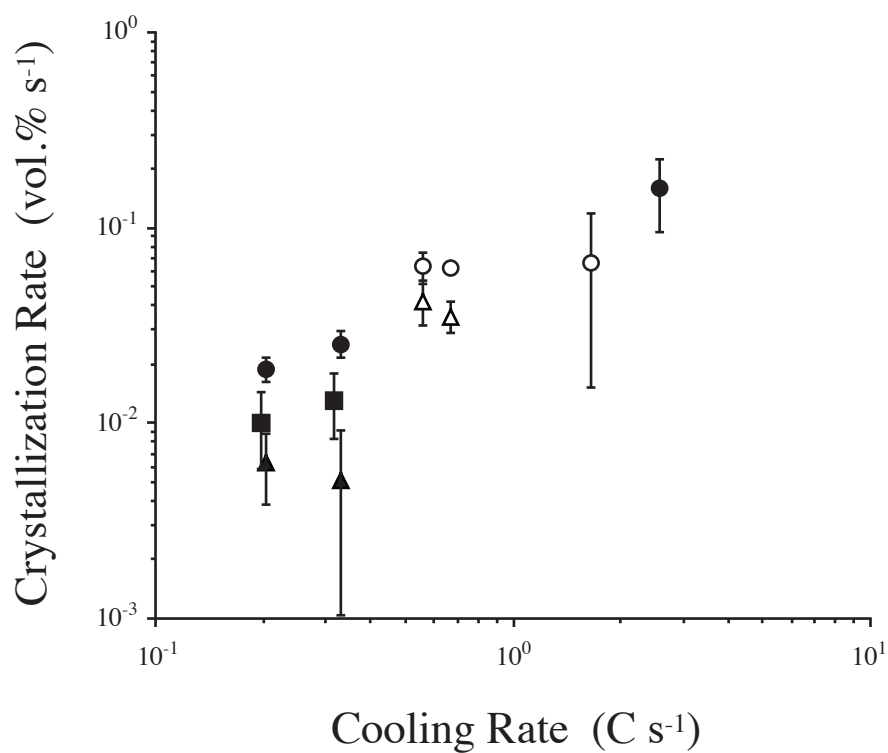


Figure 4.6. Crystallization rates of plagioclase and magnetite in large (filled symbols) and small pumice (open symbols) as a function of cooling rate. Circles are rates estimated assuming that all plagioclase grew during cooling; triangles are rates estimated assuming that some plagioclase grew before cooling (using the amount in the rims as proxies). Squares are for magnetite (offset slightly for clarity).



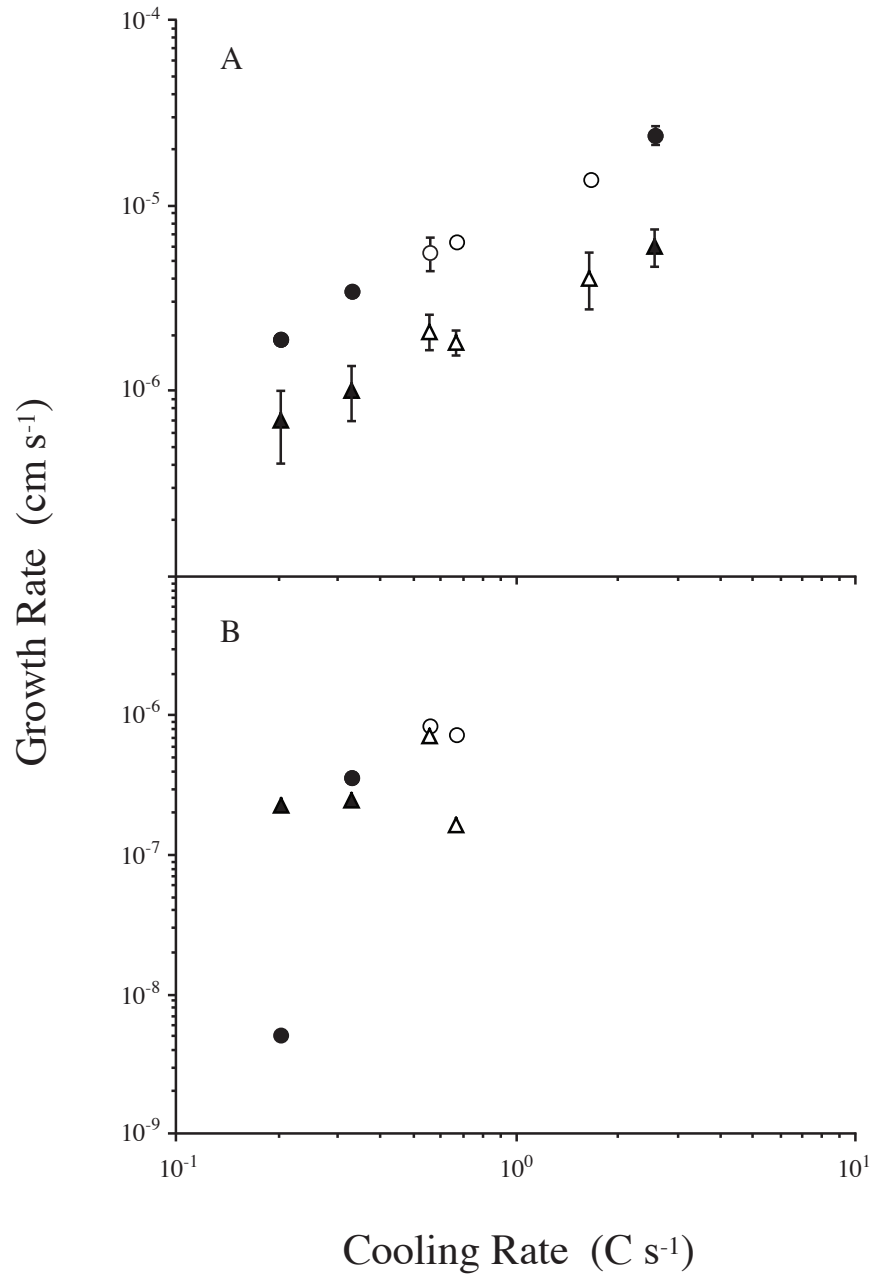


Figure 4.7. Growth rates of the long axis (circles) and short axis (triangles) of plagioclase in the large pumice (filled symbols) and the small pumice (open symbols) as a function of cooling rate. Rates in (A) are estimated assuming that all plagioclase grew during cooling; those in (B) are estimated assuming that some plagioclase grew before cooling (using the amount in the rims as proxies).

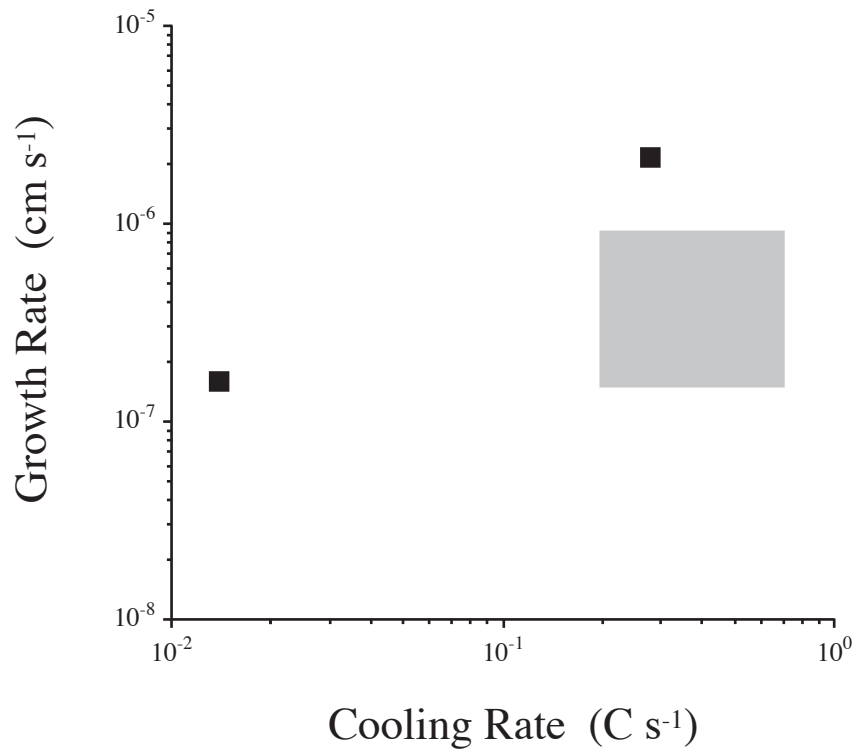


Figure 4.8. Growth rates as a function of cooling rate in Shishaldin pumice (outlined by gray box) and experiments performed on cooling basalt from Leshner et al. (1999). Note that an anomalously low growth rate from the natural data has been excluded (see Fig. 4.7).

**Table 4.1:** Crystal Contents, Sizes, and Number Densities In Basaltic Pumice

Position (mm)	$\phi_{\text{plag}}$ (vol.%)	$\phi_{\text{ox}}$ (vol.%)	$Sn$ ( $\mu\text{m}$ )	$Long$ ( $\mu\text{m}$ )	$Short$ ( $\mu\text{m}$ )	$N_V (\times 10^9)$ ( $\text{cm}^{-3}$ )	$N_P (\times 10^9)$ ( $\text{cm}^{-3}$ )
<i>Small Pumice</i>							
0 $\pm$ 0.5(8)	13 $\pm$ 10	-	2.6	27.1	7.9	6.8 $\pm$ 1.1	4.6
5 $\pm$ 1(7)	28 $\pm$ 3	-	3.0	-	-	10 $\pm$ 2	-
9 $\pm$ 1(4)	30 $\pm$ 3	-	3.3	30.6	8.7	8.6 $\pm$ 1.8	8.6
13 $\pm$ 1.5(4)	30 $\pm$ 3	-	3.2	-	-	8.7 $\pm$ 1.7	-
17 $\pm$ 1(7)	37 $\pm$ 6	-	3.4	32.0	12.1	9.3 $\pm$ 1.8	7.3
<i>Large Pumice</i>							
0 $\pm$ 1(11)	20 $\pm$ 8	-	3.1	30.2	7.4	7.3 $\pm$ 2.8	7.6
8 $\pm$ 0.5(3)	30 $\pm$ 3	1 $\pm$ 1	3.3	-	-	8.6 $\pm$ 1.6	-
18 $\pm$ 1.5(11)	25 $\pm$ 4	13 $\pm$ 5	3.9	33.8	9.9	5.3 $\pm$ 3.4	4.7
27 $\pm$ 0.5(3)	31 $\pm$ 2	14 $\pm$ 2	3.7	-	-	5.8 $\pm$ 1.1	-
38 $\pm$ 2(11)	30 $\pm$ 4	16 $\pm$ 7	3.9	30.3	11.1	5.8 $\pm$ 2.9	5.0
<i>Notes:</i> Position refers to average position of a group of images (number given in parentheses) analyzed, with the range given as the error, measured relative to the pumice rim. Crystallinity ( $\phi$ ) of plagioclase and Fe-Ti oxide microlites are listed separately. Characteristic sizes are for plagioclase only. Long and Short are the averages of the 10 longest axes of plagioclase measured, restricted to positions where more than 1000 microlites were measured. The average error on $N_P$ is 20%.							

## **Chapter 5**

### **Conclusion to Dissertation**

## Conclusion

This dissertation is an examination of mafic magma, from understanding how volatiles are recycled into the source regions to how mafic magma can erupt in a Plinian fashion and what happens to the tephra after fragmentation.

In the section on deep mantle recycling, I used Nb rather than K to constrain the amount of Cl that was present in the HIMU source after subduction. This enabled me to also constrain the amount of K present in HIMU. I found that only a small amount of Cl is recycled into the deep mantle, however the amount recycled is greater than the amount in MORB. Therefore, it appears that while subduction does remove Cl, I am seeing a small net influx of Cl into the deep mantle. In the case of K, I find that subduction removed over 90% of the amount present in altered oceanic crust resulting in a minimal amount of K present in HIMU. K does not appear to be increasing in the mantle over geologic time. I also found that that Cl/Nb ratios do not vary depending on the source, suggesting that the global Cl/Nb ratio in the mantle may be the same.

Moving to the surface, I next look at how a low viscosity melt can erupt in a Plinian fashion. I know that fragmentation requires brittle failure, but the viscosity of mafic melt should not allow this to occur. I tested the hypothesis that a rapid decompression is required for a mafic Plinian eruption. I found that one of our sample eruptions had a rapid decompression whereas the other sample eruption was not able to be bracketed. Another observation is that experimentally determined decompression rate does not correlate with magma viscosity as I initially expected it would. It appears that fast ascent is not required for mafic magmas to erupt in a Plinian fashion.

Looking at what happens to samples after fragmentation, I have shown that basaltic pumice can be affected by post-fragmentation crystallization, which can potentially overprint crystallization during ascent. Using a cooling model that outputs cooling rates as a function of pumice size, we have been able to determine growth rates for plagioclase. My growth rates are similar to those that have been previously been determined by experiments at similar cooling rates.

# Appendix 1: Experimental and Natural data for Chapter 3

F-1-D				
Label	Area	Major	Minor	Shape
image012.bmp	17.99308	7.78047	2.94449	hopper
image012.bmp	83.73702	16.77216	6.3568	hopper
image012.bmp	5.88235	3.9069	1.91703	hopper
image012.bmp	46.7128	12.6992	4.68349	hopper
image012.bmp	8.3045	8.00501	1.32087	hopper
image012.bmp	35.64014	11.65095	3.89483	hopper
image012.bmp	8.65052	7.11041	1.54902	hopper
image012.bmp	35.64014	10.66986	4.25295	hopper
image012.bmp	119.03114	20.27893	7.47353	swallowtail
image012.bmp	102.07612	18.58013	6.99497	swallowtail
image012.bmp	100.69204	26.61247	4.81748	swallowtail
image012.bmp	88.92734	34.21323	3.30942	swallowtail
image012.bmp	1858.47751	56.86403	41.61307	spherulitic
image012.bmp	2269.20415	150.99807	19.13429	spherulitic
image012.bmp	1893.07958	102.36628	23.54627	spherulitic
image012.bmp	188.92734	84.74485	2.83852	acicular
image012.bmp	9.34256	12.50419	0.95131	acicular
image012.bmp	8.99654	7.14808	1.60249	acicular
image012.bmp	30.44983	22.44418	1.72739	acicular
image012.bmp	572.31834	81.53621	8.93711	skeletal
image012.bmp	91.34948	24.27058	4.79221	skeletal
image012.bmp	306.57439	54.9333	7.10576	skeletal
image012.bmp	241.86851	30.57826	10.07109	skeletal
image012.bmp	141.52249	17.68557	10.18865	skeletal
image012.bmp	325.60554	77.80253	5.32854	skeletal
image012.bmp	36.33218	15.36907	3.00991	skeletal
image012.bmp	24.22145	12.82572	2.40452	skeletal
image012.bmp	247.75087	60.31219	5.23022	skeletal
image012.bmp	75.77855	19.07431	5.05834	skeletal
image012.bmp	212.45675	59.86903	4.51833	skeletal
image012.bmp	343.94464	32.87775	13.31977	skeletal
image012.bmp	26.29758	15.58835	2.14796	skeletal
image012.bmp	455.0173	52.04318	11.13203	skeletal
image012.bmp	399.65398	69.93399	7.27622	skeletal
image012.bmp	125.95156	23.29111	6.88531	skeletal
image012.bmp	231.48789	40.46283	7.2842	skeletal
image012.bmp	255.70934	60.5534	5.37673	skeletal
image012.bmp	155.0173	32.27081	6.11618	skeletal
image012.bmp	33.21799	8.34458	5.0685	skeletal
image012.bmp	299.30796	75.789	5.02831	skeletal
image012.bmp	400.69204	70.98452	7.18716	skeletal
image012.bmp	711.76471	115.47481	7.84801	skeletal
image012.bmp	46.02076	25.12295	2.33235	skeletal
image012.bmp	43.59862	14.29923	3.88213	skeletal
image012.bmp	194.80969	26.52076	9.35265	skeletal
image012.bmp	88.58131	16.25353	6.93912	skeletal
image012.bmp	33.91003	20.1526	2.14243	skeletal
image012.bmp	234.9481	47.32314	6.32133	skeletal

image012.bmp	1083.391	135.72267	10.16349	skeletal
image012.bmp	124.56747	55.23234	2.87158	skeletal
image012.bmp	25.60554	8.64023	3.77328	skeletal
image012.bmp	393.77163	45.50919	11.0168	skeletal
image012.bmp	387.54325	47.99978	10.27995	skeletal
Label	Area	Major	Minor	Shape
image012.bmp	78.20069	30.71286	3.24191	skeletal
image012.bmp	50.51903	9.42113	6.82751	skeletal
image012.bmp	23.52941	8.67054	3.45521	skeletal
image012.bmp	162.62976	30.263	6.84224	skeletal
image012.bmp	528.3737	41.32266	16.28033	skeletal
image012.bmp	931.14187	61.92007	19.14673	skeletal
image012.bmp	915.91696	74.94882	15.55971	skeletal
image012.bmp	470.58824	83.50061	7.17566	skeletal
image012.bmp	137.37024	40.80815	4.28604	skeletal
image012.bmp	78.54671	30.82674	3.24422	skeletal
image012.bmp	494.11765	44.52542	14.12969	skeletal
image012.bmp	87.19723	20.55503	5.40126	skeletal
image012.bmp	193.77163	33.85451	7.28759	skeletal
image012.bmp	87.19723	27.29756	4.06714	skeletal
image012.bmp	101.03806	23.06759	5.5769	skeletal
image012.bmp	225.60554	38.44413	7.47188	skeletal
image012.bmp	179.9308	19.85994	11.53553	skeletal
image012.bmp	1887.19723	193.34618	12.42773	skeletal
image012.bmp	73.70242	24.77581	3.7876	skeletal
image012.bmp	45.32872	26.18661	2.20396	skeletal
image012.bmp	241.17647	34.93017	8.79112	skeletal
image012.bmp	164.70588	40.56052	5.1703	skeletal
image012.bmp	45.67474	15.33538	3.7922	skeletal
image012.bmp	65.0519	23.63042	3.50509	skeletal
image012.bmp	95.50173	21.08592	5.76672	skeletal
image012.bmp	76.47059	18.65944	5.21802	skeletal
image012.bmp	57.78547	29.01724	2.53555	skeletal
image012.bmp	88.23529	31.80929	3.53182	skeletal
image012.bmp	216489.2734	539.25706	511.1527	area
image012.bmp	8369.55017	130.79991	81.47133	vesicles
image013.bmp	1.38504	1.82168	0.96805	hopper
image013.bmp	16.06648	4.88618	4.1866	hopper
image013.bmp	14.40443	5.44236	3.36992	hopper
image013.bmp	39.8892	9.44454	5.37755	hopper
image013.bmp	45.15235	10.29799	5.58262	swallowtail
image013.bmp	189.75069	42.00717	5.75135	swallowtail
image013.bmp	1331.30194	76.56503	22.13891	spherulitic
image013.bmp	1205.26316	70.87533	21.65194	spherulitic
image013.bmp	1230.19391	64.11845	24.42872	spherulitic
image013.bmp	132.96399	60.49722	2.79839	acicular
image013.bmp	60.94183	28.00065	2.77113	acicular
image013.bmp	83.10249	40.44956	2.61583	acicular
image013.bmp	59.27978	36.67001	2.05829	acicular
image013.bmp	100	51.67777	2.46381	acicular
image013.bmp	75.34626	11.23038	8.54235	skeletal



image013.bmp	171.74515	24.19512	9.03789	skeletal
image013.bmp	57.06371	18.61453	3.90318	skeletal
image013.bmp	119.39058	29.31044	5.1863	skeletal
image013.bmp	696.6759	87.08758	10.18555	skeletal
image013.bmp	429.08587	49.7986	10.97077	skeletal
image013.bmp	140.72022	21.32033	8.40374	skeletal
image013.bmp	1344.59834	101.31473	16.8978	skeletal
image013.bmp	184.21053	52.13174	4.49907	skeletal
image013.bmp	86.14958	20.2515	5.41634	skeletal
Label	Area	Major	Minor	Shape
image013.bmp	40.72022	15.35167	3.37726	skeletal
image013.bmp	342.38227	59.33218	7.34736	skeletal
image013.bmp	92.24377	28.13317	4.17473	skeletal
image013.bmp	111.63435	29.64951	4.79392	skeletal
image013.bmp	268.69806	46.16323	7.41103	skeletal
image013.bmp	212.18837	37.10837	7.28048	skeletal
image013.bmp	63.4349	17.79691	4.53831	skeletal
image013.bmp	67.31302	18.18544	4.71287	skeletal
image013.bmp	39.8892	12.06715	4.20882	skeletal
image013.bmp	42.93629	8.70898	6.27722	skeletal
image013.bmp	154.84765	39.2954	5.01733	skeletal
image013.bmp	174.51524	33.89031	6.55644	skeletal
image013.bmp	120.77562	19.73268	7.79297	skeletal
image013.bmp	151.52355	34.75248	5.55142	skeletal
image013.bmp	65.37396	18.54456	4.48847	skeletal
image013.bmp	61.21884	16.62052	4.68976	skeletal
image013.bmp	40.99723	8.12376	6.42551	skeletal
image013.bmp	173.4072	40.5201	5.44887	skeletal
image013.bmp	122.99169	35.09195	4.4625	skeletal
image013.bmp	104.98615	16.44768	8.12713	skeletal
image013.bmp	51.52355	12.32853	5.32114	skeletal
image013.bmp	70.91413	14.36713	6.28453	skeletal
image013.bmp	213.2964	35.83418	7.57873	skeletal
image013.bmp	342.93629	61.35686	7.1164	skeletal
image013.bmp	229.36288	31.87843	9.16086	skeletal
image013.bmp	111.63435	19.99184	7.10977	skeletal
image013.bmp	68.69806	14.46441	6.04719	skeletal
image013.bmp	247.09141	41.40679	7.59795	skeletal
image013.bmp	189.75069	40.35444	5.9869	skeletal
image013.bmp	113.01939	25.49444	5.6444	skeletal
image013.bmp	188.36565	32.95965	7.27661	skeletal
image013.bmp	68.97507	13.11799	6.69476	skeletal
image013.bmp	109.41828	19.31867	7.21145	skeletal
image013.bmp	67.31302	19.20802	4.46197	skeletal
image013.bmp	149.8615	40.14548	4.75295	skeletal
image013.bmp	29.63989	17.96537	2.10063	skeletal
image013.bmp	160.94183	32.6932	6.26789	skeletal
image013.bmp	85.87258	16.37568	6.67675	skeletal
image013.bmp	127.97784	14.61231	11.15131	skeletal
image013.bmp	130.19391	19.81642	8.36519	skeletal
image013.bmp	213.2964	62.08134	4.37454	skeletal

image013.bmp	144.59834	41.50591	4.43571	skeletal
image013.bmp	33.241	16.65751	2.54082	skeletal
image013.bmp	248.47645	31.51516	10.03866	skeletal
image013.bmp	35.18006	18.20963	2.45983	skeletal
image013.bmp	149.30748	24.46873	7.76927	skeletal
image013.bmp	122.71468	16.62234	9.39971	skeletal
image013.bmp	85.87258	11.67316	9.36647	skeletal
image013.bmp	124.65374	25.66346	6.18444	skeletal
image013.bmp	52.07756	16.25534	4.0791	skeletal
image013.bmp	549.8615	44.09195	15.87831	skeletal
image013.bmp	55.12465	14.61192	4.8034	skeletal
image013.bmp	85.31856	20.74703	5.23598	skeletal
image013.bmp	102.49307	30.69912	4.25088	skeletal
Label	Area	Major	Minor	Shape
image013.bmp	255.67867	37.62674	8.65183	skeletal
image013.bmp	193.90582	27.67585	8.92072	skeletal
image013.bmp	108.03324	12.30551	11.17809	skeletal
image013.bmp	492.24377	60.10062	10.42825	skeletal
image013.bmp	40.44321	12.08265	4.2618	skeletal
image013.bmp	217.17452	44.57587	6.20325	skeletal
image013.bmp	774.79224	89.96928	10.96481	skeletal
image013.bmp	77.83934	12.60056	7.86538	skeletal
image013.bmp	39.8892	15.77196	3.22018	skeletal
image013.bmp	32.68698	14.96675	2.78072	skeletal
image013.bmp	89.47368	30.61515	3.72108	skeletal
image013.bmp	124.65374	19.99267	7.93861	skeletal
image013.bmp	388.91967	48.3605	10.23951	skeletal
image013.bmp	89.19668	14.77671	7.68566	skeletal
image013.bmp	839.05817	58.1963	18.35721	skeletal
image013.bmp	162.32687	24.45087	8.45291	skeletal
image013.bmp	149.03047	24.29009	7.81189	skeletal
image013.bmp	171460.3878	514.21516	424.55019	area
image013.bmp	2261.49584	68.75781	41.8778	vesicles
image013.bmp	140.44321	15.81194	11.30904	vesicles
image013.bmp	4213.85042	82.30497	65.18733	vesicles
image013.bmp	1895.01385	57.17005	42.20403	vesicles
image013.bmp	14368.69806	196.31281	93.19206	vesicles

#### F-3-D

Label	Area	Major	Minor	Shape
image021.bmp	7.11111	5.66983	1.5969	hopper
image021.bmp	89.66667	16.21193	7.04217	hopper
image021.bmp	6.88889	4.11281	2.13265	hopper
image021.bmp	27.11111	9.91074	3.48298	hopper
image021.bmp	9.55556	5.74105	2.11921	hopper
image021.bmp	60.33333	14.77682	5.1986	hopper
image021.bmp	8.77778	3.95184	2.8281	hopper
image021.bmp	61.77778	10.80258	7.2814	hopper
image021.bmp	17.22222	9.30959	2.35542	swallowtail
image021.bmp	39.88889	13.16635	3.85742	swallowtail
image021.bmp	76.66667	13.45851	7.25304	spherulitic

image021.bmp	110.77778	14.84393	9.50197	spherulitic
image021.bmp	10.66667	15.16412	0.89562	acicular
image021.bmp	10.22222	11.90707	1.09308	acicular
image021.bmp	37.66667	27.90681	1.71853	acicular
image021.bmp	4.77778	7.78069	0.78184	acicular
image021.bmp	26.44444	21.47652	1.56776	acicular
image021.bmp	16.55556	12.44642	1.69359	acicular
image021.bmp	17.66667	16.78091	1.34045	acicular
image021.bmp	15.33333	17.94033	1.08822	acicular
image021.bmp	24.44444	16.13258	1.92924	skeletal
image021.bmp	51.88889	12.27404	5.38266	skeletal
image021.bmp	36.11111	19.09484	2.40788	skeletal
image021.bmp	75.44444	25.78958	3.72472	skeletal
image021.bmp	21.22222	7.804	3.46245	skeletal
image021.bmp	24.11111	8.23932	3.72594	skeletal
image021.bmp	216.77778	38.91958	7.0918	skeletal
image021.bmp	90.77778	23.44561	4.92979	skeletal
image021.bmp	96.44444	19.0793	6.43613	skeletal
image021.bmp	27.88889	8.72445	4.07008	skeletal
image021.bmp	29.33333	11.06232	3.37618	skeletal
image021.bmp	44.66667	8.82108	6.44721	skeletal
image021.bmp	209.22222	30.92238	8.6148	skeletal
image021.bmp	12.66667	5.08993	3.16855	skeletal
image021.bmp	30	15.65512	2.43992	skeletal
image021.bmp	158.55556	17.42758	11.58389	skeletal
image021.bmp	15.88889	9.49498	2.13064	skeletal
image021.bmp	50.44444	9.16511	7.00786	skeletal
image021.bmp	26.66667	14.38167	2.36086	skeletal
image021.bmp	28.55556	11.73276	3.09885	skeletal
image021.bmp	212.33333	23.28247	11.61179	skeletal
image021.bmp	36132	254.36154	180.8634	area
image021.bmp	1560.11111	57.25412	34.69436	vesicles
image021.bmp	1491.77778	49.91461	38.0528	vesicles
image021.bmp	156.88889	17.29615	11.54923	vesicles
image021.bmp	205.22222	23.52305	11.10813	vesicles
image021.bmp	110.44444	24.30345	5.7861	vesicles
image021.bmp	221.66667	34.48125	8.18517	vesicles
image021.bmp	202.66667	18.20972	14.17063	vesicles
image021.bmp	139.44444	15.17965	11.69633	vesicles
image021.bmp	140	18.79769	9.48273	vesicles
image020.bmp	15.66667	7.93989	2.5123	hopper
image020.bmp	38.44444	10.9522	4.46933	hopper
Label	Area	Major	Minor	Shape
image020.bmp	19.33333	11.59404	2.12316	swallowtail
image020.bmp	35.77778	16.29784	2.79507	swallowtail
image020.bmp	13.77778	21.25686	0.82526	acicular
image020.bmp	7.44444	9.72723	0.97444	acicular
image020.bmp	6.33333	6.4363	1.25287	acicular
image020.bmp	13.77778	16.59135	1.05732	acicular
image020.bmp	45	14.46907	3.95988	skeletal
image020.bmp	38.88889	12.66261	3.91032	skeletal

image020.bmp	51.44444	14.00383	4.67737	skeletal
image020.bmp	51.66667	17.58452	3.74102	skeletal
image020.bmp	62.44444	10.64321	7.47018	skeletal
image020.bmp	114.22222	24.37114	5.9674	skeletal
image020.bmp	25.77778	8.76569	3.74429	skeletal
image020.bmp	26	9.86323	3.35633	skeletal
image020.bmp	38	16.576	2.91886	skeletal
image020.bmp	54.22222	18.51445	3.72887	skeletal
image020.bmp	46.44444	16.89612	3.49991	skeletal
image020.bmp	215.77778	29.28451	9.38164	skeletal
image020.bmp	253.22222	24.4475	13.18796	skeletal
image020.bmp	36	17.51003	2.61774	skeletal
image020.bmp	13.33333	8.81079	1.92679	skeletal
image020.bmp	157.11111	20.48332	9.766	skeletal
image020.bmp	67.55556	14.95837	5.75025	skeletal
image020.bmp	15.77778	10.66748	1.88319	skeletal
image020.bmp	79.55556	24.67846	4.10452	skeletal
image020.bmp	9.88889	7.9184	1.59008	skeletal
image020.bmp	36	12.21833	3.75147	skeletal
image020.bmp	18.44444	9.3936	2.50002	skeletal
image020.bmp	103.33333	21.59299	6.09309	skeletal
image020.bmp	23.55556	7.31959	4.09748	skeletal
image020.bmp	104.77778	15.89336	8.39389	skeletal
image020.bmp	13.22222	4.81557	3.49596	skeletal
image020.bmp	27.88889	11.41719	3.11016	skeletal
image020.bmp	4676.77778	116.69465	51.02769	skeletal
image020.bmp	9404.22222	206.43046	58.00417	area
image020.bmp	139	18.54383	9.54389	vesicles
image020.bmp	150.66667	20.36908	9.41794	vesicles
image020.bmp	194.66667	18.18403	13.63049	vesicles
image020.bmp	25	6.77817	4.6961	vesicles

F-4-D				
Label	Area	Major	Minor	Shape
image023.bmp	21.58333	8.98251	3.05936	Tabular
image023.bmp	57.25	21.41491	3.40384	Tabular
image023.bmp	44.55556	16.45117	3.44838	Tabular
image023.bmp	50.44444	11.45047	5.60919	Tabular
image023.bmp	32.80556	20.39746	2.04777	Tabular
image023.bmp	23.72222	10.82811	2.78941	Tabular
image023.bmp	14.44444	7.15481	2.57047	Tabular
image023.bmp	60.86111	17.52025	4.42293	Tabular
image023.bmp	58.44444	14.08568	5.28294	Tabular
image023.bmp	29.27778	8.30126	4.4906	Tabular
image023.bmp	32.19444	10.43277	3.92909	Tabular
image023.bmp	33.72222	12.79392	3.35601	Tabular
image023.bmp	21.86111	10.80384	2.57635	Tabular
image023.bmp	34.58333	16.31925	2.69822	Tabular
image023.bmp	41.41667	19.35372	2.72471	Tabular
image023.bmp	12.5	6.44854	2.46808	Tabular
image023.bmp	17.47222	8.51132	2.61373	Tabular

image023.bmp	10.91667	4.65683	2.98476	Tabular
image023.bmp	15	5.53016	3.45353	Tabular
image023.bmp	20.83333	8.22691	3.22427	Tabular
image023.bmp	25.88889	10.3416	3.1874	Tabular
image023.bmp	16.25	7.79442	2.65448	Tabular
image023.bmp	13.52778	8.008	2.15086	Tabular
image023.bmp	13.91667	7.27808	2.43461	Tabular
image023.bmp	13.05556	6.49248	2.56032	Tabular
image023.bmp	22.02778	9.81141	2.85857	Tabular
image023.bmp	40.91667	8.58297	6.06978	Tabular
image023.bmp	34.36111	10.94167	3.99847	Tabular
image023.bmp	20.30556	5.67795	4.55338	Tabular
image023.bmp	16.86111	8.53776	2.5145	Tabular
image023.bmp	119.27778	26.41498	5.74936	Tabular
image023.bmp	15.25	5.50581	3.52662	Tabular
image023.bmp	28.58333	10.11246	3.59887	Tabular
image023.bmp	32.33333	8.95302	4.59823	Tabular
image023.bmp	25.63889	14.15994	2.30541	Tabular
image023.bmp	34.88889	9.15932	4.84991	Tabular
image023.bmp	31.72222	13.28912	3.03933	Tabular
image023.bmp	22.55556	7.19761	3.99002	Tabular
image023.bmp	27.08333	7.74042	4.455	Tabular
image023.bmp	38.97222	9.78278	5.07228	Tabular
image023.bmp	48.91667	13.84583	4.4983	Tabular
image023.bmp	50.72222	12.61693	5.11864	Tabular
image023.bmp	21.75	13.66822	2.02608	Tabular
image023.bmp	95.25	17.34711	6.99114	Tabular
image023.bmp	47.11111	12.42712	4.82684	Tabular
image023.bmp	23.33333	11.16382	2.66118	Tabular
image023.bmp	30.11111	13.03222	2.94184	Tabular
image023.bmp	23.52778	6.79678	4.40745	Tabular
image023.bmp	24.52778	11.07028	2.82104	Tabular
image023.bmp	29.80556	11.6956	3.24478	Tabular
image023.bmp	19.52778	6.88384	3.61187	Tabular
image023.bmp	36.25	9.33923	4.94205	Tabular
image023.bmp	84.5	24.71045	4.35398	Tabular
Label	Area	Major	Minor	Shape
image023.bmp	12.22222	4.44454	3.50133	Tabular
image023.bmp	55.61111	13.39721	5.28515	Tabular
image023.bmp	73.36111	21.01795	4.44412	Tabular
image023.bmp	111.55556	31.85168	4.45932	Tabular
image023.bmp	37.83333	11.20442	4.29928	Tabular
image023.bmp	38.91667	12.15332	4.07709	Tabular
image023.bmp	16.97222	7.30608	2.95777	Tabular
image023.bmp	11	5.36029	2.61285	Tabular
image023.bmp	7.88889	4.02316	2.49665	Tabular
image023.bmp	24.33333	8.47402	3.65614	Tabular
image023.bmp	17.63889	7.57885	2.96332	Tabular
image023.bmp	16602.63889	244.17861	86.57243	area
image024.bmp	68.55556	19.26817	4.53015	Tabular
image024.bmp	26.88889	7.94393	4.30971	Tabular

image024.bmp	57.88889	12.98654	5.6756	Tabular
image024.bmp	69.22222	29.38542	2.99933	Tabular
image024.bmp	40	13.86974	3.67199	Tabular
image024.bmp	118.55556	27.97345	5.39617	Tabular
image024.bmp	61.55556	15.68316	4.9974	Tabular
image024.bmp	53	26.33762	2.56218	Tabular
image024.bmp	68.66667	18.01473	4.8532	Tabular
image024.bmp	354	39.20031	11.49804	Tabular
image024.bmp	40	20.85428	2.44216	Tabular
image024.bmp	167.66667	26.96906	7.91573	Tabular
image024.bmp	148	25.69693	7.33315	Tabular
image024.bmp	117.66667	21.29686	7.03474	Tabular
image024.bmp	34.33333	11.78694	3.70873	Tabular
image024.bmp	34.88889	15.71527	2.82667	Tabular
image024.bmp	68.77778	13.5315	6.47161	Tabular
image024.bmp	90.88889	27.8989	4.14795	Tabular
image024.bmp	54.66667	15.14657	4.59535	Tabular
image024.bmp	24.11111	7.06019	4.34822	Tabular
image024.bmp	82.88889	22.45282	4.70041	Tabular
image024.bmp	102.33333	21.13012	6.16631	Tabular
image024.bmp	28.88889	11.75512	3.12906	Tabular
image024.bmp	105	20.48633	6.52582	Tabular
image024.bmp	19.88889	10.51947	2.40728	Tabular
image024.bmp	52.22222	15.80428	4.20718	Tabular
image024.bmp	108.66667	18.1378	7.6282	Tabular
image024.bmp	54.33333	18.32264	3.77562	Tabular
image024.bmp	76.44444	28.39119	3.42825	Tabular
image024.bmp	57.33333	20.43429	3.57238	Tabular
image024.bmp	230.66667	31.82917	9.2272	Tabular
image024.bmp	13.22222	6.60645	2.54828	Tabular
image024.bmp	60.33333	16.39035	4.68683	Tabular
image024.bmp	88.77778	20.54787	5.50108	Tabular
image024.bmp	17.77778	8.11603	2.78897	Tabular
image024.bmp	76.88889	12.8314	7.62956	Tabular
image024.bmp	71.88889	13.27754	6.89373	Tabular
image024.bmp	37.22222	12.95459	3.65838	Tabular
image024.bmp	22.33333	10.15129	2.80119	Tabular
image024.bmp	29.44444	14.06228	2.66599	Tabular
image024.bmp	52.11111	17.65837	3.75742	Tabular
image024.bmp	94.11111	20.29891	5.90307	Tabular
Label	Area	Major	Minor	Shape
image024.bmp	11.77778	4.12718	3.63346	Tabular
image024.bmp	93.22222	12.27889	9.66653	Tabular
image024.bmp	39.88889	11.34731	4.47578	Tabular
image024.bmp	22.44444	6.99702	4.08419	Tabular
image024.bmp	71.66667	15.07316	6.05373	Tabular
image024.bmp	47.77778	9.60988	6.33021	Tabular
image024.bmp	27.55556	8.94764	3.92112	Tabular
image024.bmp	7.44444	3.39158	2.79473	Tabular
image024.bmp	191.33333	23.17871	10.51021	Tabular
image024.bmp	257.11111	38.63614	8.473	Tabular

image024.bmp	179.22222	36.33517	6.28022	Tabular
image024.bmp	141.33333	39.2188	4.58839	Tabular
image024.bmp	101.77778	20.25488	6.39784	Tabular
image024.bmp	81.11111	26.71906	3.86518	Tabular
image024.bmp	87.77778	20.32077	5.4999	Tabular
image024.bmp	51.33333	12.43145	5.2576	Tabular
image024.bmp	62.22222	18.06493	4.3855	Tabular
image024.bmp	53.11111	9.84934	6.86576	Tabular
image024.bmp	39	10.62814	4.67216	Tabular
image024.bmp	47.77778	13.74595	4.42549	Tabular
image024.bmp	178.33333	26.92893	8.43186	Tabular
image024.bmp	80.55556	12.63572	8.11719	Tabular
image024.bmp	80.77778	19.76026	5.20486	Tabular
image024.bmp	35.88889	15.05242	3.03573	Tabular
image024.bmp	46.11111	12.27906	4.78135	Tabular
image024.bmp	56	26.58186	2.68233	Tabular
image024.bmp	80.44444	23.67246	4.32676	Tabular
image024.bmp	28.66667	10.50072	3.47591	Tabular
image024.bmp	57.55556	16.48477	4.44544	Tabular
image024.bmp	45.11111	12.68121	4.52932	Tabular
image024.bmp	49.11111	18.9945	3.29202	Tabular
image024.bmp	119.44444	37.95773	4.0066	Tabular
image024.bmp	64.33333	21.22659	3.85892	Tabular
image024.bmp	30.66667	13.27214	2.94195	Tabular
image024.bmp	23.44444	10.612	2.81289	Tabular
image024.bmp	22.77778	10.1641	2.85333	Tabular
image024.bmp	30.55556	8.06687	4.82275	Tabular
image024.bmp	39.22222	12.45843	4.00847	Tabular
image024.bmp	22.33333	7.24217	3.9264	Tabular
image024.bmp	32.22222	8.91772	4.60057	Tabular
image024.bmp	68.22222	13.37098	6.4964	Tabular
image024.bmp	86.33333	14.99144	7.33239	Tabular
image024.bmp	58	15.88248	4.64964	Tabular
image024.bmp	99.11111	30.15437	4.18487	Tabular
image024.bmp	37.77778	14.95822	3.21563	Tabular
image024.bmp	29.11111	12.57559	2.94741	Tabular
image024.bmp	70.88889	20.47972	4.40722	Tabular
image024.bmp	22.44444	6.71028	4.25871	Tabular
image024.bmp	32.77778	10.8894	3.83253	Tabular
image024.bmp	18.55556	8.29864	2.84693	Tabular
image024.bmp	64.33333	22.81707	3.58993	Tabular
image024.bmp	31.11111	14.42632	2.74581	Tabular
image024.bmp	22.33333	8.78508	3.23682	Tabular
image024.bmp	23.77778	13.29994	2.27631	Tabular
Label	Area	Major	Minor	Shape
image024.bmp	101.44444	27.70482	4.66212	Tabular
image024.bmp	17.66667	7.21242	3.11877	Tabular
image024.bmp	24.66667	12.52406	2.5077	Tabular
image024.bmp	10.33333	8.02685	1.6391	Tabular
image024.bmp	20.88889	8.45734	3.14479	Tabular
image024.bmp	24.88889	6.01802	5.26577	Tabular

image024.bmp	9.44444	7.47322	1.60908	Tabular
image024.bmp	62.11111	9.88637	7.99913	Tabular
image024.bmp	31.33333	7.99349	4.99092	Tabular
image024.bmp	33.55556	11.24846	3.79823	Tabular
image024.bmp	22.22222	8.12833	3.48094	Tabular
image024.bmp	52.33333	14.44567	4.61265	Tabular
image024.bmp	23.44444	11.3081	2.63973	Tabular
image024.bmp	127.88889	32.72948	4.97512	Tabular
image024.bmp	31.55556	11.42391	3.51699	Tabular
image024.bmp	40.77778	14.38899	3.60831	Tabular
image024.bmp	12.44444	4.77263	3.31992	Tabular
image024.bmp	46.11111	14.83101	3.95863	Tabular
image024.bmp	34.11111	9.81112	4.42677	Tabular
image024.bmp	41.88889	14.86818	3.58716	Tabular
image024.bmp	103.44444	22.75274	5.78873	Tabular
image024.bmp	42.66667	10.55626	5.14622	Tabular
image024.bmp	22.88889	6.12231	4.76014	Tabular
image024.bmp	21.66667	10.84518	2.5437	Tabular
image024.bmp	83.55556	11.42351	9.31292	Tabular
image024.bmp	127.11111	17.95712	9.01274	Tabular
image024.bmp	34.11111	12.39438	3.50414	Tabular
image024.bmp	44.77778	16.80729	3.39215	Tabular
image024.bmp	33	11.39845	3.68619	Tabular
image024.bmp	83.55556	22.93126	4.63935	Tabular
image024.bmp	20.66667	7.93123	3.31772	Tabular
image024.bmp	36.88889	10.42377	4.50589	Tabular
image024.bmp	46.55556	17.79872	3.33037	Tabular
image024.bmp	22.55556	7.50804	3.82505	Tabular
image024.bmp	98	20.5212	6.08042	Tabular
image024.bmp	11.33333	7.35159	1.96285	Tabular
image024.bmp	35.33333	13.25318	3.39449	Tabular
image024.bmp	23.33333	11.25107	2.64054	Tabular
image024.bmp	11.66667	6.08005	2.44315	Tabular
image024.bmp	12.33333	4.09032	3.83914	Tabular
image024.bmp	20.55556	6.77833	3.86115	Tabular
image024.bmp	36	12.38303	3.70157	Tabular
image024.bmp	15.77778	6.80843	2.95059	Tabular
image024.bmp	32.11111	10.25499	3.98685	Tabular
image024.bmp	39911.44444	374.24709	135.78417	area

#### F-6-D

Label	Area	Major	Minor
image015.bmp	104.476	21.204	6.274
image015.bmp	27.424	14.822	2.356
image015.bmp	46.227	20.127	2.924
image015.bmp	12.133	9.922	1.557
image015.bmp	153.895	25.833	7.585
image015.bmp	93.053	24.586	4.819
image015.bmp	119.634	15.872	9.597
image015.bmp	52.155	21.315	3.115
image015.bmp	41.075	8.84	5.916



image015.bmp	74.859	19.124	4.984
image015.bmp	28.399	15.733	2.298
image015.bmp	33.13	8.06	5.233
image015.bmp	12.92	5.493	2.994
image015.bmp	102.427	18.55	7.03
image015.bmp	50.15	20.963	3.046
image015.bmp	79.535	22.238	4.554
image015.bmp	41.607	10.259	5.164
image015.bmp	11.501	4.181	3.503
image015.bmp	24.144	10.974	2.801
image015.bmp	15.424	6.403	3.067
image015.bmp	8.609	8.149	1.345
image015.bmp	5.994	5.221	1.462
image015.bmp	12.521	4.475	3.562
image015.bmp	28.078	9.599	3.724
image015.bmp	55.247	21.213	3.316
image015.bmp	78.249	19.677	5.063
image015.bmp	43.213	10.018	5.492
image015.bmp	166.382	19.861	10.666
image015.bmp	15.834	14.362	1.404
image015.bmp	10.482	4.893	2.728
image015.bmp	6.958	4.809	1.842
image015.bmp	18.981	6.305	3.833
image015.bmp	32.399	10.712	3.851
image015.bmp	22.482	11.715	2.444
image015.bmp	45.097	14.866	3.862
image015.bmp	27.734	9.513	3.712
image015.bmp	4795.823	112.939	54.067

F-8-D				
Label	Area	Major	Minor	Shape
f-8-d-4.bmp	13.94444	6.31307	2.81236	hopper
f-8-d-4.bmp	59.30556	11.48718	6.57343	hopper
f-8-d-4.bmp	5.55556	3.15622	2.24115	hopper
f-8-d-4.bmp	28.88889	6.60083	5.5724	hopper
f-8-d-4.bmp	2.75	2.25628	1.55185	hopper
f-8-d-4.bmp	18.16667	5.67879	4.07314	hopper
f-8-d-4.bmp	2.36111	2.14395	1.40221	hopper
f-8-d-4.bmp	9.05556	4.27463	2.69728	hopper
f-8-d-4.bmp	19.83333	13.62614	1.85325	Swallowtail
f-8-d-4.bmp	132.77778	17.1398	9.86347	Swallowtail
f-8-d-4.bmp	67.08333	14.5581	5.86705	Swallowtail
f-8-d-4.bmp	5.88889	11.24763	0.66663	Spherillitic
f-8-d-4.bmp	94.52778	22.63889	5.31636	acicular
f-8-d-4.bmp	211.5	30.06015	8.95838	acicular
f-8-d-4.bmp	20.91667	6.99907	3.80507	acicular
f-8-d-4.bmp	265.08333	34.46168	9.79391	acicular
f-8-d-4.bmp	272.55556	49.39085	7.02617	acicular
f-8-d-4.bmp	93.75	29.90226	3.99188	acicular
f-8-d-4.bmp	81.36111	23.35914	4.43476	acicular
f-8-d-4.bmp	33.41667	8.90917	4.77569	acicular

f-8-d-4.bmp	14.69444	9.718	1.92525	acicular
f-8-d-4.bmp	31.80556	14.00324	2.89191	acicular
f-8-d-4.bmp	11.38889	10.43859	1.38915	acicular
f-8-d-4.bmp	125.19444	24.02649	6.63445	acicular
f-8-d-4.bmp	128.08333	32.56734	5.00749	acicular
f-8-d-4.bmp	225.30556	63.28868	4.53269	acicular
f-8-d-4.bmp	48.69444	21.82574	2.84067	acicular
f-8-d-4.bmp	91.52778	19.15574	6.08365	acicular
f-8-d-4.bmp	24.91667	8.71495	3.64028	acicular
f-8-d-4.bmp	35.38889	14.89373	3.02533	acicular
f-8-d-4.bmp	64.72222	27.1078	3.03997	acicular
f-8-d-4.bmp	37.80556	10.99268	4.37887	acicular
f-8-d-4.bmp	35.61111	9.90816	4.57617	acicular
f-8-d-4.bmp	302.66667	34.8527	11.05702	acicular
f-8-d-4.bmp	154.33333	31.65659	6.20734	acicular
f-8-d-4.bmp	109.02778	13.89688	9.98918	acicular
f-8-d-4.bmp	37.38889	9.0051	5.28645	acicular
f-8-d-4.bmp	34.97222	14.20258	3.13521	acicular
f-8-d-4.bmp	15.02778	4.84308	3.95078	acicular
f-8-d-4.bmp	26.55556	11.53473	2.93128	acicular
f-8-d-4.bmp	90.88889	16.78853	6.893	skeletal
f-8-d-4.bmp	51.30556	15.05791	4.3382	skeletal
f-8-d-4.bmp	36.08333	16.17039	2.84116	skeletal
f-8-d-4.bmp	21.30556	11.30584	2.39939	skeletal
f-8-d-4.bmp	22.11111	6.29831	4.46989	skeletal
f-8-d-4.bmp	9.25	7.01948	1.67783	skeletal
f-8-d-4.bmp	37	16.15189	2.91668	skeletal
f-8-d-4.bmp	29.80556	13.38304	2.83565	tabular
f-8-d-4.bmp	17416.22222	186.91977	118.63391	area
f-8-d-1.bmp	2.57117	1.93154	1.69487	hopper
f-8-d-1.bmp	22.03857	5.802	4.83632	hopper
f-8-d-1.bmp	4.22406	4.05033	1.32785	hopper
f-8-d-1.bmp	29.01745	8.44218	4.37638	hopper
Label	Area	Major	Minor	Shape
f-8-d-1.bmp	2.0202	1.67987	1.53119	hopper
f-8-d-1.bmp	8.17264	3.56587	2.91814	hopper
f-8-d-1.bmp	2.75482	2.35259	1.49093	hopper
f-8-d-1.bmp	15.51882	4.59005	4.30479	hopper
f-8-d-1.bmp	81.45087	26.52443	3.90985	hopper
f-8-d-1.bmp	131.8641	38.6264	4.34663	hopper
f-8-d-1.bmp	142.33242	46.86904	3.86659	Swallowtail
f-8-d-1.bmp	331.12948	23.6701	17.8118	Swallowtail
f-8-d-1.bmp	1605.05051	76.40253	26.74799	Swallowtail
f-8-d-1.bmp	425.1607	44.13675	12.26487	Swallowtail
f-8-d-1.bmp	5.05051	8.51106	0.75555	acicular
f-8-d-1.bmp	8.53994	9.24766	1.1758	acicular
f-8-d-1.bmp	19.10009	26.40813	0.92089	acicular
f-8-d-1.bmp	151.51515	49.3276	3.9109	skeletal
f-8-d-1.bmp	120.11019	15.74827	9.71085	skeletal
f-8-d-1.bmp	175.48209	28.62074	7.8066	skeletal
f-8-d-1.bmp	159.50413	35.3387	5.74687	skeletal

f-8-d-1.bmp	119.00826	21.45979	7.06093	skeletal
f-8-d-1.bmp	70.43159	15.69442	5.7139	skeletal
f-8-d-1.bmp	401.46924	44.77031	11.41753	skeletal
f-8-d-1.bmp	84.38935	13.62514	7.886	skeletal
f-8-d-1.bmp	367.21763	46.46761	10.06198	skeletal
f-8-d-1.bmp	54.54545	15.06225	4.61083	skeletal
f-8-d-1.bmp	362.35078	45.94746	10.04102	skeletal
f-8-d-1.bmp	35.99633	12.3229	3.71925	skeletal
f-8-d-1.bmp	202.20386	36.93597	6.97028	skeletal
f-8-d-1.bmp	411.01928	43.40382	12.05714	skeletal
f-8-d-1.bmp	173.09458	34.99246	6.29824	skeletal
f-8-d-1.bmp	239.21028	26.79972	11.36474	skeletal
f-8-d-1.bmp	226.26263	40.23446	7.16019	skeletal
f-8-d-1.bmp	33.42516	15.65534	2.71845	skeletal
f-8-d-1.bmp	51.42332	17.49679	3.74207	skeletal
f-8-d-1.bmp	152.15794	29.75633	6.51067	skeletal
f-8-d-1.bmp	153.90266	23.80474	8.23176	skeletal
f-8-d-1.bmp	57.11662	15.42526	4.71455	skeletal
f-8-d-1.bmp	62.44261	20.75417	3.83077	skeletal
f-8-d-1.bmp	91.2764	13.45298	8.63873	skeletal
f-8-d-1.bmp	71.25803	11.33414	8.00489	skeletal
f-8-d-1.bmp	26.35445	6.94195	4.83373	skeletal
f-8-d-1.bmp	39.57759	10.99384	4.58364	skeletal
f-8-d-1.bmp	141.41414	42.89692	4.19737	skeletal
f-8-d-1.bmp	53.81084	15.83978	4.32544	skeletal
f-8-d-1.bmp	34.52709	8.84116	4.97234	skeletal
f-8-d-1.bmp	129.2011	22.25916	7.39039	skeletal
f-8-d-1.bmp	79.61433	13.78152	7.35536	skeletal
f-8-d-1.bmp	38.29201	15.33623	3.17907	skeletal
f-8-d-1.bmp	114.23324	35.85684	4.05631	skeletal
f-8-d-1.bmp	25.1607	11.47345	2.79215	skeletal
f-8-d-1.bmp	20.93664	10.68962	2.49376	skeletal
f-8-d-1.bmp	21.57943	8.90788	3.08443	skeletal
f-8-d-1.bmp	11.57025	6.43477	2.28939	skeletal
f-8-d-1.bmp	22.58953	6.36405	4.51943	skeletal
f-8-d-1.bmp	98.9899	12.51307	10.0725	tabular
f-8-d-1.bmp	47049.6786	351.20795	170.56992	area
Label	Area	Major	Minor	Shape
f-8-d-5.bmp	35.20408	9.78494	4.58084	hopper
f-8-d-5.bmp	100	16.04237	7.93673	hopper
f-8-d-5.bmp	53.06122	20.48372	3.29821	Swallowtail
f-8-d-5.bmp	127.04082	26.37427	6.133	Swallowtail
f-8-d-5.bmp	103.06122	39.78987	3.29787	Swallowtail
f-8-d-5.bmp	158.16327	30.47533	6.60796	Swallowtail
f-8-d-5.bmp	108.67347	36.63922	3.77648	acicular
f-8-d-5.bmp	8.67347	19.58034	0.564	acicular
f-8-d-5.bmp	30.61224	28.1578	1.38422	acicular
f-8-d-5.bmp	95.40816	25.6752	4.73131	tabular
f-8-d-5.bmp	85.20408	18.67545	5.80898	tabular
f-8-d-5.bmp	70.40816	15.04768	5.9575	tabular
f-8-d-5.bmp	151.53061	32.29252	5.9746	skeletal

f-8-d-5.bmp	39.28571	9.04917	5.52759	skeletal
f-8-d-5.bmp	251.53061	71.28989	4.49234	skeletal
f-8-d-5.bmp	22.44898	7.16032	3.99185	skeletal
f-8-d-5.bmp	100	27.06083	4.7051	skeletal
f-8-d-5.bmp	75.5102	16.95176	5.67154	skeletal
f-8-d-5.bmp	164.28571	23.94682	8.73498	skeletal
f-8-d-5.bmp	78.57143	17.49519	5.71816	skeletal
f-8-d-5.bmp	102.04082	20.75767	6.25901	skeletal
f-8-d-5.bmp	364.79592	54.16585	8.57501	skeletal
f-8-d-5.bmp	63.26531	19.44507	4.14254	skeletal
f-8-d-5.bmp	263.26531	48.85987	6.86043	skeletal
f-8-d-5.bmp	212.2449	45.51526	5.93732	skeletal
f-8-d-5.bmp	85.71429	23.90203	4.56592	skeletal
f-8-d-5.bmp	167.85714	39.27601	5.44155	skeletal
f-8-d-5.bmp	226.02041	49.20596	5.84844	skeletal
f-8-d-5.bmp	70.40816	20.17122	4.44427	skeletal
f-8-d-5.bmp	181.12245	18.80153	12.26561	skeletal
f-8-d-5.bmp	166.32653	26.0259	8.13703	skeletal
f-8-d-5.bmp	31.63265	11.62488	3.46463	skeletal
f-8-d-5.bmp	213.77551	39.20254	6.94311	skeletal
f-8-d-5.bmp	427.55102	103.67511	5.25078	skeletal
f-8-d-5.bmp	683.67347	51.81629	16.79935	skeletal
f-8-d-5.bmp	64.79592	23.79569	3.46704	skeletal
f-8-d-5.bmp	60.20408	15.16645	5.0542	skeletal
f-8-d-5.bmp	186.73469	39.83579	5.96845	skeletal
f-8-d-5.bmp	99.4898	37.61924	3.36728	skeletal
f-8-d-5.bmp	203.57143	41.52095	6.24252	skeletal
f-8-d-5.bmp	235.71429	40.32021	7.44343	skeletal
f-8-d-5.bmp	18.36735	10.05131	2.32667	skeletal
f-8-d-5.bmp	437.2449	66.2401	8.40454	skeletal
f-8-d-5.bmp	113.77551	29.99766	4.82916	skeletal
f-8-d-5.bmp	120.91837	32.0793	4.7993	skeletal
f-8-d-5.bmp	317.34694	44.5345	9.07294	skeletal
f-8-d-5.bmp	668.87755	80.3747	10.59589	skeletal
f-8-d-5.bmp	137.2449	36.34928	4.8074	skeletal
f-8-d-5.bmp	69.38776	24.23597	3.64529	skeletal
f-8-d-5.bmp	146.42857	35.07238	5.31582	skeletal
f-8-d-5.bmp	219.38776	41.98279	6.65352	skeletal
f-8-d-5.bmp	61.22449	23.09648	3.37512	skeletal
f-8-d-5.bmp	46.42857	13.35031	4.42796	skeletal
f-8-d-5.bmp	526.02041	52.78058	12.68933	skeletal
Label	Area	Major	Minor	Shape
f-8-d-5.bmp	148.97959	37.23501	5.09431	skeletal
f-8-d-5.bmp	47.95918	16.62754	3.67243	skeletal
f-8-d-5.bmp	46.93878	14.65241	4.0788	skeletal
f-8-d-5.bmp	178.57143	47.02057	4.83542	skeletal
f-8-d-5.bmp	139.28571	38.26556	4.63456	skeletal
f-8-d-5.bmp	59.18367	12.31665	6.11814	skeletal
f-8-d-5.bmp	33.16327	12.86541	3.28204	skeletal
f-8-d-5.bmp	109.18367	15.50721	8.96467	skeletal
f-8-d-5.bmp	102.04082	20.87425	6.22405	skeletal

f-8-d-5.bmp	61.73469	18.56197	4.23463	skeletal
f-8-d-5.bmp	57.14286	20.4641	3.55533	skeletal
f-8-d-5.bmp	48.46939	21.08237	2.92724	skeletal
f-8-d-5.bmp	47.95918	19.32176	3.16035	skeletal
f-8-d-5.bmp	32.14286	12.47757	3.27993	skeletal
f-8-d-5.bmp	106.63265	31.56852	4.30077	skeletal
f-8-d-5.bmp	95.40816	21.92283	5.54114	skeletal
f-8-d-5.bmp	30.10204	14.51219	2.64103	skeletal
f-8-d-5.bmp	51.53061	18.99459	3.45418	skeletal
f-8-d-5.bmp	16.83673	7.75826	2.76314	skeletal
f-8-d-5.bmp	36.73469	16.64505	2.80997	skeletal
f-8-d-5.bmp	84.18367	21.30232	5.03166	skeletal
f-8-d-5.bmp	49.4898	16.63987	3.78683	skeletal
f-8-d-5.bmp	66.32653	22.19228	3.80536	skeletal
f-8-d-5.bmp	46.93878	13.78879	4.33427	skeletal
f-8-d-5.bmp	70.40816	24.52705	3.655	skeletal
f-8-d-5.bmp	39.79592	12.6748	3.99768	skeletal
f-8-d-5.bmp	7920.40816	115.55401	87.27154	area
f-8-d-5.bmp	101162.7551	528.88476	243.53967	area
F-9-D				
Label	Area	Major	Minor	Shape
f-9-d-6.bmp	129.14536	14.5904	11.26994	spherillitic
f-9-d-6.bmp	69.61286	13.46402	6.58302	spherillitic
f-9-d-6.bmp	24.54346	15.20282	2.05552	tabular
f-9-d-6.bmp	107.66983	25.84784	5.30371	tabular
f-9-d-6.bmp	110.59167	24.11576	5.83891	tabular
f-9-d-6.bmp	66.32579	19.24704	4.38762	tabular
f-9-d-6.bmp	92.47626	27.61418	4.26391	tabular
f-9-d-6.bmp	64.1344	20.78501	3.92872	tabular
f-9-d-6.bmp	67.05625	17.2586	4.94702	tabular
f-9-d-6.bmp	52.95836	19.42962	3.47041	tabular
f-9-d-6.bmp	39.07962	9.84063	5.05635	tabular
f-9-d-6.bmp	38.34916	11.65609	4.18903	tabular
f-9-d-6.bmp	9483.56465	183.90832	65.65689	area
f-9-d-4.bmp	12.45675	4.73067	3.35268	hopper
f-9-d-4.bmp	26.98962	6.56614	5.23355	hopper
f-9-d-4.bmp	3.46021	2.76876	1.59121	hopper
f-9-d-4.bmp	16.95502	7.22535	2.98779	hopper
f-9-d-4.bmp	167.82007	24.14383	8.85009	swallowtail
f-9-d-4.bmp	130.10381	30.39941	5.44923	swallowtail
f-9-d-4.bmp	113.14879	36.9567	3.89822	swallowtail
f-9-d-4.bmp	291.00346	24.13393	15.35254	spherillitic
f-9-d-4.bmp	64.01384	35.26048	2.31151	acicular
f-9-d-4.bmp	4.84429	9.29253	0.66375	acicular
f-9-d-4.bmp	27.68166	20.76636	1.69723	acicular
f-9-d-4.bmp	12.45675	14.09992	1.12486	acicular
f-9-d-4.bmp	29.41176	13.56832	2.75997	acicular
f-9-d-4.bmp	22.83737	21.59323	1.3466	acicular
f-9-d-4.bmp	28.3737	16.30797	2.21527	acicular
f-9-d-4.bmp	24.56747	19.03836	1.64301	acicular

f-9-d-4.bmp	3.11419	8.96426	0.44232	acicular
f-9-d-4.bmp	22.49135	12.69187	2.25632	acicular
f-9-d-4.bmp	53.2872	40.70926	1.66663	acicular
f-9-d-4.bmp	51.90311	27.32252	2.4187	acicular
f-9-d-4.bmp	39.44637	23.49579	2.1376	acicular
f-9-d-4.bmp	93.42561	47.94812	2.48087	acicular
f-9-d-4.bmp	72.66436	35.9838	2.57113	acicular
f-9-d-4.bmp	249.13495	20.39425	15.55382	skeletal
f-9-d-4.bmp	160.89965	24.58145	8.33408	skeletal
f-9-d-4.bmp	162.62976	19.66647	10.52891	skeletal
f-9-d-4.bmp	319.72318	28.27381	14.39793	skeletal
f-9-d-4.bmp	363.66782	37.5216	12.34053	skeletal
f-9-d-4.bmp	59.51557	16.75407	4.52294	skeletal
f-9-d-4.bmp	113.49481	23.12522	6.24885	skeletal
f-9-d-4.bmp	52.59516	15.19027	4.4085	skeletal
f-9-d-4.bmp	105.53633	14.75763	9.10533	skeletal
f-9-d-4.bmp	129.41176	16.98753	9.69959	skeletal
f-9-d-4.bmp	46.7128	7.90538	7.52356	skeletal
f-9-d-4.bmp	50.86505	12.85906	5.0364	skeletal
f-9-d-4.bmp	69.55017	13.04398	6.78888	skeletal
f-9-d-4.bmp	278.89273	20.89606	16.9935	skeletal
f-9-d-4.bmp	136.6782	22.79507	7.63429	skeletal
f-9-d-4.bmp	187.88927	23.41131	10.21848	skeletal
f-9-d-4.bmp	98.2699	20.4492	6.11863	skeletal
Label	Area	Major	Minor	Shape
f-9-d-4.bmp	58.82353	16.93202	4.42336	skeletal
f-9-d-4.bmp	314.18685	38.22601	10.465	skeletal
f-9-d-4.bmp	338.4083	47.39274	9.09158	skeletal
f-9-d-4.bmp	395.50173	27.41707	18.36697	skeletal
f-9-d-4.bmp	159.16955	19.96036	10.15317	skeletal
f-9-d-4.bmp	101.03806	16.61308	7.74364	skeletal
f-9-d-4.bmp	1020.0692	64.62867	20.09623	skeletal
f-9-d-4.bmp	220.76125	27.5228	10.21269	skeletal
f-9-d-4.bmp	122.14533	21.09014	7.37407	skeletal
f-9-d-4.bmp	612.80277	30.07148	25.94634	skeletal
f-9-d-4.bmp	80.96886	21.26732	4.84747	skeletal
f-9-d-4.bmp	76.81661	18.84104	5.19111	skeletal
f-9-d-4.bmp	78.89273	20.08606	5.00095	skeletal
f-9-d-4.bmp	26.29758	7.55673	4.4309	skeletal
f-9-d-4.bmp	32.87197	13.38101	3.12786	skeletal
f-9-d-4.bmp	57.43945	13.72778	5.32746	skeletal
f-9-d-4.bmp	65.0519	11.17887	7.40921	skeletal
f-9-d-4.bmp	28.3737	6.67565	5.41169	skeletal
f-9-d-4.bmp	71.6263	13.55387	6.72852	skeletal
f-9-d-4.bmp	39.44637	10.66026	4.71139	skeletal
f-9-d-4.bmp	74.04844	17.65733	5.3395	skeletal
f-9-d-4.bmp	85.81315	23.49877	4.64963	skeletal
f-9-d-4.bmp	43.59862	13.90104	3.99333	skeletal
f-9-d-4.bmp	39.44637	16.81568	2.98678	skeletal
f-9-d-4.bmp	69.20415	11.01831	7.997	skeletal
f-9-d-4.bmp	80.62284	15.62547	6.56954	skeletal

f-9-d-4.bmp	55.70934	14.6293	4.84858	skeletal
f-9-d-4.bmp	24.22145	6.80363	4.53283	skeletal
f-9-d-4.bmp	88.92734	15.80757	7.16276	skeletal
f-9-d-4.bmp	29.06574	11.21192	3.30074	skeletal
f-9-d-4.bmp	60.55363	16.18076	4.76487	skeletal
f-9-d-4.bmp	77.85467	20.67537	4.79448	skeletal
f-9-d-4.bmp	29.41176	15.98259	2.34306	skeletal
f-9-d-4.bmp	174.74048	24.00782	9.26725	skeletal
f-9-d-4.bmp	38.75433	9.80106	5.03451	skeletal
f-9-d-4.bmp	128.71972	32.15822	5.0964	skeletal
f-9-d-4.bmp	83.04498	39.17338	2.69918	skeletal
f-9-d-4.bmp	146.36678	37.69743	4.94357	skeletal
f-9-d-4.bmp	15.57093	5.8323	3.39927	skeletal
f-9-d-4.bmp	99.30796	26.12663	4.83962	skeletal
f-9-d-4.bmp	66.08997	22.34667	3.76559	skeletal
f-9-d-4.bmp	53.97924	13.94812	4.92744	skeletal
f-9-d-4.bmp	64.01384	10.25439	7.9483	skeletal
f-9-d-4.bmp	29.41176	15.63513	2.39513	skeletal
f-9-d-4.bmp	44.9827	15.58847	3.67411	skeletal
f-9-d-4.bmp	23.18339	8.50529	3.47055	skeletal
f-9-d-4.bmp	83.04498	23.71533	4.45856	skeletal
f-9-d-4.bmp	60.55363	23.71641	3.25088	skeletal
f-9-d-4.bmp	17.64706	8.27144	2.71645	skeletal
f-9-d-4.bmp	19.03114	6.26478	3.86785	skeletal
f-9-d-4.bmp	62.62976	20.90587	3.81437	tabular
f-9-d-4.bmp	270916.955	726.36679	474.88705	area
f-9-d-4.bmp	7820.0692	108.35188	91.89339	vesicules
f-9-d-4.bmp	1767.82007	50.33727	44.71554	vesicules
Label	Area	Major	Minor	Shape
f-9-d-4.bmp	55.70934	11.67292	6.07657	vesicules
f-9-d-4.bmp	233.56401	25.21068	11.79591	vesicules
f-9-d-4.bmp	598.2699	31.70396	24.02668	vesicules
f-9-d-4.bmp	4111.07266	104.74926	49.97057	vesicules
f-9-d-4.bmp	2416.609	60.49348	50.8637	vesicules
f-9-d-4.bmp	1784.08304	51.17441	44.38869	vesicules
f-9-d-4.bmp	6609.68858	124.38881	67.65654	vesicules
f-9-d-4.bmp	2108.65052	57.44821	46.73457	vesicules
f-9-d-4.bmp	341.86851	22.08784	19.70679	vesicules
f-9-d-4.bmp	141.52249	16.58288	10.86615	vesicules
f-9-d-4.bmp	9508.65052	141.24902	85.71238	vesicules
f-9-d-4.bmp	491.6955	33.99709	18.4147	vesicules
f-9-d-4.bmp	364.35986	27.67103	16.76546	vesicules
f-9-d-4.bmp	473.70242	29.429	20.49464	vesicules
f-9-d-4.bmp	679.23875	32.36885	26.71809	vesicules
f-9-d-4.bmp	2601.03806	65.16908	50.81773	vesicules
f-9-d-4.bmp	456.7474	31.8376	18.2661	vesicules
f-9-d-4.bmp	1927.68166	59.55515	41.21223	vesicules
f-9-d-4.bmp	3442.56055	73.11515	59.94933	vesicules
f-9-d-4.bmp	864.35986	34.66317	31.74947	vesicules
f-9-d-4.bmp	35180.96886	219.55102	204.02456	vesicules
f-9-d-3.bmp	24.96571	10.39588	3.05768	swallowtail

f-9-d-3.bmp	174.21125	15.52668	14.2859	spherillitic
f-9-d-3.bmp	8.5048	10.83736	0.9992	acicular
f-9-d-3.bmp	23.04527	26.52324	1.10628	acicular
f-9-d-3.bmp	31.68724	13.65158	2.95537	tabular
f-9-d-3.bmp	35.1166	13.61723	3.28348	tabular
f-9-d-3.bmp	25.10288	11.15968	2.86406	tabular
f-9-d-3.bmp	16.18656	10.24902	2.01086	tabular
f-9-d-3.bmp	43.34705	18.21029	3.03077	tabular
f-9-d-3.bmp	9.0535	4.97437	2.31733	tabular
f-9-d-3.bmp	70.50754	24.73101	3.62998	skeletal
f-9-d-3.bmp	39.64335	20.12854	2.50766	skeletal
f-9-d-3.bmp	165.70645	20.0646	10.51524	skeletal
f-9-d-3.bmp	13.71742	7.367	2.37078	skeletal
f-9-d-3.bmp	57.47599	12.11739	6.03931	skeletal
f-9-d-3.bmp	78.1893	13.45913	7.39674	skeletal
f-9-d-3.bmp	30.58985	10.6527	3.65618	skeletal
f-9-d-3.bmp	66.39232	15.49127	5.45683	skeletal
f-9-d-3.bmp	51.16598	20.06176	3.2473	skeletal
f-9-d-3.bmp	79.69822	27.54514	3.68395	skeletal
f-9-d-3.bmp	46.22771	15.39122	3.82419	skeletal
f-9-d-3.bmp	21.12483	16.14996	1.66545	skeletal
f-9-d-3.bmp	22.3594	7.0262	4.05182	skeletal
f-9-d-3.bmp	24.14266	13.60076	2.26012	skeletal
f-9-d-3.bmp	65.02058	20.60791	4.01723	skeletal
f-9-d-3.bmp	40.19204	19.40032	2.6378	skeletal
f-9-d-3.bmp	127.43484	21.71863	7.47078	skeletal
f-9-d-3.bmp	87.65432	19.08332	5.8483	skeletal
f-9-d-3.bmp	44.44444	15.53464	3.64272	skeletal
f-9-d-3.bmp	98416.32373	379.19577	330.4561	area
f-9-d-3.bmp	5680.79561	106.54802	67.88501	vesicles
f-9-d-3.bmp	4160.35665	80.81633	65.5453	vesicles
f-9-d-3.bmp	3586.28258	95.4788	47.82419	vesicles
Label	Area	Major	Minor	Shape
f-9-d-3.bmp	141.42661	16.11231	11.17592	vesicles
f-9-d-3.bmp	392.86694	31.24768	16.00803	vesicles
f-9-d-3.bmp	3749.93141	120.22806	39.71253	vesicles
f-9-d-3.bmp	4246.50206	87.1577	62.03485	vesicles
f-9-d-3.bmp	8624.00549	120.57228	91.06923	vesicles
f-9-d-3.bmp	6728.53224	106.47117	80.46341	vesicles
f-9-d-3.bmp	235.93964	19.08539	15.74019	vesicles
f-9-d-3.bmp	314.26612	23.02701	17.37682	vesicles
f-9-d-3.bmp	127.02332	32.75594	4.93746	vesicles
f-9-d-3.bmp	64.8834	16.03905	5.15069	vesicles
f-9-d-3.bmp	61.7284	15.63537	5.02675	vesicles
f-9-d-3.bmp	62.27709	23.39279	3.38966	vesicles
f-9-d-3.bmp	68.58711	12.6995	6.87648	vesicles
f-9-d-1.bmp	33.05898	16.12087	2.61103	swallowtail
f-9-d-1.bmp	59.39643	12.73949	5.93633	spherillitic
f-9-d-1.bmp	25.5144	13.99483	2.32128	tabular
f-9-d-1.bmp	32.78464	14.69821	2.83999	tabular
f-9-d-1.bmp	34.84225	13.10762	3.38448	tabular



f-9-d-1.bmp	34.0192	17.36385	2.49453	tabular
f-9-d-1.bmp	33.19616	17.19977	2.4574	tabular
f-9-d-1.bmp	24395.1989	227.06389	136.7938	area
f-9-d-1.bmp	942.93553	38.20934	31.42119	vesicules
f-9-d-1.bmp	3742.38683	76.10125	62.61336	vesicules
Natural Basaltic Andesite				
Label	Area	Major	Minor	Shape
image034.bmp	3112.10938	133.68631	29.63999	skeletal
image034.bmp	69.92188	28.95276	3.07492	tabular
image034.bmp	35.9375	18.9653	2.41267	tabular
image034.bmp	69.14062	29.7538	2.9587	tabular
image034.bmp	59.375	16.99779	4.44756	tabular
image034.bmp	15.23438	7.83539	2.47556	tabular
image034.bmp	29.29688	17.29916	2.15629	tabular
image034.bmp	7.8125	4.42069	2.25014	tabular
image034.bmp	1.5625	4.38077	0.45413	acicular
image034.bmp	1.5625	3.32817	0.59776	acicular
image034.bmp	0.39062	0.70524	0.70524	acicular
image034.bmp	7.03125	9.51017	0.94136	acicular
image034.bmp	3.125	4.95537	0.80294	acicular
image034.bmp	4.6875	3.86752	1.54319	acicular
image034.bmp	4.6875	9.32614	0.63995	acicular
image034.bmp	5.85938	7.44838	1.00161	acicular
image034.bmp	1.95312	2.79655	0.88924	acicular
image034.bmp	12.10938	16.16515	0.95379	acicular
image034.bmp	5.07812	5.71713	1.13093	acicular
image034.bmp	178.90625	25.55111	8.91509	skeletal
image034.bmp	41.01562	15.99678	3.26458	swallowtail
image034.bmp	435187.5	892.83002	620.60854	area
image034.bmp	468.75	24.97018	23.90175	vesicles
image034.bmp	439.0625	23.64385	23.64385	vesicles
image034.bmp	276.5625	20.07735	17.53869	vesicles
image034.bmp	704.6875	31.2816	28.68255	vesicles
image034.bmp	704.6875	29.9539	29.9539	vesicles
image034.bmp	926.5625	35.00516	33.70177	vesicles
image034.bmp	2325	54.96808	53.85456	vesicles
image034.bmp	7807.8125	101.95951	97.5016	vesicles
image034.bmp	24920.70312	179.38878	176.87854	vesicles
image034.bmp	1044.53125	38.66071	34.40026	vesicles
image034.bmp	681.25	30.05365	28.86154	vesicles
image034.bmp	400	23.81002	21.38998	vesicles
image034.bmp	240.625	17.50352	17.50352	vesicles
image034.bmp	681.25	30.05365	28.86154	vesicles
image034.bmp	539.0625	27.43789	25.01489	vesicles
image034.bmp	650	30.01432	27.57369	vesicles
image034.bmp	1295.3125	41.24962	39.98202	vesicles
image034.bmp	650	28.76814	28.76814	vesicles
image034.bmp	1260.9375	40.06839	40.06839	vesicles
image034.bmp	681.25	30.05365	28.86154	vesicles
image034.bmp	1460.9375	43.83212	42.43745	vesicles

image034.bmp	1550	45.093	43.76558	vesicles
image034.bmp	1726.5625	47.48824	46.29204	vesicles
image034.bmp	687.5	31.77171	27.55131	vesicles
image034.bmp	568.75	27.54538	26.28953	vesicles
image034.bmp	468.75	24.97018	23.90175	vesicles
image034.bmp	621.875	28.8245	27.46954	vesicles
image034.bmp	238.67188	18.06656	16.82038	vesicles
image034.bmp	239.0625	18.71154	16.26717	vesicles
image034.bmp	388.28125	23.23857	21.2739	vesicles
image034.bmp	596.875	27.56746	27.56746	vesicles
Label	Area	Major	Minor	Shape
image034.bmp	468.75	24.97018	23.90175	vesicles
image034.bmp	356.25	21.29769	21.29769	vesicles
image034.bmp	3865.625	72.1332	68.23303	vesicles
image034.bmp	1140.625	40.04041	36.27058	vesicles
image034.bmp	826.5625	35.0575	30.0196	vesicles
image034.bmp	539.0625	27.43789	25.01489	vesicles
image034.bmp	1326.5625	45.03486	37.50499	vesicles
image034.bmp	335.9375	22.65792	18.87768	vesicles
image034.bmp	489.0625	27.6199	22.54511	vesicles
image034.bmp	317.1875	20.09616	20.09616	vesicles
image034.bmp	798.4375	32.55562	31.22662	vesicles
image034.bmp	385.9375	22.51374	21.82627	vesicles
image034.bmp	60.9375	8.80841	8.80841	vesicles
image034.bmp	26.95312	5.85814	5.85814	vesicles
image034.bmp	293.75	19.96533	18.73318	vesicles
image034.bmp	504.6875	25.73239	24.97196	vesicles
image034.bmp	100	11.28379	11.28379	vesicles
image034.bmp	117.1875	12.55572	11.88365	vesicles
image034.bmp	768.75	32.54229	30.07787	vesicles
image034.bmp	208.98438	16.96534	15.68416	vesicles
image034.bmp	279.6875	18.87086	18.87086	vesicles
image034.bmp	217.96875	17.07085	16.25733	vesicles
image034.bmp	210.9375	16.38823	16.38823	vesicles
image034.bmp	134.375	13.7468	12.44592	vesicles
image034.bmp	48.4375	8.1272	7.58842	vesicles
image034.bmp	142.96875	13.88496	13.11012	vesicles
image034.bmp	23.4375	5.75829	5.18236	vesicles
image034.bmp	37.5	7.47171	6.3903	vesicles
image034.bmp	93.75	11.89738	10.03298	vesicles
image034.bmp	27.34375	6.16539	5.64687	vesicles
image034.bmp	84.375	10.85483	9.89694	vesicles
image034.bmp	53.51562	8.25459	8.25459	vesicles
image034.bmp	128.125	13.03609	12.51401	vesicles
image034.bmp	40.625	7.65747	6.75489	vesicles
image034.bmp	192.1875	16.25557	15.05335	vesicles
image034.bmp	155.46875	14.33711	13.80676	vesicles
image034.bmp	539.0625	27.43789	25.01489	vesicles
image034.bmp	48.4375	8.1272	7.58842	vesicles
image034.bmp	92.96875	11.14241	10.62351	vesicles
image034.bmp	184.375	15.58918	15.05875	vesicles

image034.bmp	215.625	18.11791	15.15309	vesicles
image034.bmp	84.375	10.85483	9.89694	vesicles
image034.bmp	182.03125	16.79452	13.8003	vesicles
image034.bmp	123.04688	13.06181	11.99436	vesicles
image034.bmp	117.1875	12.55572	11.88365	vesicles
image034.bmp	231.25	17.49338	16.83132	vesicles
image034.bmp	136.32812	13.17491	13.17491	vesicles
image034.bmp	142.1875	14.40928	12.56404	vesicles
image034.bmp	128.125	13.03609	12.51401	vesicles
image034.bmp	132.8125	14.96307	11.3013	vesicles
image034.bmp	75	10.04797	9.50371	vesicles
image034.bmp	81.25	10.17107	10.17107	vesicles
image034.bmp	23.4375	5.75829	5.18236	vesicles
image034.bmp	156.25	15.00799	13.25585	vesicles
Label	Area	Major	Minor	Shape
image034.bmp	170.3125	15.14345	14.31963	vesicles
image034.bmp	191.01562	16.99945	14.30686	vesicles
image034.bmp	965.625	35.06383	35.06383	vesicles
image034.bmp	13.28125	4.60853	3.66933	vesicles
image034.bmp	184.375	15.58918	15.05875	vesicles
image034.bmp	162.5	16.43876	12.5862	vesicles
image034.bmp	72.65625	11.41387	8.10495	vesicles
image034.bmp	43.75	7.46353	7.46353	vesicles
image034.bmp	33.59375	6.80516	6.28537	vesicles
image034.bmp	83.59375	11.38337	9.35003	vesicles
image034.bmp	155.46875	14.33711	13.80676	vesicles
image034.bmp	225.39062	16.94037	16.94037	vesicles
image034.bmp	92.96875	11.14241	10.62351	vesicles
image034.bmp	283.59375	19.35948	18.65147	vesicles
image034.bmp	861.32812	34.37259	31.90557	vesicles
image034.bmp	304.6875	19.96324	19.43273	vesicles
image034.bmp	100	11.28379	11.28379	vesicles
image034.bmp	344.53125	21.23577	20.65716	vesicles
image034.bmp	75	10.04797	9.50371	vesicles
image034.bmp	139.0625	14.89704	11.88558	vesicles
image034.bmp	30.85938	6.83264	5.75054	vesicles
image034.bmp	43.75	7.46353	7.46353	vesicles
image034.bmp	3633.59375	88.09422	52.5169	vesicles
image034.bmp	2487.5	101.25229	31.28012	vesicles
image034.bmp	512.5	39.94775	16.33472	vesicles
image034.bmp	554.6875	56.11423	12.58594	vesicles
image034.bmp	206.25	26.24264	10.00683	vesicles
image128.bmp	70.88889	14.27961	6.3208	spherulites
image128.bmp	56.11111	16.65477	4.28963	spherulites
image128.bmp	104.77778	14.36586	9.28641	spherulites
image128.bmp	28.55556	17.01436	2.1369	spherulites
image128.bmp	110.77778	15.39999	9.15888	spherulites
image128.bmp	128.22222	19.40236	8.41432	spherulites
image128.bmp	83.44444	11.73034	9.05726	spherulites
image128.bmp	46.11111	10.95773	5.35791	spherulites
image128.bmp	49.22222	16.12184	3.88738	skeletal

image128.bmp	18.22222	11.16154	2.07868	skeletal
image128.bmp	46.22222	16.25603	3.62032	skeletal
image128.bmp	42.88889	14.53979	3.75575	skeletal
image128.bmp	26	18.21037	1.81788	skeletal
image128.bmp	36.22222	18.96592	2.43171	skeletal
image128.bmp	8.55556	5.82801	1.86912	skeletal
image128.bmp	18.44444	7.99598	2.937	skeletal
image128.bmp	28	8.33422	4.27763	skeletal
image128.bmp	11.55556	7.77873	1.89144	skeletal
image128.bmp	10.11111	7.739	1.6635	skeletal
image128.bmp	52.55556	21.47541	3.11593	skeletal
image128.bmp	24.55556	16.27537	1.92101	skeletal
image128.bmp	11.11111	5.07432	2.78798	skeletal
image128.bmp	15.44444	5.91594	3.32398	skeletal
image128.bmp	67.66667	17.05796	5.05077	skeletal
image128.bmp	12.44444	7.34782	2.15639	skeletal
image128.bmp	38	16.05435	3.01371	skeletal
image128.bmp	16.77778	12.45061	1.71575	skeletal
Label	Area	Major	Minor	Shape
image128.bmp	21.11111	10.02694	2.68073	skeletal
image128.bmp	31.55556	12.8142	3.13541	skeletal
image128.bmp	109	25.5654	5.42855	skeletal
image128.bmp	33.44444	17.49008	2.43468	skeletal
image128.bmp	38.22222	19.82503	2.45478	skeletal
image128.bmp	36.33333	11.59485	3.98979	skeletal
image128.bmp	40.22222	21.45635	2.38682	skeletal
image128.bmp	37	17.01763	2.7683	skeletal
image128.bmp	33.33333	15.23496	2.78578	skeletal
image128.bmp	59.33333	25.43312	2.97036	skeletal
image128.bmp	10.44444	7.68617	1.73016	skeletal
image128.bmp	43.33333	18.76083	2.9409	skeletal
image128.bmp	15.44444	12.16444	1.61655	skeletal
image128.bmp	29	9.17239	4.02556	skeletal
image128.bmp	50.77778	19.32207	3.34603	skeletal
image128.bmp	28.22222	16.96129	2.11857	skeletal
image128.bmp	50.88889	22.44984	2.88616	skeletal
image128.bmp	58.66667	24.30944	3.07275	skeletal
image128.bmp	32.33333	20.18464	2.03957	swallowtail
image128.bmp	17	11.69617	1.85061	swallowtail
image128.bmp	61.66667	19.87887	3.94974	swallowtail
image128.bmp	51.33333	21.30997	3.06709	swallowtail
image128.bmp	40	21.44108	2.37533	swallowtail
image128.bmp	28.77778	25.09291	1.46021	swallowtail
image128.bmp	62.55556	33.95043	2.34601	swallowtail
image128.bmp	84	31.13472	3.43514	swallowtail
image128.bmp	52.11111	19.12488	3.4693	tabular
image128.bmp	81.33333	16.49812	6.27688	tabular
image128.bmp	39.88889	25.77137	1.97072	tabular
image128.bmp	4.22222	4.73621	1.13506	tabular
image128.bmp	9.77778	8.33512	1.49361	tabular
image128.bmp	13	14.61209	1.13277	tabular

image128.bmp	35.55556	17.60796	2.57104	tabular
image128.bmp	29.55556	18.35842	2.04981	tabular
image128.bmp	34	25.25902	1.71385	tabular
image128.bmp	6.77778	7.51481	1.14836	tabular
image128.bmp	16.55556	21.85451	0.96452	tabular
image128.bmp	19.33333	18.87998	1.30381	tabular
image128.bmp	19.88889	18.43856	1.37339	tabular
image128.bmp	10.66667	15.40565	0.88157	tabular
image128.bmp	7	9.39741	0.94842	tabular
image128.bmp	5.22222	5.84636	1.13731	tabular
image128.bmp	13.44444	13.21969	1.29489	tabular
image128.bmp	13.33333	17.10513	0.99248	tabular
image128.bmp	15.77778	11.45775	1.7533	tabular
image128.bmp	21.22222	12.80279	2.11055	tabular
image128.bmp	13.33333	8.83253	1.92204	tabular
image128.bmp	7.22222	4.99936	1.83936	tabular
image128.bmp	7.77778	6.16655	1.60592	tabular
image128.bmp	5.22222	5.31007	1.25218	tabular
image128.bmp	13.88889	5.63405	3.13875	tabular
image128.bmp	32.11111	16.59278	2.46403	tabular
image128.bmp	19	15.29975	1.58117	tabular
image128.bmp	37.22222	24.71771	1.91736	tabular
Label	Area	Major	Minor	Shape
image128.bmp	45.55556	28.14216	2.06108	tabular
image128.bmp	11.11111	8.14525	1.73685	tabular
image128.bmp	26	11.61504	2.85012	tabular
image128.bmp	30.33333	19.05851	2.02648	tabular
image128.bmp	33.66667	22.7432	1.88477	tabular
image128.bmp	6.33333	4.43432	1.81851	tabular
image128.bmp	75.11111	24.05236	3.97609	tabular
image128.bmp	54.55556	15.23057	4.56071	tabular
image128.bmp	351.33333	54.97985	8.13628	tabular
image128.bmp	6.22222	9.03127	0.87722	tabular
image128.bmp	10.11111	11.57027	1.11267	tabular
image128.bmp	18.11111	22.37726	1.0305	tabular
image128.bmp	30	23.98301	1.59268	tabular
image128.bmp	54.11111	32.18556	2.1406	tabular
image128.bmp	10.22222	13.51338	0.96314	tabular
image128.bmp	21.44444	12.55844	2.17415	tabular
image128.bmp	34.44444	18.86209	2.32509	tabular
image128.bmp	60.44444	23.33671	3.29782	tabular
image128.bmp	12.66667	13.23981	1.21812	tabular
image128.bmp	20.55556	16.86267	1.55208	tabular
image128.bmp	31.66667	27.65125	1.45814	tabular
image128.bmp	25.22222	22.95247	1.39915	tabular
image128.bmp	18	11.15146	2.05518	tabular
image128.bmp	32.55556	23.19026	1.78743	tabular
image128.bmp	12.22222	11.07764	1.4048	tabular
image128.bmp	17.11111	12.70907	1.71425	tabular
image128.bmp	5	4.66918	1.36345	tabular
image128.bmp	28.22222	27.86311	1.28965	tabular

image128.bmp	19.44444	14.10953	1.75466	tabular
image128.bmp	29	20.9175	1.76522	tabular
image128.bmp	15.33333	12.31443	1.58538	tabular
image128.bmp	27.88889	23.64421	1.50182	tabular
image128.bmp	16	11.44773	1.77955	tabular
image128.bmp	17.11111	12.20191	1.7855	tabular
image128.bmp	19.11111	16.21212	1.50092	tabular
image128.bmp	9.55556	15.0733	0.80716	acicular
image128.bmp	3.11111	6.94455	0.5704	acicular
image128.bmp	27.55556	22.27268	1.57524	acicular
image128.bmp	9.11111	12.73376	0.91101	acicular
image128.bmp	7.66667	12.04524	0.8104	acicular
image128.bmp	7.66667	12.04524	0.8104	acicular
image128.bmp	14.66667	18.66203	1.00065	acicular
image128.bmp	10.11111	20.1568	0.63869	acicular
image128.bmp	6	10.84859	0.70419	acicular
image128.bmp	6.66667	9.15934	0.92673	acicular
image128.bmp	657.88889	30.59069	27.38252	vesicles
image128.bmp	655.55556	31.05321	26.879	vesicles
image128.bmp	8.66667	3.66707	3.00914	vesicles
image128.bmp	29.11111	6.78147	5.46569	vesicles
image128.bmp	7.22222	3.3196	2.7701	vesicles
image128.bmp	5	3.88042	1.64059	vesicles
image128.bmp	42.22222	10.25699	5.24121	vesicles
image128.bmp	26.77778	6.48802	5.255	vesicles
image128.bmp	934.44444	37.77266	31.49822	vesicles
Label	Area	Major	Minor	Shape
image128.bmp	54.55556	10.04424	6.91564	vesicles
image128.bmp	23.22222	6.47429	4.56691	vesicles
image128.bmp	182.22222	22.23683	10.4337	vesicles
image128.bmp	409.55556	28.46431	18.31987	vesicles
image128.bmp	8.66667	4.19063	2.63319	vesicles
image128.bmp	3669	77.7305	60.09888	vesicles
image128.bmp	1406.88889	47.66106	37.58428	vesicles
image128.bmp	7156.55556	113.29322	80.42855	vesicles
image128.bmp	348.77778	24.10514	18.42253	vesicles
image128.bmp	25.33333	6.41605	5.0273	vesicles
image128.bmp	386.11111	31.23554	15.73887	vesicles
image128.bmp	14	4.89901	3.63856	vesicles
image128.bmp	78027.77778	384.01146	258.71117	area
image035.bmp	10.74427618	18.50357297	0.739318631	acicular
image035.bmp	6.854104849	6.882775423	1.267939475	acicular
image035.bmp	27.60167265	7.872596397	4.464033288	tabular
image035.bmp	90.77060914	26.17499716	4.415385298	skeletal
image035.bmp	39.64267419	16.82746621	2.999539405	skeletal
image035.bmp	7.780337926	8.989690989	1.101957901	acicular
image035.bmp	6.483617309	9.703408103	0.850751107	acicular
image035.bmp	20.00658324	20.32822072	1.253093747	acicular
image035.bmp	33.15906163	9.018086504	4.681637507	hopper xtal
image035.bmp	6.668861079	3.888525826	2.183616541	hopper inside
image035.bmp	7.965586438	10.92433951	0.92839509	acicular

image035.bmp	2751.275687	60.26823843	58.1240342	vesicles
image035.bmp	1589.041398	46.07145867	43.91504746	vesicles
image035.bmp	83.546012	10.76311937	9.883199126	vesicles
image035.bmp	90.58536062	10.74053657	10.7384673	vesicles
image035.bmp	743.5780103	31.86745434	29.70909046	vesicles
image035.bmp	975.8766713	36.98801358	33.59263237	vesicles
image035.bmp	371.2332667	22.85743952	20.67899738	vesicles
image035.bmp	1454.5527	43.9217811	42.16573732	vesicles
image035.bmp	173.7608803	15.05991941	14.6905984	vesicles
image035.bmp	624.2794955	28.37906217	28.0085798	vesicles
image035.bmp	139.3050981	13.75032347	12.89924373	vesicles
image035.bmp	1299.686926	41.78405953	39.60392655	vesicles
image035.bmp	1191.873672	39.20607317	38.7067791	vesicles
image035.bmp	7669.190241	105.0435241	92.95877062	vesicles
image035.bmp	258.603613	18.1473928	18.14389652	vesicles
image035.bmp	489.6055533	25.39012941	24.55226572	vesicles
image035.bmp	113.1853946	12.44262148	11.58213295	vesicles
image035.bmp	200.0658324	16.38855129	15.54327753	vesicles
image035.bmp	482.3809514	25.41687891	24.16451403	vesicles
image035.bmp	944.014335	34.88613248	34.45370526	vesicles
image035.bmp	122.2624531	17.1867869	9.05750535	vesicles
image035.bmp	50.75744266	8.229754543	7.852770391	vesicles
image035.bmp	91.14110142	11.19537446	10.36539608	vesicles
image035.bmp	102.9968544	12.122695	10.8177019	vesicles
image035.bmp	4376.995822	77.51074886	71.89925162	vesicles
image035.bmp	159.3116813	14.72061262	13.77944529	vesicles
image035.bmp	215.2560159	16.73962813	16.37267585	vesicles
image035.bmp	127834.1013	581.4253761	279.9386628	area
image134.bmp	257.66758	21.08042	15.5629	spherilite
image134.bmp	120.01837	19.55746	7.8135	spherilite
Label	Area	Major	Minor	Shape
image134.bmp	242.79155	19.66314	15.72139	spherilite
image134.bmp	50.96419	9.98985	6.49555	spherilite
image134.bmp	53.3517	14.53322	4.67408	spherilite
image134.bmp	32.04775	11.00508	3.70778	hopper xtal
image134.bmp	1.0101	1.31919	0.97492	hopper inside
image134.bmp	78.60422	26.2921	3.80654	swallowtail
image134.bmp	63.45271	39.0337	2.06976	swallowtail
image134.bmp	166.75849	43.44909	4.88672	swallowtail
image134.bmp	197.42883	60.36383	4.16432	swallowtail
image134.bmp	48.20937	18.33438	3.34792	swallowtail
image134.bmp	44.16896	17.53696	3.20681	skeletal
image134.bmp	44.81175	10.77179	5.29681	skeletal
image134.bmp	15.97796	7.37624	2.75802	skeletal
image134.bmp	34.15978	14.31504	3.03831	skeletal
image134.bmp	257.75941	37.31991	8.79395	skeletal
image134.bmp	19.00826	19.90241	1.21604	acicular
image134.bmp	2.11203	4.28794	0.62714	acicular
image134.bmp	2.29568	4.47793	0.65275	acicular
image134.bmp	21.12029	17.83155	1.50807	acicular
image134.bmp	12.48852	9.12531	1.7425	acicular

image134.bmp	14.69238	6.62401	2.82411	tabular
image134.bmp	21.4876	8.45079	3.23743	tabular
image134.bmp	29561.24885	221.74446	169.7384	area
image033.bmp	265.49587	22.49784	15.02544	skeletal
image033.bmp	106.40496	13.8414	9.78796	skeletal
image033.bmp	5.16529	3.47066	1.89493	skeletal
image033.bmp	28.30579	26.81225	1.34416	acicular
image033.bmp	14.66942	14.1685	1.31825	acicular
image033.bmp	29.75207	26.7381	1.41676	acicular
image033.bmp	19.42149	20.65856	1.197	acicular
image033.bmp	2.06612	3.99429	0.65861	acicular
image033.bmp	9.29752	11.5531	1.02466	acicular
image033.bmp	5.78512	7.90787	0.93146	acicular
image033.bmp	0.61983	1.5387	0.5129	acicular
image033.bmp	11.36364	16.00215	0.90417	acicular
image033.bmp	9.09091	13.02176	0.88889	acicular
image033.bmp	3.30579	8.33556	0.50495	acicular
image033.bmp	3.92562	8.99758	0.55551	acicular
image033.bmp	2.47934	8.0197	0.39363	acicular
image033.bmp	2.47934	5.04373	0.62588	acicular
image033.bmp	21.4876	24.22176	1.12952	acicular
image033.bmp	5.16529	8.50943	0.77287	acicular
image033.bmp	7.43802	8.41659	1.1252	acicular
image033.bmp	6.61157	7.15635	1.17631	acicular
image033.bmp	7.02479	7.81545	1.14443	acicular
image033.bmp	7.2314	11.03488	0.83438	acicular
image033.bmp	5.3719	8.92724	0.76616	acicular
image033.bmp	7.43802	8.74663	1.08275	acicular
image033.bmp	28.71901	13.40518	2.72776	swallowtail
image033.bmp	14.04959	14.933	1.19792	swallowtail
image033.bmp	9.29752	6.10213	1.93997	swallowtail
image033.bmp	2.89256	2.97217	1.23914	swallowtail
image033.bmp	35.53719	7.5685	5.97838	swallowtail
image033.bmp	51.8595	10.73988	6.14807	spherilite
Label	Area	Major	Minor	Shape
image033.bmp	14.46281	7.95065	2.31612	spherilite
image033.bmp	9.91736	4.19884	3.0073	tabular
image033.bmp	13.84298	11.57574	1.52262	tabular
image033.bmp	142.56198	13.69947	13.24982	vesicles
image033.bmp	166.73554	14.99491	14.15776	vesicles
image033.bmp	612.80992	28.14749	27.7202	vesicles
Label	Area	Major	Minor	Shape
image033.bmp	166.73554	14.99491	14.15776	vesicles
image033.bmp	182.64463	21.21542	10.96138	vesicles
image033.bmp	381.40496	31.28331	15.52329	vesicles
image033.bmp	419.83471	30.84962	17.32761	vesicles
image033.bmp	14469.21488	149.52644	123.20748	vesicles
image033.bmp	44.6281	7.89442	7.19777	vesicles
image033.bmp	12068.59504	145.21261	105.81872	vesicles
image033.bmp	177.68595	15.54486	14.5538	vesicles
image033.bmp	75.61983	10.09815	9.53463	vesicles

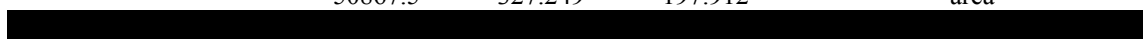


image033.bmp	1371.90083	42.71905	40.88945	vesicles
image033.bmp	61.98347	9.13143	8.64265	vesicles
image033.bmp	398.34711	23.20599	21.85605	vesicles
image033.bmp	2138.84298	55.45315	49.10919	vesicles
image033.bmp	97.52066	11.33759	10.95182	vesicles
image033.bmp	875.61983	35.02437	31.83137	vesicles
image033.bmp	1032.85124	38.58514	34.08221	vesicles
image033.bmp	546.07438	26.81179	25.93201	vesicles
image033.bmp	86.98347	10.52382	10.52382	vesicles
image033.bmp	47.10744	8.25131	7.26903	vesicles
image033.bmp	16.52893	4.58751	4.58751	vesicles
image033.bmp	343.59504	21.38305	20.45914	vesicles
image033.bmp	36.57025	7.78135	5.98388	vesicles
image033.bmp	359.50413	22.81553	20.06243	vesicles
image033.bmp	177119.8347	602.94079	374.02674	area

#### MSE-1

Area	Major	Minor	Shape
11704.198	131.706	113.148	skeletal plag
1822.963	75.924	30.571	skeletal plag
1263.062	51.667	31.126	skeletal plag
645.926	34.709	23.695	skeletal plag
267.852	22.111	15.424	skeletal plag
413.037	32.002	16.433	skeletal plag
2038.37	53.936	48.119	bad-ness
401.037	33.271	15.347	bad-ness
846.815	59.594	18.092	bad-ness
458.37	34.144	17.093	bad-ness
38052.247	264.31	183.306	area
1913.185	54.851	44.41	skeletal plag
446.123	25.801	22.015	bad-ness
56.938	10.748	6.745	bad-ness
48.296	10.815	5.686	bad-ness
26.123	7.983	4.166	bad-ness
129.827	16.262	10.165	bad-ness
19451.457	230.408	107.489	area
39.889	9.737	5.216	bad-ness
18.333	5.295	4.408	bad-ness
24.333	7.642	4.054	bad-ness
59.667	14.295	5.315	bad-ness
62.583	13.578	5.869	bad-ness
13.25	4.684	3.602	bad-ness
30.833	10.923	3.594	bad-ness
16.417	8.742	2.391	bad-ness
19.028	7.386	3.28	bad-ness
7.25	3.893	2.371	bad-ness
8.722	3.635	3.055	bad-ness
5	3.047	2.089	bad-ness
30020	237.67	160.822	area
36.944	10.455	4.499	baddness
9350.312	191.613	62.132	skeletal plag

2129.938	55.632	48.748	skeletal plag
1450.875	44.459	41.551	bad-ness
205.875	17.114	15.316	bad-ness
278.5	22.188	15.982	bad-ness
146	15.003	12.39	bad-ness
30.438	8.641	4.485	bad-ness
175.188	27.139	8.219	bad-ness
50867.5	327.249	197.912	area



MSE-2		
Label	Area	Shape
image006.bmp	28.926	hopper inside
image006.bmp	258.264	hoper xtal
image006.bmp	8.471	hopper inside
image006.bmp	126.033	hoper xtal
image006.bmp	23.554	hopper inside
image006.bmp	67.149	hoper xtal
image006.bmp	20.868	hopper inside
image006.bmp	78.719	hoper xtal
image006.bmp	15.083	hopper inside
image006.bmp	58.471	hoper xtal
image006.bmp	12.397	hopper inside
image006.bmp	44.835	hoper xtal
image006.bmp	25.413	hopper inside
image006.bmp	82.438	hoper xtal
image006.bmp	1251.653	hopper inside
image006.bmp	2142.769	hoper xtal
image006.bmp	619.215	hopper inside
image006.bmp	1126.653	hoper xtal
image006.bmp	33.678	hopper inside
image006.bmp	114.256	hoper xtal
image006.bmp	15.496	hopper inside
image006.bmp	58.884	hoper xtal
image006.bmp	38.636	hopper inside
image006.bmp	238.223	hoper xtal
image006.bmp	3.719	hopper inside
image006.bmp	53.099	hoper xtal
image006.bmp	48.347	hopper inside
image006.bmp	129.545	hoper xtal
image006.bmp	258.471	hopper inside
image006.bmp	583.058	hoper xtal
image006.bmp	60.95	hopper inside
image006.bmp	180.579	hoper xtal
image006.bmp	17.975	hopper inside
image006.bmp	73.14	hoper xtal
image006.bmp	18.595	hopper inside
image006.bmp	105.372	hoper xtal
image006.bmp	20.455	hopper inside
image006.bmp	56.612	hoper xtal
image006.bmp	76.653	hopper inside
image006.bmp	194.215	hoper xtal

image006.bmp	26.033
image006.bmp	70.041
image006.bmp	84.298
image006.bmp	180.579
image006.bmp	140.289
image006.bmp	84.091
image006.bmp	240.289
image006.bmp	14.876
image006.bmp	36.364
image006.bmp	260.744
image006.bmp	610.331
image006.bmp	298.76
image006.bmp	796.281
Label	Area
image006.bmp	67.562
image006.bmp	186.157
image006.bmp	290.289
image006.bmp	827.273
image006.bmp	97.934
image006.bmp	354.959
image006.bmp	315.909
image006.bmp	501.86
image006.bmp	131.612
image006.bmp	274.793
image006.bmp	18.802
image006.bmp	64.463
image006.bmp	824.587
image006.bmp	241.529
image006.bmp	551.86
image006.bmp	11.57
image006.bmp	47.934
image006.bmp	31.405
image006.bmp	131.198
image006.bmp	213.017
image006.bmp	485.95
image006.bmp	231.405
image006.bmp	413.223
image006.bmp	5.992
image006.bmp	10.331
image006.bmp	14.05
image006.bmp	36.983
image006.bmp	2072.314
image006.bmp	3378.306
image006.bmp	729.752
image006.bmp	1786.57
image006.bmp	52.479
image006.bmp	274.174
image006.bmp	33.471
image006.bmp	65.909
image006.bmp	20.041
image006.bmp	42.149

hopper inside  
 hopper xtal  
 hopper inside  
 hopper xtal  
 hopper inside  
 hopper xtal  
 hopper inside  
 hopper xtal  
 hopper inside  
 hopper xtal  
 hopper inside  
 hopper xtal  
 hopper inside  
 Shape  
 hopper xtal  
 hopper inside  
 hopper xtal  
 hopper inside  
 hopper xtal  
 hopper inside  
 hopper xtal  
 hopper inside  
 hopper xtal  
 hopper inside  
 hopper xtal  
 hopper inside  
 hopper xtal  
 hopper inside  
 hopper xtal  
 hopper inside  
 hopper xtal  
 hopper inside  
 hopper xtal  
 hopper inside  
 hopper xtal  
 hopper inside  
 hopper xtal  
 hopper inside  
 hopper xtal  
 hopper inside  
 hopper xtal  
 hopper inside  
 hopper xtal  
 tabular plag  
 tabular plag  
 tabular plag  
 tabular plag

image006.bmp	108.471	tabular plag
image006.bmp	57.438	tabular plag
image006.bmp	55.992	tabular plag
image006.bmp	155.785	tabular plag
image006.bmp	40.289	tabular plag
image006.bmp	74.587	tabular plag
image006.bmp	22.727	tabular plag
image006.bmp	88.43	tabular plag
image006.bmp	28.926	tabular plag
image006.bmp	19.628	tabular plag
image006.bmp	25.413	tabular plag
image006.bmp	568.802	tabular plag
image006.bmp	99.174	tabular plag
image006.bmp	70.868	tabular plag
image006.bmp	47.107	tabular plag
image006.bmp	26.033	tabular plag
image006.bmp	40.909	tabular plag
Label	Area	Shape
image006.bmp	163.223	tabular plag
image006.bmp	35.331	tabular plag
image006.bmp	150.826	tabular plag
image006.bmp	342.149	tabular plag
image006.bmp	100.207	tabular plag
image006.bmp	143.802	tabular plag
image006.bmp	185.331	tabular plag
image006.bmp	661.364	tabular plag
image006.bmp	134.917	tabular plag
image006.bmp	33.264	tabular plag
image006.bmp	258.884	tabular plag
image006.bmp	65.289	tabular plag
image006.bmp	30.785	tabular plag
image006.bmp	106.818	tabular plag
image006.bmp	56.612	vesicles and stuff
image006.bmp	78.512	vesicles and stuff
image006.bmp	98.967	vesicles and stuff
image006.bmp	669.215	vesicles and stuff
image006.bmp	475.62	vesicles and stuff
image006.bmp	130.785	vesicles and stuff
image006.bmp	296.488	vesicles and stuff
image006.bmp	2149.38	vesicles and stuff
image006.bmp	272.314	vesicles and stuff
image006.bmp	1225.826	vesicles and stuff
image006.bmp	517.355	vesicles and stuff
image006.bmp	220.455	vesicles and stuff
image006.bmp	168.595	vesicles and stuff
image006.bmp	114695.455	area
image007.bmp	111.909	hopper inside
image007.bmp	233.648	hoper xtal
image007.bmp	307.372	hopper inside
image007.bmp	581.096	hoper xtal
image007.bmp	81.285	hopper inside

image007.bmp	144.045	hoper xtal
image007.bmp	28.166	hopper inside
image007.bmp	102.268	hoper xtal
image007.bmp	60.491	hopper inside
image007.bmp	156.522	hoper xtal
image007.bmp	95.274	hopper inside
image007.bmp	211.153	hoper xtal
image007.bmp	40.643	hopper inside
image007.bmp	62.949	hoper xtal
image007.bmp	8.696	hopper inside
image007.bmp	76.371	hoper xtal
image007.bmp	234.405	hopper inside
image007.bmp	540.832	hoper xtal
image007.bmp	120.038	hopper inside
image007.bmp	421.928	hoper xtal
image007.bmp	1111.153	hopper inside
image007.bmp	2007.94	hoper xtal
image007.bmp	69.565	hopper inside
image007.bmp	376.938	hoper xtal
image007.bmp	997.921	hopper inside
image007.bmp	1868.242	hoper xtal
Label	Area	Shape
image007.bmp	105.482	hopper inside
image007.bmp	319.849	hoper xtal
image007.bmp	60.87	hopper inside
image007.bmp	143.856	hoper xtal
image007.bmp	33.27	hopper inside
image007.bmp	80.907	hoper xtal
image007.bmp	19.849	hopper inside
image007.bmp	93.384	hoper xtal
image007.bmp	216.257	hopper inside
image007.bmp	502.268	hoper xtal
image007.bmp	39.319	hopper inside
image007.bmp	35.539	hoper xtal
image007.bmp	170.132	hopper inside
image007.bmp	49.338	hoper xtal
image007.bmp	197.921	tabular plag
image007.bmp	23.251	tabular plag
image007.bmp	47.448	tabular plag
image007.bmp	58.601	tabular plag
image007.bmp	47.259	tabular plag
image007.bmp	76.749	tabular plag
image007.bmp	12.665	tabular plag
image007.bmp	78.639	tabular plag
image007.bmp	39.698	tabular plag
image007.bmp	121.172	tabular plag
image007.bmp	788.847	vesicles and stuff
image007.bmp	1486.767	vesicles and stuff
image007.bmp	282.609	vesicles and stuff
image007.bmp	2345.18	vesicles and stuff
image007.bmp	141.588	vesicles and stuff

image007.bmp	1978.072	vesicles and stuff
image007.bmp	893.573	vesicles and stuff
image007.bmp	56299.811	area
E-1		
Label	Area	Shape
image186.bmp	41.32	tabular plag
image186.bmp	52.68	tabular plag
image186.bmp	12.8	tabular plag
image186.bmp	140.12	tabular plag
image186.bmp	95.28	tabular plag
image186.bmp	22.96	tabular plag
image186.bmp	6.2	tabular plag
image186.bmp	3.48	tabular plag
image186.bmp	11.4	hopper inside
image186.bmp	135.08	hopper xtal
image186.bmp	12.76	hopper inside
image186.bmp	43.68	hopper xtal
image186.bmp	11.84	hopper inside
image186.bmp	50.36	hopper xtal
image186.bmp	20.44	hopper inside
image186.bmp	197.48	hopper xtal
image186.bmp	16.32	hopper inside
image186.bmp	119.08	hopper xtal
image186.bmp	95.12	hopper inside
image186.bmp	400.4	hopper xtal
image186.bmp	47.32	hopper inside
image186.bmp	219.6	hopper xtal
image186.bmp	37.92	hopper inside
image186.bmp	128.8	hopper xtal
image186.bmp	52.84	hopper inside
image186.bmp	235.84	hopper xtal
image186.bmp	7.84	hopper inside
image186.bmp	64.84	hopper xtal
image186.bmp	68.52	cracks and holes
image186.bmp	76.64	cracks and holes
image186.bmp	24.08	cracks and holes
image186.bmp	30.96	cracks and holes
image186.bmp	103.16	cracks and holes
image186.bmp	16974.8	area
image189.bmp	44.983	tabular plag
image189.bmp	84.083	tabular plag
image189.bmp	131.142	tabular plag
image189.bmp	508.651	tabular plag
image189.bmp	205.536	tabular plag
image189.bmp	45.675	tabular plag
image189.bmp	17.993	tabular plag
image189.bmp	167.128	tabular plag
image189.bmp	129.066	tabular plag
image189.bmp	69.55	tabular plag
image189.bmp	137.024	tabular plag











image189.bmp	116.955	skeletal plag
image189.bmp	176.471	skeletal plag
image189.bmp	315.225	skeletal plag
image189.bmp	571.972	skeletal plag
image189.bmp	179.931	skeletal plag
image189.bmp	347.059	skeletal plag
image189.bmp	497.578	skeletal plag
image189.bmp	1437.37	skeletal plag
image189.bmp	2661.938	initial plag, vesicels, cracks, ects
image189.bmp	2366.782	initial plag, vesicels, cracks, ects
image189.bmp	5220.415	initial plag, vesicels, cracks, ects
image189.bmp	4213.495	initial plag, vesicels, cracks, ects
image189.bmp	20439.792	initial plag, vesicels, cracks, ects
image189.bmp	4559.516	initial plag, vesicels, cracks, ects
image189.bmp	294967.128	area

## E-2

Label	Area	Major	Minor	Shape
image194.bmp	9569	137.459	88.635	junk
image194.bmp	3977	73.914	68.508	junk
image194.bmp	852	39.687	27.334	junk
image194.bmp	754	32.825	29.246	junk
image194.bmp	2945.5	66.337	56.535	junk
image194.bmp	823	39.562	26.487	junk
image194.bmp	5385	94.276	72.727	junk
image194.bmp	1397.5	51.04	34.862	junk
image194.bmp	556.75	36.131	19.619	junk
image194.bmp	370	39.212	12.014	junk
image194.bmp	34042	309.889	139.868	junk
image194.bmp	25650.75	232.42	140.519	junk
image194.bmp	11528	181.443	80.896	junk
image194.bmp	11950.75	181.301	83.928	junk
image194.bmp	5230.5	109.579	60.775	junk
image194.bmp	6776.5	150.544	57.313	junk
image194.bmp	4498.25	136.467	41.969	junk
image194.bmp	43253.75	253.764	217.022	junk
image194.bmp	11.5	3.991	3.669	hopper inside
image194.bmp	165.5	16.59	12.702	hoper xtal
image194.bmp	13.25	5.334	3.163	hopper inside
image194.bmp	126.75	13.289	12.144	hoper xtal
image194.bmp	25.25	5.961	5.394	hopper inside
image194.bmp	106.5	15.293	8.867	hoper xtal
image194.bmp	29	7.706	4.792	hopper inside
image194.bmp	376.5	28.943	16.563	hoper xtal
image194.bmp	61.75	13.275	5.923	hopper inside
image194.bmp	838.25	45.796	23.305	hoper xtal
image194.bmp	6	4.092	1.867	hopper inside
image194.bmp	38.25	8.501	5.729	hoper xtal
image194.bmp	21.5	6.746	4.058	hopper inside
image194.bmp	212.25	24.407	11.073	hoper xtal
image194.bmp	16.5	6.32	3.324	hopper inside

image194.bmp	171	19.155	11.366	hoper xtal
image194.bmp	43	8.04	6.81	hopper inside
image194.bmp	361.5	23.002	20.01	hoper xtal
image194.bmp	33.25	7.573	5.59	hopper inside
image194.bmp	226	21.826	13.184	hoper xtal
image194.bmp	21.25	7.254	3.73	hopper inside
image194.bmp	235	19.202	15.582	hoper xtal
image194.bmp	35.25	7.529	5.961	hopper inside
image194.bmp	96.25	11.979	10.231	hoper xtal
image194.bmp	61	16.15	4.809	hopper inside
image194.bmp	214.5	20.614	13.249	hoper xtal
image194.bmp	22	8.432	3.322	plag
image194.bmp	28.75	17.211	2.127	hopper inside
image194.bmp	181.5	26.264	8.799	hoper xtal
image194.bmp	193	19.831	12.392	tabular plag
image194.bmp	525.5	113.692	5.885	tabular plag
image194.bmp	109	57.016	2.434	tabular plag
image194.bmp	99.25	15.794	8.001	tabular plag
image194.bmp	202.75	19.598	13.172	tabular plag
image194.bmp	22.25	7.941	3.568	tabular plag
Label	Area	Major	Minor	Shape
image194.bmp	41	8.073	6.466	tabular plag
image194.bmp	45.75	7.728	7.538	tabular plag
image194.bmp	110.5	15.93	8.832	tabular plag
image194.bmp	50.25	11.298	5.663	tabular plag
image194.bmp	267.75	32.526	10.481	tabular plag
image194.bmp	33.5	8.755	4.872	tabular plag
image194.bmp	62.25	22.211	3.569	tabular plag
image194.bmp	101.25	40.401	3.191	tabular plag
image194.bmp	419.75	81.789	6.534	tabular plag
image194.bmp	183.75	57.78	4.049	tabular plag
image194.bmp	30	7.623	5.011	tabular plag
image194.bmp	133.75	21.577	7.893	tabular plag
image194.bmp	67.75	12.35	6.985	tabular plag
image194.bmp	109.75	19.766	7.07	tabular plag
image194.bmp	39.5	24.577	2.046	tabular plag
image194.bmp	66.5	13.047	6.49	tabular plag
image194.bmp	15.5	6.446	3.062	tabular plag
image194.bmp	15.25	4.97	3.906	tabular plag
image194.bmp	220	25.607	10.939	tabular plag
image194.bmp	50.5	10.037	6.406	tabular plag
image194.bmp	132.75	26.535	6.37	tabular plag
image194.bmp	87	14.129	7.84	tabular plag
image194.bmp	133	15.818	10.706	tabular plag
image194.bmp	45.25	8.282	6.956	tabular plag
image194.bmp	388.25	28.172	17.547	tabular plag
image194.bmp	86	12.191	8.982	tabular plag
image194.bmp	24.75	10.073	3.128	tabular plag
image194.bmp	154	21.853	8.973	tabular plag
image194.bmp	46	8.907	6.576	tabular plag
image194.bmp	672.75	32.19	26.61	tabular plag

image194.bmp	29.5	7.574	4.959	tabular plag
image194.bmp	13.25	7.738	2.18	tabular plag
image194.bmp	135	17.469	9.839	tabular plag
image194.bmp	730.25	41.409	22.454	tabular plag
image194.bmp	70.25	10.736	8.332	tabular plag
image194.bmp	95	18.759	6.448	tabular plag
image194.bmp	69.5	10.679	8.286	tabular plag
image194.bmp	19.5	5.859	4.238	tabular plag
image194.bmp	21	5.891	4.539	tabular plag
image194.bmp	313	39.967	9.971	skeletal plag
image194.bmp	723.5	42.601	21.624	skeletal plag
image194.bmp	1772	90.617	24.898	skeletal plag
image194.bmp	719.75	42.903	21.36	skeletal plag
image194.bmp	803	45.008	22.716	skeletal plag
image194.bmp	152.75	18.765	10.364	skeletal plag
image194.bmp	504.75	31.414	20.458	skeletal plag
image194.bmp	830	37.063	28.513	skeletal plag
image194.bmp	192.75	16.381	14.982	skeletal plag
image194.bmp	183.5	17.922	13.036	skeletal plag
image194.bmp	215	33.649	8.135	tabular plag
image194.bmp	46	8.838	6.627	tabular plag
image194.bmp	46	8.274	7.079	tabular plag
image194.bmp	32.25	10.878	3.775	tabular plag
image194.bmp	48.75	11.049	5.618	tabular plag
Label	Area	Major	Minor	Shape
image194.bmp	5.5	4.723	1.483	tabular plag
image194.bmp	7	3.853	2.313	tabular plag
image194.bmp	7.75	3.965	2.489	tabular plag
image194.bmp	9	9.328	1.228	tabular plag
image194.bmp	232344.25	702.877	420.884	area

E-4

Label	Area	Major	Minor	Shape
image195.bmp	95	22.132	5.465	hopper inside
image195.bmp	355.5	35.753	12.66	hoper xtal
image195.bmp	33.75	6.687	6.426	hopper inside
image195.bmp	85.75	11.391	9.585	hoper xtal
image195.bmp	94.5	12.672	9.495	hopper inside
image195.bmp	252	19.401	16.538	hoper xtal
image195.bmp	21	6.855	3.901	hopper inside
image195.bmp	198.75	17.443	14.508	hoper xtal
image195.bmp	10.5	5.288	2.528	hopper inside
image195.bmp	182.5	32.683	7.11	hoper xtal
image195.bmp	27	9.52	3.611	hopper inside
image195.bmp	126.75	20.959	7.7	hoper xtal
image195.bmp	36.75	7.951	5.885	hopper inside
image195.bmp	180.75	17.491	13.157	hoper xtal
image195.bmp	41.25	21.579	2.434	hopper inside
image195.bmp	230	38.755	7.556	hoper xtal
image195.bmp	157.75	23.794	8.441	hopper inside
image195.bmp	864.25	63.278	17.39	hoper xtal

image195.bmp	14.75	10.817	1.736	hopper inside
image195.bmp	263.5	25.651	13.079	hoper xtal
image195.bmp	17.5	6.859	3.249	hopper inside
image195.bmp	131	18.925	8.813	hoper xtal
image195.bmp	41	9.622	5.426	hopper inside
image195.bmp	358.75	25.541	17.884	hoper xtal
image195.bmp	2.75	3.37	1.039	hopper inside
image195.bmp	16	6.283	3.242	hoper xtal
image195.bmp	123	19.835	7.896	hopper inside
image195.bmp	497.5	33.238	19.058	hoper xtal
image195.bmp	29.5	8.285	4.534	hopper inside
image195.bmp	152	16.65	11.624	hoper xtal
image195.bmp	15.5	4.989	3.956	hopper inside
image195.bmp	59.75	9.243	8.23	hoper xtal
image195.bmp	28.5	8.967	4.047	hopper inside
image195.bmp	150.25	23.211	8.242	hoper xtal
image195.bmp	10.75	3.991	3.429	hopper inside
image195.bmp	121.5	15.964	9.691	hoper xtal
image195.bmp	534	50.083	13.576	skeletal plag
image195.bmp	1873.25	98.702	24.165	skeletal plag
image195.bmp	1068.25	55.307	24.593	skeletal plag
image195.bmp	1751.5	71.443	31.215	skeletal plag
image195.bmp	1731	92.627	23.794	skeletal plag
image195.bmp	3653.5	141.089	32.971	skeletal plag
image195.bmp	248.25	25.089	12.599	skeletal plag
image195.bmp	605.5	35.329	21.822	skeletal plag
image195.bmp	107	13.973	9.75	skeletal plag
image195.bmp	753.5	53.873	17.808	skeletal plag
image195.bmp	374.5	40.684	11.72	skeletal plag
image195.bmp	682	42.35	20.504	skeletal plag
image195.bmp	295	23.207	16.185	skeletal plag
image195.bmp	166.25	14.795	14.307	skeletal plag
image195.bmp	531.75	33.207	20.388	tabular plag
image195.bmp	295	37.453	10.029	tabular plag
image195.bmp	198.75	52.884	4.785	tabular plag
Label	Area	Major	Minor	Shape
image195.bmp	151	25.326	7.591	tabular plag
image195.bmp	127.5	28.496	5.697	tabular plag
image195.bmp	259	45.715	7.214	tabular plag
image195.bmp	115	13.383	10.941	tabular plag
image195.bmp	43.5	8.632	6.417	tabular plag
image195.bmp	21.25	6.854	3.947	tabular plag
image195.bmp	188.25	25.842	9.275	tabular plag
image195.bmp	32.75	8.187	5.093	tabular plag
image195.bmp	128.75	18.365	8.926	tabular plag
image195.bmp	121	18.495	8.33	tabular plag
image195.bmp	93.25	12.196	9.735	tabular plag
image195.bmp	67.5	14.167	6.066	tabular plag
image195.bmp	337.75	76.176	5.645	tabular plag
image195.bmp	306.75	25.223	15.484	tabular plag
image195.bmp	1063.75	117.816	11.496	tabular plag

image195.bmp	32.75	9.215	4.525	tabular plag
image195.bmp	17.5	5.268	4.23	tabular plag
image195.bmp	18	6.846	3.348	tabular plag
image195.bmp	57.5	11.999	6.101	tabular plag
image195.bmp	42.75	10.472	5.198	tabular plag
image195.bmp	55	16.757	4.179	tabular plag
image195.bmp	62.25	11.886	6.669	tabular plag
image195.bmp	109.75	27.512	5.079	tabular plag
image195.bmp	153.25	24.367	8.008	tabular plag
image195.bmp	39	10.85	4.577	tabular plag
image195.bmp	4864	85.103	72.771	junk
image195.bmp	1891.75	58.774	40.982	junk
image195.bmp	13250.75	225.882	74.691	junk
image195.bmp	127440	618.113	262.511	area

#### E-5

Label	Area	Major	Minor	Shape
image201.bmp	1334.259	63.353	26.815	junk
image201.bmp	2260.555	54.65	52.667	junk
image201.bmp	681.227	30.11	28.807	junk
image201.bmp	853.689	34.797	31.236	junk
image201.bmp	927.173	35.792	32.982	junk
image201.bmp	1375.383	45.493	38.493	junk
image201.bmp	366.18	34.504	13.513	junk
image201.bmp	115.121	25.739	5.695	junk
image201.bmp	456.172	66.518	8.732	junk
image201.bmp	17.75	6.041	3.741	hopper inside
image201.bmp	49.744	9.53	6.646	hopper xtal
image201.bmp	17.604	4.792	4.677	hopper inside
image201.bmp	99.781	13.219	9.611	hopper xtal
image201.bmp	39.883	10.678	4.756	hopper inside
image201.bmp	268.59	25.563	13.378	hopper xtal
image201.bmp	1.242	1.419	1.114	hopper inside
image201.bmp	12.491	4.364	3.644	hopper xtal
image201.bmp	11.833	5.111	2.948	hopper inside
image201.bmp	77.137	15.381	6.386	hopper xtal
image201.bmp	36.669	10.607	4.402	hopper inside
image201.bmp	164.646	27.458	7.635	hopper xtal
image201.bmp	126.589	19.539	8.249	hopper inside
image201.bmp	270.124	27.18	12.654	hopper xtal
image201.bmp	130.898	18.619	8.951	skeletal plag
image201.bmp	266.253	30.362	11.165	skeletal plag
image201.bmp	192.841	54.844	4.477	skeletal plag
image201.bmp	163.915	19.201	10.869	skeletal plag
image201.bmp	255.734	32.718	9.952	skeletal plag
image201.bmp	196.421	31.719	7.885	skeletal plag
image201.bmp	765.449	44.579	21.862	skeletal plag
image201.bmp	539.153	48.146	14.258	skeletal plag
image201.bmp	145.508	17.364	10.669	skeletal plag
image201.bmp	286.56	30.317	12.035	skeletal plag
image201.bmp	110.665	16.688	8.444	skeletal plag

image201.bmp	340.175	33.767	12.827	skeletal plag
image201.bmp	671.074	35.94	23.774	skeletal plag
image201.bmp	1179.912	43.132	34.831	skeletal plag
image201.bmp	1021.329	44.719	29.079	skeletal plag
image201.bmp	188.678	16.026	14.991	skeletal plag
image201.bmp	56.611	10.321	6.983	skeletal plag
image201.bmp	5343.828	118.203	57.562	skeletal plag
image201.bmp	148.137	24.267	7.773	tabular plag
image201.bmp	194.083	19.025	12.989	tabular plag
image201.bmp	67.787	12.726	6.782	tabular plag
image201.bmp	55.588	14.509	4.878	tabular plag
image201.bmp	27.246	9.73	3.565	tabular plag
image201.bmp	16.216	5.937	3.478	tabular plag
image201.bmp	45.654	10.812	5.376	tabular plag
image201.bmp	32.725	8.689	4.795	tabular plag
image201.bmp	18.919	6.867	3.508	tabular plag
image201.bmp	83154.565	385.053	274.964	area

#### E-6

Label	Area	Major	Minor	Shape
image206.bmp	162979	572.847	362.245	junk
image206.bmp	284875	720.892	503.146	junk
image206.bmp	211266	1377.872	195.223	junk
image206.bmp	5475	89.368	78.003	junk
image206.bmp	5782	119.822	61.44	junk
image206.bmp	548	45.665	15.279	pyroxene
image206.bmp	128.5	18.667	8.765	pyroxene
image206.bmp	1163.75	84.48	17.54	pyroxene
image206.bmp	156	15.578	12.75	pyroxene
image206.bmp	396	47.455	10.625	pyroxene
image206.bmp	67.75	13.139	6.565	pyroxene
image206.bmp	47.75	11.837	5.136	pyroxene
image206.bmp	286.5	21.46	16.998	pyroxene
image206.bmp	509.75	47.224	13.744	pyroxene
image206.bmp	170.25	21.068	10.289	pyroxene
image206.bmp	799	57.895	17.572	pyroxene
image206.bmp	724	41.227	22.36	pyroxene
image206.bmp	534.75	37.102	18.351	pyroxene
image206.bmp	442.25	28.884	19.495	pyroxene
image206.bmp	425.5	31.658	17.113	pyroxene
image206.bmp	780	39.183	25.346	pyroxene
image206.bmp	421.25	37.231	14.406	pyroxene
image206.bmp	74.5	11.212	8.46	pyroxene
image206.bmp	45.5	8.347	6.941	pyroxene
image206.bmp	24.75	8.043	3.918	pyroxene
image206.bmp	706.25	37.417	24.032	pyroxene
image206.bmp	383.5	25.672	19.02	pyroxene
image206.bmp	383.25	28.492	17.127	pyroxene
image206.bmp	132	20.189	8.325	pyroxene
image206.bmp	178	18.956	11.956	pyroxene
image206.bmp	132.25	21.246	7.925	pyroxene



image206.bmp	33	7.614	5.518	pyroxene
image206.bmp	105	13.046	10.248	pyroxene
image206.bmp	45.25	9.387	6.138	pyroxene
image206.bmp	1022.75	63.055	20.652	pyroxene
image206.bmp	38.25	10.899	4.468	pyroxene
image206.bmp	133	14.209	11.918	pyroxene
image206.bmp	168	17.433	12.27	pyroxene
image206.bmp	538.25	32.044	21.387	pyroxene
image206.bmp	102.75	13.153	9.947	hopper inside
image206.bmp	504.75	29.321	21.918	hopper xtal
image206.bmp	40.5	7.825	6.59	hopper inside
image206.bmp	333	22.055	19.224	hopper xtal
image206.bmp	33.25	10.183	4.157	hopper inside
image206.bmp	143.25	20.881	8.735	hopper xtal
image206.bmp	19.5	6.952	3.572	hopper inside
image206.bmp	246.5	24.849	12.631	hopper xtal
image206.bmp	62	24.655	3.202	hopper inside
image206.bmp	223.5	35.903	7.926	hopper xtal
image206.bmp	80.5	11.726	8.741	hopper inside
image206.bmp	557.75	31.458	22.575	hopper xtal
image206.bmp	21.25	6.244	4.333	hopper inside
image206.bmp	300	20.583	18.558	hopper xtal
Label	Area	Major	Minor	Shape
image206.bmp	15.5	6.279	3.143	hopper inside
image206.bmp	174	16.939	13.079	hopper xtal
image206.bmp	13.75	4.79	3.655	hopper inside
image206.bmp	31.5	13.651	2.938	hopper xtal
image206.bmp	161.5	21.448	9.587	hopper xtal
image206.bmp	20.25	9.52	2.708	hopper inside
image206.bmp	117.5	18.858	7.933	hopper xtal
image206.bmp	24.75	10.756	2.93	hopper inside
image206.bmp	207	18.855	13.978	hopper xtal
image206.bmp	82.25	26.152	4.004	hopper inside
image206.bmp	405.25	55.189	9.349	hopper xtal
image206.bmp	47	11.146	5.369	hopper inside
image206.bmp	167	18.094	11.751	hopper xtal
image206.bmp	43.75	10.55	5.28	hopper inside
image206.bmp	551.75	35.797	19.625	hopper xtal
image206.bmp	182	19.389	11.951	hopper inside
image206.bmp	758.5	35.745	27.018	hopper xtal
image206.bmp	65.25	9.454	8.788	hopper inside
image206.bmp	173.25	15.871	13.899	hopper xtal
image206.bmp	61.25	11.202	6.962	hopper inside
image206.bmp	189	17.269	13.935	hopper xtal
image206.bmp	72	10.819	8.473	hopper inside
image206.bmp	306.25	22.249	17.526	hopper xtal
image206.bmp	41	13.413	3.892	hopper inside
image206.bmp	471.25	42.889	13.99	hopper xtal
image206.bmp	13.25	6.945	2.429	hopper inside
image206.bmp	145.75	19.46	9.536	hopper xtal
image206.bmp	56.5	10.49	6.858	hopper inside

image206.bmp	444	29.93	18.888	hopper xtal
image206.bmp	37.25	14.011	3.385	hopper inside
image206.bmp	201.5	23.612	10.866	hopper xtal
image206.bmp	8	4.538	2.245	hopper inside
image206.bmp	53.75	11.806	5.797	hopper xtal
image206.bmp	76.5	12.244	7.955	hopper inside
image206.bmp	735.5	32.926	28.442	hopper xtal
image206.bmp	352	47.391	9.457	skeletal plag
image206.bmp	2055.75	81.692	32.041	skeletal plag
image206.bmp	147	25.316	7.393	skeletal plag
image206.bmp	258	38.269	8.584	skeletal plag
image206.bmp	209	26.571	10.015	skeletal plag
image206.bmp	655.25	55.458	15.044	skeletal plag
image206.bmp	873.5	48.755	22.811	skeletal plag
image206.bmp	399.75	25.752	19.764	skeletal plag
image206.bmp	273	46.772	7.432	skeletal plag
image206.bmp	220.25	45.293	6.191	skeletal plag
image206.bmp	388.75	58.737	8.427	skeletal plag
image206.bmp	663.75	40.059	21.097	skeletal plag
image206.bmp	1341	66.453	25.694	skeletal plag
image206.bmp	560	28.389	25.116	skeletal plag
image206.bmp	1553.25	46.171	42.834	skeletal plag
image206.bmp	757.75	64.871	14.872	skeletal plag
image206.bmp	230.5	37.63	7.799	skeletal plag
image206.bmp	555	31.785	22.232	skeletal plag
image206.bmp	425.25	25.188	21.497	skeletal plag
Label	Area	Major	Minor	Shape
image206.bmp	676.5	40.227	21.412	skeletal plag
image206.bmp	1111.5	52.199	27.112	skeletal plag
image206.bmp	921.5	44.994	26.076	skeletal plag
image206.bmp	1225.75	44.028	35.447	skeletal plag
image206.bmp	532.25	28.72	23.596	skeletal plag
image206.bmp	452.25	27.78	20.728	skeletal plag
image206.bmp	226.25	23.079	12.482	skeletal plag
image206.bmp	288.75	28.452	12.922	skeletal plag
image206.bmp	517.25	34.488	19.096	skeletal plag
image206.bmp	521.75	46.572	14.264	skeletal plag
image206.bmp	1352.25	47.631	36.147	skeletal plag
image206.bmp	680	67.25	12.874	skeletal plag
image206.bmp	301	26.722	14.342	tabular plag
image206.bmp	199	24.327	10.415	tabular plag
image206.bmp	170.75	42.111	5.163	tabular plag
image206.bmp	118.5	27.091	5.569	tabular plag
image206.bmp	311.75	36.002	11.025	tabular plag
image206.bmp	433.25	53.018	10.405	tabular plag
image206.bmp	118.5	33.948	4.444	tabular plag
image206.bmp	115.25	14.934	9.826	tabular plag
image206.bmp	258	43.942	7.476	tabular plag
image206.bmp	281	29.636	12.073	tabular plag
image206.bmp	49.25	10.166	6.168	tabular plag
image206.bmp	65.5	10.851	7.686	tabular plag

image206.bmp	182	33.151	6.99	tabular plag
image206.bmp	409.5	48.189	10.82	tabular plag
image206.bmp	107.75	16.341	8.396	tabular plag
image206.bmp	49.5	14.116	4.465	tabular plag
image206.bmp	83.75	12.497	8.533	tabular plag
image206.bmp	168	16.046	13.33	tabular plag
image206.bmp	96.5	14.28	8.604	tabular plag
image206.bmp	72	13.451	6.815	tabular plag
image206.bmp	153.75	22.322	8.77	tabular plag
image206.bmp	64	18.756	4.345	tabular plag
image206.bmp	116.5	20.037	7.403	tabular plag
image206.bmp	322	30.487	13.448	tabular plag
image206.bmp	280.75	49.047	7.288	tabular plag
image206.bmp	365.75	61.691	7.549	tabular plag
image206.bmp	852.5	79.492	13.655	tabular plag
image206.bmp	126	22.968	6.985	tabular plag
image206.bmp	170.5	55.467	3.914	tabular plag
image206.bmp	427.25	42.323	12.853	tabular plag
image206.bmp	92.25	12.286	9.56	tabular plag
image206.bmp	42.75	8.638	6.301	tabular plag
image206.bmp	89	12.316	9.201	tabular plag
image206.bmp	86	13.679	8.005	tabular plag
image206.bmp	102.5	14.813	8.81	tabular plag
image206.bmp	62.25	13.024	6.086	tabular plag
image206.bmp	44.25	9.865	5.711	tabular plag
image206.bmp	313.25	42.968	9.282	tabular plag
image206.bmp	116.75	16.199	9.177	tabular plag
image206.bmp	115.5	18.87	7.793	tabular plag
image206.bmp	124.25	17.181	9.208	tabular plag
image206.bmp	581	75.871	9.75	tabular plag
Label	Area	Major	Minor	Shape
image206.bmp	49	9.702	6.43	tabular plag
image206.bmp	128	23.138	7.043	tabular plag
image206.bmp	55.5	9.457	7.472	tabular plag
image206.bmp	124	34.873	4.527	tabular plag
image206.bmp	80	15.106	6.743	tabular plag
image206.bmp	49.75	14.428	4.39	tabular plag
image206.bmp	492	41.411	15.127	tabular plag
image206.bmp	241.25	20.971	14.647	tabular plag
image206.bmp	164.25	22.146	9.443	tabular plag
image206.bmp	327104.25	721.598	577.166	area

#### E-7

Label	Area	Major	Minor	Shape
image257.bmp	155496	468.245	422.821	junk
image257.bmp	26047	297.163	111.602	junk
image257.bmp	144325	477.608	384.751	junk
image257.bmp	99671	768.326	165.171	junk
image257.bmp	110930	663.625	212.832	junk
image257.bmp	2495	63.696	49.874	junk
image257.bmp	426	24.176	22.435	junk

image257.bmp	2056	53.381	49.039	junk
image257.bmp	321494.444	961.939	425.536	junk
image257.bmp	2770.139	124.023	28.439	junk
image257.bmp	4150.694	87.342	60.507	junk
image257.bmp	478.472	30.475	19.99	junk
image257.bmp	327.778	25.151	16.593	junk
image257.bmp	504.167	38.69	16.591	junk
image257.bmp	405.556	42.821	12.059	junk
image257.bmp	2329.167	135.652	21.862	junk
image257.bmp	1334.028	66.525	25.532	junk
image257.bmp	440.972	28.891	19.434	junk
image257.bmp	1413.194	66.118	27.214	junk
image257.bmp	5.556	2.948	2.399	hopper inside
image257.bmp	31.25	7.305	5.447	hopper xtal
image257.bmp	22.222	8.565	3.303	hopper inside
image257.bmp	72.222	13.768	6.679	hopper xtal
image257.bmp	11.111	5.743	2.463	hopper inside
image257.bmp	38.889	9.496	5.215	hopper xtal
image257.bmp	88.194	15.813	7.101	hopper inside
image257.bmp	255.556	22.984	14.157	hopper xtal
image257.bmp	13.889	5.181	3.413	hopper inside
image257.bmp	42.361	9.213	5.854	hopper xtal
image257.bmp	4.167	2.442	2.173	hopper inside
image257.bmp	25.694	7.339	4.458	hopper xtal
image257.bmp	2.778	3.064	1.154	hopper inside
image257.bmp	26.389	6.845	4.909	hopper xtal
image257.bmp	6.25	3.269	2.434	hopper inside
image257.bmp	39.583	7.834	6.433	hopper xtal
image257.bmp	5.556	4.113	1.72	hopper inside
image257.bmp	19.444	8.352	2.964	hopper xtal
image257.bmp	16.667	5.87	3.615	hopper inside
image257.bmp	55.556	9.928	7.125	hopper xtal
image257.bmp	168.75	19.549	10.991	Skeletal Xtals
image257.bmp	159.722	21.118	9.63	Skeletal Xtals
image257.bmp	86.806	11.518	9.596	Skeletal Xtals
image257.bmp	131.25	13.237	12.624	Skeletal Xtals
image257.bmp	109.028	19.759	7.026	Skeletal Xtals
image257.bmp	135.417	29.694	5.807	Skeletal Xtals
image257.bmp	47.917	9.978	6.115	Skeletal Xtals
image257.bmp	45.139	10.861	5.292	tabular plag
image257.bmp	72.222	11.538	7.97	tabular plag
image257.bmp	49.306	12.463	5.037	tabular plag
image257.bmp	29.167	6.684	5.556	tabular plag
image257.bmp	11.111	4.571	3.095	tabular plag
image257.bmp	15.972	6.223	3.268	tabular plag
image257.bmp	10.417	5.548	2.391	tabular plag
Label	Area	Major	Minor	Shape
image257.bmp	4.861	3.975	1.557	tabular plag
image257.bmp	41.667	9.943	5.336	tabular plag
image257.bmp	27.778	6.714	5.267	tabular plag
image257.bmp	27.778	6.725	5.259	tabular plag

image257.bmp	25.694	10.541	3.104	tabular plag
image257.bmp	8.333	3.765	2.818	tabular plag
image257.bmp	25	7.652	4.16	tabular plag
image257.bmp	43.056	15.691	3.494	tabular plag
image257.bmp	47.222	17.719	3.393	tabular plag
image257.bmp	30.556	11.28	3.449	tabular plag
image257.bmp	908622.917	1202.664	961.943	area

#### E-9

Label	Area	Major	Minor	Shape
image199.bmp	4775.083	120.83	50.317	junk
image199.bmp	2827.889	79.08	45.531	junk
image199.bmp	368.528	39.882	11.765	junk
image199.bmp	86.528	11.958	9.213	junk
image199.bmp	2484.417	208.936	15.14	junk
image199.bmp	149	18.708	10.141	pyroxene
image199.bmp	149.194	18.028	10.537	pyroxene
image199.bmp	446.222	48.155	11.798	pyroxene
image199.bmp	646.667	44.493	18.505	pyroxene
image199.bmp	74.917	10.554	9.038	pyroxene
image199.bmp	243.889	19.087	16.269	pyroxene
image199.bmp	251.111	26.822	11.92	pyroxene
image199.bmp	97.75	12.267	10.146	pyroxene
image199.bmp	85.056	15.756	6.873	pyroxene
image199.bmp	40.222	7.62	6.721	pyroxene
image199.bmp	30.389	7.045	5.492	pyroxene
image199.bmp	48.528	11.459	5.392	pyroxene
image199.bmp	177.556	33.03	6.844	pyroxene
image199.bmp	51.639	20.285	3.241	pyroxene
image199.bmp	12.806	6.837	2.385	Fe-Ti Oxides
image199.bmp	19.444	6.893	3.592	Fe-Ti Oxides
image199.bmp	10.111	5.729	2.247	Fe-Ti Oxides
image199.bmp	12.111	5.029	3.066	Fe-Ti Oxides
image199.bmp	12.917	6.531	2.518	Fe-Ti Oxides
image199.bmp	16.694	6.401	3.321	Fe-Ti Oxides
image199.bmp	17.806	9.206	2.463	Fe-Ti Oxides
image199.bmp	16.056	8.604	2.376	Fe-Ti Oxides
image199.bmp	4.25	4.7	1.151	Fe-Ti Oxides
image199.bmp	2.722	2.541	1.364	Fe-Ti Oxides
image199.bmp	2.028	1.807	1.429	Fe-Ti Oxides
image199.bmp	2.306	2.31	1.271	Fe-Ti Oxides
image199.bmp	4.444	2.477	2.284	Fe-Ti Oxides
image199.bmp	5.556	2.911	2.43	Fe-Ti Oxides
image199.bmp	2.861	1.995	1.826	Fe-Ti Oxides
image199.bmp	6.722	3.014	2.839	Fe-Ti Oxides
image199.bmp	2.25	2.559	1.119	Fe-Ti Oxides
image199.bmp	2.111	2.307	1.165	Fe-Ti Oxides
image199.bmp	3.028	2.32	1.661	Fe-Ti Oxides
image199.bmp	3.306	2.667	1.578	Fe-Ti Oxides
image199.bmp	1.694	1.613	1.337	Fe-Ti Oxides
image199.bmp	1.861	1.61	1.472	Fe-Ti Oxides

image199.bmp	2.778	2.583	1.369	Fe-Ti Oxides
image199.bmp	3.194	2.217	1.834	Fe-Ti Oxides
image199.bmp	1.167	1.724	0.862	Fe-Ti Oxides
image199.bmp	1.694	1.849	1.167	Fe-Ti Oxides
image199.bmp	2.667	1.992	1.704	Fe-Ti Oxides
image199.bmp	1.417	1.498	1.204	Fe-Ti Oxides
image199.bmp	1.222	2.197	0.708	Fe-Ti Oxides
image199.bmp	2.333	1.942	1.53	Fe-Ti Oxides
image199.bmp	4.639	3.858	1.531	Fe-Ti Oxides
image199.bmp	3.778	2.635	1.825	Fe-Ti Oxides
image199.bmp	4.194	2.501	2.136	Fe-Ti Oxides
image199.bmp	8.333	3.348	3.169	Fe-Ti Oxides
Label	Area	Major	Minor	Shape
image199.bmp	4.444	2.804	2.018	Fe-Ti Oxides
image199.bmp	1.5	2.207	0.865	Fe-Ti Oxides
image199.bmp	5.944	4.957	1.527	Fe-Ti Oxides
image199.bmp	12.667	7.933	2.033	Fe-Ti Oxides
image199.bmp	12.111	7.634	2.02	Fe-Ti Oxides
image199.bmp	5.333	3.349	2.028	Fe-Ti Oxides
image199.bmp	14.222	6.01	3.013	Fe-Ti Oxides
image199.bmp	1.361	2.028	0.855	Fe-Ti Oxides
image199.bmp	0.944	2.237	0.538	Fe-Ti Oxides
image199.bmp	2.333	1.942	1.53	Fe-Ti Oxides
image199.bmp	3.194	2.217	1.834	Fe-Ti Oxides
image199.bmp	3.556	2.721	1.664	Fe-Ti Oxides
image199.bmp	3.806	2.201	2.201	Fe-Ti Oxides
image199.bmp	3.778	2.346	2.05	Fe-Ti Oxides
image199.bmp	3.778	2.635	1.825	Fe-Ti Oxides
image199.bmp	4.111	2.628	1.992	Fe-Ti Oxides
image199.bmp	4.194	2.501	2.136	Fe-Ti Oxides
image199.bmp	2.778	3.377	1.047	Fe-Ti Oxides
image199.bmp	2.333	1.942	1.53	Fe-Ti Oxides
image199.bmp	894.556	34.044	33.457	Plag
image199.bmp	369.083	24.26	19.371	Plag
image199.bmp	1008.472	56.947	22.548	Plag
image199.bmp	141.556	17.9	10.069	Plag
image199.bmp	611.889	37.635	20.701	Plag
image199.bmp	548.694	42.372	16.488	Plag
image199.bmp	444.194	42.311	13.367	Plag
image199.bmp	731.167	37.073	25.111	Plag
image199.bmp	658.472	34.837	24.066	Plag
image199.bmp	418.833	26.297	20.279	Plag
image199.bmp	266.917	23.382	14.535	Plag
image199.bmp	395.25	24.272	20.733	Plag
image199.bmp	150.528	22	8.712	Plag
image199.bmp	559.611	39.606	17.99	Plag
image199.bmp	617.806	35.24	22.322	Plag
image199.bmp	302.528	30.562	12.604	Plag
image199.bmp	717.75	52.033	17.563	Plag
image199.bmp	453.972	30.982	18.657	Plag
image199.bmp	65.306	10.172	8.174	Plag

image199.bmp	58.722	11.968	6.247	Plag
image199.bmp	146.25	16.622	11.202	Plag
image199.bmp	442.333	46.57	12.094	Plag
image199.bmp	595.194	34.741	21.814	Plag
image199.bmp	878.5	42.901	26.073	Plag
image199.bmp	36408.889	240.721	192.577	area

#### Hawaiiite

Label	Area	Major	Minor	Shape
122e.tif	15.55111	10.62287	1.86393	plag
122e.tif	15.57333	12.27794	1.61498	plag
122e.tif	8.33333	6.85295	1.54829	plag
122e.tif	28.49333	19.30057	1.87968	plag
122e.tif	36.36444	19.91957	2.32438	plag
122e.tif	9.24444	10.81948	1.08789	plag
122e.tif	5.28	6.99105	0.96162	plag
122e.tif	22.16889	18.18386	1.55227	plag
122e.tif	6.48	7.10927	1.16054	plag
122e.tif	14.86222	15.8379	1.1948	plag
122e.tif	11.95556	8.23982	1.8474	plag
122e.tif	18.04	12.77918	1.7974	plag
122e.tif	12.96444	13.06099	1.26383	plag
122e.tif	10.41778	9.72892	1.36339	plag
122e.tif	16.20444	5.85555	3.52352	plag
122e.tif	4.84	7.60544	0.81027	plag
122e.tif	3.17778	2.66129	1.52034	plag
122e.tif	2.48444	4.62163	0.68445	plag
122e.tif	11.46222	11.111	1.31349	plag
122e.tif	7.55556	9.43402	1.01972	plag
122e.tif	9.92889	7.09582	1.78159	plag
122e.tif	4.49778	3.32704	1.72128	plag
122e.tif	13.48444	5.96901	2.87635	plag
122e.tif	3.81333	2.50202	1.94055	plag
122e.tif	8	6.73403	1.5126	plag
122e.tif	39.77778	14.04763	3.60535	plag
122e.tif	6.57778	5.4265	1.54337	plag
122e.tif	7.07556	3.79398	2.37452	px
122e.tif	23.77333	16.86147	1.79517	px
122e.tif	26.32889	7.66227	4.37507	px
122e.tif	6.24	4.54604	1.74768	px
122e.tif	8.44	3.60887	2.9777	px
122e.tif	5.13778	4.30055	1.52111	px
122e.tif	7.36	5.60042	1.67327	px
122e.tif	3.36	2.66075	1.60785	px
122e.tif	7.01778	7.5971	1.17615	px
122e.tif	3.84889	3.59748	1.36222	px
122e.tif	2.85778	2.09773	1.73456	px
122e.tif	2.46222	2.50296	1.25252	px
122e.tif	3.12889	2.55733	1.55781	px
122e.tif	2.68	2.00505	1.70184	px
122e.tif	3.06667	2.31089	1.68966	px

122e.tif	9.89333	5.55453	2.2678	px
122e.tif	2.82222	3.37344	1.06519	px
122e.tif	3.40444	3.43991	1.26011	px
122e.tif	1.85333	1.78862	1.31931	px
122e.tif	4.67556	3.56829	1.66833	px
122e.tif	4.40889	4.27876	1.31196	px
122e.tif	2.29333	2.79323	1.04537	px
122e.tif	12.16444	7.79084	1.98801	px
122e.tif	3.25778	2.21347	1.87395	px
122e.tif	2.19556	2.17365	1.28607	px
122e.tif	2.00444	1.77555	1.43738	px
Label	Area	Major	Minor	Shape
122e.tif	3.30222	4.26484	0.98586	px
122e.tif	1.60444	1.76576	1.15692	px
122e.tif	1.64444	1.74523	1.19971	px
122e.tif	9.02667	4.00501	2.86968	px
122e.tif	2.19556	2.39065	1.16933	px
122e.tif	6.16	3.98395	1.96869	px
122e.tif	7.90222	5.50046	1.8292	px
122e.tif	6.4	4.54552	1.79269	px
122e.tif	2.66667	1.99755	1.69973	px
122e.tif	4.79556	3.40688	1.79222	px
122e.tif	35.41333	9.04626	4.98434	px
122e.tif	2.55556	2.12144	1.53378	px
122e.tif	3.39556	2.18155	1.98178	px
122e.tif	9.81778	6.32835	1.9753	px
122e.tif	1.35556	1.43841	1.1999	px
122e.tif	1	1.2185	1.04492	px
122e.tif	0.58667	1.10909	0.67349	px
122e.tif	0.56889	1.08252	0.66912	px
122e.tif	1.01778	1.35834	0.95402	px
122e.tif	3.55111	4.31057	1.04891	px
122e.tif	2.60444	3.22075	1.0296	px
122e.tif	6.99111	5.46717	1.62815	px
122e.tif	6.29778	5.46573	1.46706	px
122e.tif	4.92889	3.73651	1.67955	px
122e.tif	0.92	1.18002	0.99268	px
122e.tif	4.51111	3.79802	1.5123	px
122e.tif	1.42222	1.41683	1.27809	px
122e.tif	1.88	2.40103	0.99694	px
122e.tif	0.46222	1.12549	0.5229	px
122e.tif	0.62222	1.4234	0.55658	px
122e.tif	0.68889	1.53158	0.57269	px
122e.tif	0.32	0.75715	0.53812	px
122e.tif	0.72889	1.0704	0.86701	px
122e.tif	0.86222	1.45686	0.75355	px
122e.tif	0.61333	1.15922	0.67366	px
122e.tif	0.46222	0.8168	0.72052	px
122e.tif	0.95111	1.21423	0.99734	px
122e.tif	1.09778	1.39728	1.00033	px
122e.tif	0.60444	0.93841	0.82012	px



122e.tif	1.12	1.76442	0.80822	px
122e.tif	1.32889	1.68069	1.00673	px
122e.tif	0.97333	1.65968	0.7467	px
122e.tif	1.10222	1.58757	0.88399	px
122e.tif	2.67111	2.99023	1.13736	px
122e.tif	1.52889	1.46632	1.32757	px
122e.tif	0.60444	0.93841	0.82012	px
122e.tif	0.56889	1.08837	0.66552	px
122e.tif	0.83556	1.56923	0.67795	px
122e.tif	1.22222	1.76848	0.87996	px
122e.tif	1.61778	2.55741	0.80543	px
122e.tif	1.13778	2.39201	0.60563	px
122e.tif	1.79556	2.11894	1.07893	px
122e.tif	1.44	1.61154	1.13771	px
122e.tif	1.79556	2.42327	0.94342	px
Label	Area	Major	Minor	Shape
122e.tif	1.34222	1.41934	1.20406	px
122e.tif	0.96	1.15785	1.05567	px
122e.tif	1.38222	1.55047	1.13508	px
122e.tif	1.79556	2.11894	1.07893	px
122e.tif	1.28	1.35068	1.20661	px
122e.tif	0.84444	1.12731	0.95376	px
122e.tif	2.52444	2.39349	1.3429	px
122e.tif	3.34667	2.19764	1.93895	px
122e.tif	1.05778	1.18852	1.13317	px
122e.tif	0.85333	1.33941	0.81118	px
122e.tif	0.8	1.26837	0.80307	px
122e.tif	0.65778	1.0511	0.79679	px
122e.tif	2.36	1.93514	1.55278	px
122e.tif	2.68444	2.11997	1.61226	px
122e.tif	2.36	1.93514	1.55278	px
122e.tif	2.84444	2.26288	1.60047	px
122e.tif	3.2	2.54896	1.59844	px
122e.tif	2.89333	2.62469	1.40356	px
122e.tif	1.93333	2.43736	1.00994	px
122e.tif	1.66667	1.65986	1.27846	px
122e.tif	1.32444	1.47427	1.14384	px
122e.tif	1.66667	1.65986	1.27846	px
122e.tif	1.83111	2.18304	1.06798	px
122e.tif	1.22667	1.45525	1.07325	px
122e.tif	1.84	2.49945	0.93731	px
122e.tif	3.48444	4.11082	1.07923	px
122e.tif	1.40444	2.6345	0.67876	px
122e.tif	1.28	1.35068	1.20661	px
122e.tif	1.72	2.18909	1.0004	px
122e.tif	1.13333	1.25936	1.14582	px
122e.tif	1.33333	1.33928	1.26759	px
122e.tif	1.26222	1.60995	0.99824	px
122e.tif	1.88444	2.54662	0.94217	px
122e.tif	3.58667	2.19925	2.07647	px
122e.tif	1.61778	1.53699	1.34016	px

122e.tif	4.39111	2.79761	1.99847	px
122e.tif	3.74667	2.84616	1.67608	px
122e.tif	2.27556	2.40387	1.20528	px
122e.tif	3.82222	2.59502	1.87536	px
122e.tif	14.13333	6.42911	2.79901	px
122e.tif	4.92	4.38443	1.42877	px
122e.tif	7.56	4.33404	2.22095	px
122e.tif	6.11111	5.17273	1.50422	px
122e.tif	9.89778	4.78592	2.63319	px
122e.tif	4.65333	4.25647	1.39195	px
122e.tif	5.76889	4.32677	1.69761	px
122e.tif	1.64444	1.64242	1.27481	px
122e.tif	6.70222	4.94414	1.72599	px
122e.tif	3.06667	4.40477	0.88645	px
122e.tif	7.71111	3.72849	2.63326	px
122e.tif	11	4.54665	3.08043	px
122e.tif	4.54222	3.60315	1.60508	px
122e.tif	12.11111	5.47474	2.81664	px
122e.tif	12.01778	4.10653	3.72614	px
Label	Area	Major	Minor	Shape
122e.tif	8.87111	5.24192	2.15475	px
122e.tif	3.98222	3.02354	1.67695	px
122e.tif	8.6	5.58029	1.96224	px
122e.tif	9.07556	7.17195	1.61119	px
122e.tif	5.71111	5.60923	1.29637	px
122e.tif	3.12	2.62107	1.51561	oxides
122e.tif	1.88	1.79638	1.33251	oxides
122e.tif	1.66222	1.88828	1.12081	oxides
122e.tif	4.01333	2.59257	1.97099	oxides
122e.tif	2.32889	1.91489	1.54851	oxides
122e.tif	1.67556	1.96119	1.0878	oxides
122e.tif	1.56444	1.52059	1.30996	oxides
122e.tif	3.71556	2.3526	2.01088	oxides
122e.tif	1.09333	1.32137	1.05351	oxides
122e.tif	1.37333	1.62895	1.07344	oxides
122e.tif	1.54667	1.50385	1.30949	oxides
122e.tif	1.02222	1.25715	1.03531	oxides
122e.tif	2739.56889	84.39546	41.33075	area
122e.tif	65.37778	9.74197	8.54463	bad
122e.tif	10.29333	4.70998	2.78258	bad
122e.tif	2.16889	1.76648	1.56329	bad
122e.tif	1.4	1.45501	1.2251	bad
122e.tif	1.40889	1.50228	1.19409	bad
122e.tif	1.94667	2.51644	0.98495	bad
122e.tif	1.2	1.61204	0.9478	bad
image003.bmp	28.17	22.38471	1.60231	plag
image003.bmp	12.78	17.3464	0.93806	plag
image003.bmp	16.32	19.46935	1.06728	plag
image003.bmp	21.33	9.7122	2.7963	plag
image003.bmp	10.88	7.80928	1.77389	plag
image003.bmp	10.18	7.34238	1.76531	plag

image003.bmp	3.5	5.13725	0.86746	plag
image003.bmp	9.89	14.63945	0.86016	plag
image003.bmp	7.26	7.25007	1.27498	plag
image003.bmp	7.42	7.54242	1.25257	plag
image003.bmp	9.48	12.9296	0.93354	plag
image003.bmp	10.55	10.77454	1.24671	plag
image003.bmp	2.73	3.67159	0.94671	plag
image003.bmp	2.58	4.85384	0.67678	plag
image003.bmp	3.25	6.55652	0.63113	plag
image003.bmp	3.14	6.15402	0.64965	plag
image003.bmp	7.47	11.63687	0.81732	plag
image003.bmp	3.53	3.67181	1.22407	plag
image003.bmp	21.06	16.15044	1.66029	plag
image003.bmp	1.43	4.6555	0.39109	plag
image003.bmp	1.41	4.34583	0.4131	plag
image003.bmp	12.7	11.42565	1.41525	plag
image003.bmp	4.92	9.13779	0.68554	plag
image003.bmp	7.44	13.83318	0.6848	plag
image003.bmp	6.38	11.09239	0.73233	plag
image003.bmp	7.88	9.25558	1.08401	plag
image003.bmp	2.34	3.01472	0.98828	plag
image003.bmp	7.11	7.38074	1.22653	plag
image003.bmp	20.8	14.20509	1.86436	plag
Label	Area	Major	Minor	Shape
image003.bmp	13.41	13.09125	1.30424	plag
image003.bmp	7.37	7.54421	1.24384	plag
image003.bmp	9.83	8.97056	1.39523	plag
image003.bmp	7.6	12.01167	0.8056	plag
image003.bmp	3.15	5.67687	0.7065	plag
image003.bmp	2.67	4.9802	0.68261	plag
image003.bmp	2.22	5.6625	0.49918	plag
image003.bmp	2.56	4.52658	0.72008	plag
image003.bmp	10.74	10.37485	1.31805	plag
image003.bmp	3.99	9.27287	0.54786	plag
image003.bmp	2.99	8.58629	0.44338	plag
image003.bmp	1.94	3.10076	0.79661	plag
image003.bmp	4.9	5.70347	1.09387	plag
image003.bmp	3.47	7.04743	0.62691	plag
image003.bmp	7.76	7.58408	1.30277	plag
image003.bmp	0.86	2.20755	0.49602	plag
image003.bmp	0.96	2.64538	0.46205	plag
image003.bmp	8.75	6.43967	1.73003	px
image003.bmp	4.66	3.72614	1.59234	px
image003.bmp	2.24	2.13009	1.33893	px
image003.bmp	2.91	2.37311	1.5613	px
image003.bmp	5.05	6.1331	1.04839	px
image003.bmp	4.36	4.5647	1.21614	px
image003.bmp	1.05	1.33996	0.99772	px
image003.bmp	2.84	2.75287	1.31354	px
image003.bmp	0.82	1.13405	0.92064	px
image003.bmp	1.93	1.76488	1.39236	px

image003.bmp	1.16	1.5265	0.96755	px
image003.bmp	2.35	2.14499	1.39493	px
image003.bmp	1.25	1.69391	0.93957	px
image003.bmp	2.62	2.39628	1.39211	px
image003.bmp	3.27	4.22061	0.98647	px
image003.bmp	3.74	3.77389	1.26181	px
image003.bmp	2.08	3.35669	0.78897	px
image003.bmp	0.5	1.16239	0.54768	px
image003.bmp	1.11	2.03388	0.69488	px
image003.bmp	0.44	0.97258	0.57602	px
image003.bmp	0.68	1.01527	0.85278	px
image003.bmp	0.47	0.84545	0.70781	px
image003.bmp	0.66	0.99921	0.841	px
image003.bmp	0.99	1.42128	0.88688	px
image003.bmp	0.68	1.52476	0.56783	px
image003.bmp	0.42	0.91293	0.58576	px
image003.bmp	0.36	0.95839	0.47827	px
image003.bmp	0.2	0.57817	0.44044	px
image003.bmp	5.34	3.49365	1.94613	px
image003.bmp	7.95	5.55683	1.82159	px
image003.bmp	0.58	0.94641	0.78029	px
image003.bmp	0.46	0.78961	0.74174	px
image003.bmp	3.41	2.43164	1.78552	px
image003.bmp	3.9	2.61583	1.8983	px
image003.bmp	2.38	3.03968	0.99692	px
image003.bmp	2.24	3.06094	0.93176	px
image003.bmp	1.34	3.68857	0.46255	px
Label	Area	Major	Minor	Shape
image003.bmp	1.22	1.62186	0.95776	px
image003.bmp	1.11	1.59276	0.88732	px
image003.bmp	0.41	0.93808	0.55648	px
image003.bmp	0.89	3.56849	0.31755	px
image003.bmp	1.14	2.36465	0.61383	px
image003.bmp	1.2	2.45382	0.62266	px
image003.bmp	1.05	1.59189	0.83982	px
image003.bmp	0.4	0.95951	0.53078	px
image003.bmp	1.05	2.00276	0.66753	px
image003.bmp	2.85	2.86218	1.26782	px
image003.bmp	1.42	1.81755	0.99475	px
image003.bmp	2.84	3.32361	1.08797	px
image003.bmp	1.45	3.11265	0.59313	px
image003.bmp	1.32	1.99962	0.8405	px
image003.bmp	0.61	1.12685	0.68924	px
image003.bmp	1.25	1.46976	1.08286	px
image003.bmp	0.93	1.58153	0.74871	px
image003.bmp	0.72	1.42169	0.64482	px
image003.bmp	1.09	3.006	0.46169	px
image003.bmp	2.61	2.31372	1.43629	px
image003.bmp	4.07	3.13368	1.65367	px
image003.bmp	3.64	2.30101	2.01416	px
image003.bmp	2.26	2.74569	1.04801	px

image003.bmp	1.6	1.98736	1.02507	px
image003.bmp	0.92	1.36082	0.86079	px
image003.bmp	1.8	1.77298	1.29265	px
image003.bmp	0.67	1.43514	0.59442	px
image003.bmp	2.78	2.23706	1.58226	px
image003.bmp	3.2	3.7418	1.08888	px
image003.bmp	1.04	1.47167	0.89977	px
image003.bmp	2.08	1.9754	1.34066	px
image003.bmp	2.04	2.32326	1.118	px
image003.bmp	1.61	1.57848	1.29867	px
image003.bmp	3.34	5.23405	0.81249	px
image003.bmp	1.7	4.31687	0.50141	px
image003.bmp	6.1	3.32988	2.33244	px
image003.bmp	2.5	2.7294	1.16623	px
image003.bmp	1.71	1.91298	1.13814	px
image003.bmp	1.88	2.80898	0.85216	px
image003.bmp	2.96	3.70887	1.01615	px
image003.bmp	1.67	1.91367	1.11112	px
image003.bmp	0.72	1.22689	0.7472	px
image003.bmp	1.94	2.13344	1.1578	px
image003.bmp	1.26	1.57691	1.01736	px
image003.bmp	0.7	1.12284	0.79376	px
image003.bmp	2.59	3.03094	1.08801	px
image003.bmp	1.73	1.96868	1.11888	px
image003.bmp	1.35	2.48466	0.69179	px
image003.bmp	1.31	1.97741	0.8435	px
image003.bmp	0.5	1.22338	0.52038	px
image003.bmp	1.51	2.35886	0.81505	px
image003.bmp	2.89	2.36333	1.55698	px
image003.bmp	2.35	2.17039	1.37861	px
image003.bmp	1.98	2.6073	0.96691	px
Label	Area	Major	Minor	Shape
image003.bmp	1.53	1.9953	0.97632	px
image003.bmp	1.92	2.77136	0.8821	px
image003.bmp	1.65	1.67938	1.25096	px
image003.bmp	5.06	6.31702	1.01988	px
image003.bmp	3.56	2.94538	1.53893	px
image003.bmp	2.51	2.93074	1.09045	px
image003.bmp	2.55	2.87648	1.12873	px
image003.bmp	2.19	1.9355	1.44066	px
image003.bmp	2.2	2.27896	1.22912	px
image003.bmp	4.11	2.9043	1.80182	px
image003.bmp	0.95	1.33647	0.90506	px
image003.bmp	1	1.42668	0.89245	px
image003.bmp	0.71	1.41035	0.64097	px
image003.bmp	0.9	1.52672	0.75058	px
image003.bmp	0.94	2.16046	0.55398	px
image003.bmp	0.76	2.25909	0.42834	px
image003.bmp	1.24	1.85148	0.85273	px
image003.bmp	0.63	1.57361	0.50974	px
image003.bmp	0.56	0.97449	0.73168	px

image003.bmp	0.38	0.7941	0.60928	px
image003.bmp	0.32	1.04012	0.39172	px
image003.bmp	0.57	1.08296	0.67015	px
image003.bmp	1.11	1.43815	0.98272	px
image003.bmp	2.03	2.52012	1.02562	px
image003.bmp	1.99	3.67818	0.68886	px
image003.bmp	1.44	3.22961	0.5677	px
image003.bmp	0.4	0.82016	0.62097	px
image003.bmp	0.53	1.05877	0.63736	px
image003.bmp	1.43	1.72594	1.05492	px
image003.bmp	0.45	0.928	0.61741	px
image003.bmp	1.89	2.64152	0.911	px
image003.bmp	1.06	2.05888	0.65552	px
image003.bmp	1.97	2.32201	1.08022	px
image003.bmp	2.59	3.29053	1.00218	px
image003.bmp	2.54	2.64637	1.22206	px
image003.bmp	2.26	2.85761	1.00697	px
image003.bmp	0.72	1.13572	0.80718	oxide
image003.bmp	1.15	1.33044	1.10055	oxide
image003.bmp	0.2	0.78163	0.32579	oxide
image003.bmp	0.37	0.92682	0.5083	oxide
image003.bmp	0.12	0.67703	0.22568	oxide
image003.bmp	0.31	0.73601	0.53627	oxide
image003.bmp	0.14	0.78987	0.22568	oxide
image003.bmp	0.26	0.62594	0.52888	oxide
image003.bmp	0.34	0.73736	0.58709	oxide
image003.bmp	0.28	0.88618	0.4023	oxide
image003.bmp	0.32	0.63831	0.63831	oxide
image003.bmp	0.26	0.62594	0.52888	oxide
image003.bmp	0.37	0.68637	0.68637	oxide
image003.bmp	0.32	0.99254	0.4105	oxide
image003.bmp	0.42	0.8648	0.61836	oxide
image003.bmp	0.64	1.02996	0.79117	oxide
image003.bmp	0.6	0.92133	0.82918	oxide
image003.bmp	0.42	0.8648	0.61836	oxide
Label	Area	Major	Minor	Shape
image003.bmp	0.79	1.09322	0.92009	oxide
image003.bmp	0.34	0.73736	0.58709	oxide
image003.bmp	0.37	0.68637	0.68637	oxide
image003.bmp	0.51	0.89867	0.72257	oxide
image003.bmp	0.37	0.92682	0.5083	oxide
image003.bmp	0.52	0.81369	0.81369	oxide
image003.bmp	0.48	0.97304	0.62809	oxide
image003.bmp	0.74	1.49895	0.62857	oxide
image003.bmp	0.51	0.89867	0.72257	oxide
image003.bmp	0.2	0.78163	0.32579	oxide
image003.bmp	0.56	1.17545	0.60659	oxide
image003.bmp	0.61	1.10956	0.69999	oxide
image003.bmp	0.26	0.62594	0.52888	oxide
image003.bmp	1.22	1.51976	1.0221	oxide
image003.bmp	0.36	0.75802	0.60469	oxide

image003.bmp	0.42	0.8648	0.61836	oxide
image003.bmp	0.31	0.73601	0.53627	oxide
image003.bmp	0.6	0.92133	0.82918	oxide
image003.bmp	0.64	1.02996	0.79117	oxide
image003.bmp	0.31	0.73601	0.53627	oxide
image003.bmp	0.21	0.51709	0.51709	oxide
image003.bmp	0.6	0.92133	0.82918	oxide
image003.bmp	0.58	1.00713	0.73325	oxide
image003.bmp	0.72	1.13572	0.80718	oxide
image003.bmp	0.61	1.10956	0.69999	oxide
image003.bmp	0.36	0.75802	0.60469	oxide
image003.bmp	0.42	1.03418	0.51709	oxide
image003.bmp	0.69	0.9373	0.9373	oxide
image003.bmp	0.72	1.13572	0.80718	oxide
image003.bmp	0.8	1.00925	1.00925	oxide
image003.bmp	0.8	1.24278	0.81961	oxide
image003.bmp	0.42	1.03418	0.51709	oxide
image003.bmp	0.58	1.00713	0.73325	oxide
image003.bmp	0.36	0.75802	0.60469	oxide
image003.bmp	0.48	0.97304	0.62809	oxide
image003.bmp	0.36	0.75802	0.60469	oxide
image003.bmp	0.64	1.02996	0.79117	oxide
image003.bmp	0.51	0.89867	0.72257	oxide
image003.bmp	0.32	0.821	0.49627	oxide
image003.bmp	0.36	0.75802	0.60469	oxide
image003.bmp	0.36	0.75802	0.60469	oxide
image003.bmp	0.28	1.1229	0.31749	oxide
image003.bmp	0.61	1.10956	0.69999	oxide
image003.bmp	0.84	1.16507	0.91799	oxide
image003.bmp	0.92	1.44255	0.81202	oxide
image003.bmp	0.34	0.73736	0.58709	oxide
image003.bmp	0.54	1.32439	0.51914	oxide
image003.bmp	0.32	0.63831	0.63831	oxide
image003.bmp	0.6	0.92133	0.82918	oxide
image003.bmp	1.36	1.58113	1.09517	oxide
image003.bmp	0.6	0.92133	0.82918	oxide
image003.bmp	0.47	1.14263	0.52373	oxide
image003.bmp	0.98	1.38066	0.90375	oxide
image003.bmp	1.02	1.30688	0.99375	oxide
Label	Area	Major	Minor	Shape
image003.bmp	0.34	0.73736	0.58709	oxide
image003.bmp	1.46	1.41555	1.31322	oxide
image003.bmp	1.12	1.41279	1.00937	oxide
image003.bmp	0.42	0.8648	0.61836	oxide
image003.bmp	0.6	0.92133	0.82918	oxide
image003.bmp	0.51	0.89867	0.72257	oxide
image003.bmp	0.31	1.23221	0.32032	oxide
image003.bmp	0.26	1.00434	0.32961	oxide
image003.bmp	0.34	0.73736	0.58709	oxide
image003.bmp	0.58	1.00713	0.73325	oxide
image003.bmp	0.36	0.75802	0.60469	oxide

image003.bmp	0.79	1.09322	0.92009	oxide
image003.bmp	0.74	1.49895	0.62857	oxide
image003.bmp	0.88	1.35081	0.82947	oxide
image003.bmp	0.48	0.97304	0.62809	oxide
image003.bmp	0.58	1.00713	0.73325	oxide
image003.bmp	1.26	1.43691	1.11648	oxide
image003.bmp	0.37	1.45251	0.32433	oxide
image003.bmp	1.22	1.51976	1.0221	oxide
image003.bmp	0.86	1.08882	1.00566	oxide
image003.bmp	0.48	1.13862	0.53675	oxide
image003.bmp	0.34	0.73736	0.58709	oxide
image003.bmp	0.72	1.13572	0.80718	oxide
image003.bmp	0.64	1.02996	0.79117	oxide
image003.bmp	0.36	0.75802	0.60469	oxide
image003.bmp	0.84	1.16507	0.91799	oxide
image003.bmp	0.56	1.17545	0.60659	oxide
image003.bmp	1.02	1.30688	0.99375	oxide
image003.bmp	0.44	0.79152	0.70779	oxide
image003.bmp	0.24	0.71416	0.42788	oxide
image003.bmp	0.96	1.19547	1.02245	oxide
image003.bmp	0.56	1.17545	0.60659	oxide
image003.bmp	0.68	1.2159	0.71207	oxide
image003.bmp	0.31	0.73601	0.53627	oxide
image003.bmp	0.32	0.821	0.49627	oxide
image003.bmp	1.02	1.30688	0.99375	oxide
image003.bmp	0.44	0.79152	0.70779	oxide
image003.bmp	0.8	1.00925	1.00925	oxide
image003.bmp	0.64	1.02996	0.79117	oxide
image003.bmp	0.48	1.13862	0.53675	oxide
image003.bmp	0.56	1.17545	0.60659	oxide
image003.bmp	0.69	0.9373	0.9373	oxide
image003.bmp	0.24	0.71416	0.42788	oxide
image003.bmp	0.6	0.92133	0.82918	oxide
image003.bmp	0.31	0.73601	0.53627	oxide
image003.bmp	0.32	0.63831	0.63831	oxide
image003.bmp	1.12	1.19416	1.19416	oxide
image003.bmp	0.34	0.73736	0.58709	oxide
image003.bmp	1.07	1.4872	0.91606	oxide
image003.bmp	0.28	0.82473	0.43227	oxide
image003.bmp	0.68	1.39029	0.62275	oxide
image003.bmp	0.32	0.821	0.49627	oxide
image003.bmp	0.6	0.92133	0.82918	oxide
image003.bmp	0.52	0.81369	0.81369	oxide
Label	Area	Major	Minor	Shape
image003.bmp	0.51	0.89867	0.72257	oxide
image003.bmp	0.88	1.80938	0.61925	oxide
image003.bmp	0.96	1.19547	1.02245	oxide
image003.bmp	1.08	1.65771	0.82952	oxide
image003.bmp	0.44	0.79152	0.70779	oxide
image003.bmp	0.48	0.97304	0.62809	oxide
image003.bmp	0.48	0.97304	0.62809	oxide



image003.bmp	0.42	1.03418	0.51709	oxide
image003.bmp	0.51	0.89867	0.72257	oxide
image003.bmp	0.36	0.75802	0.60469	oxide
image003.bmp	0.6	0.92133	0.82918	oxide
image003.bmp	0.4	1.20894	0.42127	oxide
image003.bmp	0.2	0.60447	0.42127	oxide
image003.bmp	0.26	0.62594	0.52888	oxide
image003.bmp	0.6	0.92133	0.82918	oxide
image003.bmp	0.84	1.33637	0.80032	oxide
image003.bmp	0.32	0.99254	0.4105	oxide
image003.bmp	2113.56	59.31437	45.36958	area
image003.bmp	70.57	10.1376	8.8633	bad
image003.bmp	8.47	3.66979	2.93868	bad
image003.bmp	1.96	1.85331	1.34654	bad
image003.bmp	25.85	11.52944	2.85471	plag
image003.bmp	29.54	13.6969	2.74599	plag
image003.bmp	6.56	8.32174	1.00369	plag
image003.bmp	16.01	12.03721	1.69346	plag
image003.bmp	27.86	18.20566	1.94843	plag
image003.bmp	30.04	14.6645	2.60821	plag
image003.bmp	9.67	7.8241	1.57363	plag
image003.bmp	6.9	7.72567	1.13716	plag
image003.bmp	12.94	10.77779	1.52867	plag
image003.bmp	16.39	19.11578	1.09168	plag
image003.bmp	14.98	13.51726	1.41102	plag
image003.bmp	3.1	7.01286	0.56283	plag
image003.bmp	2.94	6.319	0.59239	plag
image003.bmp	6.19	5.75257	1.37006	plag
image003.bmp	6.05	5.31419	1.44953	plag
image003.bmp	3.73	4.83245	0.98277	plag
image003.bmp	21.81	7.68344	3.61418	plag
image003.bmp	4.85	10.65504	0.57956	plag
image003.bmp	2.46	6.47206	0.48395	plag
image003.bmp	3.06	6.71194	0.58048	plag
image003.bmp	1.44	3.26452	0.56163	plag
image003.bmp	7.92	10.21568	0.98712	plag
image003.bmp	14.29	10.63331	1.71109	plag
image003.bmp	2.37	6.28169	0.48038	plag
image003.bmp	4.54	11.42944	0.50576	plag
image003.bmp	9.43	14.17046	0.8473	plag
image003.bmp	5.81	5.52122	1.33984	plag
image003.bmp	8.59	11.87363	0.92113	plag
image003.bmp	3.57	5.81635	0.7815	plag
image003.bmp	3.33	11.5851	0.36598	plag
image003.bmp	8.51	9.12569	1.18734	plag
image003.bmp	7.52	8.6859	1.10233	plag
image003.bmp	9.08	9.54254	1.21152	plag
Label	Area	Major	Minor	Shape
image003.bmp	5.31	6.86916	0.98424	plag
image003.bmp	2.67	6.38432	0.53248	plag
image003.bmp	5.86	9.95608	0.74941	plag

image003.bmp	6.8	5.96539	1.45138	plag
image003.bmp	1.36	1.54593	1.1201	plag
image003.bmp	2.42	6.03243	0.51078	plag
image003.bmp	4.53	3.46285	1.66562	plag
image003.bmp	3.94	5.16539	0.97119	plag
image003.bmp	3.22	4.00059	1.02481	plag
image003.bmp	12.07	4.41118	3.48387	plag
image003.bmp	1.37	1.60745	1.08516	px
image003.bmp	1.47	2.36903	0.79005	px
image003.bmp	0.81	1.30714	0.78899	px
image003.bmp	0.94	1.9886	0.60185	px
image003.bmp	6.05	3.11989	2.46903	px
image003.bmp	0.92	1.37764	0.85028	px
image003.bmp	1.43	1.64531	1.10662	px
image003.bmp	0.33	0.95814	0.43852	px
image003.bmp	0.45	0.89582	0.63959	px
image003.bmp	0.84	1.92735	0.55492	px
image003.bmp	0.53	1.04143	0.64797	px
image003.bmp	1.45	2.03429	0.90754	px
image003.bmp	0.94	1.88739	0.63413	px
image003.bmp	0.77	1.12042	0.87502	px
image003.bmp	0.86	1.71863	0.63713	px
image003.bmp	0.55	1.17498	0.596	px
image003.bmp	0.76	1.20251	0.8047	px
image003.bmp	0.9	1.3032	0.87931	px
image003.bmp	1.66	3.06289	0.69006	px
image003.bmp	1.33	1.56378	1.0829	px
image003.bmp	1.71	1.96175	1.10985	px
image003.bmp	1.54	1.48853	1.31727	px
image003.bmp	0.44	0.81112	0.69068	px
image003.bmp	0.27	0.68027	0.50535	px
image003.bmp	0.29	0.72705	0.50786	px
image003.bmp	0.39	0.7561	0.65674	px
image003.bmp	3.06	2.94593	1.32254	px
image003.bmp	2.1	2.62512	1.01855	px
image003.bmp	7.17	5.78611	1.57777	px
image003.bmp	1.78	1.90898	1.18722	px
image003.bmp	2.71	2.75147	1.25405	px
image003.bmp	2.16	2.38779	1.15177	px
image003.bmp	1.35	1.76308	0.97492	px
image003.bmp	1.27	1.40583	1.15022	px
image003.bmp	1.68	2.11654	1.01063	px
image003.bmp	0.62	0.98353	0.80263	px
image003.bmp	1.48	2.29632	0.82061	px
image003.bmp	1.72	2.47088	0.88631	px
image003.bmp	4.79	2.94427	2.07142	px
image003.bmp	6.38	3.9182	2.07322	px
image003.bmp	2	2.57242	0.98991	px
image003.bmp	2.27	3.26367	0.88558	px
image003.bmp	1.27	2.4062	0.67202	px
image003.bmp	0.95	1.88068	0.64316	px

Label	Area	Major	Minor	Shape
image003.bmp	5.34	3.24612	2.09453	px
image003.bmp	2.17	2.85398	0.9681	px
image003.bmp	2.44	2.58742	1.20069	px
image003.bmp	0.89	1.2449	0.91026	px
image003.bmp	0.69	1.00825	0.87134	px
image003.bmp	0.54	1.71137	0.40175	px
image003.bmp	1.26	3.26029	0.49207	px
image003.bmp	3.42	2.96669	1.46779	px
image003.bmp	1.17	2.06727	0.72061	px
image003.bmp	0.65	1.27395	0.64964	px
image003.bmp	2.32	2.66438	1.10867	px
image003.bmp	0.68	1.30621	0.66284	px
image003.bmp	0.96	2.07911	0.5879	px
image003.bmp	1.96	2.02632	1.23157	px
image003.bmp	2.12	2.81318	0.95951	px
image003.bmp	1.02	2.15647	0.60224	px
image003.bmp	1.4	1.85297	0.96199	px
image003.bmp	0.83	2.21827	0.4764	px
image003.bmp	5.6	4.35969	1.63547	px
image003.bmp	1.22	1.41584	1.09712	px
image003.bmp	1.82	2.51925	0.91984	px
image003.bmp	1.81	2.47829	0.9299	px
image003.bmp	4.01	3.13493	1.62865	px
image003.bmp	0.48	1.29227	0.47293	px
image003.bmp	0.99	1.89241	0.66608	px
image003.bmp	0.77	1.55354	0.63107	px
image003.bmp	1.16	2.68793	0.54948	px
image003.bmp	0.4	0.88344	0.57649	px
image003.bmp	0.26	0.66452	0.49817	px
image003.bmp	0.23	0.84293	0.34741	px
image003.bmp	2.26	2.17884	1.32067	px
image003.bmp	0.94	1.64853	0.72601	px
image003.bmp	0.55	1.09518	0.63942	px
image003.bmp	0.44	0.94492	0.59288	px
image003.bmp	0.48	1.12221	0.5446	px
image003.bmp	0.55	1.27287	0.55016	px
image003.bmp	1.11	1.56285	0.90431	px
image003.bmp	2.05	1.98657	1.31389	px
image003.bmp	0.51	1.1244	0.57751	px
image003.bmp	1.43	2.66934	0.68209	px
image003.bmp	0.59	1.04274	0.72042	px
image003.bmp	1.12	1.62376	0.87823	px
image003.bmp	0.5	0.81116	0.78483	px
image003.bmp	0.67	2.20941	0.38611	px
image003.bmp	0.64	1.60061	0.5091	px
image003.bmp	0.39	0.87539	0.56725	px
image003.bmp	1.39	2.1373	0.82805	px
image003.bmp	1.74	3.17913	0.69687	px
image003.bmp	0.5	1.18053	0.53926	px
image003.bmp	0.91	1.46441	0.79121	px

image003.bmp	1.9	2.51727	0.96102	px
image003.bmp	1.1	1.50143	0.93282	px
image003.bmp	1.03	1.22049	1.07452	px
image003.bmp	1.56	1.78603	1.1121	px
Label	Area	Major	Minor	Shape
image003.bmp	0.91	2.03712	0.56877	px
image003.bmp	0.23	0.86288	0.33938	px
image003.bmp	0.37	0.98946	0.47612	px
image003.bmp	0.62	1.05059	0.7514	px
image003.bmp	0.85	2.00691	0.53926	px
image003.bmp	2.37	2.61576	1.15361	px
image003.bmp	1.26	1.43691	1.11648	oxides
image003.bmp	0.56	1.17545	0.60659	oxides
image003.bmp	0.44	0.79152	0.70779	oxides
image003.bmp	0.42	0.8648	0.61836	oxides
image003.bmp	0.51	0.89867	0.72257	oxides
image003.bmp	0.26	0.62594	0.52888	oxides
image003.bmp	0.69	0.9373	0.9373	oxides
image003.bmp	0.8	1.00925	1.00925	oxides
image003.bmp	0.8	1.24278	0.81961	oxides
image003.bmp	0.26	0.62594	0.52888	oxides
image003.bmp	0.32	0.63831	0.63831	oxides
image003.bmp	0.11	0.45352	0.30882	oxides
image003.bmp	0.32	0.821	0.49627	oxides
image003.bmp	1.36	1.58113	1.09517	oxides
image003.bmp	0.6	0.92133	0.82918	oxides
image003.bmp	0.92	1.44255	0.81202	oxides
image003.bmp	0.79	1.09322	0.92009	oxides
image003.bmp	0.2	0.60447	0.42127	oxides
image003.bmp	0.68	1.39029	0.62275	oxides
image003.bmp	0.89	1.27531	0.88856	oxides
image003.bmp	0.44	0.79152	0.70779	oxides
image003.bmp	0.34	0.73736	0.58709	oxides
image003.bmp	2.74	2.48463	1.4041	oxides
image003.bmp	0.6	0.92133	0.82918	oxides
image003.bmp	0.51	0.89867	0.72257	oxides
image003.bmp	0.28	0.82473	0.43227	oxides
image003.bmp	0.52	0.81369	0.81369	oxides
image003.bmp	0.58	1.00713	0.73325	oxides
image003.bmp	0.6	0.92133	0.82918	oxides
image003.bmp	0.24	0.71416	0.42788	oxides
image003.bmp	0.32	0.63831	0.63831	oxides
image003.bmp	0.42	0.8648	0.61836	oxides
image003.bmp	0.54	1.08226	0.63529	oxides
image003.bmp	0.32	0.99254	0.4105	oxides
image003.bmp	0.32	0.821	0.49627	oxides
image003.bmp	0.6	0.92133	0.82918	oxides
image003.bmp	0.42	0.8648	0.61836	oxides
image003.bmp	0.14	0.56145	0.31749	oxides
image003.bmp	0.32	0.63831	0.63831	oxides
image003.bmp	0.6	0.92133	0.82918	oxides

image003.bmp	1.24	1.30035	1.21415	oxides
image003.bmp	0.79	1.09322	0.92009	oxides
image003.bmp	0.86	1.08882	1.00566	oxides
image003.bmp	0.6	0.92133	0.82918	oxides
image003.bmp	0.51	0.89867	0.72257	oxides
image003.bmp	0.32	0.821	0.49627	oxides
image003.bmp	0.96	1.19547	1.02245	oxides
image003.bmp	0.64	1.02996	0.79117	oxides
Label	Area	Major	Minor	Shape
image003.bmp	0.51	0.89867	0.72257	oxides
image003.bmp	0.51	0.89867	0.72257	oxides
image003.bmp	0.37	0.68637	0.68637	oxides
image003.bmp	0.14	0.78987	0.22568	oxides
image003.bmp	0.47	1.14263	0.52373	oxides
image003.bmp	0.58	1.00713	0.73325	oxides
image003.bmp	0.7	0.98646	0.9035	oxides
image003.bmp	0.14	0.56145	0.31749	oxides
image003.bmp	0.36	0.75802	0.60469	oxides
image003.bmp	0.31	0.73601	0.53627	oxides
image003.bmp	0.8	1.24278	0.81961	oxides
image003.bmp	0.34	0.73736	0.58709	oxides
image003.bmp	0.36	0.75802	0.60469	oxides
image003.bmp	0.61	1.10956	0.69999	oxides
image003.bmp	0.52	0.81369	0.81369	oxides
image003.bmp	0.68	1.2159	0.71207	oxides
image003.bmp	1.46	1.41555	1.31322	oxides
image003.bmp	0.36	0.75802	0.60469	oxides
image003.bmp	0.44	0.79152	0.70779	oxides
image003.bmp	0.24	0.71416	0.42788	oxides
image003.bmp	0.36	0.75802	0.60469	oxides
image003.bmp	0.32	0.821	0.49627	oxides
image003.bmp	0.8	1.00925	1.00925	oxides
image003.bmp	0.31	0.73601	0.53627	oxides
image003.bmp	0.51	0.89867	0.72257	oxides
image003.bmp	0.29	1.11616	0.33081	oxides
image003.bmp	0.37	0.92682	0.5083	oxides
image003.bmp	0.34	0.73736	0.58709	oxides
image003.bmp	0.86	1.08882	1.00566	oxides
image003.bmp	0.34	0.73736	0.58709	oxides
image003.bmp	0.58	1.00713	0.73325	oxides
image003.bmp	0.24	0.71416	0.42788	oxides
image003.bmp	0.36	0.75802	0.60469	oxides
image003.bmp	0.44	0.79152	0.70779	oxides
image003.bmp	0.42	0.8648	0.61836	oxides
image003.bmp	0.26	0.62594	0.52888	oxides
image003.bmp	0.32	0.821	0.49627	oxides
image003.bmp	0.16	0.49627	0.4105	oxides
image003.bmp	0.44	0.79152	0.70779	oxides
image003.bmp	0.54	1.08226	0.63529	oxides
image003.bmp	1295.76	44.29633	37.24491	area
image003.bmp	30.31	12.27572	3.14376	bad

Appendix 2: Small Pumice Data for Chapter 4

Axes measurements in Microns

0 mm	0 mm	5 mm	5 mm	9 mm	9 mm	13 mm	13 mm	17mm	17mm
Major	Minor	Major	Minor	Major	Minor	Major	Minor	Major	Minor
29.72	14.80	24.50	10.62	33.53	7.30	30.98	17.31	50.23	8.41
18.13	9.62	17.07	9.05	31.10	1.84	28.91	15.64	31.97	0.65
22.28	6.30	31.19	4.17	29.84	1.12	22.59	14.57	30.04	1.18
30.61	4.08	25.04	4.97	29.32	1.01	21.70	7.05	29.70	2.22
25.30	4.55	24.38	4.18	28.85	1.85	30.72	4.20	29.70	1.47
12.50	8.07	21.44	3.78	28.46	4.16	20.07	5.26	28.60	9.32
30.07	3.20	19.98	3.97	28.38	1.28	20.74	4.32	28.55	0.88
11.35	6.50	13.95	5.00	27.42	1.92	13.25	6.04	28.47	0.86
12.02	5.86	13.13	5.26	27.34	1.67	16.16	4.92	28.07	0.83
10.31	6.21	16.54	4.04	27.11	1.33	10.82	7.25	27.59	2.27
13.34	4.61	14.14	4.28	26.65	1.16	13.55	5.56	27.28	2.86
9.96	5.93	8.92	6.76	26.65	2.28	10.76	6.83	26.88	1.79
15.48	3.73	19.32	2.99	26.54	1.06	8.90	6.86	26.10	1.25
9.08	6.25	12.64	4.56	26.39	1.30	11.98	5.00	25.86	14.50
16.47	3.41	17.78	2.98	25.90	3.79	19.41	3.05	25.12	2.89
15.93	3.51	18.54	2.82	25.60	0.95	13.09	4.45	24.91	5.57
9.69	5.60	11.99	4.21	24.46	0.84	8.35	6.79	24.88	1.92
8.83	5.26	11.47	4.37	24.05	0.81	12.35	4.53	24.63	11.36
7.67	5.23	16.22	3.01	23.43	1.25	9.89	5.38	24.47	1.04
7.45	4.83	10.47	4.64	22.44	0.61	20.49	2.46	24.35	1.15
22.55	1.59	16.40	2.79	22.29	3.30	21.80	2.24	24.23	0.79
14.03	2.45	23.25	1.95	22.08	2.12	17.69	2.73	23.82	3.59
19.07	1.72	10.78	4.07	21.99	2.50	12.52	3.82	22.54	1.38
7.16	4.47	10.08	4.26	21.92	1.28	17.06	2.79	22.52	1.21
8.44	3.78	15.78	2.64	21.83	1.10	8.24	5.53	22.15	1.94
7.17	3.81	9.17	4.22	21.11	1.04	12.05	3.76	21.80	1.28
9.68	2.82	8.58	4.36	20.98	1.34	16.75	2.69	21.63	1.68
7.01	3.88	14.04	2.66	20.81	1.16	18.39	2.43	21.42	0.86
6.53	4.15	11.50	3.16	20.79	4.29	14.40	3.09	21.34	1.77
10.79	2.46	7.18	4.90	20.76	1.19	13.87	3.12	21.30	1.29
5.51	4.71	15.57	2.25	20.66	2.25	7.21	5.91	21.09	2.52
11.14	2.33	14.88	2.27	20.61	0.79	9.57	4.44	20.44	1.77
11.57	2.18	14.13	2.38	20.61	1.36	6.75	6.22	20.30	0.62
16.45	1.48	12.35	2.68	20.36	0.85	6.52	6.14	20.06	1.14
6.00	3.77	21.54	1.50	20.14	2.04	15.08	2.64	20.04	1.19
6.37	3.53	8.62	3.64	19.90	1.72	26.64	1.44	19.91	14.15
6.58	3.41	28.60	1.10	19.81	1.24	18.04	2.10	19.88	0.62
11.62	1.92	7.30	4.21	19.58	5.84	17.56	2.15	19.83	1.33
15.02	1.49	16.16	1.87	19.57	1.84	9.43	3.96	19.69	1.35
9.82	2.18	7.43	4.01	19.37	1.46	16.86	2.17	19.45	2.53
10.41	2.05	9.83	3.02	19.30	1.08	25.61	1.42	19.27	1.13
6.39	3.28	5.46	5.34	19.26	3.81	12.54	2.83	19.24	7.00
7.07	2.96	7.22	4.02	19.12	1.04	9.15	3.84	19.23	1.97
5.27	3.96	6.07	4.77	19.12	1.22	16.27	2.15	19.19	1.15
18.04	1.15	18.26	1.58	19.10	0.95	14.02	2.49	19.17	1.72
8.40	2.38	8.69	3.28	18.78	0.55	9.50	3.65	19.01	1.84
17.82	1.12	13.73	2.06	18.78	1.49	6.11	5.48	18.61	0.77

12.99	1.53	11.00	2.56	18.77	1.47	12.54	2.59	18.58	2.37
10.86	1.76	6.34	4.40	18.75	1.01	9.72	3.30	18.39	1.03
5.09	3.74	9.78	2.83	18.71	1.99	12.84	2.44	18.23	0.79
4.75	3.97	26.10	1.06	18.71	1.07	10.29	2.99	18.23	1.70
0 mm	0 mm	5 mm	5 mm	9 mm	9 mm	13 mm	13 mm	17mm	17mm
Major	Minor	Major	Minor	Major	Minor	Major	Minor	Major	Minor
5.94	3.07	18.82	1.44	18.50	1.46	8.22	3.61	18.13	3.68
6.65	2.73	5.67	4.72	18.43	0.71	25.62	1.14	18.01	5.99
5.99	3.02	19.23	1.37	18.43	0.64	11.50	2.51	17.99	0.77
15.01	1.21	6.89	3.80	18.23	2.05	21.81	1.33	17.98	1.44
5.06	3.57	13.80	1.88	18.14	3.43	7.51	3.81	17.87	7.11
7.97	2.26	8.11	3.12	18.10	0.66	25.40	1.12	17.83	0.65
19.97	0.89	7.23	3.44	17.96	0.73	20.90	1.35	17.83	1.90
6.01	2.96	8.53	2.91	17.88	0.52	12.11	2.32	17.82	1.37
6.17	2.81	11.84	2.05	17.81	0.97	7.64	3.63	17.73	0.93
5.73	3.02	21.74	1.11	17.61	1.07	18.80	1.47	17.67	1.57
17.08	0.97	6.97	3.39	17.50	1.07	29.24	0.92	17.64	1.06
15.20	1.08	6.19	3.82	17.40	1.33	16.46	1.64	17.62	1.17
11.09	1.48	11.23	2.09	17.39	1.29	9.64	2.74	17.59	1.56
13.26	1.22	14.40	1.63	17.36	1.13	14.33	1.84	17.55	1.07
5.30	2.96	5.50	4.23	17.31	2.17	5.93	4.36	17.54	2.06
14.65	1.05	6.10	3.77	17.15	1.05	19.62	1.31	17.53	0.94
9.64	1.59	17.95	1.26	16.98	0.79	14.92	1.72	17.52	13.54
5.76	2.62	8.29	2.72	16.90	0.57	5.49	4.60	17.38	2.15
9.98	1.50	4.75	4.62	16.79	0.98	20.32	1.21	17.24	1.38
8.96	1.67	7.03	3.06	16.68	1.71	5.97	4.11	17.20	1.87
6.98	2.13	11.21	1.91	16.56	1.65	6.90	3.50	17.14	1.04
11.74	1.26	8.54	2.47	16.55	2.33	15.88	1.48	17.09	2.35
19.22	0.77	9.74	2.14	16.50	2.44	7.66	3.05	17.06	0.79
10.51	1.40	5.41	3.71	16.50	1.64	7.32	3.18	16.96	1.70
19.01	0.77	7.64	2.48	16.46	1.12	25.40	0.90	16.96	0.62
24.53	0.59	7.64	2.48	16.27	1.16	7.72	2.94	16.92	2.63
5.95	2.39	18.78	1.00	16.27	1.23	6.50	3.49	16.81	1.14
8.22	1.69	6.09	3.06	16.25	8.65	7.61	2.90	16.79	1.82
4.39	3.12	4.73	3.87	16.25	1.50	5.20	4.22	16.73	1.03
3.77	3.59	8.00	2.28	16.24	1.24	14.91	1.47	16.73	0.80
8.94	1.50	11.15	1.62	16.02	5.26	6.65	3.19	16.66	1.18
4.46	3.00	17.05	1.04	16.02	0.90	5.82	3.63	16.54	1.34
15.18	0.88	16.01	1.10	15.97	1.05	15.33	1.37	16.52	1.47
5.92	2.26	21.06	0.84	15.95	1.32	16.09	1.30	16.50	5.82
5.73	2.30	4.85	3.60	15.91	2.01	11.45	1.83	16.46	1.40
8.10	1.63	11.58	1.50	15.89	7.22	12.50	1.67	16.43	1.54
12.70	1.01	4.67	3.72	15.89	0.80	9.28	2.24	16.36	1.05
9.88	1.29	4.69	3.69	15.84	2.84	8.34	2.47	16.30	1.52
5.34	2.31	5.30	3.25	15.71	6.19	16.41	1.25	16.28	0.73
7.46	1.64	9.73	1.76	15.70	1.55	18.77	1.07	16.26	0.88
10.59	1.15	6.40	2.67	15.69	1.12	5.86	3.42	16.25	0.56
5.18	2.31	17.10	0.99	15.67	0.88	8.63	2.32	16.16	0.52
11.15	1.07	5.95	2.85	15.66	9.74	5.65	3.53	16.12	1.13
4.29	2.76	11.31	1.49	15.58	2.31	7.01	2.83	16.11	1.54
4.83	2.45	14.49	1.16	15.56	1.11	7.57	2.62	16.07	4.96

4.13	2.84	13.33	1.25	15.49	0.92	17.95	1.10	15.98	0.81
5.91	1.95	14.84	1.12	15.11	1.09	11.13	1.78	15.97	0.93
4.08	2.79	5.74	2.89	15.09	0.75	5.10	3.84	15.91	2.54
3.54	3.17	11.82	1.40	15.09	1.34	5.82	3.34	15.84	2.56
5.26	2.12	6.66	2.48	15.05	1.57	8.02	2.36	15.82	1.52
4.71	2.36	4.59	3.59	15.04	1.48	15.37	1.22	15.81	1.19
16.54	0.67	9.31	1.76	15.04	3.26	19.96	0.94	15.74	2.90
4.07	2.69	10.21	1.60	15.04	2.75	14.14	1.32	15.73	0.65
0 mm	0 mm	5 mm	5 mm	9 mm	9 mm	13 mm	13 mm	17mm	17mm
Major	Minor	Major	Minor	Major	Minor	Major	Minor	Major	Minor
4.44	2.45	13.33	1.21	14.89	1.18	6.62	2.81	15.60	1.06
11.19	0.97	11.42	1.40	14.89	1.12	12.78	1.45	15.48	1.50
4.24	2.54	12.15	1.30	14.87	1.16	9.58	1.92	15.32	1.59
11.73	0.91	7.81	2.02	14.77	1.16	4.93	3.71	15.29	0.79
4.37	2.44	4.85	3.24	14.69	3.07	23.88	0.77	15.29	0.94
15.78	0.67	11.70	1.34	14.69	10.98	5.11	3.57	15.25	0.68
6.41	1.65	12.47	1.24	14.68	1.09	10.77	1.69	15.17	1.68
5.77	1.81	16.14	0.94	14.66	0.42	4.53	3.98	15.15	1.06
4.07	2.54	3.94	3.84	14.63	1.09	19.02	0.93	15.03	0.41
5.81	1.76	14.04	1.08	14.63	6.18	11.75	1.45	14.98	0.70
9.66	1.05	15.52	0.97	14.59	0.95	7.37	2.31	14.93	6.23
4.13	2.45	4.24	3.52	14.58	1.98	12.60	1.34	14.93	0.86
12.93	0.76	9.49	1.57	14.54	0.64	9.79	1.73	14.86	1.20
9.22	1.07	9.66	1.53	14.45	2.51	4.96	3.41	14.84	3.36
7.59	1.29	13.71	1.08	14.43	3.03	12.13	1.39	14.80	1.00
4.79	2.03	5.16	2.88	14.37	1.05	5.50	3.03	14.74	1.84
4.08	2.37	17.25	0.86	14.32	1.64	14.74	1.12	14.71	0.82
7.68	1.24	5.63	2.61	14.26	2.46	6.20	2.66	14.68	2.61
7.18	1.33	9.15	1.60	14.26	0.93	9.92	1.66	14.65	1.17
5.41	1.76	13.04	1.11	14.25	1.26	5.69	2.87	14.61	5.66
12.87	0.74	16.66	0.85	14.20	0.95	14.93	1.09	14.60	0.94
16.48	0.57	12.28	1.14	14.13	1.56	10.74	1.51	14.54	1.63
5.24	1.79	9.76	1.43	14.12	1.06	4.71	3.36	14.53	3.55
3.57	2.60	5.56	2.51	14.09	1.85	21.62	0.73	14.46	1.59
5.05	1.81	15.32	0.90	14.08	1.56	15.95	0.98	14.43	0.62
15.55	0.58	19.54	0.70	14.05	2.03	9.85	1.58	14.37	0.72
8.10	1.11	7.99	1.72	14.01	1.37	5.96	2.60	14.10	1.17
7.57	1.18	13.77	0.99	14.01	4.34	9.53	1.62	14.05	0.96
5.86	1.53	7.29	1.87	13.96	1.42	18.99	0.81	14.03	0.89
4.39	2.02	4.68	2.90	13.95	3.45	4.57	3.35	14.02	4.23
6.21	1.42	16.13	0.84	13.91	0.82	8.76	1.74	14.00	1.19
6.51	1.35	8.40	1.58	13.85	6.59	12.33	1.24	13.99	1.17
15.94	0.55	15.67	0.84	13.82	3.59	7.60	2.00	13.99	1.50
3.77	2.33	5.89	2.23	13.81	0.90	11.30	1.34	13.96	5.55
9.03	0.97	18.96	0.69	13.80	1.17	7.91	1.92	13.89	1.36
11.58	0.75	9.93	1.31	13.80	1.39	11.96	1.26	13.83	1.51
5.10	1.70	12.62	1.02	13.74	0.73	15.52	0.96	13.80	1.43
4.07	2.11	13.71	0.94	13.72	0.88	11.80	1.25	13.80	1.31
3.39	2.54	15.93	0.80	13.64	1.48	16.92	0.87	13.78	1.25
4.27	2.00	7.59	1.68	13.61	3.03	8.94	1.65	13.69	0.93
4.07	2.08	12.20	1.04	13.57	0.58	15.22	0.96	13.68	2.35



4.68	1.79	6.49	1.95	13.56	6.22	11.42	1.27	13.61	0.93
5.34	1.56	11.54	1.09	13.47	1.18	7.56	1.91	13.59	5.24
3.56	2.33	5.47	2.30	13.46	1.06	14.27	1.01	13.57	0.79
4.84	1.70	13.39	0.93	13.46	1.35	8.68	1.66	13.55	2.34
8.71	0.94	8.52	1.43	13.45	2.21	10.69	1.31	13.51	1.03
5.73	1.43	5.51	2.20	13.35	1.14	5.91	2.35	13.46	0.87
10.68	0.76	16.66	0.72	13.25	1.54	4.07	3.40	13.43	0.57
13.07	0.62	5.27	2.25	13.22	0.98	10.54	1.31	13.42	1.94
3.53	2.26	3.81	3.10	13.19	0.83	5.37	2.57	13.30	1.44
5.08	1.54	6.01	1.96	13.18	0.64	11.19	1.21	13.28	0.59
4.01	1.96	7.62	1.52	13.16	0.73	12.14	1.11	13.25	1.45
9.46	0.82	20.89	0.55	13.15	2.85	3.93	3.43	13.18	1.10
0 mm	0 mm	5 mm	5 mm	9 mm	9 mm	13 mm	13 mm	17mm	17mm
Major	Minor	Major	Minor	Major	Minor	Major	Minor	Major	Minor
6.76	1.15	7.10	1.62	13.14	1.30	7.18	1.88	13.18	0.94
13.50	0.57	8.10	1.41	13.12	1.08	4.97	2.69	13.16	0.93
4.98	1.54	9.82	1.15	13.11	1.15	8.24	1.62	13.15	0.66
8.81	0.87	8.35	1.35	13.09	0.91	5.28	2.49	13.11	2.11
4.54	1.68	10.13	1.11	13.04	2.57	9.39	1.39	13.08	0.91
6.78	1.12	4.68	2.39	12.99	0.82	16.28	0.80	13.07	1.26
4.99	1.52	10.12	1.08	12.98	1.86	10.26	1.27	13.06	3.42
11.29	0.67	11.39	0.96	12.92	1.37	10.20	1.27	13.03	0.98
4.09	1.85	3.58	3.04	12.92	1.94	5.39	2.39	12.97	0.68
5.84	1.30	16.46	0.66	12.91	1.27	9.58	1.33	12.91	0.89
4.23	1.77	9.92	1.09	12.88	1.07	13.19	0.97	12.91	2.13
3.20	2.34	7.06	1.52	12.87	1.49	3.70	3.42	12.82	6.90
4.99	1.50	7.52	1.42	12.87	1.48	14.69	0.86	12.70	0.87
3.02	2.47	13.88	0.77	12.82	1.34	5.16	2.43	12.65	0.43
7.62	0.97	16.39	0.64	12.82	0.94	3.65	3.39	12.63	0.86
4.87	1.52	12.03	0.87	12.80	1.28	8.86	1.39	12.61	0.71
4.02	1.84	5.33	1.96	12.80	1.21	5.62	2.19	12.59	0.90
10.97	0.67	6.90	1.50	12.79	1.79	12.71	0.97	12.58	1.10
4.56	1.61	10.62	0.97	12.68	2.80	16.68	0.73	12.47	0.85
6.64	1.11	5.58	1.84	12.65	0.87	14.13	0.86	12.44	1.08
6.02	1.21	14.00	0.73	12.56	1.84	4.36	2.73	12.44	1.45
4.14	1.74	14.19	0.72	12.54	0.93	14.76	0.80	12.43	4.23
7.23	1.00	9.99	1.02	12.47	1.10	3.83	3.08	12.42	0.77
6.79	1.06	4.53	2.23	12.46	1.61	7.54	1.56	12.39	1.83
14.94	0.48	9.89	1.02	12.45	4.58	12.71	0.93	12.33	1.02
4.75	1.50	6.85	1.47	12.41	1.44	15.58	0.75	12.31	1.04
10.96	0.65	4.26	2.36	12.38	1.18	16.07	0.73	12.29	0.97
3.71	1.91	3.94	2.56	12.38	1.89	6.91	1.69	12.28	1.03
4.27	1.66	11.69	0.85	12.31	3.49	8.16	1.43	12.25	1.09
5.94	1.19	14.83	0.67	12.16	1.52	15.61	0.75	12.22	1.64
8.71	0.81	6.62	1.50	12.11	1.05	5.04	2.30	12.21	2.34
2.90	2.44	3.93	2.53	12.09	3.34	11.57	1.00	12.19	1.00
4.80	1.47	7.75	1.27	12.05	0.70	5.75	2.01	12.19	1.07
3.52	1.98	14.45	0.68	12.01	1.06	8.55	1.34	12.15	2.65
3.52	1.98	4.19	2.35	11.99	0.73	3.61	3.16	12.10	1.05
6.45	1.08	8.44	1.16	11.95	1.48	9.36	1.22	12.10	0.89
8.70	0.80	9.84	1.00	11.94	1.21	17.64	0.64	12.10	0.83

3.89	1.78	8.55	1.15	11.93	4.32	3.71	3.05	12.07	0.96
9.10	0.75	3.88	2.51	11.92	2.67	15.85	0.71	12.06	2.05
4.50	1.52	18.64	0.52	11.90	0.98	10.26	1.08	12.04	1.71
9.85	0.69	9.86	0.97	11.88	1.13	10.25	1.07	12.03	1.44
8.32	0.82	7.64	1.25	11.86	2.70	12.11	0.91	12.03	1.34
13.68	0.49	6.21	1.52	11.82	1.90	10.76	1.02	12.00	0.85
9.06	0.74	5.58	1.69	11.81	1.17	5.30	2.06	11.97	0.64
5.79	1.15	6.77	1.39	11.80	1.38	14.09	0.77	11.96	2.06
6.90	0.97	8.75	1.06	11.76	0.94	4.96	2.17	11.95	1.26
13.93	0.48	3.11	2.99	11.67	1.36	8.80	1.23	11.91	0.82
3.14	2.12	6.63	1.40	11.65	0.67	6.07	1.77	11.91	1.30
4.12	1.61	4.06	2.27	11.65	0.85	9.13	1.17	11.90	0.69
11.37	0.58	3.50	2.62	11.63	3.44	10.15	1.06	11.86	1.11
6.78	0.97	8.82	1.04	11.63	1.04	12.23	0.87	11.85	0.38
6.48	1.00	9.45	0.97	11.61	0.39	9.17	1.16	11.84	3.66
8.44	0.77	5.61	1.63	11.59	0.91	5.07	2.09	11.80	1.40
0 mm	0 mm	5 mm	5 mm	9 mm	9 mm	13 mm	13 mm	17mm	17mm
Major	Minor	Major	Minor	Major	Minor	Major	Minor	Major	Minor
8.28	0.79	5.26	1.74	11.59	2.22	12.52	0.84	11.79	1.11
3.05	2.12	7.81	1.17	11.54	1.33	11.06	0.95	11.77	0.90
3.21	2.02	18.26	0.50	11.49	2.59	10.13	1.00	11.75	1.14
9.66	0.67	5.99	1.51	11.48	3.81	10.89	0.93	11.70	0.56
6.04	1.06	9.05	0.99	11.46	1.57	3.86	2.63	11.68	1.01
3.04	2.12	13.94	0.63	11.42	1.16	11.14	0.91	11.63	0.98
7.40	0.87	14.03	0.62	11.38	1.71	10.35	0.98	11.61	6.57
12.98	0.49	10.38	0.83	11.37	3.96	11.06	0.91	11.60	0.94
7.18	0.89	9.08	0.95	11.35	0.77	14.03	0.72	11.56	0.96
2.90	2.19	5.23	1.65	11.35	1.01	11.00	0.91	11.52	1.35
4.61	1.37	3.99	2.16	11.32	1.51	7.15	1.40	11.50	1.55
6.37	0.99	9.95	0.86	11.31	0.89	3.41	2.91	11.44	1.06
4.07	1.54	3.60	2.39	11.28	0.77	10.13	0.97	11.31	2.63
8.03	0.78	7.51	1.14	11.28	1.05	5.24	1.87	11.26	0.76
6.53	0.96	10.37	0.83	11.27	1.63	4.60	2.12	11.18	2.04
6.02	1.03	5.59	1.52	11.26	0.80	4.22	2.30	11.15	4.76
6.66	0.93	6.69	1.27	11.26	0.77	4.96	1.95	11.14	1.03
3.55	1.74	11.45	0.74	11.18	2.02	7.39	1.30	11.06	0.43
11.02	0.56	6.47	1.29	11.18	1.17	5.61	1.72	11.06	1.61
4.31	1.43	6.52	1.29	11.17	0.93	9.74	0.98	10.93	1.76
7.31	0.84	3.61	2.31	11.14	1.49	8.42	1.13	10.93	0.78
7.74	0.79	8.38	0.99	11.12	0.94	9.85	0.96	10.91	0.56
3.34	1.82	8.90	0.93	11.07	0.78	16.97	0.55	10.85	0.96
9.50	0.64	6.49	1.27	11.06	0.82	10.78	0.86	10.84	0.71
4.66	1.30	4.72	1.74	11.06	1.38	5.67	1.63	10.81	0.66
4.66	1.30	9.50	0.86	11.05	0.38	10.21	0.90	10.80	1.10
3.77	1.60	3.70	2.22	10.99	1.12	18.59	0.49	10.79	0.89
4.72	1.27	11.33	0.72	10.95	1.15	9.70	0.94	10.78	1.05
5.26	1.14	11.13	0.73	10.93	1.73	7.76	1.15	10.75	1.27
5.44	1.10	4.10	1.99	10.90	1.08	6.71	1.33	10.74	0.91
4.49	1.32	8.76	0.92	10.82	1.35	9.95	0.89	10.69	1.18
10.36	0.57	3.84	2.10	10.79	0.96	9.45	0.94	10.69	1.30
6.01	0.99	3.07	2.62	10.77	2.47	4.34	2.04	10.69	0.75

5.73	1.02	7.47	1.07	10.74	1.39	9.41	0.93	10.57	2.14
5.59	1.04	8.43	0.94	10.68	0.83	16.08	0.55	10.52	1.41
4.76	1.22	4.59	1.73	10.66	3.00	12.68	0.68	10.50	1.03
7.24	0.80	7.15	1.10	10.65	0.97	9.58	0.90	10.45	1.97
10.11	0.57	10.66	0.73	10.55	1.62	9.58	0.90	10.43	1.97
12.57	0.46	4.30	1.82	10.54	0.69	8.06	1.07	10.35	0.75
2.72	2.11	6.42	1.21	10.53	0.85	10.25	0.84	10.34	0.39
4.66	1.23	5.36	1.45	10.53	0.78	5.99	1.43	10.31	1.23
3.32	1.73	11.17	0.69	10.52	0.67	3.62	2.36	10.31	0.78
10.11	0.56	5.10	1.51	10.48	0.88	11.68	0.73	10.29	7.44
4.98	1.14	7.03	1.10	10.47	0.87	3.24	2.63	10.28	0.91
5.95	0.96	4.31	1.77	10.47	1.11	6.51	1.31	10.23	4.19
6.12	0.93	3.54	2.15	10.46	0.85	8.04	1.06	10.21	1.23
6.21	0.91	9.87	0.76	10.45	1.17	6.54	1.29	10.20	1.80
11.31	0.50	5.47	1.37	10.45	1.09	8.26	1.02	10.20	1.72
9.41	0.59	8.87	0.85	10.45	3.97	9.02	0.92	10.13	1.10
11.83	0.47	8.61	0.87	10.42	3.32	18.36	0.45	10.08	0.99
8.57	0.65	7.26	1.03	10.40	0.91	8.39	0.98	10.07	0.80
4.60	1.21	13.32	0.55	10.33	0.87	3.79	2.18	10.04	2.22
2.73	2.04	3.16	2.33	10.32	1.54	3.29	2.48	10.03	0.51
0 mm	0 mm	5 mm	5 mm	9 mm	9 mm	13 mm	13 mm	17mm	17mm
Major	Minor	Major	Minor	Major	Minor	Major	Minor	Major	Minor
2.79	1.98	7.73	0.95	10.30	3.15	8.39	0.97	9.99	2.58
4.39	1.26	8.55	0.85	10.29	0.96	6.82	1.19	9.92	2.32
6.11	0.90	14.12	0.51	10.28	0.90	3.78	2.14	9.84	4.62
6.95	0.78	8.91	0.81	10.27	0.84	3.35	2.39	9.82	0.82
3.48	1.57	12.70	0.57	10.27	0.94	12.05	0.66	9.80	1.26
10.68	0.50	6.67	1.08	10.25	2.79	8.44	0.93	9.76	1.32
11.47	0.46	5.27	1.36	10.24	1.88	15.19	0.52	9.76	2.95
7.69	0.69	5.47	1.31	10.20	1.94	4.08	1.92	9.75	1.53
2.65	2.00	3.04	2.36	10.20	0.94	11.54	0.67	9.75	0.94
7.26	0.73	11.82	0.60	10.19	0.93	4.63	1.66	9.70	3.34
5.21	1.01	3.73	1.91	10.18	1.21	11.18	0.68	9.67	0.72
2.83	1.85	4.68	1.50	10.18	1.56	13.52	0.56	9.65	0.68
3.52	1.49	5.32	1.32	10.12	0.77	4.95	1.54	9.65	0.51
6.87	0.76	11.89	0.59	10.06	0.94	3.15	2.39	9.64	0.54
7.77	0.67	3.46	2.02	10.04	0.65	5.50	1.36	9.63	5.88
6.68	0.78	3.32	2.11	10.04	0.73	3.22	2.31	9.59	4.61
4.81	1.08	3.94	1.77	10.01	3.43	12.82	0.58	9.57	5.50
13.48	0.39	3.24	2.14	10.01	0.34	7.97	0.93	9.56	0.75
3.31	1.57	2.89	2.40	10.00	1.07	7.64	0.96	9.55	1.49
3.96	1.29	8.33	0.83	9.99	1.17	3.01	2.42	9.52	0.90
4.59	1.11	7.11	0.97	9.98	1.13	3.32	2.19	9.52	0.67
6.60	0.77	4.88	1.41	9.94	4.06	11.43	0.64	9.50	0.56
3.39	1.50	4.17	1.64	9.86	0.83	9.27	0.78	9.49	1.52
4.39	1.15	5.03	1.35	9.82	1.51	6.96	1.04	9.47	0.68
6.74	0.75	4.48	1.51	9.80	0.57	4.62	1.57	9.44	0.94
8.70	0.58	6.70	1.00	9.80	0.68	5.97	1.21	9.32	1.32
10.74	0.46	7.06	0.95	9.79	0.87	5.89	1.22	9.31	0.97
5.55	0.89	9.80	0.68	9.78	1.17	8.42	0.84	9.26	1.75
3.63	1.36	5.95	1.11	9.77	0.68	6.18	1.14	9.24	1.65

3.56	1.38	3.64	1.81	9.67	1.17	7.44	0.94	9.20	1.13
3.35	1.46	3.39	1.94	9.67	0.58	3.85	1.80	9.17	0.98
3.79	1.28	8.51	0.77	9.67	0.56	9.99	0.69	9.16	3.55
3.79	1.28	9.45	0.69	9.64	1.14	9.60	0.72	9.09	0.70
10.07	0.48	7.86	0.83	9.62	1.77	5.46	1.26	9.05	4.50
7.04	0.69	5.87	1.11	9.61	2.19	7.75	0.89	9.02	5.48
3.31	1.45	8.64	0.75	9.61	0.84	3.02	2.27	9.01	4.74
8.33	0.58	6.64	0.98	9.60	7.91	4.53	1.52	9.01	0.75
6.36	0.76	6.88	0.94	9.60	1.09	8.99	0.76	8.98	0.82
3.56	1.35	8.11	0.80	9.60	0.87	6.96	0.99	8.96	1.01
3.69	1.29	8.59	0.74	9.60	0.73	5.46	1.25	8.96	0.67
12.04	0.39	7.65	0.83	9.56	1.11	7.40	0.92	8.95	0.93
6.55	0.72	5.53	1.15	9.48	0.53	5.52	1.23	8.95	0.74
4.06	1.16	11.61	0.54	9.48	2.79	7.46	0.91	8.93	1.24
3.11	1.50	3.99	1.57	9.48	4.30	8.62	0.79	8.93	1.68
4.88	0.96	6.04	1.04	9.44	0.55	11.24	0.60	8.91	1.06
6.32	0.73	8.10	0.77	9.42	2.98	5.37	1.25	8.90	0.67
4.79	0.96	13.61	0.46	9.20	0.50	9.71	0.69	8.90	0.29
9.35	0.49	9.13	0.68	9.20	0.90	4.58	1.47	8.89	2.28
4.88	0.94	6.23	0.99	9.18	2.51	10.35	0.64	8.87	0.69
5.29	0.87	8.08	0.75	9.16	2.70	5.77	1.15	8.85	0.56
2.77	1.66	10.02	0.60	9.16	1.22	7.09	0.93	8.84	3.29
2.63	1.74	9.57	0.63	9.13	1.95	9.01	0.73	8.84	0.86
5.01	0.91	8.16	0.73	9.10	0.49	10.49	0.62	8.80	0.61
0 mm	0 mm	5 mm	5 mm	9 mm	9 mm	13 mm	13 mm	17mm	17mm
Major	Minor	Major	Minor	Major	Minor	Major	Minor	Major	Minor
7.19	0.63	7.39	0.81	9.10	0.74	10.70	0.61	8.76	1.00
2.61	1.73	10.02	0.59	9.07	1.22	4.80	1.36	8.75	0.63
2.73	1.64	3.53	1.68	9.05	5.75	2.82	2.31	8.73	0.72
3.63	1.24	7.72	0.77	9.01	1.26	6.13	1.06	8.72	1.03
8.08	0.55	6.90	0.85	9.00	0.60	11.19	0.58	8.71	1.02
6.76	0.65	10.59	0.55	9.00	2.16	3.15	2.04	8.70	1.25
5.53	0.79	9.30	0.63	8.97	0.68	3.57	1.80	8.70	1.14
3.03	1.45	3.52	1.65	8.96	4.20	2.60	2.47	8.68	4.52
3.58	1.21	2.87	2.01	8.96	1.14	7.52	0.85	8.63	0.70
2.54	1.71	6.17	0.94	8.95	1.22	5.72	1.10	8.63	0.49
2.49	1.72	8.78	0.66	8.93	1.23	6.00	1.05	8.61	1.30
6.48	0.66	12.55	0.46	8.92	0.90	6.17	1.02	8.61	0.69
2.60	1.63	3.31	1.73	8.86	1.31	8.13	0.78	8.60	0.84
4.57	0.93	5.56	1.03	8.85	0.90	8.31	0.75	8.59	1.24
5.62	0.76	3.03	1.88	8.84	1.16	7.21	0.87	8.59	0.85
7.58	0.56	8.78	0.65	8.83	1.35	8.90	0.70	8.58	1.37
6.47	0.66	4.51	1.26	8.82	0.95	5.48	1.14	8.57	0.89
3.30	1.28	5.22	1.08	8.80	0.97	8.71	0.71	8.55	1.08
6.05	0.70	3.06	1.85	8.79	0.69	5.07	1.21	8.52	1.36
2.42	1.72	4.28	1.32	8.79	1.40	9.31	0.66	8.45	0.43
3.34	1.25	4.58	1.23	8.79	3.40	9.50	0.64	8.45	3.79
2.62	1.56	5.89	0.95	8.79	1.14	3.37	1.81	8.43	0.49
6.02	0.68	6.21	0.90	8.78	0.73	6.75	0.90	8.43	6.75
6.45	0.63	6.69	0.83	8.72	0.77	8.49	0.72	8.40	4.74
6.49	0.63	7.58	0.74	8.70	1.22	7.79	0.78	8.38	1.10

5.92	0.68	3.26	1.70	8.68	2.16	4.40	1.37	8.38	2.39
4.29	0.94	8.88	0.62	8.66	1.85	5.87	1.03	8.38	2.84
7.99	0.50	8.07	0.68	8.65	0.72	4.57	1.31	8.37	1.98
4.05	0.99	3.60	1.52	8.65	1.35	9.47	0.63	8.36	6.74
3.32	1.20	5.02	1.09	8.63	0.80	11.47	0.52	8.35	0.65
5.24	0.76	9.75	0.56	8.63	1.11	9.30	0.64	8.28	1.93
6.50	0.61	4.90	1.12	8.63	1.64	7.75	0.76	8.28	0.93
5.78	0.69	9.63	0.57	8.62	1.18	6.10	0.97	8.26	1.07
2.88	1.36	5.82	0.94	8.62	0.70	7.93	0.74	8.21	4.43
6.33	0.62	5.00	1.09	8.61	0.74	7.52	0.78	8.21	0.74
5.89	0.67	4.45	1.22	8.60	2.59	6.39	0.91	8.18	1.67
7.54	0.52	4.49	1.20	8.58	0.96	3.48	1.66	8.15	1.13
6.95	0.56	4.61	1.17	8.55	1.13	6.07	0.95	8.09	1.49
4.06	0.96	7.88	0.68	8.55	4.85	6.62	0.86	8.08	0.86
6.15	0.63	3.31	1.61	8.54	0.80	5.64	1.01	8.02	3.09
4.55	0.85	4.25	1.24	8.53	0.60	6.10	0.94	8.02	1.11
7.07	0.55	11.65	0.45	8.49	1.25	6.13	0.93	8.02	1.19
8.45	0.46	10.07	0.52	8.44	0.91	6.20	0.92	8.00	1.45
6.16	0.63	5.41	0.97	8.44	0.73	4.79	1.19	7.99	0.70
12.42	0.31	7.89	0.66	8.44	1.31	6.34	0.89	7.95	0.96
2.55	1.50	2.66	1.96	8.44	3.20	5.69	0.99	7.95	1.94
5.20	0.73	4.34	1.20	8.44	1.58	5.96	0.94	7.95	1.64
2.15	1.76	4.04	1.28	8.40	2.40	14.22	0.39	7.91	4.27
5.61	0.67	4.22	1.23	8.40	0.74	6.80	0.82	7.90	1.01
6.74	0.56	7.46	0.67	8.39	1.59	5.23	1.05	7.89	1.09
2.11	1.78	8.49	0.59	8.35	0.47	13.52	0.41	7.85	6.65
9.64	0.39	8.28	0.61	8.32	0.86	6.14	0.89	7.85	0.72
5.87	0.64	5.53	0.91	8.30	0.83	6.65	0.82	7.84	1.17
0 mm	0 mm	5 mm	5 mm	9 mm	9 mm	13 mm	13 mm	17mm	17mm
Major	Minor	Major	Minor	Major	Minor	Major	Minor	Major	Minor
2.43	1.55	2.67	1.87	8.28	1.05	6.66	0.82	7.83	3.46
3.17	1.18	3.58	1.40	8.27	0.54	2.86	1.89	7.78	1.24
5.70	0.66	2.52	1.99	8.24	1.24	8.67	0.62	7.77	1.01
2.26	1.64	2.41	2.06	8.24	0.61	4.08	1.29	7.74	0.79
2.55	1.46	2.87	1.72	8.21	1.87	4.18	1.26	7.73	1.58
5.73	0.65	2.68	1.84	8.20	0.78	9.07	0.58	7.72	1.37
7.10	0.52	5.89	0.83	8.20	0.50	6.11	0.84	7.71	1.63
5.43	0.68	7.11	0.69	8.15	1.18	5.78	0.89	7.70	1.70
4.20	0.88	4.84	1.00	8.13	1.26	2.89	1.79	7.70	0.91
4.85	0.76	4.91	0.98	8.12	0.42	6.54	0.79	7.65	0.67
6.10	0.60	8.75	0.55	8.12	0.81	7.83	0.65	7.64	1.39
4.48	0.81	6.57	0.72	8.10	0.86	11.50	0.44	7.63	1.00
7.65	0.48	5.59	0.85	8.07	0.55	3.16	1.60	7.62	3.52
7.42	0.49	6.85	0.69	8.07	0.92	3.89	1.30	7.59	0.76
7.09	0.51	3.87	1.22	8.07	0.78	6.98	0.72	7.59	1.79
3.82	0.95	10.25	0.46	8.06	0.89	4.50	1.09	7.56	0.70
4.61	0.78	3.59	1.30	8.05	1.05	4.73	1.03	7.56	1.33
6.32	0.57	8.89	0.52	8.05	0.59	4.45	1.09	7.52	2.98
5.60	0.64	6.28	0.73	8.05	0.73	5.93	0.82	7.49	1.11
5.41	0.67	6.37	0.72	8.04	2.19	3.64	1.32	7.49	0.79
4.06	0.89	6.63	0.70	8.04	0.50	8.89	0.54	7.48	1.30

6.62	0.55	8.25	0.56	8.02	0.72	6.68	0.72	7.46	2.93
4.60	0.78	3.86	1.19	8.02	0.58	6.79	0.71	7.45	0.95
5.04	0.71	5.20	0.87	8.01	1.36	8.96	0.53	7.45	1.15
4.28	0.83	4.26	1.06	8.01	1.06	6.88	0.70	7.43	0.95
5.57	0.63	7.79	0.58	8.00	0.89	7.90	0.61	7.42	0.65
7.01	0.50	6.21	0.72	8.00	1.31	10.81	0.44	7.39	2.87
7.00	0.51	4.44	1.01	7.99	1.09	4.86	0.97	7.39	1.37
7.20	0.49	8.87	0.50	7.98	1.88	6.20	0.76	7.38	0.84
5.30	0.66	9.19	0.48	7.98	0.65	6.57	0.72	7.36	3.08
2.65	1.32	6.15	0.71	7.98	0.93	5.49	0.85	7.36	0.66
6.23	0.56	7.10	0.61	7.94	1.10	2.57	1.82	7.35	6.68
3.64	0.94	7.96	0.54	7.93	1.81	5.81	0.80	7.30	0.72
2.14	1.61	4.88	0.89	7.91	5.23	8.23	0.56	7.29	0.57
6.03	0.56	5.40	0.80	7.89	1.16	10.19	0.45	7.28	2.53
4.66	0.73	8.76	0.49	7.89	5.16	5.91	0.78	7.26	1.33
3.06	1.11	6.23	0.69	7.89	0.60	8.17	0.56	7.24	2.01
3.03	1.12	9.45	0.45	7.88	0.46	5.16	0.88	7.23	0.79
5.60	0.60	2.26	1.88	7.87	1.24	8.70	0.52	7.22	1.32
1.88	1.79	4.53	0.93	7.87	1.06	3.71	1.23	7.18	0.98
4.68	0.71	5.86	0.71	7.87	0.89	3.83	1.19	7.16	0.86
3.60	0.92	4.84	0.87	7.86	1.02	10.83	0.42	7.16	0.78
3.09	1.08	5.25	0.80	7.86	0.77	6.00	0.75	7.16	0.59
6.32	0.53	7.56	0.55	7.85	0.82	4.43	1.01	7.15	0.49
2.31	1.44	5.84	0.71	7.78	0.74	6.33	0.70	7.14	1.11
5.34	0.62	7.38	0.56	7.77	0.61	4.67	0.95	7.12	1.87
5.55	0.59	2.30	1.79	7.76	0.80	4.91	0.88	7.12	0.67
6.29	0.52	2.61	1.57	7.76	1.10	5.82	0.75	7.11	0.86
4.99	0.66	5.92	0.69	7.76	1.63	7.95	0.55	7.11	1.04
7.23	0.46	2.74	1.50	7.76	1.08	10.90	0.39	7.10	0.78
4.41	0.75	4.05	1.01	7.76	0.78	10.39	0.41	7.06	1.88
4.81	0.68	6.43	0.63	7.71	1.42	7.84	0.54	7.06	1.69
2.90	1.12	7.83	0.52	7.70	0.58	4.35	0.97	6.99	3.65
0 mm	0 mm	5 mm	5 mm	9 mm	9 mm	13 mm	13 mm	17mm	17mm
Major	Minor	Major	Minor	Major	Minor	Major	Minor	Major	Minor
10.23	0.32	4.90	0.83	7.69	4.40	8.27	0.51	6.98	0.70
5.63	0.58	6.38	0.64	7.67	1.26	6.27	0.66	6.97	0.91
5.62	0.58	9.37	0.43	7.67	1.37	6.25	0.66	6.97	0.73
5.92	0.54	6.96	0.58	7.67	1.26	5.47	0.76	6.95	0.90
2.73	1.16	4.79	0.84	7.66	0.94	4.11	1.00	6.95	1.38
5.60	0.57	3.43	1.17	7.61	0.74	5.48	0.75	6.94	0.71
5.61	0.56	7.87	0.51	7.58	1.77	6.51	0.63	6.94	0.99
2.83	1.11	4.46	0.88	7.57	0.61	3.85	1.06	6.89	1.65
4.99	0.63	5.76	0.68	7.56	4.50	4.35	0.93	6.88	1.03
4.05	0.77	3.58	1.09	7.56	0.55	6.54	0.61	6.87	1.68
4.67	0.67	4.50	0.86	7.55	1.07	5.43	0.74	6.86	0.71
7.05	0.44	6.44	0.60	7.54	0.99	3.29	1.21	6.86	1.27
4.88	0.64	5.15	0.75	7.53	0.60	3.48	1.13	6.83	0.36
7.79	0.40	2.71	1.44	7.51	1.37	6.69	0.58	6.83	0.92
3.82	0.81	5.76	0.67	7.49	1.36	7.19	0.54	6.81	1.26
5.48	0.56	6.39	0.60	7.48	1.95	4.35	0.89	6.79	1.43
5.20	0.59	5.39	0.71	7.45	2.08	4.82	0.79	6.78	4.05

7.96	0.39	5.39	0.71	7.44	0.49	4.92	0.77	6.76	0.38
8.53	0.36	6.08	0.63	7.44	1.07	6.45	0.59	6.76	0.55
5.44	0.55	3.36	1.13	7.43	1.07	3.84	0.98	6.75	1.89
6.85	0.43	2.34	1.61	7.40	0.33	8.29	0.45	6.73	0.47
5.17	0.57	3.92	0.96	7.36	0.58	2.08	1.79	6.72	1.07
6.62	0.45	6.78	0.56	7.34	0.59	5.61	0.67	6.71	0.75
5.29	0.56	2.90	1.29	7.34	0.54	8.36	0.44	6.63	0.54
4.42	0.67	5.03	0.74	7.33	0.61	3.09	1.19	6.60	1.53
4.72	0.62	5.41	0.69	7.32	2.98	3.58	1.03	6.60	0.44
6.30	0.47	6.18	0.60	7.32	1.15	5.79	0.62	6.57	1.83
3.71	0.78	4.77	0.77	7.32	1.38	3.82	0.94	6.54	0.97
3.98	0.73	5.27	0.70	7.31	0.94	4.52	0.79	6.53	1.58
6.30	0.46	5.20	0.71	7.30	0.83	4.48	0.80	6.52	1.16
5.50	0.53	7.23	0.50	7.29	1.98	6.22	0.57	6.51	1.08
8.99	0.32	6.41	0.56	7.28	4.14	6.09	0.58	6.49	0.73
3.17	0.92	7.03	0.51	7.28	0.59	3.18	1.10	6.49	0.77
2.10	1.36	8.49	0.43	7.27	1.17	3.64	0.96	6.45	1.57
3.62	0.79	4.06	0.88	7.26	0.72	6.96	0.50	6.41	1.21
7.29	0.39	4.96	0.72	7.25	2.25	5.78	0.60	6.40	2.39
4.64	0.62	5.10	0.70	7.24	0.55	3.58	0.97	6.40	3.55
5.38	0.53	6.93	0.51	7.24	4.30	5.05	0.68	6.39	0.49
2.88	0.99	4.79	0.74	7.24	1.47	5.96	0.58	6.39	1.64
4.52	0.63	3.91	0.90	7.19	0.80	2.13	1.61	6.39	0.81
1.87	1.53	3.81	0.93	7.18	0.87	2.78	1.22	6.38	1.40
3.80	0.75	6.21	0.57	7.17	1.12	2.63	1.28	6.35	1.58
2.13	1.33	6.85	0.51	7.15	3.48	5.37	0.63	6.35	1.89
2.14	1.30	2.81	1.25	7.14	1.33	4.93	0.67	6.35	3.62
5.24	0.53	4.93	0.71	7.14	0.79	4.60	0.72	6.34	0.47
5.06	0.55	2.65	1.31	7.14	1.20	3.62	0.91	6.34	0.43
4.42	0.62	5.68	0.61	7.11	0.64	5.26	0.62	6.32	1.14
3.81	0.72	3.21	1.06	7.11	3.60	2.09	1.55	6.32	0.66
5.82	0.47	7.24	0.47	7.10	1.17	6.11	0.53	6.29	1.74
7.26	0.38	7.45	0.46	7.10	0.74	2.15	1.51	6.27	3.50
3.73	0.74	3.20	1.07	7.09	3.07	4.07	0.80	6.24	0.95
1.81	1.51	2.03	1.66	7.05	0.81	2.81	1.16	6.23	0.54
5.06	0.54	2.54	1.33	7.05	0.45	3.02	1.06	6.21	0.97
0 mm	0 mm	5 mm	5 mm	9 mm	9 mm	13 mm	13 mm	17mm	17mm
Major	Minor	Major	Minor	Major	Minor	Major	Minor	Major	Minor
4.55	0.60	6.89	0.49	7.05	3.45	3.41	0.94	6.19	1.96
5.22	0.52	3.33	1.01	7.04	0.45	2.14	1.48	6.18	3.71
5.21	0.52	3.35	0.99	7.03	1.08	4.86	0.65	6.17	1.62
3.09	0.87	4.28	0.78	7.01	0.55	2.16	1.44	6.16	0.68
2.04	1.30	5.97	0.56	7.00	2.75	5.59	0.55	6.15	1.07
2.74	0.97	6.16	0.53	6.99	0.89	3.45	0.90	6.12	2.16
4.42	0.60	8.89	0.37	6.99	0.61	4.88	0.64	6.10	0.98
5.06	0.52	3.66	0.90	6.96	0.95	5.52	0.56	6.10	1.51
4.62	0.57	3.87	0.84	6.95	0.83	8.03	0.38	6.09	3.21
4.55	0.58	5.58	0.58	6.95	1.14	5.09	0.60	6.06	0.77
6.23	0.42	5.50	0.59	6.93	0.90	2.86	1.06	6.05	2.68
4.85	0.54	7.65	0.43	6.91	0.58	4.05	0.75	6.05	0.63
3.15	0.83	9.33	0.35	6.90	0.35	5.13	0.59	6.04	0.80

4.52	0.58	5.40	0.60	6.90	1.16	12.57	0.24	6.02	1.14
3.28	0.80	3.49	0.91	6.89	1.60	3.22	0.93	6.01	1.06
3.02	0.86	4.52	0.71	6.88	1.00	4.54	0.66	6.01	3.34
3.42	0.75	2.71	1.16	6.86	0.15	6.57	0.45	6.01	3.43
4.09	0.63	5.06	0.62	6.85	0.69	2.65	1.11	6.00	1.37
5.34	0.48	6.98	0.44	6.84	2.62	5.26	0.55	5.99	0.86
3.69	0.70	2.66	1.17	6.83	2.37	3.50	0.83	5.97	0.59
3.10	0.82	10.36	0.30	6.81	1.30	4.25	0.67	5.95	2.04
5.85	0.43	4.62	0.66	6.81	0.44	4.36	0.66	5.93	5.10
3.76	0.67	5.27	0.58	6.80	1.96	4.26	0.67	5.92	0.53
3.55	0.70	4.13	0.73	6.78	0.78	6.30	0.45	5.91	0.77
4.07	0.61	5.32	0.57	6.77	0.85	6.04	0.46	5.90	1.10
1.92	1.29	4.14	0.72	6.77	1.00	4.80	0.58	5.89	1.17
3.69	0.66	5.86	0.50	6.72	1.15	3.80	0.73	5.86	2.48
7.84	0.31	5.78	0.51	6.72	2.21	5.26	0.52	5.86	1.20
4.10	0.59	3.90	0.76	6.72	1.87	1.91	1.44	5.85	0.71
2.55	0.96	1.98	1.48	6.71	0.73	3.62	0.75	5.83	0.78
4.54	0.54	6.16	0.46	6.70	2.17	2.14	1.27	5.83	0.92
2.30	1.06	9.09	0.31	6.69	1.90	4.08	0.65	5.81	0.87
7.70	0.31	4.69	0.60	6.68	0.63	2.81	0.95	5.80	1.28
5.36	0.45	5.04	0.56	6.67	3.67	4.38	0.61	5.79	1.09
3.00	0.79	4.74	0.59	6.66	0.86	4.78	0.56	5.78	2.51
5.35	0.44	2.67	1.04	6.65	0.98	4.58	0.57	5.77	3.04
3.41	0.70	5.44	0.51	6.64	1.27	4.20	0.62	5.74	0.89
5.18	0.45	3.03	0.89	6.64	0.70	5.46	0.47	5.73	0.86
4.12	0.57	3.02	0.89	6.59	3.79	2.93	0.87	5.72	0.99
4.71	0.50	3.27	0.81	6.58	1.36	2.86	0.89	5.71	0.25
5.19	0.44	4.76	0.55	6.54	4.12	8.41	0.30	5.71	0.97
4.31	0.53	2.93	0.90	6.53	1.53	3.25	0.78	5.71	2.98
6.03	0.38	2.40	1.09	6.53	1.53	5.43	0.47	5.69	2.68
4.58	0.50	5.12	0.51	6.51	0.97	3.95	0.64	5.68	1.34
3.74	0.61	4.01	0.65	6.51	1.08	4.87	0.51	5.67	0.76
1.85	1.22	2.00	1.28	6.50	3.81	4.20	0.59	5.59	0.81
5.38	0.42	5.56	0.46	6.49	1.58	2.50	1.00	5.58	0.82
4.60	0.49	1.96	1.28	6.47	0.99	4.11	0.61	5.58	2.02
4.22	0.54	2.62	0.95	6.46	1.08	3.24	0.76	5.58	0.52
4.45	0.51	2.87	0.86	6.46	0.55	4.01	0.61	5.57	3.55
3.38	0.67	5.97	0.41	6.46	0.94	3.66	0.66	5.53	1.33
6.41	0.35	6.10	0.41	6.45	1.46	5.79	0.41	5.49	2.92
4.67	0.49	6.33	0.39	6.43	1.46	9.71	0.24	5.49	0.63
0 mm	0 mm	5 mm	5 mm	9 mm	9 mm	13 mm	13 mm	17mm	17mm
Major	Minor	Major	Minor	Major	Minor	Major	Minor	Major	Minor
2.25	1.01	4.46	0.55	6.43	2.97	3.23	0.73	5.48	3.22
2.46	0.91	4.86	0.51	6.42	2.62	3.45	0.68	5.46	1.34
4.10	0.54	4.78	0.51	6.41	0.85	4.56	0.52	5.44	1.33
3.91	0.56	2.37	1.03	6.40	0.60	2.07	1.12	5.43	0.89
5.36	0.41	8.70	0.28	6.37	1.39	5.72	0.41	5.42	3.05
4.27	0.51	2.34	1.03	6.36	0.68	7.62	0.30	5.42	4.96
1.70	1.27	4.17	0.57	6.32	0.35	2.68	0.84	5.42	1.28
3.92	0.55	1.97	1.21	6.31	0.39	3.27	0.69	5.39	1.23
4.34	0.50	5.55	0.43	6.30	1.08	3.95	0.56	5.38	0.49



1.88	1.15	4.24	0.55	6.30	0.69	2.96	0.75	5.37	4.19
7.25	0.30	4.45	0.53	6.29	0.65	7.06	0.32	5.34	1.21
4.01	0.54	2.80	0.84	6.29	2.66	4.86	0.45	5.33	2.19
4.35	0.50	3.41	0.68	6.27	1.31	2.78	0.79	5.33	1.13
3.03	0.71	4.25	0.55	6.26	1.72	1.83	1.17	5.31	3.20
3.99	0.54	1.57	1.46	6.24	0.67	5.30	0.40	5.31	3.08
3.15	0.68	7.63	0.30	6.24	1.29	4.60	0.45	5.30	1.07
5.53	0.38	3.14	0.72	6.24	1.46	2.05	1.00	5.29	0.53
2.88	0.74	2.93	0.76	6.24	0.85	2.17	0.94	5.28	0.79
4.08	0.52	5.17	0.43	6.23	0.48	3.97	0.52	5.27	0.85
1.93	1.10	3.45	0.65	6.21	1.87	3.10	0.66	5.24	3.45
5.04	0.41	4.41	0.50	6.21	2.92	7.55	0.27	5.22	0.95
3.99	0.52	4.69	0.47	6.18	1.37	2.54	0.78	5.21	0.94
3.51	0.59	8.13	0.27	6.18	0.92	3.83	0.52	5.19	1.41
4.62	0.45	1.88	1.15	6.18	0.82	4.00	0.47	5.16	1.24
5.92	0.35	2.61	0.83	6.18	0.75	2.89	0.66	5.16	3.67
3.03	0.68	7.98	0.27	6.15	0.95	3.11	0.61	5.16	1.05
3.35	0.61	1.92	1.12	6.14	0.58	4.13	0.45	5.14	0.74
4.84	0.42	3.50	0.61	6.13	1.44	2.35	0.77	5.13	1.19
6.06	0.34	4.43	0.48	6.12	2.34	2.85	0.62	5.12	3.23
3.41	0.60	1.78	1.19	6.12	1.84	6.54	0.27	5.12	0.82
3.41	0.60	6.06	0.34	6.11	0.63	1.88	0.93	5.07	0.80
3.01	0.68	1.70	1.22	6.11	5.72	5.48	0.31	5.06	1.16
4.86	0.41	3.33	0.62	6.11	3.50	3.57	0.48	5.06	0.78
3.49	0.58	4.71	0.44	6.09	4.75	3.70	0.44	5.05	3.97
4.93	0.41	4.05	0.51	6.09	1.21	2.44	0.65	4.99	0.94
4.12	0.48	2.69	0.76	6.09	2.02	1.91	0.82	4.98	0.55
4.52	0.44	4.10	0.49	6.09	1.05	2.26	0.69	4.97	0.80
3.11	0.64	2.19	0.92	6.08	1.44	1.70	0.90	4.97	0.93
4.70	0.42	2.07	0.96	6.07	0.51	5.18	0.30	4.97	0.70
3.34	0.59	4.82	0.41	6.07	0.61	3.04	0.50	4.94	3.20
3.35	0.59	2.06	0.95	6.06	1.24	3.08	0.49	4.93	1.23
2.93	0.66	4.95	0.39	6.05	1.99	1.49	0.99	4.92	0.85
4.84	0.40	2.14	0.90	6.01	4.50	3.72	0.39	4.92	0.78
2.05	0.93	2.86	0.65	6.01	1.66	2.48	0.57	4.91	0.98
3.83	0.50	2.56	0.73	6.00	1.10	2.60	0.55	4.91	3.11
4.90	0.39	2.37	0.79	5.98	0.52	3.75	0.37	4.90	1.12
4.89	0.39	2.37	0.79	5.97	1.63	2.13	0.65	4.90	1.77
2.24	0.84	3.72	0.49	5.96	3.85	2.32	0.57	4.90	3.96
4.82	0.39	3.22	0.57	5.96	0.56	1.68	0.79	4.89	2.68
4.56	0.41	6.01	0.30	5.94	0.79	1.35	0.98	4.86	0.98
3.75	0.50	2.85	0.63	5.92	1.13	2.53	0.51	4.85	1.24
3.27	0.57	3.61	0.50	5.91	0.67	4.12	0.31	4.85	0.79
3.81	0.49	3.06	0.59	5.87	0.93	2.55	0.51	4.83	1.19
0 mm	0 mm	5 mm	5 mm	9 mm	9 mm	13 mm	13 mm	17mm	17mm
Major	Minor	Major	Minor	Major	Minor	Major	Minor	Major	Minor
4.90	0.38	2.52	0.72	5.86	0.43	1.50	0.84	4.83	3.42
3.14	0.59	4.63	0.38	5.86	0.95	2.07	0.61	4.81	1.04
2.61	0.71	3.05	0.58	5.85	0.69	4.79	0.25	4.77	3.68
3.34	0.55	2.63	0.68	5.82	1.01	3.09	0.37	4.76	2.82
4.33	0.42	2.86	0.62	5.80	0.87	2.08	0.55	4.76	1.25

3.94	0.46	3.09	0.57	5.79	0.81	2.45	0.44	4.76	1.58
6.45	0.28	3.82	0.46	5.77	0.55	3.84	0.28	4.74	0.48
3.36	0.54	3.37	0.52	5.77	0.75	2.75	0.38	4.74	1.34
3.97	0.45	1.76	0.99	5.76	1.26	1.49	0.67	4.71	0.83
5.11	0.35	4.26	0.41	5.76	0.94	2.19	0.45	4.68	0.80
2.91	0.61	5.72	0.30	5.75	0.98	3.65	0.27	4.68	3.76
3.23	0.55	2.44	0.70	5.72	3.08	2.54	0.38	4.67	1.10
2.33	0.76	2.11	0.80	5.72	1.93	1.61	0.58	4.67	3.17
3.68	0.48	2.85	0.59	5.71	3.67	1.67	0.56	4.65	0.56
3.34	0.53	3.00	0.56	5.71	0.74	1.53	0.59	4.64	3.45
2.52	0.70	3.57	0.46	5.71	0.56	1.48	0.61	4.64	1.33
1.91	0.91	1.84	0.90	5.70	0.61	1.33	0.68	4.63	2.45
3.29	0.53	2.13	0.78	5.70	0.53	1.37	0.64	4.62	3.65
4.95	0.35	3.64	0.45	5.68	0.34	1.59	0.49	4.61	2.48
2.76	0.63	4.15	0.39	5.67	1.68	3.36	0.22	4.61	0.99
1.85	0.92	6.62	0.24	5.65	1.61	2.13	0.33	4.60	0.58
3.78	0.45	4.90	0.33	5.64	0.49	2.39	0.28	4.59	2.57
3.56	0.48	4.91	0.33	5.63	1.68	2.44	0.26	4.56	0.88
3.54	0.48	2.29	0.69	5.63	0.58			4.53	1.19
2.37	0.72	3.02	0.52	5.62	2.92			4.51	0.78
2.48	0.67	3.79	0.41	5.62	1.72			4.51	0.46
2.97	0.56	2.85	0.54	5.62	0.94			4.49	0.86
3.02	0.55	1.96	0.78	5.61	1.93			4.46	1.20
3.47	0.48	4.03	0.37	5.61	0.81			4.46	1.30
2.10	0.79	1.73	0.85	5.61	1.61			4.45	0.49
2.51	0.66	2.53	0.58	5.59	0.91			4.45	1.30
4.80	0.35	3.23	0.45	5.57	0.59			4.44	1.42
2.59	0.64	7.57	0.19	5.56	0.83			4.43	4.24
2.06	0.79	2.78	0.52	5.56	0.74			4.42	0.77
2.38	0.68	5.30	0.27	5.54	1.28			4.41	0.42
3.45	0.47	5.17	0.27	5.54	1.42			4.40	1.78
1.93	0.84	5.19	0.27	5.54	3.57			4.40	0.84
1.52	1.05	2.07	0.69	5.53	0.37			4.40	2.03
2.05	0.78	3.46	0.41	5.50	0.80			4.40	3.43
3.87	0.41	2.88	0.48	5.50	0.90			4.38	1.07
3.94	0.40	3.66	0.38	5.48	0.68			4.38	2.50
2.42	0.66	3.85	0.36	5.47	0.61			4.37	1.25
2.09	0.74	2.93	0.46	5.47	0.59			4.37	1.41
2.48	0.63	2.18	0.62	5.47	0.82			4.35	0.80
3.80	0.41	4.11	0.32	5.45	2.94			4.32	1.02
4.13	0.38	1.44	0.90	5.44	1.10			4.31	1.72
2.84	0.55	1.92	0.66	5.44	0.52			4.30	1.76
2.60	0.60	2.42	0.51	5.43	0.90			4.30	3.28
3.34	0.47	2.22	0.56	5.42	1.85			4.24	0.60
3.47	0.44	4.94	0.25	5.42	0.68			4.19	3.56
2.81	0.54	2.85	0.43	5.39	3.12			4.17	1.85
5.70	0.27	1.54	0.78	5.39	0.28			4.17	0.75
4.00	0.38	1.84	0.65	5.38	1.16			4.15	1.23
0 mm	0 mm	5 mm	5 mm	9 mm	9 mm	13 mm	13 mm	17mm	17mm
Major	Minor	Major	Minor	Major	Minor	Major	Minor	Major	Minor
2.31	0.66	3.31	0.35	5.37	0.88			4.15	0.88

1.41	1.06	2.06	0.56	5.35	1.00	4.14	1.87
6.30	0.24	3.45	0.33	5.35	0.63	4.12	1.03
2.35	0.63	2.77	0.40	5.35	1.14	4.12	1.03
1.92	0.77	3.88	0.29	5.33	1.30	4.11	2.03
1.54	0.96	1.47	0.76	5.32	1.26	4.11	1.20
2.19	0.66	2.59	0.42	5.32	3.13	4.10	2.50
2.49	0.58	4.18	0.26	5.32	2.38	4.08	0.36
2.53	0.57	2.28	0.48	5.31	1.06	4.08	0.44
4.16	0.35	2.41	0.45	5.31	1.04	4.08	2.48
3.63	0.39	3.03	0.35	5.31	1.77	4.08	1.61
5.96	0.24	2.26	0.47	5.30	1.70	4.07	2.44
1.28	1.08	1.53	0.67	5.30	3.59	4.06	0.51
2.93	0.47	3.68	0.27	5.28	2.99	4.05	1.47
4.45	0.31	3.78	0.26	5.21	0.37	4.05	1.21
4.72	0.29	3.11	0.31	5.18	1.93	4.03	1.05
2.49	0.55	4.38	0.22	5.16	0.71	4.02	0.55
4.29	0.32	1.82	0.53	5.14	0.26	4.01	0.71
4.56	0.30	4.21	0.22	5.13	3.61	4.00	2.20
4.02	0.33	2.05	0.43	5.09	4.31	4.00	1.20
2.90	0.45	1.88	0.45	5.09	2.50	4.00	0.43
3.96	0.33	1.50	0.54	5.08	1.46	4.00	0.28
2.27	0.58	3.38	0.24	5.06	0.71	4.00	0.32
2.13	0.61	2.66	0.28	5.05	3.46	3.99	0.75
2.78	0.47	1.95	0.39	5.03	0.82	3.99	1.17
3.23	0.41	2.17	0.32	5.01	1.10	3.97	1.09
3.55	0.37	1.55	0.45	5.00	3.29	3.97	1.44
4.14	0.31	1.20	0.58	4.97	0.52	3.96	0.70
2.39	0.53	1.83	0.33	4.96	2.65	3.95	2.17
3.37	0.38	2.40	0.25	4.96	0.61	3.94	0.87
2.45	0.52	2.48	0.23	4.96	2.38	3.93	2.04
1.28	0.97	2.19	0.26	4.95	1.63	3.93	1.60
3.07	0.40	1.95	0.29	4.93	0.22	3.90	0.38
3.62	0.34	2.38	0.24	4.92	2.90	3.90	2.90
1.40	0.86	1.29	0.42	4.92	0.16	3.89	0.77
3.96	0.30	2.64	0.17	4.91	0.68	3.88	2.14
2.44	0.49	1.35	0.34	4.91	0.75	3.86	1.26
3.19	0.38	0.81	0.52	4.90	0.48	3.83	2.01
1.32	0.91	2.26	0.17	4.90	0.79	3.82	1.16
2.09	0.56	1.73	0.21	4.88	2.94	3.81	2.37
2.13	0.55			4.88	3.50	3.80	1.51
3.23	0.36			4.86	3.43	3.80	0.99
1.74	0.67			4.86	1.38	3.79	1.21
2.94	0.40			4.84	0.99	3.79	0.93
1.75	0.65			4.81	0.75	3.77	0.53
1.85	0.59			4.79	0.86	3.77	2.05
2.70	0.41			4.78	2.01	3.77	1.14
4.62	0.24			4.74	2.48	3.77	0.61
2.29	0.48			4.72	0.56	3.77	1.66
2.45	0.43			4.71	1.92	3.76	1.87
1.67	0.64			4.71	0.80	3.75	3.15
2.60	0.41			4.70	1.44	3.74	0.99

3.84	0.28			4.69	1.81			3.72	0.78
0 mm	0 mm	5 mm	5 mm	9 mm	9 mm	13 mm	13 mm	17mm	17mm
Major	Minor	Major	Minor	Major	Minor	Major	Minor	Major	Minor
3.21	0.32			4.68	2.76			3.71	1.90
3.32	0.31			4.68	0.76			3.70	2.69
1.67	0.61			4.68	1.26			3.70	0.69
3.66	0.28			4.68	0.51			3.70	1.60
2.28	0.45			4.68	0.70			3.70	2.00
2.97	0.35			4.68	1.49			3.69	0.25
1.59	0.65			4.67	0.66			3.69	1.04
3.33	0.30			4.67	0.38			3.69	0.67
3.76	0.26			4.66	2.45			3.67	0.57
2.14	0.46			4.66	3.54			3.65	1.16
3.24	0.29			4.66	1.36			3.63	0.35
1.54	0.62			4.65	0.71			3.62	3.54
2.10	0.46			4.65	0.51			3.62	0.61
1.67	0.55			4.64	0.30			3.62	0.76
1.03	0.89			4.64	0.65			3.62	0.35
3.09	0.30			4.63	2.87			3.62	1.99
3.03	0.30			4.63	3.99			3.61	0.76
1.45	0.61			4.63	3.42			3.59	0.50
1.76	0.50			4.62	0.47			3.59	2.41
6.18	0.14			4.61	2.20			3.59	0.38
2.52	0.35			4.61	0.81			3.59	2.15
2.72	0.33			4.59	0.42			3.59	2.26
3.02	0.28			4.58	2.85			3.57	0.93
1.82	0.47			4.58	0.48			3.53	2.60
2.60	0.33			4.58	0.56			3.50	0.70
0.96	0.85			4.57	0.36			3.50	0.61
3.31	0.25			4.57	2.08			3.49	0.68
3.31	0.25			4.56	0.42			3.48	1.38
2.03	0.40			4.56	0.98			3.43	1.48
1.83	0.44			4.56	0.65			3.42	1.87
4.59	0.18			4.56	1.21			3.40	1.72
3.19	0.25			4.54	0.27			3.39	1.55
1.99	0.41			4.53	1.48			3.38	1.43
1.74	0.47			4.53	1.02			3.38	2.93
1.61	0.48			4.52	3.59			3.38	0.40
1.12	0.66			4.51	0.77			3.37	2.10
2.41	0.31			4.50	1.88			3.37	2.10
2.20	0.34			4.50	2.12			3.37	0.71
2.07	0.36			4.47	0.57			3.36	0.73
1.54	0.46			4.43	2.92			3.33	1.07
1.19	0.59			4.41	0.33			3.33	0.89
1.74	0.41			4.39	1.26			3.32	1.91
3.10	0.23			4.39	2.06			3.31	0.73
2.19	0.32			4.38	0.52			3.31	0.90
2.71	0.26			4.37	1.39			3.30	0.44
0.94	0.72			4.37	0.67			3.30	1.98
1.01	0.63			4.36	1.21			3.30	0.32
1.08	0.59			4.36	0.71			3.30	1.50

2.13	0.30			4.36	0.58			3.29	2.73
1.18	0.54			4.35	1.61			3.28	1.89
1.37	0.46			4.34	1.57			3.25	1.39
1.43	0.44			4.32	0.48			3.23	1.15
1.08	0.56			4.30	0.81			3.23	0.70
0 mm	0 mm	5 mm	5 mm	9 mm	9 mm	13 mm	13 mm	17mm	17mm
Major	Minor	Major	Minor	Major	Minor	Major	Minor	Major	Minor
2.21	0.27			4.30	0.95			3.22	2.65
1.07	0.53			4.28	0.83			3.21	0.96
1.39	0.41			4.26	1.37			3.21	1.49
1.27	0.45			4.25	1.37			3.20	2.66
1.76	0.32			4.21	0.69			3.18	0.88
1.01	0.52			4.18	1.38			3.16	0.49
1.57	0.34			4.12	2.49			3.15	0.28
3.12	0.17			4.10	1.70			3.14	1.13
0.97	0.55			4.10	1.42			3.13	1.08
1.95	0.25			4.10	1.48			3.13	1.29
2.87	0.17			4.08	1.19			3.11	0.61
1.27	0.39			4.08	0.87			3.11	1.80
1.24	0.37			4.07	2.91			3.09	0.31
1.15	0.40			4.06	2.84			3.09	1.50
0.76	0.56			4.05	2.49			3.09	0.60
0.69	0.61			4.03	1.86			3.08	0.32
1.59	0.27			4.03	1.14			3.08	0.65
0.80	0.53			4.02	0.62			3.07	0.53
0.98	0.44			4.02	0.95			3.05	1.20
2.46	0.16			4.00	0.74			3.04	1.02
2.41	0.15			3.98	1.56			3.04	1.36
1.42	0.25			3.98	2.02			3.04	0.33
1.41	0.25			3.98	1.19			3.03	0.61
0.71	0.45			3.96	1.18			3.02	0.77
1.02	0.31			3.95	1.44			3.01	0.54
0.80	0.40			3.95	0.45			3.01	2.07
0.64	0.44			3.94	3.03			3.01	0.76
1.16	0.24			3.93	3.30			2.98	1.15
0.66	0.43			3.92	0.99			2.90	2.75
1.74	0.14			3.91	3.47			2.88	2.09
1.17	0.21			3.91	1.22			2.88	1.35
0.62	0.34			3.91	1.22			2.87	0.74
0.66	0.32			3.88	1.69			2.86	0.80
1.13	0.19			3.88	2.31			2.84	1.17
1.18	0.18			3.88	0.95			2.83	0.61
0.68	0.26			3.86	1.62			2.83	0.74
1.11	0.13			3.85	2.93			2.82	0.63
0.82	0.17			3.85	0.53			2.82	1.78
0.75	0.19			3.82	2.79			2.81	1.31
0.54	0.26			3.81	2.55			2.81	0.91
0.38	0.19			3.79	0.59			2.78	1.80
14.93	8.04			3.79	0.24			2.78	0.23
25.13	3.89			3.78	1.40			2.78	0.76
12.65	7.26			3.78	1.08			2.77	1.56

12.13	6.26			3.76	0.87			2.76	0.81
18.02	3.68			3.76	1.29			2.76	1.34
14.99	4.09			3.76	0.50			2.75	0.72
15.78	3.83			3.76	0.86			2.73	1.18
22.92	2.61			3.75	2.57			2.73	1.86
12.67	4.18			3.73	0.41			2.72	1.75
8.96	5.79			3.71	0.21			2.71	0.60
20.19	2.43			3.71	1.60			2.71	0.55
20.19	2.43			3.71	1.33			2.71	0.39
0 mm	0 mm	5 mm	5 mm	9 mm	9 mm	13 mm	13 mm	17mm	17mm
Major	Minor	Major	Minor	Major	Minor	Major	Minor	Major	Minor
13.17	3.71			3.71	1.06			2.70	0.59
11.08	4.38			3.71	1.49			2.70	0.93
9.74	4.89			3.69	0.92			2.70	0.75
28.00	1.67			3.65	0.61			2.69	0.97
9.31	4.78			3.64	0.69			2.66	0.84
7.87	5.58			3.64	1.67			2.66	0.53
19.40	2.16			3.62	0.59			2.64	1.01
18.44	2.12			3.62	0.39			2.63	0.54
8.04	4.83			3.62	0.64			2.60	1.36
21.19	1.83			3.61	1.51			2.60	0.84
18.21	2.02			3.59	0.75			2.59	2.16
15.81	2.28			3.59	1.54			2.58	0.27
10.69	3.36			3.58	0.87			2.58	0.92
19.93	1.79			3.56	0.73			2.57	0.56
24.95	1.41			3.55	2.28			2.56	2.50
13.02	2.45			3.52	1.12			2.55	1.79
9.47	3.27			3.50	0.24			2.54	0.83
8.86	3.46			3.50	0.52			2.53	0.73
28.27	1.06			3.45	0.32			2.53	0.67
10.48	2.81			3.45	0.73			2.53	0.70
12.30	2.28			3.45	0.74			2.51	0.77
11.41	2.44			3.41	0.64			2.48	0.49
7.87	3.34			3.41	0.86			2.46	0.61
7.90	3.32			3.41	0.69			2.42	1.14
17.88	1.46			3.40	0.76			2.42	0.85
15.91	1.61			3.40	0.82			2.42	0.85
15.17	1.67			3.39	0.66			2.40	0.47
21.16	1.18			3.39	0.21			2.39	0.44
14.01	1.75			3.38	0.32			2.39	1.08
8.61	2.80			3.36	2.58			2.39	0.73
12.14	1.98			3.36	0.62			2.38	0.91
24.46	0.98			3.36	2.21			2.38	0.36
5.92	3.92			3.32	2.85			2.38	0.80
14.67	1.56			3.30	0.91			2.38	0.40
5.88	3.88			3.29	0.39			2.37	0.92
20.35	1.10			3.28	0.41			2.36	0.31
9.22	2.43			3.27	2.62			2.34	0.23
7.91	2.83			3.27	2.01			2.34	1.53
23.04	0.97			3.26	0.96			2.33	0.86
9.07	2.46			3.26	0.92			2.31	0.63

10.55	2.12			3.24	0.47			2.29	0.63
9.75	2.27			3.24	0.73			2.28	0.82
13.02	1.68			3.24	1.83			2.28	0.56
8.67	2.52			3.24	0.63			2.26	1.73
14.49	1.50			3.23	0.88			2.26	1.05
8.73	2.47			3.20	0.33			2.18	0.94
10.10	2.13			3.19	2.14			2.18	0.44
15.97	1.32			3.19	1.00			2.17	0.41
13.94	1.52			3.18	1.19			2.16	0.42
15.35	1.34			3.18	1.77			2.14	0.68
15.17	1.35			3.17	1.40			2.13	1.60
13.60	1.51			3.16	1.55			2.12	1.00
11.97	1.70			3.16	0.16			2.12	0.68
0 mm	0 mm	5 mm	5 mm	9 mm	9 mm	13 mm	13 mm	17mm	17mm
Major	Minor	Major	Minor	Major	Minor	Major	Minor	Major	Minor
19.79	1.02			3.16	0.35			2.11	0.50
5.33	3.79			3.16	0.61			2.11	0.39
10.31	1.92			3.15	2.09			2.11	0.84
18.75	1.04			3.15	2.09			2.08	0.88
21.11	0.93			3.15	0.52			2.07	1.03
5.52	3.54			3.14	0.32			2.01	1.50
10.83	1.78			3.14	0.79			2.01	1.43
11.49	1.64			3.13	1.86			2.00	0.19
9.15	2.05			3.12	0.39			1.98	1.21
8.51	2.20			3.11	1.14			1.97	0.50
4.53	4.09			3.11	0.66			1.94	0.82
9.59	1.91			3.11	1.82			1.90	0.59
6.45	2.84			3.10	2.79			1.89	1.18
11.21	1.62			3.10	1.07			1.88	1.01
4.80	3.77			3.09	0.49			1.88	0.75
5.41	3.33			3.09	1.09			1.87	0.55
11.86	1.51			3.09	0.34			1.86	0.87
16.06	1.10			3.06	1.36			1.86	0.53
5.48	3.21			3.06	1.32			1.86	0.80
15.45	1.13			3.06	1.34			1.85	0.50
6.08	2.85			3.04	0.44			1.84	0.58
13.84	1.24			3.04	0.34			1.83	0.62
15.45	1.11			3.04	0.70			1.83	1.69
6.70	2.55			3.04	0.89			1.82	0.41
13.23	1.27			3.03	0.84			1.81	1.01
19.97	0.83			3.03	0.79			1.80	0.37
12.08	1.37			3.00	0.72			1.78	0.88
6.51	2.53			3.00	0.71			1.76	0.97
18.87	0.87			3.00	1.06			1.75	1.57
13.10	1.25			2.99	1.37			1.73	0.55
6.63	2.45			2.96	2.39			1.72	0.62
5.42	2.99			2.95	0.46			1.72	0.82
11.75	1.38			2.94	1.37			1.72	0.39
13.06	1.23			2.94	0.26			1.72	0.89
9.93	1.60			2.94	0.98			1.71	0.70
6.67	2.37			2.94	0.48			1.71	0.64

9.51	1.65			2.92	1.03			1.71	0.35
10.09	1.53			2.91	0.26			1.70	0.67
5.65	2.72			2.90	0.65			1.62	0.76
13.54	1.12			2.90	0.67			1.56	0.57
16.83	0.90			2.88	0.44			1.54	0.46
13.85	1.09			2.88	1.25			1.54	1.24
5.16	2.93			2.87	0.31			1.53	0.39
4.51	3.29			2.81	0.91			1.46	0.82
9.86	1.45			2.81	1.30			1.46	0.29
4.96	2.86			2.79	0.44			1.45	1.44
11.93	1.18			2.78	0.65			1.44	0.51
8.00	1.76			2.75	0.50			1.44	0.30
9.26	1.49			2.75	1.69			1.42	0.37
10.26	1.33			2.75	1.25			1.42	0.20
5.25	2.57			2.74	0.86			1.38	0.69
8.64	1.56			2.73	1.03			1.38	0.79
9.96	1.36			2.73	0.32			1.38	1.18
0 mm	0 mm	5 mm	5 mm	9 mm	9 mm	13 mm	13 mm	17mm	17mm
Major	Minor	Major	Minor	Major	Minor	Major	Minor	Major	Minor
17.95	0.75			2.73	0.30			1.35	1.20
4.79	2.78			2.71	1.20			1.34	1.11
16.74	0.78			2.70	0.39			1.34	0.16
9.65	1.36			2.70	0.39			1.32	0.54
11.72	1.12			2.70	1.44			1.32	0.80
6.15	2.13			2.69	0.63			1.28	0.66
10.65	1.22			2.68	0.53			1.28	0.47
5.66	2.29			2.68	0.67			1.26	0.59
8.74	1.48			2.67	1.31			1.23	0.52
16.15	0.78			2.66	0.32			1.20	0.47
12.39	1.01			2.66	0.97			1.17	0.54
6.39	1.94			2.65	0.65			1.16	0.73
12.34	0.99			2.64	0.92			1.14	0.56
7.90	1.55			2.62	1.15			1.09	0.55
13.91	0.87			2.56	0.75			1.06	0.97
9.38	1.29			2.56	0.73			1.03	0.65
3.70	3.27			2.56	0.64			0.95	0.89
6.95	1.73			2.56	1.43			0.94	0.56
9.56	1.26			2.54	1.07			0.94	0.42
11.64	1.03			2.52	1.28			0.93	0.15
11.21	1.06			2.51	0.28			0.89	0.44
5.10	2.33			2.51	0.14			0.85	0.17
11.09	1.03			2.50	1.10			0.84	0.25
15.58	0.73			2.50	1.13			0.71	0.15
9.28	1.23			2.50	1.53			0.67	0.48
9.73	1.17			2.49	1.59			0.38	0.19
12.34	0.92			2.48	0.80			18.97	17.19
9.98	1.13			2.47	0.50			17.49	11.31
6.27	1.77			2.47	0.31			20.09	9.10
9.98	1.10			2.44	0.38			16.50	10.80
7.62	1.43			2.44	0.49			25.96	5.73
12.54	0.87			2.44	0.77			14.58	9.60



11.06	0.98			2.41	0.51			14.49	7.44
10.13	1.07			2.41	0.75			11.64	8.58
8.95	1.20			2.38	0.53			29.94	3.30
4.55	2.35			2.38	0.53			22.42	4.30
8.94	1.18			2.37	1.24			16.06	5.86
17.16	0.61			2.36	1.08			22.54	4.13
6.91	1.52			2.34	0.15			19.83	4.68
7.78	1.34			2.32	1.75			20.12	4.46
4.37	2.37			2.31	0.54			12.03	6.30
9.60	1.07			2.29	0.91			17.11	4.37
12.78	0.79			2.27	0.48			8.92	7.90
8.92	1.13			2.27	0.70			16.31	4.17
10.17	0.99			2.27	0.16			9.12	7.08
6.28	1.59			2.25	0.52			9.67	6.13
5.96	1.67			2.24	0.50			11.58	4.96
12.47	0.79			2.23	0.57			17.50	3.18
9.16	1.08			2.23	0.48			20.81	2.60
5.58	1.76			2.20	0.87			28.96	1.86
8.84	1.10			2.20	1.49			7.93	6.43
4.73	2.01			2.19	1.19			15.89	3.09
11.77	0.80			2.18	1.60			11.13	4.38
0 mm	0 mm	5 mm	5 mm	9 mm	9 mm	13 mm	13 mm	17mm	17mm
Major	Minor	Major	Minor	Major	Minor	Major	Minor	Major	Minor
12.28	0.77			2.18	1.79			27.20	1.71
3.35	2.78			2.14	0.99			20.35	2.27
3.55	2.61			2.13	1.74			24.33	1.78
14.89	0.62			2.11	1.19			13.76	3.13
10.98	0.83			2.09	0.83			32.07	1.32
10.14	0.90			2.08	1.07			21.20	2.00
9.72	0.93			2.08	1.50			9.80	4.13
11.73	0.77			2.07	0.89			24.89	1.62
10.18	0.89			2.07	0.26			22.97	1.75
11.41	0.79			2.06	0.91			14.47	2.77
6.50	1.38			2.03	1.31			21.56	1.82
10.38	0.86			2.02	0.94			21.56	1.82
6.83	1.29			2.01	1.32			18.31	2.12
9.91	0.88			2.00	0.62			19.25	2.00
4.26	2.04			2.00	1.11			8.69	4.40
10.06	0.86			1.99	0.11			23.38	1.63
6.12	1.41			1.99	0.67			13.19	2.79
10.85	0.79			1.98	0.91			7.95	4.60
6.10	1.40			1.98	0.89			11.39	3.15
11.54	0.74			1.96	1.86			26.50	1.33
10.11	0.84			1.95	0.83			9.10	3.82
7.35	1.15			1.95	0.96			11.16	3.11
8.60	0.98			1.91	0.52			14.77	2.34
7.78	1.08			1.91	0.93			24.96	1.37
10.29	0.81			1.89	0.45			9.09	3.74
11.69	0.71			1.89	0.37			7.47	4.52
7.96	1.04			1.87	0.40			17.36	1.86
10.83	0.76			1.83	0.48			8.73	3.69

9.13	0.90			1.82	1.27			9.49	3.38
9.52	0.86			1.80	0.94			14.67	2.18
8.89	0.91			1.80	0.43			16.52	1.94
10.63	0.75			1.79	1.07			14.63	2.18
3.29	2.36			1.78	0.79			15.29	2.05
8.42	0.92			1.78	0.77			18.54	1.68
3.11	2.48			1.77	0.68			10.95	2.77
11.18	0.68			1.76	0.54			15.08	2.01
6.88	1.11			1.74	1.26			9.08	3.32
4.38	1.74			1.74	0.91			20.66	1.46
11.08	0.68			1.72	0.64			7.35	4.10
6.47	1.16			1.71	0.39			15.60	1.92
7.97	0.93			1.70	0.25			19.06	1.56
5.51	1.35			1.67	0.85			18.18	1.63
9.33	0.78			1.66	1.02			9.05	3.24
4.16	1.75			1.66	0.60			15.89	1.82
5.70	1.28			1.66	0.92			13.93	2.06
8.65	0.84			1.64	0.24			12.26	2.33
7.84	0.92			1.62	0.85			6.70	4.18
8.21	0.88			1.57	0.41			5.54	5.03
3.76	1.91			1.54	0.41			21.14	1.31
8.06	0.89			1.54	0.37			13.08	2.11
8.06	0.89			1.52	0.65			9.31	2.96
6.10	1.16			1.43	0.77			9.21	2.99
5.40	1.30			1.36	0.55			7.47	3.66
0 mm	0 mm	5 mm	5 mm	9 mm	9 mm	13 mm	13 mm	17mm	17mm
Major	Minor	Major	Minor	Major	Minor	Major	Minor	Major	Minor
5.13	1.36			1.36	0.31			5.76	4.75
8.43	0.83			1.35	0.45			7.94	3.43
8.78	0.79			1.33	0.85			9.68	2.81
11.43	0.60			1.32	0.78			7.62	3.52
6.60	1.04			1.32	0.38			13.55	1.98
3.21	2.12			1.29	0.82			18.94	1.41
5.74	1.18			1.27	0.14			8.92	2.92
8.94	0.76			1.23	0.69			18.13	1.43
6.41	1.06			1.23	0.69			14.42	1.79
8.69	0.78			1.22	0.70			18.24	1.40
6.22	1.06			1.20	0.26			16.47	1.54
7.74	0.85			1.18	0.75			17.32	1.44
11.94	0.55			1.17	0.60			12.67	1.95
5.30	1.22			1.16	0.24			14.22	1.74
7.86	0.81			1.16	0.43			8.30	2.95
3.91	1.60			1.15	0.68			21.48	1.14
7.24	0.86			1.13	0.16			8.86	2.73
7.51	0.82			1.10	0.48			7.31	3.28
12.41	0.49			1.01	0.52			14.68	1.62
3.18	1.90			0.99	0.36			15.79	1.50
8.96	0.68			0.99	0.43			8.06	2.93
4.37	1.38			0.99	0.54			10.42	2.26
5.37	1.12			0.96	0.22			13.59	1.73
5.79	1.03			0.95	0.56			5.70	4.11

5.79	1.03			0.93	0.76			7.71	3.02
7.56	0.79			0.73	0.72			7.26	3.19
5.58	1.04			0.62	0.57			14.85	1.55
4.83	1.18			31.87	9.59			16.09	1.42
7.22	0.79			25.07	5.87			16.60	1.37
6.01	0.94			25.93	5.43			6.96	3.27
6.96	0.81			17.54	7.15			11.67	1.94
5.17	1.08			17.75	7.00			12.59	1.78
7.66	0.72			27.35	4.46			11.82	1.89
3.67	1.49			13.29	9.03			17.21	1.30
7.72	0.69			11.61	9.65			15.52	1.43
7.35	0.72			16.06	6.29			8.82	2.52
2.89	1.82			31.58	3.20			8.79	2.52
8.80	0.60			31.16	2.97			7.95	2.73
3.73	1.41			16.14	4.81			13.39	1.62
6.02	0.86			19.79	3.69			13.11	1.65
9.20	0.56			16.82	3.60			20.71	1.04
11.05	0.46			27.23	2.21			6.56	3.29
6.89	0.74			18.82	2.58			7.87	2.73
2.79	1.83			25.01	1.94			6.99	3.05
6.41	0.78			14.64	3.30			11.86	1.79
3.73	1.34			26.22	1.83			12.59	1.69
6.37	0.79			14.36	3.28			12.90	1.64
6.62	0.76			7.86	5.88			5.38	3.91
9.14	0.54			11.67	3.94			7.34	2.86
5.16	0.96			9.13	5.02			12.00	1.75
4.93	1.00			9.45	4.73			15.14	1.36
5.02	0.98			8.56	5.22			10.65	1.92
7.55	0.65			20.41	2.11			14.28	1.42
0 mm	0 mm	5 mm	5 mm	9 mm	9 mm	13 mm	13 mm	17mm	17mm
Major	Minor	Major	Minor	Major	Minor	Major	Minor	Major	Minor
5.01	0.97			8.99	4.79			14.34	1.41
3.05	1.59			14.48	2.87			13.88	1.46
3.03	1.59			12.16	3.38			11.41	1.77
8.06	0.60			9.18	4.34			17.75	1.14
3.96	1.21			21.51	1.84			7.05	2.86
5.44	0.88			15.52	2.52			5.36	3.74
5.23	0.91			19.10	2.04			11.58	1.73
3.45	1.36			7.05	5.50			18.91	1.06
3.23	1.42			14.35	2.70			6.21	3.18
7.06	0.64			7.35	5.22			5.63	3.51
7.46	0.61			12.35	3.09			8.95	2.21
4.73	0.95			15.75	2.41			5.04	3.91
4.55	0.98			7.90	4.77			20.24	0.97
7.11	0.63			20.36	1.85			20.15	0.97
7.12	0.62			7.85	4.78			4.97	3.91
4.47	0.99			13.50	2.70			6.12	3.16
7.15	0.62			8.99	4.04			11.29	1.71
5.23	0.84			13.11	2.77			4.88	3.96
5.23	0.84			17.32	2.08			15.76	1.22
5.79	0.75			9.98	3.57			4.69	4.09

8.79	0.49			8.40	4.24			9.81	1.96
5.15	0.84			14.00	2.53			8.88	2.16
6.30	0.68			24.81	1.39			5.49	3.48
5.72	0.74			30.58	1.12			13.88	1.38
5.73	0.74			9.91	3.37			10.03	1.90
10.44	0.40			13.69	2.39			11.53	1.65
6.27	0.67			15.55	2.08			16.10	1.17
3.54	1.18			27.73	1.17			15.51	1.21
3.83	1.08			19.69	1.64			5.25	3.56
6.14	0.67			22.30	1.44			14.77	1.26
7.94	0.52			28.14	1.14			4.95	3.76
7.00	0.58			13.50	2.36			15.26	1.21
6.36	0.63			7.14	4.45			4.99	3.71
6.38	0.62			15.71	1.99			8.02	2.29
10.09	0.39			9.26	3.35			6.75	2.71
4.83	0.82			14.68	2.05			4.92	3.70
9.26	0.43			12.64	2.37			14.16	1.29
4.77	0.83			22.08	1.35			5.08	3.57
3.86	1.02			11.98	2.49			6.32	2.87
6.92	0.57			16.51	1.81			11.64	1.56
4.81	0.80			12.78	2.33			5.59	3.23
9.34	0.41			16.66	1.78			16.80	1.06
3.80	1.02			13.21	2.23			17.82	1.00
5.10	0.76			13.92	2.11			6.69	2.64
4.59	0.82			14.04	2.04			5.22	3.34
5.91	0.63			13.81	2.08			6.98	2.49
4.40	0.84			7.90	3.63			10.27	1.69
3.50	1.04			23.86	1.20			12.05	1.43
3.90	0.93			17.80	1.60			7.77	2.22
6.78	0.53			10.38	2.74			17.33	0.99
3.52	1.01			7.32	3.88			4.45	3.86
5.48	0.65			16.22	1.74			5.27	3.23
5.07	0.69			12.20	2.30			9.67	1.76
0 mm	0 mm	5 mm	5 mm	9 mm	9 mm	13 mm	13 mm	17mm	17mm
Major	Minor	Major	Minor	Major	Minor	Major	Minor	Major	Minor
5.09	0.68			6.36	4.40			13.85	1.23
4.51	0.76			8.79	3.17			11.54	1.47
4.23	0.81			6.33	4.37			10.42	1.62
6.01	0.57			20.54	1.34			10.25	1.65
5.56	0.61			11.16	2.47			9.86	1.70
4.85	0.70			6.37	4.32			13.68	1.22
5.10	0.65			9.62	2.86			11.08	1.50
5.10	0.65			8.56	3.14			8.74	1.91
6.87	0.46			5.42	4.96			12.97	1.28
2.51	1.25			17.55	1.52			13.08	1.27
5.97	0.53			17.28	1.54			13.67	1.18
4.92	0.64			24.23	1.10			6.39	2.53
6.55	0.47			9.05	2.91			10.24	1.57
7.59	0.41			5.21	5.04			8.58	1.87
3.81	0.81			8.32	3.15			7.66	2.07
3.44	0.89			6.62	3.96			10.05	1.57

3.85	0.78			18.42	1.39			4.77	3.31
3.49	0.86			8.31	3.04			7.39	2.13
3.98	0.74			12.39	2.04			5.29	2.97
3.25	0.90			9.37	2.67			8.71	1.80
7.97	0.37			9.53	2.60			10.90	1.44
3.57	0.81			13.96	1.76			19.67	0.80
3.61	0.79			15.30	1.59			8.26	1.90
7.60	0.38			21.58	1.12			7.12	2.20
6.10	0.46			12.02	1.99			11.41	1.37
6.53	0.43			6.63	3.57			4.58	3.40
3.22	0.86			14.81	1.59			9.69	1.60
5.32	0.52			26.88	0.86			12.68	1.22
5.80	0.48			5.16	4.48			14.17	1.09
6.88	0.40			5.84	3.89			4.48	3.44
2.86	0.95			5.33	4.25			12.16	1.26
6.64	0.40			26.37	0.85			5.24	2.89
8.53	0.31			10.74	2.09			7.79	1.94
6.26	0.42			7.00	3.20			11.96	1.26
3.34	0.78			5.50	4.07			8.97	1.68
4.85	0.53			19.07	1.17			14.03	1.07
4.79	0.54			5.85	3.78			8.10	1.85
7.65	0.33			11.14	1.99			13.38	1.12
3.61	0.70			9.08	2.44			4.98	2.98
5.00	0.51			8.68	2.53			7.02	2.11
3.29	0.73			18.05	1.22			8.98	1.64
2.15	1.11			8.53	2.57			7.44	1.98
4.19	0.57			15.02	1.46			15.39	0.96
4.29	0.53			17.87	1.22			9.26	1.57
5.38	0.39			21.55	1.01			9.50	1.53
3.32	0.63			5.48	3.93			5.91	2.44
7.72	0.27			8.01	2.67			13.44	1.07
3.90	0.49			16.46	1.29			13.77	1.04
3.36	0.57			10.97	1.94			17.96	0.80
2.38	0.80			11.36	1.83			13.14	1.09
1.54	1.20			16.36	1.26			7.97	1.79
3.58	0.51			6.10	3.37			9.22	1.54
5.08	0.36			19.12	1.06			4.18	3.38
0 mm	0 mm	5 mm	5 mm	9 mm	9 mm	13 mm	13 mm	17mm	17mm
Major	Minor	Major	Minor	Major	Minor	Major	Minor	Major	Minor
3.29	0.55			22.11	0.91			14.34	0.98
3.76	0.47			5.88	3.43			14.86	0.94
2.99	0.56			11.61	1.71			9.61	1.44
3.32	0.51			11.15	1.77			7.42	1.85
3.03	0.54			16.34	1.19			15.82	0.86
3.11	0.51			12.77	1.52			4.27	3.20
3.51	0.44			5.39	3.57			5.76	2.36
2.74	0.51			10.49	1.83			12.95	1.04
2.46	0.52			4.63	4.13			12.65	1.06
3.64	0.34			6.33	3.02			5.68	2.35
2.44	0.49			4.77	4.00			6.94	1.92
1.50	0.78			9.10	2.08			4.48	2.97

1.61	0.65			9.92	1.87			4.37	3.04
2.30	0.43			13.44	1.38			14.35	0.93
2.13	0.47			6.20	2.96			9.60	1.38
1.71	0.56			13.21	1.39			11.75	1.12
2.10	0.36			13.29	1.37			8.29	1.58
2.71	0.27			5.12	3.50			8.35	1.57
2.03	0.31			15.93	1.13			7.88	1.66
1.79	0.35			11.21	1.58			11.59	1.13
2.48	0.21			5.93	2.96			5.88	2.22
0.76	0.47			21.42	0.82			6.97	1.87
				14.53	1.20			8.95	1.44
				10.60	1.63			8.60	1.50
				18.16	0.95			13.28	0.97
				9.54	1.79			10.92	1.17
				8.84	1.93			11.66	1.09
				11.43	1.49			9.79	1.30
				14.01	1.20			5.70	2.23
				5.27	3.18			13.30	0.95
				13.87	1.20			13.86	0.92
				4.37	3.77			6.21	2.04
				8.13	2.02			4.16	3.04
				14.77	1.11			4.68	2.68
				4.24	3.85			9.19	1.36
				9.06	1.80			6.10	2.05
				12.20	1.33			7.73	1.61
				5.02	3.22			7.95	1.56
				14.60	1.11			13.47	0.92
				19.82	0.81			6.02	2.04
				4.30	3.73			12.04	1.02
				4.39	3.61			11.59	1.06
				7.12	2.23			9.84	1.24
				5.64	2.80			7.30	1.67
				10.03	1.58			7.82	1.55
				21.77	0.73			3.76	3.23
				5.49	2.87			10.44	1.16
				11.80	1.33			10.15	1.19
				20.97	0.74			7.29	1.66
				9.02	1.72			10.71	1.13
				4.93	3.13			5.05	2.38
				7.88	1.94			11.57	1.04
				14.13	1.08			14.21	0.84
0 mm	0 mm	5 mm	5 mm	9 mm	9 mm	13 mm	13 mm	17mm	17mm
Major	Minor	Major	Minor	Major	Minor	Major	Minor	Major	Minor
				10.03	1.50			12.08	0.99
				9.73	1.52			9.78	1.21
				5.58	2.61			10.99	1.07
				14.23	1.02			17.32	0.68
				6.85	2.12			9.18	1.28
				12.65	1.14			10.79	1.09
				15.79	0.91			12.89	0.91
				14.97	0.96			8.23	1.42

				10.21	1.41				15.03	0.78
				7.15	1.98				7.01	1.66
				16.29	0.86				14.99	0.78
				8.92	1.57				3.76	3.08
				16.29	0.86				6.64	1.74
				15.92	0.88				10.73	1.08
				5.17	2.67				14.32	0.80
				12.48	1.10				7.73	1.48
				14.66	0.93				9.99	1.14
				10.54	1.30				4.26	2.68
				9.60	1.42				12.64	0.90
				5.02	2.71				11.27	1.01
				14.50	0.94				8.31	1.36
				7.68	1.76				8.44	1.34
				12.16	1.11				6.86	1.65
				10.65	1.27				9.88	1.14
				10.44	1.29				7.26	1.54
				16.25	0.83				9.53	1.17
				6.74	1.99				10.43	1.07
				14.64	0.92				10.87	1.02
				21.09	0.63				3.95	2.78
				4.09	3.27				8.51	1.29
				11.31	1.18				5.95	1.84
				14.95	0.89				6.43	1.70
				10.65	1.25				8.87	1.23
				15.97	0.83				8.02	1.36
				10.01	1.32				11.15	0.98
				6.02	2.18				5.44	1.99
				6.02	2.18				10.89	0.99
				4.00	3.27				4.96	2.17
				7.31	1.78				7.17	1.50
				12.18	1.06				10.90	0.99
				9.45	1.37				8.22	1.31
				8.57	1.51				5.60	1.91
				11.17	1.15				4.93	2.16
				14.27	0.90				8.18	1.30
				8.12	1.58				7.68	1.38
				5.88	2.17				4.11	2.58
				10.60	1.20				5.57	1.90
				13.75	0.92				9.25	1.14
				9.50	1.34				3.67	2.88
				13.30	0.95				7.94	1.32
				3.64	3.46				4.41	2.38
				11.33	1.10				7.18	1.45
				4.43	2.81				9.54	1.08
0 mm	0 mm	5 mm	5 mm	9 mm	9 mm	13 mm	13 mm	17mm	17mm	
Major	Minor	Major	Minor	Major	Minor	Major	Minor	Major	Minor	
				8.04	1.54			7.58	1.36	
				4.73	2.62			7.55	1.36	
				5.52	2.24			6.93	1.47	
				13.77	0.90			3.53	2.87	

				8.40	1.47					7.05	1.43
				4.87	2.52					9.59	1.05
				4.99	2.45					4.80	2.09
				12.77	0.95					9.82	1.02
				10.04	1.21					3.60	2.78
				12.60	0.96					10.20	0.98
				4.60	2.63					11.77	0.85
				5.62	2.14					9.07	1.10
				4.30	2.80					7.26	1.37
				12.80	0.94					5.76	1.72
				4.17	2.88					4.78	2.07
				5.95	2.01					6.78	1.46
				9.74	1.23					10.65	0.92
				9.54	1.25					4.23	2.32
				5.00	2.39					7.13	1.38
				6.33	1.88					6.18	1.59
				8.07	1.47					11.78	0.83
				4.84	2.45					10.07	0.97
				9.16	1.28					8.73	1.12
				11.11	1.06					3.27	2.97
				11.11	1.06					4.79	2.03
				12.13	0.95					11.07	0.88
				3.77	3.05					9.59	1.01
				7.02	1.64					6.51	1.47
				10.00	1.15					3.49	2.75
				14.19	0.80					6.30	1.52
				8.78	1.30					3.37	2.81
				11.15	1.02					3.84	2.48
				12.24	0.93					5.66	1.67
				3.72	3.04					5.68	1.66
				10.77	1.05					9.48	0.99
				7.08	1.59					8.72	1.08
				9.79	1.15					9.61	0.98
				8.43	1.33					13.36	0.70
				8.12	1.38					12.00	0.78
				13.76	0.81					7.11	1.31
				10.84	1.03					8.38	1.11
				5.95	1.88					12.54	0.74
				5.40	2.05					7.31	1.26
				7.68	1.44					10.60	0.86
				6.77	1.63					4.84	1.87
				12.62	0.87					6.03	1.50
				3.97	2.77					4.79	1.88
				11.72	0.93					7.45	1.21
				4.65	2.35					4.27	2.10
				8.95	1.21					6.82	1.32
				3.88	2.79					9.30	0.96
				9.15	1.18					5.75	1.56
				9.51	1.13					5.10	1.75
0 mm	0 mm	5 mm	5 mm	9 mm	9 mm	13 mm	13 mm	17mm	17mm		
Major	Minor	Major	Minor	Major	Minor	Major	Minor	Major	Minor		



12.76	0.84	5.79	1.54
4.73	2.27	5.80	1.53
12.04	0.89	8.62	1.03
11.55	0.92	9.51	0.93
10.96	0.97	3.76	2.33
13.98	0.76	3.41	2.56
10.81	0.98	3.68	2.37
6.26	1.68	8.10	1.07
3.42	3.07	8.62	1.01
6.74	1.55	3.95	2.20
11.37	0.92	8.86	0.98
10.29	1.01	4.27	2.02
4.63	2.23	7.88	1.09
3.95	2.61	5.87	1.46
8.74	1.18	11.71	0.73
5.60	1.83	8.03	1.07
11.66	0.88	8.58	1.00
7.47	1.36	8.21	1.04
9.51	1.06	4.01	2.13
12.01	0.84	3.78	2.26
7.36	1.36	10.01	0.86
3.70	2.69	11.79	0.73
12.13	0.82	5.39	1.58
4.07	2.42	3.24	2.63
9.74	1.01	5.61	1.52
10.99	0.89	7.95	1.07
3.61	2.72	8.76	0.97
12.41	0.79	8.36	1.01
3.42	2.84	7.03	1.20
10.62	0.91	11.54	0.73
3.80	2.53	7.24	1.16
14.30	0.67	6.85	1.21
10.26	0.93	7.88	1.05
10.07	0.95	7.05	1.17
3.70	2.55	6.60	1.25
8.07	1.17	4.76	1.71
7.14	1.31	4.33	1.88
9.12	1.02	3.69	2.20
11.92	0.78	5.15	1.57
10.94	0.85	3.52	2.30
5.46	1.70	4.16	1.93
7.53	1.24	9.64	0.83
5.20	1.79	8.34	0.96
3.45	2.68	8.32	0.96
7.36	1.26	4.89	1.63
11.16	0.82	10.47	0.76
11.16	0.82	5.79	1.36
10.99	0.83	6.75	1.16
5.31	1.73	3.93	1.98
11.32	0.80	8.60	0.90
4.98	1.82	10.08	0.77

				13.53	0.67				5.85	1.32
				3.52	2.56				7.59	1.02
0 mm	0 mm	5 mm	5 mm	9 mm	9 mm	13 mm	13 mm	17mm	17mm	
Major	Minor	Major	Minor	Major	Minor	Major	Minor	Major	Minor	
				9.51	0.95			7.33	1.05	
				6.04	1.49			6.45	1.19	
				4.77	1.88			3.04	2.53	
				6.12	1.46			7.98	0.96	
				3.35	2.66			4.67	1.63	
				10.98	0.81			4.95	1.54	
				4.37	2.04			11.97	0.64	
				7.06	1.26			8.57	0.89	
				10.46	0.84			9.90	0.76	
				4.65	1.89			5.52	1.37	
				5.54	1.58			9.62	0.78	
				8.87	0.99			8.39	0.89	
				8.25	1.06			7.40	1.01	
				7.32	1.19			8.55	0.87	
				13.80	0.63			6.16	1.21	
				7.78	1.12			5.71	1.29	
				5.06	1.70			7.13	1.04	
				11.57	0.74			4.02	1.82	
				10.58	0.81			4.20	1.71	
				7.95	1.08			6.91	1.04	
				12.26	0.70			15.95	0.45	
				10.82	0.79			6.46	1.11	
				11.97	0.71			11.08	0.65	
				3.45	2.45			4.20	1.70	
				9.04	0.93			5.36	1.33	
				7.50	1.12			8.63	0.83	
				5.12	1.63			6.23	1.15	
				12.90	0.64			3.61	1.97	
				8.72	0.95			10.91	0.65	
				5.93	1.40			6.72	1.05	
				4.83	1.71			7.91	0.90	
				7.62	1.08			6.88	1.03	
				5.20	1.58			3.81	1.85	
				13.42	0.61			7.55	0.93	
				7.92	1.04			4.34	1.62	
				12.87	0.64			4.35	1.61	
				13.75	0.59			6.97	1.00	
				12.88	0.63			8.70	0.80	
				10.56	0.77			5.13	1.36	
				3.04	2.68			4.14	1.69	
				8.35	0.97			5.26	1.32	
				4.06	1.99			6.39	1.09	
				6.88	1.17			8.84	0.78	
				11.58	0.70			4.02	1.72	
				3.63	2.22			10.32	0.67	
				6.55	1.23			3.35	2.06	
				10.48	0.77			4.58	1.50	

				5.90	1.36			7.90	0.87
				5.66	1.42			7.39	0.92
				7.57	1.06			5.08	1.33
				3.54	2.26			2.89	2.34
				9.80	0.81			5.66	1.19
				6.43	1.23			3.94	1.71
0 mm	0 mm	5 mm	5 mm	9 mm	9 mm	13 mm	13 mm	17mm	17mm
Major	Minor	Major	Minor	Major	Minor	Major	Minor	Major	Minor
				6.53	1.21			5.97	1.13
				3.13	2.52			3.05	2.19
				5.71	1.38			6.17	1.08
				3.39	2.32			6.06	1.09
				9.04	0.86			4.72	1.40
				4.36	1.77			6.38	1.04
				13.02	0.59			6.34	1.04
				7.93	0.97			2.70	2.43
				9.49	0.80			7.43	0.88
				8.73	0.87			5.26	1.24
				3.74	2.01			9.07	0.72
				11.06	0.68			4.02	1.63
				8.25	0.91			5.39	1.21
				6.50	1.14			7.07	0.92
				5.51	1.35			4.86	1.33
				4.18	1.77			6.34	1.02
				6.20	1.19			5.96	1.08
				4.02	1.84			5.51	1.17
				5.43	1.35			6.75	0.95
				3.03	2.41			5.20	1.24
				8.52	0.85			7.26	0.88
				8.27	0.87			7.57	0.85
				4.61	1.57			4.23	1.52
				5.83	1.23			8.54	0.75
				8.28	0.87			7.33	0.87
				6.87	1.04			6.15	1.03
				3.32	2.14			7.01	0.91
				8.21	0.86			6.25	1.01
				5.56	1.27			5.62	1.12
				5.90	1.19			4.82	1.30
				4.80	1.47			3.38	1.85
				9.20	0.76			4.14	1.51
				7.54	0.93			3.95	1.59
				7.69	0.91			8.52	0.74
				4.22	1.65			9.80	0.63
				7.64	0.91			6.84	0.90
				4.39	1.57			7.80	0.79
				3.23	2.14			3.89	1.59
				8.29	0.83			4.60	1.33
				3.41	2.00			4.02	1.52
				7.75	0.88			8.12	0.75
				15.17	0.45			5.38	1.13
				6.25	1.09			5.82	1.04

				4.63	1.46			5.11	1.18
				6.59	1.02			5.21	1.16
				6.05	1.12			6.98	0.85
				3.93	1.72			3.95	1.50
				6.42	1.05			6.69	0.89
				6.20	1.08			5.51	1.07
				10.94	0.61			6.99	0.84
				5.63	1.18			6.07	0.97
				5.55	1.19			4.11	1.43
				3.24	2.05			4.44	1.31
0 mm	0 mm	5 mm	5 mm	9 mm	9 mm	13 mm	13 mm	17mm	17mm
Major	Minor	Major	Minor	Major	Minor	Major	Minor	Major	Minor
				5.25	1.26			4.56	1.27
				5.34	1.23			6.61	0.88
				6.16	1.06			5.87	0.99
				3.04	2.15			4.90	1.18
				9.47	0.69			6.86	0.84
				6.68	0.98			6.05	0.96
				5.49	1.19			7.72	0.75
				9.87	0.66			4.60	1.25
				5.66	1.14			3.22	1.79
				4.41	1.46			5.93	0.97
				6.88	0.94			7.78	0.74
				7.31	0.88			2.83	2.02
				7.31	0.88			4.50	1.27
				8.26	0.78			5.86	0.97
				6.06	1.06			3.20	1.77
				4.16	1.53			5.95	0.95
				5.91	1.08			3.34	1.70
				4.86	1.30			5.20	1.09
				3.30	1.92			10.33	0.55
				6.61	0.95			10.41	0.54
				7.71	0.81			4.17	1.34
				10.58	0.59			4.46	1.25
				6.22	1.00			3.45	1.61
				3.56	1.75			2.92	1.89
				8.22	0.76			5.07	1.08
				6.15	1.01			6.25	0.87
				7.91	0.79			3.83	1.42
				6.30	0.98			7.97	0.68
				5.14	1.21			4.81	1.12
				3.93	1.57			3.34	1.60
				7.01	0.88			3.89	1.37
				8.24	0.75			8.42	0.63
				7.71	0.79			5.29	1.00
				5.84	1.05			4.74	1.12
				2.95	2.06			4.94	1.07
				3.22	1.88			4.98	1.06
				11.06	0.55			3.38	1.56
				6.63	0.91			6.54	0.80
				6.54	0.92			6.25	0.84

				5.93	1.02			4.15	1.26
				9.90	0.61			6.96	0.75
				3.54	1.69			2.49	2.08
				8.68	0.68			7.64	0.68
				2.91	2.03			4.87	1.06
				7.27	0.81			3.77	1.37
				4.38	1.34			7.52	0.69
				4.87	1.21			2.92	1.76
				9.09	0.64			5.67	0.91
				4.26	1.37			2.92	1.76
				5.38	1.08			2.78	1.84
				8.91	0.65			2.85	1.79
				3.72	1.55			5.82	0.87
				6.86	0.84			6.28	0.81
0 mm	0 mm	5 mm	5 mm	9 mm	9 mm	13 mm	13 mm	17mm	17mm
Major	Minor	Major	Minor	Major	Minor	Major	Minor	Major	Minor
				10.32	0.55			3.16	1.61
				5.70	1.01			3.89	1.31
				3.81	1.50			7.83	0.65
				5.03	1.14			3.01	1.68
				3.51	1.61			5.58	0.91
				5.68	1.00			6.68	0.75
				2.63	2.14			3.84	1.30
				4.30	1.30			2.59	1.93
				4.10	1.37			5.10	0.98
				5.07	1.10			6.81	0.73
				3.19	1.75			4.00	1.24
				8.14	0.68			4.30	1.14
				6.72	0.83			4.02	1.21
				8.08	0.69			3.06	1.59
				5.30	1.05			6.48	0.74
				5.85	0.95			4.58	1.05
				7.39	0.75			4.48	1.08
				6.01	0.92			3.75	1.29
				6.19	0.89			5.76	0.84
				6.44	0.85			4.01	1.20
				2.94	1.86			3.52	1.36
				3.86	1.41			8.39	0.57
				3.90	1.39			3.94	1.21
				5.64	0.96			4.79	0.99
				5.53	0.97			3.15	1.50
				8.91	0.60			3.92	1.20
				6.99	0.77			5.76	0.82
				2.76	1.94			2.62	1.77
				3.32	1.60			2.64	1.76
				6.06	0.88			5.59	0.83
				6.65	0.80			3.19	1.45
				6.50	0.81			2.69	1.72
				3.68	1.42			5.13	0.90
				2.66	1.97			5.75	0.80
				6.02	0.87			3.99	1.15

				6.15	0.84			7.95	0.58
				4.97	1.04			4.47	1.02
				5.71	0.90			2.81	1.62
				3.87	1.32			2.81	1.62
				2.67	1.92			7.91	0.57
				7.21	0.71			5.40	0.83
				9.81	0.52			3.31	1.36
				6.09	0.83			4.82	0.92
				5.86	0.86			4.10	1.09
				6.64	0.75			3.20	1.38
				4.82	1.03			3.86	1.14
				2.40	2.07			4.18	1.05
				2.91	1.71			7.25	0.60
				4.61	1.08			3.63	1.20
				5.02	0.99			7.30	0.59
				3.43	1.44			3.64	1.19
				2.93	1.68			3.78	1.15
				3.19	1.53			2.43	1.78
0 mm	0 mm	5 mm	5 mm	9 mm	9 mm	13 mm	13 mm	17mm	17mm
Major	Minor	Major	Minor	Major	Minor	Major	Minor	Major	Minor
				7.75	0.63			3.03	1.42
				5.44	0.89			2.30	1.87
				7.52	0.65			3.64	1.18
				2.87	1.69			4.59	0.93
				5.21	0.93			4.24	1.00
				5.17	0.93			5.74	0.73
				12.16	0.39			7.01	0.60
				4.83	0.99			4.08	1.03
				6.28	0.76			2.65	1.58
				2.93	1.63			4.03	1.04
				6.49	0.73			4.54	0.92
				5.74	0.83			3.41	1.21
				4.91	0.97			2.77	1.49
				5.18	0.92			2.78	1.47
				3.84	1.21			2.64	1.55
				6.58	0.70			6.19	0.66
				6.15	0.74			2.73	1.49
				6.67	0.68			3.90	1.04
				3.73	1.21			4.84	0.84
				4.01	1.13			3.92	1.02
				7.13	0.63			4.07	0.98
				4.68	0.97			7.67	0.51
				2.85	1.58			6.78	0.57
				2.85	1.58			3.54	1.09
				5.64	0.80			4.49	0.86
				5.87	0.76			4.23	0.91
				3.98	1.12			5.11	0.75
				3.16	1.41			2.41	1.58
				4.19	1.06			2.77	1.36
				2.68	1.66			5.35	0.70
				9.59	0.47			6.35	0.59

				5.06	0.88			4.74	0.78
				3.31	1.34			3.75	0.98
				4.30	1.03			6.36	0.57
				4.90	0.89			3.30	1.10
				6.49	0.66			5.44	0.66
				6.97	0.62			2.31	1.55
				6.57	0.66			3.33	1.07
				6.96	0.62			3.98	0.89
				3.57	1.20			5.13	0.69
				7.29	0.59			3.12	1.12
				4.85	0.88			4.06	0.86
				6.27	0.68			6.34	0.55
				6.81	0.62			3.57	0.97
				7.45	0.56			2.62	1.32
				4.57	0.91			2.30	1.49
				3.19	1.30			1.93	1.78
				4.14	1.00			4.17	0.82
				4.20	0.98			4.91	0.70
				3.52	1.16			4.59	0.74
				2.67	1.52			8.10	0.42
				4.48	0.90			4.76	0.71
				3.57	1.13			3.18	1.06
0 mm	0 mm	5 mm	5 mm	9 mm	9 mm	13 mm	13 mm	17mm	17mm
Major	Minor	Major	Minor	Major	Minor	Major	Minor	Major	Minor
				6.43	0.61			8.10	0.41
				5.87	0.66			4.09	0.80
				5.14	0.75			2.86	1.15
				4.27	0.90			5.07	0.64
				4.41	0.86			4.01	0.80
				4.17	0.90			2.95	1.08
				3.33	1.13			2.56	1.25
				3.58	1.04			3.82	0.83
				7.62	0.49			3.82	0.83
				8.67	0.43			1.99	1.59
				2.09	1.77			3.66	0.85
				3.54	1.04			2.84	1.09
				3.99	0.91			3.40	0.90
				4.49	0.80			2.25	1.37
				4.57	0.79			2.37	1.27
				4.98	0.73			3.25	0.93
				4.05	0.89			6.08	0.50
				2.48	1.45			4.36	0.68
				2.70	1.32			3.22	0.92
				3.36	1.06			3.28	0.89
				5.94	0.59			4.05	0.72
				5.38	0.65			2.86	1.02
				7.20	0.48			5.10	0.57
				3.60	0.96			4.72	0.62
				5.89	0.59			3.50	0.84
				3.01	1.15			2.46	1.18
				4.57	0.76			2.08	1.39

				5.35	0.64				3.70	0.77
				2.55	1.35				4.01	0.71
				3.31	1.04				2.35	1.21
				4.24	0.80				2.25	1.26
				4.37	0.77				3.17	0.88
				2.50	1.32				3.24	0.87
				6.36	0.52				3.29	0.85
				3.33	0.99				2.11	1.33
				3.44	0.96				4.06	0.68
				4.76	0.69				1.97	1.39
				3.97	0.82				3.65	0.74
				3.47	0.93				4.09	0.66
				2.97	1.09				1.89	1.42
				3.65	0.88				3.73	0.72
				4.37	0.73				2.62	1.03
				3.14	1.00				4.34	0.62
				4.07	0.76				3.19	0.83
				6.32	0.49				3.25	0.81
				3.62	0.85				4.64	0.57
				2.38	1.28				1.83	1.43
				4.43	0.68				5.52	0.47
				5.38	0.56				3.11	0.82
				2.48	1.22				2.11	1.21
				3.30	0.91				2.47	1.02
				4.75	0.63				2.82	0.90
				3.11	0.96				3.15	0.80
0 mm	0 mm	5 mm	5 mm	9 mm	9 mm	13 mm	13 mm	17mm	17mm	
Major	Minor	Major	Minor	Major	Minor	Major	Minor	Major	Minor	
				5.50	0.54			2.01	1.26	
				4.72	0.63			2.25	1.11	
				5.80	0.51			1.95	1.28	
				3.24	0.90			2.76	0.89	
				4.48	0.65			2.13	1.15	
				4.23	0.69			2.73	0.89	
				3.11	0.93			3.49	0.68	
				5.06	0.57			3.64	0.65	
				3.14	0.91			4.18	0.55	
				3.89	0.72			2.27	1.01	
				3.01	0.93			1.67	1.37	
				3.99	0.70			3.11	0.74	
				3.95	0.70			4.63	0.49	
				2.46	1.12			5.18	0.43	
				5.49	0.50			2.57	0.87	
				3.30	0.82			2.02	1.10	
				4.74	0.57			3.73	0.60	
				3.62	0.75			3.32	0.65	
				5.27	0.51			2.68	0.79	
				4.29	0.62			4.30	0.49	
				2.08	1.29			2.49	0.84	
				8.62	0.31			2.62	0.78	
				3.93	0.68			4.75	0.43	



				5.73	0.46				1.97	1.02
				5.22	0.51				1.78	1.12
				7.53	0.35				2.69	0.74
				3.84	0.69				2.35	0.85
				3.44	0.76				2.35	0.85
				3.80	0.69				1.92	1.04
				4.58	0.57				1.62	1.21
				2.88	0.90				2.77	0.70
				5.06	0.51				3.36	0.55
				3.22	0.80				2.43	0.75
				4.21	0.59				2.33	0.78
				2.90	0.86				2.75	0.66
				3.61	0.68				3.18	0.57
				2.79	0.89				2.60	0.70
				5.18	0.48				1.54	1.16
				1.93	1.26				1.80	0.97
				3.31	0.74				3.78	0.45
				2.89	0.84				1.97	0.84
				3.01	0.79				1.62	1.02
				2.96	0.80				1.70	0.98
				2.85	0.83				1.40	1.16
				3.87	0.61				1.90	0.86
				4.05	0.57				2.92	0.56
				2.74	0.84				2.90	0.56
				5.27	0.43				3.18	0.51
				4.33	0.52				3.56	0.45
				2.79	0.81				2.09	0.77
				3.06	0.73				2.19	0.72
				3.27	0.68				2.21	0.70
				5.84	0.38				1.77	0.85
0 mm	0 mm	5 mm	5 mm	9 mm	9 mm	13 mm	13 mm	17mm	17mm	
Major	Minor	Major	Minor	Major	Minor	Major	Minor	Major	Minor	
				2.84	0.78			3.48	0.43	
				2.69	0.81			2.34	0.63	
				2.52	0.86			1.49	0.97	
				3.08	0.70			2.09	0.69	
				3.55	0.61			1.93	0.73	
				3.28	0.65			1.50	0.95	
				3.37	0.63			1.79	0.77	
				2.57	0.82			1.92	0.72	
				2.67	0.79			1.94	0.67	
				2.68	0.78			2.85	0.46	
				2.05	1.01			1.95	0.66	
				3.31	0.61			2.38	0.53	
				3.31	0.61			1.83	0.67	
				2.72	0.74			2.02	0.60	
				4.73	0.42			1.75	0.69	
				4.83	0.41			1.52	0.79	
				2.56	0.75			1.68	0.72	
				2.09	0.92			1.75	0.67	
				2.65	0.73			1.17	1.00	

				5.62	0.34				1.81	0.62
				5.21	0.37				1.16	0.93
				3.01	0.62				1.89	0.58
				1.68	1.11				2.17	0.47
				2.87	0.63				1.81	0.57
				3.33	0.53				2.16	0.45
				5.23	0.33				1.31	0.69
				2.85	0.59				1.11	0.73
				1.60	1.05				1.22	0.62
				2.77	0.61				1.14	0.64
				3.67	0.45				1.14	0.64
				1.96	0.85				1.62	0.41
				4.37	0.37				4.20	0.14
				3.01	0.53				1.61	0.34
				1.61	0.99				2.23	0.23
				4.32	0.36				0.72	0.38
				2.31	0.68					
				1.98	0.78					
				1.48	1.04					
				2.88	0.53					
				2.58	0.57					
				2.23	0.66					
				1.89	0.75					
				2.02	0.68					
				3.78	0.37					
				2.23	0.58					
				1.98	0.64					
				2.59	0.48					
				2.56	0.47					
				1.62	0.69					
				2.31	0.48					
				2.58	0.43					
				1.87	0.55					
				2.01	0.51					
0 mm	0 mm	5 mm	5 mm	9 mm	9 mm	13 mm	13 mm	17mm	17mm	
Major	Minor	Major	Minor	Major	Minor	Major	Minor	Major	Minor	
				1.15	0.86					
				4.21	0.22					
				2.35	0.38					
				2.25	0.39					
				1.51	0.56					
				1.66	0.51					
				1.78	0.44					
				1.02	0.77					
				1.43	0.50					
				1.14	0.64					
				1.29	0.54					
				1.12	0.62					
				2.30	0.25					
				0.97	0.50					

### Appendix 3: Large Pumice Data for Chapter 4

#### Axes measurements in Microns

0 mm	0 mm	8 mm	8 mm	18 mm	18 mm	27 mm	27 mm	38 mm	38 mm
Major	Minor	Major	Minor	Major	Minor	Major	Minor	Major	Minor
27.21	7.81	29.85	3.37	33.93	4.98	33.79	6.84	26.24	13.04
12.40	7.81	34.30	2.92	27.62	5.37	28.66	6.37	31.35	10.74
16.48	5.75	11.85	8.39	32.36	4.56	16.65	8.61	25.56	7.17
9.85	6.73	32.99	2.87	23.27	6.28	37.73	3.36	29.92	6.12
22.10	2.81	14.98	5.69	25.69	4.44	27.15	4.01	22.30	4.53
20.01	2.65	15.76	5.20	26.85	3.99	26.20	4.11	18.72	5.30
20.91	2.44	29.42	2.76	21.12	4.49	22.74	4.59	26.38	3.18
30.59	1.63	23.69	3.30	31.67	2.82	13.45	7.67	25.31	3.21
12.85	3.80	19.81	3.64	27.91	3.16	14.73	6.70	28.29	2.84
13.48	3.61	21.68	3.31	11.35	7.45	23.74	4.08	13.16	5.81
11.36	4.15	15.97	4.49	28.18	2.85	14.09	6.87	28.33	2.38
17.29	2.68	35.37	2.00	25.90	3.09	20.44	4.72	15.61	4.06
32.71	1.37	19.05	3.68	26.31	2.91	18.41	5.19	18.25	3.22
13.96	3.16	8.64	8.00	27.91	2.64	23.35	4.05	24.74	2.35
9.45	4.67	29.81	2.31	16.84	4.10	26.82	3.52	11.80	4.82
20.17	1.99	9.81	6.77	11.90	5.69	20.07	4.65	12.09	4.18
7.41	5.27	24.04	2.70	23.24	2.90	17.76	5.17	16.88	2.98
12.30	3.14	11.08	5.68	9.94	6.43	28.49	3.22	14.39	3.31
6.64	5.16	18.66	3.27	20.37	3.03	33.45	2.67	11.52	4.00
9.80	3.27	16.10	3.73	9.76	6.24	9.90	8.18	21.17	2.09
12.86	2.44	11.12	5.28	24.18	2.51	16.54	4.82	20.80	2.05
7.01	4.43	12.05	4.80	15.42	3.84	23.09	3.43	11.01	3.85
10.19	3.02	21.54	2.60	19.84	2.92	18.80	4.04	12.47	3.38
13.00	2.35	8.62	5.91	15.46	3.72	17.88	4.16	13.19	3.15
12.82	2.30	10.46	4.86	32.36	1.76	25.32	2.85	12.03	3.37
7.25	3.96	8.57	5.83	14.05	4.04	22.84	3.11	25.34	1.58
5.81	4.91	16.56	2.99	21.21	2.64	29.67	2.39	16.89	2.36
10.70	2.58	28.35	1.72	18.81	2.97	27.26	2.59	18.77	2.11
7.42	3.65	9.01	5.27	24.99	2.14	28.08	2.47	15.37	2.49
18.07	1.47	7.77	6.07	23.85	2.13	21.08	3.21	6.86	5.55
12.51	2.02	16.94	2.63	18.87	2.63	16.19	4.12	17.78	2.10
15.53	1.61	7.26	6.07	26.45	1.86	11.33	5.83	10.45	3.55
7.55	3.24	12.37	3.55	16.66	2.91	15.95	4.13	20.46	1.77
9.39	2.55	7.90	5.55	24.78	1.84	17.64	3.69	8.33	4.33
13.97	1.70	14.78	2.97	9.46	4.74	8.88	7.25	9.88	3.58
6.07	3.91	9.77	4.38	20.11	2.20	13.56	4.65	6.31	5.61
10.23	2.30	11.88	3.56	12.94	3.42	24.54	2.51	18.97	1.86
16.93	1.36	6.90	6.02	10.87	4.01	21.15	2.82	15.64	2.22
21.81	1.04	14.63	2.82	25.74	1.69	9.66	6.14	10.65	3.21
5.91	3.73	8.00	4.76	18.61	2.31	27.16	2.15	10.40	3.28
4.87	4.52	11.97	3.12	16.63	2.54	22.54	2.59	7.16	4.72
9.07	2.41	9.66	3.86	29.56	1.43	22.19	2.62	12.98	2.55
14.64	1.48	14.05	2.59	15.20	2.76	25.39	2.25	10.59	3.05
13.50	1.59	11.90	2.99	9.49	4.42	33.56	1.69	9.21	3.38
11.56	1.83	11.52	3.06	17.49	2.38	27.99	1.98	16.44	1.86
10.72	1.95	7.71	4.57	13.12	3.07	13.46	4.10	6.76	4.53
16.33	1.27	7.71	4.57	13.67	2.92	10.12	5.34	15.70	1.95

11.74	1.71	9.15	3.76	9.64	3.90	33.12	1.62	9.02	3.36
18.84	1.04	17.77	1.89	8.36	4.49	14.88	3.54	8.99	3.37
9.01	2.17	9.91	3.37	20.92	1.79	24.98	2.07	13.39	2.24
20.15	0.96	18.12	1.83	17.40	2.09	11.53	4.47	11.48	2.61
0 mm	0 mm	8 mm	8 mm	18 mm	18 mm	27 mm	27 mm	38 mm	38 mm
Major	Minor	Major	Minor	Major	Minor	Major	Minor	Major	Minor
15.36	1.25	14.78	2.21	18.21	1.99	22.18	2.32	18.67	1.60
22.42	0.84	6.70	4.83	7.15	4.99	22.48	2.28	10.08	2.96
6.79	2.79	13.30	2.43	8.78	4.00	15.28	3.09	16.55	1.79
24.26	0.78	20.03	1.60	7.59	4.60	8.56	5.45	18.90	1.55
7.94	2.32	10.01	3.14	18.63	1.87	10.53	4.36	15.45	1.89
6.31	2.88	9.06	3.46	14.97	2.32	27.34	1.66	7.83	3.65
15.20	1.19	6.02	5.08	20.89	1.64	8.22	5.52	15.14	1.88
15.73	1.15	9.49	3.18	6.38	5.16	12.95	3.48	11.64	2.36
5.63	3.15	10.47	2.85	29.42	1.11	28.95	1.54	10.59	2.60
12.23	1.42	7.50	3.95	8.59	3.76	10.55	4.22	7.01	3.91
4.93	3.42	8.71	3.36	20.89	1.55	18.55	2.38	6.14	4.46
21.78	0.76	13.45	2.12	19.30	1.66	12.17	3.59	19.18	1.42
11.29	1.46	11.43	2.50	19.52	1.64	13.40	3.19	10.35	2.50
9.31	1.76	17.30	1.60	17.48	1.81	20.89	1.97	5.77	4.47
16.94	0.96	6.66	4.15	13.01	2.43	12.06	3.41	12.30	2.09
8.32	1.95	19.50	1.39	8.02	3.90	15.01	2.72	16.04	1.59
5.54	2.91	6.60	4.09	18.62	1.68	22.84	1.79	12.85	1.97
11.49	1.40	15.31	1.75	14.58	2.13	8.77	4.64	5.85	4.32
9.28	1.71	23.67	1.11	12.12	2.50	7.55	5.35	14.95	1.69
7.64	2.07	12.91	2.03	12.35	2.45	6.85	5.78	13.99	1.79
6.90	2.29	10.02	2.61	17.87	1.66	29.82	1.31	14.70	1.69
8.24	1.91	16.71	1.54	17.15	1.70	14.39	2.68	6.87	3.61
11.45	1.35	18.41	1.39	9.73	2.98	16.96	2.27	11.99	2.05
4.56	3.34	11.10	2.31	6.84	4.15	13.61	2.75	10.48	2.34
14.75	1.03	10.24	2.44	5.55	5.11	17.50	2.14	11.94	2.05
10.79	1.40	7.23	3.46	9.33	2.94	24.29	1.50	10.09	2.42
12.34	1.20	6.74	3.63	11.02	2.43	15.05	2.41	13.96	1.73
12.92	1.14	18.12	1.32	13.53	1.98	9.22	3.91	13.68	1.73
6.60	2.22	6.72	3.48	16.33	1.61	16.65	2.16	11.96	1.96
14.85	0.98	14.44	1.61	13.92	1.87	23.10	1.55	6.70	3.46
16.40	0.88	8.16	2.80	17.18	1.51	19.42	1.82	17.25	1.34
11.52	1.25	5.88	3.87	8.50	3.02	13.03	2.66	6.99	3.28
11.34	1.24	9.67	2.35	14.32	1.77	21.26	1.62	6.91	3.32
5.11	2.74	16.23	1.40	7.95	3.18	10.39	3.31	6.28	3.61
15.39	0.88	5.22	4.29	5.76	4.33	8.56	4.00	8.45	2.67
5.99	2.20	7.31	3.07	20.04	1.23	19.59	1.73	16.22	1.37
12.43	1.03	11.61	1.87	8.57	2.84	13.91	2.41	9.42	2.36
17.15	0.75	13.59	1.60	11.40	2.13	19.18	1.72	8.72	2.55
14.39	0.86	6.60	3.29	5.98	3.96	13.81	2.38	8.07	2.74
4.32	2.86	6.35	3.40	20.97	1.13	6.28	5.22	14.53	1.51
10.37	1.18	10.09	2.13	13.01	1.80	16.80	1.87	10.07	2.10
9.96	1.21	16.81	1.26	6.21	3.74	17.20	1.81	16.71	1.26
4.34	2.75	15.44	1.36	11.84	1.95	6.74	4.61	7.31	2.78
4.98	2.38	6.16	3.40	8.48	2.68	9.41	3.23	10.16	1.98
4.02	2.92	7.01	2.96	6.40	3.51	6.99	4.34	7.44	2.69

12.96	0.90	10.55	1.94	5.51	4.04	13.66	2.21	11.66	1.71
10.48	1.11	24.29	0.84	12.52	1.78	17.35	1.74	5.33	3.71
9.74	1.19	8.07	2.50	15.77	1.39	16.48	1.82	7.21	2.72
7.30	1.58	9.02	2.23	14.05	1.53	10.58	2.82	6.94	2.82
10.28	1.12	14.09	1.42	15.56	1.33	7.27	4.04	10.06	1.94
12.03	0.94	14.02	1.42	10.48	1.98	14.53	2.00	6.83	2.86
15.62	0.72	6.18	3.19	8.54	2.42	16.46	1.74	10.53	1.85
11.73	0.95	5.24	3.65	5.97	3.44	6.84	4.17	18.16	1.07
0 mm	0 mm	8 mm	8 mm	18 mm	18 mm	27 mm	27 mm	38 mm	38 mm
Major	Minor	Major	Minor	Major	Minor	Major	Minor	Major	Minor
10.48	1.06	7.24	2.62	15.39	1.30	9.95	2.81	7.33	2.62
9.18	1.20	10.11	1.87	6.74	2.93	12.16	2.29	7.38	2.57
10.09	1.09	5.66	3.27	12.72	1.51	6.39	4.33	9.14	2.06
8.92	1.22	4.48	4.08	8.84	2.16	23.51	1.15	8.03	2.34
9.38	1.15	6.60	2.74	10.69	1.77	22.03	1.23	16.24	1.16
6.33	1.70	5.53	3.27	10.95	1.72	7.38	3.66	11.10	1.69
8.41	1.27	13.45	1.34	5.71	3.28	8.87	3.02	8.21	2.25
6.01	1.76	4.81	3.69	20.19	0.91	18.76	1.42	7.64	2.41
3.70	2.86	7.78	2.27	20.19	0.91	6.09	4.34	11.18	1.64
9.50	1.11	13.72	1.29	12.92	1.42	13.50	1.96	10.02	1.83
9.95	1.05	13.36	1.29	4.98	3.66	25.39	1.04	8.20	2.20
14.36	0.72	15.86	1.08	8.72	2.07	6.13	4.30	5.96	3.02
10.44	0.99	9.22	1.86	11.18	1.60	18.86	1.39	9.57	1.87
10.08	1.01	7.67	2.21	5.73	3.12	16.21	1.61	8.74	2.04
6.57	1.55	7.97	2.11	11.02	1.62	13.38	1.88	10.55	1.68
5.63	1.80	8.53	1.94	4.76	3.74	9.22	2.71	9.43	1.84
6.47	1.54	9.03	1.83	8.63	2.05	5.93	4.17	10.81	1.60
5.19	1.92	6.68	2.45	12.62	1.40	11.58	2.12	11.42	1.51
4.71	2.10	11.36	1.44	10.30	1.71	12.99	1.88	9.63	1.77
7.04	1.40	18.91	0.86	5.58	3.13	5.78	4.22	8.26	2.07
10.65	0.91	4.80	3.40	11.60	1.50	5.22	4.65	11.34	1.50
19.04	0.51	4.48	3.63	12.82	1.35	18.61	1.30	11.56	1.47
10.71	0.90	15.14	1.05	14.23	1.21	6.65	3.64	9.89	1.71
3.72	2.59	8.04	1.97	4.97	3.45	11.68	2.05	12.83	1.31
7.78	1.24	5.39	2.90	9.28	1.85	10.03	2.35	7.92	2.13
7.98	1.19	6.19	2.52	9.01	1.89	5.22	4.49	7.52	2.22
7.47	1.27	14.57	1.06	8.29	2.06	19.58	1.15	12.65	1.31
13.96	0.67	7.91	1.94	5.54	3.07	8.41	2.69	9.70	1.69
3.15	2.94	12.74	1.19	8.63	1.92	11.79	1.91	8.74	1.87
12.69	0.73	4.28	3.52	4.65	3.52	4.92	4.53	6.92	2.35
8.79	1.04	11.02	1.37	11.01	1.46	5.22	4.23	5.77	2.82
10.32	0.88	4.34	3.42	8.14	1.95	9.03	2.44	8.69	1.86
8.38	1.08	12.72	1.17	9.50	1.66	5.40	4.05	12.91	1.25
8.72	1.03	10.10	1.47	12.30	1.27	6.62	3.29	10.76	1.50
5.90	1.48	4.62	3.20	11.10	1.41	7.16	3.04	9.52	1.68
6.00	1.40	7.84	1.88	8.93	1.74	19.48	1.11	11.61	1.38
5.01	1.68	13.04	1.13	6.51	2.36	5.41	3.95	5.32	2.95
7.25	1.13	8.02	1.83	10.77	1.42	11.24	1.89	10.57	1.47
12.08	0.67	11.87	1.23	5.61	2.67	9.28	2.27	7.03	2.20
8.34	0.97	5.04	2.89	8.52	1.75	16.54	1.25	9.60	1.60
4.09	1.96	8.16	1.77	7.33	2.02	18.16	1.13	8.16	1.87

8.25	0.97	10.54	1.36	7.38	1.97	5.78	3.53	7.14	2.14
13.67	0.58	9.33	1.54	4.92	2.94	15.65	1.30	6.71	2.26
5.73	1.39	10.06	1.41	10.24	1.41	18.95	1.07	10.54	1.40
9.16	0.85	12.47	1.13	4.80	2.99	4.91	4.10	9.05	1.63
6.36	1.22	10.36	1.36	4.60	3.09	10.91	1.83	6.33	2.33
4.63	1.67	7.04	2.00	5.50	2.54	5.17	3.85	9.59	1.53
12.08	0.63	11.57	1.21	12.53	1.08	5.29	3.76	6.52	2.25
5.67	1.33	7.74	1.79	6.79	2.00	9.30	2.12	17.94	0.81
6.47	1.16	5.36	2.56	3.91	3.47	4.70	4.13	8.59	1.69
3.30	2.28	4.16	3.26	5.88	2.23	19.73	0.98	6.24	2.30
8.50	0.88	17.48	0.77	4.74	2.76	11.50	1.67	9.26	1.54
7.42	1.01	4.21	3.20	3.98	3.25	11.27	1.69	9.14	1.56
0 mm	0 mm	8 mm	8 mm	18 mm	18 mm	27 mm	27 mm	38 mm	38 mm
Major	Minor	Major	Minor	Major	Minor	Major	Minor	Major	Minor
8.44	0.88	9.32	1.42	5.61	2.30	18.64	1.02	8.54	1.64
7.35	1.01	13.18	1.00	6.14	2.07	6.20	3.07	7.65	1.81
4.75	1.55	14.39	0.92	7.52	1.69	10.98	1.71	5.07	2.73
9.68	0.76	4.93	2.62	6.65	1.90	6.76	2.74	6.49	2.13
3.41	2.07	9.39	1.37	10.64	1.18	8.77	2.10	3.80	3.62
6.88	1.02	16.19	0.79	5.63	2.21	16.67	1.10	6.22	2.20
6.53	1.07	5.87	2.18	9.44	1.32	4.47	4.09	5.10	2.67
10.90	0.63	5.19	2.43	4.60	2.57	5.39	3.35	6.56	2.07
3.32	2.06	3.71	3.36	3.66	3.22	5.29	3.39	5.64	2.40
8.54	0.80	14.11	0.88	10.42	1.12	5.87	3.05	7.79	1.73
5.73	1.19	4.72	2.61	4.66	2.49	9.91	1.78	5.78	2.33
7.39	0.90	5.28	2.29	5.00	2.27	9.20	1.88	4.46	3.01
3.48	1.91	16.02	0.74	5.93	1.90	8.56	2.01	7.38	1.80
11.00	0.60	15.50	0.77	6.88	1.61	10.89	1.57	4.07	3.27
10.02	0.66	4.25	2.79	7.87	1.40	9.67	1.76	8.21	1.62
3.92	1.68	5.41	2.18	10.10	1.06	34.24	0.49	8.46	1.54
3.38	1.95	10.98	1.06	6.19	1.72	5.88	2.79	5.84	2.22
6.31	1.02	4.01	2.90	7.76	1.36	15.64	1.05	5.71	2.26
5.90	1.09	4.39	2.64	4.81	2.18	4.91	3.32	5.09	2.53
9.31	0.68	6.38	1.81	8.49	1.22	13.01	1.24	4.69	2.74
11.24	0.56	4.53	2.55	19.14	0.54	5.59	2.82	10.84	1.18
4.93	1.23	10.28	1.12	4.99	2.01	6.77	2.31	5.92	2.16
4.70	1.29	6.19	1.83	7.63	1.30	4.38	3.53	10.58	1.20
9.71	0.62	7.08	1.59	3.48	2.80	5.94	2.59	5.61	2.26
7.65	0.78	8.99	1.25	6.41	1.51	26.27	0.58	3.85	3.29
5.54	1.07	17.65	0.64	7.50	1.28	10.31	1.47	4.54	2.74
4.34	1.37	7.50	1.50	6.56	1.40	11.96	1.26	6.28	1.89
6.60	0.87	16.00	0.70	8.18	1.12	6.81	2.20	3.66	3.23
5.36	1.08	13.62	0.82	6.84	1.33	7.33	2.04	5.51	2.12
6.58	0.87	12.13	0.91	11.73	0.75	11.34	1.32	10.02	1.14
5.87	0.96	8.43	1.31	7.77	1.13	6.80	2.20	8.19	1.38
4.57	1.23	3.67	2.93	7.34	1.20	4.41	3.39	6.67	1.70
6.78	0.81	12.01	0.89	6.70	1.32	4.07	3.60	3.56	3.17
6.86	0.79	3.56	2.99	5.46	1.59	18.39	0.79	9.22	1.22
10.63	0.51	3.69	2.88	3.91	2.21	4.08	3.48	5.22	2.10
5.51	0.98	7.65	1.38	6.86	1.21	17.70	0.80	10.56	1.01
3.49	1.51	8.44	1.24	3.78	2.14	12.82	1.10	3.58	2.98

2.46	2.11	8.50	1.20	6.50	1.24	19.68	0.72	7.53	1.41
9.89	0.52	4.22	2.39	7.45	1.08	12.70	1.11	9.20	1.12
6.14	0.83	10.14	0.98	11.87	0.67	7.54	1.87	4.49	2.24
8.10	0.62	7.66	1.30	9.67	0.83	9.34	1.50	6.81	1.47
6.87	0.73	8.77	1.13	9.67	0.83	4.48	3.08	5.12	1.95
7.73	0.64	15.72	0.63	6.49	1.18	11.38	1.19	10.02	1.00
10.84	0.45	8.71	1.13	7.01	1.08	8.67	1.56	9.14	1.09
8.54	0.56	3.53	2.75	5.44	1.38	14.83	0.91	4.96	2.01
10.61	0.44	6.43	1.50	3.44	2.12	7.54	1.79	5.54	1.77
8.15	0.57	6.17	1.56	5.95	1.21	8.27	1.63	6.51	1.50
8.45	0.54	3.84	2.50	4.84	1.48	9.98	1.34	10.12	0.95
4.56	0.97	6.35	1.50	4.87	1.46	4.58	2.91	9.02	1.06
8.89	0.49	15.27	0.62	4.16	1.67	4.58	2.91	6.97	1.36
7.78	0.56	8.60	1.08	2.81	2.48	17.04	0.78	6.65	1.41
7.48	0.57	6.84	1.36	5.38	1.22	13.46	0.99	6.28	1.49
7.43	0.58	4.02	2.30	3.00	2.06	17.56	0.75	6.03	1.51
0 mm	0 mm	8 mm	8 mm	18 mm	18 mm	27 mm	27 mm	38 mm	38 mm
Major	Minor	Major	Minor	Major	Minor	Major	Minor	Major	Minor
3.71	1.15	10.16	0.90	4.98	1.20	9.46	1.39	6.51	1.40
6.16	0.69	9.84	0.93	2.82	2.09	8.63	1.51	6.73	1.34
8.82	0.47	7.62	1.18	2.66	2.18	16.87	0.77	4.41	2.05
6.63	0.61	9.66	0.93	2.89	1.88	12.33	1.04	5.18	1.69
9.07	0.44	16.92	0.53	3.24	1.66	17.75	0.71	3.37	2.58
3.05	1.28	4.19	2.10	4.50	1.16	8.15	1.54	3.09	2.79
3.04	1.27	5.15	1.69	3.82	1.36	5.60	2.24	6.81	1.25
7.30	0.52	8.92	0.97	4.32	1.18	4.11	3.05	3.88	2.16
2.50	1.50	5.07	1.71	2.77	1.79	15.47	0.81	5.34	1.55
6.60	0.56	8.69	0.99	4.78	1.03	5.93	2.09	5.28	1.55
7.18	0.49	7.79	1.10	4.91	0.99	5.41	2.27	5.99	1.34
4.33	0.82	7.66	1.11	4.04	1.20	12.51	0.98	5.42	1.48
6.61	0.52	4.15	2.04	5.86	0.79	5.08	2.41	9.32	0.86
4.59	0.73	5.96	1.41	4.88	0.94	5.04	2.41	3.20	2.47
1.95	1.70	8.43	1.00	2.73	1.67	11.99	1.01	2.98	2.62
6.52	0.51	4.22	1.99	4.89	0.86	14.09	0.85	6.95	1.05
4.86	0.68	9.42	0.89	2.50	1.64	5.67	2.12	3.56	2.05
5.52	0.58	7.35	1.13	2.95	1.06	5.11	2.34	5.71	1.23
3.99	0.80	4.94	1.68	2.20	1.06	6.27	1.90	4.74	1.48
10.50	0.30	8.86	0.93	3.37	0.67	13.47	0.88	3.61	1.93
6.36	0.49	11.39	0.72	2.18	0.78	18.53	0.64	6.71	1.03
8.37	0.36	12.00	0.68	35.37	12.20	3.96	2.95	4.47	1.53
5.00	0.59	9.74	0.83	17.14	14.81	4.50	2.57	6.17	1.10
7.02	0.40	5.45	1.47	27.03	7.68	4.71	2.45	8.47	0.79
3.28	0.86	5.10	1.52	23.41	8.52	3.57	3.23	10.10	0.63
2.60	1.09	8.35	0.93	21.15	8.77	9.04	1.27	4.06	1.50
3.81	0.72	3.48	2.21	23.29	5.11	8.15	1.39	4.96	1.17
7.15	0.36	7.60	1.00	36.08	3.00	7.85	1.42	5.61	1.02
8.92	0.27	6.01	1.27	20.21	5.01	14.65	0.75	3.74	1.50
6.68	0.31	5.25	1.45	24.67	4.06	8.17	1.33	3.49	1.55
4.91	0.41	8.76	0.85	23.94	4.04	11.45	0.95	2.85	1.90
4.32	0.47	8.48	0.88	29.48	3.24	11.42	0.95	6.08	0.88
2.40	0.84	3.00	2.49	36.23	2.61	10.46	1.03	4.08	1.32

4.48	0.44	9.43	0.79	10.98	8.45	6.39	1.65	2.69	1.88
6.20	0.31	10.89	0.68	18.21	4.92	11.07	0.95	11.85	0.42
5.09	0.38	6.01	1.22	23.20	3.82	3.88	2.69	2.47	1.96
5.23	0.37	7.39	0.98	17.64	5.01	3.99	2.59	4.42	1.06
3.02	0.61	8.77	0.83	20.62	4.18	12.38	0.83	2.78	1.63
4.03	0.44	9.26	0.78	14.55	5.89	3.88	2.61	3.36	1.33
3.02	0.59	8.65	0.82	17.82	4.63	12.84	0.78	2.46	1.78
1.63	1.06	3.30	2.15	25.77	3.14	14.91	0.66	5.43	0.79
3.04	0.52	11.79	0.60	10.13	7.75	7.70	1.27	3.15	1.30
2.56	0.60	5.03	1.40	25.21	2.86	6.60	1.48	3.99	1.01
5.19	0.27	4.86	1.44	20.11	3.56	13.07	0.75	5.01	0.69
3.07	0.42	3.08	2.26	21.02	3.36	11.41	0.86	2.54	1.35
2.76	0.41	7.92	0.88	10.46	6.74	4.70	2.06	5.19	0.55
4.46	0.25	10.36	0.67	25.79	2.70	3.30	2.91	2.67	0.68
3.45	0.31	7.00	0.98	13.16	5.07	12.17	0.79	2.08	0.65
5.16	0.12	6.39	1.07	11.58	5.65	3.98	2.40	2.69	0.28
3.84	0.11	5.65	1.20	17.62	3.53	21.56	0.44	18.89	11.57
39.36	8.71	3.75	1.81	24.17	2.29	9.30	1.03	24.48	8.08
10.89	10.47	7.35	0.92	13.49	3.93	9.82	0.97	23.10	7.70
11.49	9.35	9.01	0.74	20.87	2.53	3.95	2.40	15.61	7.66
0 mm	0 mm	8 mm	8 mm	18 mm	18 mm	27 mm	27 mm	38 mm	38 mm
Major	Minor	Major	Minor	Major	Minor	Major	Minor	Major	Minor
21.31	4.84	5.25	1.26	17.75	2.96	3.64	2.60	25.07	4.17
23.38	4.35	3.24	2.04	15.81	3.20	16.35	0.57	17.05	6.04
25.13	3.59	9.51	0.70	12.45	4.05	7.17	1.29	12.65	7.18
18.96	4.63	5.74	1.15	19.11	2.63	10.29	0.88	17.95	4.70
17.00	4.75	10.93	0.59	10.22	4.85	11.77	0.77	10.31	7.41
17.48	4.26	9.40	0.68	21.39	2.31	9.23	0.98	18.44	3.94
26.54	2.67	8.75	0.73	20.43	2.39	3.57	2.54	14.74	4.88
12.57	5.64	12.49	0.51	11.21	4.22	10.77	0.84	14.92	4.76
23.95	2.89	7.74	0.81	12.49	3.78	5.48	1.65	33.78	2.02
17.55	3.86	2.92	2.14	13.11	3.59	8.41	1.07	25.66	2.50
19.93	3.19	8.10	0.77	13.44	3.49	7.64	1.17	11.68	5.27
24.41	2.59	6.69	0.93	33.86	1.36	3.26	2.74	8.67	7.04
11.75	5.38	4.28	1.45	21.89	2.08	10.28	0.87	23.13	2.60
20.93	2.71	4.27	1.44	15.99	2.84	9.52	0.93	13.68	4.36
8.75	5.94	3.67	1.67	21.30	2.12	3.87	2.27	29.22	2.01
18.54	2.79	3.64	1.68	15.24	2.85	7.55	1.17	13.24	4.34
28.18	1.83	7.79	0.77	7.35	5.89	11.70	0.75	14.60	3.94
13.06	3.93	5.27	1.14	15.51	2.65	5.69	1.53	21.62	2.57
11.36	4.44	7.28	0.83	21.37	1.89	4.27	2.03	26.00	2.12
28.81	1.66	7.09	0.82	15.33	2.62	8.97	0.96	21.72	2.53
20.76	2.29	2.94	1.99	15.30	2.61	4.33	1.98	9.55	5.74
24.00	1.95	4.61	1.27	13.02	3.06	13.42	0.63	25.92	2.11
24.21	1.87	5.75	1.01	20.86	1.89	8.34	1.02	22.97	2.31
13.64	3.26	2.51	2.28	7.94	4.92	6.17	1.37	12.89	3.86
17.55	2.48	7.13	0.80	14.28	2.66	3.90	2.15	6.97	6.62
29.32	1.41	9.14	0.63	8.36	4.51	10.09	0.83	6.95	6.54
7.13	5.77	7.43	0.77	17.39	2.16	11.32	0.73	25.55	1.73
8.67	4.69	10.43	0.55	10.06	3.66	4.37	1.88	9.18	4.79
11.27	3.56	2.81	1.99	11.18	3.21	3.62	2.26	7.11	5.95



13.57	2.96	7.33	0.75	9.11	3.85	9.67	0.84	17.86	2.33
15.57	2.44	3.44	1.60	6.54	5.30	5.22	1.55	8.24	4.99
23.30	1.63	9.30	0.59	20.58	1.68	8.90	0.90	15.49	2.62
10.84	3.41	2.41	2.27	8.70	3.92	8.18	0.98	15.37	2.60
11.86	3.08	3.27	1.66	9.55	3.57	3.24	2.47	20.30	1.94
16.43	2.21	5.85	0.93	10.53	3.19	3.24	2.46	14.68	2.66
7.67	4.73	9.01	0.60	19.11	1.72	7.48	1.06	7.62	5.11
7.44	4.86	7.77	0.69	17.79	1.84	12.83	0.61	12.70	3.05
9.16	3.91	3.08	1.74	5.88	5.43	3.04	2.58	10.10	3.80
8.46	4.20	3.80	1.40	9.07	3.52	9.05	0.87	13.97	2.70
25.78	1.36	9.38	0.57	16.37	1.95	4.52	1.73	11.65	3.20
8.86	3.95	5.15	1.02	18.18	1.74	3.46	2.23	14.55	2.54
11.86	2.94	7.20	0.73	22.10	1.41	7.54	1.02	9.85	3.69
6.79	5.07	9.83	0.53	17.72	1.76	6.24	1.23	12.00	3.02
12.54	2.74	7.71	0.67	8.70	3.52	3.28	2.32	8.31	4.36
16.34	2.07	2.76	1.88	12.73	2.38	4.66	1.63	21.43	1.66
6.28	5.36	9.83	0.53	12.07	2.50	3.23	2.32	18.34	1.93
18.22	1.83	2.62	1.97	15.30	1.96	10.92	0.69	16.80	2.10
15.11	2.20	6.34	0.81	9.35	3.18	10.69	0.70	8.16	4.31
22.19	1.50	8.47	0.61	7.93	3.73	15.32	0.48	12.72	2.75
7.16	4.63	4.40	1.16	6.26	4.70	6.23	1.16	17.86	1.95
8.22	3.96	2.54	1.99	7.80	3.77	6.70	1.07	12.87	2.67
8.87	3.65	7.40	0.68	17.53	1.67	6.83	1.05	11.83	2.84
17.13	1.87	5.36	0.93	7.91	3.67	3.65	1.95	24.44	1.37
0 mm	0 mm	8 mm	8 mm	18 mm	18 mm	27 mm	27 mm	38 mm	38 mm
Major	Minor	Major	Minor	Major	Minor	Major	Minor	Major	Minor
5.87	5.43	6.85	0.72	8.72	3.29	8.01	0.87	18.94	1.76
14.39	2.20	6.47	0.75	6.04	4.65	5.08	1.37	19.20	1.72
12.42	2.55	3.25	1.48	6.23	4.48	12.37	0.56	22.32	1.47
10.50	2.99	10.86	0.43	5.85	4.72	6.87	1.01	9.59	3.42
21.41	1.44	6.04	0.78	21.93	1.25	7.08	0.97	19.79	1.62
8.55	3.58	2.22	2.10	7.11	3.83	4.00	1.71	22.05	1.45
14.27	2.11	5.24	0.89	13.53	1.98	3.50	1.88	7.87	4.04
13.91	2.15	9.54	0.48	13.90	1.92	10.23	0.64	6.91	4.59
13.70	2.17	5.36	0.85	12.15	2.18	4.17	1.57	16.93	1.87
10.44	2.85	3.61	1.26	5.92	4.47	3.67	1.76	7.15	4.42
7.31	4.04	4.40	1.02	17.54	1.48	8.81	0.72	6.42	4.88
11.91	2.46	8.60	0.52	8.48	3.05	3.01	2.08	7.56	4.12
6.97	4.21	5.21	0.85	19.22	1.35	3.00	2.06	23.50	1.32
13.45	2.15	2.79	1.57	8.59	2.99	10.82	0.57	8.14	3.80
15.12	1.89	2.49	1.75	7.77	3.28	7.65	0.80	18.51	1.66
29.04	0.97	5.01	0.87	21.21	1.20	2.58	2.36	17.33	1.77
6.61	4.24	6.69	0.64	16.09	1.56	4.88	1.24	8.21	3.74
18.88	1.48	4.33	0.98	8.84	2.84	2.79	2.17	11.66	2.62
19.69	1.38	8.41	0.50	12.25	2.02	10.92	0.55	9.46	3.17
7.78	3.46	3.71	1.10	13.55	1.80	3.68	1.59	12.98	2.29
8.92	2.99	3.75	1.08	11.33	2.12	7.28	0.79	19.01	1.57
12.99	2.05	5.20	0.78	6.76	3.51	3.08	1.84	6.57	4.48
10.38	2.55	4.59	0.88	17.65	1.34	9.53	0.59	24.50	1.20
15.81	1.66	7.85	0.51	7.56	3.09	10.06	0.56	5.62	5.09
5.47	4.76	7.53	0.53	7.68	3.03	3.78	1.48	9.02	3.16

13.29	1.93	14.06	0.29	6.01	3.80	5.20	1.07	15.97	1.78
10.06	2.52	4.41	0.90	11.28	1.98	5.25	1.05	14.18	1.99
23.12	1.09	5.17	0.76	15.28	1.46	2.81	1.93	15.75	1.79
10.30	2.44	2.43	1.63	7.53	2.89	5.91	0.91	16.94	1.65
21.85	1.13	4.45	0.89	11.54	1.88	3.94	1.36	16.49	1.67
7.12	3.40	2.39	1.65	15.53	1.39	3.35	1.60	6.97	3.93
8.63	2.78	6.27	0.63	13.71	1.57	5.44	0.98	7.98	3.41
7.87	3.04	4.72	0.83	11.97	1.80	2.81	1.90	7.50	3.59
5.09	4.67	2.63	1.49	8.94	2.39	2.60	2.05	14.34	1.86
5.71	4.14	5.35	0.73	5.32	4.01	3.48	1.53	13.03	2.02
6.33	3.72	3.76	1.03	7.60	2.79	5.78	0.92	13.50	1.94
12.02	1.95	4.50	0.85	22.73	0.93	7.48	0.71	8.75	2.96
12.00	1.95	5.43	0.70	18.32	1.15	3.23	1.64	12.69	2.03
17.78	1.32	7.53	0.51	29.89	0.71	4.44	1.19	15.23	1.67
6.27	3.71	8.86	0.43	9.76	2.16	6.17	0.84	10.33	2.43
6.07	3.82	3.02	1.25	5.55	3.79	3.79	1.37	21.16	1.18
6.26	3.71	4.86	0.76	6.27	3.35	2.96	1.74	6.46	3.78
19.29	1.20	6.77	0.54	5.22	4.00	2.76	1.82	10.34	2.34
5.52	4.18	3.58	1.01	5.20	4.00	5.14	0.97	15.74	1.52
8.87	2.58	3.97	0.91	15.47	1.35	4.37	1.12	13.84	1.72
12.20	1.88	4.65	0.75	9.22	2.25	5.83	0.84	5.47	4.34
15.27	1.50	6.15	0.56	30.12	0.69	7.34	0.67	11.31	2.10
6.88	3.29	6.04	0.57	14.94	1.39	10.41	0.47	7.00	3.36
6.95	3.16	4.74	0.72	12.37	1.67	4.03	1.21	5.29	4.43
5.57	3.94	4.65	0.74	14.50	1.42	4.48	1.09	17.08	1.34
15.03	1.45	2.50	1.34	5.16	3.93	5.47	0.89	6.57	3.34
16.51	1.31	2.22	1.50	13.48	1.51	10.97	0.44	19.16	1.11
9.60	2.26	3.00	1.08	18.41	1.10	2.95	1.64	9.27	2.28
0 mm	0 mm	8 mm	8 mm	18 mm	18 mm	27 mm	27 mm	38 mm	38 mm
Major	Minor	Major	Minor	Major	Minor	Major	Minor	Major	Minor
18.18	1.19	4.48	0.72	12.47	1.59	9.42	0.51	14.78	1.43
8.49	2.53	5.39	0.58	12.61	1.57	4.19	1.14	13.00	1.61
16.54	1.30	3.01	1.02	6.98	2.83	5.31	0.90	14.02	1.50
9.69	2.22	2.86	1.07	9.27	2.12	4.53	1.04	10.15	2.04
5.22	4.06	4.56	0.65	10.56	1.87	2.38	1.98	6.82	3.03
17.83	1.18	3.71	0.80	9.66	2.04	2.36	1.99	19.65	1.05
12.20	1.70	3.03	0.97	7.28	2.65	7.06	0.66	4.79	4.30
14.53	1.42	3.62	0.82	7.76	2.48	2.73	1.71	25.80	0.80
5.93	3.48	5.59	0.53	9.92	1.94	4.20	1.11	12.07	1.69
9.09	2.27	1.98	1.48	9.01	2.08	3.69	1.25	4.52	4.51
19.01	1.08	5.21	0.56	10.13	1.84	8.22	0.56	8.37	2.43
7.96	2.56	5.24	0.56	5.31	3.51	7.30	0.63	16.40	1.24
13.70	1.48	4.42	0.65	5.11	3.65	4.77	0.95	7.12	2.84
6.14	3.29	4.06	0.70	14.36	1.30	2.74	1.65	13.53	1.49
15.29	1.31	2.54	1.11	11.21	1.65	2.80	1.61	5.75	3.48
17.20	1.16	2.08	1.33	8.28	2.23	4.46	1.00	17.31	1.15
20.69	0.95	3.81	0.72	7.21	2.54	2.24	2.00	10.52	1.88
6.03	3.26	2.21	1.22	10.00	1.82	9.36	0.48	12.41	1.58
13.79	1.42	2.15	1.21	7.82	2.31	4.04	1.11	14.96	1.30
7.43	2.60	4.72	0.55	12.92	1.39	3.89	1.13	15.92	1.21
12.57	1.53	1.68	1.55	5.64	3.19	3.73	1.17	15.38	1.25

6.84	2.81	5.27	0.48	7.32	2.45	8.47	0.51	20.28	0.95
21.45	0.89	3.64	0.69	8.65	2.07	5.49	0.78	5.87	3.25
14.74	1.29	3.70	0.67	5.95	3.00	4.07	1.05	11.60	1.63
17.62	1.06	4.37	0.57	6.47	2.75	3.49	1.22	6.34	2.96
6.67	2.81	2.22	1.12	6.73	2.63	2.65	1.59	5.69	3.28
4.91	3.81	2.34	1.03	7.02	2.51	2.70	1.54	10.11	1.80
10.95	1.71	4.51	0.54	6.50	2.71	6.88	0.60	5.45	3.33
10.37	1.79	4.03	0.60	12.30	1.43	5.89	0.70	15.83	1.14
17.72	1.05	4.80	0.51	10.07	1.74	4.95	0.82	5.24	3.40
9.06	2.04	4.78	0.50	6.28	2.77	2.73	1.48	19.48	0.92
20.47	0.90	5.90	0.41	9.21	1.89	4.73	0.85	10.52	1.69
26.59	0.69	3.61	0.66	9.96	1.73	9.00	0.45	17.76	1.00
7.89	2.31	2.88	0.83	9.81	1.73	4.47	0.90	9.23	1.91
6.25	2.89	3.90	0.61	8.33	2.03	5.10	0.79	12.55	1.40
6.06	2.97	2.60	0.91	5.70	2.97	6.59	0.60	15.48	1.14
19.84	0.91	3.12	0.75	8.62	1.94	4.01	0.98	15.03	1.16
7.61	2.37	4.16	0.56	7.08	2.34	8.52	0.46	4.62	3.78
18.88	0.95	3.81	0.60	10.81	1.53	2.61	1.50	13.00	1.34
5.81	3.09	3.06	0.75	11.64	1.41	4.42	0.88	11.22	1.53
13.96	1.28	1.93	1.18	13.36	1.22	8.85	0.43	23.60	0.73
19.38	0.93	4.41	0.51	8.36	1.94	5.43	0.70	8.60	1.99
10.42	1.72	5.67	0.40	5.47	2.94	8.01	0.47	14.83	1.14
9.67	1.84	1.92	1.16	9.60	1.68	3.12	1.21	4.65	3.60
5.33	3.33	1.80	1.22	4.95	3.24	5.17	0.73	13.29	1.26
5.38	3.29	1.69	1.30	5.29	2.98	7.60	0.49	7.53	2.22
12.06	1.46	1.72	1.26	7.36	2.13	2.72	1.37	11.32	1.47
8.45	2.09	3.98	0.55	4.89	3.20	5.96	0.62	14.74	1.13
8.70	2.01	2.17	1.00	9.66	1.62	3.76	0.95	4.98	3.34
7.87	2.21	3.76	0.58	5.25	2.97	10.09	0.35	17.14	0.97
5.28	3.23	2.82	0.77	8.73	1.78	2.83	1.24	8.53	1.95
16.72	1.01	3.08	0.70	4.28	3.60	3.25	1.07	13.80	1.20
4.76	3.54	3.66	0.59	8.34	1.84	5.45	0.64	4.63	3.55
0 mm	0 mm	8 mm	8 mm	18 mm	18 mm	27 mm	27 mm	38 mm	38 mm
Major	Minor	Major	Minor	Major	Minor	Major	Minor	Major	Minor
4.65	3.63	2.58	0.83	6.99	2.17	7.18	0.48	6.76	2.42
14.16	1.19	3.01	0.70	10.33	1.47	3.67	0.94	10.53	1.55
14.19	1.18	3.52	0.60	11.57	1.30	6.41	0.53	6.99	2.30
16.38	1.03	4.03	0.52	4.88	3.06	3.21	1.06	6.44	2.50
5.17	3.24	3.17	0.66	4.65	3.20	5.45	0.62	15.48	1.03
16.78	1.00	6.33	0.33	22.90	0.65	3.70	0.89	4.35	3.61
4.19	3.95	2.29	0.91	7.51	1.95	3.18	1.03	6.06	2.59
6.88	2.40	3.20	0.65	8.35	1.74	5.79	0.56	18.65	0.84
11.10	1.47	3.03	0.68	5.37	2.68	3.01	1.07	10.28	1.52
5.68	2.87	4.55	0.45	9.71	1.48	6.45	0.49	16.96	0.91
4.63	3.52	1.83	1.12	9.06	1.58	5.32	0.58	5.33	2.89
7.61	2.14	4.43	0.46	13.83	1.03	2.30	1.35	8.23	1.87
6.02	2.69	2.07	0.97	7.98	1.76	3.67	0.85	10.64	1.45
4.45	3.60	2.22	0.91	4.82	2.92	4.13	0.75	15.48	0.99
4.76	3.36	2.81	0.70	7.21	1.95	5.07	0.61	5.47	2.78
14.05	1.14	4.63	0.41	17.68	0.79	2.62	1.17	6.68	2.27
5.16	3.09	4.15	0.46	11.74	1.18	7.02	0.43	15.04	1.00

6.02	2.64	1.73	1.06	5.43	2.55	2.59	1.17	7.48	2.01
12.02	1.32	2.91	0.63	6.07	2.27	4.48	0.67	14.67	1.03
11.45	1.38	5.69	0.32	7.51	1.83	2.87	1.05	7.53	1.99
15.91	0.98	2.59	0.70	4.34	3.16	4.56	0.65	4.94	2.99
4.97	3.12	2.82	0.64	11.07	1.23	3.95	0.75	4.80	3.04
13.43	1.15	3.84	0.46	6.45	2.12	5.25	0.55	5.30	2.75
16.01	0.96	3.80	0.47	5.08	2.69	2.89	0.99	4.43	3.28
5.70	2.70	2.72	0.64	7.02	1.94	2.68	1.07	5.32	2.72
8.73	1.76	4.27	0.41	4.75	2.86	2.07	1.36	16.04	0.90
9.57	1.60	3.92	0.44	15.39	0.88	2.10	1.35	4.95	2.90
13.62	1.12	5.39	0.32	4.25	3.17	4.72	0.59	5.72	2.50
9.18	1.66	2.58	0.66	13.14	1.02	5.29	0.52	9.63	1.49
9.54	1.59	2.42	0.71	14.59	0.92	4.94	0.55	9.21	1.54
9.52	1.59	5.56	0.31	11.06	1.21	5.66	0.48	11.03	1.29
4.67	3.25	1.51	1.11	11.82	1.12	3.50	0.76	4.65	3.04
9.43	1.61	2.21	0.76	7.34	1.81	6.54	0.39	9.81	1.44
6.15	2.46	4.33	0.38	7.72	1.71	8.75	0.30	14.54	0.96
7.63	1.97	2.12	0.76	5.46	2.42	3.44	0.75	13.51	1.03
6.55	2.23	4.50	0.35	6.46	2.00	5.78	0.44	8.21	1.68
10.94	1.33	2.08	0.75	7.05	1.83	2.14	1.19	9.65	1.43
7.98	1.82	2.90	0.53	19.74	0.65	4.15	0.61	15.62	0.89
10.61	1.37	2.02	0.74	12.81	0.99	4.48	0.55	17.06	0.81
5.29	2.74	3.07	0.49	8.98	1.40	2.88	0.85	4.42	3.11
5.60	2.57	2.20	0.68	15.94	0.79	3.62	0.67	15.10	0.90
7.51	1.92	3.92	0.38	8.81	1.41	3.52	0.68	12.04	1.13
14.24	1.01	2.28	0.64	4.24	2.90	3.94	0.60	7.99	1.70
17.31	0.82	1.46	0.98	16.06	0.77	2.94	0.79	14.24	0.95
12.98	1.07	2.61	0.54	13.10	0.94	3.84	0.60	12.52	1.07
4.39	3.15	4.00	0.35	5.55	2.22	4.21	0.55	11.80	1.13
8.39	1.63	2.29	0.58	4.01	3.06	3.53	0.65	10.54	1.27
10.62	1.29	3.52	0.38	6.04	2.03	2.51	0.90	4.74	2.81
7.68	1.78	3.40	0.38	7.30	1.68	5.66	0.40	9.94	1.34
16.01	0.85	2.45	0.53	4.48	2.73	3.20	0.71	13.35	1.00
17.22	0.79	2.95	0.43	4.38	2.77	2.95	0.77	7.13	1.85
6.20	2.18	2.12	0.59	4.24	2.85	1.98	1.13	4.95	2.65
4.88	2.77	2.12	0.59	10.55	1.14	6.43	0.35	7.15	1.82
0 mm	0 mm	8 mm	8 mm	18 mm	18 mm	27 mm	27 mm	38 mm	38 mm
Major	Minor	Major	Minor	Major	Minor	Major	Minor	Major	Minor
12.64	1.06	1.51	0.80	7.36	1.64	2.81	0.80	8.34	1.55
9.77	1.36	1.34	0.91	23.65	0.51	3.32	0.66	12.17	1.06
6.57	2.02	1.83	0.65	8.36	1.43	4.27	0.51	8.08	1.60
4.69	2.82	1.51	0.78	14.85	0.81	2.11	1.02	11.97	1.07
16.47	0.80	1.32	0.90	6.47	1.84	4.76	0.45	11.97	1.07
14.47	0.91	2.68	0.42	4.70	2.52	2.86	0.74	10.55	1.21
8.62	1.52	3.75	0.30	11.40	1.04	2.16	0.95	8.10	1.57
9.40	1.37	2.36	0.47	9.56	1.24	1.91	1.07	6.54	1.94
16.50	0.78	3.57	0.30	12.51	0.94	3.72	0.55	7.33	1.73
11.39	1.13	2.75	0.38	7.34	1.60	3.84	0.53	8.43	1.50
8.93	1.44	2.90	0.36	3.71	3.15	4.57	0.44	11.87	1.07
11.15	1.15	2.57	0.40	6.10	1.92	4.12	0.48	4.10	3.04
8.64	1.48	2.03	0.49	9.49	1.23	3.82	0.51	21.57	0.58

10.16	1.26	1.89	0.46	5.92	1.97	2.70	0.73	11.64	1.07
6.52	1.95	3.19	0.26	4.28	2.72	2.08	0.94	5.51	2.22
5.15	2.46	2.08	0.40	4.37	2.60	2.74	0.70	13.63	0.90
7.97	1.59	2.53	0.31	5.67	2.01	1.58	1.22	17.45	0.70
6.40	1.97	3.60	0.20	5.95	1.91	4.03	0.47	11.95	1.00
5.63	2.23	4.82	0.15	3.84	2.95	3.99	0.47	6.86	1.74
8.67	1.45	1.32	0.54	8.60	1.31	3.46	0.54	4.53	2.63
7.57	1.65	1.76	0.37	7.54	1.49	1.94	0.95	4.18	2.83
8.27	1.51	1.28	0.51	13.79	0.79	1.68	1.07	17.29	0.68
14.18	0.88	1.55	0.42	5.83	1.88	2.96	0.60	6.82	1.73
9.18	1.34	1.45	0.43	6.70	1.63	2.59	0.69	5.82	2.02
8.40	1.47	2.07	0.20	4.61	2.36	2.17	0.79	12.26	0.95
8.85	1.39	1.62	0.21	3.87	2.80	2.87	0.60	15.46	0.76
5.96	2.06			5.75	1.88	2.38	0.70	10.30	1.13
10.09	1.21			3.70	2.90	6.46	0.26	9.29	1.25
5.94	2.05			14.57	0.73	3.02	0.55	12.51	0.92
5.44	2.24			6.49	1.63	1.53	1.07	11.15	1.04
4.10	2.95			3.88	2.72	2.02	0.77	6.94	1.67
19.62	0.62			6.06	1.74	4.17	0.37	10.63	1.07
13.26	0.91			6.86	1.53	3.49	0.45	9.86	1.15
12.93	0.93			13.24	0.78	1.71	0.91	10.35	1.09
5.14	2.34			7.71	1.33	2.25	0.68	11.51	0.98
10.60	1.13			3.44	2.95	2.04	0.75	12.37	0.91
9.16	1.31			5.89	1.72	4.82	0.30	8.37	1.33
3.93	3.04			5.88	1.72	2.76	0.53	11.09	1.00
12.31	0.97			12.82	0.78	3.44	0.41	8.22	1.35
11.74	1.02			10.05	0.99	1.40	1.00	4.19	2.62
15.80	0.75			9.50	1.05	1.69	0.79	13.56	0.81
20.30	0.58			5.65	1.75	1.80	0.74	16.39	0.66
4.70	2.52			7.96	1.23	1.42	0.94	12.62	0.86
14.60	0.81			6.11	1.60	1.82	0.72	5.85	1.84
10.30	1.14			4.30	2.26	4.76	0.27	17.36	0.62
4.93	2.38			3.67	2.65	1.75	0.73	7.54	1.41
12.07	0.97			13.26	0.73	1.41	0.88	6.60	1.60
9.89	1.18			9.92	0.98	2.88	0.42	5.41	1.94
11.32	1.03			3.64	2.66	1.30	0.93	10.50	1.00
9.53	1.23			4.87	1.98	2.61	0.45	10.53	0.99
10.85	1.08			3.74	2.57	2.60	0.44	4.76	2.20
12.21	0.95			5.64	1.69	1.96	0.59	6.85	1.52
4.70	2.46			15.57	0.61	1.24	0.90	8.26	1.26
0 mm	0 mm	8 mm	8 mm	18 mm	18 mm	27 mm	27 mm	38 mm	38 mm
Major	Minor	Major	Minor	Major	Minor	Major	Minor	Major	Minor
6.65	1.74			11.49	0.83	1.45	0.77	9.17	1.14
3.98	2.90			6.66	1.42	2.28	0.48	5.69	1.82
4.97	2.32			10.87	0.87	2.15	0.51	15.32	0.67
11.81	0.97			13.58	0.70	2.62	0.42	8.76	1.17
11.48	1.00			9.24	1.03	1.43	0.74	10.69	0.96
11.00	1.04			7.98	1.18	1.62	0.63	8.47	1.19
12.90	0.89			3.70	2.55	1.62	0.63	5.64	1.78
8.41	1.36			6.86	1.38	1.68	0.59	4.54	2.19
13.80	0.83			9.50	0.99	1.22	0.82	8.58	1.15

9.11	1.25			6.37	1.48	1.76	0.57	13.08	0.76
10.09	1.12			6.53	1.44	3.19	0.30	13.10	0.75
9.47	1.20			7.76	1.21	1.23	0.78	9.88	1.00
7.16	1.58			3.17	2.94	3.41	0.26	10.21	0.96
5.36	2.11			4.69	1.98	1.65	0.51	4.96	1.94
10.84	1.04			6.12	1.50	1.15	0.73	3.93	2.45
11.55	0.97			6.62	1.38	1.55	0.52	8.30	1.16
18.77	0.60			3.86	2.36	1.31	0.59	10.54	0.90
7.76	1.44			6.91	1.32	1.45	0.51	6.76	1.41
3.72	3.00			3.67	2.48	1.45	0.47	10.31	0.92
9.01	1.22			5.14	1.77	1.16	0.59	12.13	0.78
6.85	1.59			7.61	1.18	1.33	0.47	13.40	0.70
11.68	0.94			7.51	1.19	2.11	0.24	18.84	0.50
11.52	0.94			6.63	1.33	2.82	0.14	7.96	1.18
6.72	1.61			7.82	1.13	1.86	0.22	14.46	0.65
9.34	1.15			3.57	2.46			4.30	2.17
11.34	0.94			6.37	1.37			4.38	2.13
10.60	1.00			9.85	0.88			4.01	2.32
9.38	1.14			8.06	1.08			3.85	2.39
10.00	1.06			14.36	0.60			5.00	1.82
9.14	1.16			5.49	1.56			5.81	1.56
4.03	2.63			3.43	2.48			4.61	1.96
3.76	2.82			7.51	1.13			4.37	2.07
7.53	1.40			5.35	1.59			12.53	0.72
3.65	2.88			4.41	1.92			9.49	0.95
7.63	1.38			5.72	1.48			9.49	0.95
9.09	1.16			9.57	0.88			12.89	0.70
5.54	1.89			13.65	0.61			15.63	0.57
8.12	1.28			9.32	0.88			9.63	0.93
9.10	1.14			4.53	1.81			6.61	1.35
8.50	1.22			3.51	2.34			3.90	2.28
8.65	1.19			3.65	2.24			3.44	2.59
5.15	1.98			3.28	2.49			3.64	2.45
8.58	1.18			9.25	0.88			5.47	1.62
9.70	1.05			9.25	0.88			7.48	1.19
7.18	1.41			8.14	1.00			9.91	0.90
4.18	2.39			9.58	0.85			16.12	0.55
6.55	1.53			3.76	2.16			5.96	1.47
10.68	0.93			6.11	1.33			9.45	0.93
10.13	0.97			3.27	2.47			7.70	1.14
5.06	1.95			5.96	1.35			11.18	0.78
10.06	0.98			3.85	2.09			4.38	1.98
5.16	1.91			4.47	1.80			7.59	1.13
11.69	0.84			3.64	2.20			6.21	1.38
0 mm	0 mm	8 mm	8 mm	18 mm	18 mm	27 mm	27 mm	38 mm	38 mm
Major	Minor	Major	Minor	Major	Minor	Major	Minor	Major	Minor
3.99	2.45			4.92	1.63			9.29	0.92
11.02	0.88			3.08	2.58			11.21	0.76
7.86	1.23			8.70	0.91			9.31	0.91
4.96	1.95			11.20	0.71			3.27	2.58
10.65	0.90			10.10	0.78			8.65	0.98

8.47	1.14			6.46	1.21			12.79	0.66
7.96	1.20			9.04	0.86			8.62	0.97
8.51	1.12			3.26	2.38			11.74	0.70
7.31	1.30			8.69	0.90			5.35	1.55
4.78	1.98			6.53	1.19			7.77	1.06
3.78	2.51			5.57	1.39			11.28	0.72
3.31	2.87			3.42	2.25			8.97	0.90
8.55	1.10			4.50	1.70			8.23	0.98
12.56	0.75			7.76	0.98			11.79	0.69
10.07	0.93			9.98	0.76			8.33	0.97
6.90	1.36			3.34	2.26			7.05	1.14
6.93	1.35			8.78	0.86			5.82	1.38
7.90	1.19			7.04	1.06			13.95	0.57
7.57	1.24			4.53	1.65			3.86	2.05
6.60	1.41			3.38	2.15			11.18	0.70
4.97	1.87			10.76	0.67			6.39	1.23
9.07	1.02			9.65	0.74			7.08	1.10
9.13	1.00			4.10	1.73			16.53	0.47
8.46	1.08			6.03	1.17			10.29	0.75
8.06	1.14			3.33	2.10			3.21	2.40
9.98	0.91			3.45	2.02			11.34	0.68
7.13	1.27			3.76	1.85			5.11	1.50
3.48	2.61			9.35	0.75			14.22	0.53
4.94	1.83			5.43	1.28			10.82	0.70
3.76	2.39			3.63	1.90			10.53	0.72
11.51	0.78			8.42	0.81			10.42	0.71
7.32	1.22			3.41	1.99			8.78	0.84
15.29	0.58			8.14	0.83			8.81	0.84
8.49	1.05			3.38	2.00			2.86	2.58
3.44	2.58			4.17	1.61			5.24	1.39
7.08	1.25			3.50	1.91			6.00	1.21
8.74	1.01			2.69	2.45			4.32	1.68
8.60	1.02			8.11	0.81			12.56	0.57
10.69	0.82			2.97	2.20			4.69	1.53
9.37	0.93			13.66	0.47			3.24	2.21
7.73	1.13			3.45	1.87			4.90	1.45
3.44	2.49			3.61	1.76			2.82	2.52
12.36	0.69			4.17	1.52			6.13	1.16
5.38	1.58			9.10	0.70			12.23	0.58
8.42	1.01			2.85	2.21			10.83	0.65
9.93	0.85			2.95	2.13			13.03	0.53
4.93	1.72			2.58	2.44			3.79	1.83
9.17	0.92			3.44	1.82			7.23	0.95
5.18	1.63			2.84	2.17			14.96	0.46
5.80	1.46			4.05	1.52			3.14	2.20
4.83	1.75			5.41	1.12			7.35	0.94
4.69	1.79			8.88	0.68			3.20	2.12
7.83	1.07			3.34	1.80			10.41	0.65
0 mm	0 mm	8 mm	8 mm	18 mm	18 mm	27 mm	27 mm	38 mm	38 mm
Major	Minor	Major	Minor	Major	Minor	Major	Minor	Major	Minor
7.94	1.06			7.07	0.85			7.81	0.87

9.91	0.84	4.43	1.36	3.67	1.83
3.52	2.37	6.50	0.92	7.83	0.85
10.84	0.77	2.95	2.01	9.00	0.73
14.81	0.56	3.08	1.88	4.70	1.40
8.74	0.95	7.66	0.75	11.48	0.57
10.69	0.77	4.35	1.32	8.54	0.77
10.76	0.77	3.73	1.54	3.48	1.88
6.48	1.28	2.45	2.32	4.01	1.63
4.73	1.75	5.96	0.95	8.35	0.77
9.70	0.85	4.00	1.42	6.03	1.07
11.07	0.75	8.53	0.66	8.56	0.75
8.31	0.99	4.07	1.38	12.06	0.52
9.52	0.87	3.38	1.65	7.23	0.87
4.02	2.05	3.52	1.59	9.90	0.63
7.26	1.14	7.96	0.69	5.59	1.11
5.78	1.42	10.67	0.52	16.98	0.37
9.11	0.90	5.75	0.95	6.14	1.01
13.01	0.63	4.44	1.22	8.02	0.77
5.22	1.57	8.35	0.65	3.18	1.93
6.08	1.33	2.45	2.21	9.11	0.68
8.63	0.93	5.24	1.03	7.43	0.82
3.50	2.29	3.38	1.59	5.57	1.09
3.97	2.02	4.33	1.24	2.67	2.27
15.45	0.52	4.64	1.14	10.87	0.56
9.25	0.86	4.01	1.30	4.60	1.31
6.73	1.18	4.73	1.09	2.83	2.13
2.99	2.66	5.80	0.89	4.14	1.45
7.94	0.99	3.12	1.65	12.23	0.49
6.54	1.21	8.41	0.61	7.15	0.83
3.29	2.38	3.93	1.29	7.95	0.75
5.93	1.32	7.58	0.67	7.95	0.75
10.94	0.71	2.90	1.73	4.99	1.19
8.20	0.95	6.67	0.75	4.74	1.25
4.05	1.92	13.36	0.37	6.09	0.96
4.37	1.78	5.61	0.87	2.96	1.97
4.21	1.85	3.58	1.36	6.18	0.94
11.08	0.70	3.84	1.26	3.63	1.61
8.35	0.92	5.14	0.94	7.02	0.83
7.77	0.99	5.14	0.94	8.99	0.65
4.60	1.66	2.27	2.13	3.19	1.81
10.02	0.76	2.79	1.71	6.69	0.86
6.01	1.26	3.69	1.29	11.22	0.51
3.11	2.45	4.81	0.99	8.79	0.66
3.60	2.11	3.76	1.27	7.59	0.76
9.10	0.84	3.75	1.26	11.13	0.51
6.41	1.19	7.35	0.64	7.13	0.80
12.52	0.61	5.63	0.83	4.89	1.16
8.59	0.88	4.98	0.94	2.77	2.03
10.82	0.70	5.00	0.93	4.20	1.34
9.18	0.82	5.95	0.78	3.62	1.54
10.28	0.74	3.03	1.53	3.50	1.60



7.21	1.05			2.44	1.88			12.22	0.46
0 mm	0 mm	8 mm	8 mm	18 mm	18 mm	27 mm	27 mm	38 mm	38 mm
Major	Minor	Major	Minor	Major	Minor	Major	Minor	Major	Minor
6.68	1.13			5.75	0.79			2.99	1.86
8.03	0.94			7.64	0.60			10.22	0.54
10.04	0.75			3.01	1.50			13.92	0.39
3.08	2.43			3.24	1.40			7.51	0.72
4.53	1.63			6.81	0.66			6.12	0.89
8.17	0.91			2.19	2.05			4.92	1.11
7.27	1.02			3.61	1.24			10.54	0.52
5.04	1.47			2.53	1.76			3.10	1.76
5.03	1.47			6.01	0.74			8.66	0.62
8.09	0.91			3.74	1.18			8.79	0.62
9.33	0.78			4.45	0.99			2.81	1.91
7.45	0.97			5.90	0.74			3.74	1.44
7.64	0.94			4.05	1.08			6.76	0.79
4.25	1.68			5.43	0.79			8.69	0.61
7.26	0.98			6.48	0.67			5.21	1.01
5.94	1.19			8.10	0.53			3.59	1.47
6.63	1.07			4.61	0.94			5.05	1.04
4.53	1.56			2.55	1.69			13.08	0.40
5.93	1.19			4.41	0.96			4.82	1.07
5.84	1.21			9.68	0.44			5.90	0.87
5.88	1.20			3.57	1.19			11.49	0.45
9.32	0.75			7.41	0.57			8.00	0.64
3.51	1.99			2.95	1.44			6.14	0.84
4.30	1.61			2.95	1.44			5.13	1.00
6.41	1.08			5.99	0.71			6.07	0.85
9.72	0.71			13.21	0.32			3.45	1.46
4.25	1.62			3.23	1.29			6.46	0.78
5.76	1.19			6.68	0.62			3.15	1.60
7.93	0.86			5.38	0.76			4.78	1.05
10.01	0.68			3.15	1.29			6.52	0.77
8.15	0.84			6.07	0.67			4.05	1.24
7.49	0.91			3.92	1.04			8.55	0.58
3.64	1.86			7.18	0.57			3.49	1.42
7.90	0.86			2.04	1.97			6.82	0.72
3.57	1.90			4.86	0.83			8.38	0.59
8.91	0.76			4.89	0.82			4.71	1.04
8.94	0.75			3.42	1.17			6.47	0.75
7.05	0.95			2.37	1.67			7.81	0.62
7.20	0.93			2.72	1.46			7.88	0.62
8.12	0.82			2.61	1.51			3.38	1.42
7.18	0.92			4.00	0.98			8.86	0.54
3.72	1.78			3.31	1.18			7.15	0.66
5.65	1.16			4.59	0.85			5.37	0.88
7.54	0.86			7.60	0.51			4.59	1.02
6.74	0.96			2.26	1.71			7.37	0.62
9.11	0.71			4.07	0.95			4.87	0.94
3.53	1.83			7.78	0.49			3.51	1.31
7.82	0.83			6.53	0.58			8.09	0.56

10.20	0.63			6.19	0.61			3.03	1.50
7.09	0.90			5.49	0.68			3.47	1.30
8.48	0.75			7.99	0.46			7.58	0.59
5.47	1.16			4.44	0.84			6.36	0.71
5.77	1.10			3.10	1.20			6.07	0.73
0 mm	0 mm	8 mm	8 mm	18 mm	18 mm	27 mm	27 mm	38 mm	38 mm
Major	Minor	Major	Minor	Major	Minor	Major	Minor	Major	Minor
3.97	1.60			5.71	0.65			7.64	0.58
2.85	2.22			2.75	1.35			9.67	0.46
8.43	0.75			2.92	1.26			8.45	0.52
8.40	0.75			3.65	1.00			4.31	1.00
5.81	1.08			2.31	1.58			4.77	0.90
2.94	2.13			2.61	1.38			6.81	0.63
6.14	1.02			3.21	1.12			3.10	1.38
5.79	1.07			2.07	1.74			4.19	1.02
3.43	1.81			6.16	0.58			5.60	0.75
10.47	0.59			5.15	0.69			7.49	0.56
7.28	0.85			2.41	1.47			7.44	0.56
7.00	0.88			2.45	1.45			8.21	0.51
7.00	0.87			2.96	1.18			3.46	1.21
6.70	0.91			3.46	1.01			4.97	0.83
8.63	0.70			5.59	0.63			2.60	1.59
8.31	0.73			6.47	0.54			3.89	1.06
5.71	1.07			6.29	0.56			4.94	0.83
7.23	0.84			2.39	1.47			2.66	1.54
9.03	0.67			4.98	0.70			3.81	1.08
8.91	0.68			5.34	0.65			6.42	0.63
8.14	0.74			4.28	0.81			5.50	0.73
8.61	0.70			2.73	1.27			4.89	0.82
6.34	0.94			3.74	0.93			2.46	1.62
7.61	0.78			7.97	0.43			2.67	1.48
6.51	0.91			2.24	1.53			2.98	1.33
8.12	0.73			2.08	1.65			3.62	1.08
3.78	1.57			1.89	1.82			6.34	0.62
3.25	1.82			5.75	0.59			6.53	0.59
7.87	0.75			4.92	0.68			3.14	1.22
8.05	0.73			3.29	1.02			5.25	0.73
12.72	0.46			2.20	1.51			4.18	0.91
5.91	0.99			7.60	0.44			2.19	1.73
3.87	1.50			6.47	0.51			3.84	0.98
6.88	0.84			4.52	0.73			5.67	0.66
6.14	0.94			3.15	1.03			9.54	0.39
8.11	0.72			4.68	0.69			2.48	1.50
3.06	1.89			2.98	1.09			7.17	0.51
5.78	1.00			6.48	0.50			7.20	0.51
5.62	1.02			3.70	0.87			6.62	0.55
5.15	1.11			2.84	1.12			4.51	0.80
8.85	0.64			3.16	1.01			6.30	0.57
5.88	0.97			7.83	0.41			3.62	0.99
3.16	1.79			2.24	1.41			5.57	0.64
3.59	1.58			4.20	0.74			3.12	1.13

6.33	0.89			3.55	0.87			5.93	0.60
4.74	1.19			5.50	0.56			6.01	0.58
2.52	2.25			3.80	0.81			3.56	0.98
4.28	1.31			2.24	1.36			2.34	1.49
7.62	0.74			3.42	0.89			6.82	0.51
7.38	0.76			2.13	1.43			2.31	1.50
8.93	0.63			3.46	0.88			4.63	0.75
7.07	0.79			8.26	0.37			5.56	0.62
2.96	1.86			5.46	0.55			4.58	0.75
0 mm	0 mm	8 mm	8 mm	18 mm	18 mm	27 mm	27 mm	38 mm	38 mm
Major	Minor	Major	Minor	Major	Minor	Major	Minor	Major	Minor
3.50	1.58			2.09	1.44			4.52	0.76
6.72	0.82			7.58	0.39			4.59	0.75
3.08	1.78			2.43	1.22			4.25	0.80
6.12	0.90			2.43	1.22			7.19	0.47
7.36	0.75			4.93	0.60			3.20	1.05
4.36	1.25			3.56	0.82			5.29	0.63
8.44	0.65			3.39	0.86			4.16	0.81
6.57	0.82			4.82	0.60			3.21	1.01
2.74	1.97			7.89	0.37			2.12	1.54
5.88	0.91			3.81	0.76			2.93	1.11
9.34	0.58			2.50	1.15			2.44	1.32
7.87	0.68			5.15	0.55			5.28	0.60
7.61	0.70			3.25	0.87			5.60	0.57
8.93	0.60			2.85	0.99			2.63	1.21
3.47	1.53			4.28	0.66			7.01	0.45
5.73	0.93			2.31	1.23			6.00	0.53
2.46	2.14			5.15	0.55			2.47	1.28
6.50	0.81			1.98	1.41			4.38	0.72
3.23	1.63			4.69	0.60			4.43	0.70
3.43	1.52			5.91	0.47			2.10	1.48
4.37	1.20			2.61	1.06			5.82	0.54
6.78	0.76			4.66	0.59			7.02	0.44
5.32	0.96			4.74	0.57			4.09	0.74
6.83	0.75			2.91	0.94			2.20	1.37
7.46	0.68			3.86	0.70			3.53	0.85
6.63	0.76			4.78	0.57			3.53	0.85
6.30	0.79			7.94	0.34			2.88	1.05
3.06	1.62			6.48	0.42			7.92	0.38
3.44	1.44			6.77	0.39			5.28	0.56
6.87	0.72			5.51	0.48			3.29	0.90
4.38	1.13			4.57	0.57			2.66	1.12
7.75	0.64			5.47	0.48			3.51	0.85
2.51	1.97			2.52	1.04			7.39	0.40
6.40	0.77			4.09	0.63			2.19	1.33
7.36	0.67			6.56	0.39			4.66	0.62
7.51	0.65			3.63	0.70			2.26	1.27
4.82	1.02			2.21	1.15			3.09	0.93
8.47	0.58			3.73	0.68			3.32	0.85
6.96	0.71			2.52	1.01			6.94	0.41
5.00	0.98			4.69	0.54			4.91	0.57

3.35	1.46			1.83	1.39			4.48	0.62
3.42	1.40			1.79	1.40			4.63	0.60
5.50	0.87			1.78	1.41			5.59	0.49
6.74	0.71			3.74	0.66			4.16	0.65
4.80	1.00			4.26	0.58			4.80	0.57
5.89	0.82			3.44	0.71			2.70	1.00
9.72	0.50			6.49	0.38			2.54	1.06
2.63	1.81			2.29	1.06			3.44	0.78
7.62	0.63			3.62	0.66			3.97	0.67
3.43	1.39			2.28	1.06			3.30	0.79
4.40	1.08			6.06	0.40			2.89	0.91
5.13	0.93			4.22	0.56			4.33	0.60
5.64	0.84			4.73	0.50			5.06	0.51
0 mm	0 mm	8 mm	8 mm	18 mm	18 mm	27 mm	27 mm	38 mm	38 mm
Major	Minor	Major	Minor	Major	Minor	Major	Minor	Major	Minor
8.33	0.57			2.84	0.82			6.42	0.40
8.55	0.55			4.04	0.58			2.52	1.02
3.60	1.31			2.28	1.02			1.72	1.50
4.51	1.04			3.58	0.65			7.71	0.33
7.98	0.59			5.72	0.41			6.06	0.42
6.82	0.69			5.86	0.39			2.52	1.01
6.30	0.74			3.27	0.69			3.30	0.76
4.29	1.09			3.44	0.66			3.31	0.76
5.14	0.91			2.62	0.86			2.88	0.86
4.91	0.95			3.07	0.74			4.25	0.58
7.04	0.65			3.30	0.66			2.81	0.88
2.90	1.57			4.16	0.53			2.45	1.01
7.88	0.58			5.98	0.37			4.30	0.57
7.92	0.58			1.65	1.33			6.17	0.39
3.24	1.40			3.50	0.61			3.75	0.64
5.89	0.77			3.68	0.58			6.66	0.36
3.15	1.44			1.76	1.21			2.84	0.83
9.18	0.49			2.20	0.97			3.22	0.74
5.00	0.91			1.83	1.16			8.54	0.27
5.43	0.83			1.68	1.26			2.86	0.82
3.32	1.34			1.97	1.06			3.63	0.63
8.26	0.54			4.68	0.45			6.41	0.36
7.01	0.64			1.60	1.31			3.84	0.60
6.51	0.68			1.86	1.12			5.54	0.41
4.01	1.11			3.14	0.65			2.12	1.07
6.03	0.73			3.46	0.58			1.89	1.20
3.89	1.14			1.57	1.28			2.07	1.09
5.25	0.84			1.81	1.12			3.76	0.59
5.16	0.84			1.70	1.16			3.30	0.67
4.28	1.02			2.94	0.67			3.11	0.69
3.90	1.11			3.89	0.50			1.72	1.26
3.96	1.09			2.61	0.75			8.12	0.27
10.55	0.41			3.57	0.55			1.94	1.09
5.51	0.78			2.82	0.68			5.34	0.40
7.78	0.55			3.43	0.56			3.00	0.71
5.18	0.82			2.76	0.67			5.68	0.36

8.35	0.51			1.67	1.10			2.97	0.69
3.33	1.27			2.43	0.76			5.14	0.40
5.73	0.74			3.99	0.46			3.13	0.64
3.69	1.15			5.35	0.34			2.80	0.71
2.72	1.55			2.92	0.61			3.72	0.52
5.25	0.80			4.79	0.37			4.66	0.42
2.56	1.62			4.63	0.37			3.36	0.57
2.32	1.78			3.27	0.52			1.99	0.96
4.46	0.93			2.53	0.66			4.75	0.40
4.64	0.89			2.07	0.80			4.43	0.43
7.36	0.56			1.84	0.88			3.61	0.53
4.82	0.85			2.12	0.77			2.43	0.77
5.91	0.69			2.15	0.74			1.47	1.28
2.30	1.77			1.86	0.85			3.98	0.47
3.70	1.10			2.34	0.68			2.30	0.82
6.09	0.67			2.56	0.62			1.73	1.06
7.13	0.57			2.36	0.67			2.70	0.67
0 mm	0 mm	8 mm	8 mm	18 mm	18 mm	27 mm	27 mm	38 mm	38 mm
Major	Minor	Major	Minor	Major	Minor	Major	Minor	Major	Minor
2.94	1.36			3.09	0.52			4.16	0.43
7.69	0.52			2.65	0.59			1.99	0.89
6.03	0.66			1.38	1.13			3.80	0.47
5.77	0.69			3.69	0.42			3.95	0.44
2.36	1.68			3.27	0.48			2.06	0.82
5.49	0.72			4.05	0.38			4.10	0.41
7.99	0.50			3.03	0.51			3.54	0.47
3.27	1.21			2.87	0.54			3.23	0.49
4.12	0.96			4.58	0.34			4.19	0.38
4.78	0.82			3.24	0.48			1.57	1.01
3.96	0.99			1.90	0.80			3.03	0.51
3.07	1.26			3.20	0.47			4.11	0.38
4.26	0.91			3.40	0.45			2.26	0.69
2.73	1.41			3.94	0.39			4.37	0.36
5.74	0.67			3.58	0.41			3.64	0.42
5.66	0.68			2.48	0.60			6.35	0.24
7.07	0.54			4.53	0.33			1.93	0.79
2.30	1.65			2.16	0.69			3.19	0.47
5.09	0.74			4.09	0.35			3.27	0.45
2.56	1.48			2.76	0.53			2.19	0.68
6.23	0.61			2.65	0.55			3.82	0.39
4.01	0.93			2.22	0.64			2.70	0.54
5.47	0.68			3.08	0.46			1.72	0.84
4.61	0.81			3.07	0.45			3.61	0.39
6.04	0.61			1.33	1.04			2.36	0.60
2.81	1.31			2.16	0.64			1.54	0.90
6.49	0.57			4.06	0.34			2.93	0.46
4.65	0.78			2.31	0.58			1.91	0.68
4.98	0.73			2.62	0.51			1.57	0.83
4.11	0.89			2.15	0.61			2.73	0.48
5.46	0.67			3.19	0.41			4.16	0.29
3.18	1.13			2.79	0.46			5.06	0.24

6.97	0.52			2.88	0.44			2.77	0.42
4.92	0.73			2.87	0.44			2.04	0.57
5.27	0.68			1.38	0.93			3.07	0.37
4.36	0.82			2.67	0.46			2.19	0.52
5.24	0.68			1.83	0.68			2.77	0.41
6.86	0.52			2.86	0.43			2.77	0.41
7.04	0.50			1.70	0.73			4.00	0.28
3.21	1.07			1.42	0.85			1.81	0.61
4.23	0.80			3.46	0.35			3.11	0.35
3.74	0.91			2.67	0.44			3.94	0.26
4.29	0.79			2.58	0.45			5.12	0.20
4.43	0.77			2.07	0.56			2.36	0.43
5.43	0.62			1.78	0.66			1.44	0.71
3.89	0.86			3.02	0.39			3.60	0.28
5.13	0.65			2.86	0.41			2.21	0.45
2.88	1.16			2.43	0.47			1.82	0.52
2.16	1.54			1.81	0.62			2.02	0.47
3.42	0.97			2.57	0.44			2.08	0.44
4.80	0.68			1.51	0.75			1.18	0.78
2.04	1.61			4.06	0.26			2.42	0.38
3.69	0.89			2.33	0.46			2.51	0.35
0 mm	0 mm	8 mm	8 mm	18 mm	18 mm	27 mm	27 mm	38 mm	38 mm
Major	Minor	Major	Minor	Major	Minor	Major	Minor	Major	Minor
5.26	0.62			2.14	0.48			1.82	0.49
3.82	0.85			2.39	0.41			1.25	0.71
4.87	0.66			3.05	0.31			2.78	0.32
3.89	0.82			2.45	0.39			2.65	0.32
3.72	0.86			1.61	0.57			2.50	0.34
2.69	1.18			2.57	0.36			3.41	0.24
4.12	0.76			3.60	0.26			1.87	0.43
4.26	0.74			2.46	0.37			1.88	0.43
5.75	0.55			1.22	0.73			1.42	0.55
1.95	1.60			3.07	0.28			1.92	0.40
4.51	0.69			3.07	0.27			3.28	0.24
3.44	0.90			1.93	0.42			1.24	0.63
4.42	0.70			1.43	0.54			1.94	0.38
5.52	0.56			1.82	0.43			1.98	0.37
3.58	0.87			1.89	0.39			2.54	0.28
3.66	0.84			2.46	0.30			1.58	0.40
3.66	0.83			1.64	0.39			1.85	0.34
4.48	0.68			2.13	0.27			1.22	0.47
4.95	0.61			1.64	0.35			2.61	0.22
5.54	0.55			1.49	0.38			1.85	0.31
2.11	1.42			2.29	0.25			2.26	0.25
6.04	0.50			2.22	0.24			2.10	0.25
2.92	1.03			1.20	0.44			1.36	0.39
3.92	0.75			1.17	0.46			1.01	0.53
3.24	0.91			2.86	0.17			0.95	0.52
3.42	0.85			1.89	0.26			2.11	0.22
3.04	0.95			2.37	0.21			2.23	0.21
3.68	0.79			2.68	0.16			2.08	0.22

3.30	0.87			1.88	0.19			1.31	0.32
7.48	0.38			1.08	0.29			1.19	0.36
4.36	0.66			1.91	0.15			1.51	0.26
2.61	1.10			0.19	0.19			1.51	0.26
3.45	0.83			32.72	15.65			1.30	0.22
2.56	1.10			16.93	7.28			1.34	0.16
1.90	1.49			18.25	5.46			0.82	0.17
4.96	0.57			20.65	4.41			30.92	23.15
3.47	0.82			18.92	4.68			23.46	11.45
3.09	0.92			17.07	4.72			19.62	7.94
3.70	0.76			16.46	4.84			28.29	4.57
4.20	0.66			23.93	2.89			14.80	8.42
2.92	0.96			22.35	2.94			17.35	6.93
3.20	0.86			10.70	6.14			22.41	5.06
4.11	0.67			22.95	2.73			18.53	5.45
2.19	1.26			15.83	3.79			20.19	4.99
3.56	0.78			13.89	4.21			22.60	4.11
3.05	0.89			22.00	2.60			14.26	6.19
2.56	1.06			14.12	4.02			25.40	3.15
6.11	0.45			20.20	2.80			22.58	3.39
4.06	0.67			14.38	3.83			23.04	3.22
5.62	0.48			25.45	2.12			16.72	4.26
8.11	0.34			21.41	2.49			21.01	3.27
1.94	1.40			16.16	3.29			32.36	2.05
2.24	1.20			16.91	3.11			14.68	4.32
0 mm	0 mm	8 mm	8 mm	18 mm	18 mm	27 mm	27 mm	38 mm	38 mm
Major	Minor	Major	Minor	Major	Minor	Major	Minor	Major	Minor
2.43	1.10			8.54	6.06			11.98	4.95
4.46	0.60			10.65	4.76			18.46	3.11
5.34	0.50			12.03	4.16			11.56	4.81
1.99	1.30			16.40	2.96			18.75	2.77
2.93	0.87			12.82	3.75			7.71	6.46
5.18	0.49			17.93	2.64			16.02	3.04
4.00	0.63			14.38	3.16			7.77	6.13
2.64	0.95			18.30	2.47			19.18	2.48
2.77	0.89			13.12	3.44			17.24	2.73
4.23	0.59			14.66	3.07			10.39	4.46
5.27	0.46			18.76	2.39			9.66	4.75
3.73	0.65			16.18	2.76			15.83	2.87
3.96	0.61			15.16	2.88			17.40	2.60
4.41	0.55			22.90	1.90			23.74	1.87
7.92	0.30			11.00	3.86			12.55	3.47
2.48	0.95			16.42	2.58			6.94	6.17
2.93	0.79			7.77	5.19			20.81	2.05
5.10	0.44			9.39	4.24			16.40	2.56
2.93	0.77			33.01	1.19			10.42	4.01
3.69	0.61			17.05	2.30			18.07	2.30
4.20	0.54			13.63	2.87			8.66	4.76
3.35	0.67			7.92	4.91			20.06	2.05
2.87	0.78			12.47	3.03			10.44	3.72
2.21	1.01			7.70	4.86			8.73	4.43

3.09	0.71			6.89	5.41			8.24	4.51
2.36	0.93			22.80	1.61			13.24	2.80
2.81	0.77			8.33	4.40			7.97	4.65
2.98	0.72			16.73	2.17			14.50	2.55
6.57	0.32			9.10	3.96			14.04	2.63
1.86	1.14			21.13	1.71			13.99	2.62
3.01	0.71			7.41	4.81			11.46	3.16
2.03	1.03			19.15	1.82			15.51	2.33
5.05	0.41			12.67	2.73			8.18	4.38
3.37	0.62			9.60	3.55			12.04	2.93
2.06	1.00			18.62	1.80			15.88	2.22
2.17	0.94			7.61	4.16			13.72	2.56
5.61	0.37			9.33	3.38			10.57	3.31
3.70	0.55			8.23	3.80			15.13	2.29
3.73	0.55			9.57	3.26			16.48	2.09
2.34	0.88			16.36	1.90			27.65	1.24
2.12	0.95			8.27	3.71			26.16	1.30
3.61	0.56			22.90	1.31			17.82	1.90
3.01	0.67			8.74	3.44			11.89	2.84
3.32	0.60			13.05	2.30			8.10	4.15
3.45	0.57			20.76	1.42			16.94	1.98
2.83	0.70			10.97	2.60			10.87	3.07
3.20	0.62			5.65	5.04			13.28	2.51
2.83	0.70			9.28	3.06			16.91	1.95
4.01	0.49			13.70	2.05			13.51	2.43
4.44	0.45			13.70	2.05			7.83	4.16
1.80	1.08			8.94	3.13			13.04	2.47
2.59	0.75			15.59	1.79			10.04	3.21
2.50	0.76			14.49	1.84			6.82	4.66
0 mm	0 mm	8 mm	8 mm	18 mm	18 mm	27 mm	27 mm	38 mm	38 mm
Major	Minor	Major	Minor	Major	Minor	Major	Minor	Major	Minor
3.71	0.51			12.02	2.21			14.85	2.09
3.05	0.63			10.06	2.60			29.61	1.05
3.87	0.49			8.24	3.13			13.37	2.30
2.25	0.83			12.59	1.97			7.09	4.34
4.33	0.43			5.64	4.26			9.39	3.16
2.60	0.71			5.91	3.99			7.25	4.09
2.54	0.72			6.32	3.72			20.84	1.40
3.97	0.46			15.53	1.45			12.66	2.29
3.64	0.51			16.43	1.35			13.94	2.07
2.44	0.74			15.54	1.42			10.71	2.65
3.59	0.50			14.34	1.53			21.05	1.34
2.03	0.89			7.15	3.03			5.79	4.85
3.39	0.52			16.40	1.30			10.68	2.55
3.23	0.55			18.76	1.13			13.54	2.01
2.11	0.84			16.43	1.28			5.37	5.06
2.40	0.74			16.18	1.30			6.29	4.32
1.41	1.23			14.96	1.40			11.95	2.26
1.89	0.92			13.58	1.53			16.18	1.64
2.30	0.74			7.52	2.75			14.30	1.83
3.45	0.49			22.17	0.93			7.00	3.66



2.57	0.66			10.27	1.98			5.72	4.48
2.64	0.64			4.94	4.10			11.49	2.22
2.74	0.62			13.13	1.54			16.37	1.55
2.23	0.76			4.96	4.06			6.06	4.10
2.23	0.75			15.16	1.32			7.83	3.14
3.44	0.48			8.04	2.48			8.79	2.79
1.88	0.89			5.67	3.51			15.78	1.53
2.08	0.80			10.88	1.81			13.96	1.72
2.45	0.66			17.86	1.10			18.43	1.28
6.35	0.25			5.78	3.34			7.52	3.10
3.03	0.53			21.38	0.90			23.36	0.99
2.21	0.72			17.82	1.08			7.66	2.97
1.90	0.84			7.28	2.62			16.60	1.36
3.53	0.45			13.38	1.42			5.17	4.34
2.45	0.65			13.51	1.41			5.35	4.01
2.44	0.64			9.47	2.01			11.65	1.84
2.17	0.70			5.73	3.26			15.76	1.35
4.46	0.34			14.50	1.28			6.13	3.45
2.77	0.54			8.68	2.14			10.55	2.00
3.33	0.45			7.98	2.32			13.19	1.59
2.52	0.59			9.38	1.97			12.49	1.67
1.81	0.80			6.85	2.68			6.03	3.44
2.41	0.60			5.28	3.44			6.50	3.19
2.15	0.68			14.68	1.23			11.92	1.72
1.56	0.93			4.91	3.67			9.65	2.09
2.93	0.48			25.10	0.69			9.05	2.19
3.02	0.47			4.37	3.91			7.18	2.76
2.93	0.48			6.05	2.78			6.05	3.27
1.90	0.75			16.85	0.98			6.25	3.15
4.20	0.34			4.11	3.98			11.67	1.69
1.78	0.77			18.22	0.89			7.13	2.76
2.78	0.50			5.74	2.82			7.35	2.67
3.80	0.36			15.81	1.02			5.26	3.73
0 mm	0 mm	8 mm	8 mm	18 mm	18 mm	27 mm	27 mm	38 mm	38 mm
Major	Minor	Major	Minor	Major	Minor	Major	Minor	Major	Minor
1.92	0.70			16.45	0.95			12.39	1.57
1.77	0.76			14.76	1.06			5.99	3.24
2.35	0.57			6.70	2.31			13.26	1.44
2.27	0.58			10.19	1.50			5.47	3.48
2.65	0.49			5.48	2.79			9.92	1.91
1.69	0.75			16.91	0.90			10.09	1.88
2.78	0.46			20.04	0.74			10.75	1.75
2.31	0.55			4.55	3.24			9.69	1.93
1.46	0.85			4.74	3.06			8.69	2.14
1.66	0.75			5.05	2.84			29.23	0.62
1.33	0.90			4.19	3.40			24.03	0.75
4.30	0.28			9.00	1.55			4.79	3.77
2.41	0.50			4.55	3.06			4.85	3.72
2.75	0.44			18.35	0.76			23.73	0.76
1.76	0.66			16.52	0.84			8.85	2.02
2.95	0.40			3.86	3.58			7.09	2.50

2.55	0.46			11.56	1.19			5.77	3.03
2.06	0.55			15.23	0.90			10.55	1.66
3.60	0.31			5.41	2.54			18.06	0.96
2.59	0.42			11.37	1.21			5.23	3.28
3.10	0.35			15.26	0.89			6.70	2.56
1.92	0.57			12.73	1.06			9.54	1.79
2.97	0.37			10.21	1.32			8.94	1.91
2.09	0.52			12.46	1.08			16.31	1.03
1.88	0.57			5.09	2.63			11.63	1.44
1.81	0.59			12.05	1.10			10.95	1.51
2.55	0.42			6.95	1.91			8.27	1.99
2.11	0.49			14.39	0.91			13.74	1.19
1.70	0.60			6.01	2.18			13.35	1.22
2.34	0.42			11.48	1.14			5.14	3.15
2.13	0.45			12.77	1.02			9.70	1.66
4.03	0.24			13.87	0.93			12.25	1.30
2.13	0.45			10.88	1.18			9.24	1.72
2.64	0.35			14.43	0.88			6.34	2.49
1.70	0.54			17.01	0.75			9.40	1.67
2.34	0.36			16.30	0.76			7.05	2.22
1.30	0.63			7.13	1.74			7.27	2.15
1.95	0.42			4.30	2.88			21.24	0.73
1.88	0.41			14.57	0.84			8.40	1.84
1.05	0.71			6.40	1.91			8.41	1.83
1.05	0.71			5.14	2.38			5.12	3.00
2.14	0.33			3.87	3.14			10.61	1.45
1.18	0.54			10.18	1.19			4.69	3.27
1.84	0.35			8.54	1.42			7.98	1.91
1.53	0.39			16.65	0.72			8.54	1.78
1.45	0.42			14.95	0.80			5.23	2.88
1.63	0.37			14.89	0.80			13.80	1.09
1.61	0.31			5.08	2.35			19.18	0.78
0.98	0.33			4.48	2.67			5.08	2.95
1.08	0.29			5.38	2.22			9.51	1.57
0.58	0.42			7.51	1.58			6.83	2.17
24.14	4.63			9.86	1.20			11.81	1.25
19.80	4.58			4.94	2.39			5.27	2.78
0 mm	0 mm	8 mm	8 mm	18 mm	18 mm	27 mm	27 mm	38 mm	38 mm
Major	Minor	Major	Minor	Major	Minor	Major	Minor	Major	Minor
14.59	4.76			9.83	1.19			12.11	1.21
21.42	3.22			9.58	1.22			7.30	1.99
15.15	4.18			8.75	1.33			9.72	1.48
27.34	2.31			3.99	2.90			5.09	2.82
12.20	4.85			4.90	2.34			14.44	0.99
19.70	2.79			5.01	2.28			5.88	2.41
20.26	2.51			4.46	2.55			15.70	0.89
16.98	2.80			11.23	1.00			4.25	3.26
10.90	4.31			21.54	0.52			5.20	2.65
23.94	1.89			4.22	2.63			7.30	1.84
23.02	1.79			12.16	0.91			14.02	0.95
21.90	1.79			17.35	0.62			10.09	1.32

8.39	4.63			8.13	1.32			12.76	1.04
9.57	3.90			13.27	0.81			12.15	1.09
17.23	2.09			8.69	1.23			11.03	1.19
11.06	3.24			3.79	2.81			9.20	1.43
12.97	2.66			15.47	0.69			14.38	0.91
7.70	4.47			7.84	1.35			8.64	1.51
13.18	2.55			4.30	2.44			4.12	3.15
9.12	3.66			10.26	1.02			18.26	0.71
8.65	3.83			9.60	1.09			4.43	2.91
20.56	1.56			13.79	0.75			4.17	3.09
8.68	3.50			8.24	1.26			8.15	1.58
12.47	2.42			13.85	0.75			6.90	1.87
14.84	2.03			6.59	1.56			12.48	1.03
13.23	2.17			6.81	1.51			6.52	1.91
9.25	3.08			4.05	2.52			10.98	1.13
9.86	2.89			3.60	2.83			5.47	2.27
6.07	4.66			3.60	2.83			5.23	2.37
8.61	3.22			19.58	0.52			9.57	1.29
8.43	3.25			8.81	1.15			10.36	1.18
7.53	3.61			4.14	2.44			8.61	1.42
17.81	1.53			5.56	1.81			15.15	0.80
11.36	2.32			3.80	2.62			16.42	0.74
9.36	2.76			5.88	1.67			4.32	2.81
9.28	2.77			5.09	1.92			15.34	0.79
12.55	2.05			13.54	0.72			10.87	1.11
7.70	3.31			9.63	1.00			12.24	0.98
8.71	2.90			12.67	0.76			13.72	0.87
6.31	3.93			10.39	0.92			10.05	1.19
7.26	3.41			4.07	2.34			10.16	1.17
5.45	4.50			4.69	2.02			14.95	0.79
7.00	3.42			10.05	0.94			4.79	2.47
29.63	0.80			10.23	0.92			18.65	0.63
15.33	1.51			6.56	1.43			16.37	0.70
14.37	1.59			6.70	1.40			12.55	0.91
10.85	2.11			11.07	0.85			9.39	1.22
19.97	1.14			9.95	0.94			6.07	1.88
7.22	3.12			9.85	0.93			8.99	1.27
12.91	1.74			4.84	1.90			12.96	0.88
6.79	3.28			4.35	2.11			16.07	0.71
5.71	3.87			3.85	2.36			14.78	0.77
12.31	1.79			4.92	1.84			10.28	1.10
0 mm	0 mm	8 mm	8 mm	18 mm	18 mm	27 mm	27 mm	38 mm	38 mm
Major	Minor	Major	Minor	Major	Minor	Major	Minor	Major	Minor
6.01	3.63			7.16	1.26			4.31	2.59
13.99	1.53			9.81	0.92			4.32	2.57
21.20	1.00			3.74	2.40			3.59	3.07
7.16	2.93			11.14	0.80			5.23	2.08
10.77	1.95			3.04	2.88			3.36	3.22
11.41	1.83			9.08	0.97			6.27	1.70
18.22	1.15			11.02	0.79			12.45	0.86
6.55	3.12			8.57	1.01			6.08	1.75

15.13	1.31			9.66	0.89			11.08	0.96
7.25	2.71			6.10	1.40			6.15	1.71
5.52	3.49			14.10	0.60			5.03	2.09
21.87	0.88			13.62	0.62			4.26	2.46
4.73	3.97			3.54	2.39			3.61	2.89
9.11	2.03			7.24	1.16			3.61	2.87
8.60	2.14			15.45	0.54			12.30	0.84
5.47	3.36			14.44	0.57			13.83	0.74
4.91	3.74			8.52	0.97			6.42	1.60
24.25	0.76			12.38	0.66			7.95	1.29
12.00	1.53			13.89	0.59			3.98	2.55
4.46	4.09			6.58	1.24			5.45	1.86
4.81	3.79			4.31	1.89			5.52	1.82
9.84	1.83			11.33	0.72			5.83	1.72
9.08	1.97			3.26	2.48			12.39	0.81
5.78	3.07			7.09	1.14			12.14	0.82
4.70	3.70			3.03	2.66			7.46	1.34
18.83	0.92			9.78	0.82			9.67	1.03
21.02	0.82			3.36	2.39			9.36	1.06
5.71	3.00			5.26	1.52			3.58	2.77
5.23	3.22			10.25	0.78			6.88	1.42
7.64	2.19			7.04	1.13			6.68	1.46
5.34	3.13			5.35	1.48			8.12	1.20
5.38	3.10			14.09	0.56			7.87	1.23
17.26	0.97			7.22	1.09			17.21	0.56
5.88	2.81			7.55	1.04			4.62	2.08
6.37	2.58			14.84	0.53			15.49	0.61
7.15	2.29			8.62	0.91			10.21	0.92
5.20	3.14			7.04	1.11			8.38	1.12
5.43	3.01			9.17	0.84			12.80	0.73
7.86	2.08			20.56	0.38			6.64	1.39
18.86	0.85			8.11	0.95			6.80	1.36
5.65	2.84			12.27	0.63			5.41	1.70
16.03	1.00			12.54	0.61			3.76	2.44
10.57	1.52			11.38	0.67			6.25	1.45
13.83	1.15			13.83	0.56			8.41	1.08
4.83	3.26			3.81	2.02			3.23	2.79
5.76	2.71			15.10	0.51			16.07	0.56
9.84	1.59			7.36	1.04			18.06	0.49
21.20	0.73			5.07	1.51			14.71	0.61
5.58	2.78			7.20	1.04			11.38	0.77
13.61	1.14			4.55	1.64			10.95	0.80
4.84	3.19			4.41	1.69			12.01	0.73
4.17	3.69			3.73	1.98			3.99	2.16
10.82	1.42			13.39	0.54			10.71	0.80
0 mm	0 mm	8 mm	8 mm	18 mm	18 mm	27 mm	27 mm	38 mm	38 mm
Major	Minor	Major	Minor	Major	Minor	Major	Minor	Major	Minor
12.95	1.18			4.26	1.71			6.58	1.31
7.03	2.16			5.82	1.24			13.14	0.65
14.54	1.04			5.53	1.30			8.94	0.93
4.83	3.10			12.98	0.55			7.40	1.12

5.52	2.70			3.03	2.35			11.23	0.73
17.31	0.86			5.61	1.27			3.01	2.74
11.14	1.34			3.61	1.97			4.87	1.69
5.05	2.94			11.60	0.61			10.38	0.79
7.82	1.88			7.35	0.95			4.94	1.66
5.82	2.50			2.94	2.38			4.77	1.72
5.13	2.83			10.04	0.70			4.87	1.67
17.34	0.83			8.75	0.80			7.84	1.03
7.13	1.98			11.53	0.61			10.86	0.74
16.97	0.83			9.47	0.74			6.12	1.30
6.26	2.23			7.76	0.90			9.37	0.85
14.81	0.94			14.39	0.48			7.69	1.03
9.72	1.42			5.08	1.37			11.10	0.71
3.97	3.47			5.95	1.17			12.29	0.64
12.19	1.13			6.43	1.07			11.28	0.69
12.63	1.09			13.67	0.50			4.17	1.87
4.23	3.24			10.26	0.67			8.87	0.88
7.78	1.74			11.84	0.58			6.34	1.23
5.80	2.32			11.08	0.62			16.08	0.48
13.30	1.00			8.07	0.85			10.90	0.71
8.80	1.49			10.86	0.63			4.94	1.54
4.80	2.73			5.52	1.23			9.33	0.81
22.57	0.58			12.56	0.54			5.65	1.32
16.31	0.80			11.26	0.60			3.51	2.10
4.32	3.01			3.25	2.08			4.20	1.75
10.33	1.25			4.50	1.49			6.98	1.06
11.99	1.08			10.22	0.64			4.77	1.54
4.96	2.58			4.04	1.62			5.62	1.31
11.07	1.15			7.73	0.84			3.59	2.04
4.89	2.60			3.54	1.83			6.38	1.14
18.18	0.70			5.38	1.19			3.53	2.05
13.59	0.93			11.18	0.57			13.49	0.53
5.15	2.45			2.82	2.25			11.49	0.62
7.78	1.62			7.04	0.90			5.81	1.24
19.71	0.63			12.96	0.49			9.32	0.77
4.61	2.67			6.00	1.05			8.32	0.86
5.46	2.26			3.48	1.80			12.91	0.55
9.04	1.35			10.96	0.57			7.87	0.89
13.45	0.90			4.64	1.34			3.86	1.81
13.22	0.91			16.37	0.38			5.22	1.32
4.11	2.90			10.81	0.57			9.92	0.70
14.09	0.85			3.04	2.01			7.50	0.92
16.93	0.70			11.18	0.54			4.22	1.64
8.54	1.39			8.73	0.70			5.97	1.14
12.37	0.96			10.49	0.58			3.14	2.18
12.87	0.92			8.56	0.70			14.24	0.48
5.50	2.14			5.64	1.06			7.70	0.88
4.65	2.52			3.98	1.49			7.26	0.93
9.72	1.20			8.44	0.70			9.63	0.70
0 mm	0 mm	8 mm	8 mm	18 mm	18 mm	27 mm	27 mm	38 mm	38 mm
Major	Minor	Major	Minor	Major	Minor	Major	Minor	Major	Minor

15.45	0.76	2.82	2.10	5.13	1.31
10.66	1.10	7.68	0.77	4.35	1.53
5.20	2.24	6.40	0.92	9.30	0.72
10.01	1.16	9.34	0.63	3.07	2.14
11.17	1.03	5.07	1.16	5.92	1.11
12.17	0.94	4.52	1.29	8.43	0.77
4.07	2.81	2.97	1.95	4.25	1.53
5.95	1.89	10.78	0.53	4.37	1.49
13.81	0.81	4.00	1.44	7.04	0.91
5.24	2.14	10.52	0.54	8.53	0.75
4.04	2.78	10.66	0.53	3.00	2.13
7.07	1.58	3.32	1.71	6.99	0.91
15.87	0.70	10.41	0.55	4.30	1.45
4.94	2.23	5.15	1.10	4.81	1.29
8.75	1.25	8.81	0.64	5.31	1.16
6.15	1.78	7.02	0.80	7.49	0.82
8.25	1.33	7.68	0.73	8.94	0.68
4.81	2.27	8.09	0.70	3.50	1.75
6.58	1.66	5.15	1.09	7.03	0.87
10.09	1.07	8.12	0.68	8.53	0.71
6.08	1.76	11.90	0.47	3.94	1.53
8.63	1.24	8.74	0.63	6.37	0.95
4.47	2.38	5.43	1.01	3.50	1.71
11.66	0.91	5.11	1.06	7.45	0.80
3.43	3.08	3.28	1.66	7.73	0.77
14.76	0.71	2.61	2.09	4.57	1.29
15.15	0.69	6.79	0.80	4.05	1.46
3.56	2.92	8.26	0.65	3.52	1.67
4.17	2.49	12.44	0.43	9.17	0.64
12.99	0.79	3.71	1.45	2.84	2.07
12.40	0.83	6.84	0.79	4.81	1.21
9.47	1.08	9.42	0.57	5.59	1.05
5.22	1.95	12.10	0.44	6.54	0.89
8.87	1.15	8.31	0.64	3.34	1.73
7.73	1.32	5.13	1.03	5.93	0.97
4.32	2.35	6.02	0.88	2.77	2.09
12.60	0.80	4.88	1.07	3.33	1.72
9.48	1.05	7.58	0.69	6.47	0.88
11.68	0.85	5.52	0.95	5.63	1.00
5.14	1.91	9.89	0.53	5.09	1.10
5.53	1.77	5.88	0.88	3.02	1.85
6.85	1.43	6.66	0.77	2.82	1.99
16.12	0.61	3.67	1.39	6.14	0.91
11.54	0.85	7.20	0.71	7.93	0.69
5.68	1.71	7.51	0.68	4.65	1.18
13.68	0.70	4.73	1.07	3.99	1.37
9.90	0.97	2.49	2.04	3.27	1.67
4.51	2.10	8.29	0.61	6.89	0.79
12.42	0.76	2.61	1.92	4.72	1.15
9.03	1.04	7.77	0.64	6.51	0.84
5.47	1.70	3.37	1.49	2.64	2.05

11.26	0.83			14.00	0.36			7.73	0.69
9.28	1.00			2.66	1.87			5.26	1.00
0 mm	0 mm	8 mm	8 mm	18 mm	18 mm	27 mm	27 mm	38 mm	38 mm
Major	Minor	Major	Minor	Major	Minor	Major	Minor	Major	Minor
7.49	1.22			3.44	1.43			12.67	0.41
11.99	0.76			10.56	0.46			7.73	0.68
9.17	1.00			6.67	0.73			3.29	1.58
4.80	1.90			9.93	0.49			6.13	0.85
12.14	0.74			4.18	1.16			3.86	1.34
3.91	2.30			2.65	1.82			7.60	0.67
3.30	2.71			2.94	1.64			3.58	1.41
13.52	0.66			6.30	0.75			7.19	0.70
11.86	0.75			3.85	1.21			7.90	0.63
5.01	1.76			7.34	0.63			3.96	1.25
3.62	2.43			2.83	1.64			5.69	0.87
4.10	2.14			6.83	0.68			2.60	1.90
4.44	1.97			4.56	1.02			2.70	1.82
4.04	2.15			3.86	1.19			4.43	1.11
8.49	1.02			8.18	0.56			9.19	0.53
3.62	2.38			7.84	0.58			12.30	0.40
4.90	1.76			7.57	0.59			2.94	1.66
7.02	1.22			8.56	0.52			4.75	1.01
6.49	1.32			7.99	0.56			4.75	1.01
3.46	2.48			7.76	0.57			2.29	2.08
7.69	1.11			2.35	1.89			3.15	1.51
7.70	1.10			6.95	0.64			6.12	0.77
9.65	0.88			4.50	0.97			2.83	1.66
14.16	0.60			7.47	0.58			4.94	0.94
4.90	1.73			3.01	1.45			2.49	1.84
4.23	2.00			5.90	0.74			2.53	1.81
7.52	1.12			6.19	0.70			3.74	1.21
6.50	1.30			4.40	0.98			5.19	0.87
9.31	0.90			7.00	0.61			5.34	0.85
5.92	1.42			3.51	1.22			8.09	0.56
4.40	1.89			6.90	0.61			2.67	1.70
6.93	1.20			4.25	1.00			5.72	0.79
4.83	1.71			5.42	0.78			11.42	0.39
12.86	0.63			8.04	0.52			3.15	1.40
6.60	1.23			3.58	1.17			4.60	0.95
3.88	2.09			4.76	0.88			3.37	1.30
3.88	2.09			3.94	1.06			3.71	1.17
9.35	0.87			4.76	0.87			2.44	1.78
4.88	1.65			6.63	0.62			6.02	0.72
8.83	0.92			2.76	1.49			3.57	1.22
8.04	1.01			4.08	1.00			6.75	0.64
4.59	1.75			7.42	0.54			4.94	0.86
10.78	0.74			11.20	0.36			5.51	0.77
3.84	2.08			6.24	0.64			4.21	1.00
9.67	0.83			5.48	0.73			5.18	0.80
6.26	1.27			3.07	1.29			8.72	0.48
10.12	0.79			5.40	0.73			8.28	0.50

8.75	0.91			5.26	0.74			2.10	1.97
8.30	0.95			6.73	0.58			3.94	1.05
13.78	0.57			11.93	0.33			2.83	1.46
7.41	1.07			6.09	0.64			3.04	1.36
9.65	0.82			2.05	1.88			7.24	0.56
6.50	1.20			3.04	1.26			2.59	1.57
0 mm	0 mm	8 mm	8 mm	18 mm	18 mm	27 mm	27 mm	38 mm	38 mm
Major	Minor	Major	Minor	Major	Minor	Major	Minor	Major	Minor
8.30	0.94			5.95	0.64			5.47	0.74
12.63	0.61			4.54	0.84			2.92	1.38
8.99	0.86			10.33	0.37			5.23	0.77
3.59	2.14			6.77	0.56			3.72	1.08
4.15	1.83			5.87	0.65			4.59	0.87
4.37	1.73			4.69	0.81			2.85	1.40
13.65	0.55			6.63	0.57			4.06	0.98
6.46	1.17			5.12	0.73			2.96	1.34
9.64	0.78			3.50	1.07			2.81	1.40
16.02	0.47			12.51	0.30			3.94	1.00
10.83	0.69			7.07	0.53			3.53	1.12
11.14	0.67			6.85	0.54			5.28	0.74
6.63	1.12			3.00	1.22			8.37	0.46
11.80	0.63			3.33	1.10			6.87	0.57
5.40	1.38			5.48	0.66			9.01	0.43
4.62	1.60			6.88	0.52			6.87	0.57
12.51	0.59			5.55	0.65			2.96	1.29
8.74	0.84			5.55	0.65			4.19	0.91
8.28	0.88			6.85	0.52			4.44	0.85
5.64	1.29			2.10	1.70			7.05	0.53
10.33	0.70			4.30	0.82			2.15	1.74
8.72	0.82			4.67	0.76			2.71	1.37
13.59	0.52			3.69	0.95			4.44	0.84
5.95	1.20			2.44	1.43			5.92	0.62
7.89	0.89			4.28	0.81			4.43	0.83
10.10	0.69			2.29	1.50			2.94	1.24
6.69	1.04			4.73	0.73			3.60	1.01
6.09	1.14			5.75	0.60			2.25	1.59
9.10	0.76			5.69	0.61			6.60	0.54
4.42	1.56			10.22	0.34			3.94	0.90
18.09	0.38			4.13	0.83			4.83	0.73
7.69	0.90			7.47	0.46			4.76	0.74
10.12	0.68			2.09	1.62			2.44	1.41
9.10	0.75			2.90	1.16			4.26	0.80
5.12	1.34			8.46	0.40			4.43	0.76
7.55	0.90			7.35	0.45			4.53	0.75
8.26	0.82			2.16	1.52			6.32	0.54
5.00	1.34			5.78	0.57			9.02	0.37
3.96	1.69			6.16	0.53			5.09	0.66
8.46	0.79			4.16	0.78			3.21	1.03
3.42	1.95			2.52	1.28			3.28	1.00
4.28	1.56			5.18	0.61			3.64	0.91
5.93	1.12			11.91	0.26			2.86	1.15



10.74	0.62			3.57	0.88			5.05	0.65
11.58	0.57			4.70	0.67			2.62	1.25
10.17	0.65			2.32	1.35			8.30	0.39
10.51	0.63			3.30	0.93			3.07	1.05
7.29	0.91			5.40	0.57			3.29	0.97
9.20	0.72			2.25	1.37			3.37	0.95
11.44	0.58			2.67	1.12			4.92	0.65
6.65	0.99			2.70	1.10			5.60	0.57
8.29	0.79			3.04	0.98			3.65	0.87
8.27	0.79			2.21	1.35			2.12	1.48
0 mm	0 mm	8 mm	8 mm	18 mm	18 mm	27 mm	27 mm	38 mm	38 mm
Major	Minor	Major	Minor	Major	Minor	Major	Minor	Major	Minor
9.14	0.71			3.01	0.98			2.12	1.48
14.18	0.46			4.59	0.64			2.02	1.54
8.19	0.79			4.44	0.66			4.43	0.69
8.28	0.78			4.08	0.72			7.40	0.42
6.81	0.95			4.69	0.62			3.74	0.81
6.00	1.08			6.59	0.44			4.29	0.71
6.81	0.95			6.31	0.46			3.91	0.78
4.76	1.36			3.65	0.79			3.50	0.86
6.15	1.05			3.21	0.90			2.58	1.17
9.40	0.68			2.61	1.11			2.83	1.07
6.88	0.94			4.10	0.70			5.43	0.55
9.33	0.69			2.83	1.00			2.73	1.07
3.52	1.82			2.89	0.98			4.01	0.73
7.08	0.90			1.96	1.44			3.62	0.81
6.94	0.91			3.45	0.80			2.72	1.06
3.69	1.71			2.20	1.26			1.96	1.48
8.84	0.71			7.04	0.39			9.24	0.31
8.59	0.73			5.90	0.46			2.64	1.08
5.51	1.13			6.27	0.44			3.33	0.86
4.42	1.41			2.07	1.32			5.20	0.55
7.90	0.79			3.49	0.78			6.18	0.46
7.24	0.86			7.38	0.37			6.36	0.45
8.28	0.75			4.80	0.57			3.69	0.77
7.37	0.84			7.71	0.35			3.00	0.93
11.74	0.53			2.05	1.31			6.54	0.43
7.09	0.87			3.01	0.89			4.58	0.61
8.84	0.70			4.92	0.54			5.42	0.50
8.60	0.72			4.70	0.56			4.59	0.60
7.85	0.78			2.55	1.01			3.84	0.71
6.06	1.01			4.66	0.55			4.35	0.62
7.55	0.81			2.09	1.20			2.33	1.16
7.81	0.78			3.41	0.74			2.67	1.00
2.92	2.09			3.78	0.66			5.40	0.50
8.33	0.73			3.99	0.62			2.37	1.12
7.64	0.79			4.62	0.54			4.60	0.57
6.95	0.87			4.65	0.53			3.94	0.66
6.20	0.97			6.31	0.38			3.68	0.70
7.36	0.81			6.06	0.40			2.39	1.06
5.13	1.15			5.23	0.46			3.60	0.70

5.91	1.00			2.17	1.09			3.80	0.65
11.00	0.53			2.96	0.80			2.93	0.85
3.19	1.83			2.14	1.09			2.79	0.88
2.97	1.95			3.75	0.61			4.39	0.56
7.39	0.78			8.03	0.28			1.95	1.24
4.43	1.31			6.37	0.36			7.12	0.34
6.56	0.88			3.46	0.66			4.01	0.60
9.94	0.58			1.85	1.19			2.13	1.14
6.15	0.93			3.00	0.73			4.20	0.57
12.13	0.47			5.43	0.40			3.41	0.69
4.75	1.19			2.63	0.83			5.17	0.46
2.81	2.01			3.25	0.67			4.38	0.54
4.89	1.16			5.69	0.38			3.12	0.75
6.41	0.88			3.48	0.63			5.54	0.42
0 mm	0 mm	8 mm	8 mm	18 mm	18 mm	27 mm	27 mm	38 mm	38 mm
Major	Minor	Major	Minor	Major	Minor	Major	Minor	Major	Minor
5.07	1.10			1.65	1.32			3.54	0.65
5.91	0.94			3.73	0.57			3.43	0.66
8.59	0.65			2.72	0.79			5.31	0.42
7.10	0.78			4.69	0.45			2.71	0.83
6.27	0.88			2.32	0.90			2.55	0.85
8.17	0.67			3.90	0.53			2.55	0.85
7.76	0.70			3.89	0.53			3.48	0.63
6.53	0.84			5.76	0.35			3.30	0.66
6.76	0.81			1.79	1.13			2.36	0.91
5.46	1.00			2.91	0.70			3.79	0.57
8.56	0.63			6.27	0.32			1.68	1.26
4.42	1.22			5.53	0.36			3.77	0.56
2.40	2.24			2.28	0.86			5.80	0.36
6.67	0.81			4.56	0.43			2.89	0.73
9.70	0.55			6.05	0.32			4.97	0.41
3.75	1.42			2.18	0.90			2.30	0.88
5.36	0.99			2.86	0.67			4.22	0.48
8.64	0.62			4.07	0.47			1.53	1.30
4.38	1.21			1.52	1.25			2.34	0.85
5.10	1.04			2.52	0.75			4.05	0.49
5.98	0.89			2.33	0.80			4.33	0.46
9.41	0.57			4.61	0.40			1.78	1.12
7.40	0.71			3.47	0.54			2.79	0.70
8.16	0.65			2.02	0.92			3.22	0.61
9.11	0.58			2.04	0.92			3.29	0.60
5.42	0.98			2.07	0.89			2.66	0.74
2.41	2.18			2.52	0.73			2.20	0.88
6.77	0.78			1.90	0.92			1.67	1.15
6.58	0.80			2.78	0.63			1.93	0.98
7.41	0.70			4.37	0.40			3.61	0.52
7.09	0.73			4.08	0.43			2.46	0.76
7.11	0.73			5.21	0.33			2.11	0.89
6.74	0.76			5.69	0.31			2.16	0.85
5.33	0.96			3.71	0.47			1.89	0.97
6.28	0.82			4.68	0.37			5.76	0.31

7.10	0.72			3.60	0.47			2.94	0.61
6.65	0.77			1.61	1.04			2.92	0.61
6.87	0.75			4.02	0.41			2.52	0.70
7.22	0.71			2.56	0.64			2.96	0.59
2.77	1.84			1.73	0.95			2.34	0.74
6.19	0.82			1.52	1.04			3.05	0.56
3.61	1.40			7.93	0.20			2.27	0.75
3.18	1.59			1.61	0.97			2.14	0.79
3.78	1.34			2.79	0.55			1.59	1.04
7.89	0.64			2.82	0.53			2.34	0.71
8.97	0.56			2.74	0.55			2.63	0.63
6.80	0.74			2.63	0.57			2.76	0.60
6.23	0.81			2.00	0.75			2.30	0.72
4.90	1.03			3.59	0.41			3.57	0.46
7.33	0.68			2.04	0.71			3.26	0.51
6.88	0.72			5.26	0.28			4.22	0.38
6.33	0.79			1.36	1.05			2.79	0.58
5.04	0.98			2.57	0.55			2.94	0.53
0 mm	0 mm	8 mm	8 mm	18 mm	18 mm	27 mm	27 mm	38 mm	38 mm
Major	Minor	Major	Minor	Major	Minor	Major	Minor	Major	Minor
3.52	1.40			3.17	0.44			2.18	0.71
7.51	0.65			2.46	0.57			2.06	0.74
10.88	0.45			2.83	0.48			1.77	0.86
6.11	0.80			1.32	1.03			2.00	0.76
4.53	1.06			4.42	0.30			2.39	0.64
8.71	0.55			3.65	0.37			2.30	0.66
8.13	0.59			1.67	0.80			3.33	0.46
7.04	0.68			1.84	0.71			1.79	0.83
7.92	0.60			2.62	0.50			4.87	0.31
4.92	0.97			1.28	0.99			2.50	0.60
5.77	0.82			3.34	0.38			5.17	0.29
3.95	1.20			2.54	0.49			3.60	0.40
6.16	0.77			2.22	0.56			2.28	0.60
9.69	0.48			5.09	0.24			2.57	0.53
4.16	1.13			2.04	0.58			1.59	0.84
4.65	1.01			1.85	0.64			4.55	0.29
6.23	0.74			1.52	0.76			3.41	0.39
7.31	0.63			6.07	0.18			1.82	0.72
5.81	0.79			2.33	0.45			3.08	0.41
5.81	0.79			3.85	0.27			3.18	0.40
4.52	1.00			4.80	0.21			1.72	0.71
7.46	0.61			2.13	0.48			1.50	0.81
5.63	0.80			6.27	0.16			2.06	0.59
5.23	0.86			2.23	0.45			2.27	0.53
4.42	1.01			1.44	0.69			1.66	0.71
7.21	0.62			1.82	0.53			1.36	0.87
7.21	0.62			3.17	0.29			6.94	0.17
3.59	1.24			1.34	0.69			2.35	0.50
6.26	0.71			1.80	0.52			3.04	0.38
5.49	0.80			2.67	0.34			1.88	0.61
6.63	0.66			1.40	0.64			4.10	0.28

5.89	0.74			2.56	0.35			1.77	0.63
5.23	0.83			2.66	0.34			1.26	0.89
9.14	0.47			2.97	0.29			2.10	0.53
5.69	0.76			2.20	0.40			1.09	1.03
6.06	0.71			2.14	0.41			1.48	0.76
6.25	0.68			2.02	0.43			2.66	0.41
5.93	0.72			1.86	0.45			1.50	0.73
5.16	0.82			1.45	0.54			1.08	1.01
10.86	0.39			2.22	0.34			2.07	0.51
3.17	1.34			1.14	0.63			1.93	0.55
8.01	0.53			1.71	0.40			1.98	0.53
6.41	0.66			2.07	0.33			2.03	0.50
6.17	0.68			3.08	0.22			2.97	0.34
5.03	0.83			2.41	0.28			1.76	0.57
6.61	0.63			2.05	0.32			1.50	0.66
6.03	0.69			2.57	0.25			2.55	0.39
5.87	0.70			1.87	0.35			1.89	0.49
10.08	0.41			1.25	0.50			1.33	0.70
7.64	0.54			6.19	0.10			1.99	0.45
7.38	0.56			2.29	0.26			2.03	0.41
6.68	0.61			2.66	0.21			2.25	0.37
4.59	0.88			3.09	0.17			1.27	0.64
0 mm	0 mm	8 mm	8 mm	18 mm	18 mm	27 mm	27 mm	38 mm	38 mm
Major	Minor	Major	Minor	Major	Minor	Major	Minor	Major	Minor
6.15	0.65			1.28	0.39			3.23	0.25
7.38	0.54			4.11	0.11			2.84	0.27
8.58	0.47			3.08	0.15			1.31	0.59
7.06	0.56			0.62	0.15			1.23	0.61
8.72	0.46							1.54	0.48
6.82	0.58							1.37	0.52
6.48	0.61							1.57	0.42
2.58	1.53							1.88	0.35
7.42	0.53							2.23	0.28
4.17	0.94							3.00	0.21
5.47	0.72							1.64	0.34
4.60	0.84							1.10	0.48
3.75	1.03							1.29	0.41
3.30	1.18							1.63	0.29
3.06	1.26							2.93	0.15
6.87	0.56							1.05	0.27
6.78	0.57							0.96	0.16
7.86	0.49								
4.08	0.93								
4.46	0.85								
7.91	0.48								
5.54	0.68								
6.04	0.62								
6.32	0.60								
5.51	0.68								
6.96	0.53								
4.51	0.82								

3.01	1.22								
3.05	1.20								
6.64	0.55								
5.21	0.70								
6.22	0.58								
9.05	0.40								
2.82	1.29								
7.96	0.46								
4.45	0.82								
6.19	0.59								
2.24	1.60								
7.63	0.47								
6.87	0.52								
7.56	0.47								
7.22	0.49								
3.10	1.15								
10.14	0.35								
3.25	1.09								
3.14	1.13								
5.00	0.71								
5.72	0.62								
7.85	0.45								
4.55	0.76								
4.96	0.70								
2.60	1.33								
3.17	1.08								
0 mm	0 mm	8 mm	8 mm	18 mm	18 mm	27 mm	27 mm	38 mm	38 mm
Major	Minor	Major	Minor	Major	Minor	Major	Minor	Major	Minor
5.28	0.65								
5.48	0.62								
6.70	0.51								
4.20	0.81								
7.30	0.46								
4.06	0.82								
3.67	0.91								
4.54	0.73								
2.11	1.55								
3.62	0.90								
5.72	0.56								
7.15	0.45								
4.62	0.70								
5.24	0.61								
4.92	0.65								
3.88	0.82								
9.07	0.35								
8.68	0.36								
3.51	0.88								
5.41	0.57								
6.67	0.46								
4.51	0.67								
3.13	0.97								

3.82	0.80								
3.31	0.91								
6.51	0.46								
4.94	0.61								
8.38	0.36								
4.93	0.61								
4.73	0.63								
6.53	0.46								
5.10	0.59								
2.20	1.34								
9.12	0.32								
6.23	0.47								
5.15	0.57								
3.89	0.75								
6.02	0.47								
4.99	0.57								
4.15	0.69								
6.63	0.43								
5.19	0.55								
2.91	0.97								
4.43	0.64								
5.47	0.52								
4.59	0.61								
4.64	0.60								
3.24	0.86								
5.47	0.51								
3.66	0.76								
6.72	0.42								
4.66	0.59								
2.73	1.00								
0 mm	0 mm	8 mm	8 mm	18 mm	18 mm	27 mm	27 mm	38 mm	38 mm
Major	Minor	Major	Minor	Major	Minor	Major	Minor	Major	Minor
4.90	0.56								
3.24	0.84								
3.93	0.69								
2.65	1.02								
5.69	0.48								
2.27	1.18								
2.81	0.95								
4.64	0.57								
5.48	0.48								
3.97	0.67								
5.57	0.47								
2.90	0.90								
4.61	0.57								
4.92	0.52								
5.17	0.50								
3.02	0.84								
6.01	0.42								
4.38	0.57								
3.46	0.72								

2.35	1.04								
2.50	0.98								
5.59	0.44								
5.34	0.45								
4.59	0.53								
2.86	0.85								
3.43	0.71								
7.19	0.34								
3.50	0.68								
5.14	0.47								
4.69	0.50								
3.30	0.72								
6.50	0.36								
3.77	0.63								
3.54	0.67								
3.03	0.76								
1.89	1.22								
1.83	1.26								
4.72	0.49								
4.91	0.46								
2.15	1.05								
3.40	0.67								
4.51	0.50								
3.33	0.67								
4.35	0.51								
3.40	0.65								
2.82	0.77								
3.42	0.64								
3.98	0.54								
3.35	0.64								
1.96	1.09								
2.27	0.95								
2.36	0.90								
2.10	1.01								
0 mm	0 mm	8 mm	8 mm	18 mm	18 mm	27 mm	27 mm	38 mm	38 mm
Major	Minor	Major	Minor	Major	Minor	Major	Minor	Major	Minor
4.29	0.49								
4.28	0.49								
4.54	0.47								
3.81	0.54								
2.56	0.80								
3.21	0.63								
3.21	0.63								
2.76	0.72								
3.03	0.65								
3.81	0.51								
6.41	0.31								
1.65	1.17								
3.59	0.54								
3.10	0.61								
3.55	0.53								

4.05	0.46								
3.95	0.47								
2.01	0.91								
4.02	0.46								
1.89	0.97								
4.43	0.41								
4.00	0.44								
3.14	0.56								
2.44	0.71								
3.42	0.51								
5.57	0.31								
3.79	0.46								
1.89	0.92								
2.64	0.66								
1.89	0.92								
2.60	0.66								
3.03	0.56								
1.91	0.90								
3.67	0.46								
2.04	0.82								
1.76	0.95								
3.75	0.45								
3.61	0.46								
2.09	0.79								
3.28	0.50								
2.93	0.56								
2.67	0.60								
4.40	0.37								
3.01	0.53								
2.03	0.78								
4.36	0.36								
3.82	0.41								
3.89	0.40								
2.99	0.51								
2.51	0.58								
1.97	0.74								
2.45	0.60								
3.23	0.44								
0 mm	0 mm	8 mm	8 mm	18 mm	18 mm	27 mm	27 mm	38 mm	38 mm
Major	Minor	Major	Minor	Major	Minor	Major	Minor	Major	Minor
2.48	0.58								
2.04	0.70								
2.49	0.57								
1.41	0.97								
2.00	0.68								
2.30	0.58								
1.55	0.86								
2.70	0.48								
2.64	0.49								
3.30	0.39								
1.41	0.90								



2.72	0.47								
2.43	0.53								
4.23	0.29								
2.41	0.50								
2.92	0.42								
1.64	0.74								
2.10	0.56								
2.51	0.47								
1.52	0.78								
2.75	0.43								
1.46	0.81								
2.54	0.45								
1.66	0.66								
2.71	0.40								
3.18	0.33								
2.34	0.45								
2.09	0.51								
2.14	0.48								
1.86	0.55								
1.74	0.59								
1.69	0.59								
2.64	0.38								
2.30	0.43								
1.92	0.50								
2.83	0.34								
2.05	0.46								
1.38	0.68								
2.13	0.42								
1.13	0.79								
2.11	0.41								
1.72	0.51								
1.56	0.56								
2.62	0.32								
2.53	0.33								
1.86	0.40								
2.06	0.36								
1.35	0.55								
2.46	0.30								
1.62	0.46								
1.23	0.55								
2.27	0.30								
1.56	0.44								
0 mm	0 mm	8 mm	8 mm	18 mm	18 mm	27 mm	27 mm	38 mm	38 mm
Major	Minor	Major	Minor	Major	Minor	Major	Minor	Major	Minor
1.54	0.45								
1.92	0.36								
1.89	0.33								
1.21	0.49								
0.92	0.58								
3.00	0.18								
0.93	0.57								

1.53	0.31
1.85	0.25
1.53	0.20
0.83	0.38

## **Bibliography**

- Andrews BJ, Gardner JE, in review, Effects of caldera collapse on conduit dimensions and magma decompression rate: An example from the 1800 14C yr BP eruption of Ksudach Volcano, Kamchatka, Russia, *J. Volcanol. Geotherm. Res.*
- Alidibirov M, Dingwell DB, 2000, Three fragmentation mechanisms for highly viscous magma under rapid decompression, *Journal of Volcanology and Geothermal Research* 100: 413-421.
- Asimow PD, Ghiorso MS, 1998, Algorithmic Modifications Extending MELTS to Calculate Subsolidus Phase Relations. *American Mineralogist* 83: 1127-1131.
- Becker H, Jochum KP, Carlson RW, 2000, Trace element fractionation during dehydration of eclogites from high-pressure terrains and the implications for elements fluxes in subduction zones. *Chemical Geology*, 163: 65-99.
- Behrens H, Gaillard F, 2006, Geochemical aspects of melts: Volatiles and redox behavior. *Elements* 2: 275-280.
- Benjamin ER, Plank T, Wade JA, Kelley KA, Hauri EH, Alvarado GF, 2007, High water contents in basaltic magmas from Irazú Volcano, Costa Rica. *Journal of Volcanology and Geothermal Research* 168: 68-92.
- Bouska V, Borovec Z, Cimbalnikova A, Kraus I, Lajcakova A, Pacesova M, 1993, *Natural glasses*. Ellis Horwood Ltd., Chichester, England, 354 p.
- Bouvier AS, Metrich N, Delocle E, 2008, Slab-derived fluids in the magma sources of St. Vincent (Lesser Antilles Arc): Volatile and light element imprints, *Journal of Petrology* 49: 1427-1448.
- Cashman KV, 1993, Relationship between plagioclase crystallization and cooling rate in basaltic melts, *Contributions to Mineralogy and Petrology*, 113: 126-142.
- Castro JM, Gardner JE, 2008, Did magma ascent rates control the explosive-effusive transition at the Inyo volcanic chain, California?, *Geology* 36: 279-282.
- Chaffey DJ, Cliff RA, Wilson BM, 1989, Characterization of the St Helena Magma Source. In: Saunders and Norry (editors), *Magmatism in the Ocean Basins*. Geol. Soc. London, Spec Publ., 42: 257-276.
- Conte AM, Perinelli C, Trigila R, 2006, Cooling kinetics experiments on different Stromboli lavas: Effects on crystal morphologies and phases composition, *Journal of Volcanology and Geothermal Research*, 155:179-200.

Cohen RS, O’Nions RK, 1982, Identification of recycled continental material in the mantle from Sr, Nd, and Pb isotope investigations. *Earth and Planetary Science Letters* 61: 73-84.

Coltelli M, Del Carlo P, Vezzoli L, 1998, Discovery of a Plinian basaltic eruption of Roman age at Etna volcano, Italy. *Geology* 26: 1095-1098.

Coltelli M, Del Carlo P, Vezzoli L, 1995, Stratigraphy of the Holocene Mt. Etna explosive eruptions. *Periodico di Mineralogia* 64: 141-143.

Costantini L, Bonadonna C, Houghton BF, Wehrmann H, 2009, New physical characterization of the Fontana Lapilli basaltic Plinian eruption, Nicaragua, *Bulletin of Volcanology* 71: 337-335.

Costantini L, Houghton BF, Bonadonna C, 2010, Constraints on eruption dynamics of basaltic explosive activity derived from chemical and microtextural study: The example of the Fontana Lapilli Plinian eruption, Nicaragua, *Journal of Volcanology and Geothermal Research* 189: 207-224.

Couch S, 2003, Experimental investigation of crystallization kinetics in a haplogranite system. *American Mineralogist*, 88: 1471-1485.

Dasgupta R, Hirschmann MM, Withers AC, 2004, Deep global cycling of carbon constrained by the solubility of anhydrous, carbonated eclogite under upper mantle conditions. *Earth and Planetary Science Letters* 227: 73-85.

Danyushevsky LV, Della-Pasqua, FN, Sokolov S, 2000, Re-equilibration of melt inclusions trapped by magnesian olivine phenocrysts from subduction-related magmas: petrological implications. *Contrib. Mineral. Petrol.* 138: 68– 83.

Dale CW, Gannoun A, Buron KW, Argles TW, Parkinson IJ, 2007, Rhenium–osmium isotope and elemental behavior during subduction of oceanic crust and the implications for mantle recycling. *Earth and Planetary Science Letters* 253: 211–225.

Del Carlo P, 2001, The 122 BC Etna Plinian eruption: Magmatic processes and eruptive dynamics on the basis of chemical, petrographical and volcanological data. *Plinius* 25: 39-43.

Del Carlo P, Pompilio M, 2004, The relationship between volatile content and the eruptive style of basaltic magma: the Etna case. *Annals Geophys* 47: 1423-1432.

Devine JD, Rutherford MJ, Gardner JE, 1997, Petrologic determination of ascent rates for the 1995-1997 Soufriere Hill Volcano andesitic magma, *Geophysical Research Letters* 25: 3673-3676.

Dingwell DB, Webb SL, 1989, Structural relaxation in silicate melts and non-Newtonian melt rheology in geologic processes. *Phys Chem Minerals* 16: 508-516.

Dixon JE, Stolper EM, Holloway JR, 1995, An experimental study of water and carbon dioxide solubilities in mid-ocean ridge basaltic liquids, Part I, Calibration and solubility models, *Journal of Petrology*, 36: 1607-1631.

Edmond JM, Measures C, McDuff RE, Chan LH, Collier R, Grant B, 1979, Ridge crest hydrothermal activity and the balances of the major and minor elements in the ocean; the Galapagos data. *Earth and Planetary Science Letters* 46: 1-18.

Eiler JM, Schiano P, Kitchen N, Stolper EM, 2000, Oxygen-isotope evidence for recycled crust in the sources of mid-ocean-ridge basalts. *Nature*, 403: 530-534.

Franck S, Bounama C, 2000, Global water cycle and Earth's thermal evolution. *Journal of Geodynamics* 32: 231-246.

Ford CE, Russell DG, Craven JA, Fisk MR, 1983, Olivine-Liquid Equilibria: Temperature, Pressure and Composition dependence of the Crystal/Liquid cation partition coefficients for Mg, Fe<sup>2+</sup>, Ca and Mn. *Journal of Petrology* 24: 256-265.

Gaonac'h H, Lovejoy S, Schertzer, D, 2003, Percolating Magmas and explosive volcanism, *Geophys. Res. Lett.*, 30: 1559-1563.

Gardner CA, Cashman KV, Neal CA, 1998, Tephra-fall deposits from the 1992 eruption of Crater Peakm Alaska: implications of clast textures for eruptive processes, *Bulletin of Volcanology*, 59: 537-555.

Gardner JE, Hilton M, Carroll MR, 1999, Experimental Constraints on Degassing of Magma: Isothermal Bubble Growth During Continuous Decompression from High Pressure, *Earth and Planetary Science Letters*, 168: 201-218.

Gardner JE, Thomas RME, Jaupart C, Tait S, 1996, Fragmentation of magma during volcanic plinian eruptions, *Bulletin of Volcanology*, 58: 144-162.

Geschwind CH, Rutherford MJ, 1995, Crystallization of microlites during magma ascent: the fluid mechanics of 1980-1986 eruptions at Mount St Helens. *Bulletin of Volcanology* 57 (5): 356-370.

Ghiorso, MS, Sack, RO, 1995, Chemical Mass Transfer in Magmatic Processes. IV. A Revised and Internally Consistent Thermodynamic Model for the Interpolation and

Extrapolation of Liquid-Solid Equilibria in Magmatic Systems at Elevated Temperatures and Pressures. *Contributions to Mineralogy and Petrology*, 119: 197-212.

Giordano D, Nichols ARL, Dingwell DB, 2005, Glass transition temperatures of natural hydrous melts: a relationship with shear viscosity and implications for the welding process, *Journal of Volcanology and Geothermal Research*, 142: 105-118.

Glaze LS, Baloga SM, 1996, Sensitivity of buoyant plume heights to ambient atmospheric conditions: Implications for volcanic eruption columns, *Journal of Geophysical Research*, 101: 1529-1540.

Glaze LS, Baloga SM, Wilson L, 1997, Transport of atmospheric water vapor by volcanic eruption columns, *Journal of Geophysical Research*, 102: 6099-6108.

Goepfert K, Gardner JE, 2010, Influence of Pre-eruptive storage conditions and volatile contents on explosive Plinian style eruptions of basic magma, *Bull. Volc.* 72: 511-521.

Goepfert, 2008, Influence of Pre-eruptive storage conditions and volatile contents on explosive fragmentation of mafic Plinian eruptions. Masters Thesis, University of Texas at Austin, 72 pp.

Grove TL, Parman SW, Bowring SA, Price RC, Baker MB, 2002, The role of an H<sub>2</sub>O-rich fluid component in the generation of primitive basaltic andesites and andesites from the Mt. Shasta region, N. California. *Contributions to Mineralogy and Petrology* 142: 375–396.

Gurenko AA, Belousov AB, Trumbull RB, Sobolev AV, 2005, Explosive basaltic volcanism of the Chikurachki Volcano (Kurile arc, Russia): Insights on pre-eruptive magmatic conditions and volatile budget revealed from phenocryst-hosted melt inclusions and groundmass glasses. *J Volcanol Geotherm Res* 147:203-232.

Hammer JE, Rutherford MJ, 2002, An experimental study of the kinetics of decompression-induced crystallization in silicic melt, *Journal of Geophysical Research*, doi:10.1029/2000JB000281.

Hart S, 1988, Heterogeneous mantle domains: signatures, genesis and mixing chronologies. *Earth and Planetary Science Letters*, 90: 273-296.

Hauri EH, 2002, SIMS analysis of volatiles in silicate glasses, 2: isotopes and abundances in Hawaiian melt inclusions. *Chem. Geology* 183: 115-141.

Hauri EH, Hart SR, 1993, Re-Os isotope systematics of HIMU and EMII oceanic island basalts from the south Pacific Ocean. *Chem. Geology* 114: 353-371.

Hoffman AW, 1988, Chemical differentiation of the Earth: The relationship between mantle, continental crust and oceanic crust. *Earth and Planetary Science Letters* 90: 287-314.

Hort M, Gardner JE, 2000, Constraints on degassing of pumice clasts during Plinian volcanic eruptions based on model calculations, *Journal of Geophysical Research*, 105: 25981-26001.

Houghton BF, Gonnermann HM, 2008, Basaltic explosive volcanism: Constraints from deposits and models. *Chemie der Erde - Geochem* 68: 117-140.

Houghton BF, Wilson CJN, Del Carlo P, Coltelli M, Sable JE, Carey RJ, 2004, The influence of conduit processes on changes in style of basaltic Plinian eruptions: Tarawera 1886 and Etna 122 BC. *J. Volcanol. Geotherm. Res.* 137: 1-14.

Houghton BF, Wilson CJN, 1989, A vesicularity index for pyroclastic deposits, *Bull Volcanol* 51: 451-462.

Ihinger PD, Hervig RL, McMillan PF, 1994, Analytical methods for volatiles in glasses. *Reviews in Mineralogy*, 30: 67-121.

Ito E, Harris DM, Anderson AT, 1983, Alteration of oceanic crust and geologic cycling of chlorine and water. *Geochimica et Cosmochimica Acta* 47: 1613-1624.

Jackson MG, Dasgupta R, 2008, Compositions of HIMU, EM1, and EM2 from global trends between radiogenic isotopes and major elements in ocean island basalts. *Earth and Planetary Science Letters* 276: 175-186.

Jarrard RD, 2003, Subduction fluxes of water, carbon dioxide, chlorine, and potassium. *Geochemistry Geophysics Geosystems* 4: 1-50. doi:10.1029/2002GC000392

Jaupart C, 2000, Magma ascent at shallow levels. In, Sigurdsson, H. (ed.), *Encyclopedia of Volcanoes*, Academic Press, San Diego, CA, 237-248.

Kent AJR, Peate DW, Newman S, Stolper EM, Pearce JA, 2002, Chlorine in submarine glasses from the Lau Basin: seawater contaminations and constraints on the composition of slab-derived fluids. *Earth and Planetary Science Letters* 202: 361-377.

Koyaguchi T, Mitani NK, 2005. A theoretical model for fragmentation of viscous bubbly magmas in shock tubes. *Journal of Geophysical Research* 110 (B10): B10202. doi:10.1029/2004JB003513.

Lassiter JC, Blichert-Toft J, Hauri EH, Barszczus HG, 2003. Isotope and trace element variations in lavas from Ravivavae and Rapa, Cook-Austral islands: constraints on the

nature of HIMU- and EM-mantle and the origin of mid-plate volcanism in French Polynesia. *Chem. Geol.* 202: 115-138.

Lassiter JC, Hauri EH, Nikogosian IK, Barszczus HG, 2002, Chlorine-potassium variations in melt inclusions from Raivavae and Rapa, Austral Islands: constraints on chlorine recycling in the mantle and evidence for brine-induced melting of oceanic crust. *Earth and Planetary Science Letters* 202: 525-540.

Lejeune AM, Richet P, 1995. Rheology of crystal-bearing silicate melts – an experimental study at high viscosities. *J. Geophys. Res.* 100: 4215–4229.

Leshner CE, Cashman KV, Mayfield JD, 1999, Kinetic controls on crystallization of Tertiary North Atlantic basalt and implications for the emplacement and cooling history of lava at site 989, Southeast Greenland rifted margin, In: Larsen, H.C., R.A. Duncan, J.F. Allan, and K. Brooks (eds.), *Proceedings of the Ocean Drilling Project, Scientific Results*, 163: 135-148.

Lofgren GE, 1974, An experimental study of plagioclase crystal morphology: isothermal crystallization. *American journal of Science* 274: 243-273.

Lofgren GE, 1980, Experimental studies on the dynamic crystallization of silicate melts. In: Hargaves, RB (Ed), *Physics of magmatic processes*. Princeton University Press, Princeton, NJ, United States, pp, 487-565.

Lowenstern JB, 2003, Melt inclusions come of age: Volatiles, Volcanoes, and Sorby's Legacy, In: B. De Vivo and R.J. Bodnar (eds). *Melt Inclusions in Volcanic Systems: Methods, Applications and Problems*. *Developments in Volcanology* 5, Elsevier Press, Amsterdam, pp. 1-22.

Ludden J, 2009, Subduction fluxes through geologic time. *Applied Geochemistry* 24: 1052-1057.

Mader HM, 1998, Conduit flow and fragmentation. In: Gilbert GS, Sparks RSJ (eds) *The Physics of Explosive Volcanic Eruptions*. *Geol Soc London*: 51-71.

Mangan M, Sisson T, 2000, Delayed, disequilibrium degassing in rhyolite magma: decompression experiments and implications for explosive volcanism. *Earth and Planetary Science Letters* 183: 441-455.

Michael PJ, Schilling JG, Chlorine in mid-ocean ridge magmas-evidence for assimilation of seawater-influenced components, *Geochim. Cosmochim. Acta* 53: 3131-3143.



Morris JD, Hart SR, 1983, Isotopic and incompatible element constraints on the genesis of island arc volcanics for Cold Bay and Amak island, Aleutians, and implications for mantle structure, *Geochimica et Cosmochimica Acta* 47: 2015-2030.

Münker C, Wörner G, Yogodzinski G, Churikova T, 2004, Behaviour of high field strength elements in subduction zones: constraints from Kamchatka-Aleutian arc lavas. *Earth and Planetary Science Letters* 224: 275-293.

Namiki A, Manga M, 2008, Transition between fragmentation and permeable outgassing of low viscosity magmas, *Journal of Volcanology and Geothermal Research* 169: 48-60.  
Newman S, Lowenstern JB, 2000, VolatileCalc: a silicate melt-H<sub>2</sub>O-CO<sub>2</sub> solution model written in Visual Basic for Excel, *Computers in Geosciences*, 28: 597-604.

Nielsen RL, Michael P, and Sours-Page RE, 1998, Physical and chemical indicators of compromised melt inclusions. *Geochim. Cosmochim. Acta*, 61, 161-172.

Nielsen CH, Sigurdsson H, 1981, Quantitative methods for electron microprobe analysis of sodium in natural and synthetic glasses. *American Mineralogist* 66: 547-552.

Papale P, 1999, Strain-induced magma fragmentation in explosive eruptions. *Nature* 397: 425-428.

Pearce JA, Peate DW, 1995, Tectonic Implications of the composition of volcanic arc magmas, *Ann. Rev. Earth Planet. Sci.* 23: 251-285.

Philippot P, Agrinier P, Scambelluri M, 1998, Chlorine cycling during subduction of altered oceanic crust. *Earth Planet Sci Lett.* 161: 33-44.

Plank T, Langmuir CH, 1998, The chemical composition of subducting sediment and its consequences for the crust and mantle, *Chemical Geology* 145: 325-394.

Portnyagin M, Hoernle K, Plechov P, Mironov N, Khubunaya S, 2007, Constraints on mantle melting and composition and nature of slab components in volcanic arcs from volatiles (H<sub>2</sub>O, S, Cl, F) and trace elements in melt inclusions from the Kamchatka Arc. *Earth and Planetary Science Letters* 255: 53-69

Proussevitch AA, Sahagian DL, 1996. Dynamics of coupled diffusive and decompressive bubble growth in magmatic systems. *J. Geophys. Res.* 101: 17447-17456.

Rapp RP, Irifune T, Shimizu N, Nishiyama N, Norman MD, Inoue T, 2008, Subduction recycling of continental sediments and the origin of geochemically enriched reservoirs in the deep mantle. *Earth and Planetary Science Letters* 271: 12-23.

Regenauer-Lieb, Klaus. 2006. Water and geodynamics. in *Reviews in Mineralogy and Geochemistry* 62: 451-473.

Richard G, Monnereau M, Ingrun J, 2002, Is the transition zone an empty water reservoir? Interferences from numerical model of mantle dynamics. *Earth and Planetary Science Letters* 205: 37-51.

Roggensack K, Hervig RL, McKnight SB, Williams SN, 1997, Explosive basaltic volcanism from Cerro Negro Volcano: Influences of volatiles on eruptive style, *Science* 277: 1639-1641.

Roscoe R, 1952, The viscosity of suspensions of rigid spheres, *British Journal of Applied Physics* 3: 267. doi:10.1088/0508-3443/3/8/306

Roux PJ le, Shirey SB, Hauri EH, Perfit MR, Bender JF, 2006, The effects of variable sources, process and contaminants on the composition of northern EPR MORB (8-10°N and 12-14°N): Evidence from volatiles (H<sub>2</sub>O, CO<sub>2</sub>, S) and halogens (F, Cl). *Earth and Planetary Science Letters* 251: 209-231.

Rowe MC, Nielsen RL, Kent AJR, 2006, Anomalously high Fe contents in rehomogenized olivine-hosted melt inclusions from oxidized magmas. *American Mineralogist* 91: 82-91.

Rowe MC, Lassiter JC, 2009, Chlorine enrichment in central Rio Grande Rift basaltic melt inclusions: Evidence for subduction modification of the lithospheric mantle. *Geology* 37: 439-442.

Saal AE, Hart SR, Shimizu N, Hauri EH, Layne GD, Eiler JM, 2005, Pb isotope variability in melt inclusions from the EMI-EMII-HIMU mantle end-members and the role of the oceanic lithosphere. *Earth and Planetary Science Letters* 240: 605-620.

Sable JE, Houghton BF, Del Carlo P, Coltelli M, 2006, Changing conditions of magma ascent and fragmentation during the 122 BC basaltic Plinian eruption: Evidence from clast microtextures. *J Volcanol Geotherm Res* 158: 333-354.

Sandwell DT, Smith WHF, 1997, Global sea floor topography from satellite altimetry and ship depth soundings. *Science* 277: 1956-1962.

Shimizu N, 1978, Analysis of the zoned plagioclase of different magmatic environments: A preliminary ion-microprobe study. *Earth and Planetary Science Letters* 39: 398-406.

Sparks RSJ, Barclay J, Jaupart C, Mader HM, Phillips JC, 1994, Physical aspects of magmatic degassing. I. Experimental and theoretical constraints on vesiculation. In: Carroll MR, Holloway JR (eds) *Volatiles in magmas* 30: 413-445.

Staudigel H , Davies GR, Hart SR, Marchant KM, Smith BM, 1995, Large - Scale isotopic Sr, Nd, and O isotopic composition of altered oceanic crust at DSDP/ODP Sites 417/418, *Earth Planet. Sci. Lett.*, 130: 169–185.

Stelling P, Begét J, Nye C, Gardner J, Devine JD, George R, 2002, Geology and petrology of ejecta from the 1999 eruptions of Shishaldin Volcano, Alaska, *Bulletin of Volcanology*, 64: 548-561.

Stroncik NA, Haase KM, 2004, Chlorine in oceanic intraplate basalts: Constraints on mantle sources and recycling processes. *Geology*, v. 32 No. 11: 945-948.

Sun SS, McDonough WF, 1989, Chemical and isotopic systematics of oceanic basalts: implications for mantle composition and processes. In: Saunders and Norry (editors), *Magmatism in the Ocean Basins*. *Geol. Soc. London, Spec Pulb.*, 42: 313-345.

Sun WD, Binns RA, Fan AC, Kamenetsky VS, Wysoczanski R, Wei GJ, HU YH, Arculus RJ, 2007. Chlorine in submarine volcanic glasses from the eastern Manus basin. *Geochimica et Cosmochimica Acta*, 71: 1542-1552.

Szramek L, Gardner JE, Hort M, 2010, Cooling-induced crystallization of microlite crystals in two basaltic pumice clasts. *American Mineralogist* 95: 503-509.

Szramek L, Gardner JE, Larsen J, 2006, Degassing and microlite crystallization of basaltic andesite magma erupting at Arenal Volcano, Costa Rica, *Journal of Volcanology and Geothermal Research* 157: 182-201.

Tait S, Thomas RME, Gardner JE, Jaupart C, 1998, Constraints on cooling rates and permeabilities of pumice in an explosive eruption jet from colour and magnetic mineralogy, *Journal of Volcanology and Geothermal Research*, 86: 79-91.

Thomas N, Jaupart C, Vergnolle S, 1994, On the vesicularity of pumice. *J. Geophys. Res.* 99: 15633–15644.

Van Der Hilst RD, Widiyantoro S, Engdahl ER, 1997. Evidence for deep mantle circulation from mantle tomography. *Nature* 386: 578-584.

Vigouroux N, Wallace PJ, Kent AJR, 2008, Volatiles in High-K magmas from the western trans-Mexican Volcanic Belt: Evidence fro Fluid Fluxing and Extreme enrichment of the mantle wedge by subduction processes. *Journal of Petrology* 49: 1589-1618.

Unni CK, Schilling JG, 1978, Cl and Br degassing by volcanism along the Reykjanes Ridge and Iceland. *Nature* 272: 19-23.

Wallace P, 2005, Volatiles in subduction zone magmas: concentrations and fluxes based on melt inclusions and volcanic gas data. *Journal of Volcanology and Geothermal Research* 140: 217-240.

Walker GPL, Self S, Wilson L, 1984, Tarawera 1886, New Zealand- A basaltic Plinian fissure eruption. *J Volcanol Geotherm Res* 21: 61-78.

Wehrmann H, Bonadonna C, Freundt A, Houghton BF, Kutterolf S, 2006, Fontana tephra: A basaltic plinian eruption in Nicaragua. *Geol Soc Am Spec Pap* 412:209-223.

White WM, 2007 p 324-326 <http://www.imwa.info/geochemistry/>

White WM, Hofmann AW, 1982, Sr and Nr isotope geochemistry of oceanic basalts and mantle evolution, *Nature* 296: 821-825.

Williams SN, 1983, Plinian airfall deposits of basaltic composition. *Geology* 11: 211-214.

Willbold M, Stracke A, 2006, Trace element composition of mantle end-members: Implications for recycling of oceanic and upper and lower continental crust. *Geochemistry Geophysics Geosystems* 7: Q04004, doi:10.1029/2005GC001005.

Woodhead JD, 1996. Extreme HIMU in an oceanic setting: the geochemistry of Mangaia Island (Polynesia), and temporal evolution of the Cook-Austral hotspot. *J. Volcanol. Geotherm. Res.* 72: 1-19.

Workman RK, Hauri E, Hart SR, Wang J, Blusztajn J, 2006, Volatile and trace elements in basaltic glasses from Samoa; implications for water distribution in the mantle. *Earth and Planetary Science Letters* 241: 932-951.

Wright HMN, Weinberg RF, 2009, Strain localization in vesicular magma, Implications for rheology and fragmentation. *Geology* 37: 1023-1026.

You CF, Castillo PR, Gieskes JM, Chan LH, Spivack AJ, 2006, Trace element behavior in hydrothermal experiments: Implications for fluid processes at shallow depths in subduction zones. *Earth and Planetary Science Letters* 140: 41-52.

Zhang Y, 1999, A criterion for the fragmentation of bubbly magma based on brittle failure theory. *Nature* 402: 648-650.

Zindler A, Hart S, 1986, Chemical geodynamics. *Annu. Rev. Earth Planet Sci.* 14: 493-571.

### **Vita**

Born and raised in the Pacific Northwest, Lindsay left for college on the opposite side of the country after graduating high school at the Salem-Keizer Volcanoes Stadium. While at Bowdoin College in Maine, she discovered geology as a major and realized that all she really ever had to think about again would be volcanoes. For her Master's, she went to University of Alaska, Fairbanks, thinking why not study volcanoes in the state that has the most currently active ones in the USA? After completing her work there, she decided to move cross-country again, to Texas.

Permanent Address: 4754 Flintlock Ct NE, Salem, Oregon 97503

This manuscript was typed by the author.